frontiers | Research Topics

Perinatal derivatives and the road to clinical translation, volume II

Edited by
Ornella Parolini, Antonietta Rosa Silini and Peter Ponsaerts

Published in
Frontiers in Bioengineering and Biotechnology

ISSN 1664-8714
ISBN 978-2-83251-273-9
DOI 10.3389/978-2-83251-273-9

About Frontiers

Frontiers is more than just an open access publisher of scholarly articles: it is a pioneering approach to the world of academia, radically improving the way scholarly research is managed. The grand vision of Frontiers is a world where all people have an equal opportunity to seek, share and generate knowledge. Frontiers provides immediate and permanent online open access to all its publications, but this alone is not enough to realize our grand goals.

Frontiers journal series

The Frontiers journal series is a multi-tier and interdisciplinary set of open-access, online journals, promising a paradigm shift from the current review, selection and dissemination processes in academic publishing. All Frontiers journals are driven by researchers for researchers; therefore, they constitute a service to the scholarly community. At the same time, the *Frontiers journal series* operates on a revolutionary invention, the tiered publishing system, initially addressing specific communities of scholars, and gradually climbing up to broader public understanding, thus serving the interests of the lay society, too.

Dedication to quality

Each Frontiers article is a landmark of the highest quality, thanks to genuinely collaborative interactions between authors and review editors, who include some of the world's best academicians. Research must be certified by peers before entering a stream of knowledge that may eventually reach the public - and shape society; therefore, Frontiers only applies the most rigorous and unbiased reviews. Frontiers revolutionizes research publishing by freely delivering the most outstanding research, evaluated with no bias from both the academic and social point of view. By applying the most advanced information technologies, Frontiers is catapulting scholarly publishing into a new generation.

What are Frontiers Research Topics?

Frontiers Research Topics are very popular trademarks of the *Frontiers journals series*: they are collections of at least ten articles, all centered on a particular subject. With their unique mix of varied contributions from Original Research to Review Articles, Frontiers Research Topics unify the most influential researchers, the latest key findings and historical advances in a hot research area.

Find out more on how to host your own Frontiers Research Topic or contribute to one as an author by contacting the Frontiers editorial office: frontiersin.org/about/contact

Perinatal derivatives and the road to clinical translation, volume II

Topic editors

Ornella Parolini — Catholic University of the Sacred Heart, Rome, Italy
Antonietta Rosa Silini — Fondazione Poliambulanza Istituto Ospedaliero, Italy
Peter Ponsaerts — University of Antwerp, Belgium

Citation

Parolini, O., Silini, A. R., Ponsaerts, P., eds. (2023). *Perinatal derivatives and the road to clinical translation, volume II*. Lausanne: Frontiers Media SA.
doi: 10.3389/978-2-83251-273-9

Table of contents

frontiers | Frontiers in Bioengineering and Biotechnology

TYPE Editorial
PUBLISHED 21 December 2022
DOI 10.3389/fbioe.2022.1122728

OPEN ACCESS

EDITED AND REVIEWED BY
Ranieri Cancedda,
Independent researcher, Genova, Italy

*CORRESPONDENCE
Peter Ponsaerts,
peter.ponsaerts@uantwerpen.be

SPECIALTY SECTION
This article was submitted to Tissue Engineering and Regenerative Medicine, a section of the journal Frontiers in Bioengineering and Biotechnology

RECEIVED 13 December 2022
ACCEPTED 14 December 2022
PUBLISHED 21 December 2022

CITATION
Silini AR, Parolini O and Ponsaerts P (2022), Editorial: Perinatal derivatives and the road to clinical translation, Volume II.
Front. Bioeng. Biotechnol. 10:1122728.
doi: 10.3389/fbioe.2022.1122728

Editorial: Perinatal derivatives and the road to clinical translation, Volume II

Antonietta R. Silini[1], Ornella Parolini[2,3] and Peter Ponsaerts[4]*

[1]Centro di Ricerca E. Menni, Fondazione Poliambulanza- Istituto Ospedaliero, Brescia, Italy, [2]Department of Life Science and Public Health, Università Cattolica del Sacro Cuore, Rome, Italy, [3]Fondazione Policlinico Universitario "Agostino Gemelli" IRCCS, Rome, Italy, [4]Laboratory of Experimental Hematology, Vaccine and Infectious Disease Institute (Vaxinfectio), University of Antwerp, Antwerp, Belgium

KEYWORDS

regenerative medicine, perinatal cells, placenta, secretome, preclinical (*in vivo*) studies, clinical trials, regulatory

Editorial on the Research Topic
Perinatal derivatives and the road to clinical translation, Volume II

This Research Topic issue entitled "*Perinatal Derivatives and the Road to Clinical Translation, Volume II*" builds upon Volume I to address Research Topic that are critical for moving perinatal derivatives (PnD) from preclinical lab research towards successful clinical application. These two Research Topics are a concerted effort from members of the EU-funded COST (Cooperation in Science and Technology) Action entitled "The International Network for Translating Research on Perinatal Derivatives into Therapeutic Approaches-SPRINT". Volume II is aimed to summarize our current understandings with regard to the mechanisms and therapeutic actions of PnD, thereby 1) critically discussing basic research data that can be useful for designing clinical trials, and 2) identifying research gaps to guide future research on perinatal derivatives and streamline translation to the clinic. Finally, it will equally well put attention on current clinical trials using PnD and underline aspects that are fundamental to consider for the design of future clinical trials.

Understanding the therapeutic potential and underlying biological mechanisms is critical to allow for the identification of which PnD, either by origin, by preparation or by administration, could potentially provide the most optimal clinical benefit for a specific disease, thereby assuming that each target disease may require an optimized approach. To achieve the latter in a preclinical setting, one also needs to carefully consider—and eventually re-evaluate—the relevance and potency of classical and new *in vitro* assays to demonstrate efficacy and mode-of-action of PnD.

In the first part of this Research Topic, focusing on research and clinical studies tackling the above-described questions, Pipino et al. use an innovative in vitro model to better understand the mechanisms underlying the beneficial effects of human amniotic membrane (hAM) on diabetic foot ulcers. The applied model mimics endothelial

dysfunction that occurs during *in vivo* hyperglycemia and is based on stimulating endothelial cells obtained from the umbilical cord vein of gestational diabetic mothers (GD-HUVECs) with a pro-inflammatory stimulus. Using this model, they suggest a role for the hAM to significantly reduce inflammation and to improve endothelial cell vascular network formation. Furthermore, Odet et al. contribute with two studies on the use of hAM in medication-related osteonecrosis of the jaw (MRONJ), a complication of specific pharmacological treatments such as bisphosphonates, denosumab, and angiogenesis inhibitors. In a prospective pilot study by cryopreserved hAM was applied on a compassionate use to 8 cancer patients with MRONJ. No adverse events occurred and all patients remained asymptomatic with excellent immediate significant pain relief and no infections. In a second study published by Odet et al., a pilot porcine study investigated different techniques for surgical application of hAM in an *ex vivo* model of MRONJ. Their results demonstrate that hAM had suitable mechanical properties and was easy to handle and that implantation with complete or partial coverage was the preferred choice for the MRONJ indication. This study not only once again strongly supports the use of hAM as a graft material suitable for oral surgery, but importantly, the methods described educate surgeons on the handling of hAM in oral surgery. Taking a step further towards the use of novel cell/tissue-free regenerative medicine approaches, Costa et al. analyzed whether conditioned medium or extracellular vesicles harvested from human amniotic fluid–derived stem cells (hAFSC-CM/hAFSC-EVs) could induce cardiomyocyte renewal. In this study, hAFSC were obtained from leftover samples of 2nd trimester prenatal amniocentesis (fetal hAFSC) and from clinical waste 3rd trimester amniotic fluid during scheduled C-section procedures (perinatal hAFSC), and primed under 1% O_2 to enrich hAFSC-CM and EVs with cardioactive factors. In conclusion, this study demonstrates the promising cardiogenic effects of hAMSC-EVs and further investigations will be aimed to define their specific mechanism of action and enhance their potential translation into therapeutic opportunity. Along these lines, Dubus et al. established a protocol to obtain allogenic ECM by fully removing cell membranes and nuclei moieties from Wharton's jelly (WJ) tissue while enhancing antibacterial properties of decellularized WJ based matrix. This study paves the way for the development of a WJ bioactive antibacterial matrix for regenerative medicine.

In the second part of this Research Topic, a review series is provided as a joint effort from the COST SPRINT Action. Being well-established that PnD act multimodally through complex mechanisms of action, in this Research Topic a four-part review series on functional assays for validation of PnD, spanning biological functions such as immunomodulation, anti-microbial and anti-cancer activities, anti-inflammation, wound healing, angiogenesis, and regeneration have been prepared by COST SPRINT consortium members. These reviews highlight fundamental points that must be considered in future research and in the development of more effective PnD therapies. Papait et al. discuss several assay relevant parameters for assessing the immunomodulatory activities of PnD with a focus on T cell and monocyte/macrophage assays. Silini et al. present the most commonly used functional assays for the assessment of antitumor and antimicrobial properties of PnD, and their advantages and disadvantages in assessing the functionality. Pozzobon et al. continue the review series by discussing the importance of potency testing in validating PnD therapeutics for regenerative medicine applications in brain, bone, skeletal muscle, heart, intestinal, liver, and lung pathologies. Finally, Flores et al. further elaborate on the beneficial modes of action of PnD on inflammation, angiogenesis and wound healing, with a special focus on vascular function as well as on cutaneous and oral wound healing.

Apart from the above-mentioned overview reviews on functional assays covering a broad spectrum of disease models and their clinical pathology, a third part of this Research Topic is devoted review manuscripts covering current knowledge regarding the application of PnD to specific diseases. Lange-Consiglio et al. provide an insightful overview of the applications of PnD in human and veterinary medicine for reproductive disorders with a focus on ovarian disorders in order to restore normal ovarian function. Administration of PnD was able to reduce oxidative stress and apoptosis of granulosa cells in injured ovarian tissue, to promote recovery of the oestrus cycle and to improve endocrine function, and thus may become new therapeutic options for infertile patients in the future. Norte-Munoz et al. performed a systematic review of published preclinical and clinical studies addressing PnD in the treatment of ocular diseases. While current clinical applications mainly focus on applications using the hAM, preclinical studies however indicate a potential for other PnD, yet underlining the need for more preclinical studies and clinical trials before PnD can be fully included in the daily ophthalmic practice. In another systematic review, Pichlsberger et al. discuss the application of PnD in wound healing, thereby highlighting the advantages and limitations of the most commonly used animal models and evaluating the impact of the type of PnD, the route of administration, and the dose of cells/secretome application in correlation with the wound healing outcome. Taken together, these systematic reviews underline how further concerted actions are needed to bridge the gap between PnD basic research, pre-clinical studies and PnD translation into the clinic for their use in various disease models and/or clinical applications. Furthermore, all these systematic reviews emphasize the importance of *in vitro* characterization of PnD and provide guidelines for this and for their preclinical use (see also Volume I of this Research Topic).

As a final part of this Research Topic, Gindraux et al. provides a comprehensive analysis of current clinical trials using PnD over various disease types. Identifying several knowledge gaps, they propose an approach for clinical trial preparation and registration in a uniform and standardized way, elaborating–using a publicly-available questionnaire—on

a series of criteria that are relevant when starting a new clinical trial using PnD. This article is also important in for raising awareness to the medical field to further investigate PnD-based products in clinical practice.

Concluding, the COST SPRINT Action has here shared expertise and knowledge with the scientific community for guiding future research on PnD into streamlined translation to the clinic, thereby putting forward their therapeutic potential that will safely and surely turn into a clinical reality.

Author contributions

All authors listed have made a substantial, direct, and intellectual contribution to the work and approved it for publication.

Conflict of interest

The authors declare that the research was conducted in the absence of any commercial or financial relationships that could be construed as a potential conflict of interest.

Publisher's note

frontiers in Bioengineering and Biotechnology

SYSTEMATIC REVIEW
published: 24 September 2021
doi: 10.3389/fbioe.2021.742858

Systematic Review of the Application of Perinatal Derivatives in Animal Models on Cutaneous Wound Healing

Melanie Pichlsberger[1†], Urška Dragin Jerman[2†], Hristina Obradović[3†], Larisa Tratnjek[2†], Ana Sofia Macedo[4], Francisca Mendes[5,6], Pedro Fonte[5,6,7,8], Anja Hoegler[1], Monika Sundl[1], Julia Fuchs[1], Andreina Schoeberlein[9,10], Mateja Erdani Kreft[2†], Slavko Mojsilović[3†] and Ingrid Lang-Olip[1†]*

[1]Division of Cell Biology, Histology and Embryology, Gottfried Schatz Research Center, Medical University of Graz, Graz, Austria, [2]Institute of Cell Biology, Faculty of Medicine, University of Ljubljana, Ljubljana, Slovenia, [3]Group for Hematology and Stem Cells, Institute for Medical Research, University of Belgrade, Belgrade, Serbia, [4]LAQV, REQUIMTE, Department of Chemical Sciences-Applied Chemistry Lab, Faculty of Pharmacy, University of Porto, Porto, Portugal, [5]iBB–Institute for Bioengineering and Biosciences, Department of Bioengineering, Instituto Superior Técnico, Universidade de Lisboa, Lisboa, Portugal, [6]Associate Laboratory i4HB–Institute for Health and Bioeconomy at Instituto Superior Técnico, Universidade de Lisboa, Lisboa, Portugal, [7]Center for Marine Sciences (CCMar), Faculty of Sciences and Technology, University of Algarve, Faro, Portugal, [8]Department of Chemistry and Pharmacy, Faculty of Sciences and Technology, University of Algarve, Faro, Portugal, [9]Department of Obstetrics and Feto-maternal Medicine, Inselspital, Bern University Hospital, University of Bern, Bern, Switzerland, [10]Department for BioMedical Research (DBMR), University of Bern, Bern, Switzerland

OPEN ACCESS

Edited by:
Peter Ponsaerts,
University of Antwerp, Belgium

Reviewed by:
Chia-Ching (Josh) Wu,
National Cheng Kung University, Taiwan
Menekse Ermis Sen,
Terasaki Institute for Biomedical Innovation, United States

***Correspondence:**
Ingrid Lang-Olip
Ingrid.lang@medunigraz.at

[†]These authors have contributed equally to this work

Specialty section:
This article was submitted to Tissue Engineering and Regenerative Medicine, a section of the journal Frontiers in Bioengineering and Biotechnology

Received: 16 July 2021
Accepted: 06 September 2021
Published: 24 September 2021

Citation:
Pichlsberger M, Jerman UD, Obradović H, Tratnjek L, Macedo AS, Mendes F, Fonte P, Hoegler A, Sundl M, Fuchs J, Schoeberlein A, Kreft ME, Mojsilović S and Lang-Olip I (2021) Systematic Review of the Application of Perinatal Derivatives in Animal Models on Cutaneous Wound Healing. Front. Bioeng. Biotechnol. 9:742858. doi: 10.3389/fbioe.2021.742858

Knowledge of the beneficial effects of perinatal derivatives (PnD) in wound healing goes back to the early 1900s when the human fetal amniotic membrane served as a biological dressing to treat burns and skin ulcerations. Since the twenty-first century, isolated cells from perinatal tissues and their secretomes have gained increasing scientific interest, as they can be obtained non-invasively, have anti-inflammatory, anti-cancer, and anti-fibrotic characteristics, and are immunologically tolerated *in vivo*. Many studies that apply PnD in pre-clinical cutaneous wound healing models show large variations in the choice of the animal species (e.g., large animals, rodents), the choice of diabetic or non-diabetic animals, the type of injury (full-thickness wounds, burns, radiation-induced wounds, skin flaps), the source and type of PnD (placenta, umbilical cord, fetal membranes, cells, secretomes, tissue extracts), the method of administration (topical application, intradermal/subcutaneous injection, intravenous or intraperitoneal injection, subcutaneous implantation), and the type of delivery systems (e.g., hydrogels, synthetic or natural biomaterials as carriers for transplanted cells, extracts or secretomes). This review provides a comprehensive and integrative overview of the application of PnD in wound healing to assess its efficacy in preclinical animal models. We highlight the advantages and limitations of the most commonly used animal models and evaluate the impact of the type of PnD, the route of administration, and the dose of cells/secretome application in correlation with the wound healing outcome. This review is a collaborative effort from the COST SPRINT Action (CA17116), which broadly aims at approaching consensus for different aspects of PnD research, such as providing inputs for future standards for the preclinical application of PnD in wound healing.

Keywords: perinatal derivatives, placenta, cells, preclinical studies, animal models, wound healing, skin, cutaneous

INTRODUCTION

Human skin is the largest organ of the body that provides complex functions. It protects the body against mechanical, chemical, and physical impact, as well as dehydration. In addition, it modulates the body temperature and serves as a sensory organ. The compact part of the skin, the cutis, consists of the epidermis, a keratinized stratified squamous epithelium, and the underlying dermis, which is built from connective tissue. Below the cutis is the loosely-layered subcutis, which is enriched by adipose tissue.

Severe skin injury is the result of wounds caused by incision, excision, abrasion, burn, radiation or pressure. The degree of wounding describes the depth of damage to the respective skin layers. In first-degree wounds, only the epidermis is affected, in second-degree wounds, the epidermis and dermis are affected, and in third-degree wounds, all three skin layers including the subcutis are affected.

Skin damage is repaired by wound healing, a multistep, finely orchestrated process that includes hemostasis, inflammation, tissue growth (proliferation), and tissue remodeling (maturation) (Xue et al., 2018). This process is highly efficient in healthy individuals. However, the type, extent, and depth of injury, as well as any deviations in the fragile wound repair response, affect the healing outcome. Parameters such as aging, comorbidities (e.g., diabetes, obesity, arterial or venous insufficiencies, autoimmune diseases), and severe burn injuries constitute some of the causes that delay wound healing, often due to insufficient blood supply based on impaired wound revascularization (Demidova-Rice et al., 2012). Non-healing wounds that persist for more than 3 months are called *chronic wounds*. These types of wounds have failed to proceed through an orderly and timely reparative process to produce anatomic and functional integrity of the injured site (Lazarus et al., 1994) and are often detained in a self-perpetuating inflammatory stage that hinders progression to proliferation (Stojadinovic et al., 2008). Approximately 40 million patients worldwide suffer from chronic wounds, which are still a challenge to treat and constitute a significant financial burden on the health care system (Sen et al., 2009). Thus, new therapeutic approaches for wound healing are highly warranted.

A promising strategy for wound treatment is the application of human perinatal derivatives (PnD). PnD are birth-associated tissues such as the placenta and its annexes (human amniotic membrane (hAM), chorionic membrane, decidua, umbilical cord) and the amniotic fluid. PnD are an abundant source of extracellular matrix proteins, growth factors, and cells that have already been used in a wide variety of applications in tissue engineering and regenerative medicine (Deus et al., 2020). The application of the hAM has a long tradition in the treatment of wounds. Early studies from 1909 to 1913 reported successful use of the hAM in skin transplantation (Davis, 1909) and for treating burns and skin ulcerations as a biological dressing. Its use significantly reduced pain and increased the epithelialization rate of the traumatized skin without signs of infection (Sabella, 1913; Stern, 1913). Several clinical trials in the subsequent decades confirmed the successful use of the hAM for skin injuries (Silini et al., 2015). The twenty-first century brought the breakthrough for cell isolations from different placental regions and the progressive investigation of their therapeutic potential. Minimal criteria for the definition of PnD derived cells were described in 2008 (Parolini et al., 2008), and ongoing extensive characterization of PnD was performed (Caruso et al., 2012; Silini et al., 2020).

PnD derived cells have anti-inflammatory, immunomodulatory, anti-cancer, anti-fibrotic, anti-apoptotic, and anti-oxidant effects. They are immunologically tolerated *in vivo* and have been transplanted without signs of immunological rejection, meaning that the application does not require immunosuppressive treatment (Ueta et al., 2002; Bailo et al., 2004; Jirsova and Jones, 2017).

With the expanding knowledge that cells act by paracrine mechanisms, the released secretomes (cell-derived conditioned media, cell-derived extracellular vesicles) are gaining increasing interest. Placental cells secrete factors that are crucial for wound healing such as EGF, IL-8, and IGF-1, which modulate migration and proliferation of keratinocytes, fibroblasts, and endothelial cells (Kim et al., 2012). hAM mesenchymal stromal cells (hAMSC) and their secretomes exhibit beneficial, survival-enhancing effects on endothelial cells *in vitro* and were shown to stabilize endothelial networks in the Matrigel assay (König et al., 2012; König et al., 2015). Further, co-transplantation of hAMSC and placental endothelial cells enabled the formation of human capillaries connecting to the murine blood circulation in a mouse model *in vivo* (Kinzer et al., 2014).

As the formation of new blood vessels is critical for normal wound healing, innovations to improve wound revascularization could also lead to significant advances in wound healing therapy and patient care (Demidova-Rice et al., 2012). Improved techniques for tissue preservation, and recent advances in isolation and culture procedures for PnD derived cells paved the way for established clinical uses and investigative pre-clinical and clinical trials such as the application of placenta derived mesenchymal stromal-like cells (PDA-002) for the treatment of patients with diabetic foot ulcer wounds and peripheral arterial disease (Silini et al., 2015)[1].

This review provides a thorough overview of the application of PnD in wound healing to assess its efficacy in preclinical animal models based on different wound types. We highlight the advantages and limitations of the most commonly used animal models and evaluate the impact of the type of PnD, the delivery method and the dose of cells/secretome application in correlation with the wound healing outcome.

METHODS AND SEARCH STRATEGY TO COLLECT THE DATA

We performed a systematic literature search of the PubMed® database covering a period from 2004 to 2020 and used the Boolean search string (Supplements) in accordance with the

[1]https://clinicaltrials.gov/

consensus of the scientific network of the COST SPRINT Action (CA17116) to identify articles exploring therapeutic options of PnD in *in vivo* experimental models of wound healing. Titles and abstracts were screened to select publications including *in vivo* models evaluating the efficacy of PnD. The search was limited to original research publications available as full text in English. The publications were cross-checked for meeting the inclusion criteria by an independent study. The selection workflow was compliant with the PRISMA guidelines (Page et al., 2021a; Page et al., 2021b).

We obtained 141 manuscripts investigating the application of PnD to animal wound- or angiogenic models. We further focused on studies of cutaneous wound healing, which used human PnD. Articles with insufficient data (insufficient group sizes, no statistics, no controls, no adequate figures) were excluded. After the screening process, we identified 79 relevant articles. We observed a continuous increase in publications on the application of PnD in animal models of cutaneous wound healing during the last decade. The major part of these studies was performed in Asia (China 41%, Iran 15%, rest of Asia 22%), followed by the United States and Canada (11%), Europe (6%), South America (4%) and Africa (Egypt 1%). From the relevant articles, we extracted data concerning animal species (rodents, large animals), diabetic status (diabetic or non-diabetic animals), the type of wounds (full-thickness wounds, burns, radiation-induced wounds, skin flaps, subcutaneous pockets), the source and type of PnD (placenta, umbilical cord, fetal membranes, cells, secretomes, tissue extracts), the method and dose of administration (topical application, intradermal/subcutaneous injection, intravenous or intraperitoneal injection, subcutaneous implantation) and the use of delivery systems (e.g., hydrogels, synthetic or natural biomaterials as carriers for transplanted cells, extracts or secretomes). Data extraction was performed to meet the populations, interventions, comparators, outcomes and study designs (PICOS) criteria (McKenzie et al., 2021).

PND USED FOR CUTANEOUS WOUND HEALING IN PRECLINICAL STUDIES

Types, Dosage and Application Mode of PnD

In the papers included in this review, PnD were applied in the form of cells, cell secretomes (cell-derived conditioned media (CM), cell-derived small extracellular vesicles (sEV), tissue membranes and tissue extracts (**Figure 1**). Naming and abbreviations of the PnD types in the reviewed studies varied due to the authors' discretion. To improve the comparability of data, we harmonized terms according to the recently published consensus nomenclature for perinatal tissues and cells (Silini et al., 2020). For example, as there is no consensus on the zones of Wharton's jelly and on the experimental protocols for isolation of the cells thereof, we have used the single term *human umbilical cord mesenchymal stromal cells* (hUC-MSC), which comprises all potential cell subpopulations. The types and combinations of the PnD applied in these studies as well as the delivery systems are outlined in detail in **Tables 1–5**. Overall, in 14 of 79 studies, two different PnD types were addressed. The authors either compared the effect of different PnD (e.g., cells vs. cell-derived CM, cells vs. cell-derived sEV, cells vs. tissue), or two PnD types were applied in combination (different cell types, cells and cell-derived CM, cells and tissue).

To standardize the different dosages of PnD used in the reviewed studies, the doses are presented as the number, weight (μg), or volume (μl) of the specific PnD per wound area (cm^2), when the PnD were administered locally (topically, intradermally/subcutaneously), or per body weight (kg) of an animal, when PnD were applied systemically (intravenously or intraperitoneally). To determine the dose of locally administered PnD per cm^2, we divided the quantity of applied PnD by the wound area. In most of the studies, both the wound area and the exact quantity of PnD were indicated.

Perinatal Cells

Perinatal cells were the most commonly used PnD type in preclinical studies of cutaneous wound healing (49.5%) (**Table 1**). Mostly, hUC-MSC were used (60.4%), followed by hAMSC (12.5%) and MSC isolated from the whole placenta (hPMSC, 8.3%). Cells were applied as suspensions injected intradermally/subcutaneously or intravenously, topically by cell spraying, or seeded on electrospun or biological scaffolds, including the amniotic membrane. Cell therapy implemented by administering cells to the bloodstream may lead to the accumulation of injected cells in other organs such as the lungs (Ankrum and Karp, 2010).

Perinatal cells were applied in doses ranging from 200 cells per cm^2 up to 8 million cells per cm^2 (**Figure 2A**). The most frequently applied dose was around 2 million cells per cm^2 (mode = $1.99 \times 10^6/cm^2$, median = $1 \times 10^6/cm^2$). Regarding mode of application, lower doses of cells were used for topical application (median = $0.6 \times 10^6/cm^2$) than for subcutaneous (median = $1.78 \times 10^6/cm^2$) and intradermal (median = $3.54 \times 10^6/cm^2$) applications (**Figure 2B**). Mostly used dose for full-thickness wound model was $1.99 \times 10^6/cm^2$ (median = $1.88 \times 10^6/cm^2$), while for the other wound models the doses were usually less than $1 \times 10^6/cm^2$ (median = $0.12 \times 10^6/cm^2$ for burn wounds, $0.11 \times 10^6/cm^2$ for radiation wounds, $0.22 \times 10^6/cm^2$ for skin flaps, and $0.1 \times 10^6/cm^2$ for non-healing skin lesions). The median cell doses for mice were higher ($1.99 \times 10^6/cm^2$) than those for the rats ($0.16 \times 10^6/cm^2$). The systemic doses were 25×10^6/kg and 29×10^6/kg when applied intravenously, and 45×10^6/kg, when applied intraperitoneally (Liu et al., 2014; Abd-Allah et al., 2015; Liu et al., 2016; Shi et al., 2020). Moreover, few studies compared the effect of applying different cell concentrations. Namely, in a full-thickness skin wound model on rats, increasing the number of hAMSC injected into the wound bed from $2 \times 10^3/cm^2$ to 2×10^5 cells/cm^2, enhanced the wound healing results (Gao et al., 2020). On the other hand, in a full-thickness burn wound model on pigs, low doses, ranging from 200 to 40,000 cells per cm^2, topically applied in combination with a collagen-based scaffold, demonstrated superior wound healing of full-thickness burn wounds,

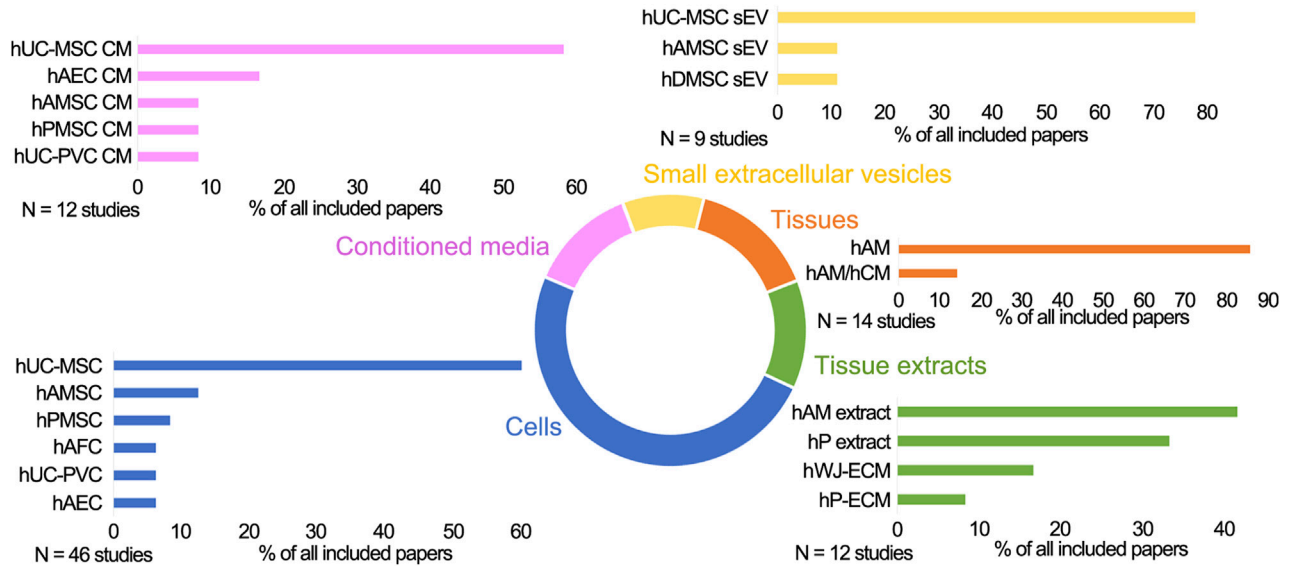

FIGURE 1 | The schematic presentation of the perinatal derivatives used in skin wound healing in preclinical studies. Cells: hUC-MSC, human umbilical cord mesenchymal stromal cells; hAMSC, human amniotic membrane mesenchymal stromal cells; hPMSC, human placenta mesenchymal stromal cells; hUC-PVC, human umbilical cord perivascular cells; hAEC, human amniotic membrane epithelial cells; hAFSC, human amniotic fluid stem cells; hAFC, human amniotic fluid cells; Conditioned media (CM) derived from hUC-MSC, hAEC, hAMSC, hPMSC, hUC-PVC; Small extracellular vesicles (sEV) derived from hUC-MSC, hAMSC, hDMSC; Tissues: hAM, human amniotic membrane; hAM/hCM, human amniotic/chorionic membrane; Tissue extracts derived from hAM, hP (human placenta), hP-ECM (human placenta-derived extracellular matrix), hWJ-ECM (human Wharton's jelly derived extracellular matrix).

compared to higher doses ($2 \times 10^5/cm^2$ to $2 \times 10^6/cm^2$) and controls (Eylert et al., 2021). In a study that compared systemic (intraperitoneal) and local (intradermal) application, the intraperitoneal injections of hPMSC showed better results than the local one, in terms of histological scores, expression of the healing promoting factors, as well as the engraftment into the wounded skin (Abd-Allah et al., 2015).

Perinatal Cell-Derived Conditioned Medium (CM)

Of the studies included in this review, 12.9% used perinatal cell-derived CM (**Table 2**). The CM derived from hUC-MSC was the most commonly used CM (58.3%). The CM is a medium collected from cell cultures and contains various cell products released by cells. These products may be proteins, non-coding RNAs, growth factors, antioxidants, proteasomes, and extracellular vesicles, which vary depending on the cell type and cell culture conditions (Maguire, 2013). The advantage of using CM collected from MSC to study regeneration lies in the ease of medium availability, storing, freezing, drying, and transporting, as well as in its lack of immunogenicity (Gunawardena et al., 2019).

CM was usually collected after 24, 48, and 72 h of cell cultivation. It was mainly applied intradermally/subcutaneously or topically and in combination with hydrogels or as a cell spray. Doses of the CM used ranged from 7 to 354 µl/cm^2. No studies examined the effects of different CM dosages on the efficacy of wound healing.

Several wound healing studies have investigated the combined treatment of cell-derived CM and corresponding cells, or have compared the efficacy of cell-derived CM versus cells alone. While both CM and its corresponding perinatal cells, alone or in combination, showed an increased rate of re-epithelization and accelerated wound closure compared to control, no significant difference in efficacy between the CM and the cells has been demonstrated (Payne et al., 2010; Shohara et al., 2012; Shrestha et al., 2013; Aguilera et al., 2014; Raj et al., 2019; Zhang et al., 2020). Only rare studies used multiple doses of CM (Payne et al., 2010; Sun et al., 2019). It was observed that frequent application of CM achieved better results on wound healing than 2-fold application (Payne et al., 2010).

Perinatal Cell-Derived Small Extracellular Vesicles (sEV)

The least used PnD type (9.6%) were perinatal cell-derived EV (**Table 3**). The cell secretome generally contains a mixture of different EV subtypes, including exosomes, apoptotic bodies and microparticles (Gangoda et al., 2015). The exosomes are the most characterized and the smallest EV. They are of endosomal origin with the size of 30–150 nm in diameter and carry many different components, such as lipids, proteins, mRNAs, non-coding RNAs, and even DNA derived from cells (reviewed in Rashed et al. (2017)). It was first thought that exosomes only play a role in removing unnecessary molecules from cells, but nowadays their involvement in a plethora of different cell responses is documented (Keller et al., 2006). According to their shape, size, and marker expression (HSP70, CD9, CD63, CD81), the EV described in the processed literature were characterized as

TABLE 1 | Application of perinatal cells in *in vivo* animal models of skin wound healing. Time points indicated in the "Outcome" column mean days (d), weeks (w) or hours (h) after treatment.

Perinatal cells					
PnD cell type	**Dosage**	**Application (carrier)**	**Wound type, animal**	**Outcome**	**References**
hAEC	3.54 × 10^6 cells/cm^2	Intradermal injection	Full-thickness, diabetic mouse Splint model	hAEC showed higher engraftment, better keratinocyte-transdifferentiation rates and accelerated wound healing (wound closure and re-epithelialization) than hASC (d28)	Jin et al. (2016)
hAFC, hAFSC	1.59 × 10^4 cells/cm^2	Topical (polyester disks covered with collagen)	Full-thickness, rat	hAFC and hAFSC achieved accelerated wound closure, epithelization, collagen fiber production, angiogenesis and the disappearance of inflammatory cells compared to controls without cells (d14, d17, d21)	Yang et al. (2013)
hAFSC	6.41 × 10^6 cells/cm^2	Intradermal/subcutaneous injection	Full-thickness, mouse	hAFSC showed a better keratinocyte-transdifferentiation and enhanced wound closure and early-stage repair of skin damage than fibroblasts and sham controls by creating a moderate inflammatory microenvironment (d21)	Sun et al. (2019)
	1.99 × 10^6 cells/cm^2	Intradermal/subcutaneous injection	Full-thickness, mouse	hAFSC enhanced re-epithelialization and collagen III contents and achieved lower numbers of myofibroblasts and less fibrotic scarring than PBS controls (best effects d14, after d21 no significance). hAFSC engrafted in the epidermis and dermis	Fukutake et al. (2019)
hAMSC	3.54 × 10^6 cells/cm^2	Intradermal injection	Full-thickness, diabetic mouse Splint model	hAMSC had higher engraftment and keratinocyte-transdifferentiation potential and induced a better healing potential (increased wound closure, re-epithelialization and cellularity) than ASC and fibroblasts (d7, d10 and d14)	Kim et al. (2012)
	0.597 × 10^6 cells/cm^2	Topical (Matrigel or Matriderm)	Full-thickness, mouse	In both application forms, hAMSC promoted neovascularization compared to control without cells. Matriderm/hAMSC enhanced wound closure (d8). Inhomogeneous distribution of Matrigel led to inadequate wound closure	Tuca et al. (2016)
	0.995 × 10^6 cells/cm^2	Topical (Matriderm or PCL/PLA, with or without Matrigel)	Full-thickness, mouse	Matriderm and PCL/PLA were suitable as carriers for hAMSC. 3 days *in vitro* culture of scaffolds with hAMSCs without Matrigel before wound application is recommended. PCL/PLA showed higher cell adherence and counteract wound contracture (d14)	Vonbrunn et al. (2020)
hUC-MSC	0.22 × 10^6 cells/cm^2	Subcutaneous injection	Skin flap, mouse	hUC-MSC were mainly distributed in the subcutaneous flap tissues and increased survival of the flap, neovascularization and expression of bFGF and VEGF (d7)	Leng et al. (2012)
	1.99 × 10^6 cells/cm^2	Subcutaneous injection (SA/Col hydrogel)	Full-thickness, mouse	SA/Col hydrogel + hUC-MSC accelerated wound closure, formation of granulation, enhanced collagen deposition and angiogenesis. Hydrogel promoted the survival of hUC-MSC, enhanced growth factors secretion, and inhibited inflammation (d7, d14)	Zhang et al. (2021)
	0.11 × 10^6 cells/cm^2	Subcutaneous injection	Radiation, rat	hUC-MSC increased neovascularization and re-epithelization (d14, d21, d28)	Liu et al. (2018)
	2.83 × 10^6 cells/cm^2	Subcutaneous injection	Full-thickness, diabetic rat	Compared to un-transduced hUC-MSC, c-Jun overexpressing hUC-MSC accelerated wound closure, enhanced angiogenesis and re-epithelialization (d7, d10, d15, d17)	Yue et al. (2020)
	1.27 × 10^6 cells/cm^2	Topical (collagen-based scaffolds, Integra® and Col)	Full-thickness, mouse	hUC-MSC accelerated angiogenesis compared to ASC and control without cells (d7, d10) and provided a suitable matrix for wound repair, without altering the inflammatory response in the animals	Edwards et al. (2014)
	0.44 × 10^6 cells/cm^2	Topical (collagen membrane)	Full-thickness, mouse	HOXA4-overexpressing hUC-MSC differentiated into epidermal cells and increased re-epithelialization of wounds and thickness of the epidermis (d7, d14, d21)	He et al. (2015)

(Continued on following page)

TABLE 1 | (*Continued*) Application of perinatal cells in *in vivo* animal models of skin wound healing. Time points indicated in the "Outcome" column mean days (d), weeks (w) or hours (h) after treatment.

Perinatal cells					
PnD cell type	**Dosage**	**Application (carrier)**	**Wound type, animal**	**Outcome**	**References**
	Not specified	Topical (collagen membrane or collagen-fibrin membrane)	Full-thickness, mouse	hUC-MSC promoted wound healing. Collagen-fibrin carriers for hUC-MSC were more efficient in wound healing than collagen membrane carriers (d5, d10, d15)	Nan et al. (2015)
	0.339 × 10^6 cells/cm^2	Topical (fibrin-based scaffold)	Full-thickness, mouse	Fibrin-based scaffolds with hUC-MSC healed slowly with no scarring. Untreated wounds or wounds treated with scaffolds without cells healed rapidly but disorderly, due to wound retraction into scarring (d15, d21, d36)	Montanucci et al. (2017)
	1.99 × 10^6 cells/cm^2	Topical (PF-127/SAP hydrogel)	Full-thickness, mouse	PF-127/SAP hydrogel enhanced engraftment of hUC-MSC in the dermis and facilitated dermis regeneration (increase in thickness, collagen fibers, hair follicles), angiogenesis and M2 macrophage formation (d8)	Deng et al. (2020)
	1.77 × 10^6 cells/cm^2	Topical (collagen scaffold)	Full-thickness, diabetic mouse Splint model	Combination of hUC-MSC therapy and hyperbaric oxygen had a collaborative effect on wound-healing, with a faster healing rate compared to hUC-MSC alone (d7)	Pena-Villalobos et al. (2018)
	0.39 × 10^6 cells/cm^2	Topical (cell spray)	Burn 3rd degree, rat	hUC-MSC increased re-epithelialization compared to control without cells. hUC-MSC were detected in the burned areas at d7, d14, d21	Pourfath et al. (2018)
	Not specified	Topical (collagen–chitosan laser drilling acellular dermal matrix)	Full-thickness, diabetic rat	hUC-MSC accelerated wound healing by activation of the Wnt signaling pathway (d7, d14, d21)	Han et al. (2019)
	200 cells/cm^2 5,000 cells/cm^2 40,000 cells/cm^2 200,000 cells/cm^2 400,000 cells/cm^2 2000,000 cells/cm^2	Topical (Integra® collagen-based scaffold)	Burn full-thickness, pig	Low dose hUC-MSC regenerated wounds most efficaciously. Best effects were achieved by 40,000 cells/cm^2 (accelerated epithelialization and vascularization, reduced signs of scarring, fibrosis, reduced numbers of macrophages compared to controls (d28)	Eylert et al. (2021)
	0.1 × 10^6 cells/cm^2	Topical (PVA hydrogel membrane)	Non-healing skin lesions, dog	hUC-MSC induced a significant progress in skin regeneration with decreased extent of ulcerated areas	Ribeiro et al. (2014)
	29 × 10^6 cells/kg	Intravenous injection	Full-thickness, diabetic rat	UC-MSC were detectable in the wound tissue (d16). They improved wound healing by regulating inflammation, trans-differentiation and providing growth factors that promote angiogenesis, cell proliferation and collagen deposition (d8, d16)	Shi et al. (2020)
	25 × 10^6 cells/kg	Intravenous injection	Burn full-thickness, rat	hUC-MSC were detectable in the wound tissue for 3 weeks. They accelerated wound healing (wound closure, vascularization, collagen deposition) and decreased inflammation (w2, w3, w6, w8)	Liu et al. (2014)
	25 × 10^6 cells/kg	Intravenous injection	Burn full-thickness, rat	hUC-MSC attenuated burn-induced excessive inflammation via secretion of ant-inflammatory protein TSG-6 which inhibits activation of P38 and JNK signaling (6, 12, 24, 48 h)	Liu et al. (2016)
a) hUC-MSC-Fib b) me-VEGF-hUC-MSC-Fib	Not specified	Topical collagen-chitosan acellular dermal matrix - tissue engineered dermis (TED)	Full-thickness, pig	me-VEGF-hUC-MSC-Fib improved the vascularization of tissue-engineered dermis and induced a higher wound healing than controls (me-hUC-MSC, empty capsule and PBS-treated group) (w3)	Han et al. (2014)
a) hUC-MSC b) hU-MSC-End	5.09 × 10^6 cells/cm^2	(a-b) Intradermal injection	Full-thickness, mouse Splint model	Transplantation of celecoxib (anti-inflammatory drug) -preconditioned hUC-MSC-End showed higher wound healing potential than hUC-MSC and hUC-MSC-End (d7)	Kaushik and Das, (2019)
hPMSC	45 × 10^6 cells/kg	Intraperitoneal and intradermal injection	Full-thickness, mouse	hPMSC enhanced wound healing through release of proangiogenic factors and decreased	Abd-Allah et al. (2015)

(Continued on following page)

TABLE 1 | (*Continued*) Application of perinatal cells in *in vivo* animal models of skin wound healing. Time points indicated in the "Outcome" column mean days (d), weeks (w) or hours (h) after treatment.

Perinatal cells					
PnD cell type	**Dosage**	**Application (carrier)**	**Wound type, animal**	**Outcome**	**References**
				proinflammatory cytokines. The intraperitoneal injections are more effective than intradermal injections (d7)	
	1.99 × 10^6 cells/cm^2	Subcutaneous injection	Full-thickness, diabetic rat	hPMSC accelerated wound closure, increased collagen deposition, granulation tissue and epidermis thickness (d15). Wound healing was accelerated by decrease of local pro-inflammatory cytokines TNF-α, IL-6 and IL-1, increase of anti-inflammatory IL-10	Wang et al. (2016)
	5.09 × 10^6 cells/cm^2	Topical (Matrigel)	Full-thickness, mouse Splint model	PDGFR-β- hPMSC displayed a superior angiogenic property and exerted enhanced therapeutic efficacy on cutaneous wound healing compared to PDGFR-β -negative hPMSC (d7, d14)	Wang et al. (2018)
hUC-PVC	7.96 × 10^6 cells/cm^2	Topical (fibrin gel)	Full-thickness, mouse	hUC-PVC accelerated re-epithelization and dermal repair and wound strength compared to treatment without cells (d7)	Zebardast et al. (2010)
	1.27 × 10^6 cells/cm^2	Topical (decellularized dermal matrix scaffold)	Full-thickness, diabetic rat	hUC-PVC accelerated wound closure rate (faster re-epithelization, more granulation tissue formation, decreased scarring and increased neovascularization than treatment without cells (d14, d21)	Milan et al. (2016)
a) hAEC-Ker + b) hUC-MSC-Fib	a) 7,500 cells/cm^2 b) 6,250 cells/cm^2	Topical (plasma-based gel)	Burn 2nd degree, full-thickness excision, rat	Scaffolds seeded with hUC-MSC-Fib and hAEC-improved re-epithelization concurrent with reduced apoptosis compared to treatment without cells (d10, d20)	Mahmood et al. (2019)
a) hAMSC b) hCP-MSC-bv c) hUC-MSC +co-application with hCP-EC	0.6 × 10^6 cells/cm^2	(a-c) Topical (Matriderm)	Full thickness, mouse	hAMSC, hCP-MSC-bv and hUC-MSC induced faster wound healing and vascularization compared to controls without cell treatment (d8). hCP-EC co-application did not further improve the advantageous effects of MSC.	Ertl et al. (2018)

Abbreviations: bFGF, basic fibroblast growth factor; col, collagen type I; hAEC, human amniotic membrane epithelial cells; hAEC-Ker, human amniotic membrane epithelial cells derived keratinocytes; hAFC, human amniotic fluid cells; hAFSC, human amniotic fluid stem cells; hAMSC, human amniotic membrane mesenchymal stromal cells; hASC, human adipose mesenchymal stromal cells; hCP-EC, human chorionic plate endothelial cells; hCP-MSC-bv, human chorionic plate mesenchymal stromal cells derived from blood vessels; hPMSC, human placenta mesenchymal stromal cells; hUC-MSC, human umbilical cord mesenchymal stromal cells; hU-MSC-End, human umbilical cord mesenchymal stromal cells -endothelial transdifferentiated; hUC-MSC-Fib, human umbilical cord mesenchymal stromal cells derived fibroblasts; hUC-PVC, human umbilical cord perivascular cells; me-VEGF- hUC-MSC-Fib, microencapsulated VEGF-gene modified human umbilical cord mesenchymal stromal cells derived fibroblasts; PCL/PLA, Poly(caprolactone)/poly(l-lactide); PDGFA, platelet derived growth factor A; PDGFR-β, platelet derived growth factor receptor β; PF-127/SAP, Pluronic F-127 hydrogel plus antioxidant sodium ascorbyl phosphate; PVA, polyvinyl alcohol; SA, sodium alginate; TED, Topical collagen-chitosan acellular dermal matrix - tissue engineered dermis; TNF-α, tumor necrosis factor α; TSG-6, TNF-stimulated gene 6 protein; VEGF, vascular endothelial cell growth factor; IL-1, IL-6, IL-10, interleukin-1, -6, -10.

exosomes. However, the International Society for Extracellular Vesicles in their position statement from 2018 (van Deun et al., 2017; Théry et al., 2018) urge authors to use an operational term for EV subtypes unless they can unequivocally prove their endosomal origin (by live imaging techniques, for example). Therefore, according to these recommendations, in this review we will refer to these EV as small EV, or sEV. The sEV derived from perinatal cells are a relatively new PnD type used for skin wound healing since they first appeared in publications only a few years ago. All included studies used sEV derived from MSC, most commonly from hUC-MSC (77.8%).

The sEV were applied mostly by subcutaneous injection in animals with burn or full-thickness wounds. The doses of sEV were predominantly expressed as μg/cm^2, except for one study where the authors used the number of particles as a measure for the sEV quantity (Bian et al., 2020). The doses were comparatively uniform throughout the analyzed studies, mainly using 100 to 156 μg/cm^2 (Zhang et al., 2015a; Zhang et al., 2015b; Zhang et al., 2016; Yang et al., 2019; Yang et al., 2020; Zhao et al., 2020) and 318 μg/cm^2 in one study (Liu et al., 2021). There were no studies that compared different dosages of sEV.

Perinatal cell-derived sEV showed similar (Zhang et al., 2015a) or even better (Zhao et al., 2020) beneficial effects on wound healing compared to perinatal cells. Gao et al. (2020) observed that sEV overexpressing micro RNA (miR)-135a significantly accelerated fibroblast cell migration by downregulating LATS2 levels to promote wound healing in rats making it the first evidence of positive miRNA effect on this process. This was

TABLE 2 | Application of perinatal cell-conditioned medium (CM) alone or compared to/combined with perinatal cells in *in vivo* animal models of skin wound healing. Time points indicated in the "Dosage" and Outcome" columns mean days (d), weeks (w) or hours (h) of/after treatment.

Perinatal cell-conditioned medium (CM)

PnD	Dosage	Application (carrier)	Wound type, animal	Outcome	References
hAEC-CM	100 µl (48 h) CM/cm^2 on d1 and d3	Subcutaneous injection	Full-thickness, mouse	hAEC-CM enhanced wound healing (closure, tissue reorganization, replacement of skin appendages), whereas CM+ ERK, JNK and AKT- inhibitors impaired wound healing (d7, d14). Control mice received PBS injection	Zhao et al. (2016)
hPMSC-CM	31.85 µl (72 h) CM/cm^2	Subcutaneous injection	Burn degree n.d., mouse	hPMSC were maintained in normoxic or hypoxic conditions. Hypoxic CM reduced scar formation, while there was no marked difference between normoxic CM and controls (normal medium) at d8	Du et al. (2016)
hUC-MSC-CM	50 µl (5 µg/ml) (48 h) CM/cm^2 every 2nd d for 8w	Topical (hydrogel)	Radiation, rat	Hydrogel containing hUC-MSC-CM accelerated wound closure, sebaceous gland cell-like regeneration and angiogenesis compared to EGF gel and negative control (w2, w4, w6, w8, wound treatment every 2 days)	Sun et al. (2019)
	(48 h) CM (volume not specified)	Topical (SA/gelatin hydrogel)	Full-thickness, rat Splint model	Hydrogel containing CM of UC-MSC transfected cells accelerated wound contraction and promoted neovascularization, skin-appendages, epithelialization compared to control (PBS or Hydrogel treatment without CM (d14)	Sabzevari et al. (2020)

Perinatal cell-conditioned medium (CM) compared to/or combined with perinatal cells

PnD	Dosage (CM harvesting time)	Application (carrier)	Wound type, animal	Outcome	References
a) hAMSC b) hAMSC-CM	2.546 × 10^6 cells/cm^2 254.6 µl (48 h) CM/cm^2	Subcutaneous injection	Burn 2nd degree, mouse	hAMSC and hAMSC-CM similarly accelerated re-epithelialization and cell proliferation compared to controls without cells or CM (d7, d14, d21), increased expression of CK19 and PCNA, inhibited heat stress-induced apoptosis through activating PI3K/AKT signaling pathway	Li et al. (2019)
a) hAEC-CM b) hAEC + hAE-CM c) hAEC + unconditioned medium	I exp. 7 µl (72 h) CM/cm^2 d1, d7 33,333 cells/cm^2 d1, d7 II exp. 10 µl (72 h) CM/cm^2 on every 2nd d or 4th d or 7th d for 3w	Topical (cell spray)	Burn partial-thickness, guinea pig	hAEC, hAEC-CM, or the combination of both improved epithelialization compared to controls without cell or CM treatment (d7 – d21). Frequent application of hAEC-CM for every day achieved better results than 2-fold application at d0 and d7	Payne et al. (2010)
a) hUC-MSC b) hUC-MSC-CM	7.07 × 10^6 cells/cm^2 212.3 µl (24 h) CM/cm^2	(a-b) Subcutaneous injection	Full-thickness, diabetic mouse	hUC-MSC and hUC-MSC-CM accelerated wound closure and angiogenesis, with similar effects at d10. CM induced better effects in wound healing and higher expression of PDGFß and KGF in wounds at d14	Shrestha et al. (2013)
a) hUC-MSC or hU-MSC-End b) hUC-MSC-CM or hU-MSC-End-CM	1.77 × 10^6 cells/cm^2 212.3 µl (48 h) CM/cm^2	(a-b) Intradermal injection	Full-thickness, mouse Splint model	hUC-MSC and CM accelerated wound closure, regeneration capacity and neovascularization. hUC-MSC-End achieved better cellular and paracrine effects than hUC-MSC (d7, d12). Effects of cells were not directly compared to the effects of CM.	Aguilera et al. (2014)
a) hUC-MSC b) hUC-MSC-CM	1.99 × 10^6 cells/cm^2 298 µl (24 h) CM/cm^2	(a-b) Subcutaneous injection	Full-thickness, diabetic mouse	hUC-MSC and hUC-MSC-CM similarly improved angiogenesis, re-epithelialization and granulation (d14). Fibroblasts or PBS served as controls	Zhang et al. (2020)

(Continued on following page)

TABLE 2 | (*Continued*) Application of perinatal cell-conditioned medium (CM) alone or compared to/combined with perinatal cells in *in vivo* animal models of skin wound healing. Time points indicated in the "Dosage" and Outcome" columns mean days (d), weeks (w) or hours (h) of/after treatment.

Perinatal cell-conditioned medium (CM)					
PnD	**Dosage**	**Application (carrier)**	**Wound type, animal**	**Outcome**	**References**
a) hUC-MSC b) hUC-MSC-CM	1.99 × 10^6 cells/cm^2 3.54 × 10^6 cells/cm^2 199 µl (72 h) CM/cm^2 354 µl (72 h) CM/cm^2	(a-b) Topical (AV/PCL scaffold) or subcutaneous injection	Full-thickness, diabetic mouse	hUC-MSC and hUC-MSC-CM applied by AV/PCL carrier or subcutaneous injection similarly achieved better effects on wound healing (re-epithelialization, collagen deposition, angiogenesis and immunomodulation) than controls (fibroblasts, fibroblast-CM, unconditioned medium (d7, d14, d28)	Raj et al. (2019)
a) hUC-MSC b) hUC-MSC-CM	6.37 × 10^4 cells/cm^2	Topical (alginate gel) with cells or CM	Full-thickness, mouse Splint model	hUC-MSC-alginate and hUC-MSC-CM-alginate achieved faster wound healing than control groups (FBS-alginate, PBS-alginate), (d10, d15)	Wang et al. (2016)
a) hUC-PVC b) hUC-PVC- CM	3.54 × 10^6 cells/cm^2 354 µl (48 h) CM/cm^2	(a-b) Intradermal injection combined with topical application	Full-thickness, mouse Splint model	hUC-PVC and hUC-PVC-CM accelerated wound closure and healing (collagen deposition and angiogenesis) compared to fibroblasts and fibroblast-CM (d4, d7, d14). Effects of cells were not directly compared to the effects of CM.	Shohara et al. (2012)

Abbreviations AV/PCL, Aloe vera/po lycaprolactone; hAEC, human amniotic membrane epithelial cells; hAMSC, human amniotic membrane mesenchymal stromal cells; hPMSC, human placenta mesenchymal stromal cells; hUC-MSC, human umbilical cord mesenchymal stromal cells; hU-MSC-End, human umbilical cord mesenchymal stromal cells-endothelial transdifferentiated; hUC-PVC, human umbilical cord perivascular cells; CM, conditioned medium derived from hAEC, hAMSC, hPMSC, hUC-MSC, hUC-MSC-End, hUC-PVC; SA, sodium alginate.

an interesting aspect, because so far, different miRNAs (including miR-135a) were mainly shown to impair wound healing (Bibby et al., 2021).

Perinatal Tissues

Perinatal tissues (of which hAM predominate with 85.7%) were applied in 15.1% of the included preclinical studies (**Table 4**). The hAM serves as a potential wound dressing due to its high biocompatibility, antimicrobial and anti-scarring properties. Its anti-inflammatory properties have been attributed to the decrease of pro-inflammatory cytokine expression (transforming growth factor ß and interleukin 10). Furthermore, it produces B defensins, elastase inhibitors, elastin, and lactoferrin with antimicrobial effects, making it highly attractive in healing leg ulcers (ElHeneidy et al., 2016). Decellularized or dehydrated perinatal tissues were used as grafts or as support for perinatal cells or cells of another origin and were applied topically. In cases where the entire full-thickness or burn wound area was covered with the hAM (Kim et al., 2009; Samadikuchaksaraei et al., 2016; Motamed et al., 2017; Song et al., 2017; Farzamfar et al., 2018; Gholipourmalekabadi et al., 2018; Kakabadze et al., 2019; Arasteh et al., 2020; Nasiry et al., 2020), the wound areas are given instead of dosages (**Table 4**). Also, in two studies where a proprietary human amnion/chorion graft (EpiFix®) was implanted subcutaneously, calculating the dosages was inapplicable (Koob et al., 2013; Koob et al., 2014).

It was shown that combinations of cells and decellularized hAM achieved better results on wound healing than either cells or hAM alone (Kim et al., 2009; Sabapathy et al., 2014; Samadikuchaksaraei et al., 2016; Motamed et al., 2017; Farzamfar et al., 2018; Gholipourmalekabadi et al., 2018; Kakabadze et al., 2019; Hashemi et al., 2020).

Perinatal Tissue Extracts

Of the included studies, 12.9% used perinatal tissue extracts (**Table 5**). The most frequently used tissue extract was hAM extract (41.7%). Tissue extracts are usually obtained by tissue lysis and centrifugation, hence they do not contain cells, but are rich in an array of proteins, minerals, amino acids, and steroid hormones (Datta and Bhattacharyy, 2012). Tissue extracts possess anti-inflammatory, antioxidant, and cytoprotective properties and stimulate proliferation and reparative processes similar to their tissues of origin (reviewed in Pogozhykh et al. (2018)).

Perinatal tissue extracts (some of which were prepared as a powder) were applied topically or by subcutaneous injection, mostly on full-thickness skin wounds, and once on either a burn wound or a skin flap model, respectively. The amount of the extracts used was usually expressed in µg of lyophilized powder or, in some cases, in µl of proprietary human placental extracts. The doses ranged from 1 µg to 83.3 µg/cm^2. In two studies that compared the application of lower and higher doses of perinatal tissue extracts, higher doses performed better in terms of wound healing rate, reduced inflammation (Momeni et al., 2018), and skin flap survival (Kwon et al., 2019). Acellular umbilical cord-derived Wharton's jelly extract (hWJ-ECM) was applied with Matrigel or in the form of a spongy scaffold in doses of 353.7 and 450 µl/cm^2, respectively, providing enhanced wound closure and re-epithelization (Bakhtyar et al., 2017; Beiki et al., 2017). In one

TABLE 3 | Application of perinatal cell-derived small extracellular vesicles (sEV) alone or compared to perinatal cells in *in vivo* animal models of skin wound healing. Time points indicated in the "Dosage" and "Outcome" columns mean days (d) or weeks (w) of/after treatment.

Perinatal cell-derived small extracellular vesicles (sEV)					
PnD	**Dosage**	**Application (carrier)**	**Wound type, animal**	**Outcome**	**References**
hUC-MSC-sEV	100 μg/cm^2	Subcutaneous injection	Burn 2nd degree, rat	hUC-MSC-sEV enhanced re-epithelization and promoted self-regulation of Wnt/β-catenin signaling during the tissue remodeling period of cutaneous regeneration compared to PBS control (w2, w4)	Zhang et al. (2016)
	100 μg/cm^2	Subcutaneous injection	Burn 2nd degree, rat	hUC-MSC-sEV promoted re-epithelization and angiogenesis compared to controls (PBS, fibroblast-Ex, d7). Proangiogenic effects were inhibited by interference of Wnt4 expression in hUC-MSC- sEV.	Zhang et al. (2015b)
	318 μg/cm^2	Subcutaneous injection	Burn 2nd degree, rat	hUC-MSC-sEV accelerated wound closure and angiogenesis compared to control (PBS, d13). Overexpression of Ang-2 in hUC-MSC-sEV further enhanced therapeutic effects. Knockdown of Ang-2 in hUC-MSC-sEV abrogated these effects	(Liu et al., 2020)
	127 μg/cm^2	Subcutaneous injection	Burn 2nd degree, mouse	hUC-MSC- sEV treated with blue light (455 nm) achieved better angiogenic effects than untreated hUC-MSC- sEV (d7)	Yang et al. (2019)
	127 μg/cm^2	Topical injection (Pluronic F127 hydrogel)	Full-thickness, diabetic rat	hUC-MSC-sEV -hydrogel and hUC-MSC- sEV -PBS accelerated the wound closure rate and vascularization compared to controls (gel, PBS). hUC-MSC- sEV -hydrogel achieved better effects than hUC-MSC- sEV -PBS (d7, d10, d14)	Yang et al. (2020)
hDMSC-sEV	2.6 × 10^10 particles/cm^2 on every 7th d for 4w	Subcutaneous injection	Full-thickness, diabetic mouse	hDMSC-sEV accelerated wound closure and collagen deposition compared to PBS controls (d14, d21)	Bian et al. (2020)
Perinatal cell-derived small extracellular vesicles (sEV) compared to perinatal cells					
PnD	**Dosage**	**Application (carrier)**	**Wound type, animal**	**Outcome**	**References**
a) hAMSC b) hAMSC-sEV c) hAMSC-miR-135a-sEV	2,222; 22,222; or 222,222 cells/cm^2 Dose of sEV not specified	a) Subcutaneous injection (collagen) (b-c) Topical (collagen)	Full-thickness, rat	hAMSC and hAMSC-sEV enhanced wound closure and epidermalization. hAMSC-miR-135a-sEV induced faster wound healing than hAMSC-sEV (d5). Higher cell dose achieved better results than lower cell dose	Gao et al. (2020)
a) hUC-MSC b) hUC-MSC-sEV	1.56 × 10^6 cells/cm^2 156 μg-sEV/cm^2	(a-b) Subcutaneous injection	Full-thickness, mouse	hUC-MSC-sEV attenuated full-thickness skin wounds by enhancing epidermal re-epithelialization and dermal angiogenesis compared to hUC-MSC (d7, d14)	Zhao et al. (2020)
a) hUC-MSC-sEV b) hUC-MSC	100 μg sEV/cm^2 0.5 × 10^6 cells/cm^2	Subcutaneous injection	Burn 2nd degree, rat	hUC-MSC and hUC-MSC-sEV similarly accelerated re-epithelialization and increased expression of CK19, PCNA, and collagen I compared to control (PBS, fibroblast, Fibroblast-sEV, d7, d14) via Wnt4 pathway. hUC-MSC-sEV reduced heat stress-induced apoptosis via activation of AKT pathway	Zhang et al. (2015a)

Abbreviations; hAMSC, human amniotic membrane mesenchymal stromal cells; hAMSC-miR-135a, human amniotic membrane mesenchymal stromal cells overexpressing miR-135a; hDMSC, human decidua mesenchymal stromal cells; hUC-MSC, human umbilical cord mesenchymal stromal cells; sEV, small extracellular vesicles derived from hAMSC, hDMSC, hUC-MSC; miR-135a-sEV, sEV overexpressing microRNA135a.

study, hybrid extracellular matrix sponges containing human placenta-derived extracellular matrix were applied within the wound area, but no volume or other quantitative value of the applied matrix was specified (Rameshbabu et al., 2018).

It was shown that amnion-derived hydrogel and amnion powder achieved better results on wound healing than AmnioGraft® (Murphy et al., 2020). The combination of the human placental extract with autologous bone marrow MSC

TABLE 4 | Application of perinatal tissues alone or compared to/combined with perinatal cells or cells of non-perinatal origin in *in vivo* animal models of skin wound healing. Stated time points in the "Outcome" column mean days (d) or weeks (w) after treatment.

Perinatal tissues

PnD		Carrier of the topical PnD application	Wound type, animal	Outcome	References
a) hAM b) hAM + silk fibroin	wa 0.2 cm^2	Topical	Full-thickness, mouse Splint model	hAM-silk fibroin scaffolds achieved better epidermal and dermal regeneration than hAM-treated and untreated wounds (d30)	Arasteh et al. (2020)
a) hAM b) hAM-S	wa 1.77 cm^2	Topical	Full-thickness, diabetic rat, non-diabetic control rat Splint model	hAM-S seemed to have better effects on the healing of diabetic wounds than hAM (d7, d14, d21)	Nasiry et al. (2020)
hAM	wa 1.69 cm^2	Topical	Full-thickness, rat	hAM promoted wound closure (d3, d5, d7), and enhanced VEGF and α- SMA expression (d7). Reduced TGF-β1 expression at an early stage (d3) alleviated wound inflammation, promoted tissue regeneration and relieved scar formation compared to PBS treated wounds	Song et al. (2017)
Dehydrated hAM/chorion (EpiFix®)	Not applicable	Subcutaneous implantation	Subcutaneous pocket model, mouse	hAM/chorion implants recruited more mesenchymal progenitor cells to the site of implantation compared to normal skin and the sham implant site (d7)	Koob et al. (2013)
Dehydrated hAM/chorion (EpiFix®)	Not applicable	Subcutaneous implantation	Subcutaneous pocket model, mouse	hAM/chorion implants displayed a steady increase in microvessels approaching that of healthy and healing skin (d28)	Koob et al. (2014)

Perinatal tissues compared to/or combined with perinatal cells

PnD	Dosage	Application	Wound type, animal	Outcome	References
a) hUC-MSC b) hUC-MSC+ hAM c) hAM	1 × 10^6 cells/cm^2 wa 1 cm^2	a) Subcutaneous injection b) Topical	Full-thickness, mouse	Combination of hUC-MSC and hAM achieved better wound healing (reduced scar formation with hair growth and improved biomechanical properties of regenerated skin) than hUC-MSC alone (d14) and untreated wounds	Sabapathy et al. (2014)
a) hUC-MSC b) hAM c) hUC-MSC+hAM	0.7 × 10^6 cells/cm^2 wa 1.54 cm^2	Subcutaneous injection or topical (b-c) Topical	Burn 3rd degree, rat	hUC-MSC/hAM combination induced better wound healing (re-epithelialization, formation of granulation tissue, and hemorrhage) than hAM and hUC-MSC alone (d14)	Hashemi et al. (2020)

Perinatal tissues combined with cells of non-perinatal origin

PnD		Carrier of the topical PnD application	Wound type, animal	Outcome	References
a) hAM b) hAM+hFib c) hAM+hASC	wa 11–18 cm^2 0.5 × 10^6 cells/cm^2	Topical	Burn 3rd degree, rat	hAM seeded with fibroblasts or with ASC similarly showed better wound healing than hAM-only and control (Vaseline gauze) (d7, d14, d20, d28, d40)	Motamed et al. (2017)
a) hAM b) hAM/silk fibroin c) hAM/silk fibroin+hASC	wa 0.79 cm^2 10,000 cells/cm^2	a) Topical (b-c) Topical silk fibroin	Burn 3rd degree, mouse	Silk fibroin accelerated wound healing compared to hAM only. hAM/silk fibroin+hASC achieved better effects	Gholipourmalekabadi et al. (2018)

(Continued on following page)

TABLE 4 | (*Continued*) Application of perinatal tissues alone or compared to/combined with perinatal cells or cells of non-perinatal origin in *in vivo* animal models of skin wound healing. Stated time points in the "Outcome" column mean days (d) or weeks (w) after treatment.

Perinatal tissues					
PnD		**Carrier of the topical PnD application**	**Wound type, animal**	**Outcome**	**References**
hAM (loaded or injected with autologous or allologous rabbit BM-MSC	wa 5.06 cm^2 88,888 cells/cm^2 on hAM 3.02 × 10^6 cells/cm^2 i.d	Topical	Full-thickness, rabbit	than hAM/silk fibroin without ASC (d7, d14, d28) and reduced post burn scars hAM grafts loaded with autologous and allologous BM-MSC similarly accelerated wound closure compared to hAM grafts with injected BM-MSC (d7, d12, d15)	Kim et al. (2009)
a) hAM b) hAM+BM-MSC c) hAM+ freeze-dried rat BM-MSC	wa 2 cm^2 number of cells per cm^2 Not specified	Topical	Radiation followed by full-thickness, rat	hAM+BM-MSC and hAM+ freeze-dried BM-MSC similarly accelerated wound closure compared to hAM only. Inflammation and exudations were absent when hAM was used in contrast to non-treated wounds (Observation period 90 days)	Kakabadze et al. (2019)
a) Dehydrated hAM (Amniofix ®) b) Amniofix ® +BM-MSC c) Amniofix ® +TGFβ3 expressing BM-MSC	wa 4 cm^2 0.1 × 10^6 cells/cm^2	Topical	Full-thickness, rat	All treatments resulted in similar wound closure (d7-d21). TGF-β3 expressing cells decreased the scar formation (d85)	Samadikuchaksaraei et al. (2016)
a) hAM b) hAM+ Men-MSC	wa 2.25 cm^2 30,000 cells/cm^2	Topical	Full-thickness, rat	Men-MSC+hAM improved wound closure, angiogenesis and re-epithelization compared to hAM-only (d14)	Farzamfar et al. (2018)

Abbreviations: α-SMA, alpha-smooth muscle actin; BM-MSC, bone-marrow mesenchymal stromal cells; hAM, human amniotic membrane; hAM-S, bioengineered 3D hAM-scaffold; hASC, human adipose mesenchymal stromal cells; hFib, human fibroblasts; hUC-MSC, human umbilical cord mesenchymal stromal cells; Men-MSC, menstrual blood mesenchymal stromal cells; TGF-β1, transforming growth factor beta-1; VEGF, vascular endothelial cell growth factor; wa, wound area covered by tissue membranes.

achieved better results on wound healing than placental extract applied without cells (Akela et al., 2013).

In vitro Characterization and Functional Testing of PnD Before Their Application in Preclinical Studies

The evaluation of the *in vitro* characterization (**Figure 3A**) displayed the sEV as the most *in vitro* characterized PnD, as they were properly characterized in all included studies. The methods used for the characterization were: transmission electron microscopy to observe their morphology (100%), Western blot to determine the expression of exosome markers (89%), and nanoparticle tracking analysis to measure the size of sEV (89%). The reputable characterization of sEV is most probably due to the exact guidelines for isolation and characterization (van Deun et al., 2017; Théry et al., 2018). Encouraging the scientific community to properly perform exosome characterization has proven to be a good practice that provides transparency to the studies, and should also be considered in other fields. Cells were also fairly well characterized *in vitro* (84.8%). The predominant methods were: flow cytometry to identify the presence of the cell surface markers (87.2%), assessment of the differentiation potential into multiple lineages to confirm their stemness (50%), and bright field microscopy to verify morphological characteristics (35.9%). Of perinatal cell-derived CM, 83.3% were characterized *in vitro*. CM was biochemically analyzed in just one of the studies (Sabzevari et al., 2020), however, we further defined CM as "*in vitro* characterized" also when the corresponding cells were identified and characterized at the molecular and morphological levels. Perinatal tissues were *in vitro* characterized with a proportion of 50%; this group also includes commercially available perinatal tissues (71.4%).

We considered commercially obtained perinatal tissues as "*in vitro* characterized," since the vendors clearly describe them. As the most commonly used perinatal tissue is the hAM, we assume that the poor percentage of the *in vitro* characterization is due to the fact that the hAM has been characterized and tested many times before. Further, identification and preparation of the hAM are unambiguous and straightforward (Jerman et al., 2014; Poženel et al., 2019; Jerman et al., 2020; Ramuta et al., 2020; Weidinger et al., 2020), whereas cells and cell-derived secretomes or sEV require precise characterization. Since the vast majority of the researchers isolated cells from the perinatal tissues by themselves, adequate characterization is mandatory to assure that a pure cell population has been isolated. The least *in vitro* characterized PnD were perinatal tissue extracts (41.7%).

TABLE 5 | Application of perinatal tissue extract alone or compared to/combined with with perinatal tissue or cells of non-perinatal origin in *in vivo* animal models of skin wound healing. Time points indicated in the "Dosage" and "Outcome" column mean days (d) or weeks (w) of/after treatment.

Perinatal tissue extracts

PnD	Dosage	Application (carrier)	Wound type, animal	Outcome	References
hAM extract	83.3 µg extract/cm^2 8.33 µg extract/cm^2	a) Topical b) Topical (chitosan hydrogel)	Burn 1st degree, rat	hAM+chitosan-gel increased cutaneous regeneration (granulation tissue, fibroblast proliferation, vascularization) compared to controls (PBS, gel) (d15, d25, d31). High concentrated hAM extract (1 mg/ml) achieved better effects than low concentrated hAM extract (0.1 mg/ml)	Momeni et al. (2018)
hAM extract	100 µg/ml wound dressing (applied volume not spec.)	Topical (PVA/SA gel)	Full-thickness, rat	hAM+PVA/SA-gel accelerated wound closure, increased re-epithelization, granulation tissue areas, neovascularization, collagen proliferation and reduced number of inflammatory cells compared to Medifoam™ hydrogel or the control (sterile gauze) (d6, d9, d12)	Choi et al. (2014)
hP extract	3.98 µl extract/cm^2	Subcutaneous injection	Full-thickness, mouse	hP extract accelerated wound healing (d3-d9) TGF-β increased in the early phase of wound healing (d6) and VEGF in the late phase (d14) compared to PBS control	Hong et al. (2010)
	3.33 µl extract/cm^2/d 0.45 and 1.35 ml/kg/d every day for 7 days	Subcutaneous injection or Intraperitoneal injection	Skin flap, rat	hP extract enhanced flap survival, angiogenesis, reduced necrotic areas, induced antioxidative response and inhibited apoptosis compared to PBS control. Daily application (d0-d6) of low dose localized or systemic hP injections or high dose. Systemic high dose HP injections showed the best effects. (d7)	Kwon et al. (2019)
a) hP extract b) Placental laminin	a) 35 µg/cm^2 b) 11 µg/cm^2	Subcutaneous injection	Full-thickness, rat	hP and placental laminin accelerated wound closure compared to PBS controls (d5, d7, d9)	Mukherjee et al. (2020)
a) hAM powder b) hAM powder+AV	2 µg hAM/cm^2 1 µg hAM + 1 µg AV/cm^2	Topical	Burn 2nd degree, rat	hAM powder, AV, and hAM+AV accelerated wound healing compared to untreated wounds (d24)	Rahman et al. (2019)
Solubilized hAM	Not specified	Topical (hyaluronic acid hydrogel)	Full-thickness, mouse	hAM-hyaluronic acid hydrogel accelerated wound closure, wound re-epithelialization, vascularization compared to controls (hydrogel, untreated). Hydrogel ± hAM counteracted wound contracture in contrast to untreated wounds (d7, d14)	Murphy et al. (2017)
hP–ECM	Not specified	Topical (hybrid with silk fibroin)	Full-thickness, rat	hP-ECM-silk fibroin scaffolds accelerated wound closure (pronounced angiogenesis, enhanced granulation tissue formation, early re-epithelialization) compared to controls (collagen-silk-fibroin scaffolds, sham) (d7, d14, d21)	Rameshbabu et al. (2018)
hWJ-ECM	450 µl/cm^2	Topical (hWJ-ECM scaffold)	Full-thickness, mouse	WJ-ECM scaffolds accelerated wound closing and re-epithelization compared to wounds without scaffolds (d7, d12) and counteract wound contracture (d18)	Beiki et al. (2017)
hWJ-ECM	353.7 µl/cm^2	Topical (Matrigel)	Full-thickness, mouse	Acellular hUC-WJ+Matrigel enhanced wound closure and augmented the differentiation of fibroblasts into myofibroblasts compared to control (DMEM-Matrigel) (d5, d7)	Bakhtyar et al. (2017)

Perinatal tissue extracts compared to perinatal tissue

PnD	Dosage	Application (carrier)	Wound type, animal	Outcome	References

(Continued on following page)

TABLE 5 | (*Continued*) Application of perinatal tissue extract alone or compared to/combined with with perinatal tissue or cells of non-perinatal origin in *in vivo* animal models of skin wound healing. Time points indicated in the "Dosage" and "Outcome" column mean days (d) or weeks (w) of/after treatment.

Perinatal tissue extracts

PnD	Dosage	Application (carrier)	Wound type, animal	Outcome	References
a) hAM powder b) hAM powder+hydrogel c) Amniograft^{R}	Not specified	Topical	Full-thickness, pig	Amnion+hydrogel and amnion powder accelerated wound healing compared to Amniograft^{R} > hydrogel only > untreated wounds > graft jacket. The treatment with graft jacket-only led to the worst healing (most wound, most contraction, least epithelialization (d28)	Murphy et al. (2020)

Perinatal tissue extracts combined with cells of non-perinatal origin

PnD	Dosage	Application (carrier)	Wound type, animal	Outcome	References
a) hPE+autologous BM-MSC b) hPE+buffy coat in autologous plasma) c) hPE+autologous plasma	Concentration of hPE not specified (commercial preparation) 1 × 10^6 cells/cm^2	Topical	Full-thickness, rabbit	hP-E+ BMSC achieved better results on wound healing (accelerated wound closure, earlier disappearance of inflammatory reaction, better epithelialization, neovascularisation, and collagen formation than the other groups (d7, d14, d21, d30)	Akela et al. (2013)

Abbreviations: AV, aloe vera; BM-MSC, bone marrow mesenchymal stromal cells; hAM, human amniotic membrane; hPE, human placenta extract; hP-ECM, human placenta extracellular matrix; hUC-WJ-ECM, human umbilical cord Wharton´s jelly extracellular matrix; PVA, polyvinyl alcohol; SA, sodium alginate.

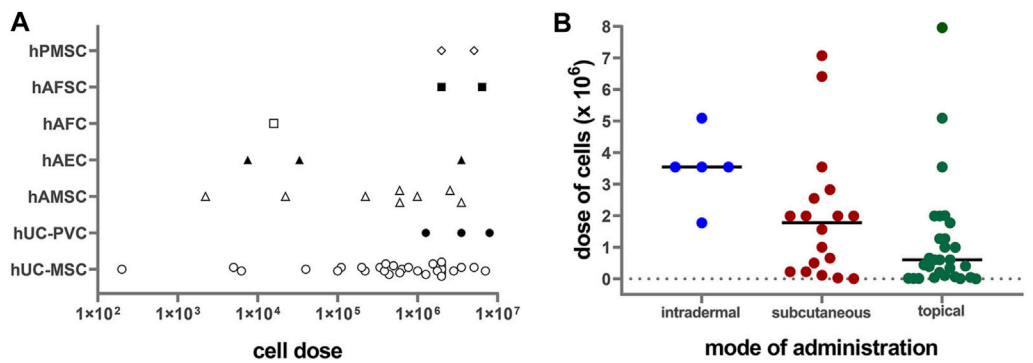

FIGURE 2 | (A) Correlation of applied PnD cell type versus cell number/cm^2 on a logarithmic scale (Log10). hUC-MSC, human umbilical cord mesenchymal stromal cells; hAMSC, human amniotic membrane mesenchymal stromal cells; hPMSC, human placenta mesenchymal stromal cells; hAFC, human amniotic fluid cells; hAFSC, human amniotic fluid cells; hUC-PVC, human umbilical cord perivascular cells; hAEC, human amniotic membrane epithelial cells. **(B)** Correlation of cell doses with the mode of administration. Lines represent median values.

In addition to *in vitro* characterization, *in vitro* functional tests were performed (**Figure 3B**). The differentiation and proliferation assays, scratch wound assay, and cytotoxicity assay were the most prevalently used to evaluate the effect of different PnD on cell cultures *in vitro*. The *in vitro* functional tests are usually quick and performed under controlled conditions. Compared to the animal models, they certainly lack the complexity of the native tissue. Nevertheless, monitoring the specific mechanisms *in vitro* is a good indicator of how the tested materials affect the biological processes *in vivo*. Among the PnD used in the preclinical studies of skin wound healing, 77.8% of the perinatal cell-derived sEV were functionally tested *in vitro*. Moreover, 58.3% of included studies performed functional tests *in vitro* on perinatal tissue extracts, and half of the studies functionally tested the perinatal cell-derived CM. On the other hand, despite being the most frequently used PnD in skin wound healing, only 41.3% of the perinatal cells were subjected to functional *in vitro* assays before their application in preclinical studies. The least *in vitro* tested PnD were perinatal tissues (21.3%).

ANIMAL MODELS OF CUTANEOUS WOUND HEALING

Animal models span various wound types, multiple animal species, and strategic scientific approaches for wound

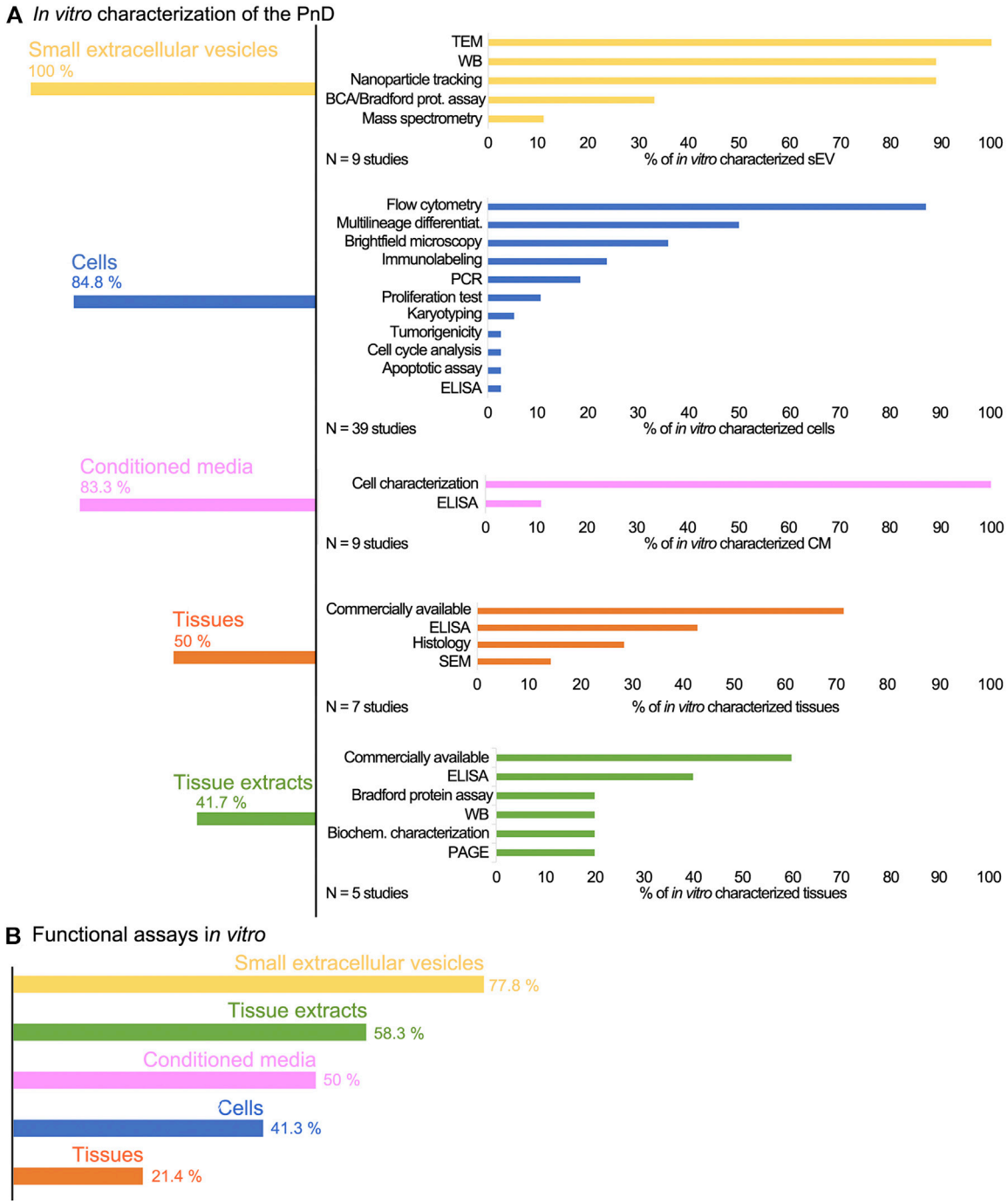

FIGURE 3 | (A) The schematic presentation of the PnD characterization and **(B)** verification *in vitro*. The sEV derived from perinatal MSC are overall the most characterized and *in vitro* tested PnD used in skin wound healing in preclinical studies. Conversely, the least characterized and *in vitro* tested PnD are the perinatal tissues. The commercially available PnD or the PnD that have been described in the previous studies by the same authors, were defined as characterized *in vitro*, although the exact data were not provided in the actual study.

treatment. According to most common problems in wound healing in humans, such as full-thickness wounds, chronic ulcers caused by diabetes, poorly healing wounds after radiation, or severe burn injuries, the animal models are adapted to these conditions as well as possible.

The herein described animal models dealt with full-thickness wounds (53 studies), burn wounds (18 studies), radiation wounds (three studies), skin flaps (two studies), and subcutaneous pockets (two studies). One case report described the application of PnD on non-healing skin lesions (**Figure 4**; **Tables 1**–**5**).

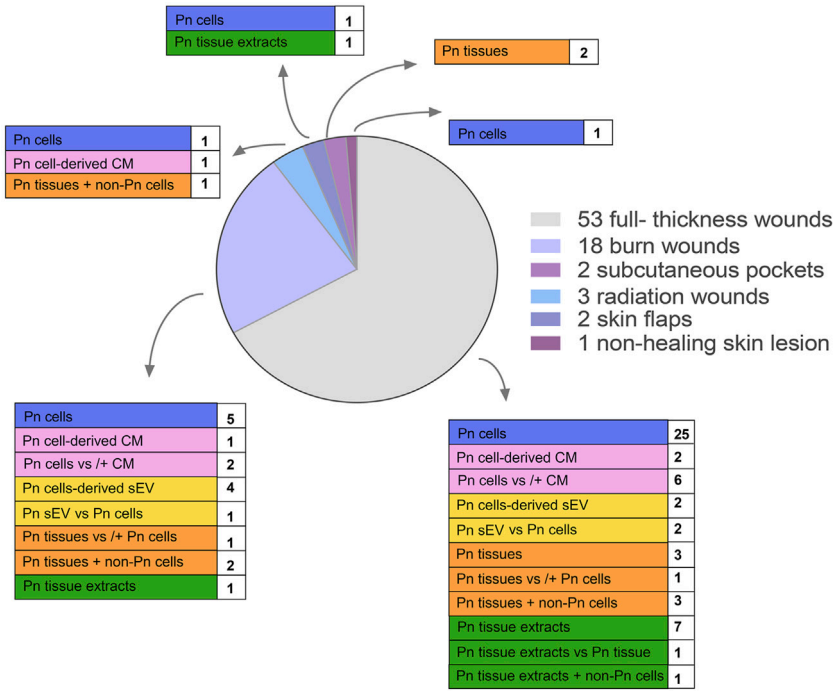

FIGURE 4 | Distribution of wound types and applied PnD types.

Wound Models

Full-Thickness Wound Models

In full-thickness wounds, all skin layers including the subcutaneous tissue, are removed. Full-thickness wounds were inflicted mainly by biopsy punches or by scalpels and surgical scissors. In addition to healthy animals, this wound type has also been applied to diabetic animals to mimic impaired healing conditions and chronic wounds.

Diabetic Wound Models

Diabetes is a major health care problem. A diabetes-related foot ulcer is one of the most challenging complications in the treatment of diabetic patients. More than half of diabetic ulcers become infected and lead to amputation in 20% of cases. (Armstrong et al., 2017). Thus, several studies use diabetic mouse and rat models to develop new strategies for treatment.

Experimental type 1 diabetes can be studied on a genetic non-obese diabetic mouse line or on mice/rats treated with streptozotocin, which destroys pancreatic beta cells. The advantage of diabetes induced by streptozotocin injection is that there is no limitation to a particular mouse or rat strain. Two studies used the non-obese diabetic/severe combined immunodeficiency (NOD/SCID) mice, which have a metabolic state similar to type 1 diabetes ((Jin et al., 2016) and (Kim et al., 2012)). One study used a streptozotocin-induced C57BL/6J mouse (Zhang et al., 2020). Four studies used diabetic rat models on streptozotocin-induced SD rats (Han et al., 2019; Shi et al., 2020; Yang et al., 2020; Yue et al., 2020). One further study used streptozotocin-induced Wistar rats (Milan et al., 2016).

Type 2 diabetes can be induced by a high-fat diet or genetically in the leptin-deficient mouse line (Boyko et al., 2017). Four studies (Shrestha et al., 2013; Peña-Villalobos et al., 2018; Raj et al., 2019; Bian et al., 2020) used leptin-deficient db/db mice as a diabetes type 2 model. Affected mice show morbid obesity, chronic hyperglycemia, pancreatic beta-cell atrophy, and hypoinsulinemia. They are polyphagic, polydipsic, and polyuric, similar to diabetic type 2 patients. This mouse line is recommended for wound healing models[2].

Wang et al. (2016) used the Goto-Kakizaki rats as a non-obese model of type 2 diabetes with metabolic, hormonal, and vascular disorders similar to human diabetes.

Burn Injury Wound Models

Burn wounds can be created by scald, contact, chemical or electrical combustion. The severity of the burn wound (**Supplementary Table S1**) depends on the temperature and exposure time of the heat source to the skin, as well as on the skin thickness.

Except for the study on pigs (Eylert et al., 2021), all burn injury wound models of the reviewed studies were performed on rodents (primarily mice and rats, with one study was performed on guinea pigs). Burn wounds were created by scalding with hot water (70°C–94°C) for 6–100 s (Liu et al., 2014; Zhang et al., 2015a;

[2]https://www.criver.com/products-services/find-model/jax-dbdb-mice?region=3616/

Zhang et al., 2015b; Du et al., 2016; Liu et al., 2016; Zhang et al., 2016; Momeni et al., 2018; Li et al., 2019; Yang et al., 2019; Liu et al., 2021) or by a heated brass rod or aluminum devices (100–105°C, for 5–30 s), where wound size and shape depend on the size and shape of the instrument used (Motamed et al., 2017; Gholipourmalekabadi et al., 2018; Pourfath et al., 2018; Mahmood et al., 2019; Rahman et al., 2019; Hashemi et al., 2020). As wounding by the brass bar technique leads to scab formation, the developed necrosis was usually excised 12–48 h before application of PnD.

In most studies, severe burn injuries of 2nd or 3rd degree were performed. Some authors described the injury as "full-thickness burn injuries" which would correspond to at least category IIa according to the severity score. In cases with extensive wounds, an injection of balanced salt solution was given to prevent shock.

Uniform partial-thickness burns cannot be reproducibly created in mice and rats due to their estrous hair cycle (Robson et al., 1980), and superficial burns in pigs heal too quickly, because the porcine epidermis is 2-fold thicker than the human equivalent (Hammond, 2000). Thus, a higher temperature is needed to create severe burn wounds in pigs. (Eylert et al., 2021) used a heated aluminum device (200°C) for 20s and digital force gauge and histologically confirmed full-thickness burn wounds 48 h post-burn via punch-biopsy. Payne et al. (2010) studied partial-thickness burn wounds on guinea pigs, which do not have hair cycles and are therefore the more satisfactory model to evaluate this wound type. Only one study investigated superficial first-degree burn wounds on rats (Momeni et al., 2018).

Some authors described the percentage of the total body surface area (%TBSA) affected by a burn. 10% TBSA wounds were performed on guinea pigs (Payne et al., 2010), 30% TBSA and 50% TBSA on rats (Liu et al., 2014; Liu et al., 2016).

Due to a large number of different parameters such as wound size, heat exposure time, application of brass bar or water, inconsistent use of the severity score, and different treatments and application modes with PnD, a comparison of investigated experiments is not possible.

Radiation-Induced Wound Models

Radiation dermatitis is a common side effect of radiotherapy. Many of the radiation-induced skin changes are minor and reversible. Nevertheless, when acute changes do not resolve, skin ulcers, fibrosis, or necrosis of underlying structures may occur. Disruption of the epithelial basement membrane and breakdown of the barrier function substantially increase the risk for these injuries (Hymes et al., 2006). The severity grade is shown in **Supplementary Table S2** according to the Classification of radiation dermatitis from the National Cancer Institute (Hymes et al., 2006).

In the studies reviewed, 3rd or 4th-grade radiation wounds were created in rats (Liu et al., 2014; Kakabadze et al., 2019; Sun et al., 2019), respectively. Radiation dose and exposure time varied between the different studies. Liu et al. (2014) administered a dose of 45 Gy for 7.5 min per animal, Sun et al. (2019) administered 40 Gy for 25 min and Kakabadze et al. (2019) used a dose of 60 Gy without specifying of the radiation duration.

Sun et al. (2019) topically applied Hydrogel containing hUC-MSC-CM every second day after radiation for 8 weeks. PnD treatment accelerated wound closure, sebaceous gland regeneration, and angiogenesis compared to EGF application and negative control (weeks 2, 4, 6, 8).

Liu et al. (2014) created ulcers and Kakabadze et al. (2019) excised the radiation areas 3 weeks post-radiation to simulate a chronic radiation injury before starting the treatment with PnD. Subcutaneous injection of hUC-MSC increased neovascularization and re-epithelization, days 14, 21, 28 after treatment (Liu et al., 2018). Topical application of decellularized hAM seeded with BM-MSC (Kakabadze et al., 2019) accelerated wound closure compared to decellularized hAM. Inflammation and exudations were absent when the decellularized hAM was used (observation period 90 days).

Due to different intervals of evaluation, only days 7 and 14 could be used for a comparison, whereby the comparison is limited by different doses of radiation, different surgical interventions post-radiation, and different time points of application of the various PnD. In all investigated works, wounds treated with PnD showed a significantly accelerated wound healing on day 14 compared to control groups.

Due to the limited data and varying methods, a clear recommendation for the optimal treatment method concerning the application of PnD for the healing of radiation-induced wounds is not possible.

Skin Flap Models

A skin flap is a full-thickness mass of skin containing superficial fascia, transplanted from a donor site to a recipient site with an intact blood supply. Skin flap surgery is a common procedure in reconstructive surgery. In this field, surgeons often struggle with ischemia-associated complications such as tissue necrosis or wound breakdown (Schmauss et al., 2018). Flap models in rodents are versatile and have a long tradition in experimental surgery. In studies included in this review, two types of skin flaps were performed: the epigastric ischemic skin flap (EIF) and the McFarlane flap.

The EIF is an axial skin flap, designed at the pedicled superficial inferior epigastric vessels. The skin flap is lifted from its remote end, and the vascular pedicle gets clamped for a specific time to induce flap ischemia. Leng et al. (Leng et al., 2012) performed the EIF on mice at a size of 3 × 6 cm and clamped the respective blood vessels for 6 h. Then, the flap was opened to remove the clamps and to enable flap reperfusion. The flap was sutured *in situ* and hUC-MSC were subcutaneously injected into the flap at 10 distributed points. After 7 days, the survival area of the flap was evaluated concerning the gross appearance, necrosis, and vascularization. hUC-MSC were detectable in the flap tissues and increased the survival of the flap, neovascularization, and expression of bFGF and VEGF compared to controls without cell treatment.

The McFarlane flap model is characterized by a cranially based and randomly perfused dorsal skin flap, which is elevated beneath the musculus panniculus carnosus. It has a defined width-to-length ratio to ensure a predictable rate of necrosis. Perforating blood vessels were electrically cauterized to ensure a completely random vascular pattern. Kwon et al. (2019) performed this model on rats with a flap size of 3 × 10 cm to investigate

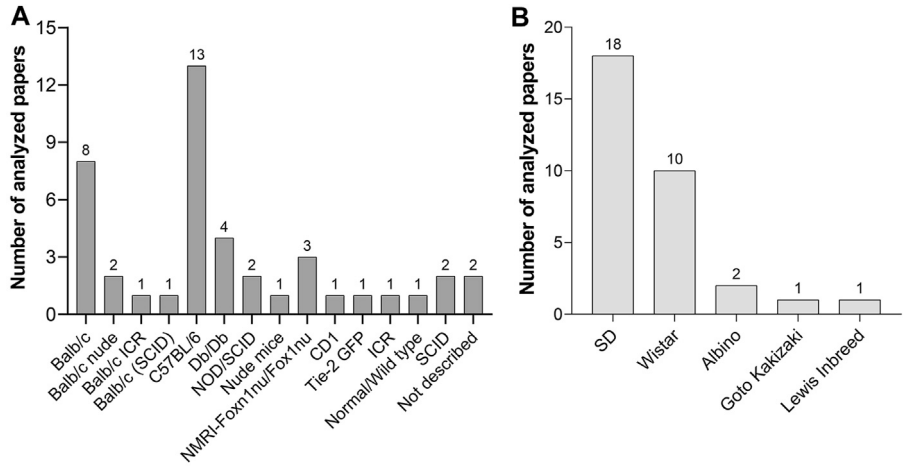

FIGURE 5 | (A) Mouse strains and **(B)** rat strains used for wound healing experiments with PnD treatment in scientific papers published between 2004 and 2020.

therapeutical effects of human placenta extract (hP-E) applied by subcutaneous or intraperitoneal injections. hP-E enhanced flap survival, angiogenesis, reduced necrotic areas, induced antioxidative response, and inhibited apoptosis compared to phosphate-buffered solution (PBS) control. Daily application (d0-d6) of low dose (10 mg/kg/d) localized or systemic hP-E injections or high dose (40 mg/kg/d) systemic hP-E injections showed the best effects of high dose administration (d7).

Although data on using PnD in skin flap models are rare, both approaches showed promising results.

Subcutaneous Pocket Model

Koob et al. (2013), Koob et al. (2014) created subcutaneous pockets in mice and implanted commercially available dehydrated human amnion/chorion-tissue allografts (Purion^{R}) at a size of 5 × 5 mm to investigate their biological and angiogenic properties. hAM/chorion implants recruited more mesenchymal progenitor cells to the site of implantation compared to uninjured skin and the sham implant site (day 7). In addition, implants displayed a steady increase in microvessels approaching that of healthy and healing skin after 28 days.

Animal Species Used for Cutaneous Wound Healing Models

Rodents

The vast majority of animal wound models (92%) were performed on rodents, with 40 and 32 studies performed on mice and rats, respectively. Only one study was performed on guinea pigs. Rodents are easy to handle and inexpensive with respect to costs for food, medication, and wound dressings. They are simple to house and have a short life cycle. Generally, smaller wounds were created on mice and rats than on larger animals, which helps to reduce the quantity of applied PnD material. However, rodents' wounds close due to the contraction of the *musculus panniculus carnosus*, a thin layer of skeletal muscle located in subcutaneous tissue, which is virtually non-existent in most regions of the human body (Zomer and Trentin, 2018). This physiological difference creates difficulties in replicating the wound closure processes of human skin, which should be considered. For long-time experiments on full-thickness wounds, anti-contractive tools should be chosen (described in the chapter *Wound Healing in Rodents*).

Mouse Strains Used in Wound Healing Studies

The C57BL/6 mouse was the most commonly used strain in the analyzed studies (**Figure 5A**). It is a general-purpose strain. Some of its characteristics are a high susceptibility to diet-induced obesity, diabetes II, and atherosclerosis. It has a nearly black coat, is easy to breed, and is robust. However, it tends to bite, and male mice remove hair from their cage mates (Sarna, 2000). Its barbering behavior may be counterproductive for an undisturbed wound healing process, as these animals might nibble on wound dressings. Most importantly, these animals are unusually sensitive to pain and cold, and analgesic medications are less effective (Mogil et al., 1999). Thus, the selection of C57BL/6 mice for wound healing experiments needs to be carefully evaluated.

Another commonly used mouse type was the albino Balb/c strain with its different inbreeds (Balb/c ICR, Balb/c (SCID), and Balb/c nude). BALB/c mice are more docile than C57BL/6 mice and are particularly well known for the production of monoclonal antibodies. BALB/c mice are used in many research fields (cardiovascular research, cancer, infectious diseases, neurobiology immunology, inflammation, autoimmunity). As most substrains display high levels of anxiety, (Griebel et al., 1993; Belzung and Berton, 1997) a familiar, calm environment is recommended.

The ICR inbred strain serves as a general-purpose strain and does not develop insulitis or diabetes. These mice were recommended amongst others for drug testing and as a control for non-obese diabetic mice[3].

[3]https://www.jax.org/strain/009122

CD1 are albino mice and are suggested as a general multipurpose model, for safety and efficacy testing, as an aging, pseudopregnancy, and surgical model[4].

SCID Mice are homozygous for the severe combined immune deficiency spontaneous mutation (*Prkdc*^{scid}). They are characterized by an absence of functional T cells and B cells, and a normal hematopoietic microenvironment. As *SCID mice* accept allogeneic and xenogeneic grafts, they are an ideal model for cell transfer experiments. Immunodeficient mice should be housed in a specific-pathogen-free environment to avoid infections[5].

Nude mice such as the Balb/c nude or the NMRI-Foxn1nu/Foxn1nu inbred are characterized by thymic aplasia, which results in immunodeficiency due to the lack of T cells. They have no rejection responses. The mutation leads to a keratinization defect of the hair follicles and the epidermis[6]. The mostly hairless phenotype helps to avoid a shaving procedure before the wound healing experiments. They are sensitive to cold and need to be kept at warm temperature conditions.

TIE-2 GFP (B6.Cg-Tg287Sato/1) strain expresses Green Fluorescent Protein under the direction of the endothelial-specific receptor tyrosine kinase (*Tek*, formerly, *Tie2*) promoter. This mouse type is especially appropriate to study neovascularisation during the wound healing process as GFP-expressing endothelial cells can be visualized via fluorescent microscopy (Wang et al., 2018).

Rat Strains Used in Wound Healing Studies

Compared to mouse strains, fewer rat strains were used in the investigated wound healing experiments (**Figure 5B**). Sprague Dawley (SD) and Wistar rats are the most popular albino rats used for laboratory research. SD rats are calm and less active than Wistar rats and are therefore easy to handle. Lewis rats are highly sensitive to the induction of autoimmune diseases as well as to diet-induced obesity and diabetes and streptozotocin-induced diabetes[7]. The Goto-Kakizaki inbred line was used as a non-obese model of type 2 diabetes.

Wound Healing in Rodents

In general, larger wounds were created on rats than on mice (one to two full-thickness wounds/animal with an average size of 1.52 vs. 2.11 cm^2 and one to two burn wounds/animal with an average size of 1.37 vs. 3.8 cm^2 in mice and rats, respectively. Larger wounds were radiation wounds created on rats (8 cm^2) and skin flaps (18 cm^2 on mice, 30 cm^2 on rats). Several approaches were developed to get similar conditions to human wound healing through the generation of granulation tissue and re-epithelialization rather than contraction of the *musculus panniculus carnosus*. One possibility is to investigate early stages of wound healing in short-term studies lasting up to 8 days post wounding, where no apparent wound contraction occurs (as performed by Tuca et al. (2016), Ertl et al. (2018)).

For longer-term experiments on full-thickness wounds, anti-contractive tools should be chosen: Splinting wound models use silicone or rigid plastic rings strapped around the wound area to the underlying muscles to prevent wound contraction. In the reviewed papers, the silicone rings were mostly sutured or fixed with glue (Kim et al., 2012; Shohara et al., 2012; Aguilera et al., 2014; Jin et al., 2016; Wang et al., 2016; Peña-Villalobos et al., 2018; Wang et al., 2018; Kaushik and Das, 2019; Arasteh et al., 2020; Nasiry et al., 2020; Sabzevari et al., 2020). Others directly sutured scaffolds loaded with PnD to the wound site (Yang et al., 2013; Edwards et al., 2014; Milan et al., 2016; Montanucci et al., 2017). Edwards et al. (2014) additionally placed a titanized mesh between the wound bed and a collagen-based scaffold (loaded with hUC-MSC) to avoid tissue contraction. However, these methods carry risks of inflammation and surgical site infection (Mulholland, 2020). Some studies did not use suturing of the scaffolds (or at least did not mention suturing) (Nan et al., 2015; Du et al., 2016; Han et al., 2019; Raj et al., 2019).

Beiki et al. (2017) observed that scaffolds produced from liquid WJ-ECM accelerated wound closing and counteract wound contracture during the observation period of 18 days. Also, a hyaluronic acid hydrogel with or without solubilized hAM counteracted wound contracture (Murphy et al., 2017). We could see from Vonbrunn et al. (2020) that the application of stiff carrier materials for PnD such as electrospun Poly(ε-caprolactone)/poly(l-lactide) (PCL/PLA) could enable uncomplicated experiments on rodents without suturing and could open new therapeutic approaches due to the anti-contractive properties of the material. Still, numerous long term-studies were performed on rodents, where no anti-contractive strategies were applied. This hinders the reproducibility of data, and the studies' outcomes seem questionable. Anti-contractive properties are strongly needed, especially if PnD were just subcutaneously injected around the wound area or are topically applied in fluid or gel-like solutions or as soft membranes.

Another problem for the reproducibility of data is that there is significant variability in the application of wound dressings. Wound dressings are used to keep the wound area free of contamination. In the majority of the analyzed studies on rodents, it is not described whether a wound dressing was applied or not (**Figure 6**). Thus, it is difficult to evaluate the wound healing progress under unspecified experimental settings. In two studies, wounds were left open (Liu et al., 2014; Liu et al., 2016).

A popular wound dressing material for rodents is a dressing with Tegaderm™ plaster. It was applied without suturing (Zebardast et al., 2010; Tuca et al., 2016; Ertl et al., 2018; Bian et al., 2020; Vonbrunn et al., 2020), sutured onto the skin (Eylert et al., 2021), or was combined with a cohesive bandage (Arasteh et al., 2020). Other possibilities for wound dressings are fat gauze or oil gauze – with and without suturing to the skin (Montanucci et al., 2017; Motamed et al., 2017; Song et al., 2017; Gao et al., 2020; Hashemi et al., 2020; Zhao et al., 2020).

[4]https://www.criver.com/products-services/find-model/cd-1r-igs-mouse?region=3616

[5]https://www.criver.com/products-services/research-models-services/animal-models/mice/immunodeficient-mice/scid-mice?region=3616

[6]https://www.jax.org/

[7]https://www.janvier-labs.com/en/fiche_produit/lewis_rat/

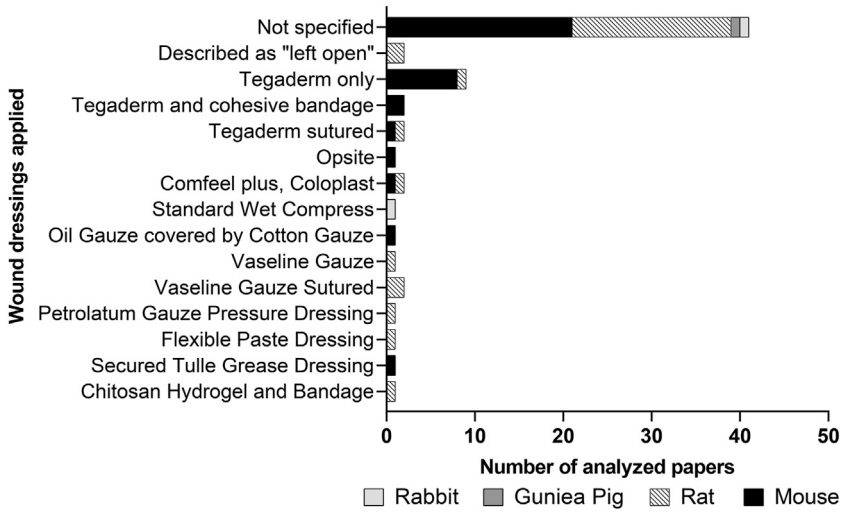

FIGURE 6 | Types of wound dressing applied to animal cutaneous wounds.

As unsutured plasters were partly detached from the wounds after a few days, we recommend removing the plasters 3 days post wounding, and thereafter leaving the wounds open to get standardized conditions for the wound healing process.

An accurate description of the advantages or disadvantages of used wound dressings in future publications would be helpful to standardize experiments and to enable comparability of the experiments concerning the healing outcome.

Wound Healing in Large Animals

On large animals, experiments were mainly performed on pigs. Pigs have the advantage that the porcine skin more closely correlates to human skin in thickness and structure than rodent skin. Wound closure in pigs is similar to wound healing in humans because the *musculus panniculus carnosus* is vestigial or absent in most body regions. Therefore, wounds heal by re-epithelialization rather than by contraction, and no anti-contractive strategies or devices are needed. However, experiments on pigs are cost-intensive and far more complex with respect to medication, anesthesia, and wound dressing, making them mainly useful for preclinical trials of therapies (Boyko et al., 2017).

As the number of animals in experiments is limited due to costs and husbandry, multiple wounds were performed on each subject.

Three studies included in the review utilized pigs as experimental animals (Han et al., 2014; Murphy et al., 2020; Eylert et al., 2021). Multiple wounds were created on the back of the animals (minimum 4, maximum not specified) and topically treated with PnD for 3–4 weeks. (Eylert et al., 2021) performed multiple full-thickness burn wounds with a size of 5 × 5 cm in diameter. It was shown that wounds treated with Integra® seeded with hUC-MSC at a low dose (40,000 cells/cm^2) regenerated wounds most efficaciously. Wounds were dressed with a layer of topical antibiotics, fat gauze, multiple layers of gauze, Tegaderm®, and a compression jacket. The initial wound margins were marked by a skin stapler. Wound dressing changes were performed two to three times per week.

Murphy et al. (2020) created eight 4 × 4 cm square-shaped full-thickness wounds on the central back and marked initial wound margins by tattooing before excision. Amnion-hydrogel and amnion powder treatments achieved the most rapid wound healing compared to commercially available Amniograft®, followed by hydrogel only, untreated wounds, or graft jacket, respectively. The treatment with the graft jacket alone led to the worst healing outcome (largest wound area, most contraction, least epithelialization). The wound dressing consisted of a topical antibiotic cream, Tegaderm® and a cast padding, cohesive bandaging, a protective saddle, and a jacket.

Han et al., 2014 (Han et al., 2014) created circular full-thickness wounds (diameter 3 cm). Collagen-chitosan-based scaffolds loaded with microencapsulated VEGF gene-modified hUC-MSC improved the vascularization of the tissue-engineered dermis and induced a better wound healing than controls (microencapsulated hUC-MSC, empty capsule, and PBS-treated group). The wound dressing was not described.

One case report described the wound treatment on dogs (Ribeiro et al., 2014). Two dogs suffering from non-healing skin lesions were treated with poly(vinyl alcohol) hydrogel (PVA) membrane supplied with low-dose UC-MSC 0.1 × 10^6 cells/cm^2. hUC-MSC induced significant progress in skin regeneration with the decreased extent of ulcerated areas.

Two studies were performed on rabbits, where full-thickness wounds were treated with rabbit BM-MSC either in combination with hAM (Kim et al., 2009) or with human placenta extract (Akela et al., 2013).

SUMMARY AND CONCLUSION

The pre-clinical evidence of our review indicates that PnD-based therapy is in general effective to promote cutaneous wound healing. The significant amount of variability between types, dosage, and application mode of PnD, as well as between the animal models, hinders the comparability of data. Perinatal cells

were the most commonly used PnD type, but only a tiny minority of studies compared the effect of applying different cell concentrations or modes of administration. Perinatal cell treatment worked at both low and high dosing, and further studies are required to evaluate the most optimal cell therapy. Treatment with perinatal cell-derived CM achieved similar beneficial effects as with cells, and frequent multiple applications of CM showed better outcomes than single- or two-fold treatments. Perinatal cell-derived sEV showed similar or even better beneficial effects on wound healing than perinatal cells. No studies compared different dosages of perinatal cell-sEV. The combination of cells and perinatal tissue membranes achieved better results on wound healing than either cells or tissue alone, and the combination of perinatal tissue extracts with cells achieved better results than tissue extracts without cells.

As an inadequate characterization of PnD may lead to a false identification of the PnD that hinders reproducibility and comparability of various studies, we propose the following guidelines for the PnD characterization before their application in pre-clinical studies:

1) A detailed and traceable cell/tissue isolation procedure – if PnD are commercially available, the company should be indicated (catalog and lot numbers, etc.).
2) Each PnD should be characterized by at least two *in vitro* methods: For cells, this should include the phenotype (morphology, immunolabeling for mesenchymal/epithelial markers, stem cell markers) and the ability to differentiate into all three germ layers (if stem cells are used). For the tissues, histology and immunolabeling to prove the identity/characteristics of the PnD, should be provided. In the case of purchased cells/tissues, the authors should indicate the main characteristics of PnD, as provided by the company.
3) Functional tests on cytotoxicity, promotion of proliferation, migration, and differentiation should be performed to ensure the quality of the PnD.
4) Dosage of PnD, characteristics of the wound, and the entire operating procedure, with mode and timing of application, should be described in detail so that the methodology is fully reproducible.

In addition, well-defined and standardized animal models are required for a comparison of outcome measures between studies. They may help to minimize redundancy in animal experimentation in line with the Replacement, Reduction, and Refinement (3R) principles for more ethical use of animals in research (Russell and Burch, 1960). The needs for standardization range from the choice of animal species and strains (with a preference for docile strains without barbering behavior and low anxiety levels) to precise experimental settings with regard to the extent and deepness of wounding and the adequate wound dressing. On rodents, anti-contractive strategies, ideally without suturing of devices, should be considered for long-term experiments (longer than 1 week) on full-thickness wounds.

An accurate description of the advantages or disadvantages of methods used in future publications would be helpful to standardize experiments and to enable comparability of the experiments concerning the healing outcome.

In conclusion, PnD have a promising potential to be widely used as a source of biological material to assist wound healing, now and in the future. Further concerted actions will be needed to bridge the gap between PnD basic research, pre-clinical studies, and their translation into the clinic. The COST SPRINT Action (CA17116) aims to provide comprehensive and evidence-based guidelines on all levels (Silini et al., 2020) to promote the safety and efficacy of the therapeutic use of PnD. The present review will contribute to the establishment of standards of care in wound healing.

DATA AVAILABILITY STATEMENT

The original contributions presented in the study are included in the article/**Supplementary Material**, further inquiries can be directed to the corresponding author.

AUTHOR CONTRIBUTIONS

ILO, MEK, SM, and PF conceptualized the review. All authors analyzed the data. MP, UJ, HO, and LT prepared the Figures and Tables. ILO wrote the Introduction. MEK, UJ, LT, HO, and SM wrote the section "PnD used for cutaneous wound healing in preclinical studies." MP and ILO wrote the section "Animal Models of cutaneous wound healing." ILO coordinated the work and compiled the manuscript. All authors contributed to revising and editing the manuscript and approved the submitted version.

FUNDING

This work was funded by: the COST Action 17116 – Sprint – International Network for Translating Research on Perinatal Derivatives into Therapeutic Approaches – CUP J56C18001930006, by the Ministry of Education, Science, and Technological Development of Republic of Serbia (Contract No. 451-03-9/2021-14/200015), by the Slovenian Research Agency (project J7-2594, and research core funding no. P3-0108), by FEDER - Fundo Europeu de Desenvolvimento Regional funds through the COMPETE 2020 - Operational Programme for Competitiveness and Internationalization (POCI), and by Portuguese funds through Fundação para a Ciência e a Tecnologia (FCT) in the framework of the project POCI-01-0145-FEDER-032610 - PTDC/MEC-DER/32610/2017. It was also supported by FCT under the project UIDB/50006/2020, UIDB/04326/2020 and UIDB/04565/2020.

SUPPLEMENTARY MATERIAL

The Supplementary Material for this article can be found online at: https://www.frontiersin.org/articles/10.3389/fbioe.2021.742858/full#supplementary-material

REFERENCES

Abd-Allah, S. H., El-Shal, A. S., Shalaby, S. M., Abd-Elbary, E., Mazen, N. F., and Abdel Kader, R. R. (2015). The Role of Placenta-Derived Mesenchymal Stem Cells in Healing of Induced Full-Thickness Skin Wound in a Mouse Model. *IUBMB Life* 67, 701–709. doi:10.1002/iub.1427

Aguilera, V., Briceño, L., Contreras, H., Lamperti, L., Sepúlveda, E., Díaz-Perez, F., et al. (2014). Endothelium Trans Differentiated from Wharton's Jelly Mesenchymal Cells Promote Tissue Regeneration: Potential Role of Soluble Pro-angiogenic Factors. *PLoS One* 9, e111025. doi:10.1371/journal.pone.0111025

Akela, A., Nandi, S. K., Das, P., Banerjee, D., Roy, S., and Datta, U. (2013). Autologous Bone Marrow-Derived Cells with Placental Extract for Healing Excisional Cutaneous Wounds in Animal Model. *Int. Wound J.* 10, 167–176. doi:10.1111/j.1742-481X.2012.00964.x

Ankrum, J., and Karp, J. M. (2010). Mesenchymal Stem Cell Therapy: Two Steps Forward, One Step Back. *Trends Mol. Med.* 16, 203–209. doi:10.1016/j.molmed.2010.02.005

Arasteh, S., Khanjani, S., Golshahi, H., Mobini, S., Jahed, M. T., Heidari-Vala, H., et al. (2020). Efficient Wound Healing Using a Synthetic Nanofibrous Bilayer Skin Substitute in Murine Model. *J. Surg. Res.* 245, 31–44. doi:10.1016/j.jss.2019.07.017

Armstrong, D. G., Boulton, A. J. M., and Bus, S. A. (2017). Diabetic Foot Ulcers and Their Recurrence. *N. Engl. J. Med.* 376, 2367–2375. doi:10.1056/NEJMra1615439

Bailo, M., Soncini, M., Vertua, E., Signoroni, P. B., Sanzone, S., Lombardi, G., et al. (2004). Engraftment Potential of Human Amnion and Chorion Cells Derived from Term Placenta. *Transplantation* 78, 1439–1448. doi:10.1097/01.TP.0000144606.84234.49

Bakhtyar, N., Jeschke, M. G., Mainville, L., Herer, E., and Amini-Nik, S. (2017). Acellular Gelatinous Material of Human Umbilical Cord Enhances Wound Healing: A Candidate Remedy for Deficient Wound Healing. *Front. Physiol.* 8, 200. doi:10.3389/fphys.2017.00200

Beiki, B., Zeynali, B., and Seyedjafari, E. (2017). Fabrication of a Three Dimensional Spongy Scaffold Using Human Wharton's Jelly Derived Extra Cellular Matrix for Wound Healing. *Mater. Sci. Eng. C* 78, 627–638. doi:10.1016/j.msec.2017.04.074

Belzung, C., and Berton, F. (1997). Further Pharmacological Validation of the BALB/c Neophobia in the Free Exploratory Paradigm as an Animal Model of Trait Anxiety. *Behav. Pharmacol.* 8, 541–548. doi:10.1097/00008877-199711000-00012

Bian, X., Li, B., Yang, J., Ma, K., Sun, M., Zhang, C., et al. (2020). Regenerative and Protective Effects of dMSC-sEVs on High-Glucose-Induced Senescent Fibroblasts by Suppressing RAGE Pathway and Activating Smad Pathway. *Stem Cel Res. Ther.* 11, 166. doi:10.1186/s13287-020-01681-z

Bibby, G., Krasniqi, B., Reddy, I., Sekar, D., and Ross, K. (2021). Capturing the RNA Castle: Exploiting MicroRNA Inhibition for Wound Healing. *FEBS J.* doi:10.1111/febs.16160

Boyko, T. V., Longaker, M. T., and Yang, G. P. (2017). Laboratory Models for the Study of Normal and Pathologic Wound Healing. *Plast. Reconstr. Surg.* 139, 654–662. doi:10.1097/PRS.0000000000003077

Caruso, M., Evangelista, M., and Parolini, O. (2012). Human Term Placental Cells: Phenotype, Properties and New Avenues in Regenerative Medicine. *Int. J. Mol. Cel Med.* 1, 64–74. PMCID: PMC3920494.

Choi, J. K., Din, F., Kim, D. W., Kim, Y. I., Kim, J. O., and Ku, J. K. (2014). Amniotic Membrane extract-loaded Double-Layered Wound Dressing: Evaluation of Gel Properties and Wound healing. *Drug. Dev. Ind. Pharm.* 40, 852–859. doi:10.3109/03639045.2013.788015

Datta, P., and Bhattacharyy, D. (2012). "Aqueous Extract of Human Placenta," in *Recent Advances in Research on the Human Placenta*. Editor J. Zheng (Rijeka, Croatia: IntechOpen Europe). doi:10.5772/31669

Davis, J. S. (1909). Skin Grafting at the Johns Hopkins Hospital. *Ann. Surg.* 50, 542–549. doi:10.1097/00000658-190909000-00002

Demidova-Rice, T. N., Durham, J. T., and Herman, I. M. (2012). Wound Healing Angiogenesis: Innovations and Challenges in Acute and Chronic Wound Healing. *Adv. Wound Care* 1, 17–22. doi:10.1089/wound.2011.0308

Deng, Q., Huang, S., Wen, J., Jiao, Y., Su, X., and Shi, G. (2020). PF-127 Hydrogel Plus Sodium Ascorbyl Phosphate Improves Wharton's jelly Mesenchymal Stem Cell-Mediated Skin Wound Healing in Mice. *Stem Cell Res.* 11, 143–158. doi:10.1186/s13287-020-01638-2

Deus, I. A., Mano, J. F., and Custódio, C. A. (2020). Perinatal Tissues and Cells in Tissue Engineering and Regenerative Medicine. *Acta Biomater.* 110, 1–14. doi:10.1016/j.actbio.2020.04.035

Du, L., Lv, R., Yang, X., Cheng, S., Ma, T., and Xu, J. (2016). Hypoxic Conditioned Medium of Placenta-Derived Mesenchymal Stem Cells Protects against Scar Formation. *Life Sci.* 149, 51–57. doi:10.1016/j.lfs.2016.02.050

Edwards, S. S., Zavala, G., Prieto, C. P., Elliott, M., Martínez, S., Egaña, J. T., et al. (2014). Functional Analysis Reveals Angiogenic Potential of Human Mesenchymal Stem Cells from Wharton's Jelly in Dermal Regeneration. *Angiogenesis* 17, 851–866. doi:10.1007/s10456-014-9432-7

Ertl, J., Pichlsberger, M., Tuca, A.-C., Wurzer, P., Fuchs, J., Geyer, S. H., et al. (2018). Comparative Study of Regenerative Effects of Mesenchymal Stem Cells Derived from Placental Amnion, Chorion and Umbilical Cord on Dermal Wounds. *Placenta* 65, 37–46. doi:10.1016/j.placenta.2018.04.004

Eylert, G., Dolp, R., Parousis, A., Cheng, R., Auger, C., Holter, M., et al. (2021). Skin Regeneration Is Accelerated by a Lower Dose of Multipotent Mesenchymal Stromal/stem Cells-A Paradigm Change. *Stem Cel Res. Ther.* 12, 82. doi:10.1186/s13287-020-02131-6

Farzamfar, S., Salehi, M., Ehterami, A., Naseri-Nosar, M., Vaez, A., Zarnani, A. H., et al. (2018). Promotion of Excisional Wound Repair by a Menstrual Blood-Derived Stem Cell-Seeded Decellularized Human Amniotic Membrane. *Biomed. Eng. Lett.* 8, 393–398. doi:10.1007/s13534-018-0084-1

Fukutake, M., Ochiai, D., Masuda, H., Abe, Y., Sato, Y., Otani, T., et al. (2019). Human Amniotic Fluid Stem Cells Have a Unique Potential to Accelerate Cutaneous Wound Healing With Reduced Fibrotic Scarring Like a Fetus. *Human Cell* 32, 51–63. doi:10.1007/s13577-018-0222-1

Gangoda, L., Boukouris, S., Liem, M., Kalra, H., and Mathivanan, S. (2015). Extracellular Vesicles Including Exosomes Are Mediators of Signal Transduction: Are They Protective or Pathogenic? *Proteomics* 15, 260–271. doi:10.1002/pmic.201400234

Gao, S., Chen, T., Hao, Y., Zhang, F., Tang, X., Wang, D., et al. (2020). Exosomal miR-135a Derived from Human Amnion Mesenchymal Stem Cells Promotes Cutaneous Wound Healing in Rats and Fibroblast Migration by Directly Inhibiting LATS2 Expression. *Stem Cel Res. Ther.* 11, 56. doi:10.1186/s13287-020-1570-9

Gholipourmalekabadi, M., Seifalian, A. M., Urbanska, A. M., Omrani, M. D., Hardy, J. G., Madjd, Z., et al. (2018). 3D Protein-Based Bilayer Artificial Skin for the Guided Scarless Healing of Third-Degree Burn Wounds *In Vivo*. *Biomacromolecules* 19, 2409–2422. doi:10.1021/acs.biomac.7b01807

Griebel, G., Belzung, C., Misslin, R., and Vogel, E. (1993). The Free-Exploratory Paradigm. *Behav. Pharmacol.* 4, 637–644. doi:10.1097/00008877-199312000-00009

Gunawardena, T. N. A., Rahman, M. T., Abdullah, B. J. J., and Abu Kasim, N. H. (2019). Conditioned media Derived from Mesenchymal Stem Cell Cultures: The Next Generation for Regenerative Medicine. *J. Tissue Eng. Regen. Med.* 13, 569–586. doi:10.1002/term.2806

Hammond, S. (2000). Transcutaneous Immunization of Domestic Animals: Opportunities and Challenges. *Adv. Drug Deliv. Rev.* 43, 45–55. doi:10.1016/s0169-409x(00)00076-4

Han, Y., Tao, R., Han, Y., Sun, T., Chai, J., Xu, G., et al. (2014). Microencapsulated VEGF Gene-Modified Umbilical Cord Mesenchymal Stromal Cells Promote the Vascularization of Tissue-Engineered Dermis: an Experimental Study. *Cytotherapy* 16, 160–169. doi:10.1016/j.jcyt.2013.10.014

Han, Y., Sun, T., Han, Y., Lin, L., Liu, C., Liu, J., et al. (2019). Human Umbilical Cord Mesenchymal Stem Cells Implantation Accelerates Cutaneous Wound Healing in Diabetic Rats via the Wnt Signaling Pathway. *Eur. J. Med. Res.* 24, 10. doi:10.1186/s40001-019-0366-9

Hashemi, S. S., Pourfath, M. R., Derakhshanfar, A., Behzad-Behbahani, A., and Moayedi, J. (2020). The Role of Labeled Cell Therapy with and without Scaffold in Early Excision Burn Wounds in a Rat Animal Model. *Iran J. Basic Med. Sci.* 23, 673–679. doi:10.22038/ijbms.2020.34324.8156

He, L., Tu, H., He, W., Guo, L. L., and Yu, S. (2015). Lentiviral-Mediated Overexpression of Homeobox A4 by Human Umbilical Cord Mesenchymal Stem Cells Repairs Full-Thickness Skin Defects. *Mol. Med. Rep.* 11, 3517–3522. doi:10.3892/mmr.2015.3208

Hong, J. W., Lee, W. J., Hahn, S. B., Kim, B. J., and Lew, D. H. (2010). The Effect of Human Placenta Extract in a Wound Healing Model. *Ann. Plast. Surg.* 35, 96–100. doi:10.1097/SAP.0b013e3181b0bb67

Hymes, S. R., Strom, E. A., and Fife, C. (2006). Radiation Dermatitis: Clinical Presentation, Pathophysiology, and Treatment 2006. *J. Am. Acad. Dermatol.* 54, 28–46. doi:10.1016/j.jaad.2005.08.054

Jerman, U. D., Veranič, P., and Kreft, M. E. (2014). Amniotic Membrane Scaffolds Enable the Development of Tissue-Engineered Urothelium with Molecular and Ultrastructural Properties Comparable to that of Native Urothelium. *Tissue Eng. C Methods* 20, 317–327. doi:10.1089/ten.TEC.2013.0298

Jerman, U. D., Veranič, P., Cirman, T., and Kreft, M. E. (2020). Human Amniotic Membrane Enriched with Urinary Bladder Fibroblasts Promote the Re-Epithelization of Urothelial Injury. *Cel Transpl.* 29, 096368972094666. doi:10.1177/0963689720946668

Jin, E., Kim, T.-H., Han, S., and Kim, S.-W. (2016). Amniotic Epithelial Cells Promote Wound Healing in Mice through High Epithelialization and Engraftment. *J. Tissue Eng. Regen. Med.* 10, 613–622. doi:10.1002/term.2069

Jirsova, K., and Jones, G. L. A. (2017). Amniotic Membrane in Ophthalmology: Properties, Preparation, Storage and Indications for Grafting-A Review. *Cell Tissue Bank* 18, 193–204. doi:10.1007/s10561-017-9618-5

Kakabadze, Z., Chakhunashvili, D., Chakhunashvili, D., Gogilashvili, K., Ediberidze, K., Chakhunashvili, K., et al. (2019). Bone Marrow Stem Cell and Decellularized Human Amniotic Membrane for the Treatment of Nonhealing Wound after Radiation Therapy. *Exp. Clin. Transpl.* 17, 92–98. doi:10.6002/ect.MESOT2018.O29

Kaushik, K., and Das, A. (2019). Cycloxygenase-2 Inhibition Potentiates Trans-differentiation of Wharton's Jelly-Mesenchymal Stromal Cells into Endothelial Cells: Transplantation Enhances Neovascularization-Mediated Wound Repair. *Cytotherapy* 21, 260–273. doi:10.1016/j.jcyt.2019.01.004

Keller, S., Sanderson, M. P., Stoeck, A., and Altevogt, P. (2006). Exosomes: from Biogenesis and Secretion to Biological Function. *Immunol. Lett.* 107, 102–108. doi:10.1016/j.imlet.2006.09.005

Kim, S. S., Song, C. K., Shon, S. K., Lee, K. Y., Kim, C. H., Lee, M. J., et al. (2009). Effects of Human Amniotic Membrane Grafts Combined with Marrow Mesenchymal Stem Cells on Healing of Full-Thickness Skin Defects in Rabbits. *Cell Tissue Res.* 336, 59–66. doi:10.1007/s00441-009-0766-1

Kim, S.-W., Zhang, H.-Z., Guo, L., Kim, J.-M., and Kim, M. H. (2012). Correction: Amniotic Mesenchymal Stem Cells Enhance Wound Healing in Diabetic NOD/SCID Mice through High Angiogenic and Engraftment Capabilities. *PLoS One* 7. doi:10.1371/annotation/f6ebe3d3-ef7c-42ce-86fe-d5a661d7f67f

Kinzer, M., Hingerl, K., König, J., Reinisch, A., Strunk, D., Huppertz, B., et al. (2014). Mesenchymal Stromal Cells from the Human Placenta Promote Neovascularization in a Mouse Model *In Vivo*. *Placenta* 35, 517–519. doi:10.1016/j.placenta.2014.04.004

König, J., Huppertz, B., Desoye, G., Parolini, O., Fröhlich, J. D., Weiss, G., et al. (2012). Amnion-derived Mesenchymal Stromal Cells Show Angiogenic Properties but Resist Differentiation into Mature Endothelial Cells. *Stem Cell Develop.* 21, 1309–1320. doi:10.1089/scd.2011.0223

König, J., Weiss, G., Rossi, D., Wankhammer, K., Reinisch, A., Kinzer, M., et al. (2015). Placental Mesenchymal Stromal Cells Derived from Blood Vessels or Avascular Tissues: what Is the Better Choice to Support Endothelial Cell Function? *Stem Cell Develop.* 24, 115–131. doi:10.1089/scd.2014.0115

Koob, T. J., Rennert, R., Zabek, N., Massee, M., Lim, J. J., Temenoff, J. S., et al. (2013). Biological Properties of Dehydrated Human Amnion/chorion Composite Graft: Implications for Chronic Wound Healing. *Int. Wound J.* 10, 493–500. doi:10.1111/iwj.12140

Koob, T. J., Lim, J. J., Massee, M., Zabek, N., Rennert, R., Gurtner, G., et al. (2014). Angiogenic Properties of Dehydrated Human Amnion/chorion Allografts: Therapeutic Potential for Soft Tissue Repair and Regeneration. *Vasc. Cel* 6, 10. doi:10.1186/2045-824X-6-10

Kwon, J. W., Hong, S. E., Kang, S. R., and Park, B. Y. (2019). Effect of Human Placental Extract Treatment on Random-Pattern Skin Flap Survival in Rats. *J. Invest. Surg.* 32, 304–313. doi:10.1080/08941939.2017.1417518

Lazarus, G. S., Cooper, D. M., Knighton, D. R., Margolis, D. J., Percoraro, R. E., Rodeheaver, G., et al. (1994). Definitions and Guidelines for Assessment of Wounds and Evaluation of Healing. *Wound Repair Regen.* 2, 165–170. doi:10.1046/j.1524-475X.1994.20305.x

Leng, X., Zhang, Q., Zhai, X., and Chen, Z. (2012). Local Transplant of Human Umbilical Cord Matrix Stem Cells Improves Skin Flap Survival in a Mouse Model. *Tohoku J. Exp. Med.* 227, 191–197. doi:10.1620/tjem.227.191

Li, J.-Y., Ren, K.-K., Zhang, W.-J., Xiao, L., Wu, H.-Y., Liu, Q.-Y., et al. (2019). Human Amniotic Mesenchymal Stem Cells and Their Paracrine Factors Promote Wound Healing by Inhibiting Heat Stress-Induced Skin Cell Apoptosis and Enhancing Their Proliferation through Activating PI3K/AKT Signaling Pathway. *Stem Cel Res. Ther.* 10, 247. doi:10.1186/s13287-019-1366-y

Liu, L., Yu, Y., Hou, Y., Chai, J., Duan, H., Chu, W., et al. (2014). Human Umbilical Cord Mesenchymal Stem Cells Transplantation Promotes Cutaneous Wound Healing of Severe Burned Rats. *PLoS One* 9, e88348. doi:10.1371/journal.pone.0088348

Liu, L., Song, H., Duan, H., Chai, J., Yang, J., Li, X., et al. (2016). TSG-6 Secreted by Human Umbilical Cord-MSCs Attenuates Severe Burn-Induced Excessive Inflammation via Inhibiting Activations of P38 and JNK Signaling. *Sci. Rep.* 6, 30121. doi:10.1038/srep30121

Liu, Z., Yu, D., Xu, J., Li, X., Wang, X., He, Z., et al. (2018). Human Umbilical Cord Mesenchymal Stem Cells Improve Irradiation-Induced Skin Ulcers Healing of Rat Models. *Biomed. Pharmacother.* 101, 729–736. doi:10.1016/j.biopha.2018.02.093

Liu, J., Yan, Z., Yang, F., Huang, Y., Yu, Y., Zhou, L., et al. (2021). Exosomes Derived from Human Umbilical Cord Mesenchymal Stem Cells Accelerate Cutaneous Wound Healing by Enhancing Angiogenesis through Delivering Angiopoietin-2. *Stem Cel Rev. Rep.* 17, 305–317. doi:10.1007/s12015-020-09992-7

Maguire, G. (2013). Stem Cell Therapy without the Cells. *Commun. Integr. Biol.* 6, e26631. doi:10.4161/cib.26631

Mahmood, R., Mehmood, A., Choudhery, M. S., Awan, S. J., Khan, S. N., and Riazuddin, S. (2019). Human Neonatal Stem Cell-Derived Skin Substitute Improves Healing of Severe Burn Wounds in a Rat Model. *Cell Biol. Int.* 43, 147–157. doi:10.1002/cbin.11072

McKenzie, J., Brennan, S., Ryan, R., Thomson, H., Johnston, R., and Thomas, J. (2021). "Chapter 3: Defining the Criteria for Including Studies and How They Will Be Grouped for the Synthesis," in *Cochrane Handbook for Systematic Reviews of Interventions Version 6.2*. Editors J. Higgins, J. Thomas, J. Chandler, M. Cumpston, T. Li, M. Page, et al. (Wiley Blackwell: London, UK). Available at: https://training.cochrane.org/handbook/current/chapter-03 (Accessed March 30, 2021).

Milan, P. B., Lotfibakhshaiesh, N., Joghataie, M. T., Ai, J., Pazouki, A., Kaplan, D. L., et al. (2016). Accelerated Wound Healing in a Diabetic Rat Model Using Decellularized Dermal Matrix and Human Umbilical Cord Perivascular Cells. *Acta Biomater.* 45, 234–246. doi:10.1016/j.actbio.2016.08.053

Mogil, J. S., Wilson, S. G., Bon, K., Eun Lee, S., Chung, K., Raber, P., et al. (1999). Heritability of Nociception I: Responses of 11 Inbred Mouse Strains on 12 Measures of Nociception. *Pain* 80, 67–82. doi:10.1016/S0304-3959(98)00197-3

Momeni, M., Zarehaghighi, M., Hajimiri, M., Khorasani, G., Dinarvand, R., Nekookar, A., et al. (2018). *In Vitro* and *In Vivo* Investigation of a Novel Amniotic-based Chitosan Dressing for Wound Healing. *Wound Rep. Reg.* 26, 87–101. doi:10.1111/wrr.12618

Montanucci, P., Di Pasquali, C., Ferri, I., Pescara, T., Pennoni, I., Siccu, P., et al. (2017). Human Umbilical Cord Wharton Jelly-Derived Adult Mesenchymal Stem Cells, in Biohybrid Scaffolds, for Experimental Skin Regeneration. *Stem Cell Int.* 2017, 1–13. doi:10.1155/2017/1472642

Motamed, S., Taghiabadi, E., Molaei, H., Sodeifi, N., Hassanpour, S. E., Shafieyan, S., et al. (2017). Cell-based Skin Substitutes Accelerate Regeneration of Extensive Burn Wounds in Rats. *Am. J. Surg.* 214, 762–769. doi:10.1016/j.amjsurg.2017.04.010

Mulholland, E. J. (2020). Electrospun Biomaterials in the Treatment and Prevention of Scars in Skin Wound Healing. *Front. Bioeng. Biotechnol.* 8, 481. doi:10.3389/fbioe.2020.00481

Mukherjee, C., Saleem, S., Das, S., Biswas, S. C., and Bhattacharyya, D. (2020). Human Placental Laminin: Role in Neuronal Differentiation, Cell Adhesion and Proliferation. *J. Biosci.* 45, 93–115. doi:10.1007/s12038-020-00043-4

Murphy, S. V., Skardal, A., Song, L., Sutton, K., Haug, R., Mack, D. L., et al. (2017). Solubilized Amnion Membrane Hyaluronic Acid Hydrogel Accelerates Full-Thickness Wound Healing. *Stem Cell Transl. Med.* 6, 2020–2032. doi:10.1002/sctm.17-0053

Murphy, S. V., Skardal, A., Nelson, R. A., Sunnon, K., Reid, T., Clouse, C., et al. (2020). Amnion Membrane Hydrogel and Amnion Membrane Powder Accelerate Wound Healing in a Full Thickness Porcine Skin Wound Model. *Stem Cell Transl. Med.* 9, 80–92. doi:10.1002/sctm.19-0101

Nan, W., Liu, R., Chen, H., Xu, Z., Chen, J., Wang, M., et al. (2015). Umbilical Cord Mesenchymal Stem Cells Combined with a Collagenfibrin Double-Layered Membrane Accelerates Wound Healing. *Wounds* 27, 134–140. PMID: 25965183.

Nasiry, D., Khalatbary, A. R., Abdollahifar, M.-A., Amini, A., Bayat, M., Noori, A., et al. (2020). Engraftment of Bioengineered Three-Dimensional Scaffold from Human Amniotic Membrane-Derived Extracellular Matrix Accelerates Ischemic Diabetic Wound Healing. *Arch. Dermatol. Res.* 313, 567. doi:10.1007/s00403-020-02137-3

Omran, E., Hieneedy, H., Halwagy, A., Al-Inany, H., Al-Ansary, M., and Gad, A. (2016). Amniotic Membrane Can Be a Valid Source for Wound Healing. *Int. J. Womens Health* 8, 225–231. doi:10.2147/IJWH.S96636

Page, M. J., McKenzie, J. E., Bossuyt, P. M., Boutron, I., Hoffmann, T. C., Mulrow, C. D., et al. (2021a). The PRISMA 2020 Statement: an Updated Guideline for Reporting Systematic Reviews. *BMJ* 372, n71. doi:10.1136/bmj.n71

Page, M. J., Moher, D., Bossuyt, P. M., Boutron, I., Hoffmann, T. C., Mulrow, C. D., et al. (2021b). PRISMA 2020 Explanation and Elaboration: Updated Guidance and Exemplars for Reporting Systematic Reviews. *BMJ* 372, n160. doi:10.1136/bmj.n160

Parolini, O., Alviano, F., Bagnara, G. P., Bilic, G., Bühring, H.-J., Evangelista, M., et al. (2008). Concise Review: Isolation and Characterization of Cells from Human Term Placenta: Outcome of the First International Workshop on Placenta Derived Stem Cells. *Stem Cells* 26, 300–311. doi:10.1634/stemcells.2007-0594

Payne, W. G., Wachtel, T. L., Smith, C. A., Uberti, M. G., Ko, F., and Robson, M. C. (2010). Effect of Amnion-Derived Cellular Cytokine Solution on Healing of Experimental Partial-Thickness burns. *World J. Surg.* 34, 1663–1668. doi:10.1007/s00268-010-0420-9

Peña-Villalobos, I., Casanova-Maldonado, I., Lois, P., Prieto, C., Pizarro, C., Lattus, J., et al. (2018). Hyperbaric Oxygen Increases Stem Cell Proliferation, Angiogenesis and Wound-Healing Ability of WJ-MSCs in Diabetic Mice. *Front. Physiol.* 9, 995. doi:10.3389/fphys.2018.00995

Pogozhykh, O., Prokopyuk, V., Figueiredo, C., and Pogozhykh, D. (2018). Placenta and Placental Derivatives in Regenerative Therapies: Experimental Studies, History, and Prospects. *Stem Cell Int.* 2018, 1–14. doi:10.1155/2018/4837930

Pourfath, M. R., Behzad-Behbahani, A., Hashemi, S. S., Derakhsahnfar, A., Taheri, M. N., and Salehi, S. (2018). Monitoring Wound Healing of Burn in Rat Model Using Human Wharton's Jelly Mesenchymal Stem Cells Containing cGFP Integrated by Lentiviral Vectors. *Iran J. Basic Med. Sci.* 21, 70–76. doi:10.22038/IJBMS.2017.19783.5212

Poženel, L., Lindenmair, A., Schmidt, K., Kozlov, A. V., Grillari, J., Wolbank, S., et al. (2019). Critical Impact of Human Amniotic Membrane Tension on Mitochondrial Function and Cell Viability *In Vitro*. *Cells* 8, 1641. doi:10.3390/cells8121641

Rahman, M. S., Islam, R., Rana, M. M., Spitzhorn, L.-S., Rahman, M. S., Adjaye, J., et al. (2019). Characterization of Burn Wound Healing Gel Prepared from Human Amniotic Membrane and Aloe Vera Extract. *BMC Complement. Altern. Med.* 19, 115. doi:10.1186/s12906-019-2525-5

Raj, V., Claudine, S., Subramanian, A., Tam, K., Biswas, A., Bongso, A., et al. (2019). Histological, Immunohistochemical, and Genomic Evaluation of Excisional and Diabetic Wounds Treated with Human Wharton's Jelly Stem Cells with and without a Nanocarrier. *J. Cel Biochem.* 120, 11222–11240. doi:10.1002/jcb.28398

Rameshbabu, A. P., Datta, S., Bankoti, K., Subramani, E., Chaudhury, K., Lalzawmliana, V., et al. (2018). Polycaprolactone Nanofibers Functionalized with Placental Derived Extracellular Matrix for Stimulating Wound Healing Activity. *J. Mater. Chem. B* 6, 6767–6780. doi:10.1039/C8TB01373J

Ramuta, T. Ž., Jerman, U. D., Tratnjek, L., Janev, A., Magatti, M., Vertua, E., et al. (2020). The Cells and Extracellular Matrix of Human Amniotic Membrane Hinder the Growth and Invasive Potential of Bladder Urothelial Cancer Cells. *Front. Bioeng. Biotechnol.* 8, 554530. doi:10.3389/fbioe.2020.554530

Rashed, M. H., Bayraktar, E., Helal, G. K., Abd-Ellah, M., Amero, P., Chavez-Reyes, A., et al. (2017). Exosomes: From Garbage Bins to Promising Therapeutic Targets. *Int. J. Mol. Sci.* 18, 538. doi:10.3390/ijms18030538

Ribeiro, J., Pereira, T., Amorim, I., Caseiro, A. R., Lopes, M. A., Lima, J., et al. (2014). Cell Therapy with Human MSCs Isolated from the Umbilical Cord Wharton Jelly Associated to a PVA Membrane in the Treatment of Chronic Skin Wounds. *Int. J. Med. Sci.* 11, 979–987. doi:10.7150/ijms.9139

Robson, M. C., DelBeccaro, E. J., Heggers, J. P., and Loy, G. L. (1980). Increasing Dermal Perfusion after Burning by Decreasing Thromboxane Production. *J. Trauma Inj. Infect. Crit. Care* 20, 722–725. doi:10.1097/00005373-198009000-00002

Russell, M. S., and Burch, R. L. (1960). The Principles of Humane Experimental Technique. *Med. J. Aust.* 1, 500. doi:10.5694/j.1326-5377.1960.tb73127.x

Sabapathy, V., Sundaram, B., Sreelakshmi, V. M., Mankuzhy, P., and Kumar, S. (2014). Human Wharton's Jelly Mesenchymal Stem Cells Plasticity Augments Scar-free Skin Wound Healing with Hair Growth. *PLoS One* 9, e93726. doi:10.1371/journal.pone.0093726

Sabella, N. (1913). Use of Fetal Membranes in Skin Grafting. *Medication Reconciliation* 83, 478–480. doi:10.1177/001452461302401011

Sabzevari, R., Roushandeh, A. M., Mehdipour, A., Alini, M., and Roudkenar, M. H. (2020). SA/G Hydrogel Containing hCAP-18/LL-37-Engineered WJ-MSCs-Derived Conditioned Medium Promoted Wound Healing in Rat Model of Excision Injury. *Life Sci.* 261, 118381. doi:10.1016/j.lfs.2020.118381

Samadikuchaksaraei, A., Mehdipour, A., Habibi Roudkenar, M., Verdi, J., Joghataei, M. T., As'adi, K., et al. (2016). A Dermal Equivalent Engineered with TGF-β3 Expressing Bone Marrow Stromal Cells and Amniotic Membrane: Cosmetic Healing of Full-Thickness Skin Wounds in Rats. *Artif. Organs* 40, E266–E279. doi:10.1111/aor.12807

Sarna, J. (2000). The Dalila Effect: C57BL6 Mice Barber Whiskers by Plucking. *Behav. Brain Res.* 108, 39–45. doi:10.1016/S0166-4328(99)00137-0

Schmauss, D., Weinzierl, A., Schmauss, V., and Harder, Y. (2018). Common Rodent Flap Models in Experimental Surgery. *Eur. Surg. Res.* 59, 255–264. doi:10.1159/000492414

Sen, C. K., Gordillo, G. M., Roy, S., Kirsner, R., Lambert, L., Hunt, T. K., et al. (2009). Human Skin Wounds: a Major and Snowballing Threat to Public Health and the Economy. *Wound Repair Regen.* 17, 763–771. doi:10.1111/j.1524-475X.2009.00543.x

Shi, R., Lian, W., Jin, Y., Cao, C., Han, S., Yang, X., et al. (2020). Role and Effect of Vein-Transplanted Human Umbilical Cord Mesenchymal Stem Cells in the Repair of Diabetic Foot Ulcers in Rats. *Acta Biochim. Biophys. Sin. (Shanghai)* 52, 620–630. doi:10.1093/abbs/gmaa039

Shohara, R., Yamamoto, A., Takikawa, S., Iwase, A., Hibi, H., Kikkawa, F., et al. (2012). Mesenchymal Stromal Cells of Human Umbilical Cord Wharton's Jelly Accelerate Wound Healing by Paracrine Mechanisms. *Cytotherapy* 14, 1171–1181. doi:10.3109/14653249.2012.706705

Shrestha, C., Zhao, L., Chen, K., He, H., and Mo, Z. (2013). Enhanced Healing of Diabetic Wounds by Subcutaneous Administration of Human Umbilical Cord Derived Stem Cells and Their Conditioned media. *Int. J. Endocrinol.* 2013, 1–10. doi:10.1155/2013/592454

Silini, A. R., Cargnoni, A., Magatti, M., Pianta, S., and Parolini, O. (2015). The Long Path of Human Placenta, and its Derivatives, in Regenerative Medicine. *Front. Bioeng. Biotechnol.* 3, 162. doi:10.3389/fbioe.2015.00162

Silini, A. R., Di Pietro, R., Lang-Olip, I., Alviano, F., Banerjee, A., Basile, M., et al. (2020). Perinatal Derivatives: Where Do We Stand? A Roadmap of the Human Placenta and Consensus for Tissue and Cell Nomenclature. *Front. Bioeng. Biotechnol.* 8, 610544. doi:10.3389/fbioe.2020.610544

Song, M., Wang, W., Ye, Q., Bu, S., Shen, Z., and Zhu, Y. (2017). The Repairing of Full-Thickness Skin Deficiency and its Biological Mechanism Using Decellularized Human Amniotic Membrane as the Wound Dressing. *Mater. Sci. Eng. C* 77, 739–747. doi:10.1016/j.msec.2017.03.232

Stern, M. (1913). The Grafting of Preserved Amniotic Membrane to Burned and Ulcerated Surfaces, Substituing Skin Grafts. *JAMA* 60, 973. doi:10.1001/jama.1913.04340130021008

Stojadinovic, A., Carlson, J. W., Schultz, G. S., Davis, T. A., and Elster, E. A. (2008). Topical Advances in Wound Care. *Gynecol. Oncol.* 111, S70–S80. doi:10.1016/j.ygyno.2008.07.042

Sun, J., Zhang, Y., Song, X., Zhu, J., and Zhu, Q. (2019). The Healing Effects of Conditioned Medium Derived from Mesenchymal Stem Cells on Radiation-Induced Skin Wounds in Rats. *Cel Transpl.* 28, 105–115. doi:10.1177/0963689718807410

Théry, C., Witwer, K. W., Aikawa, E., Alcaraz, M. J., Anderson, J. D., Andriantsitohaina, R., et al. (2018). Minimal Information for Studies of

Extracellular Vesicles 2018 (MISEV2018): a Position Statement of the International Society for Extracellular Vesicles and Update of the MISEV2014 Guidelines. *J. Extracell Vesicles* 7, 1535750. doi:10.1080/20013078.2018.1535750

Tuca, A.-C., Ertl, J., Hingerl, K., Pichlsberger, M., Fuchs, J., Wurzer, P., et al. (2016). Comparison of Matrigel and Matriderm as a Carrier for Human Amnion-Derived Mesenchymal Stem Cells in Wound Healing. *Placenta* 48, 99–103. doi:10.1016/j.placenta.2016.10.015

Ueta, M., Kweon, M.-N., Sano, Y., Sotozono, C., Yamada, J., Koizumi, N., et al. (2002). Immunosuppressive Properties of Human Amniotic Membrane for Mixed Lymphocyte Reaction. *Clin. Exp. Immunol.* 129, 464–470. doi:10.1046/j.1365-2249.2002.01945.x

van Deun, J., Van Deun, J., Mestdagh, P., Agostinis, P., Akay, Ö., Anand, S., et al. (2017). EV-TRACK: Transparent Reporting and Centralizing Knowledge in Extracellular Vesicle Research. *Nat. Methods* 14, 228–232. doi:10.1038/nmeth.4185

Vonbrunn, E., Mueller, M., Pichlsberger, M., Sundl, M., Helmer, A., Wallner, S. A., et al. (2020). Electrospun PCL/PLA Scaffolds Are More Suitable Carriers of Placental Mesenchymal Stromal Cells Than Collagen/Elastin Scaffolds and Prevent Wound Contraction in a Mouse Model of Wound Healing. *Front. Bioeng. Biotechnol.* 8, 604123. doi:10.3389/fbioe.2020.604123

Wang, S., Yang, H., Tang, Z., Long, G., and Huang, W. (2016). Wound Dressing Model of Human Umbilical Cord Mesenchymal Stem Cells-Alginates Complex Promotes Skin Wound Healing by Paracrine Signaling. *Stem Cell Int.* 2016, 1–8. doi:10.1155/2016/3269267

Wang, S., Mo, M., Wang, J., Sadia, S., Shi, B., Fu, X., et al. (2018). Platelet-derived Growth Factor Receptor Beta Identifies Mesenchymal Stem Cells with Enhanced Engraftment to Tissue Injury and Pro-angiogenic Property. *Cell. Mol. Life Sci.* 75, 547–561. doi:10.1007/s00018-017-2641-7

Weidinger, A., Poženel, L., Wolbank, S., and Banerjee, A. (2020). Sub-Regional Differences of the Human Amniotic Membrane and Their Potential Impact on Tissue Regeneration Application. *Front. Bioeng. Biotechnol.* 8, 613804. doi:10.3389/fbioe.2020.613804

Xue, M., Zhao, R., Lin, H., and Jackson, C. (2018). Delivery Systems of Current Biologicals for the Treatment of Chronic Cutaneous Wounds and Severe burns. *Adv. Drug Deliv. Rev.* 129, 219–241. doi:10.1016/j.addr.2018.03.002

Yang, J. D., Choi, D. S., Cho, Y. K., Kim, T. K., Lee, J. W., Choi, K. Y., et al. (2013). Effect of Amniotic Fluid Stem Cells and Amniotic Fluid Cells on the Wound Healing Process in a white Rat Model. *Arch. Plast. Surg.* 40, 496–504. doi:10.5999/aps.2013.40.5.496

Yang, K., Li, D., Wang, M., Xu, Z., Chen, X., Liu, Q., et al. (2019). Exposure to Blue Light Stimulates the Proangiogenic Capability of Exosomes Derived from Human Umbilical Cord Mesenchymal Stem Cells. *Stem Cel Res. Ther.* 10, 358. doi:10.1186/s13287-019-1472-x

Yang, J., Chen, Z., Pan, D., Li, H., and Shen, J. (2020). Umbilical Cord-Derived Mesenchymal Stem Cell-Derived Exosomes Combined Pluronic F127 Hydrogel Promote Chronic Diabetic Wound Healing and Complete Skin Regeneration. *Int. J. Nanomedicine* 15, 5911–5926. doi:10.2147/IJN.S249129

Yue, C., Guo, Z., Luo, Y., Yuan, J., Wan, X., and Mo, Z. (2020). c-Jun Overexpression Accelerates Wound Healing in Diabetic Rats by Human Umbilical Cord-Derived Mesenchymal Stem Cells. *Stem Cell Int.* 2020, 1–10. doi:10.1155/2020/7430968

Zebardast, N., Lickorish, D., and Davies, J. E. (2010). Human Umbilical Cord Perivascular Cells (HUCPVC). *Organogenesis* 6, 197–203. doi:10.4161/org.6.4.12393

Zhang, B., Wang, M., Gong, A., Zhang, X., Wu, X., Zhu, Y., et al. (2015a). HucMSC-Exosome Mediated-Wnt4 Signaling Is Required for Cutaneous Wound Healing. *Stem Cells* 33, 2158–2168. doi:10.1002/stem.1771

Zhang, B., Wu, X., Zhang, X., Sun, Y., Yan, Y., Shi, H., et al. (2015b). Human Umbilical Cord Mesenchymal Stem Cell Exosomes Enhance Angiogenesis through the Wnt4/β-Catenin Pathway. *Stem Cell Transl. Med.* 4, 513–522. doi:10.5966/sctm.2014-0267

Zhang, B., Shi, Y., Gong, A., Pan, Z., Shi, H., Yang, H., et al. (2016). HucMSC Exosome-Delivered 14-3-3ζ Orchestrates Self-Control of the Wnt Response via Modulation of YAP during Cutaneous Regeneration. *Stem Cells* 34, 2485–2500. doi:10.1002/stem.2432

Zhang, S., Chen, L., Zhang, G., and Zhang, B. (2020). Umbilical Cord-Matrix Stem Cells Induce the Functional Restoration of Vascular Endothelial Cells and Enhance Skin Wound Healing in Diabetic Mice via the Polarized Macrophages. *Stem Cel Res. Ther.* 11, 39. doi:10.1186/s13287-020-1561-x

Zhang, Z., Li, Z., Li, Y., Wang, Y., Yao, M., Zhang, K., et al. (2021). Sodium Alginate/Collagen Hydrogel Loaded With Human Umbilical Cord Mesenchymal Stem Cells Promotes Wound Healing and Skin Remodeling. *Cell Tissue Res.* 383, 809–821. doi:10.1007/s00441-020-03321-7

Zhao, G., Liu, F., Liu, Z., Zuo, K., Wang, B., Zhang, Y., et al. (2020). MSC-derived Exosomes Attenuate Cell Death through Suppressing AIF Nucleus Translocation and Enhance Cutaneous Wound Healing. *Stem Cel Res. Ther.* 11, 174. doi:10.1186/s13287-020-01616-8

Zhao, B., Liu, J. Q., Zhang, Z., Zhang, J., Wang, S. Y., and Han, S. C. (2018). Human Amniotic Epithelial Stem Cells Promote Wound Healing by Facilitating Migration and Proliferation of Keratinocytes via ERK, JNK and AKT Signaling Pathways. *Cell Tissue Res.* 365, 85–99. doi:10.1007/s00441-016-2366-1

Zomer, H. D., and Trentin, A. G. (2018). Skin Wound Healing in Humans and Mice: Challenges in Translational Research. *J. Dermatol. Sci.* 90, 3–12. doi:10.1016/j.jdermsci.2017.12.009

Conflict of Interest: The authors declare that the research was conducted in the absence of any commercial or financial relationships that could be construed as a potential conflict of interest.

Publisher's Note: All claims expressed in this article are solely those of the authors and do not necessarily represent those of their affiliated organizations, or those of the publisher, the editors and the reviewers. Any product that may be evaluated in this article, or claim that may be made by its manufacturer, is not guaranteed or endorsed by the publisher.

frontiers in Bioengineering and Biotechnology

REVIEW
published: 24 January 2022
doi: 10.3389/fbioe.2022.811875

Application of Perinatal Derivatives in Ovarian Diseases

Anna Lange-Consiglio[1,2], Emanuele Capra[3], Valentina Herrera[1], Ingrid Lang-Olip[4], Peter Ponsaerts[5] and Fausto Cremonesi[1,2]*

[1]Dipartimento di Medicina Veterinaria, Università Degli Studi di Milano, Lodi, Italy, [2]Centro Clinico-Veterinario e Zootecnico-Sperimentale di Ateneo, Università Degli Studi di Milano, Lodi, Italy, [3]Istituto di Biologia e Biotecnologia Agraria, Consiglio Nazionale Delle Ricerche IBBA CNR, Lodi, Italy, [4]Division of Cell Biology, Histology and Embryology, Gottfried Schatz Research Center, Medical University of Graz, Graz, Austria, [5]Laboratory of Experimental Hematology, Vaccine and Infectious Disease Institute (Vaxinfectio), University of Antwerp, Antwerp, Belgium

Reproductive diseases could lead to infertility and have implications for overall health, most importantly due to psychological, medical and socio-economic consequences for individuals and society. Furthermore, economical losses also occur in animal husbandry. In both human and veterinary medicine, hormonal and surgical treatments, as well as assisted reproductive technologies are used to cure reproductive disorders, however they do not improve fertility. With ovarian disorders being the main reproductive pathology in human and bovine, over the past 2 decades research has approached regenerative medicine in animal model to restore normal function. Ovarian pathologies are characterized by granulosa cell and oocyte apoptosis, follicular atresia, decrease in oocyte quality and embryonic development potential, oxidative stress and mitochondrial abnormalities, ultimately leading to a decrease in fertility. At current, application of mesenchymal stromal cells or derivatives thereof represents a valid strategy for regenerative purposes. Considering their paracrine/autocrine mode of actions that are able to regenerate injured tissues, trophic support, preventing apoptosis and fibrosis, promoting angiogenesis, stimulating the function and differentiation of endogenous stem cells and even reducing the immune response, are all important players in their future therapeutic success. Nevertheless, obtaining mesenchymal stromal cells (MSC) from adult tissues requires invasive procedures and implicates decreased cell proliferation and a reduced differentiation capacity with age. Alternatively, the use of embryonic stem cells as source of cellular therapeutic encountered several ethical concerns, as well as the risk of teratoma formation. Therefore, several studies have recently focussed on perinatal derivatives (PnD) that can be collected non-invasively and, most importantly, display similar characteristics in terms of regenerating-inducing properties, immune-modulating properties and hypo-immunogenicity. This review will provide an overview of the current knowledge and future perspectives of PnD application in the treatment of ovarian hypofunction.

Keywords: perinatal derivatives, ovarian diseases, secretome, extracellular vesicles, animal models

OPEN ACCESS

Edited by:
Bryan Brown,
University of Pittsburgh, United States

Reviewed by:
Anna Cargnoni,
Fondazione Poliambulanza Istituto Ospedaliero, Italy
Roberto Gramignoli,
Karolinska Institutet (KI), Sweden

****Correspondence:***
Anna Lange-Consiglio
anna.langeconsiglio@unimi.it

Specialty section:
This article was submitted to Tissue Engineering and Regenerative Medicine, a section of the journal Frontiers in Bioengineering and Biotechnology

Received: *09 November 2021*
Accepted: *05 January 2022*
Published: *24 January 2022*

Citation:
Lange-Consiglio A, Capra E, Herrera V, Lang-Olip I, Ponsaerts P and Cremonesi F (2022) Application of Perinatal Derivatives in Ovarian Diseases. Front. Bioeng. Biotechnol. 10:811875. doi: 10.3389/fbioe.2022.811875

INTRODUCTION

Reproductive disorders are caused by different factors, including social, genetic, endocrine, physiological, psychological and lifestyle habits (e.g., smoking and alcohol consumption), and may lead to infertility (Agarwal et al., 2021; Farsimadan et al., 2021). In human, both men and women are affected, with a male factor occurrence of around 30–40% and a female occurrence of around 50% (Boivin et al., 2007; Gurunath et al., 2011). Reproductive diseases include abnormal hormone production by gonads (ovaries or testes) or endocrine glands (pituitary, thyroid, or adrenals), but can also be caused by genetic or congenital abnormalities, infections, tumours and disorders of unknown cause. In male, the most common reproductive diseases are oligospermia, poor semen quality, low sperm motility, anatomical defects like block in vas deferens, infections leading to inflammation of seminal vesicles, the epididymis or the prostate, genetic abnormalities like Klinefelter, Chlamydia infections, circumcision, erectile dysfunction, genital herpes, genital warts, gonorrhoea and penis disorders (Boivin et al., 2007; Gurunath et al., 2011). In woman, the most common causes of infertility are ovarian hypofunction, irregular ovulation, poor oocyte quality, blocked fallopian tubes due to infection or endometriosis, uterine fibroids, polycystic ovaries, primary and secondary amenorrhea, pelvic inflammatory disease, hostile cervical mucus, sexually transmitted diseases, gynaecologic cancers as well as side effects of cancer chemotherapy (Boivin et al., 2007). Both male and female infertility has implications for overall health. In fact, compared to the healthy population, female infertility is often associated with other disorders such as higher rates of psychiatric disorders, endometrial cancer, polycystic ovary syndrome and patients are more likely to develop cardiovascular disease and metabolic disorders such as diabetes (Hanson et al., 2017). Male infertility on the other hand is reflected by a higher incidence of cancer.

Reproductive diseases are also subject of veterinary medicine. Reproductive performances (for example in dairy cattle) can be complicated by twinning, dystocia, stillbirth, abortion, retained placenta, metritis and ovary hypofunction. These diseases primarily affect the productivity of dairy cows by decreasing reproductive efficiency, shortening the expected productive lifespan and lowering milk production. Poor reproductive performance is a major cause of involuntary culling with negative influence on the subsequent productivity of dairy herd (Ghavi Hossein-Zadeh, 2013).

Despite assisted reproductive technologies have created enormous expectation for infertility treatment, and both hormonal and surgical treatments have been applied to (partially) cure reproductive disorders in human and veterinary medicine, there is an unmet need for awareness that these disorders do have a wider impact on long-term health in human (Hanson et al., 2017) and on the economic management of dairy farms. Therefore, the needs to identify alternative therapies is growing. Over the past 2 decades, researchers have approached the concept of regenerative medicine to restore normal sexual function and preserve fertility, principally focusing on ovarian diseases that are the main pathology in females, both human and animal.

OVARIAN DISEASES

Functionality of the ovaries through the production of hormones and gametes guarantees the health of the female reproductive system (Kim et al., 2018). In the ovarian follicle, the oocyte is surrounded by granulosa cells and cumulus cells that allow oocytes to survive, grow and mature through molecular and intercellular communications (Thabet et al., 2020). Proliferation and differentiation of granulosa cells is essential for the continuous development of follicles from primary, secondary, tertiary antral follicles up to ovulation (Li et al., 2019). Adequate functioning of the hypothalamus guarantees the hormone-releasing gonadotropins (GnRH) which at the adenohypophysis level will favour the release of follicle-stimulating hormone (FSH) and luteinizing hormone (LH) which are conveyed to the oocyte thanks to the cumulus cells equipped with receptors for these hormones. These two hormones promote the functionality of granulosa cells for the secretion of oestrogen and anti-Mullerian hormone (AMH), and follicular growth until ovulation (**Figure 1A**). Therefore, proliferation and differentiation of granulosa cells and cumulus cells are basic conditions for the continuous development of ovarian follicles (Zhang H et al., 2018). The AMH, in turn, inhibits the recruitment of primordial follicles from the dormant follicular pool into the emergent pool, thus preserving a state of coordinated ovarian follicular recruitment (Thabet et al., 2020). The AMH, which is expressed in granulosa cells, also participates in the selection of the dominant follicles and plays an important role in follicle growth (Zhang H et al., 2018). In addition, granulosa cells are an important source of oestrogen and progesterone (Li et al., 2019). In the normal developmental period of the ovarian follicular cycle, all phases of follicular atresia are closely related to the activity levels of granulosa cells. In both aging and clinical context, increased apoptosis and decreased proliferation of granulosa cells is the principal mechanism driving follicular atresia and arrest (Ding et al., 2018; Huang et al., 2020). Current knowledge on ovarian dysfunction in the human, murine and bovine reproductive system will be briefly introduced.

Human Pathology

In situations related to the life of an individual, such as age-related diseases, natural aging, aging induced by therapeutic interventions and diseases, granulosa cells can be prone to persistent senescence (Huang et al., 2020). Physiological ovarian aging is a gradual decrease in both the quantity and quality of oocytes residing within the primordial follicles (Yang et al., 2020) and is linked to ovarian aging characterized by apoptosis of oocytes, follicular atresia, cessation of menstruation and elevated plasma levels of FSH (Ding et al., 2020a; Huang et al., 2020). The condition affects 1% of women worldwide by the age of 40 years (Ding et al., 2020a; Huang et al., 2020).

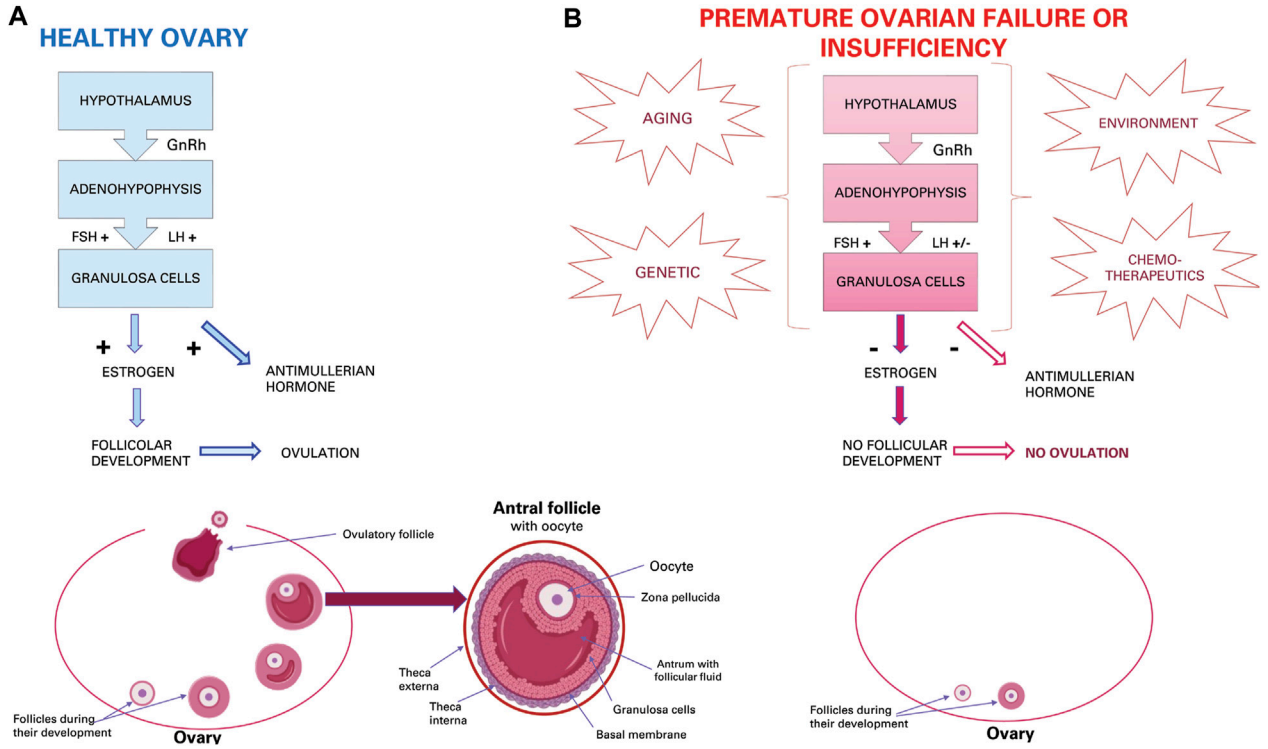

FIGURE 1 | Ovarian activity. **(A)** Physiological hormonal mechanism that induce normal granulosa activity, oestrous cycle, and ovulation. **(B)** Effect of aging, genetic, environmental and chemotherapeutic factors that induce POI or POF.

Menopause in women is an inevitable event due to ovarian aging (Huang et al., 2020), which in mammals implicates the inability to produce new oocytes after birth or during adult life since the number of oocytes is already predetermined as primordial follicles formed before birth. As such, the constant recruitment of primordial follicles and their disappearance over time depletes the ovarian reserve, leading to menopause (Yang et al., 2020). Recently, it has been shown that ovarian dysfunction could also be caused by genetic (e.g., genomic DNA alteration, mitochondrial DNA mutations and reduced telomerase activity) or environmental factors (e.g., oxidative stress, advanced glycation and chemotherapy). Especially for the latter, chemotherapeutic agents either directly affect oocytes or indirectly induce their degeneration by damaging granulosa cells (Hong et al., 2020) (**Figure 1B**). Furthermore, the process of ovarian dysfunction accelerates with increasing age (Seok et al., 2020) and may lead to various systemic complications (e.g., osteoporosis, heart disease, symptoms of menopause and metabolic syndrome) (Kim et al., 2018).

In addition to the physiological aging of the ovary, also premature ovarian aging may occur and is called "premature ovarian insufficiency" (POI) or "premature ovarian failure" (POF). This pathological condition is characterized by premature depletion of ovarian follicles (Lai et al., 2013). POF affects 1% women under the age of 40 and 0.1% of woman under 30. While about 25% of all forms of POF can be classified as iatrogenic and related to cancer treatment, more than 50% of cases remain idiopathic with unexplained aetiology (Lai et al., 2013). Patients with iatrogenic POF have abnormal ovary development that could be due to genetic disorders, such as fragile X, Turner syndrome, and some autosomal gene mutations (Li et al., 2018). Iatrogenic insults can be represented by cancer treatments, such as chemotherapy or radiotherapy, which can damage ovarian function leading to premature menopause, ovarian dysfunction, and risk of infertility (Li et al., 2018). Idiopathic or iatrogenic POI or POF is clinically characterized by oligomenorrhea or amenorrhea for at least 4 months, high levels of FSH and low levels of 17β-estradiol (E2) (Ling et al., 2019), resulting in oocyte apoptosis, follicular atresia (Ding et al., 2020b), decrease in oocyte quality and embryonic development potential, and, therefore, a decrease in fertility (Liu et al., 2012) (**Figure 1B**). In addition, the uterus and vaginal mucosa undergo atrophy due to oestrogen deficiency caused by inactive ovaries (Liu et al., 2012). Furthermore, oxidative stress and mitochondrial abnormalities have been shown to be related to follicular atresia and POI (Ding et al., 2020b). Oxidative stress induced by reactive oxygen species (ROS) is usually associated with various age-related diseases. POI is also characterized by decreased antioxidant levels and increased oxidative stress in cumulus cells, oocytes and ovaries, and oxidative stress levels are correlated with worse outcomes (Liu et al., 2012). If POI is not treated, there are many health risks, some of which are typical of menopause such as depression, anxiety, osteoporosis, increased risk of fractures, cardiovascular disease and cognitive decline

(Ling et al., 2019). In fact, most women with POF are sterile and suffer from unexpected and early menopause symptoms (Lai et al., 2013). Therefore, in contrast to the inevitable event of physiological ovarian aging, spontaneous premature cessation of ovarian function may need higher clinical and treatment attention in order not to be "permanent" (Li et al., 2018).

Experimental Models of Ovarian Diseases

Due to the poor feasibility of human studies, it is important to have ideal animal models that mimic the events that occur in human patients with POF or POI.

Usually, the mouse is chosen for its short reproductive life spans, high reproduction index, stable genetic backgrounds, and low costs. In addition, the estrous cycle of female mice is similar to that of humans, although the estrous cycle of mice is shorter than that of humans.

Mouse knockout models have been used to identify genes associated with follicle development, granulosa cell apoptosis, and subsequent damage or depletion of the follicle pool leading to POI or POF (Bouhali et al., 2011).

Since chemotherapy is a common method used to treat various malignancies and could induce ovarian failure and reduce fertility in young female patients (Ling et al., 2019), the treatment of ovarian damage has been studied in animal models, such as mice and rats, in which the disease has been induced by chemotherapy or radiotherapy as reported in **Table 1**. The most used chemotherapy drugs were cyclophosphamide or busulfan. In some papers, POI in mice was induced by ZP3 peptide, while in other cases, ovariectomized rats, or mice with physiological ovarian aging, or sterilized mice, or rats with naturally aging, or ovariectomized rats were used.

Treated animal models displayed paralleled manifestations to clinic features of human POI patients, mainly oxidative stress and apoptosis of granulosa cells, with the consequence of a significant decrease of the number of follicles, level of hormones, weight of ovaries, and number of offspring, as reported in all papers used in this review.

Physiologically, in the ovary, reactive oxygen species (ROS) are generated during ovulation and hence follicular rupture, which is considered an inflammation-like reaction. Several studies in rat and mouse models with induced POI have reported an increase of ROS levels that reduces oocyte quality due to granulosa cell apoptosis (Seok et al., 2020), which can cause a decrease in the number of follicles and a reduced level of oestrogen (Li et al., 2019) and AMH (Zhang H et al., 2018). Normally, presence of AMH allows the survival of small developing follicles, inhibits excessive follicular stimulation by FSH and acts as a regulator of follicular estrogen production. The AMH allows for the maintenance of an ovarian reserve. Then, fewer ovarian primordial follicles in a POF mouse model may be due to a decreased level of AMH in serum that increases the number of primordial follicles becoming the growing follicles. In this situation, the number of the primordial follicles ultimately decreases resulting in premature depletion of the primordial follicle pool (Zhang H et al., 2018) (**Figure 1B**), as in human POI or POF.

It is known that the follicles become atretic when 10% of granulosa cells have undergone apoptosis and this suggests that granulosa cell apoptosis plays a vital role in the development of follicular atresia (Zhang H et al., 2018). In fact, in a cyclophosphamide-induced mouse model of POF, there is a decreased expression of the antiapoptotic protein B-cell lymphoma 2 (Bcl-2) and an increased expression of the pro-apoptotic protein bcl-2-like protein 4 (Bax). These effects together induce apoptosis in follicular granulocyte cells and increased follicular atresia (Zhang H et al., 2018). In these animal models, it have been highlighted some metabolic aspects that induce POI or POF. For example, the oxidative stress can involve theca interstitial cells too and induce apoptosis and autophagy. These cells play an important role in folliculogenesis because they provide nutrients and hormones to granulosa cells through the basement membrane *via* vessels (Lu et al., 2020). The result is ovarian failure by a loss of oocyte maturation and granulosa cell luteinization (Seok et al., 2020). Granulosa cell apoptosis in POF mice may also be triggered by the endoplasmic reticulum (ER) stress response. Caspase-12 is the key molecule of regulating ER stress induced apoptosis and it is activated during ER stress. Indeed, studies in these animal models have shown that caspase-12 deficiency mice were resistant to ER stress-induced apoptosis (Li et al., 2019). Furthermore, DNA and proteins can also be damaged by oxidative stress with the consequent disruption of cellular processes (Liu et al., 2012).

In addition to mouse and rat as animal models, the cow could be used as possible and useful model to study the ovarian pathology and potential new treatments. In this species, there are spontaneous reproductive disorders (López-Gatius et al., 2006), mostly due to ovarian abnormalities, among which ovarian failure, that is the most common ovarian disorder (11.45%), followed by adhesions and cysts (6.38 and 5.22%, respectively) (Mekibib et al., 2013). Usually, cows have a dominant follicle that develops to the Graafian follicle stage which subsequently ovulates. After ovulation, this follicle will form the corpus luteum responsible for the secretion of progesterone. If a follicle of at least 8–15 mm is present on two consecutive examinations during the postpartum period and there is absence of cysts or luteal structures, it can be assumed that the cow may be affected by ovarian hypofunction and to have ovarian anovulation (Cremonesi et al., 2020). These animals are healthy but sub-fertile thus causing considerable economic damage to farms.

CLASSICAL TREATMENT OPTIONS

To date, several therapeutic approaches have been applied to POI patients to alleviate complications caused by low oestrogen levels and to improve fertility, among them 1) hormone replacement therapy (HRT), 2) cryopreservation of ovarian tissue and 3) administration of gonadotropins releasing hormone (GnRH) agonists. Hormone replacement therapy is effective for symptoms associated with low oestrogen levels but does not improve fertility (Ding et al., 2020a). Furthermore, this therapy is associated to some negative effects such as

thromboembolism, stroke, vaginal bleeding, heart disease, and breast cancer (Kim et al., 2018). For this reason, half of post-menopausal women worldwide live without reproductive hormones, such as oestrogen and progesterone (Kim et al., 2018). Although it has recently been reported that for women under the age of 60 that various risks can be reduced when this therapy is used at an appropriate timing, it still the disadvantage of being ineffective when it is stopped or not used at the correct schedule (Seok et al., 2020). Alternatively, cryopreservation of oocytes and ovarian tissue is a good option for preserving fertility, but the method is an "*ex vivo*" option and does not maintain ovarian function for an extended period (Hong et al., 2020). Finally, the administration of GnRH agonists has been proposed as a potential strategy. Although first-stage results demonstrate a significant reduction in ovarian failure induced by chemotherapy, the protective effects of GnRH agonists remain controversial (Hong et al., 2020).

There are also several other experimental approaches under investigation for POI patients. Among them, the use of phytoestrogens or herbal remedies are reported, but to date no data is available on the mechanism of action and/or long-term safety (Li et al., 2017). Similarly, application of the c-Abl kinase inhibitor imatinib, the sphingosine-based lipid signalling molecule sphingosine-1-phosphate (SIP) and the LH have been reported to prevent premature infertility (Hong et al., 2020), but future confirmatory studies will be needed. Learning from the veterinary field of medicine, cows are experimentally treated with GnRH-based treatments such as the Ovsynch protocol (López-Gatius et al., 2001; Lopez-Gatius et al., 2004; Yaniz et al., 2004) or a progesterone releasing intravaginal device (PRID) (Yániz et al., 2008), but oestrus response in affected cows is very low (usually <30%). Overall, all these methods do not fundamentally improve ovarian function and therefore the development safe and new treatments that can recover normal ovarian function would represent an important advance in reproductive biology.

TOWARDS CELLULAR THERAPIES

The field of regenerative medicine includes tissue engineering and cell therapy. Among the different cells for the treatment of diseases in both human and veterinary medicine, there are mesenchymal stromal cells (MSC) that can be collected from adult and perinatal tissues. Considering a possible transplantation, the source of these cells can be autologous or allogeneic.

Mesenchymal stromal cells are adult non-hematopoietic cells that are present in specific stem cell niches of various organs and tissues. The main properties of MSC are self-renewal and tri-lineage differentiation potential. However, upon *in vivo* administration, true engraftment of transplanted MSC, and as such tissue replacement, has only been documented in a few cases (Duffield et al., 2005; Tögel et al., 2005; Bi et al., 2007; Chimenti et al., 2010). Nevertheless, many studies have demonstrated that transplanted MSC rather act by paracrine/autocrine mechanisms, thereby regenerating injured tissues by means of trophic support. Mesenchymal stromal cell administration can prevent fibrosis and apoptosis, promotes angiogenesis, stimulates the function and differentiation of endogenous stem cells, and even decreases deleterious immune response (Huang et al., 2020). Consequently, the use of MSC has been applied in animal models for various diseases including, for example, myocardial infarction, neurological diseases, and diabetes (Wang et al., 2020). Since MSC also display immunosuppressive and anti-inflammatory properties, they are under investigation for the treatment of various inflammatory diseases, including inflammatory bowel disease, atopic dermatitis, and rheumatoid arthritis (Liao et al., 2019).

Alternative to the direct administration of autologous or allogeneic MSC is the application of MSC-derived factors to the diseased or affected organ or tissue. Although still under debate, it is highly likely that released secretome, that if collected *in vitro* is called conditioned media (MSC-CM) recapitulate the various functions of MSC that harbour their regenerative properties (Hong et al., 2020; Seok et al., 2020). Conditioned medium secreted by MSC is rich in soluble factors and insoluble components represented by extracellular vesicles (EVs) capable to attenuate tissue damage, inhibit apoptosis and fibrosis, promote angiogenesis, and to modulate immune responses (Bruno et al., 2019; Seok et al., 2020). Furthermore, MSC-CM has significant advantages compared to direct MSC application, including that 1) it can be lyophilized and transported more easily, 2) it reduces rejection problems between donor and recipient, and 3) it eliminates potential tumorigenic effects such as uncontrolled differentiation, increased metastatic capacity of tumour cells and epithelial-mesenchymal transition of tumour cells (Hong et al., 2020). The soluble factors in MSC-CM encompass chemokines, cytokines, and growth factors. On the other end, MSC-derived EVs are membranous structures with lipid bilayers of nanometre size that are normally released into the extracellular space (Thabet et al., 2020). Extracellular vesicles can be subcategorized in exosomes, which are the major subclass of EVs with sizes ranging from 50 to 120 nm and shedding vesicles or microvesicles that represent larger-sized vesicles (50–1,000 nm) (Thabet et al., 2020). Extracellular vesicles are rich in proteins, lipids, RNAs and microRNAs (miRNAs). MicroRNAs regulate diverse cellular processes by suppressing the expression of genes mainly via inhibition of their messenger RNAs (mRNAs) (Thabet et al., 2020). In this way, numerous studies have already demonstrated that EVs have intrinsic therapeutic effects in various diseases such as wound healing, inflammation, hypertension, cardiovascular disease, brain injuries and tumours (Yang et al., 2020). Similar to CM, EVs are very promising as therapeutic agents as compared to MSC, especially with regard to their low immunogenicity, lack of tumorigenicity, high clinical safety and low ethical risk compared to the cells of origin (Yang et al., 2020).

In addition to a general preference of using secretomes instead of live cell preparations, regenerative medicine is also exploring the use of alternative cellular sources in comparison to those considered to date as the gold standard, such as bone marrow and adipose tissue. Human bone marrow-MSC were the first cell type that was shown to improve ovarian function

and structure in a rat model with ovarian hypo functionality caused by chemotherapy. Subsequently, other sources such as adipose tissue (Kim et al., 2018), human menstrual blood, endometrium (Li et al., 2018) and skin (Seok et al., 2020) have been applied to rat models of ovarian dysfunction, with similar successes. Furthermore, MSC derived from bone marrow and adipose tissue also displayed positive effects on damaged ovarian tissue in a POF mouse model, thereby promoting an increase in E2 level, suppressing apoptosis and promoting angiogenesis (Kim et al., 2018).

From a clinical point of view, the collection of bone marrow and adipose tissue requires invasive procedures. Moreover, the actual cell yield for transplantation is rather low to insufficient due to decreased proliferation and a reduced differentiation capacity with age for these adult somatic cell types (Lange-Consiglio et al., 2012). An alternative source could be pluripotent stem cells, including embryonic stem cells (ESC) and induced pluripotent stem cells (iPSC), which proliferate rapidly and can give rise to three germ layer lineages. Another interesting feature of pluripotent stem cells is their ability to differentiate into germ cells, which have undergone meiosis and produce gametes (Lai et al., 2013). However, murine ESC *in vitro* have not supported the completion of meiosis and ESC-derived oocyte maturation ultimately fails *in vitro* (Lai et al., 2013). Furthermore, these cells do have limited use in clinical trials due to ethical concerns, allograft rejection problem, and risk of teratoma formation (Lin et al., 2015). Recently, the use of perinatal derivatives (PnD) in the development of cellular and acellular therapies for ovarian diseases has become a topic of interest in medical research.

PERINATAL DERIVATIVES (PnD)

The term "perinatal" refers to the tissues associated with birth that are collected from the term placenta (chorionic villi, chorionic plate) and extra-foetal tissues (including amniotic and chorionic membrane, amniotic fluid, and umbilical cord). The term derivatives refers to both living cells as well as their secretome or conditioned medium, including extracellular vesicles (Silini et al., 2020). Perinatal tissues, as compared to BM, represent an important source of MSC because they are a readily available source whose collection is painless and non-invasive, with minimal ethical issues as they are usually discarded at birth (Papait et al., 2020). In general, perinatal MSC show similar characteristics of bone marrow-MSC, including proliferation potential, self-renewal capacity, differentiation potential into multiple cell types, and chemotactic migration potential to sites of injury (Ling et al., 2019). Interestingly for regenerative medicine purposes, their higher proliferation rate as compared to adult tissue derived MSC can be explained by a more primitive developmental stage for these cells (Ilancheran et al., 2009). In addition, long-term *in vitro* culture does not seem to alter their phenotype and genetic stability (Sabapathy et al., 2014), which is not always the case for bone marrow-MSC.

In addition to the same characteristics of MSC, PnD also display several phenotypic characteristics of ESCs (Ling et al., 2019). For example, amniotic fluid-MSC express octamer-binding transcription factor 4 (OCT4), but unlike ESC they do not develop into teratomas (Xiao et al., 2014). It has also been suggested that several types of PnD can be used for allogeneic transplantation without rejection because they show hypo immunogenicity and the ability to modulate immune responses (Li et al., 2017; Ling et al., 2019). Compared to bone marrow-MSC, that are not able to exert suppressive effects if they are not previously exposed to inflammatory stimuli, PnD do not require "licensing" with inflammatory stimuli such as interferon (IFN) and tumor necrosis factor-α (TNF-α) (Lange-Consiglio et al., 2020; Papait et al., 2020). Moreover, PnD produce higher levels of cytokines and growth factors as compared to bone marrow-MSC and adipose-MSC, including granulocyte colony-stimulating factor (G-CSF), regulated on activation, normal T cell expressed and secreted (RANTES) and interleukin (IL)-6/-8/-10 (Seok et al., 2020). Therapeutic effects of PnD have already been highlighted in hepatic diseases, optic nerve crush injury (Seok et al., 2020), tendon lesion (Lange-Consiglio et al., 2013) and in many other diseases (Silini et al., 2017). These therapeutic effects include anti-fibrosis, anti-inflammation and anti-apoptosis effects (Lange-Consiglio et al., 2016; Kim et al., 2019). Given this knowledge, exploring the use of PnD as a potential innovative therapy in ovarian diseases is highly encouraged.

MATERIALS AND METHODS

A search was performed on PubMed to identify all papers describing the use of PnD by means of the following combination of terms, within the 2004–2021 time limit: (placenta OR placental OR "perinatal tissue" OR "neonatal tissue" OR decidua OR amnion OR "amniotic fluid" OR "amniotic membrane-derived" OR "human amniotic membrane" OR "umbilical cord" OR "Wharton's jelly" OR "Wharton jelly" OR "Whartons jelly" OR chorion OR "chorionic membrane" OR "fetal membrane" OR "fetal tissue" OR "villous stroma") AND ("stem cells" OR "progenitor cells" OR "stroma cells" OR "stromal cells" OR "mesenchymal cells" OR "amnion epithelial cells" OR "amniotic epithelial cells" OR "amniotic membrane-derived cells" OR "amniotic membrane transplantation" OR "extracellular vesicles" OR exosomes OR microvesicles OR secretome OR "conditioned medium" OR scaffold OR "protein extracts" OR "extract") NOT ("umbilical cord blood" OR "cord blood" OR hematopoietic OR haematopoietic OR review [Publication Type]) AND (animal OR "*in vivo*" OR preclinical OR pre-clinical OR mouse OR mice OR rat OR rodent OR rabbit OR sheep OR ovine OR swine OR pig OR horse OR equine OR cow OR bovine OR dog OR canine OR fish OR primate OR primates OR organoids OR "decellularized matrix" OR "de-cellularized matrix" OR "decellularised matrix" OR "de-cellularised matrix"). Articles in languages other than English, guidelines, reviews, and scientific video protocols were excluded.

Fifty-six manuscripts focusing on reproductive diseases were selected covering ovary ($n = 39$), utero ($n = 9$), testicle ($n = 6$) and mammary ($n = 2$) diseases. Considering the limited number of manuscripts using PnD in different reproductive disorders, in

this review, the attention was focused on the therapies with PnD in the treatment of ovarian diseases.

OVARIAN DISEASES AND PnD THERAPY

Several recent discoveries have shown the potential of cell therapy to restore chemotherapy-induced ovarian failure in mouse or rat animal models. Chemotherapy can induce granulosa cell apoptosis, follicular loss, vascular damage and tissue fibrosis, ultimately leading to ovarian failure (Ling et al., 2019). Over the years, cellular therapy has been suggested to display positive therapeutic effects via different mechanisms. From direct differentiation into oocytes or granulosa cells when aiming at ESC/iPSC therapy, to restoration of ovarian function through the paracrine effect when aiming at MSC therapy (Ling et al., 2019), with the latter obviously being most accessible for clinical application. As described above, considering the limitations using adult and embryonic stem cells, several studies have recently investigated the use of human perinatal cells derived from amniotic fluid, amniotic membrane, umbilical cord and placenta, including chorionic plate and villous chorion. All these PnD share the following characteristics: they are easy to obtain, there is abundant starting material, they display low immunogenicity, they are easy culture, they do not display oncogenicity and there are no ethical restrictions (Liu et al., 2012). Characteristics of currently used perinatal cells derived from different sources and their putative mode of action in the therapeutic treatment of POI or POF are thereafter described and summarized in **Table 1**.

Placenta MSC (PMSC). Transplantation of PMSC can significantly restore ovarian function by altering 1) the expression levels of folliculogenesis-related genes, 2) the number of follicles (Kim et al., 2018) and 3) by promoting ovulation with more oocytes collected after 6 weeks of PMSC transplantation versus control (Li et al., 2018). These pre-clinical observations in animal models are related to the anti-apoptotic (Zhang H et al., 2018) and antioxidant effects of PMSC as well as their homing activity, which positively impacts POI by the secretion of epidermal growth factor (EGF). The EGF secretion will inhibit ROS by upregulating nuclear factor erythroid 2–related factor 2 (NRF2) and heme oxigenase-1 (HO-1) expression, and by inhibiting phosphatase and tensin homolog (PTEN) expression (Ding et al., 2020b). There is also evidence that PMSC transplantation decreases apoptosis of granulosa cells by increasing the inhibin B (INHBB) levels, as it was shown that low levels of INHBB increase apoptosis of granulosa cells (Luo et al., 2020). Furthermore, PMSC transplantation also attenuates granulosa cell apoptosis by inhibiting excessive activation of the ER stress pathway. In this context, it has been shown that caspase-12 is significantly inhibited in the ovaries of POF mice upon PMSC transplantation (Li et al., 2019). Also the phosphatidylinositol 3-kinase/protein-kinase B (PI3K/Akt) signalling pathway plays an important role in folliculogenesis and controls the survival, loss, and activation of primordial follicles in the oocyte (Yin et al., 2018). After PMSC transplantation in POF mice, the PI3K/Akt signalling pathway promotes the recovery of ovarian function by modifying the ratios of Th17/Tc17 and Th17/Treg cells, which are involved in the pathogenesis of inflammatory and autoimmune diseases (Yin et al., 2018). In summary, PMSC could facilitate the development of follicles and oocytes in ovarian disease by multiple mechanisms, including the reduction of cellular stress, the prevention of apoptosis and the modulation of inflammatory responses (Li et al., 2018). Further evidence comes from the interesting observation that PMSC cultured in 3D spheroidal cultures, as compared to 2D cultured PMSC, significantly increase the number of ovarian follicles, the production of E2 and the expression levels of folliculogenesis-related genes in a shorter time frame, when grafted in mice with chemotherapy-induced POF (Kim et al., 2018). Moving towards the application of acellular PnD therapeutic products, administration of human placental extracts (hPE) have been shown to favour weight gain of the ovary, a reduction of the number of atretic follicles, an increase of serum levels of the hormones E2 and progesterone, a reduction of serum levels of FSH and a decrease of apoptosis in granulosa cells. Furthermore, it has also been shown that treatment with hPE downregulates phospho-Rictor (*p*-Rictor), BCL2 associated agonist of cell death (Bad), Bax, peroxisome proliferator activated receptors (PPAR) and upregulates *p*-Akt and phosphor-forkhead boxO3a (*p*-Foxo3a). These effects together can promote protection of granulosa cells from apoptosis, prevent follicular atresia, and relieve symptoms of cycloheximide induced ovarian damage (Zhang BF et al., 2018).

Amniotic membrane cells (AMC). For AMC it is important to distinguish between amniotic epithelial cells (AEC) and amniotic mesenchymal cells (AMSC). Administration of both cell types has demonstrated a positive effect on POF. Interestingly, AMSC displayed a greater therapeutic activity than AEC, especially in the cycloheximide mouse model. This is most likely due to the large amount of collagen secreted by AMSC, which promoted enhanced engraftment and increased proliferation of transplanted AMSC (Ding et al., 2017). The latter is further supported *in vitro*, where AMSC favour a better proliferation rate of granulosa cells (Ding et al., 2017). Notwithstanding, AEC transplantation was also able to inhibit TNF-α-mediated apoptosis in granulosa cells and to reduce inflammation in chemotherapy-induced ovarian damage (Zhang and Liu, 2015).

Amniotic fluid MSC (AF-MSC). Cheng et al. (2012) reported that hAF-MSC cultured in medium containing 5% porcine follicular fluid can differentiate into oocyte-like cells. In addition, these cells were able to restore folliculogenesis that included four stages: primordial germ cells and oogonia formation, follicle formation, follicular growth and follicular maturation. In each of these stages, AF-MSC displayed increased ovarian marker expression: primordial germal cell oogonia (Forkhead Box L2: FOXL2 and cytochrome P450 family 19 subfamily A member: CYP19A1), follicle formation (MutS Homolog 4: MSH4 and stromal antigen 3: STAG3), follicular growth (growth differentiation factor 9: GDF9 and AMH) and follicular maturation (follicle stimulating hormone receptor: FSHR and bone morphogenetic protein 15: BMP15). Moreover, these oocyte-like cells can increase the level of E2 and AMH (Huang et al., 2020). These hormones strongly correlate

TABLE 1 | Different sources of perinatal derivatives and their action in the treatment of POI or POF.

Author	Animal	Source	Secretome	Dose	Via	Outcome
Li et al. (2019)	POF mice by ZP3 peptide	hPMSC		1×10^6 hPMSCs	tail vein	hPMSC suppress GCs apoptosis-induced by ER stress IRE1α signaling pathway contributing to ovarian function recovery
Zhang H et al. (2018)	POF mice by ZP3 protein	hPMSC		1×10^6 hPMSC	tail vein	hPMSC increase the expression of *AMH* and *FSHR*; decrease the level of FSH, LH and AZPAb; increase the level of E2 and AMH; decrease granulosa cell apoptosis; lower number of atretic follicles but more normal follicles
Seok et al. (2020)	Ovariectomized rat model	hPMSC		5×10^5/ml hPMSC	tail vein	hPMSC promote a decreased expression of oxidative stress markers (*H O -1* and *H O -2*) and increase expression of antioxidant markers (*SOD1* and *catalase*); increase of E2 and AMH; increase of expression of genes related to development follicles (*Nobox*, *Lhx8*, *Nano3*); increase of number of follicles
Luo et al. (2020)	POF mice by cyclophosphamide	hPMSC		1×10^6/ml hPMSC	tail vein	hPMSCs induce increase of amounts of INHBB and FSHR and reduce the apoptosis of granulosa cells
Yin et al. (2018)	POF mice by ZP3 protein	hPMSC		1×10^6 hPMSC	tail vein	hPMSC increase E2 and AMH levels, while decrease the levels of FSH, LH and AZPAb; increase of expression of *p-Akt;* decrease apoptosis in granulosa cells; decrease of the ratios of Th17/Tc17 and Th17/Treg cells and decrease of the serum levels of IL-17
Ding et al. (2017)	POF mice by cyclophosphamide	hAEC and hAMSC		no dose reported	tail vein	hAMSC promote granulosa cell proliferation better than hAECs
Zhang and Liu (2015)	POF mice by cyclophosphamide and busulfan	hAEC		2×10^6/ml hAEC	tail vein	hAEC inhibit TNF-α-mediated granulosa cell apoptosis; reduced inflammatory reaction in ovaries; promote follicle development; increase cumulus oocyte complexes number; improved ovarian mass and increased the number of follicles; increase the number of pups born
Huang et al. (2020)	Mice with physiological ovarian aging	hAF-MSC			intra-ovary	hAF-MSC increase follicle numbers and improve hormone levels. They increase mRNA and protein expression levels of ovarian markers at four stages of folliculogenesis and inhibit DNA damage genes expression
Lai et al. (2013)	Sterilized mice	hAF-MSC		$2–5 \times 10^3$ cells	intra-ovary	hAF-MSC restore ovarian morphology. Restored ovaries displayed many follicle-enclosed oocytes at all stages of development. hAFCs survive and differentiate into granulosa cells

(Continued on following page)

TABLE 1 | (*Continued*) Different sources of perinatal derivatives and their action in the treatment of POI or POF.

Author	Animal	Source	Secretome	Dose	Via	Outcome
Liu et al. (2012)	POF mice by cyclophosphamide	hAF-MSC		1×10^3 cell spheres/μl	intra-ovary	hAF-MSC have a normal cell cycle distribution and undergo cell division *in vivo*
Xiao et al. (2014)	POF mice by cyclophosphamide and busulfan	AF-MSC		5×10^5 AFC in 5 μL	in ovary	AF-MSC increase the number of primordial and antral follicles and decrease the number of atretic follicles; increase of the number of estrous cycles and the number of litters
Lu et al. (2020)	POI rats by cisplatin	hUC-MSC		2×10^6 hUMSCs	tail vein	hUC-MSC significantly increase the number of normal follicles and greatly reduce the number of atresia follicles. The number of apoptotic theca interstitial cells significantly decrease and the hormone level of E2 increase
Li et al. (2017)	Naturally aging rat	hUC-MSC		1×10^6/ml (1 ml per animal). Second treatment after 48h	tail vein	hUC-MSC increase E2 and AMH while FSH decrease; ovarian structure improved and follicle number increased; ovarian expression of *HGF*, *VEGF*, and *IGF-1* protein elevate significantly
Wang et al. (2020)	POF rat induced by ovarian antigen	hUC-MSC		0.25×10^6/ml, 1.00×10^6/ml, or 4.00×10^6/mL	tail vein	The estrus cycle of rats returne to normal and follicular development is significantly improved after transplantation of UC-MSC. In addition, serum concentrations of 17-estradiol (E2), progesterone (P4), and anti-Mullerian hormone (AMH) increase significantly with treatment. Transplantation of UC-MSC also reduce the apoptosis of granulosa cells. hUC-MSC promote proliferation of granulosa cells in dose dependent manner; upregulate expression of *Bcl-2*, *AMH*, and *FSHR* and downregulated the expression of *caspase-3*
Zheng et al. (2019)	POF mice by cyclophosphamide	hUC-MSC		5×10^6 hUCC	intravenously	hUC-MSC induce increase of E2, AMH, and GnRH levels; prolong estrous; decrease *caspase-3* expression; prevent loss of secondary follicles; increase *TrkA* expression and decrease *FSHR* expression; improve pregnant rate and embryos numbers
Shen et al. (2020)	POI mice by cyclophosphamide	hUC-MSC		1×10^6 cells/mL	tail vein	hUC-MSC induce increase of ovarian weight; increase of E2 and decrease of FSH; increase of number of follicles; mice resume the normal estrous cycle

(Continued on following page)

TABLE 1 | (*Continued*) Different sources of perinatal derivatives and their action in the treatment of POI or POF.

Author	Animal	Source	Secretome	Dose	Via	Outcome
Zhu et al. (2015)	POF rats by cyclophosphamide	hUC-MSC		1×10^6 cells/ml	tail vein and ovary	hUC-MSC induce increase of the number of secondary and antral follicles; higher level of E2 and lower levels of FSH; fertility is restored, and their offspring develop normally, but the litter size of the tail vein injection group is higher than that of ovary injection group
Yin et al. (2020)	POF mice by cyclophosphamide and busulfan	UC-MSC		1×10^6 UCC	tail vein	UC-MSC increase E2 and AMH level; *HO-1* expressed in UCCs help recover the ovarian function activating the JNK/Bcl-2 signal pathway-regulated autophagy and upregulating the circulating of $CD8^+CD28^-$ T cells
Yang Y et al. (2019)	POF mice by cyclophosphamide	UC-MSC		2×10^5 UCC with or without collagen scaffold	in ovary	Collagen-UC-MSC increase E2 and AMH levels, increase ovarian volume, and number of antral follicles; promote granulosa cell proliferation and ovarian angiogenesis with the increased expression of CD31
Song et al. (2016)	POI rats by cyclophosphamide	hUC-MSC		2×10^6 cells/mL	tail vein	hUC-MSC increase the level of E2 and AMH and decrease the level of FSH; significant increase in secondary follicles; reduction of apoptotic cells
Kim et al. (2018)	Ovariectomized rats	hParietal decidua-MSC and their spheroids		1×10^5 cells	intra-ovary	Parietal decidua-MSC transplantation significantly increase the estradiol level and enhance folliculogenesis-related gene expression levels. Spheroid-cultured PMSCs enhance therapeutic potential via increased engraftment efficiency
Li et al. (2018)	POF mice by cyclophosphamide	hChorionic plate-MSC		2×10^6 cells/kg in 200 μl once week for 4 weeks	tail vein	hChorionic plate-MSC restore the level of E2 and FSH and increase the number of follicles and oocytes
Zhang BF et al. (2018)	POF mice by cyclophosphamide	human placental extracts (HPE)		different doses (0.6-1.2-2.4 ml/kg)	intraperitoneally	HPE induce higher ovarian weight, lower number of atretic follicles, higher serum levels of the hormones E2 and progesterone, and lower apoptosis and serum levels of LH and FSH in granulosa cells
Ding et al. (2020b)	POF mice by cyclophosphamide	hPMSC	CM (no dose reported)	1×10^6 hPMCs	caudal vein	hPMSC promote recovered follicular numbers and increase expression of oocyte markers
Zhang et al. (2017)	POF mice by busulfan	hAEC	hAEC-CM	2×10^4 hAEC and concentrated hAEC-CM (from a total of 2×10^4 cells)	orthotopically/ovary injection	hAEC and hAEC-CM promote healthy and mature follicles in ovaries; increase the expression of *AMH*, *MVH*, *BMP15* and *HAS2*

(Continued on following page)

TABLE 1 | (*Continued*) Different sources of perinatal derivatives and their action in the treatment of POI or POF.

Author	Animal	Source	Secretome	Dose	Via	Outcome
Yao et al. (2016)	POF mice by busulphan	hAEC	hAEC-CM	4×10^6 hAEC or corresponding CM	IP injection	hAEC or hAEC-CM increase follicle number and expression of both *VEGFR1* and *VEGFR2*. They increase detection of CD34 marker and angiogenesis; induce expression of *SRY* gene; increase the number of litters per pregnancy
Ling et al. (2019)	POF mice by cyclophosphamide	hAMSC	hAMSC-CM	4×10^6 AMSCs in 0.6 ml or 100 µl of hAMSC-CM	hAMSCs in tail vein; hAMSC-CM in ovary	hAMSC decrease *Bax* expression and increase *Bcl-2* and endogenous *VEGF* expression in ovarian cells; they inhibit GC apoptosis, and promote angiogenesis and follicular development
Thabet et al. (2020)	POI rats by cyclophosphamide	AF-MSC	EVs da AF-MSC	0.5×10^6 of AFC in 0.5 ml or the amount of EVs secreted by these cells	in ovary	AF-MSC and EVs equally restore total follicular counts, AMH levels, regular estrous cycles, and fruitful conception, while it both diminish *caspase 3* and *PTEN* levels
Xiao et al. (2016)	POF mice by busulfan	AF-MSC	exosomes from AF-MSC	5×10^5 EGFP-AFC or 125 µg of exosomes proteins (an approximate amount produced by 5×10^5 cells overnight)	in ovary	Exosomes have anti-apoptotic effect on granulosa cells; increase the number of primordial follicles; prevent ovarian follicular atresia; reduce the numbers of atretic follicles. miR-10a directly targets *Bim* and results in the down regulation of *Casp9*, which are crucial factors in apoptotic pathway. miR-146a, miR-17, miR-21a and miR-29b also contribute to anti-apoptosis through targeting various genes involved in apoptotic pathway
Yang et al. (2020)	Old mice	hUC-MSC	exosomes from hUC-MSC	10 mg of hUCC-exos	in ovarian bursa	Exosomes activate oocyte PI3K/mTOR signaling pathway and accelerate follicular development evaluated by related genes; increase oocyte production and improve oocyte quality; increase of number of puppies for female
Hong et al. (2020)	POF mice by cisplatino	hUC-MSC	hUC-MSC-CM	30–50 µl hUCC-CM daily from P5 to P9	intraperitoneally	hUC-MSC-CM decrease apoptosis of oocytes and granulosa cells, and increase *G-CSF*, *GM-CSF*, *Cxcl1*, *Ccl2*, *Ccl7*, and *Il23a* expression
Ding et al. (2020b)	POF mice by cyclophosphamide	hUC-MSC	Exosomes	10^{12} prticles/ml	ovaries	hUC-MSC exosomes induce GC proliferation and decrease ROS. miR-17-5P represses *PARP1*, *γH2AX*, and *XRCC6* by inhibiting *SIRT7*

(Continued on following page)

TABLE 1 | (*Continued*) Different sources of perinatal derivatives and their action in the treatment of POI or POF.

Author	Animal	Source	Secretome	Dose	Via	Outcome
Yang Z et al. (2019)	POF mice by busulfan	hUC-MSC	MVs from hUC-MSC	150 μg of hUCC-MVs	caudal vein	MVs induce increase of the body weight and number of ovarian follicles; increase of E2 level and decrease of FSH level; upregulate mRNA expression levels of angiogenesis-related cytokines, including *VEGF*, *IGF-1*, and *angiogenin* cytokines (*VEGF*, *IGF*, and *angiogenin*); increase expression of total *AKT*, *p-AKT*, and *VEGF*.

with the size of the follicular pool (Lai et al., 2013) and repress apoptosis in granulosa cells in animals with ovarian physiological aging (Huang et al., 2020). Although further research is needed, AF-MSC may sustain the number of healthy ovarian follicles in POF mice either by promoting *de novo* folliculogenesis, by inhibiting follicular atresia or a combination of both (Xiao et al., 2014).

Umbilical cord-MSC (UC-MSC). Transplantation of UC-MSC in a POF rat model induced the return to normal oestrus cycle with follicular development, increased serum concentrations of E2, progesterone (P4) and AMH, reduced apoptosis and increased proliferation of granulosa cells. Furthermore, transplantation of UC-MSC up-regulated increased expression of Bcl-2, AMH and FSHR in the ovary of POF rats and downregulated the expression of caspase-3 (Zheng et al., 2019; Wang et al., 2020). Umbilical cord cells can also alleviate POI injury by inhibiting apoptosis of theca-interstitial cells by suppression of the autophagy signalling pathway adenosine monophosphate-activated protein kinase/mechanistic target of rapamycin (AMPK/mTOR) (Lu et al., 2020) and increasing nerve growth factor (NGF) and nerve growth factor receptor (TrkA) levels. The TrkA receptor predominantly activates PI3K and mitogen-activated protein kinase (MAPK) to promote cell survival and proliferation (Zheng et al., 2019). The PI3K/Akt signalling pathway regulates oocyte growth and the survival and development of primordial follicles, promotes the proliferation and differentiation of granulosa cells, and inhibits apoptosis, and these processes are critical for the normal development and physiological functions of the ovaries (Zheng et al., 2019). Furthermore, UC-MSC can reduce the degree of apoptosis and improve the endocrine function of mouse ovaries (Shen et al.,

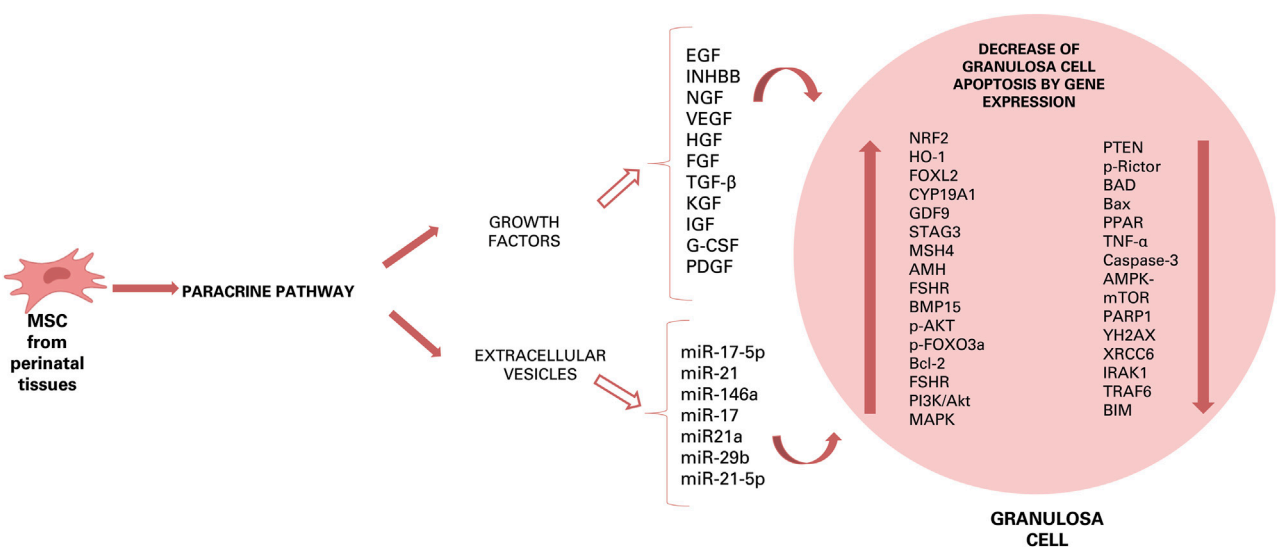

FIGURE 2 | Hypothesis of action of PnD and their effect on ovarian diseases. Growth factors and components of EVs can induce different effects: anti-apoptotic, antioxidant, pro-angiogenetic, restoration of hormonal levels, autophagy and anti-inflammatory by down- or up-regulation of some gene expression or by increase or decrease of some factor. The results of this effects are the increase of cumulus oocyte complexes number, of ovarian mass, of number of follicles, of number of estrous cycles and, then, of number of pups born.

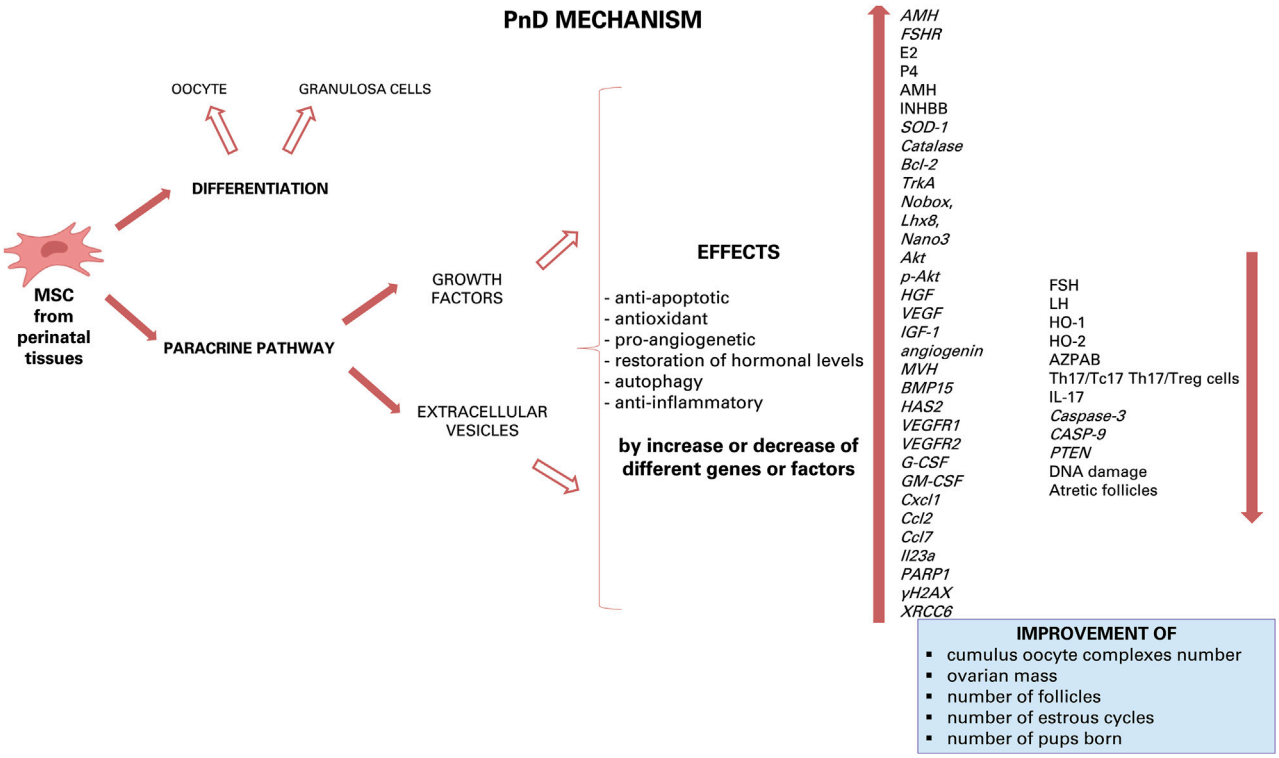

FIGURE 3 | Hypothesis of apoptosis mechanism of PnD. Inside the granulosa cells, some growth factors and some miRNAs can induce down- or up-regulation of some gene expression.

2020) restoring fertility and offspring that develop normally (Zhu et al., 2015). Finally, the mechanism of action of UC-MSC may also be attributable to the action of the HO-1 gene expressed by these cells. The HO-1 has potent anti-inflammatory, antioxidant, and immunoregulatory properties. Moreover, HO-1 also participates in the physiology of the ovary itself, as well as in the secretion of gonadotropins from the pituitary gland. Studies have demonstrated that HO-1 helps recover the ovarian function of POF mice with UC-MSC transplantation *via* activation of the Jun N-terminal kinase (JNK)/Bcl-2 signal pathway. This pathway regulates autophagy and increases the number of circulating $CD8^+CD28^-$T cells. These $CD8^+CD28-$T cells display typical immunosuppressive function and can induce immunological tolerance in transplantation, demonstrating immunologic suppression in organ transplants (Yin et al., 2020). Interestingly for future research, UCC have recently been grafted in ovary of POF induced mice in with the support of a collagen scaffold, hereby demonstrating a greater therapeutic effect compared the UC-MSC grafting without scaffold support (Yang Y et al., 2019).

THE IMPORTANCE OF PnD SECRETOMES IN OVARIAN DISESEAS

Although recent studies have shown that AMSC transplantation in rats with chemotherapy-induced POI restored ovarian function, grafted cells were only detectable in the interstitium of the ovaries and not in the follicles. Indeed, these cells did not express the typical oocyte and granulosa cell markers, which are zona pellucida sperm-binding protein 3 (ZP3) and FSHR, respectively. These results suggest that grafted AMSC do not differentiate into oocytes or granulosa cells but are able to improve ovarian function *via* a paracrine mechanism (Ling et al., 2019). This paracrine effect is most likely related to the secretion of growth factors able to reduce apoptosis of granulosa cells and to recover follicular development with increase of serum levels of AMH and E2 and decreased FSH (Song et al., 2016) (**Figure 2**). Several studies have shown that also the AM is a source of multiple growth factors, including vascular endothelial growth factor (VEGF), hepatocyte growth factor (HGF), fibroblast growth factor 2 (FGF2), transforming growth factor beta (TGF-ß), keratinocyte growth factor (KGF), insulin growth factor (IGF-1) and G-CSF, which were highly likely to play important roles in repairing ovarian injury and restoring ovarian function in animals with POI (Zhang et al., 2017; Li et al., 2018). These growth factors have been shown to inhibit apoptosis and to stimulate proliferation of granulosa cells, to upregulate Bcl-2 expression, to downregulate Bax expression, and to promote local VEGF expression in the ovaries of POI rats with the result of angiogenesis and follicular growth (Ling et al., 2019). Next to the AM, also AF-MSC secrete molecules among which TGF-b (Yoon et al., 2010), vascular endothelial growth factor and glia cell-derived neurotrophic factor (GDNF), which

are required for follicular development and can inhibit follicular cell apoptosis and follicle atresia (Xiao et al., 2014).

Further evidence for the importance of the secretome of grafted cell types comes from the observation that transplantation of UCC improve the ovarian reserve function of perimenopausal rats through secretion of cytokines such as VEGF, HGF and IGF-1, whose expression distinctly increased after umbilical cord-MSC transplantation. VEGF is a powerful survival factor for ovarian granulosa cell apoptosis and ovarian follicular atresia (Li et al., 2017), while HGF, expressed both in thecal cells and granulosa cells of rat ovaries, may play its function as a modulator of the mesenchymal-epithelial cell transition between theca cells and granulosa by facilitating cell proliferation and steroid hormone production. A complete HGF system also supports granulosa cells growing via an anti-apoptotic effect. The IGF-1 is expressed in growing granulosa cells and healthy follicle and is necessary for the proliferation of granulosa cells at the early stage of folliculogenesis (Li et al., 2017).

Concluding, to data there are many substances produced by various PnD that can have a beneficial effect by paracrine action on ovarian disease, with each of them triggering important pathways in cell/tissue protection and/or regeneration. Some effects of these substance can be anti-apoptotic, antioxidant, pro-angiogenetic, restoring of hormonal levels, autophagic and-anti-inflammatory (**Figure 3**). The future goal will be to further dissect each of these modes of action and to derive an optimal therapeutic scheme.

Ovarian Diseases and Conditioned Medium Therapy

In the context that PnD secrete many molecules and act by paracrine mechanism, as discussed above, the application of CM derived from perinatal (stem) cells has gained interest as a novel therapy for POI or POF. Several studies have indeed shown the potential use of CM over cell transplantation. For example, injection of CM secreted by AEC significantly increased the number of secondary and mature follicles, as well as upregulated follicle growth related genes expression (AMH; mouse vasa homologue: MVH; BMP15 and hyaluronan synthase 2: HAS2) (Zhang et al., 2017). Furthermore, daily (for 5 days) intraperitoneal administration of CM derived from UC-MSC daily upregulated G-CSF expression in granulosa cells. This factor plays important roles in ovulation, oocyte maturation, development of preimplantation embryos, trophoblast invasion and attenuates oxidative stress-induced cell apoptosis through the PI3K/Akt pathway (Hong et al., 2020). According to Akdemir et al. (2014), G-CSF can also reduce follicle loss. Lastly, administration of CM derived from AEC improved follicle number and fertility in mice with POI. This beneficial effect was induced by regulating expression of VEGFA and its receptors, thus inducing angiogenesis and increased follicular growth (Yao et al., 2016). Since it has been demonstrated that AEC secrete a variety of growth factors, such as epidermal and fibroblast growth factors (HB-EGF, EGF- 2, bFGF, FGF-4, FGF-6, and FGF-7), angiogenic growth factors (VEGF, VEGF-D, VEGF-R2, and VEGF-R3), insulin like growth factors (IGF-1, IGF-ISR, IGFBP-1, and IGFBP-4) and platelet-derived growth factors (PDGF-AA, PDGF-BB, PDGFRa, and PDGFRb), ovaries damaged by chemotherapy would need not only VEGFA for restoration, but most likely also other growth factors secreted by AEC (Yao et al., 2016).

Ovarian Diseases and Extracellular Vesicle Therapy

With the recognition that conditioned medium, and thus secreted factors, are an important key mechanism of the therapeutic action of cellular therapies, also the paracrine activity of EVs has gained increasing interests (Liu et al., 2012). For example, transplantation of EVs secreted by UCC into the ovary of mice with chemotherapy-induced POI promotes angiogenesis and formation of new blood vessels. This was correlated with increased mRNA expression levels of VEGF, IGF-1 and angiogenin in the ovaries of POI-EV mice as compared to non-treated POI mice (Yang Z et al., 2019).

Among the different types of EVs, exosomes are powerful cell-to-cell communicators with low immunogenicity and no tumorigenicity. These small 40–150 nm EV have a cargo consisting of several molecules including mediators of inflammation, tropic factors, signalling molecules, mRNA, miRNA and long non-coding RNA (lncRNA) (Yang et al., 2020).

Among this large cargo of different types of factors, it has been shown that exosomes released by human umbilical MSC suppress apoptosis of ovarian granulosa cells and regulate the immune response by miRNAs (Sun et al., 2017; Ding et al., 2020b). One miRNA that is highly expressed in exosomes derived from hU-MSC and involved in the therapeutic effect on ovary is miR-17-5P. Injection of this miRNA increases follicle number, ovarian size and foetus number (Ding et al., 2020b). In addition, miR-17-5P restores ovarian function, reduces oxidative stress in granulosa cells by inhibiting the expression of mRNA SIRT7 and its downstream target genes [poly (ADP-ribose) polymerase 1: PARP1; γH2A histone family member X: γH2AX and X-Ray Repair Cross Complementing 6: XRCC6]. These genes are critical mediators of DNA repair: PARP1 is involved in repairing DNA damage, follicular development, and atresia formation (Ding et al., 2020b). In addition, PARP inhibition reduces ROS production; γH2AX is involved in embryonic development, stem cell self-renewal and aging; XRCC6 protects cells from DNA damage and represses BAX induced apoptosis (Ding et al., 2020b).

Another miRNA, which is abundant in AF-MSC, is miRNA-21 and is directly involved in ovarian physiology (Thabet et al., 2020). Treatment with AF-MSC and EVs can be superimposed as in both cases there is an improvement in follicular regeneration thanks to the restoration of AMH levels, an increase in follicles, regular oestrus cycles and conception in rat models with premature ovarian dysfunction. This action occurs by decreasing the expression of PTEN and PI3K/PTEN and caspase 3 proteins (Thabet et al., 2020). Others interesting miRNAs abundantly present in exosome secreted from AF-MSC are miR-146a and miR-10a, which inhibit apoptosis in

damaged granulosa cells and prevent follicle atresia in mice with POF due to chemotherapy (Xiao et al., 2016). It has been shown that miR-146a regulates apoptosis *via* the downregulation of the expression of target genes interleukin-1 receptor-associated kinase 1 (Irak1) and TNF receptor associated factor 6 (Traf6), while miR-10a modulates cell apoptosis through the suppression of pro-apoptotic factor, Bcl-2-like protein 11 (Bim) (Xiao et al., 2016). Other miRNAs, such as miR-17, miR-21a and miR-29b have anti-apoptotic action by downregulating the expression of some genes and thus preventing follicular atresia (Xiao et al., 2016). Additional evidence from *in vitro* studies have shown that the increased recruitment of primordial follicles was related to miR-146a-5p or miR-21-5p that stimulate the oocyte PI3K and mTOR signalling (Yang et al., 2020). Concluding, all these studies evidence the efficacy of MSC-derived exosomes in preclinical animal models of reproductive diseases, and, although more research is needed, may provide effective treatments for reproductive diseases.

CONCLUSION AND LIMITS

Reducing infertility rates in humans and animals requires ongoing research efforts. This review highlights how research is focusing on stem cell therapy, mainly with PnD, which exert protective effects primarily through the paracrine signalling. The results of the papers used for this review suggest that PnD reduce oxidative stress and apoptosis of the granulosa cells in injured ovarian tissue, promoting the recovery of the oestrus cycle and improvement of endocrine function in treated animals. The findings may provide a theoretical basis for infertile patients who may benefit from PnD treatment in the future.

However, to date, the potential of cell therapy to restore ovarian failure has been tested in mouse or rat animal models that do not fully offer realistic disease models as they do not share the heterogeneity of the human population including genetics and physiological variations, as well as the complex interactions of these with the environment. Therefore, many effects remain to be explored before the possible translation of PnD therapies in human medicine. It would be necessary to employ large animal models to answer several key questions, including the optimal route of administration as it is not yet clear which path(s) allows optimal engraftment of injected cells. Usually, in the rat or mouse model, the route of administration is the tail vein that is not overlapping in human species. A hypothetical large animal could be the pig that presents the advantage of having similarities with the human in terms of gastrointestinal anatomy, metabolism and physiology. For this reason, pigs are widely used as models in organ transplantation and other surgical procedures or as preclinical models in drug discovery and numerous naturally occurring and generated genetic models of human disease (Ribitsch et al., 2020). Another large animal could be the cow that is affected by spontaneous ovarian pathology but,unfortunately, it has never been treated with MSC from any source.

Moreover, it must also be determined whether a single dose is sufficient or whether multiple doses need to be administered. However, in case of the latter, it is not clear at the moment whether risks of adverse immune reactions may arise, especially in human. Regarding the PnD, it would be important to know if different time window for the collection and different culture system of the cells of origin can influence the efficacy of these cells. In addition, considering the paracrine mechanism of action of MSCs, the use of CM or EVs, which can reduce some risks due to cell administration of allogeneic cells, must be further explored.

The mode of isolation and storage of the EVs, the dosage, the route and frequency of their administration, and the safety of post-transplantation have yet to be studied. In addition, it would be important to determine the appropriate modality of delivery of their miRNAs and the timing for treatment. According to data by Xiao et al. (Xiao et al., 2016), the protection of granulosa cells against apoptosis is crucial within 72 h after chemotherapy treatment to prevent POF. It may even be beneficial to administer miRNAs prior to chemotherapy treatment to achieve maximum efficacy.

Furthermore, there are still some obstacles to the application of exosomes for the treatment of POI or for other pathologies: it is necessary to identify a less expensive method of production and purification and to better study the immunomodulatory and homing effects (Ling et al., 2019; Ding et al., 2020a).

Moreover, in future therapies, the use of miRNAs alone is envisaged, but miRNAs play complicated roles in maintaining homeostasis, and their systematic administration in high doses could cause serious side effects (Xiao et al., 2016). Indeed, EVs induce angiogenesis and, as it is well known, angiogenesis plays a critical role in tumour growth, and it is uncertain whether high doses of EVs can cause serious adverse effects, such as ovarian cancer. Therefore, more work on the efficiency and safety of the *in vivo* use of EVs must be done before it can be applied in clinical practice (Yao et al., 2016).

AUTHOR CONTRIBUTIONS

AL-C and FC: conceived and designed, financial support. AL-C: critically analyzed the literature, wrote the manuscript. EC and VH: critically analyzed the literature and realized table. IL-O and PP: critically analyzed the literature and realized figures. All authors critically reviewed and approved the final manuscript.

FUNDING

This study was funded by the Department of Veterinary Medicine of Università degli Studi di Milano, Italy.

ACKNOWLEDGMENTS

This publication is based upon work from COST Action 17116 “SPRINT”, supported by COST (European Cooperation in Science and Technology)—www.cost.eu”. This work contributes to the COST Action CA17116 International Network for Translating Research on Perinatal Derivatives into Therapeutic Approaches (SPRINT), supported by COST.

REFERENCES

Agarwal, A., Baskaran, S., Parekh, N., Cho, C.-L., Henkel, R., Vij, S., et al. (2021). Male Infertility. *Lancet* 397, 319–333. doi:10.1016/s0140-6736(20)32667-2

Akdemir, A., Zeybek, B., Akman, L., Ergenoglu, A. M., Yeniel, A. O., Erbas, O., et al. (2014). Granulocyte-colony Stimulating Factor Decreases the Extent of Ovarian Damage Caused by Cisplatin in an Experimental Rat Model. *J. Gynecol. Oncol.* 25, 328–333. doi:10.3802/jgo.2014.25.4.328

Bi, B., Schmitt, R., Israilova, M., Nishio, H., and Cantley, L. G. (2007). Stromal Cells Protect against Acute Tubular Injuryviaan Endocrine Effect. *JASN* 18, 2486–2496. doi:10.1681/ASN.2007020140

Boivin, J., Bunting, L., Collins, J. A., and Nygren, K. G. (2007). International Estimates of Infertility Prevalence and Treatment-Seeking: Potential Need and Demand for Infertility Medical Care. *Hum. Reprod.* 22, 1506–1512. doi:10.1093/humrep/dem046

Bouhali, K., Dipietromaria, A., Fontaine, A., Caburet, S., Barbieri, O., Bellessort, B., et al. (2011). Allelic Reduction of Dlx5 and Dlx6 Results in Early Follicular Depletion: a New Mouse Model of Primary Ovarian Insufficiency. *Hum. Mol. Genet.* 20, 2642–2650. doi:10.1093/hmg/ddr166

Bruno, S., Chiabotto, G., Favaro, E., Deregibus, M. C., and Camussi, G. (2019). Role of Extracellular Vesicles in Stem Cell Biology. *Am. J. Physiol. Cell Physiol.* 317, C303–C313. doi:10.1152/ajpcell.00129.2019

Cheng, X., Chen, S., Yu, X., Zheng, P., and Wang, H. (2012). BMP15 Gene Is Activated during Human Amniotic Fluid Stem Cell Differentiation into Oocyte-like Cells. *DNA Cel Biol.* 31, 1198–1204. doi:10.1089/dna.2011.1396

Chimenti, I., Smith, R. R., Li, T.-S., Gerstenblith, G., Messina, E., Giacomello, A., et al. (2010). Relative Roles of Direct Regeneration versus Paracrine Effects of Human Cardiosphere-Derived Cells Transplanted into Infarcted Mice. *Circ. Res.* 106, 971–980. doi:10.1161/CIRCRESAHA.109.210682

Cremonesi, F., Bonfanti, S., Idda, A., and Lange-Consiglio, A. (2020). Platelet Rich Plasma for Regenerative Medicine Treatment of Bovine Ovarian Hypofunction. *Front. Vet. Sci.* 7, 517. doi:10.3389/fvets.2020.00517

Ding, C., Li, H., Wang, Y., Wang, F., Wu, H., Chen, R., et al. (2017). Different Therapeutic Effects of Cells Derived from Human Amniotic Membrane on Premature Ovarian Aging Depend on Distinct Cellular Biological Characteristics. *Stem Cel Res. Ther.* 8, 173. doi:10.1186/s13287-017-0613-3

Ding, C., Zou, Q., Wang, F., Wu, H., Chen, R., Lv, J., et al. (2018). Human Amniotic Mesenchymal Stem Cells Improve Ovarian Function in Natural Aging through Secreting Hepatocyte Growth Factor and Epidermal Growth Factor. *Stem Cel Res. Ther.* 9 (1), 65. doi:10.1186/s13287-018-0781-9

Ding, C., Zhu, L., Shen, H., Lu, J., Zou, Q., Huang, C., et al. (2020a). Exosomal miRNA-17-5p Derived from Human Umbilical Cord Mesenchymal Stem Cells Improves Ovarian Function in Premature Ovarian Insufficiency by Regulating SIRT7. *Stem Cells* 38 (9), 1137–1148. doi:10.1002/stem.3204

Ding, C., Zou, Q., Wu, Y., Lu, J., Qian, C., Li, H., et al. (2020b). EGF Released from Human Placental Mesenchymal Stem Cells Improves Premature Ovarian Insufficiency via NRF2/HO-1 Activation. *Aging* 12 (3), 2992–3009. doi:10.18632/aging.102794

Duffield, J. S., Park, K. M., Hsiao, L.-L., Kelley, V. R., Scadden, D. T., Ichimura, T., et al. (2005). Restoration of Tubular Epithelial Cells during Repair of the Postischemic Kidney Occurs Independently of Bone Marrow-Derived Stem Cells. *J. Clin. Invest.* 115, 1743–1755. doi:10.1172/JCI22593

Farsimadan, M., Riahi, S. M., Muhammad, H. M., Emamvirdizadeh, A., Tabasi, M., Motamedifar, M., et al. (2021). The Effects of Hepatitis B Virus Infection on Natural and IVF Pregnancy: A Meta-analysis Study. *J. Viral. Hepat.* 28, 1234–1245. doi:10.1111/jvh.13565

Ghavi Hossein-Zadeh, N. (2013). Effects of Main Reproductive and Health Problems on the Performance of Dairy Cows: a Review. *Span J. Agric. Res.* 11, 718–735. doi:10.5424/sjar/2013113-4140

Gurunath, S., Pandian, Z., Anderson, R. A., and Bhattacharya, S. (2011). Defining Infertility-A Systematic Review of Prevalence Studies. *Hum. Reprod. Update* 17, 575–588. doi:10.1093/humupd/dmr015

Hanson, B., Johnstone, E., Dorais, J., Silver, B., Peterson, C. M., and Hotaling, J. (2017). Female Infertility, Infertility-Associated Diagnoses, and Comorbidities: a Review. *J. Assist. Reprod. Genet.* 34, 167–177. doi:10.1007/s10815-016-0836-8

Hong, L., Yan, L., Xin, Z., Hao, J., Liu, W., Wang, S., et al. (2020). Protective Effects of Human Umbilical Cord Mesenchymal Stem Cell-Derived Conditioned Medium on Ovarian Damage. *J. Mol. Cel Biol.* 12 (5), 372–385. doi:10.1093/jmcb/mjz105

Huang, B., Ding, C., Zou, Q., Lu, J., Wang, W., and Li, H. (2020). Human Amniotic Fluid Mesenchymal Stem Cells Improve Ovarian Function during Physiological Aging by Resisting DNA Damage. *Front. Pharmacol.* 11, 272. doi:10.3389/fphar.2020.00272

Ilancheran, S., Moodley, Y., and Manuelpillai, U. (2009). Human Fetal Membranes: a Source of Stem Cells for Tissue Regeneration and Repair? *Placenta* 30 (1), 2–10. doi:10.1016/j.placenta.2008.09.009

Kim, T.-H., Choi, J. H., Jun, Y., Lim, S. M., Park, S., Paek, J.-Y., et al. (2018). 3D-cultured Human Placenta-Derived Mesenchymal Stem Cell Spheroids Enhance Ovary Function by Inducing Folliculogenesis. *Sci. Rep.* 8, 15313. doi:10.1038/s41598-018-33575-9

Kim, J., Jun, J., Park, S., Yang, S., Bae, S., and Kim, G. (2019). Dynamic Regulation of miRNA Expression by Functionally Enhanced Placental Mesenchymal Stem Cells Promotes Hepatic Regeneration in a Rat Model with Bile Duct Ligation. *Int. J. Mol. Sci.* 20, 5299. doi:10.3390/ijms20215299

Lai, D., Wang, F., Chen, Y., Wang, L., Wang, Y., and Cheng, W. (2013). Human Amniotic Fluid Stem Cells Have a Potential to Recover Ovarian Function in Mice with Chemotherapy-Induced Sterility. *BMC Develop. Biol.* 13, 34. doi:10.1186/1471-213X-13-34

Lange-Consiglio, A., Corradetti, B., Bizzaro, D., Magatti, M., Ressel, L., Tassan, S., et al. (2012). Characterization and Potential Applications of Progenitor-like Cells Isolated from Horse Amniotic Membrane. *J. Tissue Eng. Regen. Med.* 6, 622–635. doi:10.1002/term.465

Lange-Consiglio, A., Tassan, S., Corradetti, B., Meucci, A., Perego, R., Bizzaro, D., et al. (2013). Investigating the Efficacy of Amnion-Derived Compared with Bone Marrow-Derived Mesenchymal Stromal Cells in Equine Tendon and Ligament Injuries. *Cytotherapy* 15, 1011–1020. doi:10.1016/j.jcyt.2013.03.002

Lange-Consiglio, A., Perrini, C., Tasquier, R., Deregibus, M. C., Camussi, G., Pascucci, L., et al. (2016). Equine Amniotic Microvesicles and Their Anti-inflammatory Potential in a Tenocyte Model *In Vitro*. *Stem Cell Develop.* 25, 610–621. doi:10.1089/scd.2015.0348

Lange-Consiglio, A., Romele, P., Magatti, M., Silini, A., Idda, A., Martino, N. A., et al. (2020). Priming with Inflammatory Cytokines Is Not a Prerequisite to Increase Immune-Suppressive Effects and Responsiveness of Equine Amniotic Mesenchymal Stromal Cells. *Stem Cel Res. Ther.* 11 (1), 99. doi:10.1186/s13287-020-01611-z

Li, J., Mao, Q., He, J., She, H., Zhang, Z., and Yin, C. (2017). Human Umbilical Cord Mesenchymal Stem Cells Improve the reserve Function of Perimenopausal Ovary via a Paracrine Mechanism. *Stem Cel Res. Ther.* 8, 55. doi:10.1186/s13287-017-0514-5

Li, J., Yu, Q., Huang, H., Deng, W., Cao, X., Adu-Frimpong, M., et al. (2018). Human Chorionic Plate-Derived Mesenchymal Stem Cells Transplantation Restores Ovarian Function in a Chemotherapy-Induced Mouse Model of Premature Ovarian Failure. *Stem Cel Res. Ther.* 9, 81. doi:10.1186/s13287-018-0819-z

Li, H., Zhao, W., Wang, L., Luo, Q., Yin, N., Lu, X., et al. (2019). Human Placenta-derived Mesenchymal Stem Cells Inhibit Apoptosis of Granulosa Cells Induced by IRE1α Pathway in Autoimmune POF Mice. *Cell Biol. Int.* 43 (8), 899–909. doi:10.1002/cbin.11165

Liao, W., Tang, X., Li, X., and Li, T. (2019). Therapeutic Effect of Human Umbilical Cord Mesenchymal Stem Cells on Tubal Factor Infertility Using a Chronic Salpingitis Murine Model. *Arch. Gynecol. Obstet.* 300, 421–429. doi:10.1007/s00404-019-05209-6

Lin, K. Y., Peng, S. Y., Chou, C. J., Wu, C. C., and Wu, S. C. (2015). Engraftment of Mouse Amniotic Fluid-Derived Progenitor Cells after In Utero Transplantation in Mice. *J. Formos. Med. Assoc.* 114, 1105–1115. doi:10.1016/j.jfma.2014.04.005

Ling, L., Feng, X., Wei, T., Wang, Y., Wang, Y., Wang, Z., et al. (2019). Human Amnion-Derived Mesenchymal Stem Cell (hAD-MSC) Transplantation Improves Ovarian Function in Rats with Premature Ovarian Insufficiency (POI) at Least Partly through a Paracrine Mechanism. *Stem Cel Res. Ther.* 10, 46. doi:10.1186/s13287-019-1136-x

Liu, T., Huang, Y., Guo, L., Cheng, W., and Zou, G. (2012). CD44+/CD105+ Human Amniotic Fluid Mesenchymal Stem Cells Survive and Proliferate in the Ovary Long-Term in a Mouse Model of Chemotherapy-Induced Premature Ovarian Failure. *Int. J. Med. Sci.* 9 (7), 592–602. doi:10.7150/ijms.4841

López-Gatius, F., Santolaria, P., Yániz, J., Rutlant, J., and López-Béjar, M. (2001). Persistent Ovarian Follicles in Dairy Cows: a Therapeutic Approach. *Theriogenology* 56, 649–659. doi:10.1016/s0093-691x(01)00596-9

Lopez-Gatius, F., Murugavel, K., Santolaria, P., Lopez-Bejar, M., and Yaniz, J. L. (2004). Pregnancy Rate after Timed Artificial Insemination in Early post-partum Dairy Cows after Ovsynch or Specific Synchronization Protocols. *J. Vet. Med. Ser. A* 51, 33–38. doi:10.1111/j.1439-0442.2004.00594.x

López-Gatius, F., García-Ispierto, I., Santolaria, P., Yániz, J., Nogareda, C., and López-Béjar, M. (2006). Screening for High Fertility in High-Producing Dairy Cows. *Theriogenology* 65, 1678–1689. doi:10.1016/j.theriogenology.2005.09.027

Lu, X., Bao, H., Cui, L., Zhu, W., Zhang, L., Xu, Z., et al. (2020). hUMSC Transplantation Restores Ovarian Function in POI Rats by Inhibiting Autophagy of Theca-Interstitial Cells via the AMPK/mTOR Signaling Pathway. *Stem Cel Res. Ther.* 11, 268. doi:10.1186/s13287-020-01784-7

Luo, Q., Liu, R., Wang, L., Hou, Y., and Zhang, H. (2020). The Effects of Inhibin B in the Chemotherapy Drug-Induced Premature Ovarian Insufficiency Mice and hPMSCs Treatment. *Reprod. Sci.* 27, 1148–1155. doi:10.1007/s43032-019-00128-y

Mekibib, B., Desta, T., and Tesfaye, D. (2013). Gross Pathological Changes in the Reproductive Tracts of Cows Slaughtered at Two Abattoirs in Southern Ethiopia. *J. Vet. Med. Anim. Health* 5, 46–50. doi:10.5897/JVMAH

Papait, A., Vertua, E., Magatti, M., Ceccariglia, S., De Munari, S., Silini, A. R., et al. (2020). Mesenchymal Stromal Cells from Fetal and Maternal Placenta Possess Key Similarities and Differences: Potential Implications for Their Applications in Regenerative Medicine. *Cells* 9 (1), 127. doi:10.3390/cells9010127

Ribitsch, I., Baptista, P. M., Lange-Consiglio, A., Melotti, L., Patruno, M., Jenner, F., et al. (2020). Large Animal Models in Regenerative Medicine and Tissue Engineering: To Do or Not to Do. *Front. Bioeng. Biotechnol.* 8, 972. doi:10.3389/fbioe.2020.00972

Sabapathy, V., Sundaram, B., Vm, S., Mankuzhy, P., and Kumar, S. (2014). Human Wharton's Jelly Mesenchymal Stem Cells Plasticity Augments Scar-free Skin Wound Healing with Hair Growth. *PLoS One* 9 (4), e93726. doi:10.1371/journal.pone.0093726

Seok, J., Park, H., Choi, J. H., Lim, J.-Y., Kim, K. G., and Kim, G. J. (2020). Placenta-derived Mesenchymal Stem Cells Restore the Ovary Function in an Ovariectomized Rat Model via an Antioxidant Effect. *Antioxidants* 9, 591. doi:10.3390/antiox9070591

Shen, J., Cao, D., and Sun, J.-L. (2020). Ability of Human Umbilical Cord Mesenchymal Stem Cells to Repair Chemotherapy-Induced Premature Ovarian Failure. *World J. Stem Cell* 12 (4), 277–287. doi:10.4252/wjsc.v12.i4.277

Silini, A. R., Magatti, M., Cargnoni, A., and Parolini, O. (2017). Is Immune Modulation the Mechanism Underlying the Beneficial Effects of Amniotic Cells and Their Derivatives in Regenerative Medicine? *Cel Transpl.* 26, 531–539. doi:10.3727/096368916x693699

Silini, A. R., Di Pietro, R., Lang-Olip, I., Alviano, F., Banerjee, A., Basile, M., et al. (2020). Perinatal Derivatives: Where Do We Stand? A Roadmap of the Human Placenta and Consensus for Tissue and Cell Nomenclature. *Front. Bioeng. Biotechnol.* 8, 610544. doi:10.3389/fbioe.2020.610544

Song, D., Zhong, Y., Qian, C., Zou, Q., Ou, J., Shi, Y., et al. (2016). Human Umbilical Cord Mesenchymal Stem Cells Therapy in Cyclophosphamide-Induced Premature Ovarian Failure Rat Model. *Biomed. Res. Int.* 2016, 1–13. doi:10.1155/2016/2517514

Sun, L., Li, D., Song, K., Wei, J., Yao, S., Li, Z., et al. (2017). Exosomes Derived from Human Umbilical Cord Mesenchymal Stem Cells Protect against Cisplatin-Induced Ovarian Granulosa Cell Stress and Apoptosis *In Vitro*. *Sci. Rep.* 7, 2552. doi:10.1038/s41598-017-02786-x

Thabet, E., Yusuf, A., Abdelmonsif, D. A., Nabil, I., Mourad, G., and Mehanna, R. A. (2020). Extracellular Vesicles miRNA-21: a Potential Therapeutic Tool in Premature Ovarian Dysfunction. *Mol. Hum. Reprod.* 26 (12), 906–919. doi:10.1093/molehr/gaaa068

Tögel, F., Hu, Z., Weiss, K., Isaac, J., Lange, C., and Westenfelder, C. (2005). Administered Mesenchymal Stem Cells Protect against Ischemic Acute Renal Failure through Differentiation-independent Mechanisms. *Am. J. Physiol. Renal Physiol.* 289, F31–F42. doi:10.1152/ajprenal.00007.2005

Wang, Z., Wei, Q., Wang, H., Han, L., Dai, H., Qian, X., et al. (2020). Mesenchymal Stem Cell Therapy Using Human Umbilical Cord in a Rat Model of Autoimmune-Induced Premature Ovarian Failure. *Stem Cell Int.* 2020, 1–13. doi:10.1155/2020/3249495

Xiao, G.-Y., Liu, I.-H., Cheng, C.-C., Chang, C.-C., Lee, Y.-H., Cheng, W. T.-K., et al. (2014). Amniotic Fluid Stem Cells Prevent Follicle Atresia and rescue Fertility of Mice with Premature Ovarian Failure Induced by Chemotherapy. *PLoS One* 9, e106538. doi:10.1371/journal.pone.0106538

Xiao, G.-Y., Cheng, C.-C., Chiang, Y.-S., Cheng, W. T.-K., Liu, I.-H., and Wu, S.-C. (2016). Exosomal miR-10a Derived from Amniotic Fluid Stem Cells Preserves Ovarian Follicles after Chemotherapy. *Sci. Rep.* 6, 23120. doi:10.1038/srep23120

Yang, W., Zhang, J., Xu, B., He, Y., Liu, W., Li, J., et al. (2020). HucMSC-derived Exosomes Mitigate the Age-Related Retardation of Fertility in Female Mice. *Mol. Ther.* 28, 1200–1213. doi:10.1016/j.ymthe.2020.02.003

Yang Y, Y., Lei, L., Wang, S., Sheng, X., Yan, G., Xu, L., et al. (2019). Transplantation of Umbilical Cord-Derived Mesenchymal Stem Cells on a Collagen Scaffold Improves Ovarian Function in a Premature Ovarian Failure Model of Mice. *Vitro Cell Dev. Biol. Anim.* 55, 302–311. doi:10.1007/s11626-019-00337-4

Yang Z, Z., Du, X., Wang, C., Zhang, J., Liu, C., Li, Y., et al. (2019). Therapeutic Effects of Human Umbilical Cord Mesenchymal Stem Cell-Derived Microvesicles on Premature Ovarian Insufficiency in Mice. *Stem Cel Res. Ther.* 10, 250. doi:10.1186/s13287-019-1327-5

Yaniz, J., Murugavel, K., and Lopez-Gatius, F. (2004). Recent Developments in Oestrous Synchronization of Postpartum Dairy Cows with and without Ovarian Disorders. *Reprod. Domest. Anim.* 39, 86–93. doi:10.1111/j.1439-0531.2004.00483.x

Yániz, J., López-Gatius, F., Bech-Sàbat, G., García-Ispierto, I., Serrano, B., and Santolaria, P. (2008). Relationships between Milk Production, Ovarian Function and Fertility in High-Producing Dairy Herds in north-eastern spain. *Reprod. Domest. Anim.* 43 (Suppl. 4), 38–43. doi:10.1111/j.1439-0531.2008.01227.x

Yao, X., Guo, Y., Wang, Q., Xu, M., Zhang, Q., Li, T., et al. (2016). The Paracrine Effect of Transplanted Human Amniotic Epithelial Cells on Ovarian Function Improvement in a Mouse Model of Chemotherapy-Induced Primary Ovarian Insufficiency. *Stem Cell Int.* 2016, 1–14. doi:10.1155/2016/4148923

Yin, N., Wang, Y., Lu, X., Liu, R., Zhang, L., Zhao, W., et al. (2018). hPMSC Transplantation Restoring Ovarian Function in Premature Ovarian Failure Mice Is Associated with Change of Th17/Tc17 and Th17/Treg Cell Ratios through the PI3K/Akt Signal Pathway. *Stem Cel Res. Ther.* 9, 37. doi:10.1186/s13287-018-0772-x

Yin, N., Wu, C., Qiu, J., Zhang, Y., Bo, L., Xu, Y., et al. (2020). Protective Properties of Heme Oxygenase-1 Expressed in Umbilical Cord Mesenchymal Stem Cells Help Restore the Ovarian Function of Premature Ovarian Failure Mice through Activating the JNK/Bcl-2 Signal Pathway-Regulated Autophagy and Upregulating the Circulating of CD8+CD28− T Cells. *Stem Cel Res. Ther.* 11, 49. doi:10.1186/s13287-019-1537-x

Yoon, B. S., Moon, J.-H., Jun, E. K., Kim, J., Maeng, I., Kim, J. S., et al. (2010). Secretory Profiles and Wound Healing Effects of Human Amniotic Fluid-Derived Mesenchymal Stem Cells. *Stem Cell Develop.* 19, 887–902. doi:10.1089/scd.2009.0138

Zhang, H., and Liu, K. (2015). Cellular and Molecular Regulation of the Activation of Mammalian Primordial Follicles: Somatic Cells Initiate Follicle Activation in Adulthood. *Hum. Reprod. Update* 21, 779–786. doi:10.1093/humupd/dmv037

Zhang BF, B. F., Hu, Y., Liu, X., Cheng, Z., Lei, Y., Liu, Y., et al. (2018). The Role of AKT and FOXO3 in Preventing Ovarian Toxicity Induced by Cyclophosphamide. *Plos One* 13, e0201136. doi:10.1371/journal.pone.0201136

Zhang, Q., Bu, S., Sun, J., Xu, M., Yao, X., He, K., et al. (2017). Paracrine Effects of Human Amniotic Epithelial Cells Protect against Chemotherapy-Induced Ovarian Damage. *Stem Cel Res. Ther.* 8, 270. doi:10.1186/s13287-017-0721-0

Zhang H, H., Luo, Q., Lu, X., Yin, N., Zhou, D., Zhang, L., et al. (2018). Effects of hPMSCs on Granulosa Cell Apoptosis and AMH Expression and Their Role in

the Restoration of Ovary Function in Premature Ovarian Failure Mice. *Stem Cel Res. Ther.* 9, 20. doi:10.1186/s13287-017-0745-5

Zheng, Q., Fu, X., Jiang, J., Zhang, N., Zou, L., Wang, W., et al. (2019). Umbilical Cord Mesenchymal Stem Cell Transplantation Prevents Chemotherapy-Induced Ovarian Failure via the NGF/TrkA Pathway in Rats. *Biomed. Res. Int.* 2019, 1–9. doi:10.1155/2019/6539294

Zhu, S.-F., Hu, H.-B., Xu, H.-Y., Fu, X.-F., Peng, D.-X., Su, W.-Y., et al. (2015). Human Umbilical Cord Mesenchymal Stem Cell Transplantation Restores Damaged Ovaries. *J. Cel. Mol. Med.* 19, 2108–2117. doi:10.1111/jcmm.12571

Conflict of Interest: The authors declare that the research was conducted in the absence of any commercial or financial relationships that could be construed as a potential conflict of interest.

Publisher's Note: All claims expressed in this article are solely those of the authors and do not necessarily represent those of their affiliated organizations, or those of the publisher, the editors and the reviewers. Any product that may be evaluated in this article, or claim that may be made by its manufacturer, is not guaranteed or endorsed by the publisher.

GLOSSARY

AEC amniotic epithelial cells

AF amniotic fluid

AF-MSC amniotic fluid mesenchymal stromal cells

AM amniotic membrane

AM-MSC amniotic membrane-MSC

AMH anti-Mullerian hormone

AMPK/mTOR adenosine monophosphate-activated protein kinase/ mechanistic target of rapamycin

AMSC amniotic mesenchymal cells

AT adipose tissue

Bad BCL2 associated agonist of cell death

Bax bcl-2-like protein 4

Bim Bcl-2-like protein 11

BM bone marrow

BMP15 bone morphogenetic protein 15

CM conditioned media

CYP19A1 cytochrome P450 family 19 subfamily A memberE2: 17β-estradiol

EGF epidermal growth factor

ER endoplasmic reticulum

ESC embryonic stem cells

EV extracellular vesicles

FGF2 fibroblast growth factor 2

FOXL2 Forkhead Box L2

FSH follicle-stimulating hormone

FSHR follicle stimulating hormone receptor

G-CSF granulocyte colony-stimulating factor

GDF9 growth differentiation factor 9

GDNF glia cell-derived neurotrophic factor

GnRH gonadotropins releasing hormone

HAS2 hyaluronan synthase 2

CP human chorionic plate

hCV human villous chorion

HGF hepatocyte growth factor

HO-1 heme oxigenase-1

hPE human placental extracts

IFN interferon

IGF-1 insulin growth factor

IL interlukin

INHBB inhibin B

iPS induced pluripotent stem cells

Irak1 interleukin-1 receptor-associated kinase 1

JNK Jun N-terminal kinase

KGF keratinocyte growth factor

LH luteinizing hormone

MAPK mitogen-activated protein kinase

miRNAs microRNAs

mRNAs messenger RNAs

MSC mesenchymal stromal cells

MSH4 MutS Homolog 4

MVH mouse vasa homologue

NGF nerve growth factor

NRF2 nuclear factor erythroid 2–related factor 2

OCT4 octamer-binding transcription factor 4 physiological ovarian aging

PARP1 poly [ADP-ribose] polymerase 1

PDGF platelet-derived growth factors

p-Foxo3a p-Akt and phosphor-forkhead boxO3a

PI3K/Akt phosphatidylinositol 3-kinase/protein-kinasi B

PMSC Placenta MSC

PnD perinatal derivatives

POF premature ovarian failure

POI premature ovarian insufficiency

PPAR peroxisome proliferator activated receptors

p-Rictor phospho-Rictor

PRID progesterone releasing intravaginal device

PTEN phosphatase and tensin homolog

RANTES regulated on activation, T cell expressed and secreted

ROS reactive oxygen species

SIP sphingosine-1-phosphate

STAG3 stromal antigen 3

TGF-ß transforming growth factor-ß

TNF-α tumor necrosis facor-α

Traf6 TNF receptor associated factor 6

TrkA nerve growth factor receptor

UC umbilical cord

UC-MSC umbilical cord-MSC

VEGF vascular endothelial growth factor

XRCC6 X-Ray Repair Cross Complementing 6

ZP3 zona pellucida sperm-binding protein 3

γH2AX γH2A histone family member X

frontiers in Bioengineering and Biotechnology

ORIGINAL RESEARCH
published: 11 March 2022
doi: 10.3389/fbioe.2022.828424

Decellularization of Wharton's Jelly Increases Its Bioactivity and Antibacterial Properties

*M. Dubus[1,2], L. Scomazzon[1], J. Chevrier[1], A. Montanede[1], A. Baldit[3], C. Terryn[4], F. Quilès[5], C. Thomachot-Schneider[6], S. C. Gangloff[1,7], N. Bouland[8], F. Gindraux[9], H. Rammal[1,2], C. Mauprivez[1,2,10] and H. Kerdjoudj[1,2]**

[1]Biomatériaux et Inflammation en Site Osseux (BIOS) EA 4691, Université de Reims Champagne Ardenne, Reims, France, [2]UFR d'Odontologie, Université de Reims Champagne Ardenne, Reims, France, [3]Laboratoire d'étude des Microstructures et de Mécanique des Matériaux (LEM3), UMR CNRS 7239, Université de Lorraine, Metz, France, [4]Plateau Technique PICT, Université de Reims Champagne Ardenne, Reims, France, [5]CNRS, LCPME, Université de Lorraine, Nancy, France, [6]Groupe d'Étude des Géomatériaux et Environnement Naturels, Anthropiques et Archéologiques (GEGENAA), Université de Reims Champagne Ardenne, Reims, France, [7]UFR de Pharmacie, Université de Reims Champagne Ardenne, Reims, France, [8]Service d'anatomopathologie, UFR de Médecine, Université de Reims Champagne Ardenne, Reims, France, [9]Laboratoire de Nanomédecine, Imagerie, Thérapeutique, Université Bourgogne Franche-Comté, Besançon, France, [10]Centre Hospitalier Universitaire de Reims, Pôle Médecine Bucco-dentaire, Hôpital Maison Blanche, Reims, France

OPEN ACCESS

Edited by:
Peter Ponsaerts, University of Antwerp, Belgium

Reviewed by:
Omar Aljitawi, University of Rochester, United States
Sina Naserian, Hôpital Paul Brousse, France

***Correspondence:**
H. Kerdjoudj
halima.kerdjoudj@univ-reims.fr

Specialty section:
This article was submitted to Tissue Engineering and Regenerative Medicine, a section of the journal Frontiers in Bioengineering and Biotechnology

Received: *03 December 2021*
Accepted: *08 February 2022*
Published: *11 March 2022*

Citation:
Dubus M, Scomazzon L, Chevrier J, Montanede A, Baldit A, Terryn C, Quilès F, Thomachot-Schneider C, Gangloff SC, Bouland N, Gindraux F, Rammal H, Mauprivez C and Kerdjoudj H (2022) Decellularization of Wharton's Jelly Increases Its Bioactivity and Antibacterial Properties. Front. Bioeng. Biotechnol. 10:828424. doi: 10.3389/fbioe.2022.828424

The field of regenerative medicine has recently seen an emerging trend toward decellularized extracellular matrix (ECM) as a biological scaffold for stem cell-delivery. Human umbilical cord represents a valuable opportunity from both technical and ethical point of view to obtain allogenic ECM. Herein, we established a protocol, allowing the full removal of cell membranes and nuclei moieties from Wharton's jelly (WJ) tissue. No alterations in the ECM components (*i.e.,* collagen, GAG content, and growth factors), physical (*i.e.,* porosity and swelling) and mechanical (*i.e.,* linear tensile modulus) properties were noticed following WJ processing. Furthermore, no effect of the tissue processing on macromolecules and growth factors retention was observed, assuring thus a suitable bioactive matrix for cell maintenance upon recellularization. Based on the *in vitro* and *in vivo* biodegradability and stromal cell homing capabilities, decellularized WJ could provide an ideal substrate for stromal cells adhesion and colonization. Interestingly, the tissue processing increased the antibacterial and antiadhesive properties of WJ against *Staphylococcus aureus* and *Staphylococcus epidermidis* pathogens. Altogether, our results indicate that decellularized WJ matrix is able to limit Staphylococcus-related infections and to promote stromal cell homing, thus offering a versatile scaffold for tissue regenerative medicine.

Keywords: Wharton's jelly, decellularization, biocompatibility, bioactivity, antibacterial, *in vivo*

1 INTRODUCTION

With a length and a diameter of about 40 and 1.5 cm, the umbilical cord connects the placenta to the developing fetus, ensuring thereby its nourishment, and oxygenation. The umbilical cord stroma contains a unique stem cell-rich gelatinous substance called Wharton's jelly (WJ). Ensuring the umbilical cord flexibility, the major role of WJ is the resistance to torsional, and compressive stresses imposed upon the umbilical vessels during fetal development (Pennati, 2001). Besides its protective role, the WJ is a rich reservoir of mesenchymal stromal cells and growth factors, and contains significant amounts of extracellular matrix (ECM) components such as collagen, hyaluronic acid, and

several glycosaminoglycans (Nanaev et al., 1997; Franc et al., 1998; Sobolewski et al., 2005). With its immunologically-privileged status, the WJ lends credence to its use as an allograft for difficult-to-heal wounds. To this end, fresh or cryopreserved WJ patches have been used in clinical practice with proven reparative effects following skin graft procedure and treatment of foot ulcers and diabetic ulcers with osteomyelitis. (Caputo et al., 2016; Raphael, 2016; Marston et al., 2019; Tettelbach et al., 2019). Such an attractive combination of biomechanical, immunological and biochemical features makes WJ a versatile candidate material for the regenerative medicine field.

Regenerative medicine provides tools such as multifunctional scaffolds in the aim of avoiding bacterial infection repairing injuries. (Renth and Detamore, 2012). The effectiveness of scaffold -based therapy comes from the ability of the scaffold to recapitulate healthy tissue cues that drive tissue repair and regeneration. Several studies aim at developing innovative bio-inspired scaffolds in order to counteract ECM loss following degeneration and to support functional recovery by endogenous damaged microenvironment. In such scenario, the potential therapeutic scaffold would be the native ECM; an acellular component of tissue that provides the structural support and biochemical cues for determining a cell's fate. (Hinderer et al., 2016; Yu et al., 2016; Gilpin and Yang, 2017; Damodaran and Vermette, 2018; Spang and Christman, 2018). Furthermore, the bloodless scaffold could become the object of bacterial adhesion, and a large number of bacterial adhesions will form a biofilm resistant matrix, making it difficult to cure, and causing a relapse in infection. To process the ECM as a tool in regenerative therapy, the excised tissue must first undergo physical, chemical and/or enzymatic treatments to remove cellular components, and nuclear moieties. Therefore, the resulting decellularized ECM is thought to be an ideal and safe system to deliver chemokines and growth factors, and to provide adequate structural, and biomechanical microarchitecture in the damaged microenvironment. (Crapo et al., 2011; Keane et al., 2015). However, the consequences of ineffective or incomplete decellularization could result in host's foreign body reaction, which would lead to the formation of fibrous capsule. (Keane et al., 2012; Hussein et al., 2016).

Successful commercialization of any tissue product relies on the effective preservation of key biological components essential to maintain the intended therapeutic action of the tissue. The main disadvantage of WJ as a tissue source is its transientness as it is only available in the active form during a short time period immediately postpartum. An effective solution to this problem may be provided by its careful decellularization. Few studies showed that decellularized WJ provides a biocompatible framework with suitable features for cartilage, (Penolazzi et al., 2020), liver, (Kehtari et al., 2019), neural tissue (Kočí et al., 2017), and wound (Beiki et al., 2017) repair and regeneration. Despite significant reduction in DNA content following the decellularization, the reported values, of about several micrograms per milligram of dry tissue, are not in full agreement with Crapo *et al.*, suggesting values of about 50 ng/mg of dry tissue as safety threshold to avoid host's adverse reaction. (Crapo et al., 2011). To achieve such requirement, substantial disruption of the WJ matrix (*i.e.,* powdered and hydrogel based matrix) were reported. (Jadalannagari et al., 2017; Basiri et al., 2019; Lin et al., 2020). In other studies, WJ derived products were reported in combination with diverse polymers and ceramics, enhancing the biological activities of the scaffold. (Martínez et al., 2017; Basiri et al., 2019). In the present study, a novel protocol was developed to remove all cellular components from WJ and to generate implantable and less host reactive WJ-based patches. For better storage, the resulting patches were freeze-dried and the effects of the tissue processing on the structural, biochemical and biomechanical properties were further investigated. The biological performance of WJ-based patches was assessed *in vitro* and *in vivo*. As mentioned above, WJ was successfully used to treat foot ulcers and diabetic ulcers with osteomyelitis, and its regenerative capabilities were mainly attributed to the presence of stromal cells, growth factors and hyaluronic acid. (Marston et al., 2019). The intrinsic antimicrobial properties of WJ is still an unexplored field. Herein and to our knowledge, we report for the first time, the antibacterial properties of decellularized WJ-based patches, opening the route for the development of new and affordable WJ-bioactive antibacterial matrix for regenerative medicine.

2 MATERIAL AND METHODS

2.1 Wharton's Jelly Preparation

2.1.1 Wharton's Jelly Collection

Human umbilical cord harvesting was approved ethically and methodologically by our local Research Institution and was conducted with informed patients (written consent) in accordance with the usual ethical legal regulations (Article R 1243-57). All procedures were done in accordance with our authorization and registration number DC-2014-2262 given by the National "Cellule de Bioéthique". Fresh human umbilical cords, obtained after full-term births, were washed several times with Phosphate Buffered Saline (PBS, Gibco, and France) to remove blood components, dissected, and vascular structures removed. Wharton's jelly matrix (WJ) was then peeled off the amniotic surrounding membrane, and preserved at -20°C.

2.1.2 Wharton's Jelly Decellularization

After two cycles of freezing/defrosting (−20°C/20°C), samples were subjected to a decellularization protocol comprising hypotonic treatment with 1% Triton X-100 in distilled water (VWR, France) for 1 h then enzymatic treatment with 0.2 mg/ml of DNase (Sigma, France) at 37°C for 24 h under stirring. All processing residuals were removed by rinsing twice with PBS for 10 min under stirring. Finally, decellularized Wharton's jelly (d-WJ) samples were frozen at −20°C then −80°C before freeze-drying process. Freeze-dried devitalized WJ (WJ) was used as control.

2.2 Effectiveness of Decellularization Processing

2.2.1 DAPI Staining

The efficiency of the decellularization protocol was verified by nuclei staining with 4,6-diamidino-2-phenylindole (DAPI, 100 ng/ml, 1: 3,000 dilution) for 5 min and fluorescence microscopy imaging (Axiovert 200 M microscope, Zeiss, Oberkochen, Germany, Objective ×10).

2.2.2 DNA Quantification

DNA was extracted from samples using MasterPure™ DNA Purification Kit (Epicentre® Biotechnologies) in accordance with the manufacturer protocol. Freeze-dried samples were weighed prior to DNA extraction. Extracted DNA was then assessed by measuring the absorbance at 260 and 280 nm (Nanodrop®, Thermo Scientific) with 260/280 nm absorbance ratio for all measured samples comprised between 1.8 and 2. DNA concentration was calculated according to tissue weight (ng of DNA/µL/mg of dry tissue).

2.2.3 Histology

Samples were embedded in paraffin and cut into 4 µm sections (rotation microtome RM 2055, Leica Microsystems). Hematoxylin-eosin-safran (HES), Blue Alcian (at pH 1.5 and 2.5) and Masson's trichrome (MT) stainings were performed separately on consecutive tissue sections and images were taken using VS 120 OLYMPUS scanner.

2.2.4 Collagen Quantification

Total collagen content of samples was evaluated using a colorimetric total collagen assay kit (BioVision, France) in accordance with the manufacturer protocol. Briefly, samples were homogenized with distilled water and hydrolyzed with 12 M HCl for 3 h at 120°C. Hydrolyzed samples (15 µl) were transferred in a 96-well plate and were evaporated then 100 µl of the Chloramine T reagent were added to each sample. After 5 min, 100 µl of the p dimethylaminobenzaldehyde reagent were added to each well and the plate was incubated for 90 min at 60°C. Finally, the absorbance was measured at 560 nm using a microplate reader (FLUOstar Omega microplate reader, BMG Labtech). The total collagen concentration was calculated using kit standard curve and normalized according to the weight of dry sample (mg of collagen/mg of dry tissue).

2.2.5 Glycosaminoglycans Quantification

Sulphated and non-sulphated glycosaminoglycans (GAGs) were quantified in samples using a colorimetric Alcian Blue method. Briefly, 1 ml of 0.5% (w/v) Alcian Blue 8GX (Sigma, France) in HCl 0.1 M (pH 1.5 or pH 2.5) was added to samples and incubated overnight on orbital shaker (300 rpm). After centrifugation (10 min at 12,000 *g*), supernatant was removed and 250 µl of HCl 6 M were added to samples, incubated overnight on orbital shaker at room temperature and the absorbance of the extracted Alcian Blue was measured at 600 nm. The concentrations of sulphated and non-sulphated GAGs were determined, respectively, according to a chondroitin sulfate B sodium (Sigma) standard range (Alcian blue pH 1.5), and a hyaluronic acid (RenovHyal®) standard range (Alcian blue 2.5). GAG concentrations were normalized according to the weight of dry sample (µg of GAG/mg of dry tissue).

2.2.6 Infrared Spectroscopy

Spectra were recorded in reflection mode between 4,000 and 800 cm^{-1} on a Bruker Vertex 70v spectrometer equipped with a Hyperion 2000 microscope and a ×15 objective controlled by the OPUS 7.5 software. A KBr beam splitter and a MCT detector were used. The resolution of the single beam spectra was 4 cm^{-1}. The number of bidirectional double-sided interferogram scans was 64, which corresponds to a 40 s accumulation. All interferograms were Fourier processed using the Mertz phase correction mode and a Blackman-Harris three-term apodization function. Measurements were performed at 21 ± 1°C in an air-conditioned room. Water vapor subtraction was performed. Masks of 300 × 220 µm were used to record 58 spectra located at different areas of the freeze-dried samples. An average spectrum was then calculated from the 58 spectra of every sample, and baseline was corrected on the average spectra by concave elastic correction (4 iterations, 64 baseline points) between 4,000 and 800 cm^{-1} before further analysis of the average spectra.

2.3 Physical and Mechanical Features

2.3.1 Scanning Electron Microscopy

Freeze-dried samples were sputtered with a thin gold–palladium film using a JEOL ion sputter JFC 1100 instrument. Scanning electron microscopy with a field emission gun (FEG-SEM) investigations were performed with a FEG-SEM (JEOL JSM-7900F, France), and images were acquired from secondary electrons at primary beam energy at 5 kV.

2.3.2 Second Harmonic Generation Imaging

Two-photon excitation laser scanning confocal microscopy and second harmonic generation (SHG) were performed under circular polarization. Images of PBS- rehydrated samples were obtained with a confocal microscope (LSM 710-NLO, Carl Zeiss SAS, and Germany) coupled with CHAMELEON femtosecond Titanium-Sapphire Laser (Coherent, United States). Samples were excited at 860 nm and SHG signal was collected in 420–440 nm spectral window with ×20 objective (ON: 0.8). SHG gray level was quantified from resulting images with ImageJ.

2.3.3 Mercury Intrusion Porosimetry

Pore access radii distribution and the total porosity of samples were assessed by mercury intrusion porosimetry (Micromeretics AutoPore IV 9500, Hexton, United Kingdom). The measured pore access radius ranges from 183 µm (0.003 MPa) to 0.003 µm (227 MPa). Thus, pores larger or thinner than these sizes are not considered by this technique. The incremental curve gives the mean pore radius for which the intrusive volume is maximal. The cumulative curve allows plotting the pore threshold that corresponds to the pore access allowing filling of the main part of the porous network. When both radii are close, the pore distribution can be considered as unimodal.

2.3.4 Swelling Properties

Swelling ratio of samples was determined by a fluid absorption method. Freeze-dried samples were weighted and immersed in PBS for 5 min at room temperature. Hydrated samples were weighted after removing PBS excess and the equilibrium swelling ratio (Q) was calculated using the following equation,

$$Q = \frac{Wwet - Wdry}{Wdry}$$

"*W*" corresponds to the weight of samples.

2.3.5 Mechanical Properties

The mechanical properties of samples were tested through quasi static tensile tests up to failure. The loading sequence was divided into two steps: 1) a dry test under elastic limits with an imposed strain around 1.6% to avoid any damages followed by 2) a PBS hydrated at 37°C one allowing a full mechanical response characterization. (Dubus et al., 2020). In between both steps, 5 min were given for the sample to accommodate prior to be tested with 1.6% strain loads and eventually up to failure. All loadings were performed at a 0.01 mm s^{-1} velocity to remain in the quasi static framework. A Universal Testing Machine Zwicky 0.5 equipped with a 10 N loadcell was used to measure samples' response. The engineering stress and strain definition was used to process the force displacement curves and measure the linear elastic moduli.

2.4 Degradation Studies

In vitro degradation assessment of samples were performed by collagenase and hyaluronidase treatments. Freeze-dried samples (10 mg) were immersed in collagenase type II (Gibco, France) or hyaluronidase (Sigma, France) solution (1 mg/ml) for 6, 24, 48, and 72 h at 37°C. After incubation, the supernatant was discarded, and the remaining samples was freeze-dried. The mass of samples was determined before and after degradation to evaluate the percentage of remaining mass after degradation. The remaining hyaluronic acid was determined by Alcian Blue at pH 2.5 as previously described.

2.5 Bioactivity

2.5.1 Mass Spectrometry

Freeze-dried samples were soaked in 1 ml of fetal bovine serum (FBS) free α-MEM (Lonza, France) for 72 h and the released macromolecules were analyses by mass spectrometry. Each supernatant was precipitated with DOC/TCA and resuspended in 50 µl Urea, 6M, Tris, 50 mM, and pH 8.0. From these, 20 µl were processed as follows: Cysteine residues were reduced by addition of 4 mM DTT for 45 min, alkylated by addition of IAA at 40 mM for another 45 min and IAA was blocked by addition of another 40 mM DTT for 10 min 180 µl Tris, 50 mM, $CaCl_2$, and 1 mM were added together with 100 ng sequencing grade trypsin and digestion was allowed overnight at 37°C. Samples were acidified by addition of 10 µl TFA 10%. Samples were fractionated by nanoHPLC on an Ultimate 3000 system equipped with a 20 µl sample loop, a pepMap 100 C18 desalting precolumn and a 15 cm pepMap RSLC C18 fractionation column (all from Dionex). Samples (6.4 µl) were injected using the µl pickup mode and eluted by a 2–45% ACN gradient over 60 min at 300 nL/min. Fractions (340, 9 s each) were collected on a ProteineerFcII (Bruker) over 51 min and eluted fractions were directly mixed on MTP-1536 BC target (Bruker) spots to α-cyano-4-hydroxycinnamic acid (Bruker). LC-MALDI runs were processed using dedicated automatic methods piloted by WARP-LC software on an Autoflex speed MALDI-TOF/TOF mass spectrometer (Bruker), first in MS mode only, in the 700–3,500 mass range, using next-neighbour external calibration for all MALDI spots. MS runs were used for label-free relative quantification strictly as described. (Riffault et al., 2015). On this basis, masses found significantly changed between experimental groups were selected for MS/MS analysis in LIFT mode. Thereafter, all masses with S/N > 6 from one single run were also processed for LIFT fragmentation and all resulting fragmentation data were used for database interrogation. Peptide assignments were performed from TOF/TOF spectra by Mascot interrogation (Matrix Science) of the Swissprot human proteome database piloted in Mascot (Matrix Science) and compiled by Proteinscape (Bruker) with a mass tolerance of 50 ppm in TOF mode and 0.8 Da in TOF/TOF mode, with optional cysteine carbamidomethylation, methionine oxidation and with trypsin cut allowing one mis-cleavage. The minimal mascot score for peptides was set to 20 and that for proteins was set to 80. Protein change calculations and statistics were also performed strictly as previously. (Riffault et al., 2015). Identification results were cross-validated by interrogating an irrelevant database using the same criteria.

2.5.2 ELISA

Freeze-dried samples were soaked in 1 ml of FBS-free α-MEM and 1 ml of α- MEM supplemented with 10% of FBS for 72 h and the released vascular endothelial growth factor (VEGF), hepatic growth factor (HGF) and transforming growth factor beta (TGF-β) were determined using human Duoset® VEGF, HGF, and TGF-β (R&D systems) respectively, according to the manufacturer's instructions. α- MEM supplemented with 10% of FBS and incubated for 72 h at 37°C was used as control. Absorbances were measured at 450 nm using a microplate reader (FLUOstar Omega microplate reader, BMG Labtech). Released amount of growth factors was calculated from the corresponding standard curve.

2.6 Antibacterial Activity

For all bacterial experiments, *Staphylococcus aureus* (*S. aureus*, SH1000) and *Staphylococcus epidermidis* (*S. epidermidis,* CIP 53.124) were grown on Trypto-casein Soy (TCS) agars (Biokar) at 37°C. Both strains were then grown for 18 h in nutritive broth at 37°C and optical densities of each culture were adjusted to absorbance at 600 nm = 1 before experiments.

2.6.1 Agar Diffusion Testing

Bacterial cultures were diluted at 1/500 in nutritive broth and 2 ml were poured onto a TCS agar and excess liquid was withdrawn. Freeze-dried samples (5 mm-diameter) were UV-decontaminated for 20 min, that placed onto the plate once the agar was completely dry. Plates were then incubated at 37°C for 24 h and pictures were taken to determine the zones of microbial growth inhibition.

2.6.2 Bacteria Adhesion

Bacterial cultures were diluted at 1/500 in nutritive broth and 1 ml were deposited on UV-decontaminated freeze-dried samples

placed into a 24-well plate. After 24 h of culture at 37°C, samples were rinsed with nutritive broth, immersed in 2 ml of nutritive broth and then sonicated for 5 min (40 kHz). Serial dilutions were further plated on TCS agars plates and the rate of viable adhered bacteria was determined after colony count.

2.6.3 Confocal Laser Scanning Microscopy

For the visualization of alive and adhered *S. aureus* and *S. epidermidis* on samples, bacteria were labeled with Syto 9 fluorescent dye (Thermo Fischer) for 30 min. Bacteria were then imaged by confocal laser scanning microscopy (CLSM, Zeiss LSM 710 NLO, ×20 objective, Numerical Aperture 0.8, and Germany).

2.7 Biocompatibility

2.7.1 Cell Culture

In this study, human Wharton's jelly stromal cells (WJ-SCs) and human fibroblasts were used for *in vitro* studies. WJ-SCs were enzymatically isolated from fresh human umbilical cords obtained after full-term births and cultured in α-MEM supplemented with 10% decomplemented FBS, 1% Penicillin/Streptomycin/Amphotericin B and 1% Glutamax® (*v/v*, Gibco, France) as previously described (Mechiche Alami et al., 2014). Human gingival derived fibroblasts were isolated from gingival fragments, obtained during teeth removal Fibroblasts were cultured in DMEM-Glutamax® (Gibco, France) supplemented with 10% FBS and 1% Penicillin/Streptomycin.

2.7.2 Cytotoxicity Tests

WJ-SCs and fibroblasts were cultured in 24 well chamber culture for 24 h, then 1 mg of UV-decontaminated freeze-dried samples were added in culture wells. WJ-SCs and fibroblasts cultured on tissue culture plastic without any sample were used as controls. According to the ISO/EN 10993 part 5 guideline, the cytotoxicity of sample released agents was monitored on cells by WST-1® (water-soluble tetrazolium salt-1®, Roche Diagnostics) assay and in culture supernatants by LDH (lactate dehydrogenase, Roche Diagnostics). Briefly, after 24 h of contact with samples, WST-1® was performed on cells in accordance with the manufacturer protocol, and supernatants were transferred to new culture wells before absorbance measurement at 440 nm using a FLUOstar Omega microplate reader (BMG Labtech) against a background control as blank. A wavelength of 750 nm was used as the correction wavelength. LDH activity was evaluated following the manufacturer's instructions in cell supernatants. Absorbance was measured at 492 and 700 nm.

2.7.3 Cell Proliferation Assay

Cell proliferation assay was performed with 10^4 WJ-SCs seeded on UV-decontaminated (20 min) 5 mm-diameter-samples. WST-1® and DNA extraction were performed after 7, 10, and 15 days of culture. DNA was extracted using MasterPure™ DNA Purification Kit as previously described. Bio-Gide® collagen membrane (Giestlich Pharma, France) was used as a control for cell proliferation experiments.

2.7.4 Cell Morphology and Tissue Colonisation

After 15 days of culture on d-WJ, WJ-SCs were fixed with 4% (w/v) paraformaldehyde (Sigma-Aldrich) at 37°C for 10 min. For morphology evaluation, cells were then permeabilized with 0.5% (v/v) Triton X-100 for 5 min. Alexa® Fluor-488 conjugated-Phalloidin® (1/100 dilution in 0.1% Triton X-100) was used to stain F-actin for 45 min at room temperature. Nuclei were counter-stained with 4,6-diamidino-2-phenylindole (DAPI, 100 ng/ml, 1/3 000 dilution) for 5 min. Stained cells were mounted and imaged by confocal laser scanning microscopy (CLSM, Zeiss LSM 710 NLO, 20× objective, Numerical Aperture 1.4, and Germany). For tissue colonisation evaluation, samples were embedded in paraffin and cut into 4 µm sections and HES staining was performed as previously described.

2.7.5 Subcutaneous Implantation

All animal studies were carried out following the guidelines approved by the Committee on Animal Care Bourgogne Franche-Comté University (N° 2010-2206-02314). *In vivo* biological response to d-WJ was assessed with immunocompetent 8 weeks males Wistar rats (n = 4). UV-decontaminated (30 min) d-WJ membranes were cut with a scalpel into some pieces weighing around 10 mg. The d-WJ membranes were subcutaneously sutured and each rat received two d-WJ (according to 3R rules). After 3 weeks of implantation, the rats were sacrificed and the implanted membranes and the surrounding connective tissues and skin were resected from the underlying muscles. Samples were fixed in 4% paraformaldehyde, embedded in paraffin and cut into 4 µm sections as previously described. HES and MT staining were performed separately on consecutive tissue sections and images were taken using VS 120 OLYMPUS scanner.

2.8 Statistical Analyses

All statistical analyses were performed using GraphPad Prism software. The efficiency of decellularization was confirmed with at least six independent umbilical cords. Biochemical and swelling properties were determined from four independent umbilical cords. Bioactivity and mechanical characterization of samples were performed with five and six independent umbilical cords, respectively. For bacterial studies, at least three independent bacterial preculture were carried out for each bacterial strain and all samples were tested for each preculture in triplicate. All results were represented as histograms (mean ± SEM), statistical analysis were performed using Mann & Whitney test. For each test, a value of $p < 0.05$ was accepted as statistically significant p (rejection level of the null-hypothesis of equal means).

3 RESULT AND DISCUSSION

Healthy perinatal tissues are promising biological scaffolds as they are inexpensive, and universally available. Among these tissues, the human umbilical cord is expected to offer outstanding assets for tissue engineering by serving as a bioactive platform for supporting endogenous cell adhesion, growth, and differentiation. (Beiki et al., 2017; Jadalannagari et al., 2017; Kehtari et al., 2019; Penolazzi et al., 2020). Herein, the functional and technical justification for using decellularized

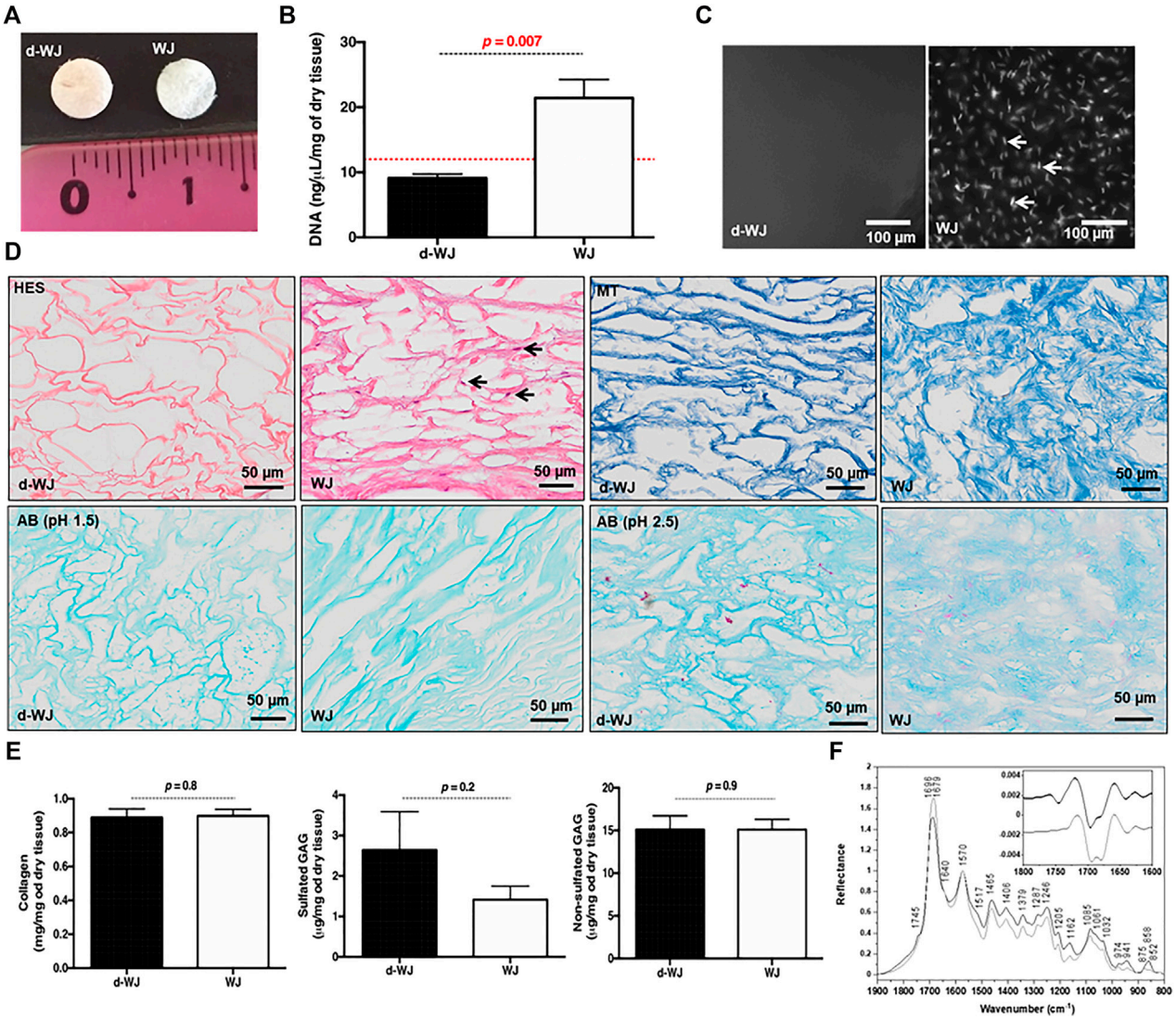

FIGURE 1 | Structural characterization of d-WJ. **(A)**: Macroscopical view of d-WJ and WJ control. **(B)**: Nuclei moieties quantification in d-WJ and WJ, indicating a significant decrease in DNA content within d-WJ (red dashed line indicates the limit of detection of the used kit; n = 6, Mann & Whitney test). **(C)**: Fluorescence microscopy observation of DAPI stained nuclei samples, indicating the absence of nuclear structures in d-WJ and the presence of nuclei in WJ samples as highlighted by white arrows (scale bars = 100 µm). **(D)**: Hematoxylin-eosin-safran (HES, in upper left, black arrows highlighting stained nuclei), Masson's trichrome (MT in upper right), Alcian Blue (AB at pH 1.5 in lower left and at pH 2.5 in lower right) of paraffin embedded d-WJ and WJ control (scale bars = 50 µm). **(E)**: Biochemical assays for collagen, sulphated and non-sulphated glycosaminoglycans, indicating a preservation in ECM components within d-WJ (n = 4, Mann & Whitney test). **(F)**: Infrared (IR) micro-spectroscopy spectra of d-WJ (grey) and WJ control (black) Spectra are normalized to one for the amide II band at 1,570 cm^{-1}. Insert represents second derivative spectra of d-WJ (grey) and WJ control (black) in the 1800–1,600 cm^{-1} region.

WJ (d-WJ) as a biodegradable matrix instead of viable WJ tissue resides from its versatility and flexibility of use as an advanced biological scaffold with a wide range of applications, surpassing thereby the limitations of donor shortage and adverse host reaction. After stripping the surrounding superfluous tissues (*i.e.* sub-amniotic envelop and blood vessels) and technical optimization, the selected decellularization consisted of a combination of Triton X-100 (a milder non-ionic detergent, which targets the lipid–lipid and lipid–protein interactions, leaving the protein–protein interaction intact) and nuclease (DNase). For further clinical and commercial benefit (*i.e.* ease of transportation logistics and storage requirements), (Moore et al., 2017), d-WJ samples were freeze-dried. The physical, mechanical and biological properties of d-WJ were compared to those obtained for devitalized WJ control.

3.1 Structural Integrity

The effective removal of cells and nucleic moieties from WJ (**Figure 1A**) was assessed by DNA quantification and histological staining (**Figures 1B–D**). The nucleic acids were hardly distinguished in d-WJ as indicated by hematoxylin-eosin-safran (HES) (**Figure 1D**) and 4,6-diamidino-2-phenylin-dole

TABLE 1 | Assignments of principal micro-infrared vibrational bands of the 1800–800 cm^{-1} region of the spectra of d-WJ and WJ.

Infrared wavenumber from 2nd derivative spectra (cm^{-1})		Tentative assignment	Main associated compound
d-WJ	WJ		
—	1745	νC = O (esters)	Phospholipids
1,696	1,696	Amide I	Collagen, β-turn
1,679	1,679	Amide I	Collagen, β-sheet
1,639	1,640	Amide I, δH_2O	Collagen, α-helix and random, Water
1,614	1,614		β-sheets, amino acid side chains (Glu, Arg)
1,570	1,572	Amide II	Collagen
1,517	1,515	Amide II	β-sheets
1,465	1,465	δCH_n	Collagen
1,406	1,406	νCOO^-	Collagen, GAGs
1,380	1,379	δCH_3	Collagen
1,343	1,343	δCH_3, Amide III	Collagen
1,316	1,316	Amide III	Collagen
1,287	1,287	Amide III	Collagen
1,246	1,246	Amide III, νsSO_2, and νsPO_2	Collagen, GAGs, phospholipids and nucleic acids
1,205	1,205	Amide III	Collagen
1,162	1,162	νC-O	Collagen (carbohydrate moiety), GAGs
1,085	1,085	νC-O, νsPO_2	Collagen (carbohydrate moiety), GAGs
1,061	1,061	νC-O	Collagen (carbohydrate moiety), GAGs
1,032	1,032	νC-O	Collagen (carbohydrate moiety, hydroxyproline), GAGs
974	975	C-O	Collagen (carbohydrate moiety)
941	941	C-O-C skeletal	Collagen (carbohydrate moiety)
875	875	C-C	Collagen
—	858	C-O-S	GAGs
852	852	C-O-S	GAGs (chondroitin-4-sulphate)

(Key: ν, stretching; δ, bending; ω, wagging; a, antisymmetric; s, symmetric; sh, shoulder; GAGs, glycosaminoglycans).

(DAPI) (**Figure 1C**) staining and corroborated by DNA content analysis (**Figure 1B**). Extracted DNA from d-WJ was 9.12 ± 1.41 ng/μl, below the limit detection of the used kit (*i.e.* 12 ng/μl), while extracted DNA from WJ was 21.42 ± 6.35 ng/μl/mg of dry tissue. Thus, the total DNA content of WJ was 664.12 ± 210.75 ng/mg of dry tissue which is above the threshold of 50 ng/mg (Crapo et al., 2011). These results indicate a successful removal of nuclei components from the d-WJ using Triton X-100 and DNase treatments.

Preservation of the ECM integrity after decellularization was a paramount goal in this study. Herein, the ECM components (*i.e.* total collagen and sulphated and non-sulphated glycosaminoglycans (GAGs)) were analysed qualitatively and quantitatively. Qualitative Masson's Trichrome and Alcian Blue staining showed that d-WJ resulted in primarily collagen and both sulphated and non-sulphated GAGs (**Figure 1D**). The quantitative biochemical investigations indicated that d-WJ composition is consistent with the ones reported for WJ as a great amount of collagen (0.88 ± 0.09 *vs* 0.89 ± 0.06 mg/mg of dry tissue), sulphated GAGs (3.14 ± 1.50 *vs* 1.6 ± 0.62 μg/mg of dry tissue) as well as non-sulphated GAGs (15.09 ± 3.29 *vs* 15.11 ± 1.94 μg/mg of dry tissue) was noticed (**Figure 1E**). To sum up, our results suggest that the used decellularization method fully meets modern criteria of decellularization. (Crapo et al., 2011; Keane et al., 2015).

Chemical composition of d-WJ was measured by infrared (IR) micro-spectroscopy (**Figure 1F**). The band assignments, gathered in **Table 1**, were performed with the help of the second derivative spectra, and in accordance with the literature. (Cortizas and López-Costas, 2020; Belbachir et al., 2009; Petibois et al., 2006; Foot and Mulholland, 2005; Gough et al., 2003; Haxaire et al., 2003; Chirgadze et al., 1975). In comparison with WJ, d-WJ spectra revealed the absence of phospholipid shoulder (located at 1745 cm^{-1}, corresponding to cell components) along with a reduction in bands intensities close to 1,240 and 1,085 cm^{-1} (partially assigned to PO_2 stretching bands from phospholipids and nucleic acids), confirming the effectiveness of the decellularization. The effect of the tissue processing on the ECM integrity was also investigated. The general shape of the spectra was close to those already reported in the literature for collagen. (Cortizas and López-Costas, 2020; Petibois et al., 2006). Indeed, both d-WJ and WJ control spectra showed major bands around 1,685 and 1,570 cm^{-1}, assigned mainly to amide I and II bands from collagen, respectively. Amide I band is very sensitive to the secondary structure of collagen. Two main bands were resolved at 1,696 and 1,679 cm^{-1} in the second derivative spectra (**Figure 1F** insert), assigned to β-turns and β-sheets of collagen, respectively, (Belbachir et al., 2009), revealing an apparent difference in their relative intensities following the decellularization. Indeed, ratio β-turns to β-sheets decreased from the WJ spectrum to d-WJ spectrum, suggesting a potential alteration of the collagen upon decellularization. Spectra also exhibit absorption bands between 1,170 and 800 cm^{-1}, which arise mainly from the ν(C–O) and ν(C–O–C) absorptions of the carbohydrate moieties from collagen and GAGs. (Haxaire et al., 2003; Petibois et al., 2006). Spectra of d-WJ showed lower absorption intensities compared to WJ spectra, indicating a partial loss of GAGs content.

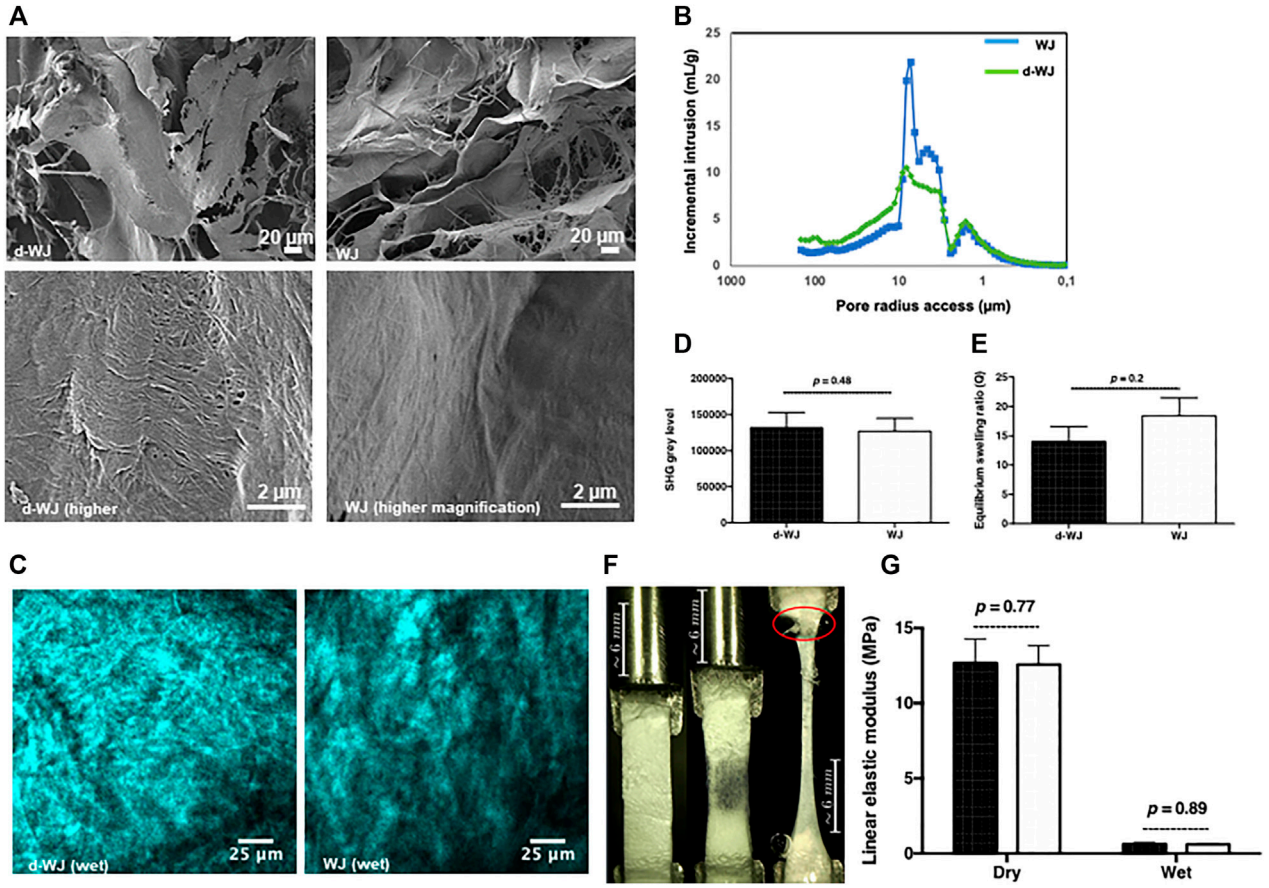

FIGURE 2 | Physical and mechanical characterization of d-WJ. **(A)**: Scanning electron microscopy views at low magnification (in upper line) and high magnification (in lower line; scale bars = 20 and 100 µm, respectively). **(B)**: Mercure intrusion porosity, **(C,D)**: Two-photon excitation laser scanning confocal microscopy and second harmonic generation imaging (Scale bars = 25 µm) and signal quantification, respectively, indicating no alteration in collagen integrity within d-WJ ($n = 4$, Mann & Whitney test). **(E)**: Equilibrium swelling ratio of d-WJ in PBS, showing a preservation in hydration capabilities of d-WJ ($n = 4$, Mann & Whitney test). **(F)**: Mechanical testing photographs (in red is indicated the rupture at the fixation site) and **(G)**: Linear elastic modulus of d-WJ (black bars) in dry and wet experimental conditions, showing no noticeable difference in d-WJ mechanical response *versus* WJ (white bars; $n = 6$, Mann & Whitney test).

Interestingly, GAGs were still left after decellularization as it is shown for example by the occurrence of the band at 852 cm^{-1}, the latter being specific for chondroitin-4-sulphate. (Allen et al., 1977; Foot and Mulholland, 2005).

3.2 Physical and Mechanical Features

The firmness of the umbilical cord is related to the fibrous collagenic nature of WJ. (Converse et al., 2018). Herein, we investigated the collagen structure by scanning electron microscopy (SEM) and Two-photon excitation laser scanning confocal microscopy and second harmonic generation (SHG). SEM micrographs of the cross-section and surface of the d-WJ demonstrated the nanofibrous architecture of d-WJ with variable porosity, close to WJ features (**Figure 2A**). Deep amino acid composition of WJ, performed by ion exchange chromatography (data not shown), showed that WJ did not exhibit similar composition with fibrillar type I collagen. Thus, the collagen fibril periodicity of ~100 nm could be attributed to type VI collagen while unspecific bending periodicity fibrils could be attributed to type V collagen. (Nanaev et al., 1997; Franc et al., 1998).

Mercury intrusion porosimetry method confirmed the highly porous microstructure of d-WJ with an average total porosity of about 78.9% close to the WJ total porosity (79.8%). However, the pore access distribution differed between the two samples. d-WJ showed a decrease in the main pore access between 3 and 9 µm while the amount of the larger pore access (>10 µm) increased (**Figure 2B**). Collagen orientation plays a crucial role in the structural and mechanical features of the tissue. SHG have seen a surge in use in biomedical research, allowing the simultaneous visualization of endogenous auto-fluorescent unstained samples and hyper-polarizable fibrillar protein. (Cicchi et al., 2013). Thus, 3D images of the organization of collagen fibers with micrometer resolution were given by polarized-SHG visualization. Despite the effect of decellularization on the secondary structure of collagen, d-WJ showed a strong SHG signal with a disordered structure close to WJ (**Figures 2C,D**). However, collagen fibres were hardly

distinguished on our experimental setup (*i.e.* PBS hydrated tissues). Thus, the provided signal could be attributed to the centrosymmetric type I, type III and type VI collagen. (Ricard-Blum et al., 2018; Reed et al., 2019). The diminished SHG in decellularized porcine urinary bladder being correlated to a strong disruption of the collagen structure, (Hwang et al., 2017), SHG signals from d-WJ are thus indicative of the absence of structural damages in the fibrillar collagen.

Water absorption capacity is one major consideration in biomedical field. WJ is a porous matrix with canalicular structures occupied mainly by hyaluronic acid. (Sobolewski et al., 1997). Therefore, the interaction with water forms a highly viscous fluid within the pore space of the matrix. (Ferguson and Dodson, 2009). To address how much and how quickly matrices absorb the fluids from their surroundings, swelling properties of the d-WJ were evaluated. Water absorption reached the equilibrium swelling within 5 min. By calculating the swelling ratio, a slight decrease was observed for d-WJ in comparison with WJ (14.0 ± 6.7 and 18.5 ± 9.2, respectively; p = 0.2; **Figure 2E**), confirming the preservation of GAGs content following the decellularization.

From its structural basis point of view (*i.e.* collagen, sulphated and non-sulphated GAGs), the highly hydrated WJ possesses a strong mechanical resistance and elasticity. (Pennati, 2001). The linear elastic modulus, a linear approximation of the stress strain curve translating the linear elastic response of the tissue, was monitored in dry and wet conditions for an average strain load of 1.59% to avoid sample damage. The results showed a decrease in linear elastic modulus from 12.69 ± 3.87 MPa in dry condition to 0.64 ± 0.22 MPa in wet condition for d-WJ and a decrease from 12.57 ± 3.08 to 0.61 ± 0.11 MPa in wet condition for WJ (**Figures 2F,G**). Previous studies reported an increase in tissue stiffness following the decellularization, because of the relative increase in collagen content and reduction of other components (*i.e.* water and GAG). (Totonelli et al., 2012; Frazão et al., 2020). The linear elastic modulus of d-WJ close to WJ is in accordance with the above cited biochemical characterization. Altogether, these results demonstrated that by eliminating the cell and nuclei moieties, the macrostructure and the mechanical integrity of d-WJ was not compromised.

3.3 Degradation

Biodegradability is an important factor for matrices designing in regenerative medicine. Collagenase and hyaluronidase are usually used to partially mimic the *in vivo* biodegradation conditions for collagen and hyaluronic acid based tissues such as cartilage. (Lau et al., 2019). Regarding the composition of WJ, herein, the effect of decellularization on WJ degradation was examined by treating d-WJ with collagenase, hyaluronidase, and enzyme free-phosphate buffer solution (PBS). As for WJ, d-WJ was completely degraded in collagenase after 72 h of incubation since a negligible amount was harvested. At 48 h of incubation, samples retained 8 ± 2% of collagen for d-WJ and 14 ± 4% for WJ (p = 0.2). Samples maintained in hyaluronidase and PBS did not show a loss in their weight over a week (**Table 2**) *in vivo* (Lau et al., 2019). Herein, collagenase and hyaluronic acid were used in much higher concentrations than found in physiological conditions, but they allowed to accelerate the biodegradation and to observe the effect in shorter time. Our results revealed that d-WJ was sensitive to the collagenase action but seemed resistant to hydrolysis probably due the presence of insoluble collagen constituents. (Sobolewski et al., 1997). The absence of weight loss in hyaluronidase could be attributed to the low content in hyaluronic acid in WJ matrix (several μg) in comparison with collagen (several mg) (**Figure 1E**). To verify the resistance of WJ degradation in hyaluronidase, we quantified the remanent non-sulphated GAGs in samples after 2 h of incubation. Our results showed that only 29 ± 13% of non-sulphated GAGs was retained in d-WJ *versus* 49 ± 13% in WJ (p = 0.2). Despite the increase in pore size in d-WJ that could induce a higher diffusion of enzymes within the tissue, our results did not reveal a major effect of the decellularization on the *in vitro* matrix biodegradability.

3.4 Bioactivity

WJ holds great potential in treating a variety of chronic wounds with a minimal scar formation. (Hanselman et al., 2015). Few empirical clinical studies have reported that transplantation of umbilical cord facilitates epithelial wound healing and reduces inflammation, scarring, and angiogenesis. (Marston et al., 2019; Tettelbach et al., 2019; Caputo et al., 2016). Macromolecules derived from WJ-ECM are believed to promote resolution of inflammatory processes, to support stromal cell recruitment, and to inhibit myofibroblasts. (Gupta et al., 2020). Herein, we supposed that when WJ is exposed to the biological fluid, most of the permeable molecules immediately enter the fluid due to the osmotic pressure, increasing the tissue bioactivity. In this context, to detect the bioactivity of d-WJ, tissues were soaked in bovine serum free α-MEM and bovine serum supplemented α-MEM culture media for 72 h and the released macromolecules and growth factors were respectively analysed by mass spectrometry and ELISA. Mass spectrometry showed a passive release of structural and adhesive proteins involved in wound healing process and antimicrobial response such as collagen, fibronectin, tenascin, lumican, periostin, Keratin type I and II, Fibulin and Fibrinogen beta chain (**Figure 3A**). Interestingly no spontaneous release of these proteins was detected for WJ. The obtained mass spectrometry results are in accordance with Jadalannagari *et al.*, who detected these molecules after WJ matrix degradation. (Jadalannagari et al., 2017). The retention of growth factors naturally occurring in the d-WJ was demonstrated by ELISA analysis of culture medium. Vascular endothelial growth factors (VEGF), hepatic growth factors (HGF) and transforming growth factors beta (TGF-β) were detected in the supernatant (**Figure 3B**). An increase in VEGF and HGF release in the culture medium was noticed for d-WJ in comparison with WJ. Our results suggest that d-WJ is more exposed to the culture medium diffusion into WJ matrix, allowing the release of bioactive molecules. The detection of the released molecules in d-WJ could be due to the increase in the pore size following the decellularization. Furthermore, it is well known that growth factors bind to sulphated GAG compound(s) such as heparan sulphate, chondroitin sulphate to form complexes with ECM components. In our experiments, the growth factors were not detected in the absence of bovine serum. Therefore, we concluded that the action of proteases and/or glycosidases naturally present in bovine serum may release and activate growth factors within the

TABLE 2 | *In vitro* degradation testing in collagenase, hyaluronidase, and in phosphate buffer.

Conditions	Time of incubation (h)	d-WJ (%)	WJ (%)
Weight lost following incubation in PBS	72	neglecting	neglecting
Remaining weight following collagenase treatment	48	8 ± 2^{NS}	14 ± 4
Weight lost following hyaluronidase treatment	72	neglecting	neglecting
Remaining non-sulphated GAGs following hyaluronidase treatment	2	29 ± 13^{NS}	49 ± 13

(GAGs, glycosaminoglycans; PBS, Phosphate buffer solution; NS, non-significant difference, n = *6, Mann & Whitney).*

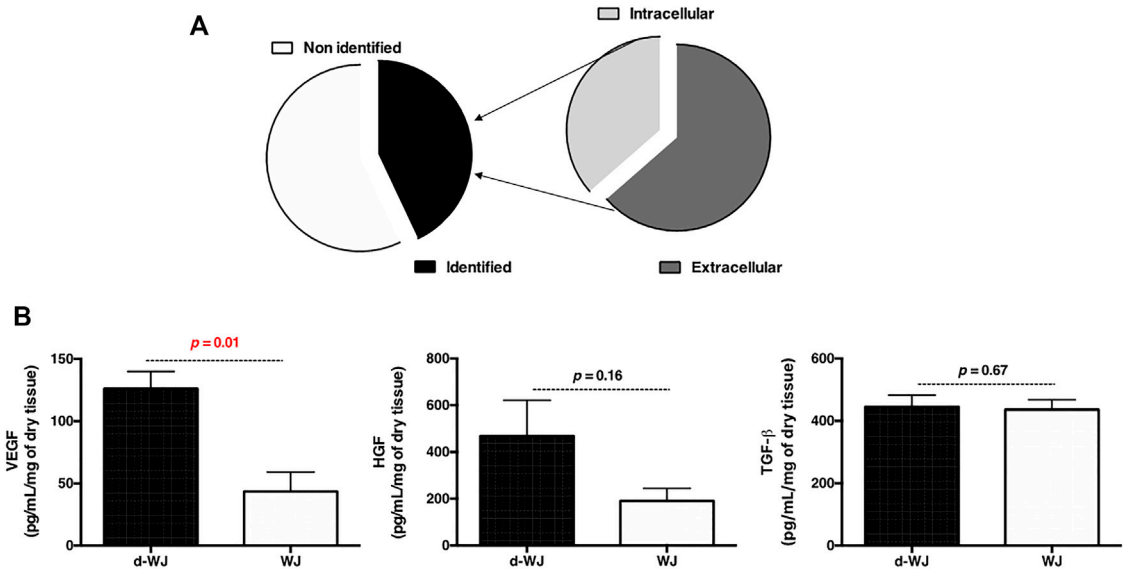

FIGURE 3 | Bioactivity of d-WJ matrix. **(A)**: Mass spectrometry analysis of released macromolecules in d-WJ supernatant. **(B)**: ELISA analysis of released growth factors, showing an increase growth factors release from d-WJ (n = 5, Mann & Whitney test).

tissue. Taken together, these results suggest that d-WJ are bioactive matrix, suitable for regenerative medicine strategies.

3.5 Antibacterial Activity

As mentioned previously, WJ shows promising results in clinic following treatment of diabetic ulcers with osteomyelitis. (Marston et al., 2019; Tettelbach et al., 2019; Caputo et al., 2016; Raphael, 2016). Osteomyelitis is most commonly caused by the *Staphylococcus aureus* (*S. aureus*) and *epidermidis* (*S. epidermidis*), opportunistic pathogens responsible for a tremendous burden on the healthcare system. One of the reasons that Staphylococci are problematic is their well-known ability to attach to surfaces and develop into recalcitrant community structures, often referred to as a "biofilm". Mass spectrometry revealed the passive release of antimicrobial molecules involved in the bacterial agglutination (*i.e.* Fibrinogen beta chain). (Hanington and Zhang, 2011; Sun et al., 2014). Consequently, we evaluated the antibacterial effect of d-WJ against *S. aureus* and *S. epidermidis* strains. Performed agar diffusion test highlighted the presence of a zone of microbial growth inhibition for both pathogens in contact with d-WJ, while WJ did not demonstrate any inhibition zone (**Figure 4A**). These results suggest a rapid diffusion of antimicrobial molecules from d-WJ such as fibrinogen beta chain Bacterial adhesion to d-WJ was then evaluated and showed a clear inherent antiadhesive effect of d-WJ in comparison with WJ (**Figures 4B,C**). On d-WJ, adherent *S. aureus* and *S. epidermidis* were respectively 23 and 26 times less than that on WJ ($p < 0.001$). Taken together, these results suggest that d-WJ had an intrinsic antibacterial effect against *Staphylococcus* strains. In addition to the release of antibacterial agents from d-WJ, we thought that the hyaluronic acid (Marcuzzo et al., 2017) component of the d-WJ extracellular matrix might be responsible for the reduction of the bacterial adhesion. Further experiments are needed to decipher the exact antibacterial action of d-WJ against *Staphylococcus* strains.

3.6 Biocompatibility *in vitro* and *in vivo*

Decellularized allografts are classified by regulatory agencies FDA as a human cell or tissue product and therefore does not require investigational new drug or device exemption approval. (Moore et al., 2017; Sutherland et al., 2015). However, they require biocompatibility testing prior to the clinical use. (Hussein et al., 2016). Consequently, the cytocompatibility d-WJ was investigated. WJ derived

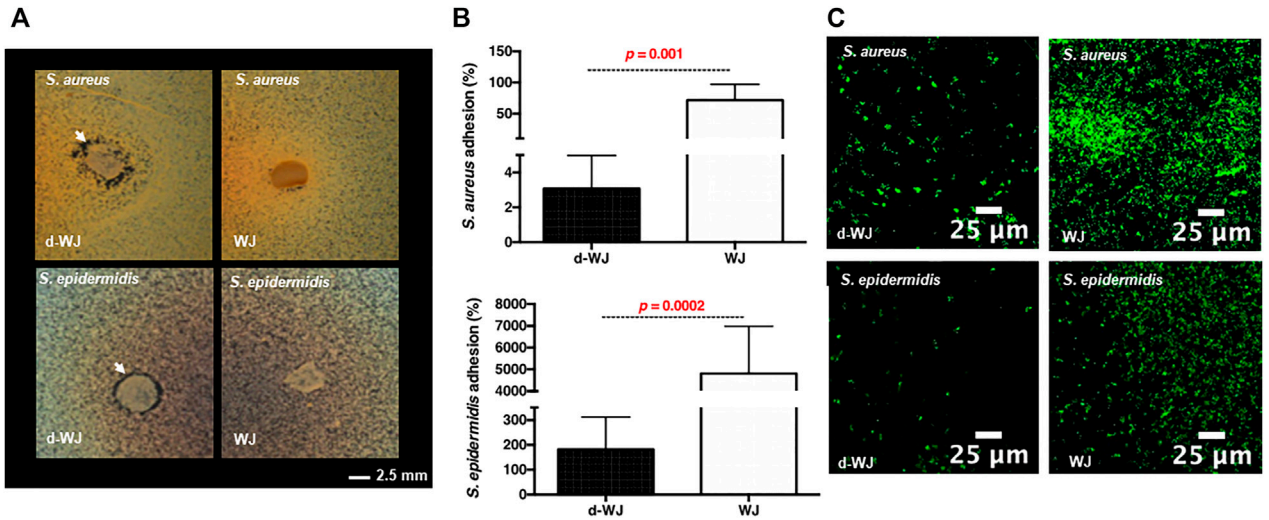

FIGURE 4 | Antibacterial properties of d-WJ. **(A)**: Agar diffusion test, white arrows indicate zone of bacterial growth inhibition of *S. aureus* and *S. epidermidis* around d-WJ. **(B)**: percentage of adhered bacteria on d-WJ matrix, and **(C)**: Confocal laser microscopy visualization of Syto-9® labelled bacteria on d-WJ matrix (green color), indicating a significant decrease in bacteria adhesion on d-WJ (n = 9, Mann & Whitney test, scale bars = 25 µm).

stromal cells (WJ-SCs) and gingival fibroblasts were cultured in 24 well chamber culture for 24 h, then 1 mg of either d-WJ or WJ was added in culture well. WJ-SCs and fibroblasts cultured on tissue culture plastic in the absence of WJ samples were used as controls. According to the ISO/EN 10993 part 5 guideline, the cytotoxicity of d-WJ was monitored by WST-1® (water-soluble tetrazolium salt-1®) assay and LDH (lactate dehydrogenase) release in culture supernatants. When compared to plastic positive control, both WJ-SCs and fibroblasts cultured in the presence of d-WJ remained above 70% of cell viability, threshold considered as an indicator of cytotoxic phenomenon. Furthermore, no increase in the LDH release was observed (**Figures 5A,B**). Taken together, our results indicated the absence of toxic agents release (*i.e.* Triton X-100) following the tissue processing. It is generally accepted that an increase in the WST-1® absorbance at 450 nm reflects a proliferating state of cells. Herein, we noticed an increase in fibroblast metabolic activity in the presence of d-WJ, while no increase in the release of LDH was observed, and suggesting a potential increase in fibroblast proliferation (**Figure 5B**). This proliferation could be attributed to the released growth factors from d-WJ, confirming thus its bioactive features. Preparing an appropriate matrix with good biocompatibility and mechanical properties that mimics the native microenvironment of cells is one of the key elements in regenerative medicine. It is known that there is a broad range of interactions between mesenchymal stromal cells and their niche, ensuring the stromal cell's function. (Shakouri-Motlagh et al., 2017). WJ-SCs possess regenerative capability close to the bone marrow derived stromal cells. The question remains unanswered whether the d-WJ could be recolonized by WJ-SCs. Therefore, WJ-SCs were cultured on d-WJ at a density of 10^4 cells/5 mm diameter of samples. Clinical device collagen membrane (Bio-Gide®) was used as a control. The cell proliferation was monitored by WST-1® assay and DNA quantification at day 7, 10, and 15 of culture, using independent samples for each test and time point. While WST-1® and DNA quantification did not show significant variation of each test and time point in d-WJ (p = 0.7), while an increase in cell content was observed on the Bio-Gide® positive control (p < 0.0003) over the studied time (**Figures 5C,D**).

Despite the small pore size of d-WJ (ranging from 10 to 184 µm), histological section and laser scanning confocal microscopy showed the presence of WJ-SCs within d-WJ (**Figures 5E,F**). WJ-SCs morphological examination of adhered WJ-SCs on d-WJ showed elongated cells on the top of d-WJ (**Figure 5G**). To sum up, these results suggest that d-WJ could simulate the natural niche and microenvironment of WJ-SCs, bringing them closer to their best function similar to what they do in the body. Thus, d-WJ could serve as a platform for WJ-SCs delivery.

Finally, we sought to investigate *in vivo* the tissue response of the recipient organism following d-WJ implantation. Thus, d-WJ was tested according to ISO/EN 10993 part 6 guidelines, by using subcutaneous implantation. Perinatal tissues including the umbilical cords are described as "unrecognized as a foreign material". (Hanselman et al., 2015; Ramuta et al., 2021). We have thus intentionally chosen immunocompetent rat for this study, in order to be able to take immunological reactions into consideration. In all animals, wounds were closed with no wound infection or other complications. Hair growth was normal in the operation field. No inflammatory response, no connective tissue capsule and good histocompatibility were noticed at the studied time point; d-WJ was completely replaced with the reparative granulation tissue. In addition, multinucleated giant cells were not found around the implanted d-WJ. Masson's Trichrome

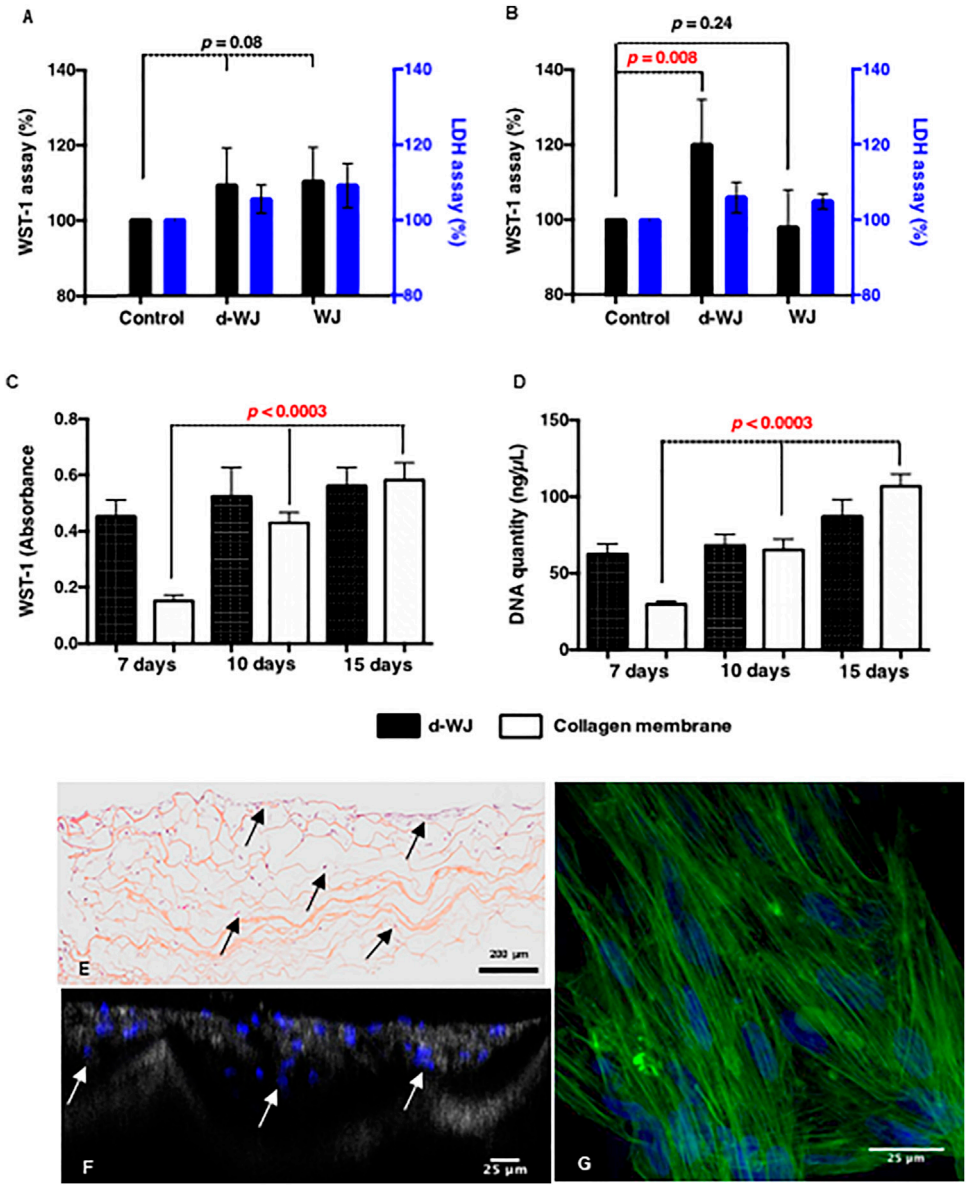

FIGURE 5 | In vitro biocompatibility of d-WJ. **(A,B)**: Metabolic activities (black bars) and LDH release (blue bars) of WJ-SCs and fibroblasts, respectively in the presence of d-WJ and WJ control, indicating the absence of cytotoxic release of Triton X-100 from d-WJ (n = 6, Mann & Whitney test). **(C)**: WJ-SCs proliferation assay and **(D)**: DNA quantification of WJ-SCs cultured on d-WJ (black bars) and Bio-Gide® positive control (white bars), showing the absence of WJ-SCs proliferation on d-WJ (n = 6, Mann & Whitney test). **(E, F)**: Cross sections of WJ-SCs cultured on d-WJ stained respectively with HES and DAPI. Arrows indicate cells within the d-WJ. **(G)**: Confocal microscopy view of WJ-SCs cultured on d-WJ labelled with phalloidin (in green) and DAPI (in blue). Scale bars = 200 µm **(E)** and 25 µm **(F,G)**.

staining did not indicate the presence of collagen matrix, suggesting the total degradation of the implanted d-WJ (**Figure 6A**). The healing process involves many closely coordinated regenerative reactions, counting hemostasis, the migration of fibroblasts and endothelial cells, inducing the tissue remodeling and degradation of collagen fibers. (Stoica et al., 2020). HES staining revealed the presence of blood vessels and fibroblast-*like* cells (**Figures 6B,C**). These results confirmed the *in vitro* and *in vivo* biocompatibility of d-WJ.

4 CONCLUSION

The present work showed that a fully decellularized matrix can be obtained from human Wharton's jelly. Decellularized WJ matrix exhibited overall desirable tissue engineering characteristics. Decellularization process increased the bioactivity of the WJ matrix, inducing a significant release of angiogenic VEGF as well as a passive release of macromolecules with an antibacterial effect against *S. aureus* and *S. epidermidis* strains. Further researches are needed to elucidate which WJ derived macromolecules cause the

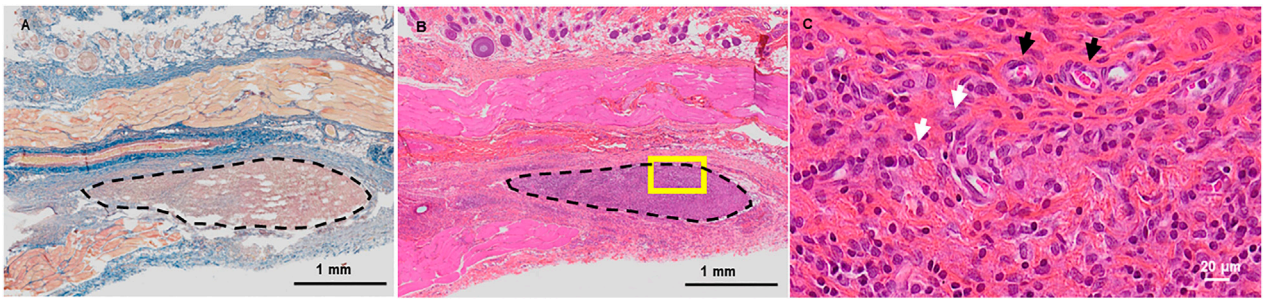

FIGURE 6 | In vivo Biocompatibility of d-WJ. **(A)**: Masson's Trichrome staining. **(B, C)**: Hematoxylin-eosin-safran staining. Dashed delimitations indicate the implanted d-WJ. Picture in C represents a higher magnification of the yellow square in **(B)**. White and black arrows indicate fibroblasts and blood vessels, respectively. Scale bars = 1 mm **(A,B)** and 20 µm **(C)**.

potent antibacterial effect. Biodegradability and stromal cell homing capabilities reinforced with excellent mechanical and physical properties render d-WJ ideal for stem cell therapy and stem cell delivery applications. In large scale future studies, the investigation of the potential use of d-WJ as an antibacterial therapeutic dressing for scar-free wound healing might promote faster and safer translation of d-WJ into clinical practice. Furthermore, the hybridization of autologous blood product such as platelet rich plasma (Barkestani et al., 2021) or autologous stem cells could increase the bioactive potential of d-WJ (Aubert et al., 2017).

DATA AVAILABILITY STATEMENT

The raw data supporting the conclusion of this article will be made available by the authors, without undue reservation.

ETHICS STATEMENT

The animal study was reviewed and approved by Committee on Animal Care Bourgogne Franche-Comte University (N° 2010-2206-02314).

AUTHOR CONTRIBUTIONS

MD, LS, JC, AM, AB, CT, FQ, CT, NB, and FG participated in experiments designing and performance: MD (decellularization process and matrix characterizations), LS (biocompatibility studies), JC (bacterial experiments), AM (matrix degradation), AB (biomechanical experiment and design), CT (SHG images), FQ (infrared studies), CT (porosity experiment), and FG (*in vivo* studies). MD, SG, HR, CM, and HK participated in study design and manuscript writing. All authors reviewed the results and approved the final version of the manuscript.

FUNDING

This work was supported by SATT Nord (Umbregen project) and Région Grand Est (ERMES project).

ACKNOWLEDGMENTS

The authors are grateful to the staff of Reims Maternity Hospital for providing umbilical cords, the staff of the pole bucco-dentaire of Reims hospital for providing gingiva and the staff of the Core PICT (URCA) for SHG and SEM imaging. The authors thank Dr. J. B. Vincourt from the Proteomics Core Facility of UMS2008/ US40 IBSLor (Université de Lorraine, CNRS, INSERM), F-54000 Nancy, France" for MALDI analysis, Dr. C. Boulagnon for histological analysis and Dr. F. Reffuveille for microbiological assay assistance.

REFERENCES

Allen, W. S., Otterbein, E. C., and Wardi, A. H. (1977). Isolation and Characterization of the Sulfated Glycosaminoglycans of the Vitreous Body. *Biochim. Biophys. Acta (Bba) - Gen. Subjects* 498, 167–175. doi:10.1016/0304-4165(77)90097-6

Aubert, L., Dubus, M., Rammal, H., Bour, C., Mongaret, C., Boulagnon-Rombi, C., et al. (2017). Collagen-Based Medical Device as a Stem Cell Carrier for Regenerative Medicine. *Ijms* 18, 2210. doi:10.3390/ijms18102210

Barkestani, M. N., Naserian, S., Uzan, G., and Shamdani, S. (2021). Post-decellularization Techniques Ameliorate Cartilage Decellularization Process for Tissue Engineering Applications. *J. Tissue Eng.* 12, 2041731420983562. doi:10.1177/2041731420983562

Basiri, A., Farokhi, M., Azami, M., Ebrahimi-Barough, S., Mohamadnia, A., Rashtbar, M., et al. (2019). A Silk Fibroin/decellularized Extract of Wharton's Jelly Hydrogel Intended for Cartilage Tissue Engineering. *Prog. Biomater.* 8, 31–42. doi:10.1007/s40204-019-0108-7

Beiki, B., Zeynali, B., and Seyedjafari, E. (2017). Fabrication of a Three Dimensional Spongy Scaffold Using Human Wharton's Jelly Derived Extra Cellular Matrix for Wound Healing. *Mater. Sci. Eng. C* 78, 627–638. doi:10.1016/j.msec.2017.04.074

Belbachir, K., Noreen, R., Gouspillou, G., and Petibois, C. (2009). Collagen Types Analysis and Differentiation by FTIR Spectroscopy. *Anal. Bioanal. Chem.* 395, 829–837. doi:10.1007/s00216-009-3019-y

Caputo, W. J., Vaquero, C., Monterosa, A., Monterosa, P., Johnson, E., Beggs, D., et al. (2016). A Retrospective Study of Cryopreserved Umbilical Cord as an Adjunctive

Therapy to Promote the Healing of Chronic, Complex Foot Ulcers with Underlying Osteomyelitis. *Wound Rep. Reg.* 24, 885–893. doi:10.1111/wrr.12456

Chirgadze, Y. N., Fedorov, O. V., and Trushina, N. P. (1975). Estimation of Amino Acid Residue Side-Chain Absorption in the Infrared Spectra of Protein Solutions in Heavy Water. *Biopolymers* 14, 679–694. doi:10.1002/bip.1975.360140402

Cicchi, R., Vogler, N., Kapsokalyvas, D., Dietzek, B., Popp, J., and Pavone, F. S. (2013). From Molecular Structure to Tissue Architecture: Collagen Organization Probed by SHG Microscopy. *J. Biophoton.* 6, 129–142. doi:10.1002/jbio.201200092

Converse, G. L., Li, D., Buse, E. E., Hopkins, R. A., and Aljitawi, O. S. (2018). Wharton's Jelly Matrix Decellularization for Tissue Engineering Applications. *Methods Mol. Biol.* 1577, 25–33. doi:10.1007/7651_2017_61

Cortizas, A. M., and López-Costas, O. (2020). Linking Structural and Compositional Changes in Archaeological Human Bone Collagen: An FTIR-ATR Approach. *Sci. Rep.* 10, 17888. doi:10.1038/s41598-020-74993-y

Crapo, P. M., Gilbert, T. W., and Badylak, S. F. (2011). An Overview of Tissue and Whole Organ Decellularization Processes. *Biomaterials* 32, 3233–3243. doi:10.1016/j.biomaterials.2011.01.057

Damodaran, R. G., and Vermette, P. (2018). Tissue and Organ Decellularization in Regenerative Medicine. *Biotechnol. Prog.* 34, 1494–1505. doi:10.1002/btpr.2699

Dubus, M., Kerdjoudj, H., Scomazzon, L., Sergheraert, J., Mauprivez, C., Rahouadj, R., et al. (2020). Mechanical Behaviour of a Membrane Made of Human Umbilical Cord for Dental Bone Regenerative Medicine. *Comput. Methods Biomech. Biomed. Eng.* 23, S88–S90. doi:10.1080/10255842.2020.1812169

Ferguson, V. L., and Dodson, R. B. (2009). Bioengineering Aspects of the Umbilical Cord. *Eur. J. Obstet. Gynecol. Reprod. Biol.* 144, S108–S113. doi:10.1016/j.ejogrb.2009.02.024

Foot, M., and Mulholland, M. (2005). Classification of Chondroitin Sulfate A, Chondroitin Sulfate C, Glucosamine Hydrochloride and Glucosamine 6 Sulfate Using Chemometric Techniques. *J. Pharm. Biomed. Anal.* 38, 397–407. doi:10.1016/j.jpba.2005.01.026

Franc, S., Rousseau, J.-C., Garrone, R., van der Rest, M., and Moradi-Améli, M. (1998). Microfibrillar Composition of Umbilical Cord Matrix: Characterization of Fibrillin, Collagen VI and Intact Collagen V. *Placenta* 19, 95–104. doi:10.1016/s0143-4004(98)90104-7

Frazão, L. P., Vieira de Castro, J., Nogueira-Silva, C., and Neves, N. M. (2020). Decellularized Human Chorion Membrane as a Novel Biomaterial for Tissue Regeneration. *Biomolecules* 10, 1208. doi:10.3390/biom10091208

Gilpin, A., and Yang, Y. (2017). Decellularization Strategies for Regenerative Medicine: From Processing Techniques to Applications. *Biomed. Res. Int.* 2017, 9831534. doi:10.1155/2017/9831534

Gough, K. M., Zelinski, D., Wiens, R., Rak, M., and Dixon, I. M. C. (2003). Fourier Transform Infrared Evaluation of Microscopic Scarring in the Cardiomyopathic Heart: Effect of Chronic AT1 Suppression. *Anal. Biochem.* 316, 232–242. doi:10.1016/s0003-2697(03)00039-3

Gupta, A., El-Amin, S. F., Levy, H. J., Sze-Tu, R., Ibim, S. E., and Maffulli, N. (2020). Umbilical Cord-Derived Wharton's Jelly for Regenerative Medicine Applications. *J. Orthop. Surg. Res.* 15, 49. doi:10.1186/s13018-020-1553-7

Hanington, P. C., and Zhang, S.-M. (2011). The Primary Role of Fibrinogen-Related Proteins in Invertebrates Is Defense, Not Coagulation. *J. Innate Immun.* 3, 17–27. doi:10.1159/000321882

Hanselman, A. E., Tidwell, J. E., and Santrock, R. D. (2015). Cryopreserved Human Amniotic Membrane Injection for Plantar Fasciitis. *Foot Ankle Int.* 36, 151–158. doi:10.1177/1071100714552824

Haxaire, K., Maréchal, Y., Milas, M., and Rinaudo, M. (2003). Hydration of Polysaccharide Hyaluronan Observed by IR Spectrometry. I. Preliminary Experiments and Band Assignments. *Biopolymers* 72, 10–20. doi:10.1002/bip.10245

Hinderer, S., Layland, S. L., and Schenke-Layland, K. (2016). ECM and ECM-like Materials - Biomaterials for Applications in Regenerative Medicine and Cancer Therapy. *Adv. Drug Deliv. Rev.* 97, 260–269. doi:10.1016/j.addr.2015.11.019

Hussein, K. H., Park, K.-M., Kang, K.-S., and Woo, H.-M. (2016). Biocompatibility Evaluation of Tissue-Engineered Decellularized Scaffolds for Biomedical Application. *Mater. Sci. Eng. C* 67, 766–778. doi:10.1016/j.msec.2016.05.068

Hwang, J., San, B. H., Turner, N. J., White, L. J., Faulk, D. M., Badylak, S. F., et al. (2017). Molecular Assessment of Collagen Denaturation in Decellularized Tissues Using a Collagen Hybridizing Peptide. *Acta Biomater.* 53, 268–278. doi:10.1016/j.actbio.2017.01.079

Jadalannagari, S., Converse, G., McFall, C., Buse, E., Filla, M., Villar, M. T., et al. (2017). Decellularized Wharton's Jelly from Human Umbilical Cord as a Novel 3D Scaffolding Material for Tissue Engineering Applications. *PLoS One* 12, e0172098. doi:10.1371/journal.pone.0172098

Keane, T. J., Londono, R., Turner, N. J., and Badylak, S. F. (2012). Consequences of Ineffective Decellularization of Biologic Scaffolds on the Host Response. *Biomaterials* 33, 1771–1781. doi:10.1016/j.biomaterials.2011.10.054

Keane, T. J., Swinehart, I. T., and Badylak, S. F. (2015). Methods of Tissue Decellularization Used for Preparation of Biologic Scaffolds and *In Vivo* Relevance. *Methods* 84, 25–34. doi:10.1016/j.ymeth.2015.03.005

Kehtari, M., Beiki, B., Zeynali, B., Hosseini, F. S., Soleimanifar, F., Kaabi, M., et al. (2019). Decellularized Wharton's Jelly Extracellular Matrix as a Promising Scaffold for Promoting Hepatic Differentiation of Human Induced Pluripotent Stem Cells. *J. Cel. Biochem.* 120, 6683–6697. doi:10.1002/jcb.27965

Kočí, Z., Výborný, K., Dubišová, J., Vacková, I., Jäger, A., Lunov, O., et al. (2017). Extracellular Matrix Hydrogel Derived from Human Umbilical Cord as a Scaffold for Neural Tissue Repair and its Comparison with Extracellular Matrix from Porcine Tissues. *Tissue Eng. Part. C Methods* 23, 333–345. doi:10.1089/ten.TEC.2017.0089

Lau, C. S., Hassanbhai, A., Wen, F., Wang, D., Chanchareonsook, N., Goh, B. T., et al. (2019). Evaluation of Decellularized Tilapia Skin as a Tissue Engineering Scaffold. *J. Tissue Eng. Regen. Med.* 13, 1779–1791. doi:10.1002/term.2928

Lin, L., Xu, Y., Li, Y., Gong, X., Wei, M., Zhang, W., et al. (2020). Nanofibrous Wharton's Jelly Scaffold in Combination with Adipose-Derived Stem Cells for Cartilage Engineering. *Mater. Des.* 186, 108216. doi:10.1016/j.matdes.2019.108216

Marcuzzo, A. V., Tofanelli, M., Boscolo Nata, F., Gatto, A., and Tirelli, G. (2017). Hyaluronate Effect on Bacterial Biofilm in ENT District Infections: a Review. *Apmis* 125, 763–772. doi:10.1111/apm.12728

Marston, W. A., Lantis, J. C., Wu, S. C., Nouvong, A., Lee, T. D., McCoy, N. D., et al. (2019). An Open-Label Trial of Cryopreserved Human Umbilical Cord in the Treatment of Complex Diabetic Foot Ulcers Complicated by Osteomyelitis. *Wound Rep. Reg.* 27, 680–686. doi:10.1111/wrr.12754

Martínez, C., Fernández, C., Prado, M., Ozols, A., and Olmedo, D. G. (2017). Synthesis and Characterization of a Novel Scaffold for Bone Tissue Engineering Based on Wharton's Jelly. *J. Biomed. Mater. Res.* 105, 1034–1045. doi:10.1002/jbm.a.35976

Mechiche Alami, S., Velard, F., Draux, F., Siu Paredes, F., Josse, J., Lemaire, F., et al. (2014). Gene Screening of Wharton's Jelly Derived Stem Cells. *Biomed. Mater. Eng.* 24, 53–61. doi:10.3233/bme-140974

Moore, M. C., Van De Walle, A., Chang, J., Juran, C., and McFetridge, P. S. (2017). Human Perinatal-Derived Biomaterials. *Adv. Healthc. Mater.* 6, 10. doi:10.1002/adhm.201700345

Nanaev, A. K., Kohnen, G., Milovanov, A. P., Domogatsky, S. P., and Kaufmann, P. (1997). Stromal Differentiation and Architecture of the Human Umbilical Cord. *Placenta* 18, 53–64. doi:10.1016/s0143-4004(97)90071-0

Pennati, G. (2001). Biomechanical Properties of the Human Umbilical Cord. *Biorheology* 38, 355–366.

Penolazzi, L., Pozzobon, M., Bergamin, L. S., D'Agostino, S., Francescato, R., Bonaccorsi, G., et al. (2020). Extracellular Matrix from Decellularized Wharton's Jelly Improves the Behavior of Cells from Degenerated Intervertebral Disc. *Front. Bioeng. Biotechnol.* 8, 262. doi:10.3389/fbioe.2020.00262

Petibois, C., Gouspillou, G., Wehbe, K., Delage, J.-P., and Déléris, G. (2006). Analysis of Type I and IV Collagens by FT-IR Spectroscopy and Imaging for a Molecular Investigation of Skeletal Muscle Connective Tissue. *Anal. Bioanal. Chem.* 386, 1961–1966. doi:10.1007/s00216-006-0828-0

Ramuta, T. Ž., Tratnjek, L., Janev, A., Seme, K., Starčič Erjavec, M., and Kreft, M. E. (2021). The Antibacterial Activity of Human Amniotic Membrane against Multidrug-Resistant Bacteria Associated with Urinary Tract Infections: New Insights from Normal and Cancerous Urothelial Models. *Biomedicines* 9, 218. doi:10.3390/biomedicines9020218

Raphael, A. (2016). A single-centre, Retrospective Study of Cryopreserved Umbilical Cord/amniotic Membrane Tissue for the Treatment of Diabetic Foot Ulcers. *J. Wound Care* 25, S10–S17. doi:10.12968/jowc.2016.25.sup7.s10

Reed, D. A., Yotsuya, M., Gubareva, P., Toth, P. T., and Bertagna, A. (2019). Two-Photon Fluorescence and Second Harmonic Generation Characterization of Extracellular Matrix Remodeling in Post-Injury Murine Temporomandibular Joint Osteoarthritis. *PLoS ONE* 14, e0214072. doi:10.1371/journal.pone.0214072

Renth, A. N., and Detamore, M. S. (2012). Leveraging "Raw Materials" as Building Blocks and Bioactive Signals in Regenerative Medicine. *Tissue Eng. B: Rev.* 18, 341–362. doi:10.1089/ten.teb.2012.0080

Ricard-Blum, S., Baffet, G., and Théret, N. (2018). Molecular and Tissue Alterations of Collagens in Fibrosis. *Matrix Biol.* 68-69, 122–149. doi:10.1016/j.matbio.2018.02.004

Riffault, M., Moulin, D., Grossin, L., Mainard, D., Magdalou, J., and Vincourt, J.-B. (2015). Label-Free Relative Quantification Applied to LC-MALDI Acquisition for Rapid Analysis of Chondrocyte Secretion Modulation. *J. Proteomics* 114, 263–273. doi:10.1016/j.jprot.2014.10.026

Shakouri-Motlagh, A., Khanabdali, R., Heath, D. E., and Kalionis, B. (2017). The Application of Decellularized Human Term Fetal Membranes in Tissue Engineering and Regenerative Medicine (TERM). *Placenta* 59, 124–130. doi:10.1016/j.placenta.2017.07.002

Sobolewski, K., Bańkowski, E., Chyczewski, L., and Jaworski, S. (1997). Collagen and Glycosaminoglycans of Wharton's Jelly. *Neonatology* 71, 11–21. doi:10.1159/000244392

Sobolewski, K., Małkowski, A., Bańkowski, E., and Jaworski, S. (2005). Wharton's Jelly as a Reservoir of Peptide Growth Factors. *Placenta* 26, 747–752. doi:10.1016/j.placenta.2004.10.008

Spang, M. T., and Christman, K. L. (2018). Extracellular Matrix Hydrogel Therapies: *In Vivo* Applications and Development. *Acta Biomater.* 68, 1–14. doi:10.1016/j.actbio.2017.12.019

Stoica, A. E., Chircov, C., and Grumezescu, A. M. (2020). Nanomaterials for Wound Dressings: An Up-To-Date Overview. *Molecules* 25, 2699. doi:10.3390/molecules25112699

Sun, J.-J., Lan, J.-F., Shi, X.-Z., Yang, M.-C., Yang, H.-T., Zhao, X.-F., et al. (2014). A Fibrinogen-Related Protein (FREP) Is Involved in the Antibacterial Immunity of Marsupenaeus Japonicus. *Fish Shellfish Immunol.* 39, 296–304. doi:10.1016/j.fsi.2014.05.005

Sutherland, A. J., Converse, G. L., Hopkins, R. A., and Detamore, M. S. (2015). The Bioactivity of Cartilage Extracellular Matrix in Articular Cartilage Regeneration. *Adv. Healthc. Mater.* 4, 29–39. doi:10.1002/adhm.201400165

Tettelbach, W., Cazzell, S., Sigal, F., Caporusso, J. M., Agnew, P. S., Hanft, J., et al. (2019). A Multicentre Prospective Randomised Controlled Comparative Parallel Study of Dehydrated Human Umbilical Cord (EpiCord) Allograft for the Treatment of Diabetic Foot Ulcers. *Int. Wound J.* 16, 122–130. doi:10.1111/iwj.13001

Totonelli, G., Maghsoudlou, P., Garriboli, M., Riegler, J., Orlando, G., Burns, A. J., et al. (2012). A Rat Decellularized Small Bowel Scaffold that Preserves Villus-Crypt Architecture for Intestinal Regeneration. *Biomaterials* 33, 3401–3410. doi:10.1016/j.biomaterials.2012.01.012

Yu, Y., Alkhawaji, A., Ding, Y., and Mei, J. (2016). Decellularized Scaffolds in Regenerative Medicine. *Oncotarget* 7, 58671–58683. doi:10.18632/oncotarget.10945

Conflict of Interest: The authors declare that the research was conducted in the absence of any commercial or financial relationships that could be construed as a potential conflict of interest.

Publisher's Note: All claims expressed in this article are solely those of the authors and do not necessarily represent those of their affiliated organizations, or those of the publisher, the editors and the reviewers. Any product that may be evaluated in this article, or claim that may be made by its manufacturer, is not guaranteed or endorsed by the publisher.

frontiers | Frontiers in Bioengineering and Biotechnology

ORIGINAL RESEARCH
published: 08 June 2022
doi: 10.3389/fbioe.2022.902038

Investigating the Paracrine Role of Perinatal Derivatives: Human Amniotic Fluid Stem Cell-Extracellular Vesicles Show Promising Transient Potential for Cardiomyocyte Renewal

*Ambra Costa[1], Carolina Balbi[2,3,4], Patrizia Garbati[1], Maria Elisabetta Federica Palamà[1], Daniele Reverberi[5], Antonella De Palma[6], Rossana Rossi[6], Dario Paladini[7], Domenico Coviello[8], Pierangela De Biasio[9], Davide Ceresa[10], Paolo Malatesta[1,10], Pierluigi Mauri[6], Rodolfo Quarto[1,10], Chiara Gentili[1], Lucio Barile[4,11,12] and Sveva Bollini[1]**

[1]Experimental Biology Unit, Department of Experimental Medicine (DIMES), University of Genova, Genova, Italy, [2]Laboratory of Cellular and Molecular Cardiology, Istituto Cardiocentro Ticino, Ente Ospedaliero Cantonale, Lugano, Switzerland, [3]Center for Molecular Cardiology, University of Zurich, Zurich, Switzerland, [4]Laboratories for Translational Research, Ente Ospedaliero Cantonale, Bellinzona, Switzerland, [5]Molecular Pathology Unit, IRCCS Ospedale Policlinico San Martino, Genova, Italy, [6]Proteomics and Metabolomics Unit, Institute for Biomedical Technologies (ITB-CNR), Milan, Italy, [7]Fetal Medicine and Surgery Unit, IRCCS Istituto Giannina Gaslini, Genova, Italy, [8]Laboratory of Human Genetics, IRCCS Istituto Giannina Gaslini, Genova, Italy, [9]Prenatal Diagnosis Perinatal Medicine Unit, IRCCS Ospedale Policlinico San Martino, Genova, Italy, [10]Cellular Oncology Unit, IRCCS Ospedale Policlinico San Martino, Genova, Italy, [11]Laboratory for Cardiovascular Theranostics, Istituto Cardiocentro Ticino, Ente Ospedaliero Cantonale, Lugano, Switzerland, [12]Faculty of Biomedical Sciences, Università Svizzera Italiana, Lugano, Switzerland*

OPEN ACCESS

Edited by:
Antonietta Rosa Silini, Fondazione Poliambulanza Istituto Ospedaliero, Italy

Reviewed by:
Valeria Chiono, Polytechnic University of Turin, Italy
Assunta Pandolfi, University of Studies G.d'Annunzio Chieti and Pescara, Italy

***Correspondence:**
Sveva Bollini
sveva.bollini@unige.it

Specialty section:
This article was submitted to Tissue Engineering and Regenerative Medicine, a section of the journal Frontiers in Bioengineering and Biotechnology

Received: *22 March 2022*
Accepted: *27 April 2022*
Published: *08 June 2022*

Citation:
Costa A, Balbi C, Garbati P, Palamà MEF, Reverberi D, De Palma A, Rossi R, Paladini D, Coviello D, De Biasio P, Ceresa D, Malatesta P, Mauri P, Quarto R, Gentili C, Barile L and Bollini S (2022) Investigating the Paracrine Role of Perinatal Derivatives: Human Amniotic Fluid Stem Cell-Extracellular Vesicles Show Promising Transient Potential for Cardiomyocyte Renewal. Front. Bioeng. Biotechnol. 10:902038. doi: 10.3389/fbioe.2022.902038

Cardiomyocyte renewal represents an unmet clinical need for cardiac regeneration. Stem cell paracrine therapy has attracted increasing attention to resurge rescue mechanisms within the heart. We previously characterized the paracrine effects that human amniotic fluid–derived stem cells (hAFSC) can exert to provide cardioprotection and enhance cardiac repair in preclinical models of myocardial ischemia and cardiotoxicity. Here, we analyze whether hAFSC secretome formulations, namely, hAFSC conditioned medium (hAFSC-CM) over extracellular vesicles (hAFSC-EVs) separated from it, can induce cardiomyocyte renewal. c-KIT+ hAFSC were obtained by leftover samples of II trimester prenatal amniocentesis (fetal hAFSC) and from clinical waste III trimester amniotic fluid during scheduled C-section procedures (perinatal hAFSC). hAFSC were primed under 1% O_2 to enrich hAFSC-CM and EVs with cardioactive factors. Neonatal mouse ventricular cardiomyocytes (mNVCM) were isolated from cardiac tissue of R26pFUCCI2 mice with cell cycle fluorescent tagging by mutually exclusive nuclear signal. mNVCM were stimulated by fetal versus perinatal hAFSC-CM and hAFSC-EVs to identify the most promising formulation for *in vivo* assessment in a R26pFUCCI2 neonatal mouse model of myocardial infarction (MI) *via* intraperitoneal delivery. While the perinatal hAFSC secretome did not provide any significant cardiogenic effect, fetal hAFSC-EVs significantly sustained mNVCM transition from S to M phase by 2-fold, while triggering cytokinesis by 4.5-fold over vehicle-treated cells. Treated mNVCM showed disorganized expression of cardiac alpha-actinin, suggesting cytoskeletal re-

arrangements prior to cell renewal, with a 40% significant downregulation of *Cofilin-2* and a positive trend of polymerized F-Actin. Fetal hAFSC-EVs increased cardiomyocyte cell cycle progression by 1.8-fold in the 4-day-old neonatal left ventricle myocardium short term after MI; however, such effect was lost at the later stage. Fetal hAFSC-EVs were enriched with a short isoform of Agrin, a mediator of neonatal heart regeneration acting by YAP-related signaling; yet *in vitro* application of YAP inhibitor verteporfin partially affected EV paracrine stimulation on mNVCM. EVs secreted by developmentally juvenile fetal hAFSC can support cardiomyocyte renewal to some extension, *via* intercellular conveyance of candidates possibly involving Agrin in combination with other factors. These perinatal derivative promising cardiogenic effects need further investigation to define their specific mechanism of action and enhance their potential translation into therapeutic opportunity.

Keywords: perinatal derivatives, human amniotic fluid stem cells, extracellular vesicles, secretome, paracrine effects, myocardial renewal, regenerative medicine

1 INTRODUCTION

Cardiac disease can arise from alterations in the heart structure and function, such as myocardial infarction (MI), chemotherapy-derived cardiotoxicity, and congenital heart defects, all progressively leading to heart failure. The main challenge related to MI is the loss of functional contractile cardiomyocytes during a prolonged ischemic insult. Regenerative therapies aiming at promoting cell cycle re-entry and proliferative activity of resident cardiomyocytes have been broadly explored to overcome the challenge of defective myocardial repair following injury. Targeting myocardial renewal to enhance adult cardiomyocyte proliferation represents an unmet clinical need for modern cardiac regenerative medicine. Alternative approaches have been based by either analyzing in details molecular mechanisms regulating cardiomyocyte division during proficiently active developmental cardiogenesis, to much more unresponsive postnatal and adult stages, or by applying exogenous stimulation to resurge their embryonic proliferative potential. While adult mammalian cardiomyocytes show a very limited—and therapeutically irrelevant—renewal potential during adulthood (Cabrol et al., 1989; Bergmann et al., 2009), the neonatal murine heart presents remarkable regenerative activity after injury within the very first days from birth. Nevertheless, such significant renewal potential suffers a sharp decline, starting as soon as postnatal day 4 (P4) to become completely downregulated by postnatal day 7 (P7). Indeed, the 7-day-old (P7) mouse pup represents the limit of the neonatal cardiac regenerative window, being more similar to the adult heart in activating defective cardiac repair over restorative myocardial renewal (Porrello et al., 2011, 2013; Lam and Sadek, 2018). Mature cardiomyocytes seem to experience a sort of "memory loss" in their embryonic/postnatal mechanisms driving active proliferation. Therefore, defining a feasible approach to "rejuvenate" cardiomyocyte renewal program by *ad hoc* stimulation would represent a major goal in translational cardiac regenerative medicine.

In this scenario, stem- and progenitor cell–based strategies have been implemented to stimulate endogenous mechanism of cardiac regeneration *via* paracrine stimulation. Mesenchymal stromal progenitor cells obtained from leftover samples of human amniotic fluid (namely, human amniotic fluid–derived stem cells, hAFSC) are perinatal derivatives with attractive features for tissue repair. In recent years, hAFSC have been proposed as potential therapeutics given the encouraging evidence obtained by their application in several experimental disease settings (Borlongan, 2017; Loukogeorgakis and De Coppi, 2017; Bollini et al., 2018; Narakornsak et al., 2019; Fang et al., 2020). Ethical concerns associated with their isolation are minimal, since they can be easily obtained from either leftover sample from II trimester prenatal diagnosis *via* routine amniocentesis (fetal hAFSC) or from III trimester clinical waste amniotic fluid during scheduled cesarean delivery at term (perinatal hAFSC). Moreover, their remarkable high self-renewal potential and capacity to withstand long-term cryopreservation support them as appealing candidate source for regenerative medicine. Notably, hAFSC have been shown to sustain tissue recovery by exerting proliferative, anti-inflammatory, and trophic influence. The relevant paracrine effects of the fetal hAFSC secretome (namely the total amount of soluble factors that cells can secrete in their culture medium, i.e., the cell-conditioned medium, hAFSC-CM), including their released membrane-derived extracellular vesicles (hAFSC-EVs) have been assessed in preclinical models of injury, as comprehensively reviewed in Costa et al. (2022). Indeed, the emphasis on mesenchymal stromal cell–based therapy has moved toward the profiling of their secreted EVs, since they have been generally described to convey enriched trophic factors and regulating RNAs orchestrating intercellular communication and have a functional impact on target cells. This has been the case for hAFSC-EVs as well. In particular, our group has comprehensively profiled the cardioprotective potential of fetal hAFSC. We have demonstrated that fetal hAFSC secretome formulations administered in preclinical murine models of disease soon after ischemic myocardial injury (i.e., MI) or cardiotoxic insult (i.e., by means of exposure of the anthracycline drug doxorubicin), resulted in long-lasting paracrine effects preserving resident cardiomyocyte viability,

while limiting fibrosis, improving local angiogenesis, rescuing cardiac function, and enhancing cardiac endogenous antioxidant defense (Lazzarini et al., 2016; Balbi et al., 2019a; Villa et al., 2021).

In this study, we wanted to investigate whether the hAFSC secretome could also exert significant cardiogenic effects, in addition to the relevant cardioprotective potential we have already observed. Since hAFSC represent "developmentally juvenile" progenitors, paracrine stimulation by their secretome may counteract postnatal loss of myocardial renewal and unlock cardiomyocyte proliferative memory. Here, we consider investigating the cardioactive influence of hAFSC secretome in the responsive neonatal murine heart model, by using a transgenic mouse with genetically driven fluorescent tracing of the different cell cycle phases based on FUCCI (fluorescent ubiquitylation–based cell cycle indicator) technology (Abe et al., 2013). While fetal hAFSC and their cardioprotective effects have been broadly characterized, a putative cardio-proliferative role of the perinatal hAFSC counterpart has not yet been defined. Hence, in order to provide comprehensive profiling of the myocardial renewal potential of the different hAFSC secretome formulations (hAFSC-CM and hAFSC-EVs), we have compared more immature II trimester fetal hAFSC, obtained from prenatal screening, over III trimester perinatal hAFSC obtained at term, in order to identify the most suitable perinatal derivative for future translational studies.

2 MATERIALS AND METHODS

2.1 R26pFUCCI2 Mouse Model

R26pFUCCI2 mice [(CDB0203T) http:www.clst.riken.jp/arg/reporter_mice.html], first described in Abe et al. (2013), were obtained following MTA (material transfer agreement) with Dr. Yasuhide Furuta, RIKEN Center for Life Science Technologies and provided as courtesy of Prof. Shrinivas Shankar and Prof. Paul Riley from University of Oxford, United Kingdom. FUCCI (fluorescent ubiquitylation–based cell cycle indicator) technology allows the discrimination of cell cycle phases (G1 versus S/G2/M) by dual color imaging *via* a nuclear fluorescent signal. R26pFUCCI mice constitutively express *mCherry-hCdt1* and *mVenus-hGeminin* constructs as a single transgene under the Rosa26 promoter. Cdt1, chromatin licensing and DNA replication factor 1, is a key regulator in the assembly of pre-DNA replication complexes in the G1 phase, and it is controlled during the S phase by the protein Geminin, which inhibits it, thus guaranteeing that DNA is replicated only once in each cell cycle (Wohlschlegel et al., 2000). Therefore, this transgenic model licenses the distinction between cells in the G1 phase, as labeled with mCherry fluorescent red nuclear expression, from those transitioning through the S phase into mitosis by the mVenus green nuclear signal (Abe et al., 2013). Mice were housed and maintained in a controlled environment in the Animal Facility at IRCCS Ospedale Policlinico San Martino, Genova, Italy, according to International Standards of Animal Welfare, as ruled by the Italian Ministry of Health (DM.146/2009-A). Animal maintenance, handling, and all procedures were performed in strict compliance to all applicable international, national, and/or institutional guidelines for the care and use of animals (D. Lgs. 26/2014, D. Lgs. 116/92, legislative transposition of Directive 2010/63/EU of European Parliament and of Council of 22 September 2010). Heterozygous R26pFUCCI2$^{+/-}$ mice were obtained from crossing R26pFUCCI2$^{+/-}$ males with wild-type C57Bl6/J or FVB females, according to specific animal license authorization (62/2019-PR and 230/2019-PR from the Italian Ministry of Health). Mice genotype was assessed using the Phire Tissue Direct PCR Master Mix (Thermo Fisher Scientific), following manufacturer's instructions. Primer sequences are available on request.

2.2 *In vitro* Cell Culture

2.2.1 Human Amniotic Fluid-Stem Cell Isolation and *in vitro* Culture

Human amniotic fluid stem cells (hAFSC) were isolated from leftover samples of human amniotic fluid (hAF) collected during routine amniocentesis at II trimester gestation for prenatal screening (fetal hAFSC), or as clinical waste material (perinatal hAFSC) from scheduled cesarean section delivery in the III trimester, from the Prenatal Diagnosis Perinatal Medicine Unit, IRCCS Ospedale Policlinico San Martino, from the Fetal and Perinatal Medical and Surgery Unit, and from the Human Genetics Laboratory, IRCCS Istituto Giannina Gaslini Hospital, in Genova, Italy. All donors provided informed written consent for research use of the leftover hAF specimen, according to authorization previously granted from the local ethical committee (P.R. 428REG 2015) and in compliance with Helsinki Declaration guidelines. II trimester fetal hAF samples were obtained from female donors with average age of 38.30 ± 0.40 years old (n = 32); III trimester perinatal hAF samples were obtained from female donors with average age of 34.25 ± 1.31 years old (n = 10). Clusters of adherent mesenchymal stromal cells (MSC) were obtained from hAF samples (hAF-MSC). hAF-MSC expressing normal karyotype were further processed by immunomagnetic sorting for c-KIT expression (CD117 MicroBead Kit, Miltenyi Biotechnology) to obtain c-KIT$^+$ hAFSC, as previously reported (Lazzarini et al., 2016; Balbi et al., 2017, 2019b; Costa et al., 2021; Villa et al., 2021). c-KIT$^+$ hAFSC (here indicated as hAFSC) were cultured in the minimal essential medium (MEM)-alpha with 15% fetal bovine serum (FBS, Gibco—Thermo Fisher Scientific), 18% Chang B and 2% Chang C medium (Irvine Scientific), 1% l-glutamine, and 1% penicillin/streptomycin (Gibco—Thermo Fisher Scientific) in incubator at 37°C with 5% CO_2 and 20% O_2 atmosphere. hAFSC were cultured up to five passages *in vitro* before being primed to isolate their secretome.

2.2.2 Mouse Neonatal Ventricular Cardiomyocyte Isolation and Culture

Primary cultures of R26pFUCCI2 neonatal mouse ventricular cardiomyocytes (mNVCM) were obtained from 1-day-old murine heart tissue. Neonatal mice were obtained by crossing R26pFUCCI2$^{+/-}$ males with wild-type FVB females (according to authorization n. 62/2019-PR). mNVCM were isolated by enzymatic digestion with papain and thermolysin enzymes

using the Pierce Primary Cardiomyocyte Isolation Kit (Thermo Fisher Scientific), following manufacturer's instructions. Primary R26pFUCCI2$^{+/-}$ mNVCM were seeded at density of 0.25×10^6 cells/cm^2 on either an 8-well-PCA (PolyCycloAlkanes) detachable chamber slide (Sarsted, Germany) or on a 24-well plate coated with a 0.2% gelatin (Sigma-Aldrich) and fibronectin (1:1000 dilution) solution. mNVCM were cultured in DMEM for primary cell (Thermo Fisher Scientific) with 10% heat-inactivated fetal bovine serum, (FBS, Gibco—Thermo Fisher Scientific) and 1% penicillin/streptomycin (Gibco—Thermo Fisher Scientific) in incubator at 37°C with 5% CO_2 and 20% O_2 atmosphere.

2.3 Isolation and Concentration of hAFSC Secretome Formulations

Fetal and perinatal hAFSC were seeded at 2,000 cells/cm^2 in T-75 and T-150 tissue-culture flasks (Eppendorf). Cells were cultured *in vitro* under normoxic (20% O_2, 5% CO_2 at 37°C) or hypoxic (1% O_2, 5% CO_2 at 37°C) conditions in CellXpert® C170i and Galaxy® 48R CO_2 Eppendorf incubators for 24 h in a serum-free medium (SF: high glucose DMEM, supplemented with 1% l-glutamine and 1% penicillin/streptomycin, Gibco—Thermo Fisher Scientific), as a priming strategy to enhance the secretion of cardioactive paracrine factors, as we previously reported (Lazzarini et al., 2016; Balbi et al., 2017, 2019b; Costa et al., 2021; Villa et al., 2021). Fetal and perinatal hAFSC–conditioned medium (fetal and perinatal hAFSC-CM) was collected, centrifuged at 300 × g for 10 min and 2,000 × g for 20 min to remove cell debris, and further concentrated by means of ultrafiltration using 3 kDa selective cutoff membranes (Amicon Ultra-15, Millipore) at 3,000 × g for 90 min.

hAFSC-EVs were separated and concentrated by serial ultracentrifugation from hAFSC-CM. In brief, hAFSC-CM was centrifuged at 10,000 × g for 40 min; pellet was then discarded, and the liquid phase was further processed by ultracentrifugation in an Optima L-90K at 100,000 × g for 120 min using a swinging-bucket SW55Ti rotor (all Beckmann Coulter). The pellet containing the separated and concentrated hAFSC-EVs was then washed in phosphate-buffered saline (1X PBS) solution by a final step of centrifugation at 100,000 × g for 120 min and then resuspended in 0.22 µm filtered 1X PBS. Concentration of proteins within hAFSC-CM and on hAFSC-EV surface was assessed using the bicinchoninic acid (BCA) assay (Thermo Fisher Scientific); the albumin (BSA) solution provided by the manufacturer was diluted in PBS to prepare protein standards with defined concentration (5, 25, 50, 125, and 250 µg/ml) to set the reference calibration curve for a specific working range hAFSC secretome formulations, and the control SF vehicle medium were diluted in PBS and incubated with the BCA working reagent solution, according to the manufacturer's instruction. Samples were acquired on a Gen5 Microplate Reader (Agilent Technologies) at wavelength 570 nm to evaluate hAFSC-CM and hAFSC-EV yield. A nanoparticle tracking analysis (NTA) on hAFSC secretome formulations was performed on the ZetaView analyzer (Particle Metrix) in order to assess EV particle amount in the secretome dosage used for the *in vitro* experiments.

2.4 *In vitro* Stimulation of mNVCM by Fetal Versus Perinatal hAFSC Secretome Formulations

Isolated R26pFUCCI2 mNVCM were seeded as 0.25×10^6 cells/cm^2 on 8-well-PCA detachable chamber slides (Sarsted, Germany), corresponding to 200,000 mNVCM in 200 µl of media per well. Furthermore, 48 h after seeding, cells were stimulated by 80 µg/ml fetal or perinatal hAFSC-CM or by 5 µg/ml fetal or perinatal hAFSC-EVs for further 48 h in SF conditions (DMEM for primary cell with 1% penicillin/streptomycin, all Gibco—Thermo Fisher Scientific). Vehicle solution (SF medium) was considered as control condition (Ctrl) treatment. The hAFSC secretome dosage employed for these experiments was based on our previous findings about their stimulatory potential (Balbi et al., 2019a; 2019b) further details are available on request. In each well, mNVCM were treated with 16 µg hAFSC-CM or 1 µg hAFSC-EVs in 200 µl SF final medium volume. The hAFSC-CM and hAFSC-EV dosages were enriched with a comparable amount of EV particles (hAFSC-CM: $5.82 \times 10^8 \pm 4.43 \times 10^8$ particles; hAFSC-EVs: $8.19 \times 10^8 \pm 1.60 \times 10^8$ particles, $p > 0.05$, **Supplementary Figure S1A**). Schematic of *in vitro* experimental design is reported in **Supplementary Figure S1B**. Cardiomyocyte cell cycle progression was evaluated 72 h after hAFSC secretome stimulation by immunostaining. A FUCCI nuclear signal was correlated with expression of cardiomyocyte-specific sarcomeric markers (cardiac alpha-actinin and cardiac troponin I); mNVCM were fixed in 4% paraformaldehyde (PFA) solution (Sigma Aldrich) and then incubated with a primary antibody against GFP (green fluorescent protein, ab13970, Abcam) followed by Alexa Fluor 488–conjugated secondary antibody (A-11039, Thermo Fisher Scientific) to enhance the mVenus probe signal, indicating progression through S up to M phases, and with an anti-sarcomeric cardiac alpha-actinin primary antibody (αAct, ab9465, Abcam) followed by Alexa Fluor 594–conjugated secondary antibody (A-11032, Thermo Fisher Scientific). To detect cytokinetic events, a primary antibody against Aurora B kinase, a chromosomal passenger protein binding to protein involved in cleavage furrow and midbody formation, (AuBK, ab2254, Abcam) followed by Alexa Fluor 647–conjugated secondary antibody (A-32733, Thermo Fisher Scientific) was used. The paracrine potential of fetal versus perinatal hAFSC-CM and hAFSC-EVs to support cardiomyocyte cell cycle progression was assessed as the percentage of αAct-positive cells (mNVCM) expressing nuclear mVenus signal (as enhanced by anti-GFP antibody) over the total αAct-positive cells by counting at least five independent fields in each condition at ×20 magnification. Cytokinesis events were detected as percentage of αAct-positive cells (mNVCM) expressing Aurora B kinase localizing at the mid-body by counting at least five independent fields in each condition at ×40 magnification. In a second set of experiments, R26pFUCCI2$^{+/-}$ mNVCM were treated with a YAP pathway inhibitor [10 µM Verteporfin solution, Tocris, as from (Bassat et al., 2017)] prior to hAFSC secretome stimulation. R26pFUCCI2 mNVCM were treated with or without YAP inhibitor in the SF medium for 48 h and treated

with 5 μg/ml hAFSC-EVs (corresponding to 1 μg hAFSC-EVs for 200,000 mNVCM in 200 μl of final medium volume) for further 48 h (as illustrated in schematic in **Supplementary Figure S1C**) in the SF medium. mNVCM were analyzed at 72 h posttreatment. mNVCM were fixed in 4% paraformaldehyde solution (Sigma Aldrich) and incubated with primary antibody against GFP (ab13970, Abcam) followed by Alexa Fluor488–conjugated secondary antibody (A-11039, Thermo Fisher Scientific) and with anti-cardiac troponin I primary antibody (TnI, ab47003, Abcam) followed by Alexa Fluor 647–conjugated secondary antibody (A-32733, Thermo Fisher). Immunostaining images were acquired on an Axiovert microscope equipped with Axiovision software (Carl Zeiss). Signal intensity was analyzed and measured with ImageJ software [https://imagej.nih.gov/ij/, (ImageJ, 2021)]. Cardiomyocyte cell cycle progression was assessed as the percentage of cTnI-positive cells (mNVCM) expressing a nuclear mVenus signal (as enhanced *via* anti-GFP antibody) over the total cTnI-positive cells by counting at least five independent fields in each condition at ×20 magnification.

2.5 Gene Expression Profile of mNVCM

The gene expression profile of R26pFUCCI2$^{+/-}$ mNVCM stimulated by hAFSC secretome over vehicle solution-treated cells as control was investigated using real-time qRT-PCR. mNVCM were seeded on 24-well plate as 500,000 cells/well and then stimulated by 5 μg/ml hAFS-EVs (corresponding to 2 μg per well in 400 μl of final medium volume). Total RNA from mNVCM stimulated with hAFSC secretome over vehicle-treated ones was extracted using the Qiazol Lysis Reagent (Qiagen), according to manufacturer's indications. cDNA was obtained by using the iScript Reverse Transcription Supermix for RT-qPCR (Bio-Rad). Real-time qRT-PCR was carried out on a 7500 Fast Real-Time PCR System (Applied Biosystems) using the Syber Green Master Mix (BrightGreen 2X qPCR, Abm). The following primer sequences were used: mouse *cofilin-2* (*Cfl2*, forward: 5′-CCGACCCCTCCTTCTTCT CG-3′ and reverse: 5′-GTAACTCCAGATGCCATAGTG C-3′) and mouse *beta-2 microglobulin* as a housekeeping reference (*β2M*, forward: 5′-CTGCTACGTAACACAGTTCCA CCC-3′ and reverse: 5′-CAT GATGCTTGATCACATGTCTCG-3′). *Cfl2* expression was evaluated by means of the 2^{-ddCt} method with vehicle solution–treated control mNVCM (Ctrl) as a calibrator.

2.6 Evaluation of F-Actin and G-Actin in mNVCM

To investigate mNVCM cytoskeleton re-arrangement following stimulation with the hAFSC secretome over vehicle solution as control, the amount of polymerized F-Actin over monomeric G-Actin was analyzed as indication of cardiomyocyte cell cycle progression (Torrini et al., 2019). mNVCM were seeded on a 24-well plate as 500.000 cells/well, which were then stimulated by 5 μg/ml hAFSC-EVs (corresponding to 2 μg per well in 400 μl of medium final volume). The F-Actin/G-Actin *In Vivo* Assay Biochem Kit (Cytoskeleton) was used as per manufacturer's instructions. mNVCM proteins were boiled with Laemmli SDS sample buffer 6x (VWR International), separated on 4–20% Mini-PROTEAN®TGX™ Precast Gel, and transferred onto a polyvinylidene difluoride (PVDF) membrane with a semi-dry transfer system (all from Bio-Rad). Membrane were incubated with F-Actin/G-Actin antibody provided in the assay and then with IRDye® 800CW goat anti-rabbit secondary antibody (LI-COR Biosciences). Infrared signals were detected using the Odyssey CLx Detection System (LI-COR Biosciences). Quantification was performed using an Odyssey CLx analyzer (LI-COR Biosciences).

2.7 Analysis of hAFSC Secretome Cardioactive Potential in a Preclinical Neonatal Mouse Model of Myocardial Infarction

Transgenic R26pFUCCI2 neonatal mice were obtained by crossing heterozygous R26pFUCCI$^{+/-}$ males with C57Bl6/J wild-type females. 4-day-old (P4) and 7-day-old (P7) R26pFUCCI2 pups were used for *in vivo* experiments in strict compliance with national and European international standards of animal care and according to required authorization from the Italian Ministry of Health (authorization n. 230/2019-PR). The preclinical mouse model of myocardial infarction (MI) was performed according to Del Campo et al. (2022). In brief, neonatal mice were anesthetized under analgesia by an initial step of inhalation of 3% isoflurane in oxygen, followed by exposure to a short period of controlled hypothermia. MI was performed by permanent ligation of the left anterior descending coronary artery (LAD). In the sham control group (Sham MI) animals underwent the same surgical procedure without coronary artery ligation. In treated mice, soon after coronary ligation, 4.5 μg fetal hAFSC-EVs in 20 μl of 1X PBS solution (fetal hAFSC-EVs) versus an equal volume of vehicle solution (1X PBS, Ctrl) were administered by intraperitoneal injections. The indicated hAFSC-EV dosage was based on our previous findings (Balbi et al., 2019a). Hearts were harvested after 3 and 7 days from MI, and the three experimental groups were assessed by histological and immunostaining analyses (Sham MI: $n = 4$ for each stage and time point analysis; fetal hAFSC-EVs: $n = 8$ for each stage and time point analysis; Ctrl: $n = 8$ for P4 pups at day 3 and day 7; fetal hAFSC-EVs: $n = 8$ for P7 at day3; Ctrl: $n = 9$ for P7 pups at day 3; $n = 8$ for P7 pups at day 3 and day 7). Cardiac tissue was fixed in 4% paraformaldehyde (PFA) solution, incubated in a 30% sucrose–PBS solution overnight, and snapped-frozen in liquid nitrogen for cryo-sectioning. Furthermore, 6-μm cryo-sections were processed for hematoxylin and eosin staining to confirm myocardial injury. Immunostaining was performed to evaluate resident cardiomyocytes re-entering the cell cycle by using the primary antibody against cardiac troponin I (cTnI, ab47003, Abcam) followed by Alexa Fluor 647–conjugated secondary antibody (A-32733, Thermo Fisher Scientific), together with a primary antibody against green fluorescent protein (GFP, ab13970, Abcam) followed by Alexa Fluor 488–conjugated secondary antibody (A-11039, Thermo Fisher Scientific) to enhance the mVenus nuclear signal. Immunostaining images were acquired on an Axiovert microscope equipped with Axiovision software (Carl Zeiss).

Signal intensity was analyzed and measured with ImageJ software [https://imagej.nih.gov/ij/, (ImageJ, 2021)]. mVenus-positive and cTnI-positive resident cells (S-M phase cardiomyocytes) were evaluated as cells/field by counting at least five independent fields for each tissue section at ×20 magnification.

2.8 Characterization of hAFSC-EVs

2.8.1 Bioinformatic Analysis of miRNA Profile

Bioinformatic analysis of miRNA predicted targets was performed on RNA sequencing data obtained from the comprehensive fetal hAFSC-EV profiling previously performed (Costa et al., 2021); results of multiple sources were aggregated using the miRNAtap R package (Package "miRNAtap", 2022 Title miRNAtap: microRNA Targets-Aggregated Predictions, 2022).

2.8.2 Western Blotting

Total protein from hAFSC-EVs was extracted by lysing samples with ice-cold RIPA (radioimmunoprecipitation assay) buffer supplemented with SIGMA FAST™ Protease Inhibitors and Phosphatase Inhibitor Cocktail 3 and 2 (all from Sigma). Total protein concentration was determined using the QuantiPro™ BCA Assay Kit (Sigma). Proteins were boiled with Laemmli SDS sample buffer 6x (VWR International), separated on 4–20% Mini-PROTEAN®TGX™ Precast Gel, and transferred onto a PVDF membrane with a semi-dry transfer system (all from Bio-Rad Europe).

hAFSC-EVs were characterized for the expression of canonical markers of small EVs. Membranes were incubated with rabbit anti-TSG101 (Tumor Susceptibility Gene 101) antibody (ab125011, Abcam); rabbit anti-Syntenin-1 antibody (ab19903, Abcam) and rabbit anti-ALIX (ALG-2-interacting protein X) antibody (ab186429, Abcam). A rabbit anti-GRP94 (Glucose-Regulated Protein 94) antibody (ab238126, Abcam) was used as contamination control. Agrin (Agrn) protein expression was investigated in fetal and perinatal hAFSC and in their corresponding secreted EVs. As normalizing control, Syntenin-1 was considered as small EV reference marker (Kugeratski et al., 2021). Membranes were incubated with primary rabbit anti-Agrin antibody (ab85174, Abcam) and primary rabbit anti-Syntenin-1 antibody (ab133267, Abcam). Membranes were following incubated with IRDye® 800CW goat anti-rabbit secondary antibody (LI-COR Biosciences, Lincoln, Nebraska, United States). Infrared signal was detected using Odyssey CLx Detection System (LI-COR Biosciences). Quantification was performed using Odyssey CLx analyzer (LI-COR Biosciences).

2.8.3 Flow Cytometry Analysis

The presence of CD9, CD81 and CD63 tetraspanin antigens on hAFSC-EV surface was also evaluated by flow cytometry, according to the protocol optimized by (Gorgun et al., 2019). Fetal and perinatal hAFSC-EVs were labeled with the lipophilic fluorescent dye CFSE (CFSE: Vybrant CFDA SE Cell Tracer Kit, Invitrogen) according to the manufacturer's instructions in combination with one of the following fluorochrome-conjugated antibodies for 15 min at room temperature: PE-Cy7™-conjugated mouse anti-human CD63; PE-conjugated mouse anti-human CD9; BV421-conjugated mouse anti-human CD81; PE-Cy7™-conjugated mouse IgG1 κ and PE-mouse IgG1, Clone 40 isotype controls (all BD Biosciences). Fetal and perinatal hAFSC-EVs (n = 3) were analyzed on a BD FACSAria II equipped with three lasers (405, 488 and 640 nm) and data analyzed by FACSDiva software, v8.0 (all BD Biosciences). Instrument setting was defined by using a mixture of fluorescent beads of varying diameters [Megamix-Plus FSC and Megamix-Plus SSC (BioCytex)] following manufacturer's instructions.

2.9 Statistical Analyses

All values are presented as mean ± s.e.m. (standard error of mean) of at least three (n = 3) independent experiments. Comparisons were drawn by one-way ANOVA followed by *post hoc* Tukey's multiple comparisons test for mNVCM stimulation or by t-Test when comparing fetal versus perinatal hAFSC-CM/EVs. Statistical analysis was performed using GraphPad Prism Version 8.0.2 (GraphPad Software) with statistical significance set at $^*p < 0.05$.

3 RESULTS

3.1 Fetal hAFSC-EVs Sustain mNVCM Cell Cycle Re-Entry and Renewal *in vitro*

The myocardial renewal potential of the fetal versus perinatal hAFSC-CM and hAFSC-EV formulations was first evaluated *in vitro* by stimulating R26pFUCCI2$^{+/-}$ mNVCM with 80 μg/ml of hAFSC-CM and 5 μg/ml of hAFSC-EVs over vehicle control solution (Ctrl, SF medium). Primary culture of R26pFUCCI2$^{+/-}$ mNVCM showed 70% enrichment of sarcomeric alpha-actinin (αAct)-positive cardiomyocytes over contaminating cardiac cells (i.e., cardiac fibroblasts, epicardial and endothelial cells as obtained from enzymatic digestion of the neonatal heart). mNVCM were evaluated by immunostaining as the percentage of αAct-positive cells with mVenus probe nuclear signal as engaging of cell cycle activity from phase S up to M, (**Figure 1A** and corresponding **Supplementary Figure S2**). While stimulation by the fetal hAFSC-CM resulted in a positive trend in the proportion of mNVCM re-entering the cell cycle, fetal hAFSC-EVs induced a significant 2.0-fold increase ($^*p < 0.05$) in the progression into M phase, when compared to untreated cells (Ctrl). On the contrary, the secretome formulations obtained from the more mature perinatal hAFSC did not exert relevant cardiogenic effect.

We then evaluated the expression of Aurora B kinase (AuBK) enzyme, a mitotic checkpoint for appropriate chromosome segregation during cell proliferation. We noticed that regardless the treatment received, the great majority (i.e., from 88% up to 94%) of mNCVM with mVenus nuclear also co-expressed AuBK within the nucleus (**Figure 1B**). Localization of AuBK in well-developed cleavage furrow and at middle stage midbody in between mNVCM was then analyzed as indication of commitment to cytokinesis and cell division; a 4.5-fold increase in the percentage of mNVCM

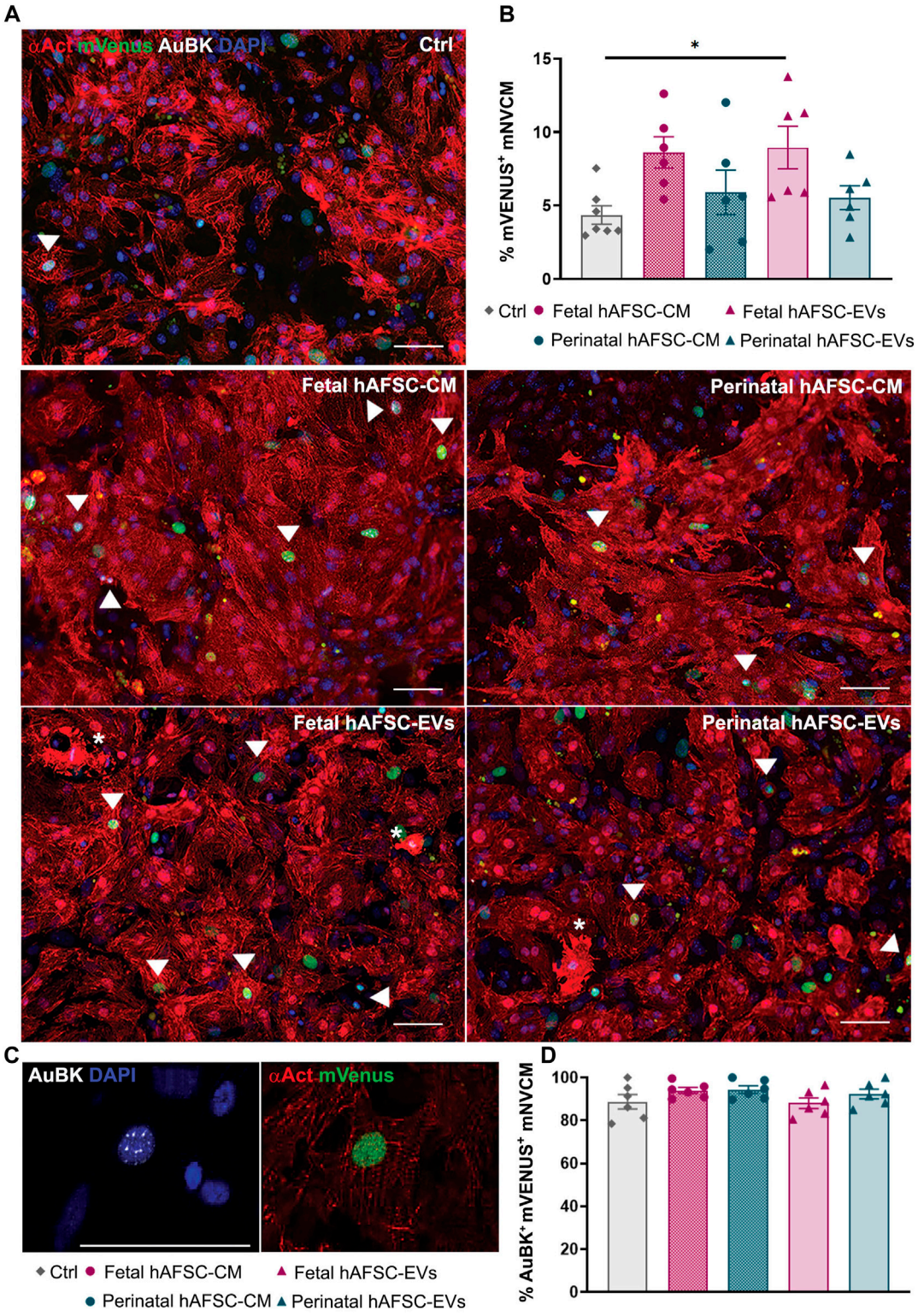

FIGURE 1 | *In vitro* mNVCM cell cycle re-entry following stimulation by fetal versus perinatal hAFSC secretome formulations. **(A)** Representative images of R26pFUCCI2$^{+/-}$ mNVCM in vehicle-treated control conditions (SF medium, Ctrl) or following treatment with fetal or perinatal hAFSC-CM or hAFSC-EVs by immunostaining for sarcomeric alpha-actinin (αAct, red), mVenus-Geminin (mVenus, green), Aurora B kinase (AuBK, white), and DAPI (blue), scale bar: 50 μm. White arrows point at αAct-positive cells (mNVCM) with mVenus nuclear signal; white asterisks indicate mNVCM with disarranged α-actinin expression as sarcomeric disassembly feature. **(B)** Analysis of mVenus-positive and αAct-positive cells (mVenus^{+} mNVCM) expressing αAct cells following stimulation with fetal or perinatal hAFSC

(*Continued*)

FIGURE 1 | secretome formulations over vehicle-treated cells (Ctrl). All values are expressed as mean ± s.e.m percentage mVenus-positive and αAct-positive cells (% mVenus$^+$ mNVCM) of independent experiments (Ctrl: 4.36 ± 0.62%, n = 7; fetal hAFSC-CM: 8.62 ± 1.06%, n = 6; perinatal hAFSC-CM: 5.90 ± 1.51%, n = 6; fetal hAFSC-EVs: 8.95 ± 1.45%, n = 6; perinatal hAFSC-EVs: 5.54 ± 0.80%, n = 6; *p = 0.0455). **(C)** Representative image of nuclear AuBK expression co-localizing with mVenus signal in αAct-positive cells (mNVCM); scale bar: 50 μm. **(D)** Evaluation of mVenus-positive and αAct-positive cells showing AuBK nuclear signal (AuBK$^+$ mVenus$^+$ mNVCM) following stimulation with fetal versus perinatal hAFSC secretome formulations over vehicle-treated control condition (Ctrl). All values are expressed as mean ± s.e.m. percentage of AuBK-positive and mVenus-positive mNVCM (%AuBK$^+$ mVenus$^+$ mNVCM) of n = 6 independent experiments (Ctrl: 88.73 ± 3.39%; fetal hAFSC-CM: 93.99 ± 1.44%; perinatal hAFSC-CM: 94.37 ± 1.76%; fetal hAFSC-EVs: 88.06 ± 2.50%; perinatal hAFSC-EVs: 92.26 ± 2.23%).

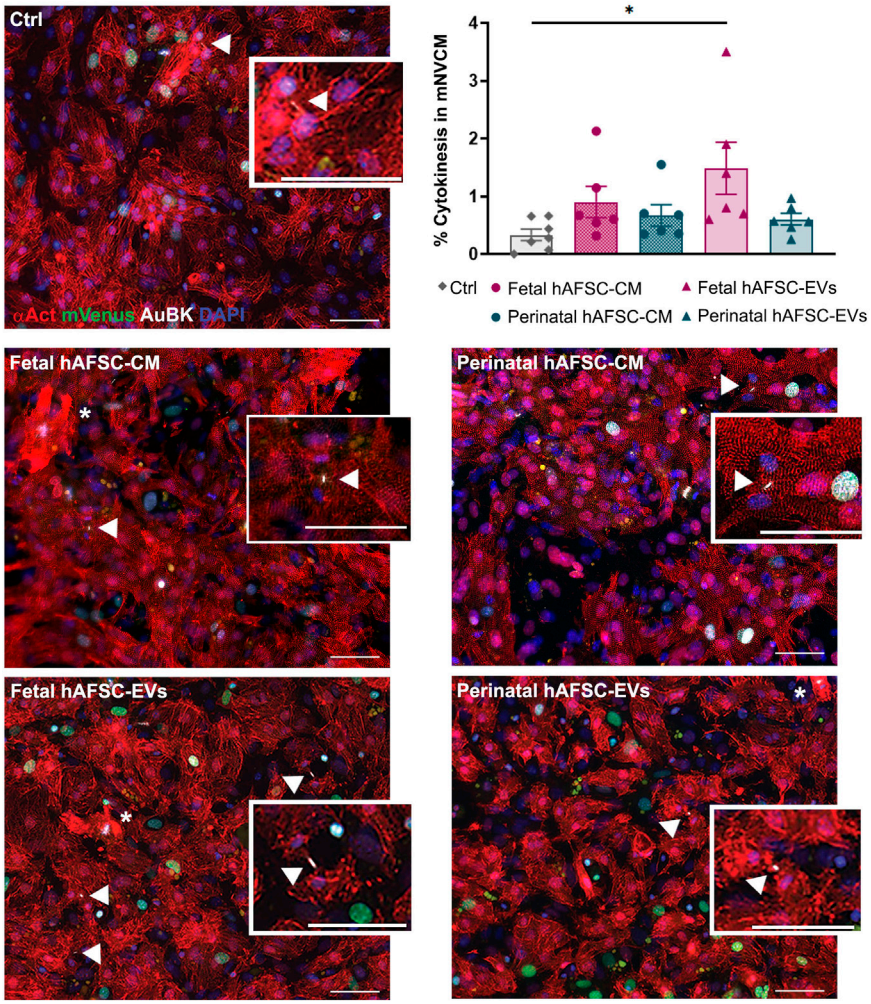

FIGURE 2 | *In vitro* cytokinesis of mNVCM following stimulation by fetal versus perinatal hAFSC secretome formulations. Representative images of AuBK localization at cell mid-body in R26pFUCCI2$^{+/-}$ mNVCM in vehicle-treated control conditions (SF medium, Ctrl) or following treatment with fetal or perinatal hAFSC-CM or hAFSC-EVs by immunostaining for sarcomeric α-actinin (αAct, red), mVenus-Geminin (mVenus, green), Aurora B kinase (AuBK, white), and DAPI (blue), scale bar: 50 μm. White arrows indicate AuBK expression at cell mid-body, corresponding to the completion of cytokinesis in αAct-positive cells (mNVCM), as illustrated in the inlet magnification, scale bar: 50 μm; white asterisks indicate mNVCM with disarranged α-actinin expression as sarcomeric disassembly feature. Upper right panel: evaluation of αAct-positive cells (mNVCM) with AuBK expression at cleavage furrows following stimulation with fetal versus perinatal hAFSC secretome formulations over vehicle-treated control condition (Ctrl). All values are expressed as mean ± s.e.m. percentage of dividing cardiomyocytes (% Cytokinesis in mNVCM) in independent experiments (Ctrl: 0.33 ± 0.09%, n = 7; fetal hAFSC-CM: 0.90 ± 0.27%, n = 6; perinatal hAFSC-CM: 0.67 ± 0.18%, n = 6; fetal hAFSC-EVs: 1.48 ± 0.45%, n = 6; perinatal hAFSC-EVs: 0.60 ± 0.10%, n = 6; *p = 0.0202).

(αAct-positive cells) expressing AuBK at midbody was detected only when cells were stimulated by fetal hAFSC-EVs (*$p < 0.05$, **Figure 2** and corresponding **Supplementary Figure S3**), over vehicle control treatment.

3.2 Fetal hAFSC-EVs Influence Cytoskeleton Re-Organization in mNVCM

Some mNVCM treated with hAFSC secretome formulations showed disorganized expression of cardiac alpha-actinin

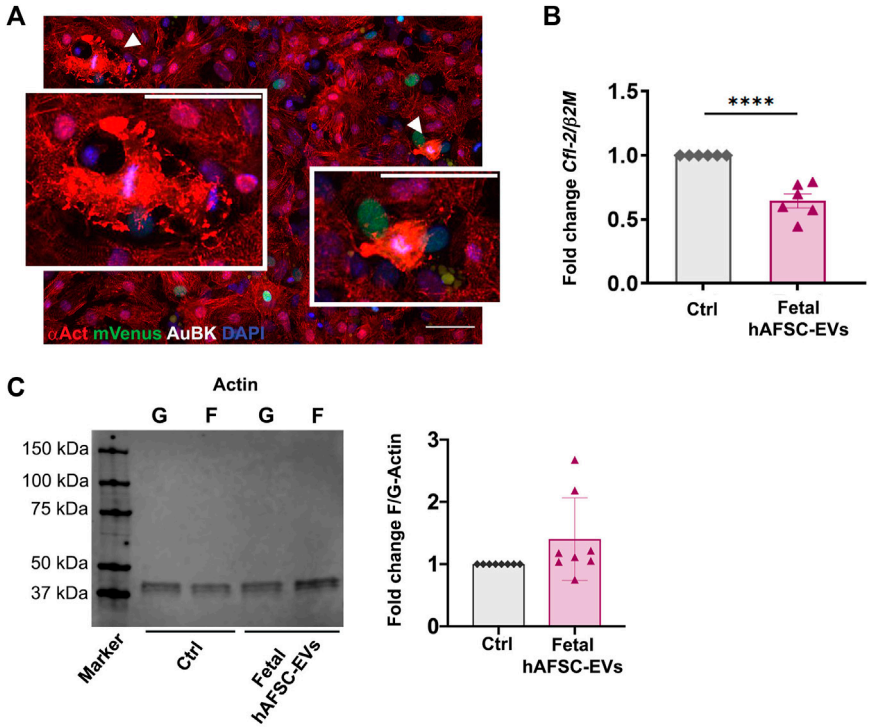

FIGURE 3 | Analysis of actin cytoskeleton regulation in mNVCM following fetal hAFSC-EV stimulation **(A)** Representative immunostaining pictures of mNVCM with sign of sarcomeric disassembly following fetal hAFSC-EV treatment as seen in **Figure 1A**; white arrows indicate mNVCM with disarranged expression of sarcomeric α-actinin (αAct, red) and intense Aurora B kinase signal (AuBK, white) associated to the chromosomal material (DAPI, blue), scale bar: 50 and 25 μm in the inlet. **(B)** Real-time qRT-PCR analysis of mNVCM stimulated by fetal hAFSC-EVs over vehicle-treated control cells (Ctrl) for *Cofilin-2 (Cfl-2)* gene expression as normalized to Beta 2 Microglobulin (β2M), as housekeeping reference. All values are expressed as mean ± s.e.m of *CFL-2/β2M* fold change for $n = 6$ independent experiments with Ctrl group as calibrator (Ctrl: 1; fetal hAFSC-EVs: 0.64 ± 0.13; $^{****}p < 0.001$). **(C)** Left panel: representative image of Western Blot analysis of G-Actin (G) and F-Actin (F) expression in mNVCM treated with fetal hAFSC-EVs (fetal hAFSC-EVs) over vehicle solution control (Ctrl); right panel: evaluation of F-Actin/G-Actin in mNVCM treated with fetal hAFSC-EVs over vehicle solution control. All values are expressed as mean ± s.e.m of fold change of F-Actin/G-Actin ratio (Fold Change F/G-Actin) of $n = 8$ independent experiments by densitometry on protein band intensity with Ctrl group as calibrator (Ctrl: 1; fetal hAFSC-EVs: 1.40 ± 0.23). kDa: kilo Dalton.

(**Figure 1A** and **Figure 2**, with details at higher magnification in **Figure 3A**, and corresponding **Supplementary Figures S2, S3**), suggesting cardiomyocyte sarcomeric disassembly, as required for cell cycle re-entry. In these mNVCM, AuBK localized within the nucleus overlapping the DAPI signal as suggesting being associated with chromosomal material at mitotic metaphase/anaphase (**Figure 3A**). Since immunostaining analyses defined fetal hAFSC-EVs as the most influencing secretome formulation, we further investigated their paracrine effect on mNVCM cytoskeleton re-organization. mNVCM treated with fetal hAFSC-EVs showed a significant decrease with a 0.6-fold ($^{****}p < 0.0001$) gene expression of *Cofilin-2* (*Cfl-2*), a modulator of actin cytoskeleton antagonizing cardiomyocyte proliferation (Torrini et al., 2019), over vehicle-treated Ctrl cells considered as reference (**Figure 3B**). Fetal hAFSC-EVs are enriched with microRNAs (miRNAs) within their cargo, as we have recently reported in (Costa et al., 2021). Additional bioinformatic analysis, suggested that some of the mostly enriched miRNAs within fetal hAFSC-EVs (miR-93-5p; miR-152-3p; miR-200b-3p; miR-429; miR-199a-3p; miR-20a-5p; miR-425-5p) preferentially target the *CFL-2* gene (**Supplementary Figure S4A**). Cofilin-2 regulates the actin cytoskeleton by promoting conversion of polymerized F-Actin back into monomeric G-Actin (Torrini et al., 2019); we then assessed the ratio between G-Actin and F-Actin in treated mNVCM; cells stimulated by fetal hAFSC-EVs showed a mild trend in the increase of polymerized F-Actin compared to the monomeric G form, as evaluated by the F/G ratio fold change (**Figure 3C**).

3.3 Fetal hAFSC-EVs can Sustain Resident Cardiomyocyte Cell Cycle Progression in a Preclinical Neonatal Mouse Model of Myocardial Infarction in the Short Term

The cardioactive paracrine potential of fetal hAFSC-EVs was evaluated in a 4-day-old (P4) and 7-day-old (P7) R26FUCCI2$^{+/-}$ neonatal mouse model of myocardial infarction (MI), at 3 and 7 days post injury. The myocardium of R26pFUCCI2$^{+/-}$ pups was evaluated by immunostaining for the expression of cardiac troponin I (cTnI)-positive cardiomyocytes with nuclear signal by the mVenus probe marking the engaging of cell cycle activity (from phase S up to completion of phase M).

MI injury did not represent a trigger sufficient to induce resident cardiomyocytes to initiate their renewal program at

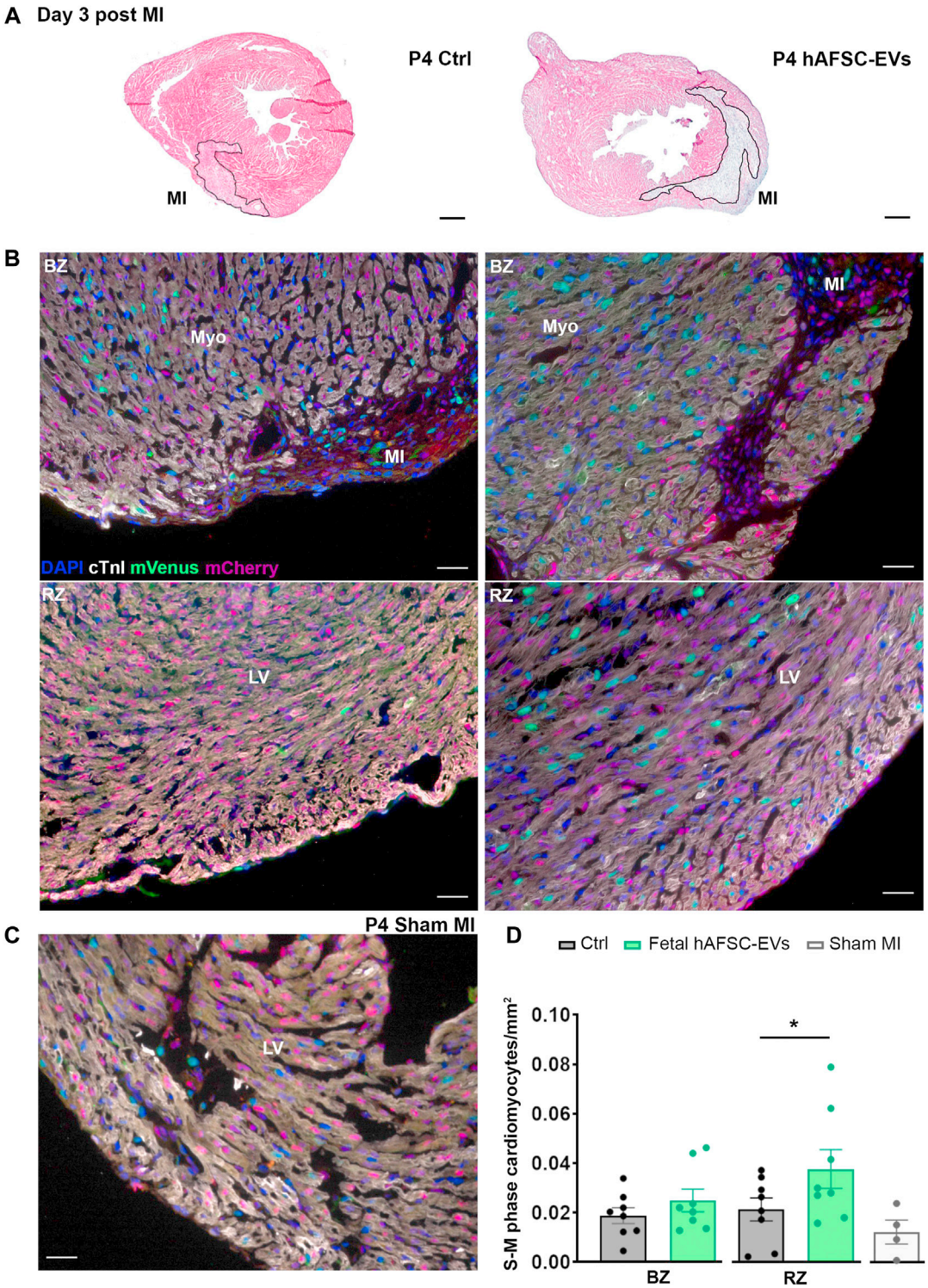

FIGURE 4 | In vivo cardiogenic effect of fetal hAFSC-EVs on P4 neonatal mouse heart at 3 days post MI. **(A)** Representative pictures of hematoxylin and eosin staining on cryo-sections of R26pFUCCI2$^{+/-}$ 4-day-old (P4) mouse myocardial tissue in: vehicle-treated control condition (PBS solution, left panel, Ctrl) and following intraperitoneal injection of 4.5 µg fetal hAFSC-EVs (hAFSC-EVs, right panel); myocardial infarct area (MI) is traced in black, scale bar: 300 µm. **(B)** Representative pictures of immunostaining analysis on cryo-sections of R26pFUCCI2$^{+/-}$ 4-day-old (P4) mouse myocardial tissue in: vehicle-treated control condition (PBS solution, left panel, Ctrl), following intraperitoneal injection with 4.5 µg fetal hAFSC-EVs (hAFSC-EVs, right panel), or in Sham control condition [**(C)**, Sham MI] for DAPI (blue), cardiac troponin I (cTnI, white), mVenus-Geminin (mVenus, green), and mCherry-Cdt1 (mCherry, red), at 3 days post MI (P4 d3); scale bar: 50 µm. **(D)** Evaluation of mVenus-positive and cTnI-positive resident cells (S-M phase cardiomyocytes/mm^2) within the myocardial tissue of mice receiving fetal hAFSC-EVs treatment compared to vehicle

(*Continued*)

FIGURE 4 | Ctrl solution in the MI border zone (BZ, upper panel) and in the remote zone (RZ, lower panel) of the left ventricle (LV). All values are expressed as mean ± s.e.m. of cTnI-positive cardiomyocytes expressing mVenus-positive nuclei per mm^2 (P4 d3 Ctrl BZ: 0.01879 ± 0.003214, RZ Ctrl: 0.02138 ± 0.004657; P4 d3 hAFSC-EVs BZ: 0.02492 ± 0.004609, RZ: 0.03770 ± 0.007848; $n = 8$ mice per experimental group; P4 d3 Sham MI 0.01230 ± 0.004847, $n = 4$ mice; $^{*}p = 0.0477$). Myo: myocardium; MI: myocardial infarction; LV: left ventricle.

either P4 or P7 stages as compared to the sham-operated (Sham MI) control group (**Figures 4**, **5**, and **Supplementary Figures S5, S6**).

While intraperitoneal administration of fetal hAFSC-EVs soon after MI did not exert any effect on resident cardiomyocytes within the left ventricle (LV) close to the infarct area (namely the border zone, BZ, **Figure 4**), a 1.8-fold ($^{*}p < 0.05$) increase in cardiomyocyte cell cycle progression was appreciated within the viable myocardium (the LV remote zone, RZ) following hAFSC-EVs treatment over Ctrl vehicle solution administration, at 3 days from injury (**Figure 4**). When investigating the fetal hAFSC-EV regenerative effect at later stage, 7 days after MI in the P4 mouse pups, no difference was appreciated between pups receiving hAFSC-EVs over the Ctrl group in either the RZ or the BZ areas (**Supplementary Figure S5**). Yet, hAFSC-EV stimulatory effect in sustaining cardiomyocyte cell cycle progression in the remote myocardium was detected within a week over sham-operated control group ($^{\$}p < 0.05$, **Supplementary Figure S5**).

Likewise, the amount of mVenus-positive endogenous cardiomyocytes in the P7 myocardium was comparable between the Ctrl and the fetal hAFSC-EV–treated group in the injury BZ. Resident cardiomyocyte cell cycle progression in the RZ of P7 mouse pups receiving hAFSC-EVs showed a mild positive trend compared to the corresponding area in the Ctrl group 3 days post MI, while being upregulated by 2-fold ($^{*}p < 0.05$) over the most unresponsive part of the injured myocardial tissue, the border zone (**Figure 5**). hAFSC-EV–induced myocardial response in the short term after MI was also found significantly improved, when compared to sham-operated controls ($^{\$}p < 0.05$, **Figure 5**). Yet, this paracrine effect was reduced within a week from injury and treatment, with no significant improvement in resident cardiomyocyte cell cycle re-entry following treatment (**Supplementary Figure S6**).

3.4 Fetal hAFSC-EVs Are Enriched With Agrin as Potential Molecular Candidate of Action

Extracellular vesicles separated and concentrated from hAFSC-CM confirmed the canonical small EV phenotype, with expression of the multivesicular body biogenesis protein TSG101 and Syntenin-1, as reference markers (Kugeratski et al., 2021), while lacking the endoplasmic reticulum antigen GRP94 and showing heterogenous distribution of exosomal tetraspanins over their size range, with enriched expression of CD81 in both small (100–160 nm size, $^{****}p < 0.0001$) and large EVs (160–900 nm size, $^{**}p < 0.01$, $^{****}p < 0.0001$) and CD63 in small EVs (100–160 nm size, $^{\#}p < 0.05$, **Supplementary Figures S4B,C**).

We previously characterized the proteomic cargo of both fetal and perinatal hAFSC-EVs, with indication of different enrichment of the first ones over the latter for some extracellular matrix components, including the proteoglycan Agrin (Costa et al., 2021). From our immunostaining analyses on treated mNVCM, fetal hAFSC-EVs demonstrated to be the most cardioactive secretome formulation in stimulating cardiomyocyte cell cycle activity. Here we also confirmed the presence of a short Agrin isoform (less than 75 kDa), as significantly enriched ($^{****}p < 0.0001$) within fetal hAFSC-EVs over perinatal ones by about an additional 40% (**Figure 6A**). Agrin has been described as important mediator for heart regeneration in neonatal mice as inducing nuclear YAP translocation, thus promoting the activation of cardiomyocyte renewal (Bassat et al., 2017). Therefore, to validate a putative mechanism of action of the most cardioactive fetal hAFSC-EVs *via* Agrin–YAP signaling axis, Verteporfin, a specific YAP pathway inhibitor, was used on mNVCM stimulated *in vitro*. Cell cycle progression traced by nuclear mVenus expression in $R26FUCCI2^{+/-}$ mNVCM ($n = 7$) was analyzed under the following treatment: vehicle control solution (1X PBS, Ctrl), fetal hAFSC-EVs alone (Fetal hAFSC-EVs) and fetal hAFSC-EVs with addition of YAP inhibitor (Fetal hAFSC-EVs + YAP inhibitor). Fetal hAFSC-EV stimulation increased the percentage of $mVenus^{+}$ mNVCM by about 2.84-fold over the Ctrl group ($^{**}p < 0.01$). The presence of the YAP inhibitor during hAFSC-EV treatment resulted in a decreasing trend of cardiogenic effect by about 40%, suggesting a possible, yet mild, putative involvement of YAP signaling in the hAFSC-EV paracrine mechanism (**Figure 6B**).

4 DISCUSSION

This study shows that immature fetal hAFSC obtained from leftover samples of II trimester prenatal diagnosis amniocentesis secrete extracellular vesicles as their most cardioactive secretome formulation to support cell cycle re-entry and proliferation of murine cardiomyocytes. We have recently reported that fetal and perinatal hAFSC share a comparable phenotype and secretory efficiency, with a different profile in the paracrine cargo of their secretome formulations, according to the gestational stage of cell isolation (Costa et al., 2021). Here we further confirm that the secretome formulation of more immature cells are endowed with enhanced cardiogenic paracrine potential over their corresponding perinatal counterpart, pointing at fetal hAFSC as candidate cell source for future translational studies.

We previously demonstrated that both the whole fetal hAFSC secretome (hAFSC-CM) and the extracellular vesicles derived from it (hAFSC-EVs) can sustain cardiomyocyte cell cycle re-entry up to the S phase by bromodeoxyuridine (BrdU) uptake, in a preclinical mouse model of myocardial infarction (MI),

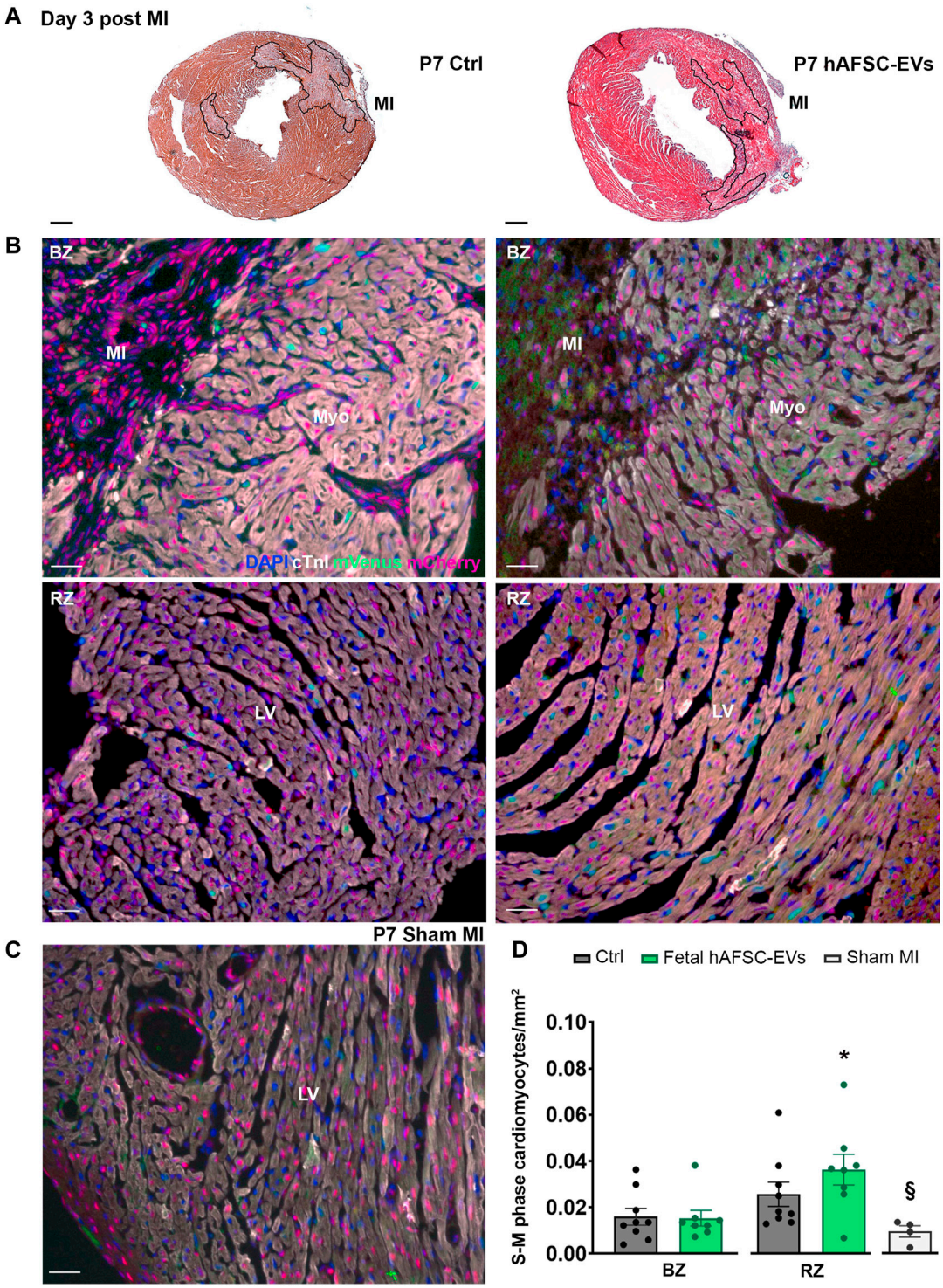

FIGURE 5 | *In vivo* cardiogenic effect of fetal hAFSC-EVs on P7 neonatal mouse heart at 3 days post MI. **(A)** Representative pictures of hematoxylin and eosin staining on cryo-sections of R26pFUCCI2$^{+/-}$ 7-day-old (P7) mouse myocardial tissue in: vehicle-treated control condition (PBS solution, left panel, Ctrl) and following intraperitoneal injection of 4.5 µg fetal hAFSC-EVs (hAFSC-EVs, right panel); myocardial infarct area (MI) is traced in black, scale bar: 300 µm. **(B)** Representative pictures of immunostaining analysis on cryo-sections of R26pFUCCI2$^{+/-}$ 7-day-old (P7) mouse myocardial tissue in: vehicle-treated control conditions (PBS solution, left panel, Ctrl), following intraperitoneal injection with 4.5 µg fetal hAFSC-EVs (hAFSC-EVs, right panel) or in Sham control conditions [**(C)**, Sham MI, for DAPI (blue), cardiac troponin I (cTnI, white), mVenus-Geminin (mVenus, green), and mCherry-Cdt1 (mCherry, red), at 3 days post MI (P7 d3), scale bar: 50 µm. **(D)** Evaluation of mVenus-positive and cTnI-positive resident cells (S-M phase cardiomyocytes/mm^2) receiving hAFSC-EVs treatment compared to vehicle Ctrl solution in the MI border zone (BZ,

(*Continued*)

FIGURE 5 | upper panel) and in the remote zone (RZ, lower panel) of the left ventricle (LV). All values are expressed as mean ± s.e.m. of cTnI-positive cardiomyocytes expressing mVenus-positive nuclei per mm^2 (P7 d3 Ctrl BZ: 0.01595 ± 0.003586, RZ: 0.02566 ± 0.005207, $n = 9$ mice; P7 d3 hAFSC-EVs BZ: 0.01529 ± 0.003393; RZ: 0.03629 ± 0.0.006650, $n = 8$ mice; P4 d3 Sham MI 0.009442 ± 0.002469, $n = 4$ mice; $^{*}p = 0.0312$ hAFSC-EVs RZ versus Ctrl BZ and $^{*}p = 0.0304$ hAFSC-EVs RZ versus hAFSC-EVs BZ; $^{§}p = 0.0218$ Sham MI versus hAFSC-EVs RZ). Myo: myocardium; MI: myocardial infarction; LV: left ventricle.

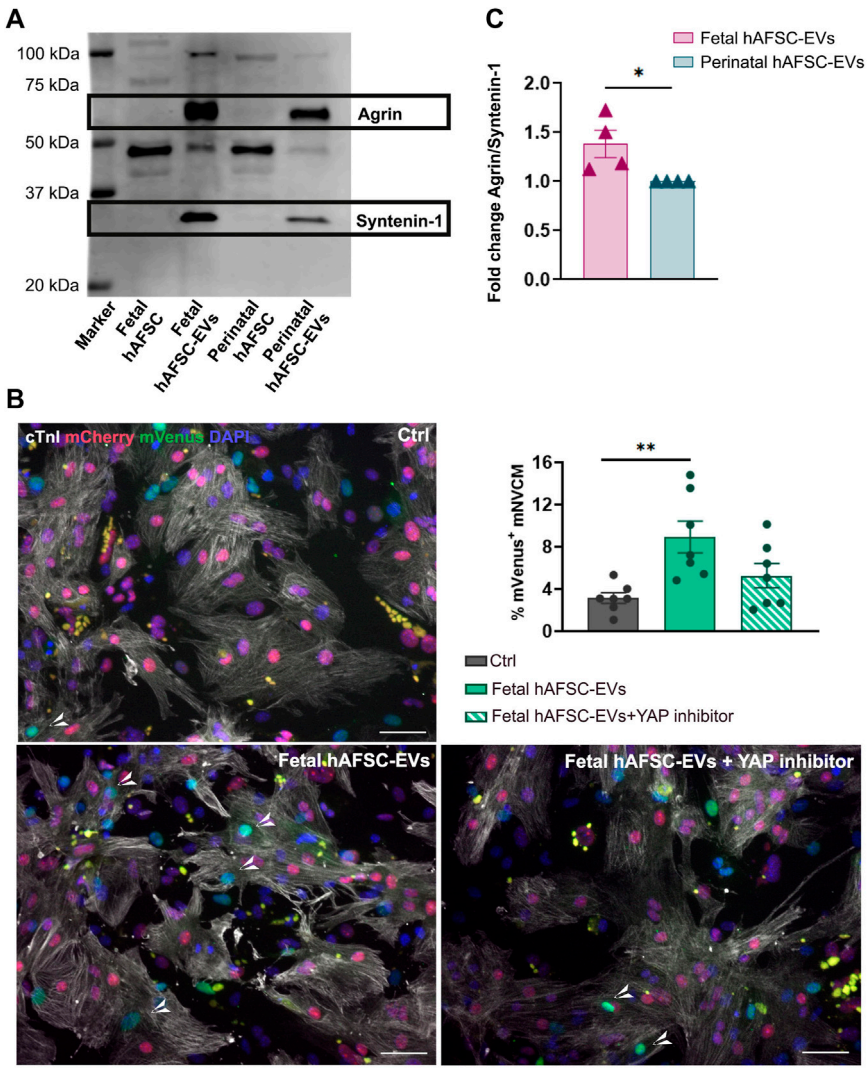

FIGURE 6 | Agrin as molecular candidate of hAFSC-EV effect on mNVCM. **(A)** Left panel: representative Western blot of Agrin expression within fetal hAFSC-EVs over perinatal hAFSC-EVs, normalized to the presence of the small EV marker Syntenin-1; right panel: densitometry analysis of protein band signal by Agrin over Syntenin-1–fold change expression as mean ± s.e.m. (Fold Change Agrin/Syntenin-1) of $n = 4$ independent experiments (fetal hAFSC-EVs: 1.38 ± 0.14; perinatal hAFSC-EVs as calibrator: 1; $^{*}p = 0.0348$). **(B)** Representative images of R26pFUCCI2$^{+/-}$ mNVCM following treatment with fetal hAFSC-EVs with or without YAP pathway inhibitor (10 μM Verterporfin solution) or in vehicle-treated control condition (PBS solution, Ctrl) by immunostaining for cardiac troponin I (cTnI, white); mCherry-Cdt1 (mCherry, red), mVenus-Geminin (mVenus, green) and DAPI (blue), scale bar: 50 μm. **(C)** Percentage of mVenus-positive and cTnI-positive cells (mVenus^{+} mNVCM) stimulated with fetal hAFSC-EVs alone or with YAP inhibitor (fetal hAFSC-EVs + YAP inhibitor) compared to vehicle-treated cells (PBS solution, Ctrl). All values are expressed as mean ± s.e.m. percentage of mVenus^{+} mNVCM (% mVenus^{+} mNVCM) of $n = 7$ independent experiments (Ctrl: 3.14 ± 0.50%; fetal hAFSC-EVs: 8.92 ± 1.50%; fetal hAFSC-EVs + YAP inhibitor: 5.27 ± 1.15%; $^{**}p = 0.0054$).

extending such effect to up of 28 days after single intramyocardial injection (Balbi et al., 2019a). While such encouraging results suggested some degree of regenerative potential in the fetal hAFSC secretome, BrdU uptake presents some concerns, as merely indicating integration within DNA and thus tracing cell engagement to S phase, without providing any information regarding further true commitment to G2/M phase. To overcome such limit, here we employed a specific

transgenic mouse model, known as R26pFUCCI2 mouse, described for the first time by (Abe et al., 2013). FUCCI labeling technology represents a useful tool to investigate cardiomyocyte cell cycle dynamics by means of mutually exclusive fluorescent nuclear signals, as recently reported by others as well (Alvarez et al., 2019; Baniol et al., 2021; Del Campo et al., 2022). The heterozygous R26pFUCCI2 mouse model used in our study is endowed with constitutive expression of a transgene probe system targeting the cell cycle–regulating protein, Cdt1 and its inhibitor Geminin, which are implicated in the DNA replication system (Wohlschlegel et al., 2000). The expression levels of these two proteins are inversely proportional and they change during cell cycle progression. Cdt1 levels are the highest in G1 phase and they decrease after the S phase. In contrast, Geminin levels peak during S and G2 phase, but drop drastically during late mitosis and G1 phase. Thus, R26pFUCCI2 system allows the fluorescent labeling of cell cycle G1 phase by expression of nuclear mCherry-Cdt1 and S/G2/M phases by expression of nuclear mVenus-Geminin (Abe et al., 2013).

Notably, while the whole fetal hAFSC secretome—as the cell-conditioned medium, hAFSC-CM—showed promising trend in the increase of responsive R26pFUCCI2 neonatal cardiomyocytes re-entering cell cycle advancement, only fetal hAFSC-EVs concentrated and separated from it significantly enhanced cell progression over G1 phase in culture. Notably, we have previously demonstrated the different cardiovascular potential of hAFSC-CM versus hAFSC-EVs in the adult mouse model of acute MI, where total hAFSC secretome exerted distinct pro-angiogenic effects that the EV counterpart was not able to evoke in the injured myocardium; *viceversa*, hAFSC-EVs showed enhanced cardioprotective rescue capacity in supporting cardiac function in the long-term (Balbi et al., 2019a). Since the total amount of particles within the hAFSC-CM and hAFSC-EV formulations was not statistically different, the different cardiogenic effect we appreciated in this study, may be related to the modulatory activity of soluble factors other than the EVs which are present in the hAFSC-CM. Nuclear co-expression of the chromosomal passenger enzyme Aurora B kinase further indicated that most of stimulated cardiomyocytes were actually proceeding over S and G2 phases into mitotic prophase (Adams et al., 2001; Murata-Hori et al., 2002). Moreover, fetal hAFSC-EVs demonstrated to actively trigger true cardiomyocyte division, as shown by Aurora B kinase expression in the cell midbody structure, thus indicating cytokinesis being in progress. hAFSC secretome stimulation also induced the expression of an altered structural phenotype in the cardiomyocytes treated *in vitro*, with sign of sarcomeric disassembly by disorganized expression of cardiac alpha-actinin, suggesting cardiomyocyte de-differentiation, a phenotypic feature required for cell cycle re-entry and renewal. Fetal hAFSC-EVs targeted the actin cytoskeleton architecture by significantly decreasing *Cofilin-2* gene expression while mildly sustaining F-actin polymerization, as consequence. Indeed, Cofilin-2 represents a key regulator of cardiomyocyte cell cycle re-entry by modulating actin polymerization and antagonizing actin polymerization into F filaments, thus increasing the G-Actin pool within the cytoplasm; in particular, it has been previously described that miR-199-a-3p targets *Cofilin-2* so to induce sarcomere disassembly and trigger cardiomyocyte proliferation (Torrini et al., 2019). Notably, additional bioinformatics analyses on the RNA content within the fetal hAFSC-EV cargo previously reported in (Costa et al., 2021) indicated that the 100 most enriched miRNA in the EVs, including miR-199-a-3, preferentially target the *Cofilin-2* gene.

The early postnatal murine heart is endowed with significant regenerative activity following critical injury, such as MI, by means of efficient resident cardiomyocyte renewal and division. Nonetheless, this regenerative program is active only within a very narrow postnatal window, with complete loss of effect after the first week from birth (P7). The 7-day-old (P7) mouse pup represent the limit of the neonatal cardiac regenerative window, being more similar to the adult heart in activating defective cardiac repair over restorative myocardial renewal (Porrello et al., 2013; Aurora et al., 2014; Lam and Sadek, 2018). In order to validate *in vivo* the results obtained on neonatal cardiomyocytes cultured *in vitro*, the cardiogenic potential of fetal hAFSC-EVs to unlock and extend such limit was assessed in a preclinical model of myocardial infarction in both P4 (i.e., representing half-way the decrease of regenerative potential) and P7 mouse pups (indicating the termination of the postnatal regenerative window). Fetal hAFSC-EVs induced an increase in resident cardiomyocyte cell cycle activity within the short-term following injury (i.e., 3 days after MI in P4 and P7 murine heart). Notably, cardiomyocyte cell cycle progression was appreciated in the left ventricle myocardium not closely related to the injured area, as suggesting that the developmental renewal program was reinstated in those viable cells organizing the regenerative advancing front as during zebrafish heart regeneration (Kikuchi et al., 2010; Yin et al., 2012). Fetal hAFSC-EV cardiogenic effect was blunted after 7 days from injury. We cannot exclude that such transient cardiogenic effect may be influenced by technical limitations in the hAFSC-EV delivery route and in the lack of follow-up treatments over time, to sustain their cardioactive influence. Here we chose to deliver fetal hAFSC-EVs *via* intraperitoneal (i.p.) administration, over more invasive intramyocardial injection, in compliance with the 3R's principle.

As a matter of fact, different routes have been investigated in order to deliver mesenchymal stromal cell–EVs (MSC-EVs) in several preclinical model of disease, including intravenous administration, and local and intraperitoneal injections, as comprehensively reviewed in (Akbari et al., 2020). Intraperitoneal administration in particular has been applied in some recent studies investigating the regenerative activity of MSC-EVs in newborn rodent preclinical models. EVs obtained from rat bone marrow- and human umbilical cord MSC have been administered daily by i.p. injections in neonatal rats developing bronchopulmonary dysplasia early after birth and counteracted disruption of alveolarization, promoted angiogenesis and ameliorated pulmonary hypertension and right ventricular hypertrophy (Braun et al., 2018; Chaubey et al., 2018). Likewise, i.p. delivery of human umbilical cord MSC EVs exerted beneficial effects by preserving cochlear hair

cells in mice receiving chronic cisplatin injection as preclinical model of ototoxicity-induced hearing loss (Tsai et al., 2021). Furthermore, i.p. injection of murine adipose tissue MSC-EVs in a preclinical model of inflammatory bowel disease (IBD) in mice with dextran sulfate sodium-induced acute colitis decreased colon injury and reduced TNF-α expression, while increasing Treg cells and TGF-β and IL-10 levels in the spleen and lymph nodes (Heidari et al., 2021). While i.p. delivery is generally well-tolerated in rodent preclinical models of disease, thus supporting overall survival and recovery, it may also present specific drawbacks. Indeed, hAFSC-EVs may struggle to reach the injured myocardial tissue, due to off-target biodistribution in other tissues, with unspecific or delayed outcome. As a matter of fact, i.p. delivery has been shown to be remarkably effective when targeting organs associated with the peritoneum cavity. On the other side, systemic delivery *via* intravenous (i.v.) infusion may provide a more clinically compliant option for follow-up treatments, offering prompt systemic distribution and improving the chances of cardiac homing; however, this approach does not prevent possible side effects either. Moreover, small EVs delivered systemically *via* i.v. administration have demonstrated limited half-life in the mouse circulation, up to very few minutes (Takahashi et al., 2013).

Another relevant aspect to be acknowledged about our *in vivo* delivery protocol is that we could not provide follow-up treatment. The main reason was to avoid any additional stress in the mother caused by frequent manipulation of the treated pups, thus prompting her to neglect them. Likewise, although progenitor-derived EVs have been broadly described as immunological inert and immunomodulatory agents, we cannot then exclude that repeated i.p. treatments may increase the risk of local sensitization leading to *in situ* activation of immune cells.

When fetal hAFSC-EVs were administered by intramyocardial delivery soon after MI, we reported long-lasting beneficial effects within the adult cardiac tissue with increased BrDU uptake in resident cardiomyocyte (Balbi et al., 2019a). Indeed, the relevance of local delivery in supporting paracrine stimulation on resident cardiomyocyte renewal seems to be highlighted by independent work as well, in which epicardial-derived progenitor cell–EVs were able to maintain a proliferative response *in vivo* for a bit longer, during and beyond the P7 murine neonatal window, following their direct intracardiac injection during MI, despite this limiting the sample size (Del Campo et al., 2022). While direct and localized injection may increase the efficiency of local targeting, this approach is likely quite invasive and hardly clinically feasible, especially for chronic cardiac disease and heart failure. Therefore, suitable alternatives should be optimized in order to define a paracrine therapy protocol ensuring therapeutic efficacy together with great potential for translational medicine and their successful application in the clinical scenario. In light of these considerations, customized engineering of the hAFSC-EV surface for the specific targeting of cardiomyocytes and the injured myocardium may represent a desirable strategy. This should be further combined with the design of *ad hoc* biocompatible hydrogel formulations for prolonged and controlled EV release *in vivo*, in order to increase stability, retention and to overcome the need of multiple follow-up administrations in the long term.

In our previous study assessing the cardioprotective role of hAFSC-EVs in the preclinical adult mouse model of MI, we demonstrated that a single intramyocardial administration of EVs resulted in the significant rescue of cardiac function in the long-term, without any collateral effects (Balbi et al., 2019a). We appreciated that it would have been relevant to evaluate whether hAFSC-EVs could exert the same cardioactive paracrine influence on the neonatal injured myocardium as well; nonetheless, cardiac function imaging on such juvenile MI model may represent a technical challenging task in our setting.

The regenerative competence of stem- and progenitor cell–EVs is acquired from their cargo of paracrine mediators, which are sorted in the vesicle by the parental secreting cell as mirroring its potential. From the earlier molecular profiling we have performed on fetal versus perinatal hAFSC secretome formulations, we revealed that they shared a stable signature group of miRNAs (Costa et al., 2021). Nevertheless, additional bioinformatic analyses performed here indicated that immature fetal hAFSC-EVs may harbor a more cardiogenic regulatory RNA content targeting *Cofilin-2* and cytoskeleton re-organization. While we previously appreciated that perinatal hAFSC-EVs can deliver soluble factors involved in endothelial cell migration, immune-modulation and neurotrophic potential stimulation (Costa et al., 2021), here we confirmed that fetal hAFSC-EVs, as the most cardiogenic secretome formulation, are significantly enriched with a short isoform of the extracellular matrix proteoglycan Agrin. Indeed, Agrin has been shown to be a master regulator during neonatal heart regeneration in mice, as acting *via* the YAP signaling axis and promoting murine and human cardiomyocyte cell division (Bassat et al., 2017). In order to assess whether Agrin may be a candidate molecular effector underlying the cardioactive paracrine potential of fetal hAFSC-EVs, functional *in vitro* analyses were performed. Stimulating primary neonatal cardiomyocytes with fetal hAFSC-EVs in combination with the YAP inhibitor Verteporfin (Bassat et al., 2017) resulted in a negative trend of their cell cycle re-entry. Although we noticed some degree of inhibition in the hAFSC-EV cardiogenic paracrine effect, we may have to consider that some additional therapeutic mechanisms may be involved, such as a combinatorial effect involving Agrin and miRNAs within the EV cargo. Moreover, since the Agrin isoform detected on hAFSC-EVs is a shorter fragment of such protein, which may sound consistent with a 72 kDa cell-secreted variant similarly reported by others (Rivera et al., 2018), we cannot exclude that this isoform may not specifically or exclusively act on the target cardiomyocytes *via* YAP signaling. Therefore, additional detailed analyses on stimulated cardiomyocytes are necessary to pinpoint the specific molecular mechanism of action of fetal hAFSC-EVs, in order to enhance it. Further development will require comprehensive characterization of the ratio between hAFSC-EV functional activity and their appropriate dosing, as well as specific potency assays. Another limit we may acknowledge refers to the *in vivo* delivery system, which needs

to be optimized in order to prolong and strengthen the transient cardiogenic potential of hAFSC-EVs so to ensure long-lasting and myocardial-specific results, while at the same time avoiding off-target systemic effects. This could be achieved by either engineering hAFSC-EV surface to implement their specific tropism toward cardiomyocytes or by developing biocompatible releasing systems to ensure hAFSC-EVs *in vivo* prolonged administration.

5 CONCLUSION

Collectively, our data suggests that fetal hAFSC can produce small EVs endowed with relevant cardiogenic effects to sustain myocardial renewal. Despite II trimester and III trimester hAFSC may present overlapping secretory efficiency, developmentally more immature fetal hAFSC-EVs have shown to be the more promising cardioactive fraction in supporting cardiomyocyte cell cycle re-entry. Yet, further functional analyses should be considered to better understand the molecular mechanism of action underlying the paracrine capacity of fetal hAFSC-EVs, in order to strengthen their potential and explore them as targeted delivery therapeutics for cardiac regenerative medicine. From a translational perspective, this study suggests that while fetal hAFSC-EVs may retain some degree of restorative capacity in supporting cardiomyocytes toward progression of the cell cycle up to true cell division, such effect may not therapeutically fulfill the expectations for adult patients experiencing myocardial infarction/cardiac dysfunction. Nevertheless, the fetal hAFSC-EV cardiogenic potential could be rather exploited in the neonatal scenario, where fetuses or newborns affected by congenital heart malformation with alteration of resident cardiomyocytes, may benefit of an innovative paracrine approach based on fetal hAFSC-EV prompt administration at/soon after birth or *in utero*. Such strategy may pave the way to promote myocardial tissue restoration by means of cell-free, EV-based advanced medicinal products, in combination with standard *in utero* or early postnatal reconstructive surgical interventions.

DATA AVAILABILITY STATEMENT

Publicly available data sets were analyzed in this study. This data can be found at: Gene Expression Omnibus repository (www.ncbi.nlm.nih.gov/geo/) with accession number: GSE168152.

ETHICS STATEMENT

The studies involving human participants were reviewed and approved by the Regional Ethic Committee (P.R. 428REG2015), according to the guidelines of the Declaration of Helsinki for the use of leftover and clinical waste samples of human amniotic fluid. Samples of human amniotic fluid were obtained following written informed consent from donors. The patients/participants provided their written informed consent to participate in this study. The animal study was reviewed and approved by Italian Ministry of Health; authorizations n. 230/2019-PR and n. 62/2019-PR.

AUTHOR CONTRIBUTIONS

AC: experimental design of the study, methodology, investigation, data acquisition, analysis, writing of the manuscript; CB, PG, and DR: methodology, investigation, data acquisition, and analysis; MP, ADP, RR, DaC, PaM, and PiM: data analysis; DP, DoC, PDB, and CG: technical support; RQ: review and editing of manuscript; LB: critical discussion and review and editing of manuscript; SB: conceptualization of the study, methodology, investigation, supervision, and project administration, review and editing of manuscript, and funding acquisition. All authors have read and agreed to the published version of the manuscript.

FUNDING

This research was funded by the University of Genova, Genova, Italy, "Curiosity Driven" grant for the project: "Triggering CARDIOmyocyte renewal by harnessing Stem cell paracrine potential (CARDIO-STAR)" to SB.

ACKNOWLEDGMENTS

Authors would like to acknowledge RIKEN Center for Life Science Technologies, Kobe, Japan and Dr. Yasuhide Furuta for the R26pFUCCI2 mouse strain (Acc. No. CDB0203T; http: www.clst.riken.jp/arg/reporter_mice.html), as from *Abe T*, *et al. Visualization of cell cycle in mouse embryos with Fucci2 reporter directed by Rosa26 promoter. Development 140(1):237–246 (2013)*. Authors would also like to acknowledge Prof. Shrinivas Shankar and Prof. Paul Riley from the Department of Physiology, Anatomy and Genetics, British Heart Foundation, Oxbridge Centre of Regenerative Medicine, University of Oxford, UK for providing R26pFUCCI2 male mice. Schematics in **Supplementary Figure S1** and in the graphical abstract have been produced using Smart—Servier Medical Art (https://smart.servier.com/). This study contributes to the aims of the Horizon 2020 COST Action CA17116 SPRINT- *International Network for Translating Research on Perinatal Derivatives into Therapeutic Approaches* in which CB and SB are involved.

SUPPLEMENTARY MATERIAL

The Supplementary Material for this article can be found online at: https://www.frontiersin.org/articles/10.3389/fbioe.2022.902038/full#supplementary-material

REFERENCES

Abe, T., Sakaue-Sawano, A., Kiyonari, H., Shioi, G., Inoue, K. I., Horiuchi, T., et al. (2013). Visualization of Cell Cycle in Mouse Embryos with Fucci2 Reporter Directed by Rosa26 Promoter. *Dev* 140, 237–246. doi:10.1242/dev.084111

Adams, R. R., Carmena, M., and Earnshaw, W. C. (2001). Chromosomal Passengers and the (Aurora) ABCs of Mitosis. *Trends Cell Biol.* 11, 49–54. doi:10.1016/S0962-8924(00)01880-8

Akbari, A., Jabbari, N., Sharifi, R., Ahmadi, M., Vahhabi, A., Seyedzadeh, S. J., et al. (2020). Free and Hydrogel Encapsulated Exosome-Based Therapies in Regenerative Medicine. *Life Sci.* 249. doi:10.1016/J.LFS.2020.117447

Alvarez, R., Wang, B. J., Quijada, P. J., Avitabile, D., Ho, T., Shaitrit, M., et al. (2019). Cardiomyocyte Cell Cycle Dynamics and Proliferation Revealed through Cardiac-specific Transgenesis of Fluorescent Ubiquitinated Cell Cycle Indicator (FUCCI). *J. Mol. Cell. Cardiol.* 127, 154–164. doi:10.1016/J.YJMCC.2018.12.007

Aurora, A. B., Porrello, E. R., Tan, W., Mahmoud, A. I., Hill, J. A., Bassel-Duby, R., et al. (2014). Macrophages Are Required for Neonatal Heart Regeneration. *J. Clin. Invest.* 124, 1382–1392. doi:10.1172/JCI72181

Balbi, C., Lodder, K., Costa, A., Moimas, S., Moccia, F., van Herwaarden, T., et al. (2019a). Reactivating Endogenous Mechanisms of Cardiac Regeneration via Paracrine Boosting Using the Human Amniotic Fluid Stem Cell Secretome. *Int. J. Cardiol.* 287, 87–95. doi:10.1016/j.ijcard.2019.04.011

Balbi, C., Lodder, K., Costa, A., Moimas, S., Moccia, F., van Herwaarden, T., et al. (2019b). Supporting Data on *In Vitro* Cardioprotective and Proliferative Paracrine Effects by the Human Amniotic Fluid Stem Cell Secretome. *Data Br.* 25, 104324. doi:10.1016/j.dib.2019.104324

Balbi, C., Piccoli, M., Barile, L., Papait, A., Armirotti, A., Principi, E., et al. (2017). First Characterization of Human Amniotic Fluid Stem Cell Extracellular Vesicles as a Powerful Paracrine Tool Endowed with Regenerative Potential. *Stem Cells Transl. Med.* 6, 1340–1355. doi:10.1002/sctm.16-0297

Baniol, M., Murganti, F., Smialowska, A., Panula, J., Lázár, E., Brockman, V., et al. (2021). Identification and Characterization of Distinct Cell Cycle Stages in Cardiomyocytes Using the FUCCI Transgenic System. *Exp. Cell Res.* 408, 112880. doi:10.1016/J.YEXCR.2021.112880

Bassat, E., Mutlak, Y. E., Genzelinakh, A., Shadrin, I. Y., Baruch Umansky, K., Yifa, O., et al. (2017). The Extracellular Matrix Protein Agrin Promotes Heart Regeneration in Mice. *Nature* 547, 179–184. doi:10.1038/nature22978

Bergmann, O., Bhardwaj, R. D., Bernard, S., Zdunek, S., Barnabé-Heider, F., Walsh, S., et al. (2009). Evidence for Cardiomyocyte Renewal in Humans. *Science* 324, 98–102. doi:10.1126/science.1164680

Bollini, S., Silini, A. R., Banerjee, A., Wolbank, S., Balbi, C., and Parolini, O. (2018). Cardiac Restoration Stemming from the Placenta Tree: Insights from Fetal and Perinatal Cell Biology. *Front. Physiol.* 9, 385. doi:10.3389/fphys.2018.00385

Borlongan, C. (2017). Amniotic Fluid as a Source of Engraftable Stem Cells. *Brain Circ.* 3, 175. doi:10.4103/BC.BC_24_17

Braun, R. K., Chetty, C., Balasubramaniam, V., Centanni, R., Haraldsdottir, K., Hematti, P., et al. (2018). Intraperitoneal Injection of MSC-Derived Exosomes Prevent Experimental Bronchopulmonary Dysplasia. *Biochem. Biophys. Res. Commun.* 503, 2653–2658. doi:10.1016/J.BBRC.2018.08.019

Cabrol, C., Gandjbakhch, I., Pavie, A., Bors, V., Rabago, G., Muneretto, C., et al. (1989). Heart Transplantation: Update. *Clin. Transpl.*, 79–87. Available at: https://pubmed.ncbi.nlm.nih.gov/2487627/(Accessed March 9, 2022).

Chaubey, S., Thueson, S., Ponnalagu, D., Alam, M. A., Gheorghe, C. P., Aghai, Z., et al. (2018). Early Gestational Mesenchymal Stem Cell Secretome Attenuates Experimental Bronchopulmonary Dysplasia in Part via Exosome-Associated Factor TSG-6. *Stem Cell Res. Ther.* 9, 173. doi:10.1186/S13287-018-0903-4

Costa, A., Ceresa, D., De Palma, A., Rossi, R., Turturo, S., Santamaria, S., et al. (2021). Comprehensive Profiling of Secretome Formulations from Fetal- and Perinatal Human Amniotic Fluid Stem Cells. *Int. J. Mol. Sci.* 22, 3713. doi:10.3390/IJMS22073713

Costa, A., Quarto, R., and Bollini, S. (2022). Small Extracellular Vesicles from Human Amniotic Fluid Samples as Promising Theranostics. *Int. J. Mol. Sci.* 23, 590. doi:10.3390/IJMS23020590

Del Campo, C. V., Liaw, N. Y., Gunadasa-Rohling, M., Matthaei, M., Braga, L., Kennedy, T., et al. (2022). Regenerative Potential of Epicardium-Derived Extracellular Vesicles Mediated by Conserved miRNA Transfer. *Cardiovasc. Res.* 118, 597–611. doi:10.1093/CVR/CVAB054

Fang, Y. H., Wang, S. P. H., Chang, H. Y., Yang, P. J., Liu, P. Y., and Liu, Y. W. (2020). Progress and Challenges of Amniotic Fluid Derived Stem Cells in Therapy of Ischemic Heart Disease. *Int. J. Mol. Sci.* 22, 1–12. doi:10.3390/IJMS22010102

Gorgun, C., Reverberi, D., Rotta, G., Villa, F., Quarto, R., and Tasso, R. (2019). Isolation and Flow Cytometry Characterization of Extracellular-Vesicle Subpopulations Derived from Human Mesenchymal Stromal Cells. *Curr. Protoc. Stem Cell Biol.* 48, e76. doi:10.1002/cpsc.76

Heidari, N., Abbasi-Kenarsari, H., Namaki, S., Baghaei, K., Zali, M. R., Ghaffari Khaligh, S., et al. (2021). Adipose-derived Mesenchymal Stem Cell-Secreted Exosome Alleviates Dextran Sulfate Sodium-Induced Acute Colitis by Treg Cell Induction and Inflammatory Cytokine Reduction. *J. Cell. Physiol.* 236, 5906–5920. doi:10.1002/JCP.30275

ImageJ (2021). Image Processing and Analysis in Java. Available at: https://imagej.nih.gov/ij/(Accessed March 10, 2021).

Kikuchi, K., Holdway, J. E., Werdich, A. A., Anderson, R. M., Fang, Y., Egnaczyk, G. F., et al. (2010). Primary Contribution to Zebrafish Heart Regeneration by Gata4(+) Cardiomyocytes. *Nature* 464, 601–605. doi:10.1038/NATURE08804

Kugeratski, F. G., Hodge, K., Lilla, S., McAndrews, K. M., Zhou, X., Hwang, R. F., et al. (2021). Quantitative Proteomics Identifies the Core Proteome of Exosomes with Syntenin-1 as the Highest Abundant Protein and a Putative Universal Biomarker. *Nat. Cell Biol.* 23, 631–641. doi:10.1038/S41556-021-00693-Y

Lam, N. T., and Sadek, H. A. (2018). Neonatal Heart Regeneration: Comprehensive Literature Review. *Circulation* 138, 421–423. doi:10.1161/CIRCULATIONAHA.118.033648

Lazzarini, E., Balbi, C., Altieri, P., Pfeffer, U., Gambini, E., Canepa, M., et al. (2016). The Human Amniotic Fluid Stem Cell Secretome Effectively Counteracts Doxorubicin-Induced Cardiotoxicity. *Sci. Rep.* 6, 29994. doi:10.1038/srep29994

Loukogeorgakis, S. P., and De Coppi, P. (2017). Concise Review: Amniotic Fluid Stem Cells: The Known, the Unknown, and Potential Regenerative Medicine Applications. *Stem Cells* 35, 1663–1673. doi:10.1002/stem.2553

Murata-Hori, M., Tatsuka, M., and Wang, Y. L. (2002). Probing the Dynamics and Functions of Aurora B Kinase in Living Cells during Mitosis and Cytokinesis. *Mol. Biol. Cell* 13, 1099. doi:10.1091/MBC.01-09-0467

Narakornsak, S., Aungsuchawan, S., Pothacharoen, P., Puaninta, C., Markmee, R., Tancharoen, W., et al. (2019). Amniotic Fluid: Source of Valuable Mesenchymal Stem Cells and Alternatively Used as Cryopreserved Solution. *Acta histochem.* 121, 72–83. doi:10.1016/J.ACTHIS.2018.10.009

Package "miRNAtap"(2022). miRNAtap: microRNA Targets-Aggregated Predictions. Available at: https://git.bioconductor.org/packages/miRNAtap (Accessed March 9, 2022).

Porrello, E. R., Mahmoud, A. I., Simpson, E., Hill, J. A., Richardson, J. A., Olson, E. N., et al. (2011). Transient Regenerative Potential of the Neonatal Mouse Heart. *Science* 331, 1078–1080. doi:10.1126/science.1200708

Porrello, E. R., Mahmoud, A. I., Simpson, E., Johnson, B. A., Grinsfelder, D., Canseco, D., et al. (2013). Regulation of Neonatal and Adult Mammalian Heart Regeneration by the miR-15 Family. *Proc. Natl. Acad. Sci.* 110, 187–192. doi:10.1073/pnas.1208863110

Rivera, C., Zandonadi, F. S., Sánchez-Romero, C., Soares, C. D., Granato, D. C., González-Arriagada, W. A., et al. (2018). Agrin Has a Pathological Role in the Progression of Oral Cancer. *Br. J. Cancer* 118, 1628–1638. doi:10.1038/S41416-018-0135-5

Takahashi, Y., Nishikawa, M., Shinotsuka, H., Matsui, Y., Ohara, S., Imai, T., et al. (2013). Visualization and *In Vivo* Tracking of the Exosomes of Murine Melanoma B16-BL6 Cells in Mice after Intravenous Injection. *J. Biotechnol.* 165, 77–84. doi:10.1016/J.JBIOTEC.2013.03.013

Torrini, C., Cubero, R. J., Dirkx, E., Braga, L., Ali, H., Prosdocimo, G., et al. (2019). Common Regulatory Pathways Mediate Activity of MicroRNAs Inducing Cardiomyocyte Proliferation. *Cell Rep.* 27, 2759–2771.e5. doi:10.1016/j.celrep.2019.05.005

Tsai, S. C. S., Yang, K. D., Chang, K. H., Lin, F. C. F., Chou, R. H., Li, M. C., et al. (2021). Umbilical Cord Mesenchymal Stromal Cell-Derived Exosomes Rescue the Loss of Outer Hair Cells and Repair Cochlear Damage in Cisplatin-Injected Mice. *Int. J. Mol. Sci.* 22, 6664. doi:10.3390/IJMS22136664

Villa, F., Bruno, S., Costa, A., Li, M., Russo, M., Cimino, J., et al. (2021). The Human Fetal and Adult Stem Cell Secretome Can Exert Cardioprotective Paracrine Effects against Cardiotoxicity and Oxidative Stress from Cancer Treatment. *Cancers (Basel)* 13, 3729. doi:10.3390/CANCERS13153729

Wohlschlegel, J. A., Dwyer, B. T., Dhar, S. K., Cvetic, C., Walter, J. C., and Dutta, A. (2000). Inhibition of Eukaryotic DNA Replication by Geminin Binding to Cdt1. *Science* 290, 2309–2312. doi:10.1126/SCIENCE.290.5500.2309

Yin, V. P., Lepilina, A., Smith, A., and Poss, K. D. (2012). Regulation of Zebrafish Heart Regeneration by miR-133. *Dev. Biol.* 365, 319–327. doi:10.1016/J.YDBIO.2012.02.018

Conflict of Interest: The authors declare that the research was conducted in the absence of any commercial or financial relationships that could be construed as a potential conflict of interest.

Publisher's Note: All claims expressed in this article are solely those of the authors and do not necessarily represent those of their affiliated organizations, or those of the publisher, the editors, and the reviewers. Any product that may be evaluated in this article, or claim that may be made by its manufacturer, is not guaranteed or endorsed by the publisher.

frontiers | Frontiers in Bioengineering and Biotechnology

ORIGINAL RESEARCH
published: 05 July 2022
doi: 10.3389/fbioe.2022.854845

Effect of the Human Amniotic Membrane on the Umbilical Vein Endothelial Cells of Gestational Diabetic Mothers: New Insight on Inflammation and Angiogenesis

Caterina Pipino[1]†, Ángel Bernabé-García[2†], Ilaria Cappellacci[1], Javier Stelling-Férez[2,3], Pamela Di Tomo[1], Manuela Santalucia[1], Carlos Navalón[2], Assunta Pandolfi[1‡] and Francisco José Nicolás[2]*‡*

[1]Center for Advanced Studies and Technology-CAST (ex CeSI-MeT), Department of Medical, Oral and Biotechnological Sciences, University G. D'Annunzio Chieti-Pescara, StemTeCh Group, Chieti, Italy, [2]Regeneration, Molecular Oncology and TGFß, IMIB-Arrixaca, Hospital Clínico Universitario Virgen de La Arrixaca, Murcia, Spain, [3]Department of Nutrition and Food Technology, UCAM, Murcia, Spain

One of the most relevant diabetes complications is impaired wound healing, mainly characterized by reduced peripheral blood flow and diminished neovascularization together with increased inflammation and oxidative stress. Unfortunately, effective therapies are currently lacking. Recently, the amniotic membrane (AM) has shown promising results in wound management. Here, the potential role of AM on endothelial cells isolated from the umbilical cord vein of gestational diabetes-affected women (GD-HUVECs), has been investigated. Indeed, GD-HUVECs *in vivo* exposed to chronic hyperglycemia during pregnancy compared to control cells (C-HUVECs) have shown molecular modifications of cellular homeostasis ultimately impacting oxidative and nitro-oxidative stress, inflammatory phenotype, nitric oxide (NO) synthesis, and bioavailability, thus representing a useful model for studying the mechanisms potentially supporting the role of AM in chronic non-healing wounds. In this study, the anti-inflammatory properties of AM have been assessed using a monocyte–endothelium interaction assay in cells pre-stimulated with tumor necrosis factor-α (TNF-α) and through vascular adhesion molecule expression and membrane exposure, together with the AM impact on the nuclear factor kappa-light-chain-enhancer of activated B cell (NF-kB) pathway and NO bioavailability. Moreover, GD-HUVEC migration and tube formation ability were evaluated in the presence of AM. The results showed that AM significantly reduced TNF-α-stimulated monocyte–endothelium interaction and the membrane exposure of the endothelial vascular and intracellular adhesion molecules (VCAM-1 and ICAM-1, respectively) in both C- and GD-HUVECs. Strikingly, AM treatment significantly improved vessel formation in GD-HUVECs and cell migration in both C- and GD-HUVECs. These collective results suggest that AM positively affects various critical pathways in inflammation and angiogenesis, thus providing further validation for ongoing clinical trials in diabetic foot ulcers.

Keywords: amniotic membrane (AM), HUVECs, diabetes, wound healing, inflammation, angiogenesis

OPEN ACCESS

Edited by:
Peter Ponsaerts, University of Antwerp, Belgium

Reviewed by:
Gaia Spinetti, MultiMedica Holding SpA (IRCCS), Italy
Sveva Bollini, University of Genoa, Italy

****Correspondence:***
Caterina Pipino
caterina.pipino@unich.it
Francisco José Nicolás
franciscoj.nicolas2@carm.es

†These authors have contributed equally to this work and share first authorship

‡These authors have contributed equally to this work and share last authorship

Specialty section:
This article was submitted to Tissue Engineering and Regenerative Medicine, a section of the journal Frontiers in Bioengineering and Biotechnology

Received: *14 January 2022*
Accepted: *11 May 2022*
Published: *05 July 2022*

Citation:
Pipino C, Bernabé-García Á, Cappellacci I, Stelling-Férez J, Di Tomo P, Santalucia M, Navalón C, Pandolfi A and Nicolás FJ (2022) Effect of the Human Amniotic Membrane on the Umbilical Vein Endothelial Cells of Gestational Diabetic Mothers: New Insight on Inflammation and Angiogenesis. Front. Bioeng. Biotechnol. 10:854845. doi: 10.3389/fbioe.2022.854845

INTRODUCTION

Hyperglycemia-induced endothelial dysfunction contributes to the development of inflammation and impaired angiogenesis in diabetes mellitus (Kolluru et al., 2012). Diabetic patients have lower ability to metabolize glucose resulting in hyperglycemic conditions making them more susceptible to inflammation and infection (Kolluru et al., 2012) which may contribute to diabetic wound impairment. It is estimated that 15% of patients with diabetes may develop foot ulcers, responsible for 50% of all diabetes-related hospitalization with negative effects on quality of life and a significant impact also on the healthcare economics (Ahmad, 2016). The formation of skin ulceration in a diabetic foot is a severe medical condition that, without correct healing, can lead to amputation (Bandyk, 2018). Many factors may contribute to impaired wound healing, among which are altered inflammatory response, decreased angiogenesis, progressive skin connective tissue atrophy, and oxidative stress (Tentolouris et al., 2021).

After wounding, endothelial cells are activated, a wide spectrum of cell surface adhesion molecules are overexpressed and leukocytes, neutrophils, and macrophages are recruited to perform the inflammatory and proliferative phases (Okonkwo and Dipietro, 2017). One of the major mediators of this event is the activation of nuclear factor kappa-light-chain-enhancer of activated B cell (NF-kB) pathway triggering, in turn, the upregulation of the expression of the vascular cell adhesion molecules (VCAM-1) and intercellular cell adhesion molecules (ICAM-1) in response to various inflammatory cytokines (Di Tomo et al., 2012).

In addition to inflammation, delayed healing of diabetic wounds is also characterized by impaired angiogenesis responses (Abaci et al., 1999; Waltenberger et al., 2000; Eelen et al., 2015) leading to chronic wounds due to a lack of preventive and adequate interventions. Moreover, nitric oxide (NO) plays a key role in regulating many aspects of inflammatory responses and angiogenesis (Wallace, 2005). Indeed, it is well known that NO is able, under normal conditions, to promote angiogenesis, migration, and proliferation of fibroblast, epithelial cells, endothelial cells, and keratinocytes (Efron et al., 2000). In diabetic foot ulcers (DFUs), hyperglycemia increases vascular super dioxide (O2-) production leading to NO inactivation that subsequently contributes to vascular dysfunction and foot ulcer development (Boykin, 2010).

Therefore, strategies to reduce inflammation and to simultaneously enhance neovascularization may dramatically improve the quality of life of these patients and significantly reduce the global biomedical burden. Nowadays, among recent DFU therapeutic applications, the amniotic membrane (AM) is one of the most promising ones (Zelen 2013; Valiente et al., 2018; Tettelbach et al., 2019; Doucette et al., 2020). AM, as a wound dressing, has been used for over a century and it is an ideal biological graft. AM is made up of a single epithelial cell layer, a thick basement membrane, and an avascular stroma (Silini et al., 2020). So far, many studies regarding the application of AM in DFU have been performed not only to test new possible applications but also to identify processing protocols (Lakmal et al., 2021). However, the role of AM and the mechanisms underlying inflammation and angiogenesis are not fully understood. Thus, to know the effect of AM on endothelial cells during AM treatment of DFUs would be desirable to understand its role in this condition.

Recently, the availability of cellular models representing endothelium affected by hyperglycemic conditions had become very useful to investigate the mechanisms of the disease and assay concrete therapeutic options. Interestingly, we have employed cultured endothelial cells that *in vivo* were exposed to chronic hyperglycemia during pregnancy (Di Fulvio et al., 2014).

Indeed, our previous results showed that these cells, isolated from the human umbilical cord veins of women affected by gestational diabetes (GD-HUVECs), exhibit epigenetic modifications leading to a durable pro-inflammatory phenotype potentially predisposing to endothelial dysfunction (Di Fulvio et al., 2014; Di Tomo et al., 2021). Thus, GD-HUVECs can be used as a valuable model for studying the diabetic endothelium typical of DFUs. Moreover, HUVECs have been commonly used to study molecular and signaling mechanisms related to angiogenesis, a wound repair fundamental process that involves endothelial cell activation, migration, and proliferation (Medina-Leyte et al., 2020).

In this study, by stimulating GD-HUVECs with a pro-inflammatory stimulus such as a low level of tumor necrosis factor-alpha (TNF-α), we have generated an environment like the one found in diabetic foot ulcer endothelium. Therefore, by using this model we have investigated mechanisms through which AM can affect inflammation, migration, and angiogenesis to better understand its positive role in the diabetic chronic wound environment.

MATERIALS AND METHODS

HUVEC Cultures and Experimental Protocol

This study was carried out on HUVECs isolated from the umbilical cord veins of newborns delivered between the 36th and the 40th gestational week at the Hospital of Chieti and Pescara (Italy) from randomly selected mothers affected by gestational diabetes (GD) and healthy Caucasian mothers (control, C), according to previously published methods (Ucci et al., 2019). All procedures agreed with the ethical standards of the Institutional Committee on Human Experimentation (reference number 1879/09COET) and with the Declaration of Helsinki principles. The protocol was approved by the Institutional Review Board and informed consent was signed by each participating subject. Briefly, umbilical cords were collected immediately after delivery, then umbilical cord veins were cannulated and perfused with 1 mg/ml collagenase1A at 37°C and HUVECs collected in a endothelial growth medium (HUVEC medium) composed by DMEM/M199 (1:1) supplemented with 1% L-glutamine, 1% penicillin–streptomycin, and 20% fetal bovine serum (FBS). Then, the cell suspension was centrifuged at 1,200 rpm for 10 min and the cell pellet was resuspended in a HUVEC medium and plated on 1.5% gelatin-coated tissue culture plates. Primary C-HUVECs and GD-HUVECs were characterized as

von Willebrand factor positive and alpha-smooth muscle cell actin negative; for all experiments, the cells were *in vitro* used between the 3rd and 5th passage.

Related to the amniotic membrane, the samples and data from patients included in this study, who gave the written informed consent, were collected, processed, and provided by the Biobanco en Red de la Región de Murcia, BIOBANC-MUR, registered on the Registro Nacional de Biobancos with registration number B.0000859, and were processed following the standard operating procedures with an appropriate approval of the Ethical and Scientific Committees.

HUVECs were grown on 1.5% gelatin-coated tissue culture plates (Sigma-Aldrich) in a complete low-glucose (1 g/L) DMEM and M199 medium (ratio 1:1) supplemented with 20% FBS, 10 μg/ml heparin and 50 μg/ml endothelial cell growth factor, 1% penicillin/streptomycin, and 1% L-glutamine (all from Biowest, Nuaillé, France) (standard medium).

All experiments were performed in technical triplicate using at least three different cellular strains (n = 3) of C- and GD-HUVECs following the experimental protocols illustrated in **Supplementary Figure S1**.

AM Collection and Storage

The amniotic membrane was prepared as previously described (Ruiz-cañada et al., 2017). Briefly, the term placenta from healthy donor mothers, average age of 36, was obtained from uncomplicated cesarean section. The fetal membranes were washed in physiological saline solution (PSS) (B.Braun, Barcelona, Spain) supplemented with 50 μg/ml amphotericin (Bristol-MyersSquibb, Madrid, Spain), 48 μg/ml clotrimazole (Almirall-Prodesfarma, Barcelona, Spain), 50 μg/ml tobramycin (Laboratorios Normon, Madrid, Spain), and 50 μg/ml vancomycin (Laboratorios Hospira, Madrid, Spain) and rapidly transferred to the laboratory under sterile conditions. Under a laminar flow cabinet, the amnion was mechanically peeled from the chorion, washed three to four times with 200 ml of PBS (Biowest, Nuaillé, France), and flattened onto the sterile nitrocellulose paper (Pierce, Thermo Fisher Scientific, Waltham, MA United States) with the amniotic epithelium surfaced up, and the spongy layer facing and sticking to the nitrocellulose paper. Then, the paper with adhered membrane was cut into 1 cm × 1 cm fragments. Freshly cut AM fragments were separated from paper pieces and placed in a sterile vial containing a freezing solution made of 10% dimethyl sulfoxide (DMSO) (Sigma-Aldrich, St Louis, MO, United States), 4% human albumin (Grifols, Bercelona, Spain) in the DMEM (Biowest, Nuaillé, France) medium and then frozen at −80°C and later preserved in liquid nitrogen until further use. On the day of the experiment, AM pieces were thawed at 37°C, then the pieces were washed three times with DMEM, and placed at 37°C in a 7.5% CO_2 incubator for 2 hours for the re-vitalization of the amniotic membrane cells. Then, the appropriate number of AM pieces, related to the number of cells/culture plate area, was used for the desired experiment. Briefly, for the use of the amniotic membrane, we established a ratio of number of pieces of amniotic membrane per cultivated cell surface. The AM (1 square centimeter pieces) was used following this rationale: one piece of AM in a well of a 24 well plate (cell migration and Matrigel tube formation assays), three pieces for a 6 well plate well (flow cytometry assay, Western blot, monocyte adhesion assay, and gene expression assay) or five to six pieces in a 5 cm diameter plate (immunofluorescence assay). For the experiment replicates, a different AM donor was employed each time.

Ribonucleic Acid Isolation and Real-Time Polymerase Chain Reaction

The gene expression of adhesion molecules was performed in serum-starved cells (medium with 0.5% FBS) that had been incubated for 24 h with AM and then treated with TNF-α (1 ng/ml) for 2, 6, or 24 h. Following treatments, RNA was extracted using the RNeasy-mini system (Qiagen). Afterward, 1 μg of RNA was retro-transcribed using iScript reagents (Bio-Rad). The resulted cDNA was used to perform a quantitative real-time PCR (RT-PCR) using the SYBR premix ex Taq kit (Takara Bio Europe) according to the manufacturer's instructions to analyze the inflammation-associated genes (**Table 1**). Each analysis was normalized with glyceraldehyde 3-phosphate dehydrogenase (*GAPDH*) gene expression according to the 2-ΔΔCt method. The experiment was carried out on three different strains for C-HUVECs and three different strains for GD-HUVECs, each in technical triplicate.

Immunofluorescence Assay and Confocal Laser Scanning Microscopy Analysis

Control HUVECs and GD-HUVECs were grown until they reached 50% confluence on round glass coverslips placed in 5 cm diameter Petri dishes, using a standard medium (20% FBS, as aforesaid). At this point, the cells were PBS-washed, and the medium was replaced by the reduced FBS medium to begin a 24-h serum-starvation period. At the same time, five to six –AM pieces (1 cm^2) were placed over the cell-seeded glass coverslips floating on the culture medium. After 24 h, control coverslips were removed from the Petri dish and fixed with paraformaldehyde 4% (AppliChem GmbH, Darmstadt, Germany) in PBS (Biowest, Nuaillé, France) for 15 min. TNF-α (1 ng/ml) was added to the remaining coverslips at the 1 ng/ml final concentration. The coverslips were removed from the medium and fixed (as aforesaid) at the indicated times. Immunofluorescence was carried out as previously described (Alcaraz et al., 2015), briefly after blocking, the cells were incubated for 1 h (RT) with the proper antibody diluted in blocking buffer, washed and further incubated with the appropriate fluorescent-conjugated secondary antibodies in combination with Alexa Fluor 594 or Alexa Fluor 468 conjugated phalloidin depending on the secondary antibody used for the antigen detection (Molecular Probes, Thermo Fisher Scientific, Waltham, MA, United States) and Hoechst 33258 (Fluka, Biochemika, Sigma-Aldrich, St Louis, MO, United States) for 30 min. Finally, the samples were examined, and representative images were taken using the confocal microscope Leica TCS SP8 MP (Leica, Wetzlar, Germany). The acquisition of images was performed using Leica Application Suite X (LAS X) software. The antibodies used

TABLE 1 | Primers used for quantitative PCR.

Gene name (GeneCards®)/primer name	Primer sequence 5′–3′
CCL2 Fw	AGACTAACCAGAAACATCC (Sigma KiCqStart)
CCL2 Rev	ATTGATTGCATCTGGCTG (Sigma KiCqStart)
GAPDH Fwd	AGCTCAGGCCTCAAGACCTT
GAPDH Rev	AAGAAGATGCGGCTGACTGT
ICAM1 Fwd	ACCATCTACAGCTTTCCG (Sigma KiCqStart)
ICAM1 Rev	TCACACTTCACTGTCACC (Sigma KiCqStart)
SELE Fwd	GAGAATTCACCTACAAGTCC (Sigma KiCqStart)
SELE Rev	AGGCTTGAACATTTTACCAC (Sigma KiCqStart)
VCAM1 (mix Fwd/Rev)	Proprietary sequence (Qiagen QuantiTect®) QT00018347

CCL2, C-C motif chemokine ligand 2. GADPH, glyceraldehyde-3-phosphate dehydrogenase. ICAM1, intercellular adhesion molecule 1. SELE, Selectin E. VCAM1, vascular cell adhesion molecule 1.

were anti-NF-kB (Abcam, ab16502, Cambridge, United Kingdom) and Anti-paxillin (Santa Cruz Biotechnology, sc-365379 Heidelberg, Germany). For proper assessment and interpretation of NF-kB nuclear translocation intensity, the maximum intensity projection of 7 z-stacks was used. The experiment was carried out on three different strains for C-HUVECs and three different strains for GD-HUVECs, each in technical triplicate.

Flow Cytometry Analysis

At the basal state and after stimulations, non-permeabilized cells were detached by 5 mM EDTA, washed, and re-suspended in 0.5% BSA solution. The cells were treated and incubated with anti-VCAM-1 PE conjugate (Santa Cruz Biotechnology, sc-13160, 1:100) and with anti-ICAM-1 FITC conjugate (Santa Cruz Biotechnology, sc-107, 1:100) as previously described (Ucci et al., 2019). One test tube for the basal state and one for the TNF-α-treated condition were incubated with anti-VCAM-PE and anti-ICAM-FITC isotypes (normal mouse IgG2a FITC-conjugated and normal mouse IgG1 PE-conjugated, Santa Cruz Biotechnology, 1:100) as negative controls. Flow cytometry analysis was performed on a BD FACS Canto II flow cytometer (BD Biosciences) and for each sample 1×10^4 events were analyzed using FACSDiva v 6.1.3 (BD Biosciences) and FlowJo 8.3.3 software (Tree Star Inc., Ashland, United States). All the results are expressed as mean fluorescence intensity (MFI) ratio ±standard deviation (SD). Each value was calculated by dividing the MFI of positive events by the MFI of negative events (MFI of secondary antibody). The experiment was carried out on four different strains for C-HUVECs and four different strains for GD-HUVECs, each in technical triplicate.

Monocyte-HUVEC Adhesion Assays

The adhesion assay was performed in C- and GD-HUVECs under the basal condition and after incubation for 24 h with AM. In detail, the cells were grown in six-well tissue culture plates (200.000 cells/well) and, when confluent, the cells were serum-starved (0.5% FBS), then stimulated with TNF-α (1 ng/ml) for 16 h, and finally AM was added for 24 h. Three pieces of 1 cm^2 AM were added per well.

Monocytes (U937 cell lines, European Collection of Authenticated Cell Cultures, ECACC) were used to evaluate the adhesion to HUVEC monolayers as previously described (Di Tomo et al., 2015; Ucci et al., 2019). Briefly, the medium was removed from each HUVEC well, then the cells were gently washed with DMEM, and 1 million of monocyte suspension was added to each well and incubated on HUVECs for 20 min with gentle shaking at room temperature. Finally, monocyte suspension was collected and HUVECs were gently washed, then the adherent monocytes on HUVECs were fixed with paraformaldehyde 1%. To identify the number of adherent monocytes for each tested strain, 12 counts for every experimental condition were performed (employing at least 3 different randomly selected high-power fields, ×10 magnification) using a quadrant. For this experiment, four different strains for C-HUVECs and four different strains for GD-HUVECs were used.

Western Blot

Control- and GD-HUVECs were seeded in 6 well plates using the standard medium (20% FBS). Then, the cells were PBS-washed, and the medium was replaced by 0.5% FBS to begin a 24-h serum-starvation period. At the same time, three AM pieces (1 cm^2) were placed over the cell by floating on the culture medium. After 24 h, then TNF-α (1 ng/ml) was added for 1 and 3 h. Briefly, for protein extraction, the cells were washed with cold PBS and lysed using RIPA buffer (Sigma-Aldrich) supplemented with phosphatase inhibitors (I and II) and protease inhibitors (all from Sigma-Aldrich). The protein concentration of the lysates was determined using the Qubit Protein Assay kit (Invitrogen). The membranes were blocked with 5% BSA, followed by immunoblotting with the primary antibody against rabbit anti-p-NF-kB p65 (Ser536) (^{93}H1) (1:1000, Cell Signaling Technology), overnight at 4°C, followed by rabbit horseradish peroxidase-conjugated secondary antibody (1:5000) (Santa Cruz Biotechnology). Then, the membranes were stripped and immunoblotted with the primary antibody against rabbit anti-NF-kB p65 (1:1000, Cell Signaling Technology), followed by rabbit horseradish peroxidase-conjugated secondary antibody (1:5000) (Santa Cruz Biotechnology). The immune complexes were visualized by means of the ECL Plus detection reagent (Thermo Scientific), and data were processed and quantified using UVITEC Alliance software. Protein densities were divided by β-actin densities (mouse monoclonal anti-β-actin, 1:10000), and the resulting

ratio was considered as an index of p-NF-kB expression in arbitrary units. The experiment was carried out on three different strains for C-HUVECs and three different strains for GD-HUVECs, each in technical triplicate.

cGMP Determination

Intracellular cyclic 3′-5′ guanosine monophosphate (cGMP) levels were evaluated using a commercially available Elisa kit (Cayman Chemical) as previously shown (Di Tomo et al., 2012). The experiment was carried out on six different strains for C-HUVECs and six different strains for GD-HUVECs, each in technical triplicate.

Matrigel Tube Formation Assay

Control- and GD-HUVECs were plated (2.5×10^4 cells/well) in the growth factor–reduced basement membrane matrix gel, also called Matrigel (BD Biosciences), coated 96-well plates using the 10% FBS HUVEC culture medium. Preliminary experiments were conducted to identify the suitable number of cells per well and the best serum concentration. After plating, the cells were incubated for 20 min at 37°C inducing cellular adhesion to Matrigel and then, in the respective wells, AM pieces were added to floating in the culture medium. Six hours later representative photographs were acquired using an inverted microscope (Olympus). Images were processed using ImageJ software (Angiogenesis analyzer tool) to analyze angiogenic parameters (i.e., number of segments, meshes, and master junctions) in the basal state and following the amniotic membrane incubation in three different strains of C-HUVECs and three different strains of GD-HUVECs in technical triplicate.

Wound Healing Scratch Assay

For the wound healing scratch assay, C- and GD-HUVECs were seeded on 24 well plates and grown for 2 days, then the growth medium was changed for complete DMEM with 1% FBS for 24 h before the wound healing scratch assay. The wound was made by scratching a line across the bottom of the dish on a confluent cell's monolayer using a sterile p-200 pipette tip. The cells were rinsed very gently with PBS and then cultivated in the medium with 1% FBS with the addition of AM pieces floating in the culture medium. Pictures were taken at ×10 magnifications using an inverted microscope (Olympus). To quantify migration, the area of the gap obtained by scratching a line across the bottom of the dish was quantified using ImageJ software (http://rsbweb.nih.gov/ij/). After each treatment, the area of the same gap was measured again. The difference between the initial and final areas was calculated. That difference was represented in each treatment and bigger differences indicate better migration. The experiment was carried out on three different strains for C-HUVECs and three different strains for GD-HUVECs, each in technical triplicate.

Statistical Analysis

The results are presented as the means ± standard deviation (SD) or standard error of the mean (SEM) of at least three different experiments using at least three different cellular strains ($n = 3$) both of C-HUVECs and GD-HUVECs. The ANOVA test followed by the Tukey's multiple comparison test for *post hoc* comparisons was used to analyze the differences between C- and GD-HUVECs and between the different treatments. The significance was defined as a p-value less than 0.05.

RESULTS

Amniotic Membrane Decreases the Expression of Genes Involved in Inflammation

The gene expression of several genes involved in inflammation was performed to evaluate the ability of AM in preventing TNF-α-triggered inflammatory response in endothelial cells.

The cells, either C-HUVECs or GD-HUVECs, were first treated with AM for 24 h and then stimulated with TNF-α up to 24 h. The cells had a strong response to the TNF-α stimulation of all genes tested, and it was significant that *VCAM-1* and E-selectin (*SELE*) had a stronger response in GD-HUVECs compared to C-HUVECs ($p < 0.001$), for the rest of the genes, there was no apparent expression differences between C-HUVECs and GD-HUVECs (**Figure 1**). Strikingly, in all cases, a pronounced attenuation to the response to TNF-α was seen in samples previously treated with AM in both C-HUVECs and GD-HUVECs. Giving special attention results in the response to the expression of *VCAM-1* and *SELE* where the previous treatment with AM markedly attenuated the response to TNF-α (**Figures 1A,D**). All these data indicate that AM causes a decrease in the transcriptional response of HUVECs to TNF-α for the expression of these four genes involved in inflammation.

Amniotic Membrane Reduces the Membrane Exposure of Endothelial Adhesion Molecules

To further validate these findings, VCAM-1 and ICAM-1 membrane exposure, the main mechanism behind the interaction between monocytes and endothelial cells, was evaluated. In order to reproduce the inflammatory milieu observed in DFUs, the amniotic membrane potential (24 h of incubation) was tested on C- and GD-HUVECs under basal conditions, as well as in cells previously treated with 1 ng/ml of TNF-α for 16 h. **Figure 2A** shows a significant increase in both VCAM-1 ($p < 0.0001$) and ICAM-1 ($p < 0.0001$) membrane exposure following treatment with TNF-α, in both cell populations, compared to basal conditions. If anything, there was a trend of higher expression of both molecules in GD-HUVECs compared to C-HUVECs. Noticeably, 24 h AM incubation produced a significant decrease in VCAM-1 and ICAM-1 protein exposure to the cell cytosolic membrane promoted by TNF-α, in both C- (VCAM-1 $p < 0.0001$ and ICAM-1 $p < 0.05$, **Figure 2A**) and GD-HUVEC populations (VCAM-1 $p < 0.0001$ and ICAM-1 $p < 0.001$, **Figure 2A**).

To measure the real impact on monocyte adhesion of the variation caused by AM on the expression of the endothelial

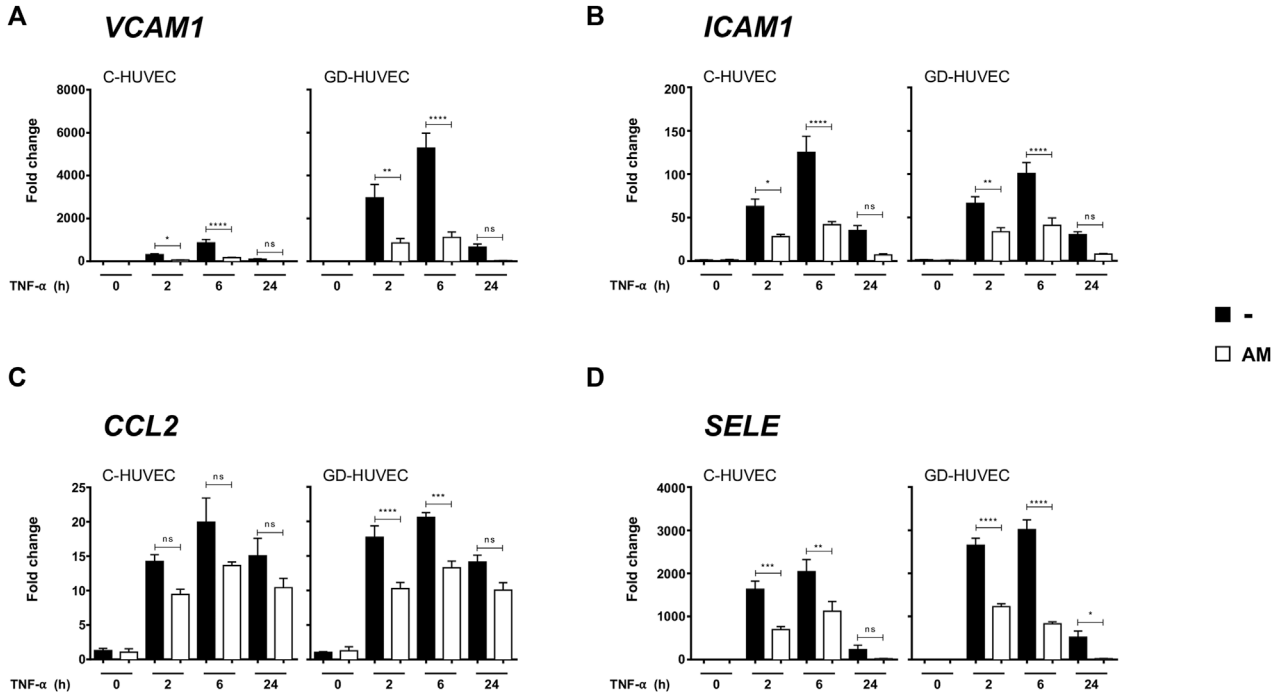

FIGURE 1 | AM reduces the expression of genes involved in inflammation. Gene expression analysis of *VCAM-1* **(A)**, *ICAM-1* **(B)**, *CCL2* **(C)**, and *SELE* **(D)**, from C- and GD-HUVECs untreated and after TNF-α stimulation of cells that had been pretreated or not with AM for 24 h. Quantitative data in the histograms **(A–D)** show the mRNA relative expression (target gene expression normalized with GAPDH expression using the 2-ΔΔCt method). Each measurement is defined as the mean ± SD using three different strains for C-HUVECs and three different strains for GD-HUVECs ($n = 3$). ANOVA and Tukey's multiple comparison test: $^{*}p < 0.05$, $^{**}p < 0.01$, $^{***}p < 0.001$ and $^{****}p < 0.0001$.

adhesion molecules, the binding of U937 monocyte cell line to AM-treated C- and GD-HUVECs was investigated. Of note, the representative high-power field pictures showed that AM treatment induces a reduction in the monocyte adhesion rate that was very evident when comparing TNF-α-treated cells to the same treatment supplemented with AM (**Figure 2B**). Additionally, AM caused an improvement in cells' morphology compared to cells under basal conditions (**Figure 2B**). The quantification of adhered monocytes in pictures showed that, under basal conditions, the monocyte adhesion rate was higher in GD-HUVECs than that in C-HUVECs ($p < 0.05$), indicating the GD-HUVEC pro-inflammatory phenotype. Next, a trend of reduction in monocyte–endothelial cell interaction was observed following AM incubation in both cell populations, especially in GD-HUVECs ($p < 0.05$). As expected, 16 h of TNF-α stimulation significantly enhanced the number of adhered monocytes both in C- and GD-HUVEC cultures, as compared to basal ($p < 0.0001$). Strikingly, 24 h of AM incubation, following TNF-α pre-treatment, induced a significant reduction of monocyte adhesion in both C- and GD-HUVECs ($p < 0.01$ and $p < 0.0001$, respectively) (**Figure 2C**).

Altogether, these data indicate that AM produces a powerful effect on the attenuation of TNF-α expression of endothelial adhesion molecule genes. This is reflected in the number of adhesion molecules detected at the cytosolic membrane of the cells that causes strong differences in the adhesion of monocytes.

Amniotic Membrane Attenuates the Phosphorylation of NF-kB and Its Nuclear Translocation in Response to TNF-α

NF-kB, a major mediator of vascular inflammation, is involved in the expression of critical molecules participating in the adhesion of monocytes to HUVECs (Di Tomo et al., 2012). To further investigate the possible link between the anti-inflammatory role of AM and the attenuation of TNF-α signaling, we looked at NF-kB phosphorylation during TNF-α stimulation. As expected, TNF-α treatment produced a neat increase in NF-kB phosphorylation that was clearly attenuated when cells had been pretreated with AM for 24 h (**Figures 3A**,**B**). Moreover, stimulation of both C-HUVECs and GD-HUVECs with TNF-α caused a very evident NF-kB nuclear translocation at 1 and 3 hours (**Figure 3C**). Consistently with phosphorylation data, 24 hours of preincubation with AM significantly decreased the nuclear translocation of NF-kB in response to TNF-α stimulation in both C- and GD-HUVECs, this was especially evident at time 3 hours (**Figure 3C**).

These data suggest that the effect seen on the expression of the genes and further protein localization at the cytosolic membrane of HUVECs could be related to the differential phosphorylation

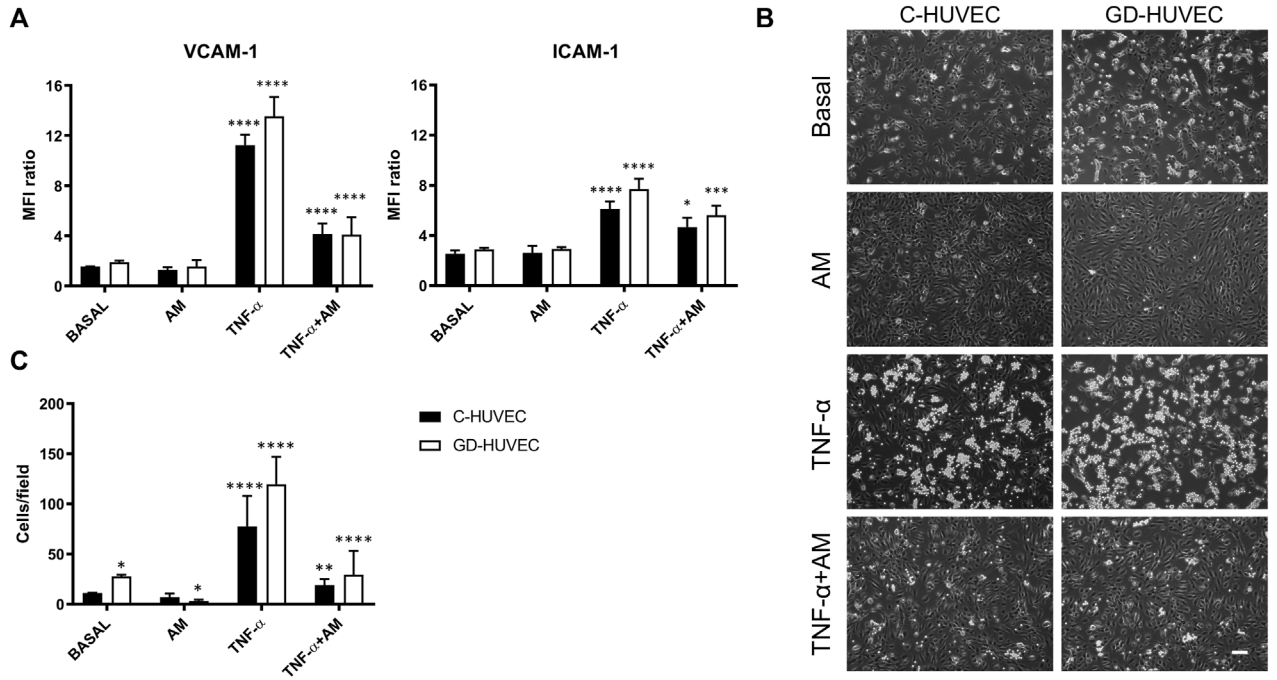

FIGURE 2 | Effect of AM on VCAM-1 and ICAM-1 membrane exposure and TNF-α-induced monocyte adhesion in C- and GD-HUVECs analyzed by flow cytometry. **(A)** VCAM-1 and ICAM-1 membrane exposure in C- and GD-HUVECs untreated (basal) and treated for 16 h with 1 ng/ml of TNF-α with or without AM incubation (24 h). Quantitative data in the histograms show the mean fluorescence intensity (MFI) ratio between the signal and the background noise. The experiments were performed using five different cellular strains for C- and five different cellular strains for GD-HUVECs ($n = 5$). ANOVA and Tukey's multiple comparison test: $^{*}p < 0.05$ TNF-α + AM vs. TNF-α; $^{***}p < 0.001$ TNF-α+AM vs. TNF-α; $^{****}p < 0.0001$ TNF-α vs. basal and vs. AM; $^{****}p < 0.0001$ TNF-α + AM vs. TNF-α. **(B)** Monocyte-endothelial cell interaction on C- and GD-HUVECs untreated (basal) and incubated with AM (24 h) after TNF-α stimulation for 16 h. Representative pictures of C- and GD-HUVECs for each experimental condition. Bar represents 100 μm. Quantitative data, in the histogram **(C)**, show the number of adherent U937 cells obtained by analyzing the microscope images of four different cellular strains for both C-HUVECs and GD-HUVECs ($n = 4$), each including 12 counts per condition. Each measurement is defined as the mean ± SD of adherent monocytes. ANOVA and Tukey's multiple comparison test: $^{*}p < 0.05$ basal GD-HUVEC vs. basal C-HUVEC and AM GD-HUVEC vs. basal GD-HUVEC; $^{**}p < 0.01$ TNF-α + AM vs. TNF-α; $^{****}p < 0.0001$ TNF-α vs. basal and vs. AM, TNF-α + AM vs. TNF-α.

and translocation of NF-kB in response to TNF-α depending on whether the cells had been previously treated with AM.

Amniotic Membrane Improves NO Bioavailability

Nitric oxide deficiency has been proven as an important mechanism associated with vascular inflammation and it is responsible for poor healing in DFU patients (Ahmad 2016). Thus, we evaluated whether AM may modulate NO bioavailability in HUVECs by means of measurement of cGMP levels. As shown in **Figure 4**, following 24 h of AM treatment, basal cGMP levels slightly increased in both C- and GD-HUVECs. As expected, when both cell cultures were pre-treated with TNF-α, cGMP levels decreased ($p < 0.05$) and, interestingly, the NO bioavailability was significantly increased by AM incubation. Of note, preincubation with L-NAME, the inhibitor of constitutive isoforms of nitric oxide synthase (NOS), produced a clear inhibition of both ionomycin (positive control) and AM stimulating effect, which was completely abolished by L-NAME preincubation (**Figure 4**). Altogether these data suggest that AM was able to counteract the effect of TNF-α increasing NO bioavailability through eNOS enzymatic activity.

Amniotic Membrane Stimulates Matrigel Tube Formation in GD-HUVECs

HUVECs are the most used cells to perform the Matrigel tube formation assay, a test of powerful utility to screen the angiogenic activity of vascular endothelial cells *in vitro*. Since diabetic foot ulcers are characterized by impaired blood vessel formation, the AM capacity in improving endothelial cell network-like structure generation, using the Matrigel tube formation assay, was evaluated. To validate the AM effect, several angiogenic parameters were analyzed following vessel formation as shown in the representative images in **Figure 5A**.

The effect of AM on C- and GD-HUVEC tubulation is shown in **Figure 5A**. To better understand the consequences of AM application, several parameters were tested, measured, and their values are represented (**Figures 5B–G**). Under basal conditions, the total isolated branch length (**Figure 5B**) and the number of isolated segments (**Figure 5C**) were increased in GD-HUVECs compared to control ones ($p < 0.05$), thus supporting the

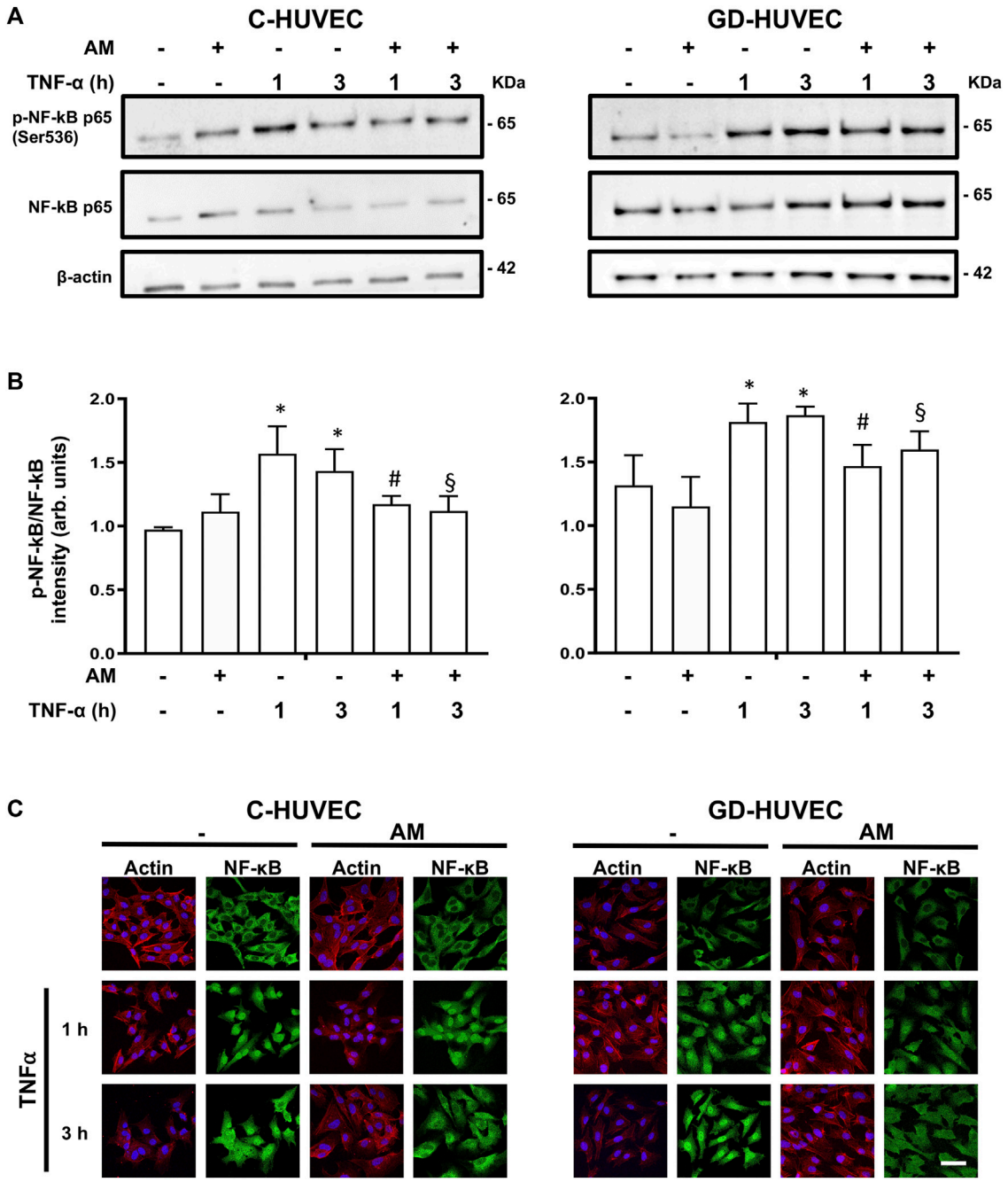

FIGURE 3 | Amniotic membrane attenuates TNF-α-induced NF-κB phosphorylation and nuclear translocation. Sub-confluent C-HUVECs and GD-HUVECs were serum-starved, treated with AM for 24h, then TNF-α was added at 1 and 3 h. **(A)** Protein extract was analyzed for WB for the mentioned antibodies. **(B)** Histograms show Western blot quantification of NF-κB phosphorylation experiments (n = 3); *p< 0.05 vs basal; #p< 0.05 vs TNF-α 1 h; §p< 0.05 vs TNF-α 3 h. **(C)** Samples were immunostained with a specific antibody against NF-κB and co-staining with Hoechst-33258 and phalloidin to reveal nuclei and he actin cytoskeleton, respectively. This experiment was repeated at least three times. Representative images are shown.

hypothesis of impaired angiogenesis in GD-HUVECs. Of note, the AM incubation induced a trend in the reduction of isolated branch length and isolated segments in GD-cells, therefore, indicating the potential of AM in improving the network formation (**Figures 5B,C**).

For all the other parameters analyzed (**Figures 5D,E**), under the basal conditions, GD-HUVECs showed a reduced level, thus further supporting the hypothesis of reduced angiogenesis in diabetic cells. Importantly, the AM incubation enhanced the number of segments in GD-HUVECs (p < 0.01, **Figure 5D**),

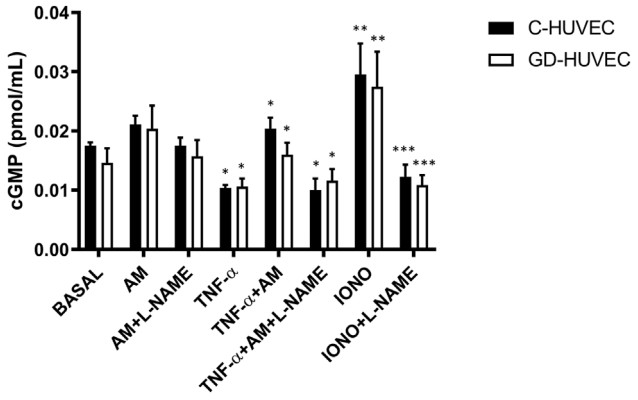

FIGURE 4 | Effect of AM on intracellular cGMP levels measured by ELISA in untreated (basal) and TNF-α-stimulated C- and GD-HUVECs after preincubation for 24 h with AM. Ionomycin (2 μM, 24 h) was used as a positive control. L-NAME (1 mmol/L) was added 45 min before AM and Ionomycin. Data are expressed as pmol/well and results by mean ± SEM, n = 4. ANOVA and Tukey's multiple comparison test: $^{*}p < 0.05$ TNF-α vs. basal; TNF-α+AM vs. TNF-α; TNF-α +AM+L-NAME vs. TNF-α+AM; $^{**}p < 0.01$ IONO vs. basal; $^{***}p < 0.001$ IONO+L-NAME vs. IONO.

as well as the number of meshes was improved ($p < 0.05$, **Figure 5E**). Again, the number of master junctions and the number of nodes (**Figures 5F,G**) increased after AM exposure in GD-HUVECs compared to the basal condition ($p < 0.01$), thus indicating an improvement in network interconnections. On the contrary, C-HUVECs did not show any significant variation in the parameters analyzed.

Overall, the analysis performed here showed impaired vessel formation in GD-HUVECs as demonstrated by the low rate of interconnections and all the analyzed elements were improved following 6 h of AM incubation.

AM Stimulates Cell Migration in GD-HUVECs

AM has a positive effect on the cell migration of different cell types that is faithfully reflected in the tangible rearrangement of migration machinery (Alcaraz et al., 2015; Bernabé-García et al., 2017; Ruiz-Cañada et al., 2018). Indeed, AM is able to induce the overexpression and activation of very important proteins for cell migration, such as c-Jun (Castellanos et al., 2017).

Many endothelial cell functions are mediated by the ability of endothelial cells to migrate, either to the site of new blood vessels or to repair a vessel wound (Lamalice et al., 2007). In angiogenesis, which is considered to be particularly important for vascular formation in adults, the migration of vascular endothelial cells is deeply involved (Serini et al., 2003; Folkman 2007; Clapp et al., 2009).

Here, first, we measured cell migration on C- and GD-HUVECs using the wound healing scratch assay (**Figure 6**). Following 24 h, the wounded area was examined by phase-contrast microscopy. Interestingly, the amniotic membrane significantly enhanced cell migration in both C- and GD-

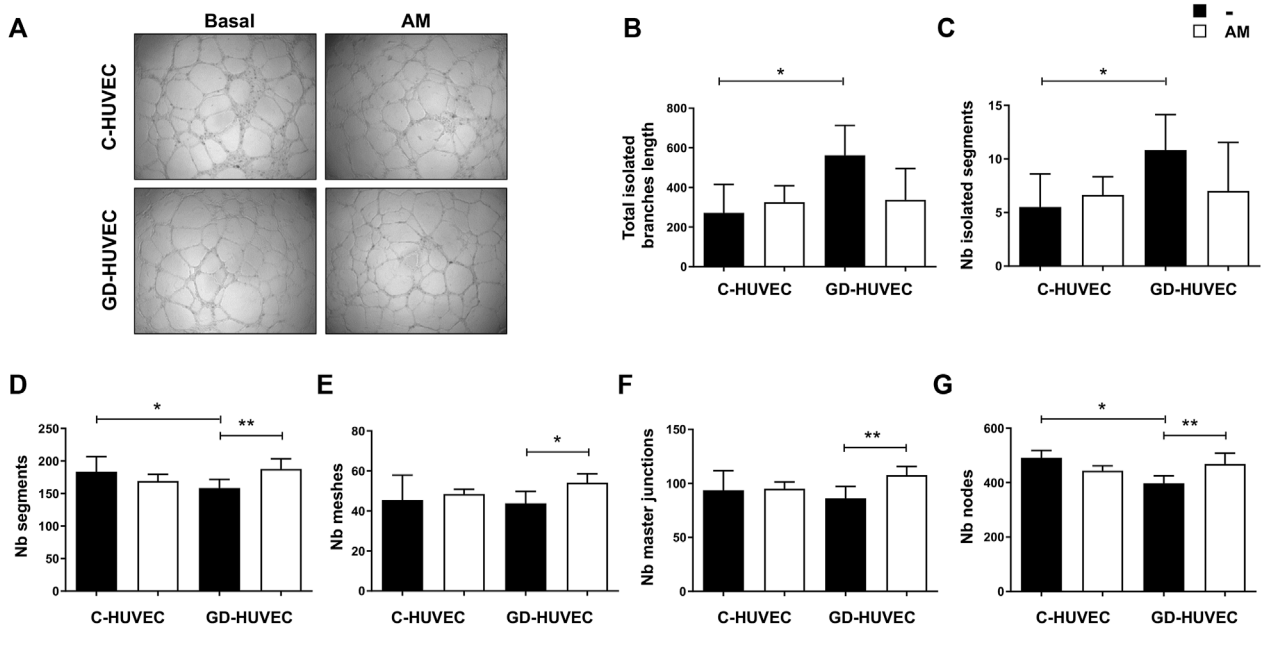

FIGURE 5 | Effect of AM on tube-like structure formation capacity on Matrigel. **(A)** Representative images of C- and GD-HUVECs for both experimental conditions. **(B–G)** Different angiogenic parameters analyzed in C- and GD-HUVECs under basal conditions and after 6 h of AM incubation. Each value is expressed as mean ± SD using three different cellular strains for C-HUVECs and three different cellular strains for GD-HUVECs ($n = 3$). ANOVA and Tukey's multiple comparison test: $^{*}p < 0.05$, $^{**}p < 0.01$.

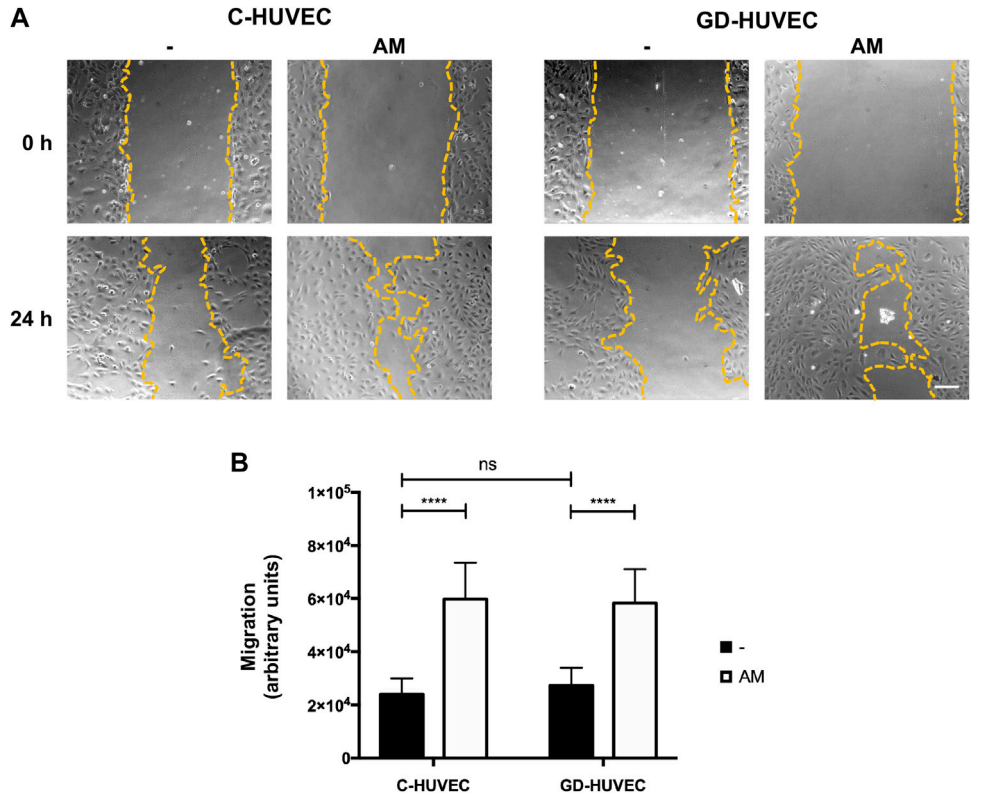

FIGURE 6 | AM induces cell migration in C- and GD-HUVECs. **(A)** HUVECs were wounded and allowed to migrate for the indicated time in the presence or absence of AM. Representative scratch assay from each experimental condition are shown. The wound edges are outlined in yellow. **(B)** Quantification of the difference of migration between 0 and 24 h. ANOVA and Tukey's multiple comparison test: ****$p < 0.0001$.

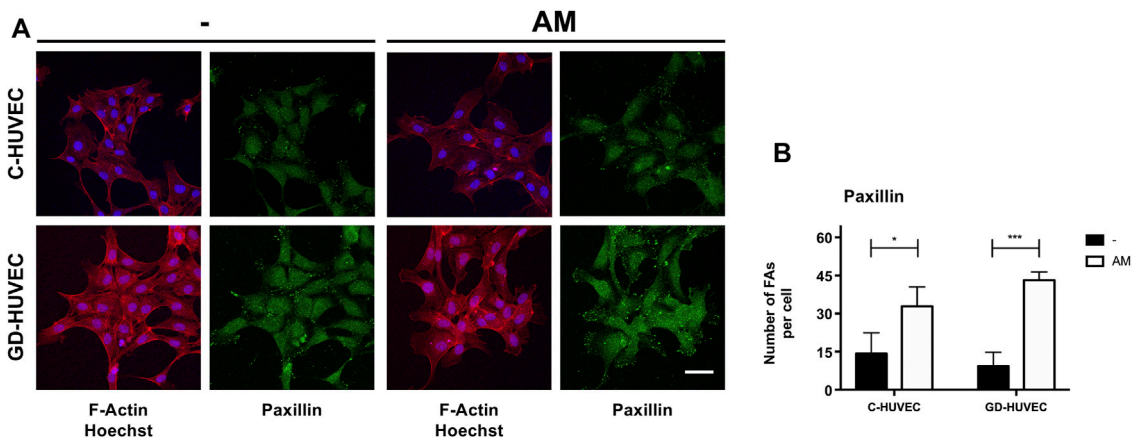

FIGURE 7 | AM induces an active remodeling of focal adhesions (FAs). **(A)** Sub-confluent C-HUVECs and GD-HUVECs were serum-starved cultured for 24 h in presence or absence of AM. Then, samples were immunostained with a specific antibody against paxillin and co-stained with Hoechst-33258 and phalloidin to reveal nuclei and the actin cytoskeleton, respectively. All images were acquired using a confocal microscope and processed using ZEN software. These experiments were repeated at least three times. Representative images are shown. Bar represents 50 μm. **(B)** Focal adhesion (FA) quantification of Paxillin. All images were analyzed through ImageJ software. The plots represent the mean of several technical replicates of three C-HUVEC and three GD-HUVEC strains ($n = 3$). The number of FAs as the region of interests (ROIs) was selected and measured. *$p < 0.05$ and ***$p < 0.001$.

HUVECs (**Figure 6B**, $p < 0.0001$). Then, we studied the subcellular localization of paxillin, a protein involved in the formation of focal adhesion that allows the monitorization of the formation and disassembly of cell adhesions (Mayor and Etienne-Manneville, 2016). When the cells migrate, paxillin-marked focal adhesions reduce their size and become more abundant, suggesting a rapid turnover of these structures to favor cell migration (Mayor and Etienne-Manneville, 2016). The examination of C- and GD-HUVECs treated with AM showed a clear increase in the number of focal adhesions (FAs) with an apparent lower size (**Figures 7A,B** and **Supplementary Figure S2**).

These data would be coherent with an increment of cell motility that may explain the better tubulation experienced by GD-HUVECs in the presence of AM.

DISCUSSION

In the present study, we investigated the potential anti-inflammatory and pro-angiogenic role of AM by using the *in vitro* model of endothelial cells derived from the umbilical cord vein of gestational diabetes women (GD-HUVECs), a precious cellular model of endothelial dysfunction taking place during *in vivo* hyperglycemia (Di Tomo et al., 2021). This study was based on the evidence that the progression of a non-healing phenotype in DFUs is closely linked to increased inflammation, reduced cell migration, and poor vascular networks (Okonkwo and Dipietro, 2017).

The use of placental-based tissues is proposed to aid in healing through the reduction of inflammation, the enhancement of cell migration into the wound environment, the stimulation of cell proliferation, and the improvement of angiogenesis (Pipino et al., 2013; Castellanos et al., 2017).

Chronic wounds fail to proceed to closure for various reasons, impaired vascularization is one of them, and that causes a long-lasting inflammatory process, alterations in the proliferative phase, and cell senescence (Castellanos et al., 2017). The benefits of AM in human therapy have been well established either by using it as a whole dressing or by using AM extracts accompanied by any matrix vehicle (Parolini and Caruso, 2011; Murphy et al., 2017). Apart from its immunomodulatory/anti-inflammatory effects, AM exhibits anti-bacterial properties and low immunogenicity (Parolini et al., 2009). Several clinical studies have used AM for the curing of burn injuries, skin wounds, DFU, chronic leg ulcers, and ocular surface reconstruction (Ornella Parolini et al., 2009; Insausti et al., 2010). In a direct collaboration with the diabetic foot ulcer unit of the Hospital Clínico Universitario Virgen de la Arrixaca (Murcia, Spain), we followed the evolution of 11 patients with DFU that had been treated with AM. A very successful outcome of the treatment shows the wound healing acceleration and a positive evolution of different DFUs upon AM treatment (Valiente et al., 2018).

In 2017, Laurent et al. (2017) , performed a meta-analysis which included different clinical trials to test AM effects on diabetic patients' foot ulcers. The results showed that the amniotic membrane treatment combined with the standard of care (SOC) is preferable, compared to SOC alone, in terms of efficiency and timing, thus highlighting all the aforementioned properties of AM (Laurent et al., 2017). However, the specific regulatory mechanisms behind the AM efficacy in diabetic wounds are not completely understood (Koob et al., 2014).

The management of inflammation is crucial in resolving chronic wounds. Here, we found that the level of several genes involved in inflammation decreased upon AM treatment. Of note, the decreased level of *VCAM-1* and *ICAM-1* and even more their reduced membrane exposure following AM addition is of particular interest since it is known that these adhesion molecules are found elevated in non-healing DFUs (Kolluru et al., 2012).

To further investigate the amniotic membrane's anti-inflammatory activity, we determined the monocyte endothelial cell interaction rate, which plays a crucial role in the formation of atheroma. Indeed, the adhesion of circulating monocytes to the endothelial cells, mediated by the interaction with adhesion molecules, is considered one of the earliest events in atherosclerosis (Čejková et al., 2016). After attaching to the endothelium, monocytes subsequently invade the vascular wall and play a central role in triggering the inflammation. Moreover, inflammation has been shown to delay wound healing, therefore, the inhibition of monocyte adhesion to the vessel results in reduced secondary damages, such as reduced inflammation, being beneficial to the wound healing (Cowin et al., 2021).

Here, we found that stimulation with a low concentration of TNF-α induced an increase in the monocyte–endothelial cell interaction that was further enhanced in GD-HUVECs. The presence of AM reduced the amount of adhered monocyte in both cell populations; however, it was especially significative in GD-HUVECs.

NF-κB plays a crucial role in the expression of proinflammatory molecules such as cytokines, chemokine, and adhesion molecules (Dinh and Lewis, 2019) and several studies have demonstrated its involvement in metabolic disorders and atherosclerosis (Di Tomo et al., 2012), phenomena that could be prevented or ameliorated by several pharmacological or natural approaches (Di Pietro et al., 2020). Interestingly, here we found that, following TNF-α-stimulation, AM pre-treatment of HUVECs significantly reduced NF-κB phosphorylation and nuclear translocation in both control cells and GD-HUVECs, thus further confirming the capability of AM in reducing inflammation.

Then, we evaluated the potential role of AM in modulating nitric oxide bioavailability which is involved in the modulation of the NF-κB pathway and thus in the vascular homeostasis balance. Of note, in GD-HUVECs chronically exposed to high glucose and inflammation, impaired nitric oxide synthase (eNOS) activity and enhanced reactive oxygen species (ROS) production are responsible for reduced bioavailability of nitric oxide thus leading to pro-atherogenic alterations (Pandolfi and De Filippis, 2007). Interestingly, in our cellular model, these effects were associated with an ability of AM to enhance NO bioavailability thus protecting HUVECs from TNF-α-induced inflammation.

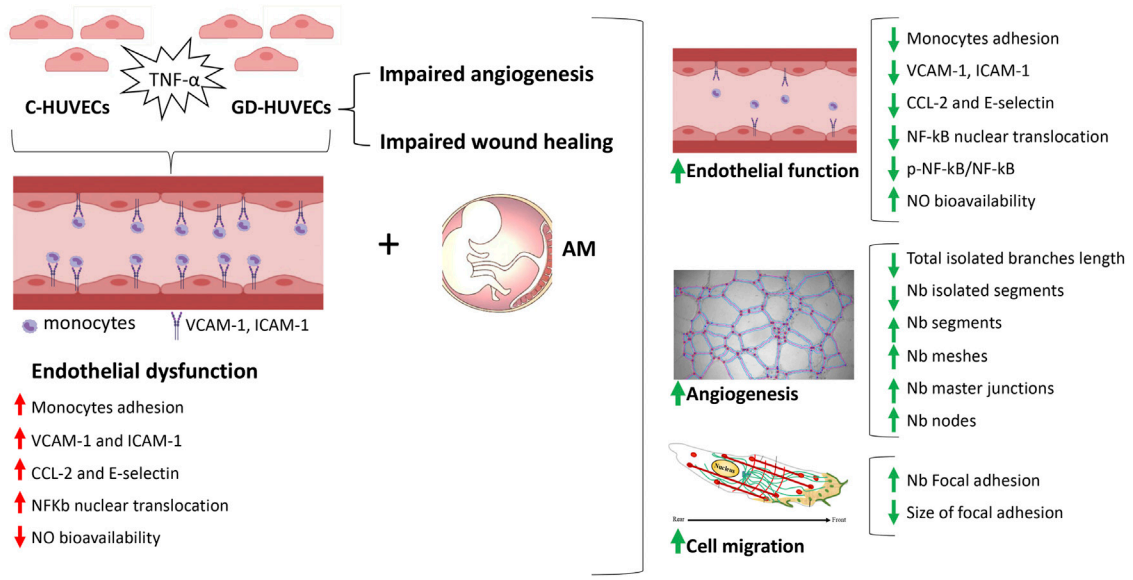

FIGURE 8 | Schematic representation of the main findings from the study. Gestational diabetes endothelial cells (GD-HUVECs) have shown increased inflammation leading to endothelial dysfunction as well as impaired angiogenesis and wound healing. By using this cellular model that reproduces a typical diabetic foot ulcer endothelium, the amniotic membrane (AM) was able to restore endothelial function, enhance angiogenesis, and improve wound healing.

On the other hand, the AM angiogenic effect is rather controversial. Indeed, AM shows anti-angiogenic features in ophthalmology (Jirsova and Jones, 2017) and pro-angiogenic properties when used to treat skin wounds and DFUs. This is probably due to the simultaneous presence of both pro- and anti-angiogenic molecules in AM. Therefore, the specific AM effect changes among conditions and target tissues (Niknejad and Yazdanpanah, 2014).

In the present study, the AM capacity to improve endothelial cells' migration and vessel formation was assessed. Supported by these observations, we focused our study on the impaired angiogenic phase that occurs in diabetic wounds. Therefore, the AM role in vessel formation was investigated using the Matrigel tube formation assay. It is worthy of note that the analysis of some angiogenic parameters such as the number of isolated segments and length of isolated branches shows that GD-HUVECs induced the formation of poor interconnected tubes compared to C-HUVECs. On the contrary, as compared to C-HUVECs, the number of segments, meshes, and master junctions and the number of nodes were reduced in GD-HUVECs, further assessing impaired angiogenesis in these cells. Additionally, GD-HUVEC data clearly showed basal impaired angiogenesis when compared to control cells. This further supports the idea that chronic hyperglycemia, *per se*, may strongly reduce the angiogenesis in GD-HUVECs. Of note, all these parameters were improved in GD-HUVECs following incubation with AM, leading to a better vascular network formation. Moreover, it should be noticed that from the data obtained by angiogenic analysis, most of the parameters in C-HUVECs were not ameliorated following AM incubation. Our explanation to these findings is that C-HUVECs already possess an intrinsic sufficient capability to achieve a full network. On the contrary, the impaired networking capacity of GD-HUVECs, was improved after incubation with AM, thus reaching the same levels of C-HUVECs. Collectively, these observations are consistent with our previous findings and may explain some of the reported beneficial effects of AM *in vivo* when applied to DFUs (Valiente et al., 2018). Also, these results are suggestive of the induction of a series of events leading to a better angiogenesis produced by AM in DFUs.

Some interesting studies reported the capability of AM in improving the migration of keratinocytes (Ruiz-Cañada et al., 2018), however, only some studies investigated the effect of AM on HUVECs migration (Koob et al., 2014; Duan-Arnold et al., 2015) but never in GD-HUVECs. When tested, AM was beneficial for the migration of both C- and GD-HUVECs. However, to our surprise, we could not detect differences between the type of cells in the migration either before or after AM stimulation.

The migrating effect of AM can also be evaluated by looking at the quality and quantity of focal adhesions (FAs). Indeed, the effect of AM on HaCaT and Mv1Lu migrating cells was a reduction in size and increment in numbers of FAs at the time of cell migration (Bernabé-García et al., 2017). This is due to a rapid formation and disassembly of cell adhesion sites that are required, and it is observed in actively migrating cells (Mayor and Etienne-Manneville, 2016). Cell migration is coordinated by a complex of proteins that localizes to sites of cell–matrix interaction, the FAs (Critchley 2000; Geiger et al., 2001). Paxillin is a key cytosolic protein that coordinates the binding of integrin cell attachment sites to the actin cytoskeleton (López-Colomé et al., 2017). Paxillin also takes part in FAs, and it is essential to integrate different signals related to cell migration (Huang et al., 2003). In HaCaT cells, AM induces paxillin

phosphorylation at Ser-178 and also produces an intense remodeling of FA paxillin staining, which are critical for cell migration (Bernabé-García et al., 2017). In the presence of AM, a clear remodeling of focal adhesions was observed when those were revealed by paxillin staining. Hence, altogether, the fact that this migration intensively related protein gets remodeled in the presence of AM is suggestive that a migration process is stimulated by the presence of AM. The strong FA remodeling effect of AM, measured as the number of paxillin structures, was equally effective in C- and GD-HUVECs, in agreement with the data of migration for both types of cells. To this end, however, whether AM promoted migration could add an extra advantage in resolving DFUs, should be deeply investigated either in *in vivo* models or patients. Altogether, this work confirms that the use of AM is a desirable strategy in DFUs and it provides further insights to elucidate the therapeutic effects of AM observed in preclinical studies.

CONCLUSION

In this study, we shed light on the mechanisms related to the AM capability to heal inflammation and improve angiogenesis in endothelial cells obtained from the umbilical cord vein of gestational diabetic mothers, supporting preclinical results. Although further research is needed to evaluate how these findings translate to diabetic foot ulcer patients, all together, these results carried out through an innovative *in vitro* cellular model, assess the role of the amniotic membrane to induce a significant reduction of the inflammation typical of chronic diabetic foot ulcers and to improve endothelial cell vascular network formation (**Figure 8**).

DATA AVAILABILITY STATEMENT

The original contributions presented in the study are included in the article/**Supplementary Materials**, further inquiries can be directed to the corresponding authors.

AUTHOR CONTRIBUTIONS

CP: conception and design, collection and assembly of data, data analysis and interpretation, manuscript writing, and final approval of the manuscript. ÁB-G, IC, and JS-F: collection and assembly of data and data analysis and interpretation. PDT, MS, and CN: collection and assembly of data. AP: conception and design, financial support, administrative support, provision of study material, and final approval of the manuscript. FN: conception and design, financial support, administrative support, provision of study material, data analysis and interpretation, manuscript writing, and final approval of the manuscript. All authors gave the final approval of the version to be submitted and read and approved the final manuscript version.

FUNDING

This work was supported by Instituto de Salud Carlos III, Fondo de Investigaciones Sanitarias, Plan Estatal I+D+I, and Instituto de Salud Carlos III-Subdirección General de Evaluación y Fomento de la Investigación (grant no. PI17/02,164) https://www.isciii.es; Fondos FEDER (EDRF) "Una manera de hacer Europa" A way of making Europe; POR FESR ABRUZZO 2014–2020 Asse I Determinazione (SANI) number 39 DPG013/12,222,017; and PON-MISE Sustainable Growth Funding-DD 27/09/2018 (grant no. 21, ex 230). AB-G was supported with funds from Instituto de Salud Carlos III-Subdirección General de Evaluación y Fomento de la Investigación (grant no. PI17/02,164). JS-F was supported with a "Contrato Predoctoral para la Formación de Personal Investigador" from Universidad Católica San Antonio de Murcia (UCAM). CN was supported by funds from F-Séneca de la Region de Murcia and Social European Fund program: "Programa Regional de Talento Investigador y su Empleabilidad." CP was supported by MIUR - PON AIM "Attraction and International Mobility" Linea 2 (Attrazione dei ricercatori), profilo 2.1, and by Ministero della Sanità Programma di Ricerca Finalizzata 2019 (GR-2019-12369702). BIOBANC-MUR was supported by the "Instituto de Salud Carlos III (proyecto PT20/00109), by "Instituto Murciano de Investigación Biosanitaria Virgen de la Arrixaca, IMIB," and by "Consejeria de Salud de la Comunidad Autónoma de la Región de Murcia.

ACKNOWLEDGMENTS

The authors are indebted to the Hospital Clínico Universitario Virgen de la Arrixaca (Spain) and to the Hospitals of Chieti and Pescara (Italy) that strongly supported this research. They are particularly grateful for the generous contribution of the patients and the collaboration of Biobank Network of the Region of Murcia, BIOBANC-MUR, registered on the Registro Nacional de Biobancos with registration number B.0000859.

SUPPLEMENTARY MATERIAL

The Supplementary Material for this article can be found online at: https://www.frontiersin.org/articles/10.3389/fbioe.2022.854845/full#supplementary-material

REFERENCES

Abacı, A., Oguzhan, A., Kahraman, S., Eryol, N. K., Unal, S., Arınc, H., et al. (1999). Effect of Diabetes Mellitus on Formation of Coronary Collateral Vessels. *Circulation* 99 (17), 2239–2242. doi:10.1161/01.CIR.99.17.2239

Ahmad, J. (2016). The Diabetic Foot. *Diabetes & Metabolic Syndrome Clin. Res. Rev.* 10 (1), 48–60. doi:10.1016/j.dsx.2015.04.002

Alcaraz, A., Mrowiec, A., Insausti, C. L., Bernabé-García, Á., García-Vizcaíno, E. M., López-Martínez, M. C., et al. (2015). Amniotic Membrane Modifies the Genetic Program Induced by TGFß, Stimulating Keratinocyte Proliferation and Migration in Chronic Wounds. *PLoS ONE* 10 (8), e0135324. doi:10.1371/journal.pone.0135324

Bandyk, D. F. (2018). The Diabetic Foot: Pathophysiology, Evaluation, and Treatment. *Seminars Vasc. Surg.* 31 (2–4), 43–48. doi:10.1053/j.semvascsurg.2019.02.001

Bernabé-García, Á., Liarte, S., Moraleda, J. M., Castellanos, G., and Nicolás, F. J. (2017). Amniotic Membrane Promotes Focal Adhesion Remodeling to Stimulate Cell Migration. *Sci. Rep.* 7 (1), 1–12. doi:10.1038/s41598-017-15509-z

Boykin, J. V. (2010). Wound Nitric Oxide Bioactivity. *J. Wound, Ostomy & Cont. Nurs.* 37 (1), 25–32. doi:10.1097/won.0b013e3181c68b61

Castellanos, G., Bernabé-García, Á., Moraleda, J. M., and Nicolás, F. J. (2017). Amniotic Membrane Application for the Healing of Chronic Wounds and Ulcers. *Placenta* 59, 146–153. doi:10.1016/j.placenta.2017.04.005

Čejková, S., Králová Lesná, I., and Poledne, R. (2016). Monocyte Adhesion to the Endothelium Is an Initial Stage of Atherosclerosis Development. *Cor Vasa* 58 (4), e419–e425. doi:10.1016/j.crvasa.2015.08.002

Clapp, C., Thebault, S., Jeziorski, M. C., and Martínez De La Escalera, G. (2009). Peptide Hormone Regulation of Angiogenesis. *Physiol. Rev.* 89, 1177–1215. doi:10.1152/physrev.00024.2009

Cowin, A. J., Bayat, A., Murray, R. Z., and Kopecki, Z. (2021). Editorial: Inflammation in Healing and Regeneration of Cutaneous Wounds. *Front. Immunol.* 12 (November), 10–12. doi:10.3389/fimmu.2021.806687

Critchley, D. R. (2000). Focal Adhesions - The Cytoskeletal Connection. *Curr. Opin. Cell Biol.* 12 (1), 133–139. doi:10.1016/s0955-0674(99)00067-8

Di Fulvio, P., Pandolfi, A., Formoso, G., Di Silvestre, S., Di Tomo, P., Giardinelli, A., et al. (2014). Features of Endothelial Dysfunction in Umbilical Cord Vessels of Women with Gestational Diabetes. *Nutr. Metabolism Cardiovasc. Dis.* 24 (12), 1337–1345. doi:10.1016/j.numecd.2014.06.005

Di Pietro, N., Baldassarre, M. P. A., Cichelli, A., Pandolfi, A., Formoso, G., and Pipino, C. (2020). Role of Polyphenols and Carotenoids in Endothelial Dysfunction: An Overview from Classic to Innovative Biomarkers. *Oxidative Med. Cell. Longev.* 2020, 1–19. doi:10.1155/2020/6381380

Di Tomo, P., Alessio, N., Falone, S., Pietrangelo, L., Lanuti, P., Cordone, V., et al. (2021). Endothelial Cells from Umbilical Cord of Women Affected by Gestational Diabetes: A Suitable *In Vitro* Model to Study Mechanisms of Early Vascular Senescence in Diabetes. *FASEB J.* 35, e21662. doi:10.1096/fj.202002072RR

Di Tomo, P., Canali, R., Ciavardelli, D., Di Silvestre, S., De Marco, A., Giardinelli, A., et al. (2012). β-Carotene and Lycopene Affect Endothelial Response to TNF-α Reducing Nitro-Oxidative Stress and Interaction with Monocytes. *Mol. Nutr. Food Res.* 56 (2), 217–227. doi:10.1002/mnfr.201100500

Di Tomo, P., Di Silvestre, S., Cordone, V. G. P., Giardinelli, A., Faricelli, B., Pipino, C., et al. (2015). Centella Asiatica and Lipoic Acid, or a Combination Thereof, Inhibit Monocyte Adhesion to Endothelial Cells from Umbilical Cords of Gestational Diabetic Women. *Nutr. Metabolism Cardiovasc. Dis.* 25 (7), 659–666. doi:10.1016/j.numecd.2015.04.002

Dinh, T., and Lewis, C. (2019). Amnion Applications in the Foot and Ankle. *Clin. Podiatric Med. Surg.* 36 (4), 563–576. doi:10.1016/j.cpm.2019.06.004

Doucette, M., Payne, K. M., Lough, W., Beck, A., Wayment, K., Huffman, J., et al. (2020). Early Advanced Therapy for Diabetic Foot Ulcers in High Amputation Risk Veterans: A Cohort Study. *Int. J. Low. Extrem. Wounds* 21, 111–119. Wounds 1534734620: 1–9. doi:10.1177/1534734620928151

Duan-Arnold, Y., Uveges, T. E., Gyurdieva, A., Johnson, A., and Danilkovitch, A. (2015). Angiogenic Potential of Cryopreserved Amniotic Membrane Is Enhanced Through Retention of All Tissue Components in Their Native State. *Adv. Wound Care* 4 (9), 513–522. doi:10.1089/wound.2015.0638

Eelen, G., De Zeeuw, P., Simons, M., and Carmeliet, P. (2015). Endothelial Cell Metabolism in Normal and Diseased Vasculature. *Circ. Res.* 116 (7), 1231–1244. doi:10.1161/CIRCRESAHA.116.302855

Efron, D. T., Most, D., and Barbul, A. (2000). Role of Nitric Oxide in Wound Healing. *Curr. Opin. Clin. Nutr. Metabolic Care* 3, 197–204. doi:10.1097/00075197-200005000-00006

Folkman, J. (2007). Angiogenesis: An Organizing Principle for Drug Discovery? *Nat. Rev. Drug Discov.* 6, 273–286. doi:10.1038/nrd2115

Geiger, B., Bershadsky, A., Pankov, R., and Yamada, K. M. (2001). Transmembrane Crosstalk Between the Extracellular Matrix and the Cytoskeleton. *Nat. Rev. Mol. Cell Biol.* 2 (11), 793–805. doi:10.1038/35099066

Huang, C., Rajfur, Z., Borchers, C., Schaller, M. D., and Jacobson., K. (2003). JNK Phosphorylates Paxillin and Regulates Cell Migration. *Nature* 424 (6945), 219–223. doi:10.1038/nature01745

Insausti, C. L., Alcaraz, A., García-Vizcaíno, E. M., Mrowiec, A., López-Martínez, M. C., Blanquer, M., et al. (2010). Amniotic Membrane Induces Epithelialization in Massive Posttraumatic Wounds. *Wound Repair Regen.* 18 (4), 368–377. doi:10.1111/j.1524-475X.2010.00604.x

Jirsova, K., and Jones, G. L. A. (2017). Amniotic Membrane in Ophthalmology: Properties, Preparation, Storage and Indications for Grafting-A Review. *Cell Tissue Bank.* 18 (2), 193–204. doi:10.1007/s10561-017-9618-5

Kolluru, G. K., Bir, S. C., and Kevil, C. G. (2012). Endothelial Dysfunction and Diabetes: Effects on Angiogenesis, Vascular Remodeling, and Wound Healing. *Int. J. Vasc. Med.* 2012, 1–30. doi:10.1155/2012/918267

Koob, T. J., Lim, J. J., Massee, M., Zabek, N., Rennert, R., Gurtner, G., et al. (2014). Angiogenic Properties of Dehydrated Human Amnion/Chorion Allografts: Therapeutic Potential for Soft Tissue Repair and Regeneration. *Int. J. Mol. Sci.* 18, 1419. doi:10.1186/2045-824X-6-10

Lakmal, K., Basnayake, O., and Hettiarachchi, D. (2021). Systematic Review on the Rational Use of Amniotic Membrane Allografts in Diabetic Foot Ulcer Treatment. *BMC Surg.* 21 (87), 1–8. doi:10.1186/s12893-021-01084-8

Lamalice, L., Le Boeuf, F., and Huot, J. (2007). Endothelial Cell Migration During Angiogenesis. *Circulation Res.* 100, 782–794. doi:10.1161/01.RES.0000259593.07661.1e

Laurent, I., Astère, M., Wang, K. R., Cheng, Q.-f., and Li, Q. F. (2017). Efficacy and Time Sensitivity of Amniotic Membrane Treatment in Patients with Diabetic Foot Ulcers: A Systematic Review and Meta-Analysis. *Diabetes Ther.* 8, 967–979. doi:10.1007/s13300-017-0298-8

López-Colomé, A. M., Lee-Rivera, I., Benavides-Hidalgo, R., López, E., and López, E. (2017). Paxillin: A Crossroad in Pathological Cell Migration. *J. Hematol. Oncol.* 10 (1), 1–15. doi:10.1186/s13045-017-0418-y

Mayor, R., and Etienne-Manneville, S. (2016). The Front and Rear of Collective Cell Migration. *Nat. Rev. Mol. Cell Biol.* 17 (2), 97–109. doi:10.1038/nrm.2015.14

Medina-Leyte, D. J., Domínguez-Pérez, M., Mercado, I., Villarreal-Molina, M. T., Jacobo-Albavera, L., and Jacobo-Albavera, L. (2020). Use of Human Umbilical Vein Endothelial Cells (HUVEC) as a Model to Study Cardiovascular Disease: A Review. *Appl. Sci.* 10 (3), 938. doi:10.3390/app10030938

Murphy, S. V., Skardal, A., Song, L., Sutton, K., Haug, R., Mack, D. L., et al. (2017). Solubilized Amnion Membrane Hyaluronic Acid Hydrogel Accelerates Full-Thickness Wound Healing. *Stem Cells Transl. Med.* 6 (11), 2020–2032. doi:10.1002/sctm.17-0053

Niknejad, H., and Yazdanpanah, G. (2014). Opposing Effect of Amniotic Membrane on Angiogenesis Originating from Amniotic Epithelial Cells. *J. Med. Hypotheses Ideas* 8 (1), 39–41. doi:10.1016/j.jmhi.2013.08.002

Okonkwo, U., and Dipietro, L. (2017). Diabetes and Wound Angiogenesis. *Ijms* 18 (7), 1419–1515. doi:10.3390/ijms18071419

Pandolfi, A., and De Filippis, E. A. (2007). Chronic Hyperglicemia and Nitric Oxide Bioavailability Play a Pivotal Role in Pro-Atherogenic Vascular Modifications. *Genes Nutr.* 2 (2), 195–208. doi:10.1007/s12263-007-0050-5

Parolini, O., and Caruso, M. (2011). Review: Preclinical Studies on Placenta-Derived Cells and Amniotic Membrane: An Update. *Placenta* 32, S186–S195. doi:10.1016/j.placenta.2010.12.016

Parolini, O., Soncini, M., Evangelista, M., and Schmidt, D. (2009). Amniotic Membrane and Amniotic Fluid-Derived Cells: Potential Tools for Regenerative Medicine? *Regen. Med.* 4 (2), 275–291. doi:10.2217/17460751.4.2.275

Pipino, C., Shangaris, P., Resca, E., Zia, S., Deprest, J., Sebire, N. J., et al. (2013). Placenta as a Reservoir of Stem Cells: An Underutilized Resource? *Br. Med. Bull.* 105, 43–68. doi:10.1093/bmb/lds033

Ruiz-Canada, C., Bernabe-García, Á., Liarte, S., Insausti, C. L., Angosto, D., Moraleda, J. M., et al. (2017). Amniotic Membrane Stimulates Cell Migration by Modulating Transforming Growth Factor-β Signalling. *J. Tissue Eng. Regen. Med.* 12 (3), 808–820. doi:10.1002/term.2501

Ruiz-Canada, C., Bernabe-Garcia, A., Liarte, S., Insausti, C. L., Angosto, D., Moraleda, J. M., et al. (2018). Amniotic Membrane Stimulates Cell Migration by Modulating Transforming Growth Factor-β Signalling. *J. Tissue Eng. Regen. Med.* 12 (3), 808–820. doi:10.1002/term.2501

Serini, G., Ambrosi, D., Giraudo, E., Gamba, A., Preziosi, L., and Bussolino, F. (2003). Modeling the Early Stages of Vascular Network Assembly. *EMBO J.* 22 (8), 1771–1779. doi:10.1093/emboj/cdg176

Silini, A. R., Di Pietro, R., Lang-Olip, I., Alviano, F., Banerjee, A., Basile, M., et al. (2020). Perinatal Derivatives: Where Do We Stand? A Roadmap of the Human Placenta and Consensus for Tissue and Cell Nomenclature. *Front. Bioeng. Biotechnol.* 8 (December), 1–33. doi:10.3389/fbioe.2020.610544

Tentolouris, N., Edmonds, M. E., Jude, E. B., Vas, P. R. J., Manu, C. A., Tentolouris, A., et al. (2021). Editorial: Understanding Diabetic Foot Disease: Current Status and Emerging Treatment Approaches. *Front. Endocrinol.* 12 753181. doi:10.3389/fendo.2021.753181

Tettelbach, W., Cazzell, S., Reyzelman, A. M., Sigal, F., Caporusso, J. M., and Agnew, P. S. (2019). A Confirmatory Study on the Efficacy of Dehydrated Human Amnion/Chorion Membrane dHACM Allograft in the Management of Diabetic Foot Ulcers: A Prospective, Multicentre, Randomised, Controlled Study of 110 Patients from 14 Wound Clinics. *Int. Wound J.* 16, 19–29. doi:10.1111/iwj.12976

Ucci, M., Di Tomo, P., Tritschler, F., Cordone, V. G. P., Lanuti, P., Bologna, G., et al. (2019). Cordone, Paola Lanuti, Giuseppina Bologna, Sara Di Silvestre, et al Anti-Inflammatory Role of Carotenoids in Endothelial Cells Derived from Umbilical Cord of Women Affected by Gestational Diabetes Mellitus. *Oxidative Med. Cell. Longev.* 2019, 1–11. doi:10.1155/2019/8184656

Valiente, M. R., Nicolás, F. J., García-Hernández, A. M., Mora, C. F., Blanquer, M., Alcaraz, P. J., et al. (2018). Cryopreserved Amniotic Membrane in the Treatment of Diabetic Foot Ulcers: A Case Series. *J. Wound Care* 27 (12), 806–815. doi:10.12968/jowc.2018.27.12.806

Wallace, J. L. (2005). Nitric Oxide as a Regulator of Inflammatory Processes. *Mem. Inst. Oswaldo Cruz* 100 (Suppl. 1), 5–9. doi:10.1590/S0074-02762005000900002

Waltenberger, J., Lange, J., and Kranz, A. (2000). Vascular Endothelial Growth Factor-A-Induced Chemotaxis of Monocytes Is Attenuated in Patients with Diabetes Mellitus. *Circulation* 102 (2), 185–190. doi:10.1161/01.CIR.102.2.185

Zelen, C. M. (2013). An Evaluation of Dehydrated Human Amniotic Membrane Allografts in Patients with DFUs. *J. Wound Care* 22 (7), 347–351. doi:10.12968/jowc.2013.22.7.347

Conflict of Interest: The authors declare that the research was conducted in the absence of any commercial or financial relationships that could be construed as a potential conflict of interest.

Publisher's Note: All claims expressed in this article are solely those of the authors and do not necessarily represent those of their affiliated organizations, or those of the publisher, the editors, and the reviewers. Any product that may be evaluated in this article, or claim that may be made by its manufacturer, is not guaranteed or endorsed by the publisher.

frontiers | Frontiers in Bioengineering and Biotechnology

ORIGINAL RESEARCH
published: 22 July 2022
doi: 10.3389/fbioe.2022.936074

Tips and Tricks and Clinical Outcome of Cryopreserved Human Amniotic Membrane Application for the Management of Medication-Related Osteonecrosis of the Jaw (MRONJ): A Pilot Study

*Stéphane Odet[1], Christophe Meyer[1,2], Camille Gaudet[1], Elise Weber[1], Julie Quenot[1], Stéphane Derruau[3,4], Sebastien Laurence[3,5], Lisa Bompy[6], Marine Girodon[6], Brice Chatelain[1], Cédric Mauprivez[3,7,8], Esteban Brenet[9], Halima Kerdjoudj[7,8], Narcisse Zwetyenga[6], Philippe Marchetti[10,11], Anne-Sophie Hatzfeld[10,11], David Toubeau[12], Fabienne Pouthier[13,14], Xavier Lafarge[15,16], Heinz Redl[17,18], Mathilde Fenelon[19,20], Jean-Christophe Fricain[19,20], Roberta Di Pietro[21,22], Charlotte Ledouble[3,7,8], Thomas Gualdi[23], Anne-Laure Parmentier[23], Aurélien Louvrier[1,14] and Florelle Gindraux[1,2]**

[1]Service de chirurgie maxillo-faciale, stomatologie et odontologie hospitalière, CHU Besançon, Besançon, France, [2]Laboratoire de Nanomédecine, Imagerie, Thérapeutique EA 4662, Université Bourgogne Franche-Comté, Besançon, France, [3]Pôle Médecine bucco-dentaire, Hôpital Maison Blanche, CHU Reims, Reims, France, [4]Université de Reims Champagne-Ardenne, Laboratoire BioSpecT EA-7506, UFR de Pharmacie, Reims, France, [5]Université de Reims Champagne Ardenne, Biomatériaux et Inflammation en Site Osseux, Pôle Santé, URCA, HERVI EA3801, UFR de Médecine, Reims, France, [6]Chirurgie Maxillo-Faciale - Stomatologie - Chirurgie Plastique Réparatrice et Esthétique - Chirurgie de la main, CHU de Dijon, Dijon, France, [7]Université de Reims Champagne Ardenne, Biomatériaux et Inflammation en Site Osseux, Pôle Santé, URCA, BIOS EA 4691, Reims, France, [8]UFR d'Odontologie, Université de Reims Champagne Ardenne, Reims, France, [9]Service d'ORL et chirurgie cervico-faciale, CHU Reims, Reims, France, [10]Banque de Tissus CBP CHU Lille, Lille, France, [11]Institut de Cancérologie ONCOLILLE CANTHER, UMR9020 CNRS–U1277 Inserm—Université de Lille, Lille, France, [12]Banque de Tissus, CHU Rouen, Rouen, France, [13]Activité d'Ingénierie Cellulaire et Tissulaire (AICT), Établissement Français du Sang Bourgogne Franche-Comté, Besançon, France, [14]Université Bourgogne Franche-Comté, INSERM, EFS BFC, UMR1098, RIGHT Interactions Greffon-Hôte-Tumeur/Ingénierie Cellulaire et Génique, Besançon, France, [15]Établissement Français du Sang Nouvelle-Aquitaine, Bordeaux, France, [16]INSERM U1035, Université de Bordeaux, Biothérapie des Maladies Génétiques Inflammatoires et Cancers (BMGIC), Bordeaux, France, [17]Ludwig Boltzmann Institute for Experimental and Clinical Traumatology/AUVA, Research Center, Vienna, Austria, [18]Austrian Cluster for Tissue Regeneration, Vienna, Austria, [19]Univ. Bordeaux, INSERM, BIOTIS, U1026, Bordeaux, France, [20]CHU Bordeaux, Service de chirurgie orale, Bordeaux, France, [21]Department of Medicine and Ageing Sciences, Gabriele D'Annunzio University of Chieti-Pescara, Chieti, Italy, [22]StemTeCh Group, Gabriele D'Annunzio Foundation, University of Chieti-Pescara, Chieti, Italy, [23]Inserm CIC 1431, CHU Besançon, Besançon, France

Medication-related osteonecrosis of the jaw (MRONJ) is a complication of certain pharmacological treatments such as bisphosphonates, denosumab, and angiogenesis inhibitors. There are currently no guidelines on its management, particularly in advanced stages. The human amniotic membrane (hAM) has low immunogenicity and exerts anti-inflammatory, antifibrotic, antimicrobial, antiviral, and analgesic effects. It is a source of stem cells and growth factors promoting tissue regeneration. hAM acts as an anatomical barrier with suitable mechanical properties (permeability, stability, elasticity, flexibility, and resorbability) to prevent the proliferation of fibrous tissue and promote early neovascularization at the surgical site. In oral surgery, hAM stimulates healing and facilitates the proliferation and differentiation of epithelial cells in the oral mucosa and

OPEN ACCESS

Edited by:
Antonietta Rosa Silini, Fondazione Poliambulanza Istituto Ospedaliero, Italy

Reviewed by:
Michele Magremanne, Cliniques Universitaires Saint-Luc, Belgium
Assunta Pandolfi, University of Studies G. d'Annunzio Chieti and Pescara, Italy

***Correspondence:**
Florelle Gindraux
fgindraux@chu-besancon.fr

Specialty section:
This article was submitted to Tissue Engineering and Regenerative Medicine, a section of the journal Frontiers in Bioengineering and Biotechnology

Received: *04 May 2022*
Accepted: *13 June 2022*
Published: *22 July 2022*

Citation:
Odet S, Meyer C, Gaudet C, Weber E, Quenot J, Derruau S, Laurence S, Bompy L, Girodon M, Chatelain B, Mauprivez C, Brenet E, Kerdjoudj H, Zwetyenga N, Marchetti P, Hatzfeld A-S, Toubeau D, Pouthier F, Lafarge X, Redl H, Fenelon M, Fricain J-C, Di Pietro R, Ledouble C, Gualdi T, Parmentier A-L, Louvrier A and Gindraux F (2022) Tips and Tricks and Clinical Outcome of Cryopreserved Human Amniotic Membrane Application for the Management of Medication-Related Osteonecrosis of the Jaw (MRONJ): A Pilot Study. Front. Bioeng. Biotechnol. 10:936074. doi: 10.3389/fbioe.2022.936074

therefore its regeneration. We proposed using cryopreserved hAM to eight patients suffering from cancer (11 lesions) with stage 2–3 MRONJ on a compassionate use basis. A collagen sponge was added in some cases to facilitate hAM grafting. One or three hAMs were applied and one patient had a reapplication. Three patients had complete closure of the surgical site with proper epithelialization at 2 weeks, and two of them maintained it until the last follow-up. At 1 week after surgery, three patients had partial wound dehiscence with partial healing 3 months later and two patients had complete wound dehiscence. hAM reapplication led to complete healing. All patients remained asymptomatic with excellent immediate significant pain relief, no infections, and a truly positive impact on the patients' quality of life. No adverse events occurred. At 6 months of follow-up, 80% of lesions had complete or partial wound healing (30 and 50%, respectively), while 62.5% of patients were in stage 3. Radiological evaluations found that 85.7% of patients had stable bone lesions ($n = 5$) or new bone formation ($n = 1$). One patient had a worsening MRONJ but remained asymptomatic. One patient did not attend his follow-up radiological examination. For the first time, this prospective pilot study extensively illustrates both the handling and surgical application of hAM in MRONJ, its possible association with a collagen sponge scaffold, its outcome at the site, the application of multiple hAM patches at the same time, and its reapplication.

Keywords: human amniotic membrane, osteonecrosis, oral mucosa, allograft, bisphosphonates, denosumab, antiangiogenic drugs

1 INTRODUCTION

The human amniotic membrane (hAM) is the innermost layer of fetal membranes. It is composed of a single layer of epithelial cells, a basement membrane, and an avascular stroma, underlayered by the chorion. The thickness of hAM varies among individuals and depends on the location of the sample (70–180 μm thick) (Chen et al., 2012; Gremare et al., 2019). hAM is not homogeneous (Centurione et al., 2018). It contains amniotic epithelial cells and amniotic mesenchymal stromal cells (Parolini et al., 2008) and variable quantities of growth factors (Russo et al., 2011; Mcquilling et al., 2017). Basic preservation methods for hAM are cryopreservation, lyophilization, and storage in a dry form (Jirsova and Jones, 2017). Cell survival after cryopreservation, despite the addition of cryoprotective agents, is questionable (Laurent et al., 2014b).

The beneficial effects of hAM have been widely described in the literature. It is a biocompatible scaffold with suitable mechanical properties (permeability, stability, elasticity, flexibility, resorbability, and transparency) (Chen et al., 2012; Fenelon et al., 2021). Additionally, it possesses antifibrotic (Ricci et al., 2013), antiscarring (Mamede et al., 2012), antimicrobial (Chen et al., 2019), anti-inflammatory (Bailo et al., 2004; Wolbank et al., 2007), and analgesic properties (Rama et al., 2001; Dua et al., 2004; Gajiwala and Gajiwala, 2004). It modulates angiogenesis, having both pro- and antiangiogenic properties (Mamede et al., 2012; Gholipourmalekabadi et al., 2019), and induces epithelialization and wound healing (Mamede et al., 2012; Gholipourmalekabadi et al., 2019). Finally, it has low immunogenicity (Kubo et al., 2001), which makes it suitable as an allograft.

To date, ophthalmology is one of the most popular hAM indications in routine use to treat ocular surface diseases, including conjunctival surface reconstruction, corneal surface reconstruction, and as a substrate for the *ex vivo* expansion of limbal and conjunctival stem cells (Mamede et al., 2012). Since the mid-1990s, there has been a growing interest in using hAM for oral surgery to accelerate tissue regeneration. Two systematic reviews of literature explored the different indications for hAM use in this specific field (Fenelon et al., 2018; Odet et al., 2021), highlighting two types of application as "implanted graft material" or "covering graft material." The first one applies to gingival recession, bone furcation defects, bone defects in interproximal areas, and surgical wounds after implant surgery; the second involves mandibular vestibuloplasty or mucosal defects.

Medication-related osteonecrosis of the jaw (MRONJ) is a complication caused by various treatments including bone antiresorptive agents (bisphosphonates and denosumab) and angiogenesis inhibitors (sunitinib, bevacizumab, among others). Clinically, symptoms can not only include pain, infection (often relapsing) with pus discharge, halitosis, and bone exposure but also serious local, regional (cellulitis, osteitis, and oro-cutaneal fistulas), or systemic infections and bone fractures. MRONJ is divided into four stages: zero (no bone exposure, only nonspecific clinical signs), one (asymptomatic bone exposure), two (bone exposure with pain or local infection), and three (symptomatic bone exposure with local, regional, or systemic infection, bone fracture, and orocutaneous fistulas). Following the American Association of Oral and Maxillofacial Surgeons (AAOMS) 2014 recommendations, conservative treatment is needed for stages 0–2, while surgical

treatment is needed only for stage 2 MRONJ resistant to conservative treatments and for stage 3 MRONJ. There is currently no consensus on the management of MRONJ.

One case report and one case-control study (Ragazzo et al., 2018; Ragazzo et al., 2021) explored the use of hAM in 26 patients affected by MRONJ. They showed promising results in terms of wound healing, clinical outcomes, and significantly improved quality of life and pain, measured on a visual analog scale (VAS). The limits of the case-control study are the mixing of 1) stages (from 1a to 3, based on the Italian Society for Oral Pathology and Medicine/Italian Society for Maxillofacial Surgery (SIPMO/SICMF) classification), 2) diagnoses (cancer and osteoporosis), and 3) the route of drug administration (per os, intravenous (IV) and subcutaneous) and type of drugs (bone antiresorptive agents and angiogenesis inhibitors) that probably impacts the rate of healing (Pichardo and van Merkesteyn, 2016; Aljohani et al., 2018; Giudice et al., 2018). In addition, the study was performed at a single healthcare facility, reducing the bias. Last, the modalities of hAM application (side, folding, number, *etc*.) were not described.

Based on Lindenmair's study (Lindenmair et al., 2010) and Eilbl's patent (Eibl and Redl, 2011), we considered hAM an innovative medication for bone repair. Meanwhile, we have accumulated extensive experience with hAM and perinatal tissues (Gindraux and Obert, 2010; Obert et al., 2012; Gindraux et al., 2013; Laurent et al., 2014a; Laurent et al., 2014b; Gindraux et al., 2017; Laurent et al., 2017; Centurione et al., 2018; Fénelon et al., 2018; Laurent et al., 2018; Bourgeois et al., 2019; Fenelon et al., 2019; Gualdi et al., 2019; Fenelon et al., 2020; Gulameabasse et al., 2020; Passaretta et al., 2020; Silini et al., 2020; Fénelon et al., 2021a; Odet et al., 2021; Fenelon et al., 2021; Etchebarne et al., 2021; Gindraux, 2021; Dubus et al., 2022a; Dubus et al., 2022b). Because the use of hAM in bone repair still requires some adaptations (Fenelon et al., 2021; Etchebarne et al., 2021), we looked for a disease that could benefit from both wound healing and bone repair as endpoints. MRONJ was that disease.

Thus, we focused on hAM application in oral surgery and established a nomenclature with four theoretical types of hAM surgeries: "implantation," "apposition," "whole covering graft material," and "partial covering graft material" (Odet et al., 2021). Later, we investigated and demonstrated these applications in a pilot study on fresh porcine mandible specimens to assist our clinical practices (Odet et al., 2021).[1] We noted that hAM suturing was not possible in the MRONJ context, leading us to revise the previous nomenclature. Thus, only two techniques were retained: "hAM implantation with complete coverage" and "hAM implantation with partial coverage" https://youtu.be/GKy3I-n3NRQ.

Here, we did a prospective 6-month pilot study to evaluate the clinical outcome of hAM in terms of wound healing, bone reexposure, pain relief (and thus the quality of life), signs of inflammation, and infection control in patients suffering from stage 2 or stage 3 MRONJ on a compassionate use basis. In addition, we collected potential adverse events and evaluated bone healing or MRONJ recurrence by imaging techniques. Consequently, we describe multiple applications and reapplication of hAM and the use of a collagen sponge to assist hAM surgery, which we believe has not been described in oral surgery, and since the use of hAM in oral surgery is not quite detailed as it is in ophthalmology (Dua and Azuara-Blanco, 1999; Letko et al., 2001; John, 2003), we illustrated different methods of hAM application and we compiled the related difficulties.

2 MATERIALS AND METHODS

2.1 Ethical Considerations

This study followed the Declaration of Helsinki on medical protocols and ethics. Patients underwent surgical treatment and follow-up in three different healthcare facilities in France: Besançon University Hospital (Centre Hospitalier Universitaire de Besançon), Reims University Hospital (Centre Hospitalier Universitaire de Reims), and Dijon University Hospital (Centre Hospitalier Universitaire de Dijon).

Each patient had no further therapeutic option available because of impaired health due to their main disease (cancers). Additionally, some patients refused the standard surgical treatment since we could not guarantee the outcome. They were informed of the risks associated with surgical treatment (pain, infection, bleeding, and edema in the short term, as well as possible local complications related to the location and extent of the lesions such as the occurrence of an oroantral communication) and received a detailed description of the procedure. All patients signed an informed consent form prior to surgery and authorized the collection of clinical data and photographic documentation. Ethics committee approval was obtained as part of the clinical randomized trial amniOST.

2.2 Study Design and Eligibility Criteria

This study was designed as a prospective 6-month follow-up study for eight patients with stage 2 or 3 MRONJ treated with hAM on a compassionate use basis in the three French hospitals between November 2020 and April 2021. Only stage 2 or 3 MRONJ (AAOMS 2014 classification) patients with surgical treatment failure or bad prognosis due to altered general health were included.

Stage 0 or 1 MRONJ patients or stage 2 or 3 MRONJ patients with no prior surgical treatment were excluded.

Patients were enrolled in a regular prospective follow-up calendar, which consisted of visits on days 7 and 14 and at months 1, 2, 3, and 6. They were either operated on as outpatients or hospitalized the day before and a few days after surgery for immediate postoperative care. Additional recall visits were scheduled, when necessary.

2.3 Cohort Characteristics

Clinical data including age, gender, diagnosis, symptoms (pain, acute sinusitis due to local inflammation, infection), general

[1]Odet, S., Meyer, C., Solecki, L., Weber, E., Chatelain, B., Euvrard, E., et al. (2021). Human Amniotic Membrane Application in Oral Surgery - an *Ex Vivo* Pilot Study. Front. Bioeng. Biotech. submitted manuscript.

TABLE 1 | Patient and MRONJ data and follow-up.

Patient number	Age	Gender	Centre	Diagnosis	Therapy	MRONJ stage	Symptoms and general condition	VAS	Number of treated lesions					Infection post-surgery	Wound healing 2 weeks post-surgery	Wound healing 1 month post-surgery	Wound healing 3 months post-surgery	Wound healing 6 months post-surgery	MRONJ relapse, bone healing, and/or neoformation 6 months post-surgery	Additional information	
								Preoperative	One week after surgery	Two weeks after surgery	One month after surgery	Six months after surgery								During the follow-up	Reintervention
1	49	M	Besançon	Renal cancer	Subcutaneous denosumab and oral sunitinib	3	Pain, infection, halitosis, bone exposure (nearly 8 cm in left and righ mandible), discontinuation of chemotherapy, malnutrition	9	1	1	0	0	2	No	Bone reexposure (1.5 cm) in sectors 3 and 4 in the premolar area, epithelialization in progress in the posterior parts of the mandible	Persistence of a bilateral 1.5 cm bone exposure in the premolar areas of sectors 3 and 4. Complete epithelialization of the posterior parts of the surgical site	Partial wound healing for the two lesions	Partial wound healing for the two lesions	MRONJ aggravation in sector 4, with mandibular fracture 4.5 months after surgery	Absence of infection. Back to normal nutrition (weight gain +10 kg). Chemotherapy restart. Mandibular fracture 4 months after surgery	No
2	55	F	Besançon	Breast cancer	IV bisphosphonates and subcutaneous denosumab	2	Intense pain, bone exposure in the anterior part of the mandible, infectious episodes	7 (under morphine medication)	2	0	0	0	1 and then the same extended lesion	No	Complete bone reexposure	Persistence of a clean bone exposure	No wound healing for the first application of hAM/ Complete wound healing for the second one	Complete wound healing with the second hAM application	Complete bone healing after first surgery on the anterior part of the mandible. Complete bone healing on sector 4 after hAM reapplication	Important tobacco consumption early after surgery. Absence of infection. Discontinuation in morphine medication after surgery	Yes, 5 months after surgery: hAM reapplication on sectors 3 and 4
3	88	M	Dijon	Prostate cancer	Subcutaneous denosumab	2	Bone exposure left mandible, halitosis	1	0	0	0	0	1	No	Complete wound healing, almost complete epithelialization, hAM almost completely resorbed	—	—	Partial wound healing	No radiological examination. Patient still asymptomatic	Visits after 2 weeks missed, the last follow-up at 6 months. Absence of infection. Bone reexposure on the lingual part of the surgical site	No
4	70	F	Dijon	Breast cancer	IV bisphosphonates and subcutaneous denosumab	3	Mandibular osteitis with a cutaneous fistula facing the MRONJ site, 10 cm bone exposure in the anterior sector of the mandible	0	0	0	0	0	1	Administration of antibiotics for weeks (preoperative osteitis)	Complete bone reexposure	Complete bone exposure	No wound healing	No wound healing	Complete bone healing	Absence of infection	Yes, 8 months after surgery: infrahyoid flap
5	71	F	Reims	Breast cancer	Subcutaneous denosumab	3	Pain, 2 cm bone exposures in the anterior part of the mandible, infection with a cutaneous fistula facing the MRONJ site	9	0	0	0	0	1	No	Almost complete epithelialization	Complete epithelialization, surgical site healed	Complete wound healing	Complete wound healing	Stability in MRONJ lesions	Absence of infection. Presence of two painless outgrowths on the anterior part of the mandible 4.5 months after surgery	No
6	69	F	Reims	Breast cancer	IV bisphosphonates and subcutaneous denosumab	2	3 MRONJ lesions: left maxillary (with chronic sinusitis), left and right mandible	2	1	0	0	0	Only left maxillary	No	Epithelialization in progress, minimal bone exposure in the anterior part of the surgical site, hAM not completely resorbed in the posterior part	Complete epithelialization, surgical site healed	Complete wound healing	Complete wound healing	Osseous neoformation on MRONJ site	Absence of infection	No

(Continued on following page)

TABLE 1 | (*Continued*) Patient and MRONJ data and follow-up.

Patient number	Age	Gender	Centre	Diagnosis	Therapy	MRONJ stage	Symptoms and general condition	VAS	Number of treated lesions				Infection post-surgery	Wound healing 2 weeks post-surgery	Wound healing 1 month post-surgery	Wound healing 3 months post-surgery	Wound healing 6 months post-surgery	MRONJ relapse, bone healing, and/or neoformation 6 months post-surgery	Additional information	
								Preoperative	One week after surgery	Two weeks after surgery	One month after surgery	Six months after surgery							During the follow-up	Reintervention
7	76	F	Reims	Multiple myeloma	IV bisphosphonates	3	Infection, halitosis, 5 cm bone exposure in left mandible	0	0	0	0	0	No	Collagen sponge and hAM not visible, wound healing in progress in the anterior part, granulation tissue with bone exposure on the vestibular and lingual sides in the posterior part	Complete healing of the anterior part, persistence of a bone exposure in the posterior part	Partial wound healing	Partial wound healing	Stability in MRONJ lesions	Absence of infection. Lack of oral hygiene after surgery	No
8	62	F	Reims	Multiple myeloma	IV Bisphosphonates	3	Infection, halitosis, 5 cm bone exposure in left mandible	1	0	0	0	0	No	Collagen sponge and hAM not visible, wound healing in progress in the posterior part, intraoperative bone exposure in the anterior part	Healing of the posterior part, persistence of a bone exposure in the anterior part	Partial wound healing	Partial wound healing	Stability in MRONJ lesions	Absence of infection	No

M: Male; F: female; IV: intravenous; SC: subcutaneous; VAS: visual analog scale; hAM: human amniotic membrane.

condition, MRONJ stage, and treatment response for MRONJ are reported in **Table 1**.

Two patients were males and six were females. Their age ranged from 49 to 88 years old (mean age: 68 ± 12.2).

As seen in **Table 1**, patient 1 (P1) suffered from renal cancer and was treated with subcutaneous denosumab and oral sunitinib; P2, P4, P5, and P6 suffered from breast cancer and were treated with IV bisphosphonates and subcutaneous denosumab or subcutaneous denosumab alone; P3 suffered from prostate cancer and was treated with subcutaneous denosumab; P7 and P8 suffered from multiple myeloma and were treated with IV bisphosphonates.

P1, P4, P5, P7, and P8 suffered from stage 3 MRONJ; P2, P3, and P6 from stage 2 MRONJ. P1 had bilateral posterior mandibular MRONJ; thus, both lesions were treated; P2, P4, and P5 had anterior mandibular MRONJ. P3, P7, and P8 had a left mandible (or sector 3) MRONJ. P6 had 3 MRONJ sites in the left maxilla (or sector 2), left mandible, and right mandible (or sector 4). Only his symptomatic sites—left maxilla—were treated.

Before the inclusion in the study, all patients suffered from painful bone exposure, with P2 being treated with morphine. All patients had one or more episodes of infection before surgery. All patients completed a 6-month follow-up.

2.4 hAM Preservation and Preparation

The hAM was cryopreserved and obtained from AICT bank from French Blood Center at Besançon (Établissement Français du Sang, EFS), Tissue Bank of Lille University Hospital (Banque de Tissus du CHRU de Lille), and Tissue Bank of Rouen University Hospital (Banque de Tissus CHU de Rouen) (**Table 2**).

A piece of hAM of 4.7 cm in diameter (from AICT Bank and Tissue Bank of Lille) or a squared 3 × 3 cm piece (from Tissue Bank of Rouen) was transported with dry ice blocks to ensure its cryopreservation at −80°C. Both hAM pieces were stored in glycerol on nitrocellulose support, the epithelial side facing the support. Upon receipt, they were thawed for 2 h at room temperature for AICT bank and 30 min for Tissue Banks of Lille and Rouen. Three 5 min rinses in saline or hypotonic injection solution were done for allografts from AICT bank and one 1 min rinse for those from Tissue Banks of Lille and Rouen.

2.5 Surgical Procedures

2.5.1 MRONJ Removal and Tissue Debridement

Surgery was performed either under local or general anesthesia or both to prevent pain upon waking.

After intra- and extraoral disinfection with Povidone-iodine, local injections without vasoconstrictors were made around the MRONJ sites. After crestal incisions on each side of the bone exposure, a full-thickness muco-periosteal flap was raised—at least 2–3 mm—to access bone tissue but with minimal flap length. Bone samples were harvested and sent for bacterial and histological analysis.

Necrotic bone was then removed—completely if possible, by exposing bleeding bone—using a motorized round burr under saline irrigation or by simply performing a sequestrectomy when necessary. The remaining bone was regularized, preserving the patient's mucosa after suturing and during wound healing. Tissue

TABLE 2 | hAM and surgical data.

Patient number	Tissue Bank	hAM size	hAM number	hAM cutting	Difficulties during surgery	Use of a collagen sponge	Water-Tight closure
1	Besançon	4.7 cm diameter disk	3	No	hAM detachment from the nitrocellulose support with forceps, spoiling both hAM and the support, impossibility to orient hAM properly, difficulty to manipulate hAM once detached from the support	No	Yes
2	Besançon	4.7 cm diameter disk	1	No	None	No	Yes
3	Lille	4.7 cm diameter disk	1	No	Difficulties to orient hAM once detached from the support	No	No
4	Rouen	3.0 × 3.0 cm square	3	No	Difficulties to close the wound hermetically without tension	No	Yes
5	Lille	4.7 cm diameter disk	1	No	Difficulties to orient hAM once detached from the support	No	Yes
6	Lille	4.7 cm diameter disk	1	No	None	Yes	No
7	Lille	4.7 cm diameter disk	1	No	None	Yes	No
8	Lille	4.7 cm diameter disk	1	No	None	Yes	No

hAM: human amniotic membrane.

debridement was also achieved by removing the altered mucosal edges, if necessary.

2.5.2 hAM Handling

The hAM was detached from the nitrocellulose support and applied with its mesenchymal side facing the bone and its epithelial side facing the gingiva. Two manipulators were necessary, one to detach the hAM with two forceps while the other held the support with another set of forceps (**Figure 1A**).

Three options for hAM handling were identified:

- Option 1: on the surgical site, the surgeon held the hAM with the two forceps, while the other unfolded it with two other forceps.
- Option 2: two surgeons applied the hAM flat on the surgical site with "four hands" (**Figure 1B**).
- Option 3: a resorbable collagen sponge (Pangen®, Urgo Medical, France) was used to supplement hAM handling and application (**Figure 1C**).

2.5.3 hAM Surgery

hAM and surgical data are summarized in **Table 2**.

In all surgeries, the hAM was tucked between the bone and the mucosa (**Figure 2**). For P6, P7, and P8, the hAM was applied flat on the collagen sponge and sutured at its ends using resorbable 5/0 Vicryl sutures, with the mesenchymal side facing the sponge, and the epithelial side facing the gingiva (**Figure 3A**).

The number of hAMs used depended on the defect size. One hAM was applied in P2, P3, and P5 to P8, and three hAMs were applied in P1 and P4. They were applied without being trimmed or cut.

Depending on the quantity of necrotic bone removed, the gingiva was sutured above the hAM as tightly as possible, without tension, leaving it more or less exposed in the oral cavity. Water-tight closure was possible in four cases (P1, P2, P4, and P5) (**Figures 4A–E**), whereas the hAM was left exposed in the oral cavity in P2, P6, P7, and P8 (**Figures 5A–E**). In P1 and P5, the hAM sides were hard to define because the hAM was folded upon itself.

2.6 Postsurgical Care

Patients had a 2-week antibiotic course prescribed (Amoxicillin + clavulanic acid, 1 g *3/day, and in case of allergies: Clindamycin 600 mg *3/day). P4 had a 6-week-long antibiotic course because of osteitis. Every patient has also been prescribed Chlorhexidine mouth rinses for 10 days.

2.7 Clinical Evaluation and Outcome Measures

2.7.1 Bone Reexposure

At each follow-up visit, the primary endpoint was determined through a clinical evaluation of bone reexposure (measured with a soft plastic ruler) and the extent of wound healing.

2.7.2 Pain, Signs of Inflammation, and Infection Control

Secondary endpoints were evaluated at each follow-up visit (**Table 1**):

- Pain, rated by the patient using a VAS, from 0 to 10 (0 = no pain at all, 10 = worst pain imaginable).
- Signs of inflammation, which were evaluated clinically, with the presence of local erythema and an easily hemorrhagic surgical site.
- Infection, defined as the presence of purulent discharge, abscess, or cellulitis on clinical examination.

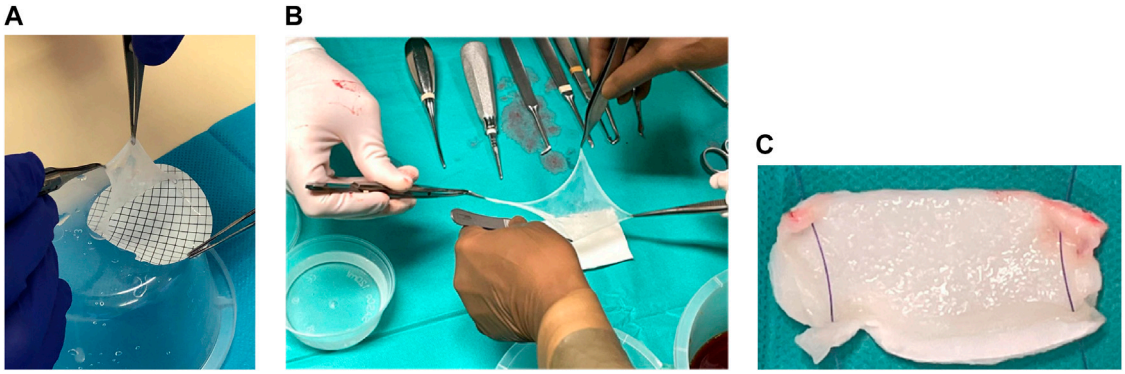

FIGURE 1 | (A) hAM detachment from the nitrocellulose support. **(B)** hAM application technique option 2: Two operators applied the hAM flat on the surgical site with "four hands." **(C)** hAM application technique option 3: hAM was sutured to a collagen sponge (Pangen®, Urgo medical, France).

2.7.3 Adverse Events

Any adverse events (local or systemic, mild, or serious) were documented throughout the follow-up period: edema, erythema, hematoma, hemorrhage, infection, allergy to the hAM or one of its preservation agents, deep vein thrombosis, pulmonary embolism, upper or lower limb ischemia, and secondary bed rest.

2.7.4 MRONJ Relapse, Bone Healing, and/or New Bone Formation

Orthopantomography was done preoperatively and at 3 and 6 months after surgery coupled with Cone Beam Computed Tomography (CBCT) when necessary to assess MRONJ relapse, bone healing, and/or new bone formation. One patient (P6) underwent Positron emission tomography–computed tomography (PET-CT), prescribed as part of her cancer diagnosis and follow-up.

2.8 Statistical Analysis

The Wilcoxon signed-rank test for paired data was applied. Statistical significance was assumed for a p value of < 0.05.

3 RESULTS

3.1 Bone Reexposure and Wound Closure

When nonwatertight sutures were made, leaving the hAM exposed in the oral cavity, the allograft started to resorb within the first week postoperatively and was not visible after 2 weeks. As reported in **Table 1**, complete wound closure was observed in three patients (P3, P5, and P6) 2 weeks after surgery. P3 missed did not attend his postoperative visits past 2 weeks. His last follow-up visit occurred at 6 months postoperatively: he remained asymptomatic with bone reexposure on the lingual part of the surgical site. In P5, wound healing was identifiable from day 4 (**Figure 6A**); two painless granulation tissue masses appeared at the grafted site 4.5 months after surgery (**Figure 6B**). These outgrowths were painless, erythematous, and bled easily when touched during clinical examination but did not delay the wearing of a mandibular prosthesis.

Partial bone reexposure was reported in three patients (P1, P7, and P8) 1 week after surgery. In P1, both treated lesions had partial bone reexposure (less than one-third relative to preoperatively) located on the anterior part of the wound. The patient, unfortunately, broke the left horizontal branch of his mandible after 4 months (probably because the remaining bone thickness was less than 1 cm, with only the basilar cortical bone) but remained asymptomatic. We decided not to treat this fracture surgically, only to monitor it. At the 6-month follow-up visit, this fracture remained asymptomatic. In P7, the anterior mandibular part healed properly; the posterior mandibular part healed partially with granulation tissue and no bone exposure in the median part, whereas the lingual and vestibular parts of the alveolar crest were reexposed. In P8, the collagen membrane was still identifiable 3 days after surgery (**Figure 3B**). Ten days after surgery, the posterior mandibular part had healed correctly, but the bone was still reexposed in the anterior mandibular part (**Figure 3C**).

Complete wound dehiscence occurred in two patients (P2 and P4) 1 week after surgery. However, these patients remained asymptomatic. P2 (who had wound dehiscence in the anterior sector of the mandible) later suffered from a painful bone reexposure in the premolar area in right mandibular, with symptoms of an infection. Thus, 5 months after the first application, hAM was reapplied on the reexposed lesion combined with a single hAM application on the new MRONJ lesion in the right mandibular. The whole surgical site was closed tightly. On day 7, partial bone reexposure was noticed in the premolar area. After 1 month, the whole surgical site was almost completely reepithelialized. After 3 months, the patient was completely pain-free, the surgical site was clean, and no adverse effect was noticed.

At both 3 and 6 months, complete wound healing was observed for P2 (who had undergone hAM reapplication), P5, and P6. Partial wound healing was observed in P1, P3 (at his unique follow-up at 6 months), P7, and P8. P4 did not show signs of wound healing, only bone healing at 6 months, evaluated radiologically.

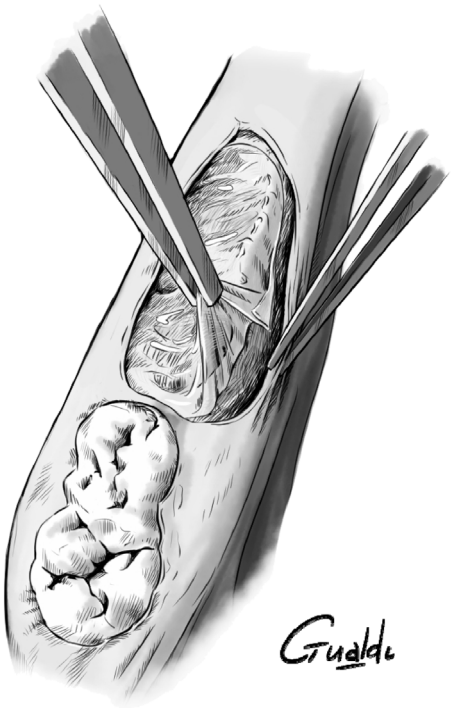

FIGURE 2 | hAM burying between bone and gingiva.

3.2 Pain and Infection

Before surgery, the mean VAS pain score was 3.5/10 (±3.61 SD) with one patient being treated with morphine (**Table 1**). All patients had persistent chronic pain, and out of eight patients, four had a score >2 and six had a score >1. The use of hAM in this context was able to significantly reduce the pain perception between the preoperative measure and the 1-week postsurgery measure (p = 0.03). The score decreased for all of them, with the largest decrease being from 9 to 1 for P1. Pain relief was complete (0/10) for all patients at 1 month. At 6 months, P3 did not report having any pain during the follow-up visits he missed.

As the first example of high pain levels, P1, who suffered from renal cancer, evaluated his pain at 8 to 9/10 on VAS, seriously altering his quality of life. He was fed by a nasogastric tube and suffered from malnutrition, leading to the discontinuation of his chemotherapy treatment. He experienced immediate pain relief after surgery, with a 0/10 score on VAS. Even though he had a 1 cm long wound dehiscence on both sides, his nasogastric tube was taken out after 3 weeks. He was then able to eat a soft-food diet, which he had not been able to do for 1 year. He gained 10 kg in 2 months and was able to resume chemotherapy for his renal cancer. At the 6-month follow-up visit, even with his mandible fracture, the patient remained pain-free and the surgical sites (MRONJ sites in left and right mandibular sectors) were uninfected.

As a second example, P2, who was suffering from breast cancer, evaluated her pain at 7/10 on VAS despite being treated with morphine. One week after surgery, she was completely asymptomatic and had ceased her morphine medication. As above, 3 months after hAM reapplication, the patient was completely pain-free.

As a third example, P5 evaluated her pain intensity at 7/10 and suffered from multiple infection episodes with cellulitis and oral fistulas with purulent discharge, causing halitosis. She had immediate pain relief after surgery and had no pain 1 week later. She did not experience any infections afterward. As shown above, the two outgrowths were painless and benign without impacting her dental prosthesis wear and allowing her to resume a normal diet.

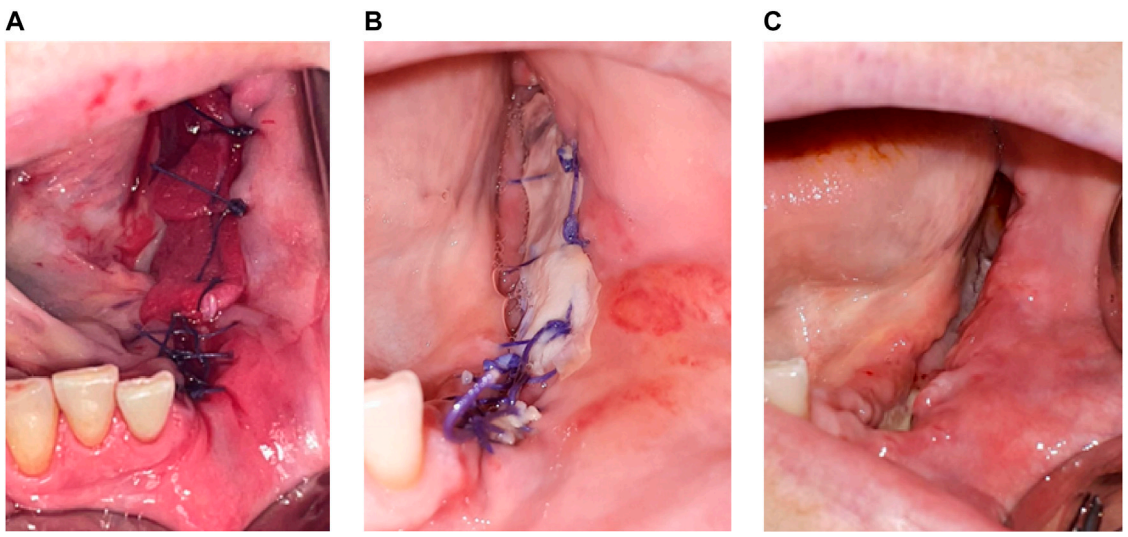

FIGURE 3 | *Patient 8* **(A)** hAM application, sutured on a collagen sponge. **(B)** Three days post-surgery. **(C)** Ten days post-surgery, with the reepithelialization on more than $^{2}/_{3}$ of the surgical site.

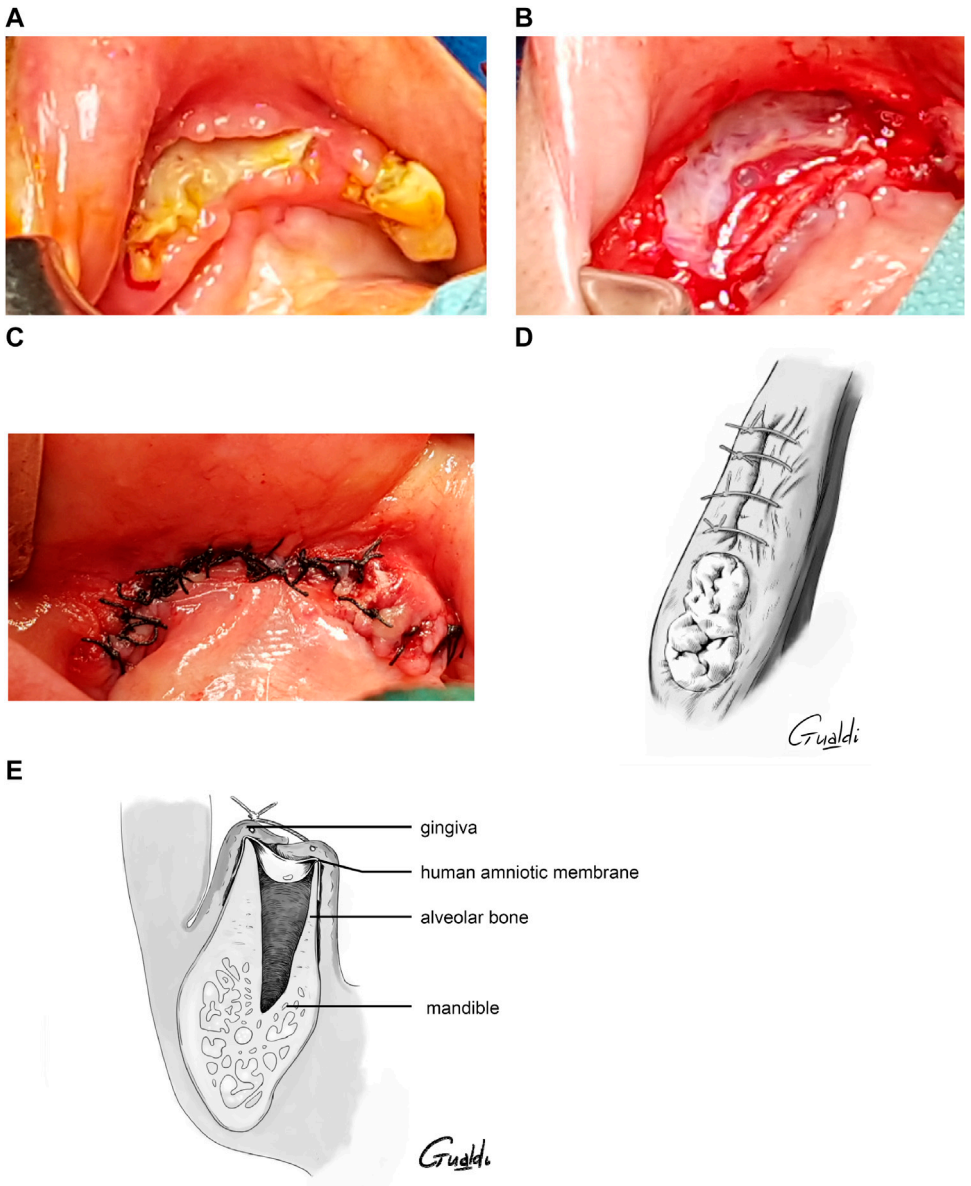

FIGURE 4 | *Patient 2* **(A)** Anterior mandibular stage 2 MRONJ. **(B)** hAM application. **(C)** Hermetical sutures from "hAM implantation with complete coverage" nomenclature (Odet et al., 2021). Here the sutures were done above the implanted hAM which was not visible. **(D)** Upper view and **(E)** Sagittal section illustrations of "hAM implantation with complete coverage" nomenclature.

Besides pain relief, no symptoms of infection were noticed during the whole follow-up in all patients.

3.3 Local Inflammation and Adverse Events

In all patients and even after multiple hAM applications or reapplication, no inflammatory symptoms and no erythema were noticed by the surgeons at the surgical sites early after surgery; also, the wound was not hemorrhagic (**Table 1**). No adverse events were reported. Painless, erythematous, and easily hemorrhagic outgrowths spontaneously appeared in P5's mouth but we were unable to attribute these tissue extensions to the hAM application in an inflammatory and infectious disease such as MRONJ.

3.4 MRONJ Relapse, Bone Healing, and/or New Bone Formation

In five cases (P2, P4, P6, P7, and P8), the bone healed completely without MRONJ recurrence, with or without complete reepithelialization above the surgical site (**Table 1**). In P2, 5 months after the first hAM application, complete bone healing was observed on the anterior part of the mandible, and 6 months after the hAM

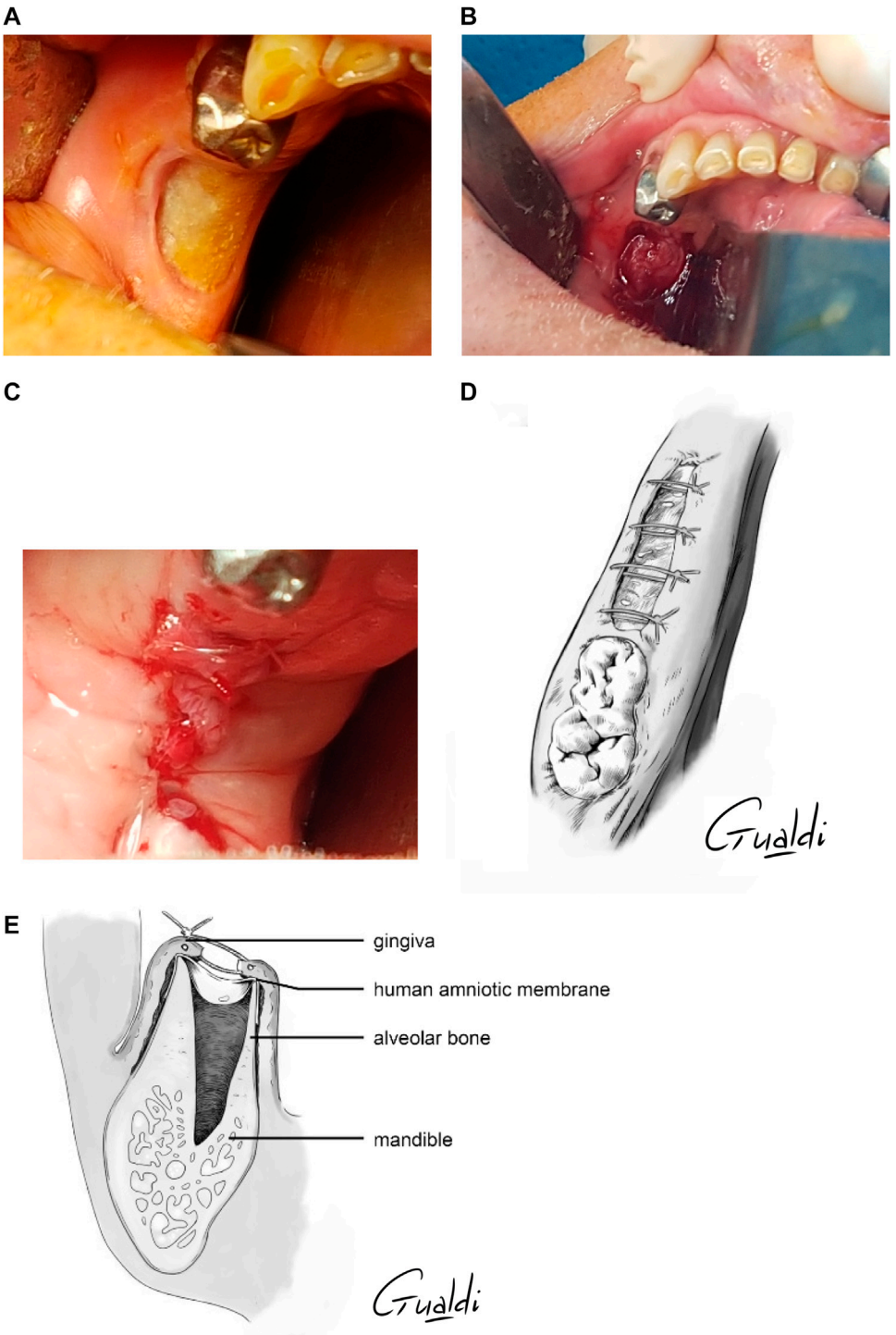

FIGURE 5 | *Patient 3* **(A)** Sector 3 posterior stage 2 MRONJ. **(B)** hAM application. **(C)** Non-hermetic sutures from "hAM implantation with partial coverage" nomenclature (Odet et al., 2021). Here the gingiva was sutured above the hAM, but leaving the hAM exposed in the oral cavity. **(D)** Upper view and **(E)** Sagittal section illustrations of "hAM implantation with partial coverage" nomenclature.

reapplication, complete bone healing was observed in the right mandibular. As another example, P6 had a preoperative, 3-month, and 6-month postoperative PET-CT. The preoperative examination showed a hypermetabolic signal at the MRONJ site in the left maxilla, with an inflammatory and infected left maxillary sinus (**Figures 7A–C**). Three months after surgery, this hypermetabolic signal

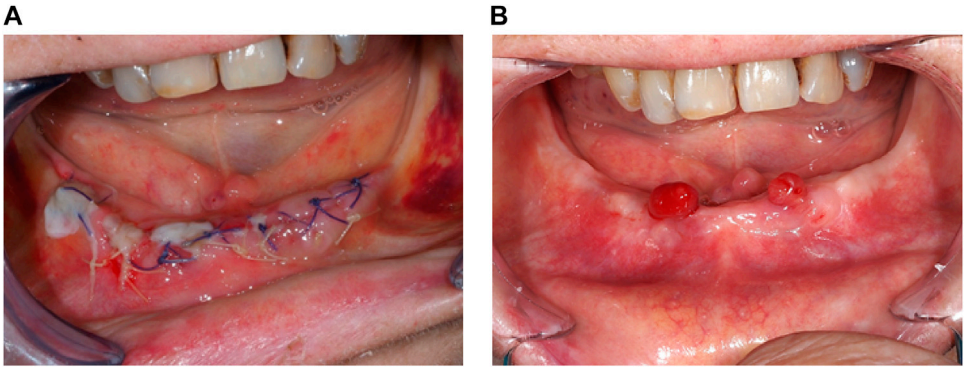

FIGURE 6 | *Patient 5* **(A)** Wound healing beginning at Day 4. **(B)** Two painless and benign granulation tissues 4.5 months post-surgery.

completely disappeared, and the left maxillary sinus was no longer infected (**Figures 7D,E**). The 6-month postoperative orthopantomography showed new bone formation (**Figure 7F**). Since this patient was asymptomatic, no further surgical treatment was performed.

Bone healing was incomplete in two patients. P1, who had an extensive preoperative MRONJ, had an asymptomatic relapse of MRONJ in the left and right mandible after 3 months, with a mandibular fracture after 4.5 months documented by CBCT. In P5, the MRONJ site was extensive and minimum bone resection was possible. Postoperative imaging showed that the MRONJ had stabilized 6 months after surgery. P3 did not have any radiological examinations.

4 DISCUSSION

Our study evaluated the benefits of using hAM in MRONJ on wound healing, quality of life (pain relief and infection control in our study), and signs of inflammation. Here, the application of hAM in patients who have exhausted all treatment options offered immediate pain relief and improved quality of life. Due to the clinical status of these patients, these first observations were already a positive result beyond the management of the lesions.

Among the eight patients treated in the context of compassionate use, three patients had a complete closure of the surgical site with proper reepithelialization at 2 weeks. Epithelialization started 1 week after surgery and was complete 1 month after, consistent with observations in other oral surgery indications (Odet et al., 2021). As one of these three patients missed several follow-up visits, the complete healing rate at 1 month (2 patients out of 7: 28.6%) was lower than in Ragazzo's cohort (78%) at the same time point (Ragazzo et al., 2021). Also, three asymptomatic patients had partial wound dehiscence 1 week after surgery and partial healing 3 months later.

In our study, complete healing at 3 months was found in 25% (2 patients out of 8) or 33% (3 lesions out of 9) of the subjects, whereas partial healing was found in 37.5% (3 patients out of 8) or 44% (4 lesions out of 9) of the subjects. At 6 months, thanks to hAM reapplication in P2, 80% of the lesions had complete or partial wound healing (30 and 50%, respectively) while 62.5% of patients were in stage 3. Our multicenter study was carried out in the context of compassionate use. Indeed, there are few surgical treatment options for MRONJ management, other than extensive flaps covering the surgical site. These flaps were too invasive for patients with impaired health. Additionally, these patients had a low healing capacity because of their cancer, had received multiple IV courses of chemotherapy, and mainly had stage 3 MRONJ (62.5%). On the contrary, Ragazzo's cohort was done at a single hospital and combined 1) all stages with a different SIPMO/SICMF classification (eight patients in stage 1, 13 patients in stage 2, and two patients in stage 3), 2) various diagnoses (cancer and osteoporosis), and 3) various routes of drug administration (per os, IV and subcutaneously) and type of drugs (bone antiresorptive agents and angiogenesis inhibitors). However, it is widely accepted that healing is easier for stage 1 and stage 2 MRONJ patients suffering from osteoporosis treated with per os bone antiresorptive drugs (Pichardo and van Merkesteyn, 2016; Aljohani et al., 2018; Giudice et al., 2018). Similarly, a small single-center cohort study ($N = 5$) has reported complete mucosal coverage with a healing rate of 80% at 3 months in stage 2 MRONJ cases, which are easier to heal (Canakci et al., 2021). Two asymptomatic patients had complete wound dehiscence 1 week after surgery. One was probably due to a fragile and very low-quality gingiva (due to chronic infection and inflammation) and to resumption of smoking right after the surgery (patient 2). In this case, another necrotic site was noted during a follow-up visit in the right mandible. Since this site was painful, we decided to remove the necrotic bone and to reapply hAM on the whole area of exposed bone. After this reapplication, complete wound epithelialization was noted after 1 month and maintained over time. In patient 4, the wound dehiscence was probably related to a mechanical issue (excessive tension on the gingival sutures) and to the location of the MRONJ lesion (on the lingual part of the alveolar crest where tongue movements could hinder wound healing). Bone healing was achieved for this last patient at 6 months.

Complete wound reepithelialization is linked to bone healing. In our study, the bone lesions were stable in 71% of the patients (5 out of 7 patients); new bone formation was observed in one

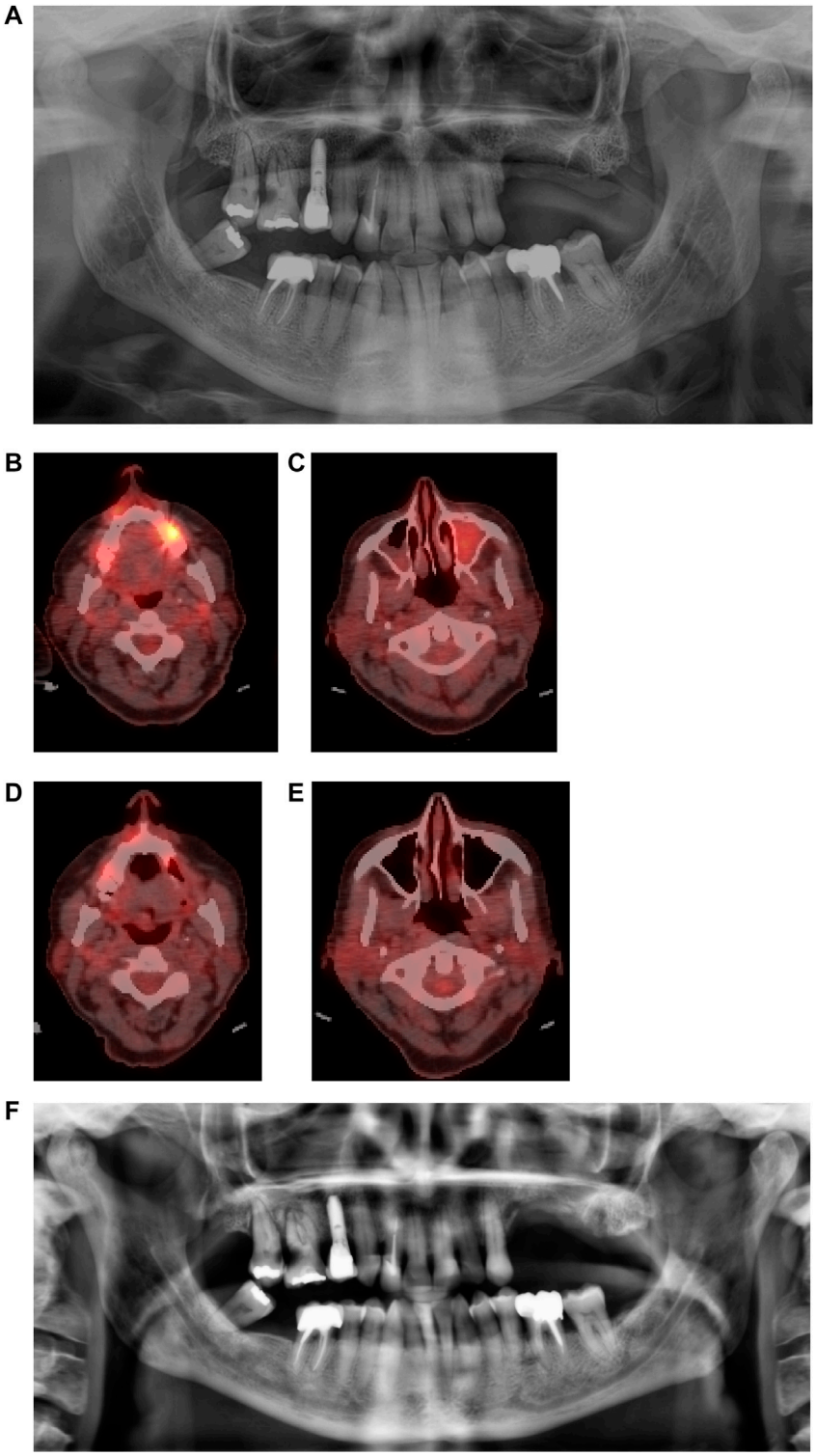

FIGURE 7 | *Patient 6* **(A)** Pre-operative orthopantomography (OPT) showing a stage 2 sector 2 MRONJ; **(B,C)** Positron-Emission Tomography (PET) before surgery, showing a hypermetabolic signal regarding the MRONJ site in sector 2, and an inflammatory left maxillary sinus; **(D,E)** Three months post-operative PET, with a considerable decrease of the hypermetabolic signal and a healthy left maxillary sinus. **(F)** Six months post-operative OPT with osseous neoformation in sector 2.

patient (14%) and the MRONJ got worse in one patient. The total of bone lesion stability and new bone formation (86%) was similar to the partial and complete wound healing rate of MRONJ lesions (80%) at the same time point.

Multiple studies have evaluated bone healing, particularly in MRONJ. The main imaging tools used for both diagnosis and follow-up are orthopantomography and CBCT (Falco et al., 2021; Bouland et al., 2021; Canakci et al., 2021; Ragazzo et al., 2021). Here, we report the use of PET-CT to follow bone repair in one patient who was undergoing this exam for the monitoring of her cancer. The main advantage of PET-CT is that it provides a map of the level of metabolic activity, which can be used at a surgical site and its surrounding structures (Fleisher et al., 2016). In addition, the use of single-photon emission computed tomography (SPECT) has also been reported in the literature and seems to detect metabolic changes as well, whereas CBCT seems to be more accurate in detecting morphological changes (Malina-Altzinger et al., 2019. Çanakçi is the only one who provided detailed postoperative radiological findings after hAM application, with three patients having no extension of bone destruction on both orthopantomography and CBCT after 6 months (Canakci et al., 2021). The radiological findings of the two remaining cases were not provided. Histology has been used to evaluate postextractive alveolus healing following the procedure for socket preservation in a patient receiving oral Bisphosphonates for more than 6 years (Falco et al., 2021). However, like the American Association of Oral and Maxillofacial Surgeons (AAOMS) recommendations (Ruggiero et al., 2014), we agree that an osseous or mucosal biopsy to follow the wound healing process in MRONJ patients is too invasive and could impact the healing process or reinfect the treated lesions.

Addressing persistent and chronic pain is one of the major goals of MRONJ management. hAM has been widely described as being able to reduce the pain experienced by patients (Mamede et al., 2012). It acts as a biological dressing that protects the exposed nerve (Farhadihosseinabadi et al., 2018) and has analgesic effects often reported in the oral surgery field (Odet et al., 2021). In our cohort, all patients had persistent and chronic pain. All were significantly asymptomatic in terms of pain and infection symptoms during the entire follow-up period. Remarkably, pain relief was obtained quickly after surgery, improving quality of life at the same time. Normal nutrition and, when necessary, chemotherapy could be restarted. Our results are consistent with those reported by Ragazzo et al. (2021), where 25 out of 26 patients had complete pain relief at 7 days postoperatively. Additionally, they reported that pain at rest and quality of life improved significantly in the hAM group compared to the resection surgery group.

Infection, often associated with pain and quality of life, is another big challenge in MRONJ management. hAM exerts an antimicrobial effect and therefore protects the wound from infection (Thomas, 2013). It expresses natural antimicrobial molecules such as β-defensins and elafin (King et al., 2007) and has an inhibitory effect against several bacteria (group A *Streptococcus* or *Staphylococcus aureus*) (Kjaergaard et al., 2001), resulting in an antibacterial effect. Its close adherence to the wound surface may also help to prevent contamination (Diaz-Prado et al., 2009). This close adhesion is also known to maintain a moist environment, which contributes to the pain-relieving effect of hAM (Jirsova and Jones, 2017).

hAM is a suitable option for postsurgery applications in wound healing, burn injuries, and ophthalmology (Dadkhah Tehrani et al., 2020) as bacterial infection and biofilm growth are common in these sites (Chen et al., 2012; Mamede et al., 2012). In the last years, our basic knowledge of the antimicrobial activity of fetal membranes has increased (Ramuta et al., 2021) with strong evidence in periodontal disease (Ashraf et al., 2019). Compared to the Ragazzo study (2021), we monitored for infection and reported no infection episodes during the entire follow-up period in our patients.

hAM has low immunogenicity (Kubo et al., 2001), which makes it suitable as an allograft. In our cohort, no matter how many hAMs were applied, no sign of inflammation—monitored by the presence of erythema as well as a tendency for the surgical site to be hemorrhagic—was observed. For patient 5, the outgrowths that spontaneously appeared could either be granulation tissue, due to probable subgingival inflammation, which is easily hemorrhagic clinically, or a botriomycoma, a benign vascular tumor. We were unable to attribute these outgrowths to the hAM application in the context of an inflammatory and infectious disease such as MRONJ. This patient's follow-up was reassuring. Confident with hAM grafting and the absence of adverse events, we experimented for the first hAM reapplication in the same patient, on the initial lesion whose first application had failed and on a new one. As mentioned in a prior study (Odet et al., 2021), hAM size, number, and reapplication are essential information about the product's pharmacology. Here, neither hAM number nor reapplication induced any sign of inflammation or adverse events, and its reapplication seems to have a dose effect. Çanakçi et al. also reported successful results in two patients who had two MRONJ lesions treated with hAM (Canakci et al., 2021).

The second goal of our study was to describe in detail and illustrate, for the first time in the literature, our hAM application method and its related difficulties. Here, from a technical point of view, the hAM was difficult to detach from its nitrocellulose support. Ophthalmologists are assisted by a microscope and blunt forceps. For oral surgery, two surgeons and blunt forceps were necessary. Three methods of hAM handling were identified. In the first one, the hAM's orientation was not easy to preserve because the hAM had folded on itself. The "four hands application technique" or a collagen sponge solved the problem. Therefore, we reported for the first time in literature the innovative use of a collagen sponge to improve hAM handling, orientation, and protection in the oral cavity.

Once applied, it was easy to tuck the hAM between the bone and mucosa, as it was remarkably adherent to the gingiva sutured above it. Indeed, we never sutured the hAM directly to the adjacent mucosa, due to the hAM's fragility. In four cases, the mucosa closure was water-tight. When not possible, less water-tight sutures without tension were applied, leaving the hAM exposed in the oral cavity or protected by the collagen sponge. In this case, clinical hAM resorption was observed and occurred after 7–10 days, as is typical in other oral surgery cases (Odet et al., 2021).

Here, we confirmed that "hAM implantation with complete coverage" and "hAM implantation with partial coverage" are the most suitable techniques for MRONJ surgery as already identified in our pilot study on porcine mandible specimens (Odet et al., submitted). From the four theoretical types of surgery established in our previous nomenclature (Odet et al., 2021), the apposition technique—where the hAM is applied without burying or suturing, left exposed in the mouth and stabilized by any means (cross stitches, pressure dressing, palatal plates, etc.,)—is feasible when gingival suturing or MRONJ lesion localization are inadequate, as occurred with patient 4. The other techniques that involve hAM suturing do not seem to be suitable for MRONJ management.

Complementary treatments to surgery, such as autologous platelet concentrates (APCs), have been developed to improve the healing of bone tissue and reduce recurrence. Like hAM, APCs release growth factors such as vascular endothelial growth factor, epidermal growth factor, platelet-derived growth factors, basic fibroblast growth factor, and transforming growth factor b1. Among APCs, platelet-rich fibrin (PRF), which is simple and inexpensive to prepare, was used to treat MRONJ after bone resection with questionable conclusions (Giudice et al., 2018). Its application, although not described in detail in the literature, is like hAM. Studies have evaluated mucosal integrity, absence of infection, and pain relief and showed a significant difference between the two groups in favor of PRF only at 1 month ($p < 0.05$), whereas no differences were found at 6 and 12 months ($p > 0.05$) (Giudice et al., 2018). Recently, Fortunato et al. reported in a systematic review that APC treatment produced a complete response in 302 lesions (88%), partial response in 23 lesions (6.7%), and negative response in 19 lesions (5.5%), although the clinical evaluations performed at the follow-up visits varied in their time points (1–94 months). The outcome of surgery alone as a treatment was a complete response in 37 lesions (64%), partial response in 14 lesions (24%), and negative response in seven lesions (12%). These findings are not sufficient to establish the effectiveness of APCs in the prevention and treatment of MRONJ. The authors concluded that randomized controlled trials with a large sample size are needed.

The limits of the PRF compared to hAM are 1) its autologous origin so nonqualifiable potential, 2) its nonelastic properties, and 3) the lack of suturing potential. To this end, a case report has described how to improve its potential with an adipose-tissue stromal vascular fraction containing mesenchymal stromal cells and endothelial progenitor cells (Bouland et al., 2021).

hAM is an allogenic tissue with regenerative components through growth factors and stem cells which possess the required properties for MRONJ management in line with pain relief, infection control, and wound healing. In addition, its route of application and resorbability seems to be more consistent when compared to PRF.

5 CONCLUSION

hAM seems to be a promising alternative for MRONJ surgical treatment. It enhances epithelialization, as six of our eight patients showed at least partial wound healing, with granulation tissue or actual gingiva covering the operated site. The patients had significant relief from pain and infectious symptoms, drastically improving their quality of life, and being able to eat again or resume chemotherapy. We detailed and illustrated the surgical application modalities and the obstacles that could be circumvented through the use of a collagen sponge, for example. We did not identify any barriers to the application of multiple hAM patches at the same time and their reapplication in one patient. This very good tolerance suggests that hAM transplantation should be employed as soon as possible without waiting for patients to reach stage 3, in order to increase the likelihood of a complete cure. In addition, reapplication seems to be a good option for the most affected patients, if required. This study will be soon followed by a multicenter randomized controlled trial in five centers in France (grant PHRCI-2020).

DATA AVAILABILITY STATEMENT

The original contributions presented in the study are included in the article/Supplementary Material; further inquiries can be directed to the corresponding author.

ETHICS STATEMENT

Ethical review and approval was not required for the study on human participants in accordance with the local legislation and institutional requirements. The patients/participants provided their written informed consent to participate in this study.

AUTHOR CONTRIBUTIONS

FG, SO, ChM, CG, BC, SD, SL, CéM, HK, NZ, XL, HR, MF, J-CF, and AL elaborated the design of the study. SO, EW, JQ, SD, SL, LB, MG, and CL performed the surgery on the patients and engaged their responsibility. FM, A-SH, DT, and FP provided the hAM and required authorizations. SO, CG, XL, and FP elaborated the adverse event questionnaire. RD revised the radiological examinations. A-LP was responsible for statistics. TG made the illustrations. SO and FG wrote the manuscript. All authors contributed to manuscript revision, and read and approved the submitted version.

FUNDING

This study was supported by a grant from the French Ministry of Health (PHRCI-2020). This publication is based upon work from COST Action 17,116 "SPRINT", supported by COST (European Cooperation in Science and Technology) www.cost.eu.

ACKNOWLEDGMENTS

The authors are grateful to Mr. Thomas Gualdi (thomas-gualdi.fr) for the high quality of his illustrations, Franck Daval (Bibliothèque Universitaire Santé, Université Bourgogne Franche-Comté, F-25000 Besançon, France) for the bibliographic support, and Joanne Archambault, Ph.D., for English language assistance.

REFERENCES

Aljohani, S., Gaudin, R., Weiser, J., Tröltzsch, M., Ehrenfeld, M., Kaeppler, G., et al. (2018). Osteonecrosis of the Jaw in Patients Treated with Denosumab: A Multicenter Case Series. *J. Cranio-Maxillofacial Surg.* 46, 1515–1525. doi:10.1016/j.jcms.2018.05.046

Ashraf, H., Font, K., Powell, C., and Schurr, M. (2019). Antimicrobial Activity of an Amnion-Chorion Membrane to Oral Microbes. *Int. J. Dent.* 2019, 1269534. doi:10.1155/2019/1269534

Bailo, M., Soncini, M., Vertua, E., Signoroni, P. B., Sanzone, S., Lombardi, G., et al. (2004). Engraftment Potential of Human Amnion and Chorion Cells Derived from Term Placenta. *Transplantation* 78, 1439–1448. doi:10.1097/01.tp.0000144606.84234.49

Bouland, C., Meuleman, N., Widelec, J., Keiani-Mothlagh, K., Voisin, C., Lagneaux, L., et al. (2021). Case Reports of Medication-Related Osteonecrosis of the Jaw (MRONJ) Treated with Uncultured Stromal Vascular Fraction and L-PRF. *J. stomatology, oral Maxillofac. Surg.* 122, 212–218. doi:10.1016/j.jormas.2020.05.024

Bourgeois, M., Loisel, F., Obert, L., Pluvy, I., and Gindraux, F. (2019). Can the Amniotic Membrane Be Used to Treat Peripheral Nerve Defects? A Review of Literature. *Hand Surg. Rehabilitation* 38, 223–232. doi:10.1016/j.hansur.2019.05.006

Canakci, F. G., Er, N., Duygu, G., and Varol, G. F. (2021). Surgical Management of Stage-2 Medicationrelated Osteonecrosis of the Jaw with Transplantation of Human Amniotic Membrane: Preliminary Results. *J. Stomatol. Oral Maxillofac. Surg.* 123 (3), e28. doi:10.1016/j.jormas.2021.09.011

Centurione, L., Passaretta, F., Centurione, M. A., De Munari, S., Vertua, E., Silini, A., et al. (2018). Mapping of the Human Placenta: Experimental Evidence of Amniotic Epithelial Cell Heterogeneity. *Cell Transpl.* 27, 12–22. doi:10.1177/0963689717725078

Chen, B., Jones, R. R., Mi, S., Foster, J., Alcock, S. G., Hamley, I. W., et al. (2012). The Mechanical Properties of Amniotic Membrane Influence its Effect as a Biomaterial for Ocular Surface Repair. *Soft Matter* 8, 8379–8387. doi:10.1039/c2sm26175h

Chen, W., Yang, S., Li, S., Lang, J. C., Mao, C., Kroll, P., et al. (2019). Self-Assembled Peptide Nanofibers Display Natural Antimicrobial Peptides to Selectively Kill Bacteria without Compromising Cytocompatibility. *ACS Appl. Mat. Interfaces* 11, 28681–28689. doi:10.1021/acsami.9b09583

Dadkhah Tehrani, F., Firouzeh, A., Shabani, I., and Shabani, A. (2020). A Review on Modifications of Amniotic Membrane for Biomedical Applications. *Front. Bioeng. Biotechnol.* 8, 606982. doi:10.3389/fbioe.2020.606982

Díaz-Prado, S., Rendal-Vázquez, M. E., Muiños-López, E., Hermida-Gómez, T., Rodríguez-Cabarcos, M., Fuentes-Boquete, I., et al. (2009). Potential Use of the Human Amniotic Membrane as a Scaffold in Human Articular Cartilage Repair. *Cell Tissue Bank.* 11, 183–195. doi:10.1007/s10561-009-9144-1

Dua, H. S., and Azuara-Blanco, A. (1999). Amniotic Membrane Transplantation. *Br. J. Ophthalmol.* 83, 748–752. doi:10.1136/bjo.83.6.748

Dua, H. S., Gomes, J. A. P., King, A. J., and Maharajan, V. S. (2004). The Amniotic Membrane in Ophthalmology. *Surv. Ophthalmol.* 49, 51–77. doi:10.1016/j.survophthal.2003.10.004

Dubus, M., Scomazzon, L., Chevrier, J., Ledouble, C., Baldit, A., Braux, J., et al. (2022a). Antibacterial and Immunomodulatory Properties of Acellular Wharton's Jelly Matrix. *Biomedicines* 10 (2), 227. doi:10.3390/biomedicines10020227

Dubus, M., Scomazzon, L., Chevrier, J., Montanede, A., Baldit, A., Terryn, C., et al. (2022b). Decellularization of Wharton's Jelly Increases its Bioactivity and Antibacterial Properties. *Front. Bioeng. Biotechnol.* 10, 828424. doi:10.3389/fbioe.2022.828424

Eibl, J., and Redl, H. (2011). *Process for Differentiating Stem Cells of the Amniotic Membrane*, WO2011EP02653.

Etchebarne, M., Fricain, J. C., Kerdjoudj, H., Di Pietro, R., Wolbank, S., Gindraux, F., et al. (2021). Use of Amniotic Membrane and its Derived Products for Bone Regeneration: A Systematic Review. *Front. Bioeng. Biotechnol.* 9, 661332. doi:10.3389/fbioe.2021.661332

Falco, A., Bataccia, F., Vittorini Orgeas, L., Perfetti, F., Basile, M., and Di Pietro, R. (2021|). A Clinical and Histological Study about the Socket Preservation in a Patient under Oral Bisphosphonates Treatment: A Case Report. *Biology (Basel)* 10 (4), 262. doi:10.3390/biology10040262

Farhadihosseinabadi, B., Farahani, M., Tayebi, T., Jafari, A., Biniazan, F., Modaresifar, K., et al. (2018). Amniotic Membrane and its Epithelial and Mesenchymal Stem Cells as an Appropriate Source for Skin Tissue Engineering and Regenerative Medicine. *Artif. Cells Nanomed Biotechnol.* 46, 431–440. doi:10.1080/21691401.2018.1458730

Fenelon, M., B Maurel, D., Siadous, R., Gremare, A., Delmond, S., Durand, M., et al. (2019). Comparison of the Impact of Preservation Methods on Amniotic Membrane Properties for Tissue Engineering Applications. *Mater. Sci. Eng. C* 104, 109903. doi:10.1016/j.msec.2019.109903

Fénelon, M., Catros, S., and Fricain, J. C. (2018). What Is the Benefit of Using Amniotic Membrane in Oral Surgery? A Comprehensive Review of Clinical Studies. *Clin. Oral Invest.* 22, 1881–1891. doi:10.1007/s00784-018-2457-3

Fénelon, M., Catros, S., Meyer, C., Fricain, J.-C., Obert, L., Auber, F., et al. (2021). Applications of Human Amniotic Membrane for Tissue Engineering. *Membranes* 11, 387. doi:10.3390/membranes11060387

Fénelon, M., Chassande, O., Kalisky, J., Gindraux, F., Brun, S., Bareille, R., et al. (2018). Human Amniotic Membrane for Guided Bone Regeneration of Calvarial Defects in Mice. *J. Mater Sci. Mater Med.* 29, 78. doi:10.1007/s10856-018-6086-9

Fenelon, M., Etchebarne, M., Siadous, R., Grémare, A., Durand, M., Sentilhes, L., et al. (2021). Comparison of Amniotic Membrane versus the Induced Membrane for Bone Regeneration in Long Bone Segmental Defects Using Calcium Phosphate Cement Loaded with BMP-2. *Mater. Sci. Eng. C* 124, 112032. doi:10.1016/j.msec.2021.112032

Fenelon, M., Etchebarne, M., Siadous, R., Grémare, A., Durand, M., Sentilhes, L., et al. (2020). Assessment of Fresh and Preserved Amniotic Membrane for Guided Bone Regeneration in Mice. *J. Biomed. Mater Res.* 108, 2044–2056. doi:10.1002/jbm.a.36964

Fleisher, K. E., Pham, S., Raad, R. A., Friedman, K. P., Ghesani, M., Chan, K. C., et al. (2016). Does Fluorodeoxyglucose Positron Emission Tomography with Computed Tomography Facilitate Treatment of Medication-Related Osteonecrosis of the Jaw? *J. Oral Maxillofac. Surg.* 74, 945–958. doi:10.1016/j.joms.2015.10.025

Gajiwala, K., and Gajiwala, A. L. (2004). Evaluation of Lyophilised, Gamma-Irradiated Amnion as a Biological Dressing. *Cell Tissue Bank.* 5, 73–80. doi:10.1023/b:catb.0000034076.16744.4b

Gholipourmalekabadi, M., Farhadihosseinabadi, B., Faraji, M., and Nourani, M. R. (2019). How Preparation and Preservation Procedures Affect the Properties of Amniotic Membrane? How Safe Are the Procedures? *Burns* 46 (6), 1254–1271. doi:10.1016/j.burns.2019.07.005

Gindraux, F. (2021). "Human Amniotic Membrane Potential for Bone Repair: from the Lab to the Clinic," in The 29th Annual Meeting of the European Orthopaedic Research Society (EORS). Rome, Italy, September 15–17, 2020. Editor O. Proceedings.

Gindraux, F., Laurent, R., Nicod, L., Billy, B., Meyer, C., Zwetyenga, N., et al. (2013). Human Amniotic Membrane: Clinical Uses, Patents and Marketed Products. *Recent Pat. Regen. Med.* 3, 193–214. doi:10.2174/22102965113039990021

Gindraux, F., and Obert, L. (2010). "Human Amniotic Membranes: Benefits for Bone Repair/regeneration," in *Bioreconstruction : de l'os à la peau Tome 2*. France: Sauramps Médical, 85–91.

Gindraux, F., Rondot, T., De Billy, B., Zwetyenga, N., Fricain, J.-C., Pagnon, A., et al. (2017). Similarities between Induced Membrane and Amniotic Membrane: Novelty for Bone Repair. *Placenta* 59, 116–123. doi:10.1016/j.placenta.2017.06.340

Giudice, A., Barone, S., Giudice, C., Bennardo, F., and Fortunato, L. (2018). Can Platelet-Rich Fibrin Improve Healing after Surgical Treatment of Medication-Related Osteonecrosis of the Jaw? A Pilot Study. *Oral Surg. Oral Med. Oral Pathology Oral Radiology* 126, 390–403. doi:10.1016/j.oooo.2018.06.007

Grémare, A., Jean-Gilles, S., Musqui, P., Magnan, L., Torres, Y., Fénelon, M., et al. (2019). Cartography of the Mechanical Properties of the Human Amniotic Membrane. *J. Mech. Behav. Biomed. Mater.* 99, 18–26. doi:10.1016/j.jmbbm.2019.07.007

Gualdi, T., Laurent, R., Moutarlier, V., Fenelon, M., Nallet, A., Pouthier, F., et al. (2019). *In Vitro* osteodifferentiation of Intact Human Amniotic Membrane Is Not Beneficial in the Context of Bone Repair. *Cell Tissue Bank.* 20, 435–446. doi:10.1007/s10561-019-09778-3

Gulameabasse, S., Gindraux, F., Catros, S., Fricain, J. C., and Fenelon, M. (2020). Chorion and Amnion/chorion Membranes in Oral and Periodontal Surgery: A Systematic Review. *J. Biomed. Mater Res. B Appl. Biomater.* 109 (8), 1216–1229. doi:10.1002/jbm.b.34783

Jirsova, K., and Jones, G. L. A. (2017). Amniotic Membrane in Ophthalmology: Properties, Preparation, Storage and Indications for Grafting-A Review. *Cell Tissue Bank.* 18, 193–204. doi:10.1007/s10561-017-9618-5

John, T. (2003). Human Amniotic Membrane Transplantation: Past, Present, and Future. *Ophthalmol. Clin. N. Am.* 16, 43–65. doi:10.1016/s0896-1549(02)00110-4

King, A. E., Paltoo, A., Kelly, R. W., Sallenave, J.-M., Bocking, A. D., and Challis, J. R. G. (2007). Expression of Natural Antimicrobials by Human Placenta and Fetal Membranes. *Placenta* 28, 161–169. doi:10.1016/j.placenta.2006.01.006

Kjaergaard, N., Hein, M., Hyttel, L., Helmig, R. B., Schønheyder, H. C., Uldbjerg, N., et al. (2001). Antibacterial Properties of Human Amnion and Chorion *In Vitro*. *Eur. J. Obstetrics Gynecol. Reproductive Biol.* 94, 224–229. doi:10.1016/s0301-2115(00)00345-6

Kubo, M., Sonoda, Y., Muramatsu, R., and Usui, M. (2001). Immunogenicity of Human Amniotic Membrane in Experimental Xenotransplantation. *Invest. Ophthalmol. Vis. Sci.* 42, 1539–1546.

Laurent, R., Brennan, M., Renaud, A., D'arros, C., Obert, L., Layrolle, P., et al. (2014a). Osteodifferentation of Intact Human Amniotic Membrane through a Jet Sprayed Polycaprolactone Nanofibre Scaffold. *Bone & Jt. J. Orthop. Proc. Suppl.* 96-B, 113.

Laurent, R., Nallet, A., De Billy, B., Obert, L., Nicod, L., Meyer, C., et al. (2017). Fresh and *In Vitro* Osteodifferentiated Human Amniotic Membrane, Alone or Associated with an Additional Scaffold, Does Not Induce Ectopic Bone Formation in Balb/c Mice. *Cell Tissue Bank.* 18, 17–25. doi:10.1007/s10561-016-9605-2

Laurent, R., Nallet, A., Obert, L., Nicod, L., and Gindraux, F. (2014b). Storage and Qualification of Viable Intact Human Amniotic Graft and Technology Transfer to a Tissue Bank. *Cell Tissue Bank.* 15, 267–275. doi:10.1007/s10561-014-9437-x

Laurent, R., Nicod, L., Layrolle, P., De Billy, B., Obert, L., and Gindraux, F. (2018). Osteogenic Potential and Immunogenicity of Human Amniotic Membrane: *In Vivo* and *In Vivo* Studies. *Orthop. Proc.* 96-B (11).

Letko, E., Stechschulte, S. U., Kenyon, K. R., Sadeq, N., Romero, T. R., Samson, C. M., et al. (2001). Amniotic Membrane Inlay and Overlay Grafting for Corneal Epithelial Defects and Stromal Ulcers. *Arch. Ophthalmol.* 119, 659–663. doi:10.1001/archopht.119.5.659

Lindenmair, A., Wolbank, S., Stadler, G., Meinl, A., Peterbauer-Scherb, A., Eibl, J., et al. (2010). Osteogenic Differentiation of Intact Human Amniotic Membrane. *Biomaterials* 31, 8659–8665. doi:10.1016/j.biomaterials.2010.07.090

Malina-Altzinger, J., Klaeser, B., Suter, V. G. A., Schriber, M., Vollnberg, B., and Schaller, B. (2019). Comparative Evaluation of SPECT/CT and CBCT in Patients with Mandibular Osteomyelitis and Osteonecrosis. *Clin. Oral Invest.* 23, 4213–4222. doi:10.1007/s00784-019-02862-8

Mamede, A. C., Carvalho, M. J., Abrantes, A. M., Laranjo, M., Maia, C. J., and Botelho, M. F. (2012). Amniotic Membrane: from Structure and Functions to Clinical Applications. *Cell Tissue Res.* 349, 447–458. doi:10.1007/s00441-012-1424-6

Mcquilling, J. P., Vines, J. B., and Mowry, K. C. (2017). *In Vitro* assessment of a Novel, Hypothermically Stored Amniotic Membrane for Use in a Chronic Wound Environment. *Int. Wound J.* 14 (6), 993–1005. doi:10.1111/iwj.12748

Obert, L., Genestier, L., Froidevaux, L., Averlant, E., Laurent, R., Wajszczak, L., et al. (2012). "Amniotic membrane for bone repair? Reflection around of the Masquelet technique to one stage/Membrane amniotique pour la réparation osseuse? Réflexion autour de la simplification de la technique de Masquelet à une chirurgie," in *Technique de Masquelet* (France: Sauramps Médical).

Odet, S., Louvrier, A., Meyer, C., Nicolas, F. J., Hofman, N., Chatelain, B., et al. (2021). Surgical Application of Human Amniotic Membrane and Amnion-Chorion Membrane in the Oral Cavity and Efficacy Evaluation: Corollary with Ophthalmological and Wound Healing Experiences. *Front. Bioeng. Biotechnol.* 9, 685128. doi:10.3389/fbioe.2021.685128

Parolini, O., Alviano, F., Bagnara, G. P., Bilic, G., Bühring, H.-J., Evangelista, M., et al. (2008). Concise Review: Isolation and Characterization of Cells from Human Term Placenta: Outcome of the First International Workshop on Placenta Derived Stem Cells. *Stem Cells* 26, 300–311. doi:10.1634/stemcells.2007-0594

Passaretta, F., Bosco, D., Centurione, L., Centurione, M. A., Marongiu, F., and Di Pietro, R. (2020). Differential Response to Hepatic Differentiation Stimuli of Amniotic Epithelial Cells Isolated from Four Regions of the Amniotic Membrane. *J. Cell Mol. Med.* 24, 4350–4355. doi:10.1111/jcmm.14928

Pichardo, S. E. C., and Van Merkesteyn, J. P. R. (2016). Evaluation of a Surgical Treatment of Denosumab-Related Osteonecrosis of the Jaws. *Oral Surg. Oral Med. Oral Pathology Oral Radiology* 122, 272–278. doi:10.1016/j.oooo.2016.03.008

Ragazzo, M., Trojan, D., Spagnol, L., Paolin, A., and Guarda Nardini, L. (2018). Use of Amniotic Membrane in the Treatment of Patients with BRONJ: Two Case Reports. *J. Surg. Case Rep.* 2018, rjy073. doi:10.1093/jscr/rjy073

Ragazzo, M., Val, M., Montagner, G., Trojan, D., Fusetti, S., and Guarda Nardini, L. (2021). Human Amniotic Membrane: an Improvement in the Treatment of Medication-Related Osteonecrosis of the Jaw (MRONJ)? A Case–Control Study. *Cell Tissue Bank.* 23 (1), 129–141. doi:10.1007/s10561-021-09922-y

Rama, P., Giannini, R., Bruni, A., Gatto, C., Tiso, R., and Ponzin, D. (2001). Further Evaluation of Amniotic Membrane Banking for Transplantation in Ocular Surface Diseases. *Cell Tissue Bank.* 2, 155–163. doi:10.1023/a:1020158206073

Ramuta, T. Ž., Šket, T., Starčič Erjavec, M., and Kreft, M. E. (2021). Antimicrobial Activity of Human Fetal Membranes: From Biological Function to Clinical Use. *Front. Bioeng. Biotechnol.* 9, 691522. doi:10.3389/fbioe.2021.691522

Ricci, E., Vanosi, G., Lindenmair, A., Hennerbichler, S., Peterbauer-Scherb, A., Wolbank, S., et al. (2013). Anti-fibrotic Effects of Fresh and Cryopreserved Human Amniotic Membrane in a Rat Liver Fibrosis Model. *Cell Tissue Bank.* 14, 475–488. doi:10.1007/s10561-012-9337-x

Ruggiero, S. L., Dodson, T. B., Fantasia, J., Goodday, R., Aghaloo, T., Mehrotra, B., et al. (2014). American Association of Oral and Maxillofacial Surgeons Position Paper on Medication-Related Osteonecrosis of the Jaw–2014 Update. *J. Oral Maxillofac. Surg.* 72, 1938–1956. doi:10.1016/j.joms.2014.04.031

Russo, A., Bonci, P., and Bonci, P. (2011). The Effects of Different Preservation Processes on the Total Protein and Growth Factor Content in a New Biological Product Developed from Human Amniotic Membrane. *Cell Tissue Bank.* 13, 353–361. doi:10.1007/s10561-011-9261-5

Silini, A. R., Di Pietro, R., Lang-Olip, I., Alviano, F., Banerjee, A., Basile, M., et al. (2020). Perinatal Derivatives: Where Do We Stand? A Roadmap of the Human Placenta and Consensus for Tissue and Cell Nomenclature. *Front. Bioeng. Biotechnol.* 8, 610544. doi:10.3389/fbioe.2020.610544

Thomas, B. S., and Chopra, A. (2013). Amniotic Membrane: A Novel Material for Regeneration and Repair. *J. Biomimetics Biomaterials Tissue Eng.* 18, 1–8.

Wolbank, S., Peterbauer, A., Fahrner, M., Hennerbichler, S., Van Griensven, M., Stadler, G., et al. (2007). Dose-dependent Immunomodulatory Effect of Human Stem Cells from Amniotic Membrane: a Comparison with Human Mesenchymal Stem Cells from Adipose Tissue. *Tissue Eng.* 13, 1173–1183. doi:10.1089/ten.2006.0313

Conflict of Interest: The authors declare that the research was conducted in the absence of any commercial or financial relationships that could be construed as a potential conflict of interest.

frontiers | Frontiers in Bioengineering and Biotechnology

TYPE Review
PUBLISHED 04 August 2022
DOI 10.3389/fbioe.2022.965006

OPEN ACCESS

EDITED BY
Wolfgang Holnthoner,
Ludwig Boltzmann Institute for Experimental and Clinical Traumatology, Austria

REVIEWED BY
Alfred Gugerell,
Medical University of Vienna, Austria
Betül Çelebi Saltik,
Hacettepe University, Turkey

*CORRESPONDENCE
Günther Eissner,
guenther.eissner@ucd.ie
Sergio Liarte,
sdll1@um.es

†These authors have contributed equally to this work

SPECIALTY SECTION
This article was submitted to Tissue Engineering and Regenerative Medicine, a section of the journal Frontiers in Bioengineering and Biotechnology

RECEIVED 09 June 2022
ACCEPTED 07 July 2022
PUBLISHED 04 August 2022

CITATION
Flores AI, Pipino C, Jerman UD, Liarte S, Gindraux F, Kreft ME, Nicolas FJ, Pandolfi A, Tratnjek L, Giebel B, Pozzobon M, Silini AR, Parolini O, Eissner G and Lang-Olip I (2022), Perinatal derivatives: How to best characterize their multimodal functions in vitro. Part C: Inflammation, angiogenesis, and wound healing. *Front. Bioeng. Biotechnol.* 10:965006. doi: 10.3389/fbioe.2022.965006

Perinatal derivatives: How to best characterize their multimodal functions *in vitro*. Part C: Inflammation, angiogenesis, and wound healing

Ana I. Flores[1†], Caterina Pipino[2†], Urška Dragin Jerman[3†], Sergio Liarte[4]*, Florelle Gindraux[5,6], Mateja Erdani Kreft[3], Francisco J. Nicolas[4], Assunta Pandolfi[2], Larisa Tratnjek[3], Bernd Giebel[7], Michela Pozzobon[8], Antonietta R. Silini[9], Ornella Parolini[10,11], Günther Eissner[12]* and Ingrid Lang-Olip[13]

[1]Regenerative Medicine Group, Research Institute Hospital 12 de Octubre (imas12), Madrid, Spain, [2]Center for Advanced Studies and Technology (CAST), Department of Medical, Oral and Biotechnological Sciences, University G. d'Annunzio Chieti-Pescara, StemTech Group, Chieti, Italy, [3]University of Ljubljana, Faculty of Medicine, Institute of Cell Biology, Ljubljana, Slovenia, [4]Laboratorio de Regeneración, Oncología Molecular y TGF-β, IMIB-Arrixaca, Murcia, Spain, [5]Service de Chirurgie Maxillo-Faciale, Stomatologie et Odontologie Hospitalière, CHU Besançon, Besançon, France, [6]Laboratoire de Nanomédecine, Imagerie, Thérapeutique EA 466, Université Bourgogne Franche-Comté, Besançon, France, [7]Institute for Transfusion Medicine, University Hospital Essen, University of Duisburg-Essen, Essen, Germany, [8]Department of Women's and Children's Health, University of Padova, Padova, Italy and Foundation Institute of Pediatric Research Fondazione Città Della Speranza, Padova, Italy, [9]Centro di Ricerca E. Menni, Brescia, Italy, [10]Department of Life Science and Public Health, Università Cattolica del Sacro Cuore, Rome, Italy, [11]Fondazione Policlinico Universitario "Agostino Gemelli" IRCCS, Rome, Italy, [12]Systems Biology Ireland, School of Medicine, Conway Institute, University College Dublin, Dublin, Ireland, [13]Division of Cell Biology, Histology and Embryology, Gottfried Schatz Research Center, Medical University of Graz, Graz, Austria

Perinatal derivatives (PnD) are birth-associated tissues, such as placenta, umbilical cord, amniotic and chorionic membrane, and thereof-derived cells as well as secretomes. PnD play an increasing therapeutic role with beneficial effects on the treatment of various diseases. The aim of this review is to elucidate the modes of action of non-hematopoietic PnD on inflammation, angiogenesis and wound healing. We describe the source and type of PnD with a special focus on their effects on inflammation and immune response, on vascular function as well as on cutaneous and oral wound healing, which is a complex process that comprises hemostasis, inflammation, proliferation (including epithelialization, angiogenesis), and remodeling. We further evaluate the different *in vitro* assays currently used for assessing selected functional and therapeutic PnD properties. This review is a joint effort from the COST SPRINT Action (CA17116) with the intention to promote PnD into the clinics. It is part of a quadrinomial series on functional assays for validation of PnD, spanning biological functions, such as immunomodulation, anti-microbial/anti-cancer activities, anti-inflammation, wound healing, angiogenesis, and regeneration.

KEYWORDS

perinatal derivatives, mesenchymal stromal cells, amniotic epithelial cells, amniotic membrane, functional assays, inflammation, angiogenesis, wound healing

1 Introduction

Stem and progenitor cells from various tissues are increasingly being used in regenerative medicine and immunotherapies. For the expansion of these strategies, many researchers are putting effort on developing methods and technologies based on perinatal derivatives (PnD), which comprise perinatal tissues and thereof derived cells and secretomes. Besides perinatal mesenchymal stromal cells (MSC), also other perinatal tissues and cells, such as human amniotic membrane epithelial cells (hAEC), human amniotic fluid cells (hAFC), human parietal decidua (hPD) cells, or processed membranes (human amniotic membrane (hAM) or human amnio-chorionic membrane (hACM)) were already used or are under investigation for therapeutical treatment. Perinatal endothelial cells (EC) are predominantly isolated from the human umbilical vein (HUVEC), due to easier obtention and higher yield (Silini et al., 2020). Consequently, research using HUVEC is gaining momentum in the PnD field for the development of technologies useful for the vascular component regeneration and as an *in vitro* platform to validate the functional role of other PnD in the context of inflammation and angiogenesis (Pipino et al., 2022).

PnD portrait important advantages over products obtained from adults regarding their naïvity, availability and accessibility. This review aims to address the most widely studied PnD with a special focus on their functional *in vitro* validation in the field of inflammation, angiogenesis and cutaneous as well as oral wound healing to support their use in specific pre-clinical and clinical settings.

The anti-inflammatory properties of PnD make them highly attractive for treating inflammatory, autoimmune, and degenerative diseases (Silini et al., 2013; Cargnoni et al., 2021; Yang et al., 2021). Inflammation is the body's defense mechanism to harmful stimuli, such as pathogens or damaged tissues. When the immune system is activated, inflammatory cells transmigrate from the vessels into damaged tissues (Medzhitov, 2008). There are two types of inflammation, acute inflammation characterized by a rapid response and chronic inflammation, which is a persistent but slowly evolving response. Immune cells from both, innate and adaptive response, play important roles in the pathogenesis of inflammatory diseases (Marshall et al., 2018). Chemokines as produced by damaged tissue recruit different immune cells, including eosinophils, macrophages, neutrophils, and T lymphocytes, contributing to inflammation. The resolution of inflammation is carried out by acting at different levels, such as through a decrease in the proliferation and maturation of immune cells, an increase in phagocytosis and apoptosis of immune cells, and an inhibition of the secretion of proinflammatory mediators. To behave as an anti-inflammatory agent, PnD should sense the inflammatory conditions, express and secrete anti-inflammatory molecules, and interact with immune cells. Accumulating evidence from preclinical and clinical trials indicates that PnD exert anti-inflammatory therapeutic effects in numerous autoimmune and inflammatory diseases such as graft versus host disease (GVHD), rheumatoid arthritis, multiple sclerosis, systemic lupus erythematosus, and respiratory diseases (Ringden et al., 2018; Yang et al., 2021; Ma et al., 2022).

Inflammation and angiogenesis, the formation of new blood vessels, are critical steps in the complex process of wound healing. Hemostasis, the first phase of wound healing, leads to vasoconstriction and the formation of a blot clot that stops bleeding. The following inflammatory phase leads to the accumulation of neutrophils and macrophages at the wound to defend bacteria and remove foreign substances, respectively. In addition, the adaptive immune system is activated. In the subsequent proliferative phase, fibroblasts multiply and deposit extracellular matrix, and angiogenesis, a critical component of acute wound healing, occurs. Re-epithelialization takes place as epithelial cells migrate from the periphery to the center of the wound. Further extracellular matrix deposition leads to a transition of the inflammatory state to a growth state, and a cross-linking of collagen, as well as scar maturation, finally leads to remodeling (Diegelmann and Evans, 2004; Dash et al., 2018). Similar processes have also been described in mucosal wound healing. Delayed wound healing is often due to insufficient blood supply based on impaired wound revascularization (Demidova-Rice et al., 2012). Further, chronic, non-healing wounds are detained in a self-perpetuating inflammatory stage that hinders progression to proliferation (Stojadinovic et al., 2008). Thus, chronic wounds are still a challenge to treat, although already more than a hundred years ago the hAM was used as a biological dressing for treating burns and skin ulcerations. Since then, while its use for the treatment of e.g. ocular ulcers is popular worldwide, its suitability for the management of skin ulcers is less well-recognized (Castellanos et al., 2017).

Improved techniques for tissue preservation, as well as advances in isolation and culture procedures for PnD cells facilitate the way for early phase clinical trials in diverse indications, such as the application of PLacental-eXpanded (PLX-PAD) stromal cells for the muscle recovery after hip arthroplasty (Winkler et al., 2022), multiple sclerosis (Lublin et al., 2014), pulmonary fibrosis (Chambers et al., 2014), and also COVID-19 (Hashemian et al., 2021; Sadeghi et al., 2021).

The focus of this review lies in the functional *in vitro* testing of PnD, which should be carried out before their application in

animal models and subsequent clinical studies, to produce a treatment which is safe, effective and available for patients.

2 Mechanism of action

2.1 PnD effects on inflammation and the immune response

PnD can downregulate inflammation by acting on several key players in innate and adaptative immunity. PnD reduce inflammatory conditions *in vitro* by suppressing the proliferation, secretion of inflammatory cytokines, and cytotoxic activity of different immune cell subpopulations, as well as by inducing T cells and monocytes to acquire anti-inflammatory functions. These anti-inflammatory effects can be measured *in vitro* in cell-to-cell contact studies between PnD and immune cells (Erkers et al., 2013; Vellasamy et al., 2013), in non-contact transwell studies via secretion of soluble factors or by using conditioned medium (CM) of PnD cultures (Magatti et al., 2008; Gu et al., 2013). It is also important to understand that PnD can act constitutively (Magatti et al., 2008; Rossi et al., 2012; Pianta et al., 2015), and they can react to local inflammatory stimuli. To functionally assess this, an *in vitro* inflammatory environment created by the addition of Interferon γ (IFNγ) and/or Tumour Necrosis Factor (TNF), Interleukin (IL) 1β, IL6, granulocyte-macrophage- colony stimulating factor (GM-CSF) or a mixture of all of these can be used to see if the cell morphology, size, immunophenotype and proliferation capabilities of PnD are altered (Mebarki et al., 2021). Furthermore, this simulated pro-inflammatory environment can be used to study the inhibitory capacity of PnD on T cell proliferation (Mebarki et al., 2021).

2.1.1 Assessment of PnD effects on the innate immune response

Innate immune cells, such as macrophages, neutrophils, dendritic cells, and natural killer cells can be regulated by PnD (Abumaree et al., 2017; De La Torre et al., 2018; Edinger et al., 2018; Torre and Flores, 2020). Anti-inflammatory assays are focused on the evaluation of cell viability, maturation and/or activation of immune cells.

Macrophages play an important role in the initiation, preservation, and cessation of inflammation through production of several cytokines and growth factors. Generally based on their cytokine profile and cell surface markers (see below) macrophages show two different phenotypes: the predominantly pro-inflammatory M1 phenotype and the generally anti-inflammatory M2 phenotype The macrophage activity switches from pro-inflammatory (M1) to anti-inflammatory (M2) during the inflammatory process, and an imbalance of this change at the end of an inflammatory process is associated with a range of inflammatory diseases (Fujiwara and Kobayashi, 2005; Lee, 2018). Some studies have reported that PnD can induce anti-inflammatory effects by regulating macrophage functions. To study whether direct or indirect contact of PnD with macrophages induces a switch to an M2-like anti-inflammatory phenotype, a transwell chamber membrane culture system can be used. The effects of adding CM of unstimulated PnD to differentiated monocytes can also be evaluated. Firstly, $CD14^+$ monocytes are isolated from peripheral blood mononuclear cells (PBMC) and differentiated into M1 macrophages by the addition of GM-CSF or lipopolysaccharide (LPS). Secondly, macrophages and PnD are co-cultured in the transwell chamber system and the M2 phenotype can be characterized by flow cytometric analyses of morphological changes and the expression of M2 cell surface markers (CD14, CD36, CD86, CD163, CD204, CD206, B7-H4 and CD11 b), the co-stimulatory molecules (CD40, CD80 and CD86) and the co-inhibitory molecules (CD273, CD274 and B7-H4), and major histocompatibility complex (MHC-II) molecules (Abumaree et al., 2013; Huang et al., 2019). The anti-inflammatory phenotype in M2-like macrophages can also be evaluated by qRT-PCR looking for an increased expression of the M2 cell surface markers, and by Enzyme-Linked Immunosorbent Assay (ELISA) examining increased secretion of IL-10 and arginase (Arg)-1, and decreased secretion of IL-1β, IL-12 (p70) and MIP-1α, TNF, inducible nitric oxide synthase (iNOS), and IL-6 (Abumaree et al., 2013; Huang et al., 2019). Furthermore, since the clearance of apoptotic cells is critical for the resolution of inflammation, it is possible to assess whether PnD increase the phagocytic activity of M2 macrophages. Phagocytosis of apoptotic cells is then evaluated by fluorescence microscopy (Abumaree et al., 2013) or the ability of M2 macrophages to take up zymosan particles as measured with the CytoSelect™ Phagocytosis Kit (Abumaree et al., 2013). The immortalized human monocyte/macrophage cell line THP-1 is another useful cell model system to study the effect of PnD on activated macrophages (He et al., 2012). THP-1 cells are pre-treated with phorbol-12-myristate-13-acetate (PMA) to induce macrophage differentiation and then activated with LPS (Shu et al., 2015). After direct coculture with PnD or their CM, Western blot can be used to detect diminished levels of the proinflammatory cytokines TNF and IL-1β, and the inhibition of the mitogen-activated protein kinase (MAPK)/NF-κB signaling pathway (Hu et al., 2013). Macrophages can induce changes in the phenotype of PnD, and these changes can be evaluated by flow cytometry as an induction in secretion of the inflammatory proteins IL8, IL-12, and Monocyte Chemoattractant Protein 1 (MCP-1), and of anti-inflammatory proteins IL-10, indoleamine-pyrrole-2,3-oxygenase (IDO) and B7H4 (Abumaree et al., 2013).

Neutrophils along with macrophages provide the innate cell-mediated immunity and inflammatory responses at sites of injury. Indeed, cytokines secreted by macrophages attract neutrophils to the injured area to initiate the inflammatory

response that in turn will recruit additional innate immunity cells and molecules. To assess the role of PnD in neutrophil and macrophage migration *in vitro*, their chemotactic activity towards recombinant macrophage inflammatory protein (MIP)-2 could be tested in the presence of CM of PnD using migration assay chambers (Li et al., 2005). To study whether PnD induce neutrophil-like N2-type polarization in an inflammatory environment, a trans-well system is used under stimulation of neutrophils with pro-inflammatory LPS. In these *in vitro* systems, two different cell models of neutrophils can be used, neutrophils freshly isolated from human blood, and the human leukemia cell line (HL-60) that is an incomplete differentiated cell line that must undergo differentiation to become functional neutrophils (Babatunde et al., 2021), HL-60 cells differentiate into neutrophils with DMSO, and subsequent stimulation with LPS induces a polarized N1 phenotype. qPCR and Western blot are used to determine the neutrophil surface molecules associated with a polarized N2-phenotype as well as the levels of secreted pro-inflammatory and anti-inflammatory factors (Wang et al., 2020). Furthermore, PnD also have direct effects on major functions of neutrophils. Co-culture of freshly isolated human blood neutrophils with PnD can serve to demonstrate the increased phagocytic capacity of neutrophils and, at the same time, their decreased oxidative burst capacity as another method to validate the anti-inflammatory function of PnD (Magatti et al., 2018; Alipour et al., 2020). However, there are not many studies addressing the anti-inflammatory role of PnD on neutrophils despite the increasing evidence revealing unsuspected roles of neutrophils in many physiological and pathological processes (Nicolas-Avila et al., 2017), and more studies are needed.

As part of the anti-inflammatory effects of PnD, the inhibition of the differentiation and maturation of monocytes to dendritic cells (DC) has been reported. Monocytes isolated from peripheral blood are differentiated to immature dendritic cells (iDC) in the presence of IL-4 and GM-CSF, and iDCs develop into mature dendritic cells (mDC) in the presence of LPS. Both processes are inhibited by PnD, by direct or indirect contact with the DC using a transwell culture system, or by the addition of CM of PnD (Magatti et al., 2009; Croxatto et al., 2014; Abomaray et al., 2015). Furthermore, PnD induce the switch to an anti-inflammatory phenotype in both iDC and mDC. This change can be measured by flow cytometry, observing a decrease in the expression of co-stimulatory molecules (CD40, CD80, CD83 and CD86) and an increase in the expression of co-inhibitory molecules (B7H3, B7H4, CD273, CD274), and of the immunosuppressive enzyme IDO (Abomaray et al., 2015). Likewise, PnD block the production of pro-inflammatory cytokines by iDC and mDC such as TNF, IL-6, IL-12 and IL-23, IFNγ, C-X-C motif chemokine ligand 10 (CXCL10), CXCL9 and chemokine C-C motif ligand (CCL5) while the secretion of IL-10 is increased, as determined in cell culture supernatants using the ELISA assay (Magatti et al., 2009; Abomaray et al., 2015; Magatti et al., 2015). Phagocytic activity of iDC is essential for the elimination of the cellular components released after a tissue injury, which -if accumulated- would cause inflammation. Phagocytic activity of iDC is induced by PnD and can be determined by CytoSelect™ phagocytosis functional assay (Abomaray et al., 2015). DC are antigen presenting cells capable of inducing an efficient T cell response to specific antigens, being an important mediator of the innate and adaptive immune response. To directly determine the impact of DC co-cultured with PnD on T-cell proliferation, a mixed lymphocyte reaction (MLR) is used, and T cell proliferation can be quantified by ^{3}H thymidine uptake (Croxatto et al., 2014; Magatti et al., 2015; Talwadekar et al., 2015). Then, PnD induce an anti-inflammatory phenotype on DC which will down-regulate the activity and proliferation of T cells, presenting *in vitro* evidence of their role in modulating the immune response in immunological diseases.

In most of these studies, monocytes are isolated from human PBMC, and only few of them used an established cell line model. Although it is well known that the composition of human PBMC depend on the donor's physiological status and its use supposes a high variability across donors (Kleiveland, 2015), they are the gold standard tool for isolating monocytes to investigate the role of immune cells in inflammatory diseases. However, although monocyte-like cells do not fully replicate the genotypic and phenotypic properties of human peripheral blood monocytes (Riddy et al., 2018), they represent a simplified surrogate and readily available cell model, especially when human blood is not available, which makes them a valuable and convenient model for repeated testing.

Natural killer cells (NK cells) are large granular lymphocytes with cytotoxic activity against injured cells, and their activation results in the secretion of pro-inflammatory cytokines, suggesting that NK cells can either drive inflammation or restrain adaptive immune responses to prevent excessive inflammation or even autoimmunity (Brandstadter and Yang, 2011; Zitti and Bryceson, 2018; Moloudizargari et al., 2021). Analysis of cellular crosstalk between PnD and NK cells has yielded contradictory results probably due to either the different origin of PnD and the different microenvironmental conditions to which the cells are exposed during pregnancy (Abumaree et al., 2019) or due to different PnD:NK and NK/tumor cells ratios used in each study (Moloudizargari et al., 2021), or to the different cell type used for cytotoxicity testing (Boissel et al., 2008). Despite this, it is valuable to know how PnD interact with NK cells in culture. It is possible to determine whether the coculture modulates NK cell proliferation, NK-activated receptor expression (NKp30, NKp44, NKp46, NKG2D, and CD69) and/or NK cell cytotoxicity on tumor cell lines (Chatterjee et al., 2014; Croxatto et al., 2014; Li et al., 2015). Furthermore, the profile of cytokine production by NK cells may be affected by coculture with PnD resulting in changes in the expression of pro-inflammatory molecules that can be measured by RT-PCR and/or ELISA assay (Li et al., 2015; Abumaree et al., 2019).

Furthermore, the suppressive activity of PnD can be measured by their release of anti-inflammatory molecules such as IL-10 and prostaglandin E2 (PGE2) when cocultured with NK cells (Chatterjee et al., 2014; Li et al., 2015). Interestingly, IL-2 preactivated NK cells exert cytotoxic effects on PnD despite expressing high levels of HLA-I, whereas nonactivated NK cells did not lyse the PnD, suggesting that an inflammatory environment is necessary for the NK cytolytic activity against PnD (Abumaree et al., 2018; Abumaree et al., 2019).

2.1.2 Assessment of PnD effects on the adaptative immune response

PnD have anti-inflammatory properties acting on the adaptive response and these are measured as their ability to inhibit the proliferation and cytokine production of T lymphocytes as well as their ability to modulate T cell differentiation. The anti-inflammatory properties of PnD can be studied using *in vitro* models of inflammatory diseases, such as ocular allergic inflammation (Solomon et al., 2005), inflammation of human middle ear epithelial cells (HMEEC) by airway pollutants (Kim et al., 2019; Kim et al., 2020), atopic dermatitis (Kim et al., 2020) or demyelinating diseases (Bravo et al., 2016). The anti-inflammatory effects of PnD after co-culture can be analyzed by fibroblast proliferation measured with the [^{3}H]-thymidine incorporation assay (Solomon et al., 2005) or T cell proliferation measured by the MTT assay (Bravo et al., 2016). The inhibitory effects can be analyzed by RT-PCR and ELISA showing the down-regulation of inflammatory cytokines released by fibroblasts, such Trasnforming Growth Factor (TGF)-β1, GM-CSF, IL-8, IL6, TNF, IL1β, and thymus as well as activation-regulated chemokines (TARC) (Solomon et al., 2005; Kim et al., 2019; Kim et al., 2020) or down-regulation of the inflammatory cytokine IL17 released by T cells (Bravo et al., 2016). In addition, the levels of PnD-expressed anti-inflammatory genes in these inflammatory systems, such as PGE2, TGFβ, and Vascular Endothelial Growth Factor (VEGF), can also be measured (Kim et al., 2019).

As described throughout this chapter, the anti-inflammatory potential of PnD is primarily assessed by determining self-secreted cytokines, as well as the production of pro- and anti-inflammatory cytokines by immune cells. ELISA and flow cytometry are the most widely used and best validated methods to measure cytokines and other inflammatory mediators. However, these methods are time-consuming, require a long sample preparation time, and do not allow the measurements of multiple cytokines at the same time in the same sample and in real-time. Recently, multiplex arrays (Luminex-based) have been developed from traditional ELISAs which allows the measurement of multiple cytokines in the same sample at the same time, and using only a small volume (Leng et al., 2008). Other commonly used immunoassays include Meso Scale Discovery (MSD), cytometric bead array (CBA), time-resolved fluorescence resonance energy transfer (TR-FRET), AlphaLISA, and FirePlex which have different sensitivities and multiplexing capabilities (Platchek et al., 2020). These technologies could represent more reliable and simpler strategies to assess the effect of PnD on immune cells.

2.2 PnD effects on inflammation and the vascular function

Among PnD, endothelial cells derived from the placenta (hP-EC) and umbilical cord, such as HUVEC represent a precious easy access *ex vivo* model of the human vasculature (Silini et al., 2020). HUVEC applications range from cardiovascular to metabolic as well as wound healing and angiogenesis-related diseases (Medina-Leyte et al., 2020). In addition, Gestational Diabetes (GD)-HUVEC exposed *in vivo* even transiently (during pregnancy) to hyperglycemia, exhibit some epigenetics modifications leading to a durable pro-inflammatory phenotype (Di Fulvio et al., 2014; Di Pietrantonio et al., 2021). HUVEC have been used to study the pro- and anti-atherogenic effect of several molecules in the early stages of atherosclerosis (Di Tomo et al., 2015; Di Pietro et al., 2020). Therefore, they represent a valuable *in vitro* model to assess the role of PnD in the above diseases through the following functional assays.

Due to a pro-oxidant state of Gestational Diabetes (GD)-HUVEC can be stimulated with an oxidative stress agent and compared to control HUVEC. $O2^-$ production and intracellular accumulation of reactive oxygen species (ROS) are measured to assess the antioxidant effect of PnD. While these methods allow to assess the general oxidative status, more integrative approaches evaluating potential antioxidant effects with higher sensitivity as well as the identification of permanent markers of oxidative stress are required (Pipino et al., 2020). Therefore, the levels of DNA/RNA damage, lipid peroxidation, and protein oxidation/nitration such as nitrotyrosine expression associated with impaired vascular nitric oxide (NO) secretion and availability may give a more reliable scenario regarding alteration of the oxidative balance (Di Fulvio et al., 2014; Alshabibi et al., 2018; Di Pietrantonio et al., 2021).

In endothelial dysfunction, the early stage of atherogenesis, there is a close interaction between oxidative stress and inflammation. Increased monocyte adhesion to the endothelium is among the mechanisms predisposing to endothelial dysfunction, the early predictor of plaque formation and atherosclerosis. The Monocyte-HUVEC Adhesion Assay can be performed in C- and GD-HUVEC in the basal state and after incubation with PnD before stimulation with an inflammatory stimulus such as low doses of TNF. Subsequently, cells from the monocytic cell line U937 are added to evaluate their adhesion to HUVEC monolayers (Di Tomo et al., 2015). Moreover, by qPCR and western blot/flow cytometry any inflammation-related gene and protein, such as

Vascular Cell Adhesion Molecule 1 (VCAM-1) and Intercellular Adhesion Molecule 1 (ICAM-1), can be evaluated. Indeed, it is noteworthy that the level of these adhesion molecules increases during inflammation. More importantly, VCAM-1 and ICAM-1 membrane exposure, the main mechanism behind the interaction between monocytes and endothelial cells, can be analyzed by flow cytometry (Di Tomo et al., 2015).

Furthermore, it is accepted that impaired NO synthesis and/or its availability in HUVEC may result in endothelial dysfunction (Pandolfi and De Filippis, 2007). To assess NO bioavailability, the intracellular cGMP level, a biological target of NO activity, is mainly evaluated by using a commercial enzyme immunoassay (EIA) kit (Di Pietro et al., 2020). It has been demonstrated that HUVEC chronically exposed to high glucose and inflammation, as well as treated with the proinflammatory stimulus TNF-α, display decreased levels of cGMP (Ucci et al., 2019) Therefore, this assay is useful to assess the role of PnD in changes of NO bioavailability, which is involved in the modulation of the Nuclear Factor kappa-light-chain-enhancer of activated B cells (NF-κB) nuclear translocation, relevant to further evaluate the potential ability of PnD in inhibiting the inflammatory pathway (Ucci et al., 2019). However, accurate NO detection and quantification are critical to understanding health and disease. Consequently, more than one of the aforementioned assays should be performed for a clear comprehension of anti-inflammatory PnD effects.

Although these assays are widely used for reproducible determinations, the results obtained may be partially affected by the passage number and donor variability of endothelial cells. To overcome these issues, experiments may be performed on multiple endothelial cell strains or immortalized endothelial cells, showing a more uniform response.

Moreover, in some inflammatory diseases, the release of several pro-inflammatory chemokines may inhibit neovascularization. The capability of PnD to regulate the chemokine environment by inhibiting the pro-inflammatory chemokines and/or by increasing the pro-angiogenic ones, may enhance new vessel formation. The most conventional way of assessing PnD' capacity in decreasing inflammation while improving endothelial cell network-like structures is the Matrigel tube formation assay (Ma et al., 2021; Nensat et al., 2021). This assay, together with the evaluation of cell migration through a scratch assay (Bernabe-Garcia et al., 2017), can be performed to assess the potential therapeutic efficacy of PnD in angiogenesis-related disease, such as diabetic foot ulcers (Castellanos et al., 2017). Besides the rapid and easy well-established method and the comparably easy cell culture and measurement, this assay is only partially representative of real cell environments. Although many laboratories commonly use this method to obtain first evidence of angiogenic and antiangiogenic agents, some limitations may occur such as difficult in vessel quantification through a specific plugin of ImageJ software as well as standardization due to Matrigel lot-to-lot variability (Nowak-Sliwinska et al., 2018). The latter may be prevented by selecting a specific lot with preferred protein and endotoxin concentrations.

Overall, all the HUVEC assays mentioned here were recently published in a study performed to assess the anti-inflammatory and pro-angiogenic role of hAM in GD-HUVEC. The results obtained strongly elucidate the mechanisms through which hAM can affect inflammation, migration, and angiogenesis thus providing additional validation for ongoing clinical trials in diabetic foot ulcer (Pipino et al., 2022).

In addition, to overcome limitations of 2D cell culture assays, HUVEC can be used *in vitro* to create 3D spheroid structures for functional screening purposes (Kocherova et al., 2019) or blood vessel tissue engineering (Moby et al., 2007; Paternotte et al., 2013). Finally, endothelial cells and the anti-inflammatory influence of PnD can also be analyzed even more physiologically under shear stress conditions in dedicated flow chambers with a computer-guided pump system and video microscopy (Zantl and Horn, 2011; Munir et al., 2015). However, all these methods do not acknowledge the multicellularity in the perivascular microenvironment. An *in vitro* solution to this problem would be vascularized spheroids or organoids which are currently under investigation.

2.3 PnD effects on cutaneous wound healing

Substantial evidence from several clinical trials shows how the application of hAM or other PnD on wounds and ulcers of diverse etiology has proven to be of benefit (Colocho et al., 1974; Singh et al., 2004; Hasegawa et al., 2007; Mermet et al., 2007; Silini et al., 2015). Additionally, a combination of PnD or even extra-cellular vesicles from PnD have been used for chronic wounds (Bakhtyar et al., 2018; Hashemi et al., 2019). All that evidence makes hAM and derived products the most researched so far in terms of wound healing treatment. Nevertheless, to fully understand the capabilities of hAM and other PnD to promote wound healing, several *in vitro* systems have been developed. Most chronic wounds show decreased proliferation and migration, mainly affecting keratinocytes, but also fibroblasts and endothelial cells. In consequence, those experimental settings mainly focus on evaluating the pro-proliferative, pro-migratory and pro-angiogenic effects that hAM or other PnD may have.

In addition, *in vivo* wound healing assays using animal models constitute an integrative benchmark in which PnD′ effects on inflammation and the immune component, such as angiogenesis and dermal as well as epidermal cell migration and proliferation, have to cooperate to show real functional effectiveness. The application of human PnD in animal studies of cutaneous wound healing was extensively reviewed

TABLE 1 Functional tests on perinatal cells.

Perinatal cells

PnD Cell type	Functional *in vitro* tests	Outcome	Reference
hAFSC	Establishment of skin equivalent	hAFSC differentiated into keratinocytes expressing K5, K14, K10, and involucrin after 30 days of culture in a keratinocyte-inducing medium and formed a complete pluristratified skin epithelium under air-liquid culture conditions on a collagen matrix with integrated HDF.	(Sun et al., 2015)
hAMSC	Cell adhesion on a scaffold	hAMSC were grown on Matriderm and PCL/PLA scaffolds. PCL/PLA yielded a higher number of attached cells and more favorable growing conditions for hAMSC than Matriderm.	(Vonbrunn et al., 2020)
hUC-MSC	(i) Cell proliferation assay (ii) Scratch wound assay	c-Jun silencing in hUC-MSC inhibited (i) cell proliferation and (ii) migration, while c-Jun overexpression enhanced proliferation but not migration of hUC-MSC.	(Yue et al., 2020)
	Cell differentiation assay	hUC-MSC were transfected with a lentivirus expressing HOXA4 and cultured for 21 days. Expression of the epidermal cell-specific markers, cytokeratins 14 and 18, was detected by immunohistochemistry and flow cytometry.	(He et al., 2015)
	Establishment of skin equivalent	hUC-MSC were seeded on the surface of fibrin gel scaffolds and cultured for 7–10 days. The established equivalent resembled the normal skin architecture.	(Montanucci et al., 2017)
	(i) Cell proliferation assay (ii) Cell viability assay (iii) Scratch wound assay	(i-iii) SAP improved the survival, proliferation, and migration of the hUC-MSC encapsulated in Pluronic F-127 hydrogel (drug delivery scaffold).	(Deng et al., 2020)
	(i) Cell proliferation (ii) Cell viability assay (iii) Cell adhesion on a scaffold	(i, ii) Activation of the Wnt signaling pathway promoted survival of hUC-MSC (proliferation, viability) seeded on a CCLDADM scaffold. (iii) Cells attached and grew uniformly when seeded onto the CCLDADM scaffold.	(Han et al., 2019)
	(i) Cell proliferation assay (ii) Scratch wound assay (iii) Tube formation assay	455-nm blue light exposure effectively promoted (i) proliferation, (ii) migration, and (iii) tube formation of HUVEC co-cultured with hUC-MSC.	(Yang et al., 2019)
	Chemotaxis assay	hUC-MSC seeded in 3D alginate gel gradually migrated from the top to the bottom of the gel, but could not migrate out from the gel during 7 days of observation.	(Wang et al., 2016b)
	Soft agar tumorigenicity test	Even after repeated passaging the cells have not acquired tumor formation capabilities.	(Sabapathy et al., 2014)
a) hUC-MSC b) hU-MSC-End	(i) Cell proliferation assay (ii) Chemotaxis assay (iii) CAM assay	hUC-MSC-End showed increased (i) proliferation, (ii) migration and (iii) vasculogenesis compared to hUC-MSC.	(Kaushik and Das, 2019)
hPMSC	Transwell co-culture assay Chemotaxis assay	Co-culturing of hPMSC with HDF inhibited LPS-induced activation of NF-κB signal in HDF. hPMSC expressing PDGFR-β exhibited enhanced chemotactic migration compared to hPMSC without expressing PDGFR-β.	(Wang et al., 2016a) (Wang et al., 2018)
a) hAEC b) hUC-MSC	Cell differentiation assay	hAEC and hUC-MSC were able to differentiate into keratinocytes and fibroblasts, respectively, after 15 days of culturing in an inducing medium. This was shown by the expression of various specific markers by immunolabeling and RT-PCR.	(Mahmood et al., 2019)

Abbreviations: CCLDADM: collagen–chitosan laser drilling acellular dermal matrix, hAEC: human amniotic membrane epithelial cells, hAFSC: human amniotic fluid stem cells, hAMSC: human amniotic membrane mesenchymal stromal cells, HDF: human dermal fibroblasts, hPMSC: human placenta mesenchymal stromal cells, hUC-MSC: human umbilical cord mesenchymal stromal cells, hU-MSC-End: human umbilical cord mesenchymal stromal cells -endothelial transdifferentiated, HUVEC: human umbilical cord vein endothelial cells, LPS: lipopolysaccharides, NF-κB: nuclear factor kappa-light-chain-enhancer of activated B-cells, PCL/PLA: Poly(caprolactone)/poly(L-lactide), PDGFR-β: platelet derived growth factor receptor β, SAP: sodium ascorbyl phosphate.

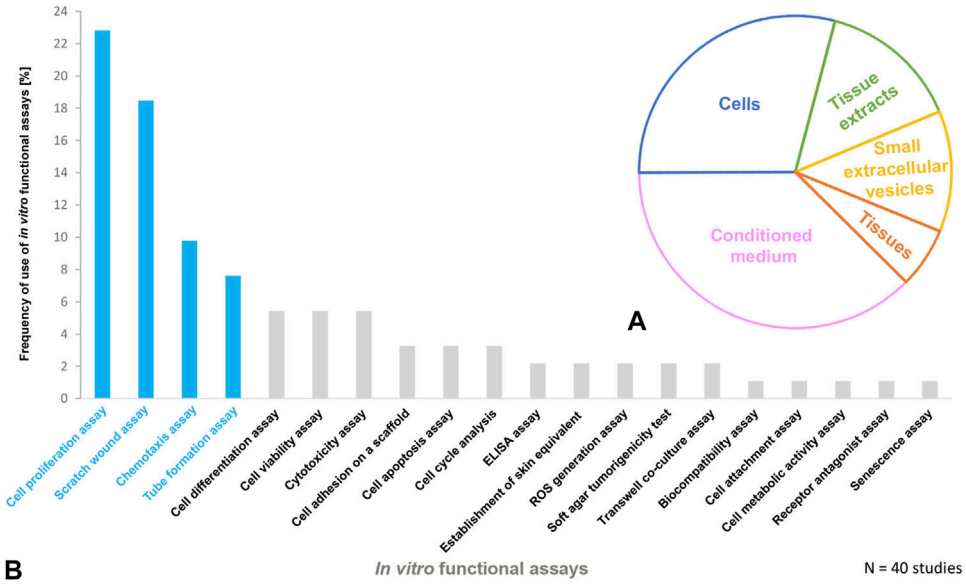

FIGURE 1
Perinatal derivatives and *in vitro* functional assays used for cutaneous wound healing in animals **(A)** The schematic presentation of PnD functionally tested *in vitro* and **(B)** frequency of use of *in vitro* functional assays in animal studies of cutaneous wound healing. The most frequently used functional assays are highlighted in blue.

by Pichlsberger et al. (Pichlsberger et al., 2021). In approximately 50% of the included studies (Pichlsberger et al., 2021) the PnD were functionally tested *in vitro* before they were applied to animal wounds. Herein we focus on the *in vitro* functional assays used in these studies. The outcome of these *in vitro* assays, the types and combinations of the PnD applied as well as the references are outlined in detail in Tables 1–5. As naming and abbreviations of the PnD types in the reviewed studies varied due to the authors' discretion, we harmonized terms according to the recently published consensus nomenclature for PnD to improve the comparability of data (Silini et al., 2020). Among the included studies, the majority of the *in vitro* tested PnD were cells (38%) mainly MSC isolated from the umbilical cord, amnion, amniotic fluid, placenta, but also cells derived from the amniotic fluid, and the amniotic epithelium. Further functional tests were performed on cellular secretomes (29%), followed by cell-derived small extracellular vesicles (sEVs, 15%) derived from MSC of the umbilical cord or decidua, tissue extracts (13%) and tissue membranes (amnion or amnion/chorion, 6%) (Figure 1A). We did not discriminate between the different subtypes of extracellular vesicles (EV) including exosomes etc., but chose the term sEVs instead, according to the recommendations of the International Society for Extracellular Vesicles to use an operational term for EV subtypes unless their endosomal origin was proven (Van Deun et al., 2017; Thery et al., 2018). Overall, these studies used twenty different functional assays to evaluate PnD *in vitro* (**Figure 1B**). The most frequently performed functional assays were: 1) cell proliferation assay, 2) scratch wound assay, 3) chemotaxis assay and 4) angiogenesis assays. These assays are considered the gold standard for the evaluation of wound healing *in vitro* since they analyze important processes that occur during wound healing, such as proliferation and migration of the cells at the wound edges and the re-epithelialization of the wound surface.

From the pathological point of view, an important limiting factor for wound healing could be the development of an altered keratinocyte behavior (Raja et al., 2007). In that sense, many authors have measured the ability of amnion or other PnD in promoting keratinocyte migration in *vitro*. Next to the well-known Boyden chamber migration assay (Mcquilling et al., 2019), the wound healing scratch assay is frequently used. By design, based on measuring the gap generated by mechanically tearing a cultured cell monolayer, the scratch assay allows for easy monitoring and quantification of cell migration and wound closure (Liarte et al.,

TABLE 2 Functional tests on perinatal cell-conditioned medium (CM) alone or compared to/or combined with perinatal cells.

Perinatal cell-conditioned medium (CM)

PnD	Functional *in vitro* tests	Outcome	Reference
hAEC-CM	scratch wound assay	hAEC-CM substantially accelerated the migration of HDF.	(Jin et al., 2016)
hPMSC-CM	(i) Cell proliferation assay (ii) Scratch wound assay	Hypoxic hPMSC-CM inhibited the (i) proliferation and (ii) migration of HDF compared to normal medium and normoxic CM.	(Du et al., 2016)
hUC-MSC-CM	(i) Cell cycle analysis (ii) Cell differentiation assay (iii) Cell proliferation assay	(i) hUC-MSC-CM caused a G0/G1-phase cell cycle arrest of HUVEC. (ii) HUVEC treated with hUC-MSC-CM had a significantly down-regulated expression of genes for IFN, TNF, IL-1, and IL-6, while the key genes involved with angiogenesis (VEGF, EGF, bFGF, and KDR) were up-regulated. (iii) hUC-MSC-CM significantly increased the proliferation of HUVEC.	(Sun et al., 2019)
	Cytotoxicity assay	50 and 100% (*V*/V) concentrations of the hUC-MSC-CM had a cytotoxic effect on HDF, contrary to 25% CM.	(Sabzevari et al., 2020)
hAMSC-CM	(i) Scratch wound assay (ii) Tube formation test	(i) hAMSC-CM significantly increased the migration rate of HDF and HUVEC. (ii) HUVEC treated with hAMSC-CM formed significantly longer tubes compared to untreated controls.	(Kim et al., 2012b)

Perinatal cell-conditioned medium (CM) compared to / or combined with perinatal cells

PnD	Functional in vitro tests	Outcome	Reference
a) hAMSC b) hAMSC-CM	(i) Cell apoptosis assay (ii) Cell proliferation assay (iii) Scratch wound assay (iv) Soft agar tumorigenicity test (v) Tube formation assay	hAMSC and hAMSC-CM (i) inhibited heat stress-induced apoptosis in HaCAT cells and HDF through activation of PI3K/AKT signaling and (ii) promoted their proliferation by activating GSK3β/β-catenin signaling. (iii) Higher HaCAT and HDF cell migration was observed in the presence of hAMSC and hAMSC-CM as compared to the control medium. (iv) hAMSC did not display tumorigenicity *in vitro*. (v) hAMSC-CM promoted HUVEC tube formation.	(Li et al., 2019)
a) hUC-MSC b) hUC-MSC-CM	(i) Chemotaxis assays (ii) Scratch wound assay (iii) Transwell co-culture assay (iv) Tube formation assay	(i,ii, iv) Raw264.7 macrophages activated by hUC-MSC-CM enhanced chemotaxis, migration and angiogenesis of HUVEC with diabetic dysfunction. (iii) hUC-MSC and hUC-MSC-CM are capable of switching macrophages from the M1 phenotype to the M2 phenotype. The action of hUC-MSC-CM on macrophages or endothelial cells was inhibited by neutralizing antibodies against PGE2 or by the inhibition of PGE2 secretion from hUC-MSC.	(Zhang et al., 2020)
	(i) Cell metabolic activity assay (ii) Cell adhesion on a scaffold (iii) Tube formation test (iv) CAM assay	(i, ii) hUC-MSC seeded on scaffolds maintained higher metabolic activity than adipose tissue MSC during 48 h serum starvation. (iii, iv) hUC-MSC-CM promoted angiogenesis.	(Edwards et al., 2014)

(Continued on following page)

TABLE 2 (*Continued*) Functional tests on perinatal cell-conditioned medium (CM) alone or compared to/or combined with perinatal cells.

Perinatal cell-conditioned medium (CM) compared to / or combined with perinatal cells

PnD	Functional in vitro tests	Outcome	Reference
a) hAEC-CM	(i) Cell cycle analysis	(ii) hAEC-CM accelerated the migration and proliferation of keratinocytes and induced increased activity of phospho-ERK, phospho-JNK, and phospho-AKT. The blockade of phospho-AKT inhibited migration induced by hAEC-CM. (i, iii) Coculturing of keratinocytes with hAEC promoted keratinocyte proliferation by up-regulation of Cyclin D1, Cyclin D3 and Mdm2.	(Zhao et al., 2016)
b) hAEC	(ii) Scratch wound assay		
	(iii) Transwell co-culture assay		

Abbreviations: bFGF: basic fibroblast growth factor, CAM: chick chorio allantoic membrane, CM: conditioned medium derived from hAEC, hAMSC, hPMSC, hUC-MSC, hUC-MSC-End, EGF: epidermal growth factor, HaCAT: immortalized human keratinocytes, hAEC: human amniotic membrane epithelial cells, hAMSC: human amniotic membrane mesenchymal stromal cells, HDF: human dermal fibroblasts hPMSC: human placenta mesenchymal stromal cells, hUC-MSC: human umbilical cord mesenchymal stromal cells, hU-MSC-End: human umbilical cord mesenchymal stromal cells-endothelial transdifferentiated, HUVEC: human umbilical cord vein endothelial cells, IL-1, IL-6: interleukin-1, -6, KDR: kinase insert domain receptor, PGE2: prostaglandin E2, TNF: tumor necrosis factor, VEGF: vascular endothelial cell growth factor. Perinatal cell-conditioned medium (CM).

2018). The unique advantage of this assay is the fact that cells at the wound edge can be studied microscopically at any time, allowing for the characterization of distinct morphology and topological changes in living cultures, along with the precise detection of the expression of key factors involved in wound healing on fixed cultures (Bernabe-Garcia et al., 2017). Of note, the wound healing scratch assay can be applied on almost any cell line growing in monolayers. For instance, in the specific case of skin wounds, most of the preclinical experience with amnion and other PnD is based on the effects of well stablished human keratinocyte cell lines, such as the spontaneously transformed aneuploid immortal human cell line HaCaT (Boukamp et al., 1988). However, several reports also apply the scratch method onto human fibroblasts (Bakhtyar et al., 2018; Rahman et al., 2019). In the case of keratinocytes, HaCaT offers unparalleled characteristics by being phenotypically similar to primary keratinocytes, while still allowing routine culture procedures (Boukamp et al., 1988). Numerous papers show that HaCaT keratinocytes had not only allowed to certify the benefits of amnion on migration (Alcaraz et al., 2015; Kitala et al., 2019; Rahman et al., 2019) but also to understand how amnion treatment effects appear to be restricted to the edge of the artificial wound *in vitro* (Ruiz-Canada et al., 2018). These results support the notion that migration effects of amnion are not systemic, but local. This is in line with clinical observations that the effects of amnion treatment of human patients' wounds were limited to the wound edge (Insausti et al., 2010). Moreover, the HaCaT scratch assay in combination with immunological methods allows for the precise detection of key proteins participating in the migration machinery, such as Paxilline H, demonstrating that among its effects, amnion treatment triggers focal adhesion molecule rearrangement in cells at the very edge of the wound and is thus promoting local cell migration (Bernabe-Garcia et al., 2017). Altogether, the possibilities provided by the wound healing scratch assay offer uncontested capacity to obtain high quality data in a comprehensive manner, opening opportunity for precise correlations between what is macroscopically observed in the chronic wounds and the behavior of cells observed *in vitro*, as shown for the HaCaT cells, (Ruiz-Canada et al., 2021).

A proper development of the underlying dermal tissue is a prerequisite for keratinocyte proliferation as an important limiting factor for correct healing and wound closure. Therefore, fibroblast and endothelial cell proliferation also needs to be assessed. Using different methodologies, from image analysis to comparative cell counting, including cell cycle analysis and cell suspension absorbance determination, numerous papers evaluate the effects of amnion treatment and coincide in finding positive effects on keratinocyte and fibroblast proliferation (Alcaraz et al., 2015; Murphy et al., 2017; Kitala et al., 2019; Rahman et al., 2019).

In contrast, comparably little is known about the effects of amnion or other PnD on endothelial cell proliferation. However, studies assessing this component mostly apply methods based on the analysis of *in vitro* tube formation and branching by endothelial cells in culture (Hu et al., 2018; Bullard et al., 2019). Tube formation assay, an *in vitro* angiogenesis assay, is often used in wound healing experiment designs since the formation of new vessels significantly contributes to tissue recovery. The 3D-tube formation assay on gelled basement membrane extract is a powerful *in vitro* technique for evaluating angiogenesis. This assay involves endothelial cell adhesion, migration, protease activity, and tube formation (Arnaoutova and Kleinman, 2010). Also, 2D co-culture models are meaningful assays to evaluate the functionality of the respective PnD type. For example, endothelial cells showed a significantly increased formation of vessel-like structures in direct co-culture with MSC derived from placental blood vessels as compared to human amniotic membrane mesenchymal stromal cells

TABLE 3 Functional tests on Perinatal cell-derived small extracellular vesicles (sEV) alone or compared to perinatal cell-conditioned medium (CM).

Perinatal cell-derived small extracellular vesicles (sEV)

PnD	Functional *in vitro* tests	Outcome	Reference
hUC-MSC-sEV	(i) Cell differentiation assay (ii) Cell proliferation assay	(i) hUC-MSC-sEV inhibited α-SMA and collagen I and III expression in HDF cultivated at high cell density. (ii) hUC-MSC-sEV restrict HaCaT and HDF proliferation at high cell densities, but promote cell proliferation at low densities.	(Zhang et al., 2016)
	(i) Cell proliferation assay (ii) Cytotoxicity assay (iii) Scratch assay (iv) Tube formation assay (v) Chemotaxis assay	hUC-MSC-sEV promoted the (i, ii) proliferation, (iii, v) migration, and (iv) tube formation of a HUVEC-derived cell line in a dose-dependent manner.	(Zhang et al., 2015)
	(i) Cell proliferation assay (ii) Chemotaxis assay (iii) Tube Formation Assay	hUC-MSC-sEV promoted (i) the proliferation, (ii) migration and (iii) tube-formation of HUVEC. hUC-MSC-sEV contained Ang-2, and treatment with hUC-MSC-sEV enhanced the expression of the Ang-2 in HUVEC through exosome-mediated Ang-2 transfer.	(Liu et al., 2021)

Perinatal cell-derived small extracellular vesicles (sEV) compared to perinatal cell-CM

PnD	Functional *in vitro* tests	Outcome	Reference
a) hUC-MSC-sEV	(i) Cell apoptosis assay	hUC-MSC-CM and hUC-MSC-sEV (i) decreased H_2O_2-induced cell apoptosis of HaCaT by inhibiting AIF and upregulating PARP-1 and poly ADP-ribose, (ii) increased HaCaT proliferation, in contrast to hUC-MSC-sEV-dp. (iii) hUC-MSC-CM improved the viability of HaCaT. (iv, vi) hUC-MSC-sEV and hUC-MSC-CM promoted cell migration relative to the hUC-MSC-sEV-dp. (vi) (v) ROS intensity in the hUC-MSC-sEV group and hUC-MSC-CM group was lower than in the control group.	(Zhao et al., 2020)
b) hUC-MSC-CM	(ii) Cell proliferation assay (iii) Cell viability assay (iv) Chemotaxis assay (v) ROS generation assay (vi) Scratch wound assay		
	(i) Cell proliferation assay (ii) Scratch wound assay	(i) hUC-MSC-sEV/Pluronic F-127 hydrogel promoted HUVEC proliferation better than hUC-MSC-sEV and hUC-MSC-CM. (ii) hUC-MSC-sEV and CM groups showed greater cell migration than the Pluronic F-127 hydrogel and control group. The hUC-MSC-sEV/Pluronic F-127 hydrogel group exhibited the best performance.	(Yang et al., 2020)
a) hDMSC-sEV b) hDMSC-CM	Cell cycle assay Cell differentiation assay Cell proliferation assay Scratch wound assay Senescence assay ROS generation assay	(i) hDMSC-sEV enhanced proliferation of HG aged HDF, (iv) increased their migration rate, (ii) promoted differentiation of HG-aged HDF into myofibroblasts (increased α-SMA and collagen I protein expression), (v) inhibited senescence associated β-galactosidase expression and (vi) inhibited ROS generation in HG aged HDF. hDMSC-CM improved (iii) proliferation and (iv) migration of HDF. The sEV blocker GW4869 reduced both effects, indicating that hDMSC-sEV in hDMSC-CM probably enhance the proliferation and migration abilities of HDF.	(Bian et al., 2020)

Abbreviations; Ang-2: angiopoietin-2, AIF: apoptosis-inducing factor, α-SMA: alpha-smooth muscle actin, CM: conditioned medium derived from hDMSC, hUC-MSC, HaCAT: immortalized human keratinocytes, HDF: human dermal fibroblast, hDMSC: human decidua mesenchymal stromal cells, HG: high glucose, hUC-MSC: human umbilical cord mesenchymal stromal cells, PARP-1: poly ADP, ribose polymerase 1, ROS: reactive oxygen species, sEV: small extracellular vesicles derived from hDMSC, hUC-MSC, sEV-dp: conditioned medium depleted from small extracellular vesicle. Perinatal cell-derived small extracellular vesicles (sEV).

TABLE 4 Functional tests on perinatal tissues.

Perinatal tissues

PnD	Functional *in vitro* tests	Outcome	Reference
Dehydrated hAM/chorion (EpiFix®)	(i) Cell proliferation assay (ii) Chemotaxis assay (iii) ELISA assay	(i) Dehydrated hAM/chorion extracts caused a dose-dependent increase in HDF proliferation. (ii) Dehydrated hAM/chorion tissue allografts promoted migration of hMSC. (iii) Growth factors such as EGF, bFGF and TGF-1 were able to elute from dehydrated hAM/chorion into the saline.	(Koob et al., 2013)
Dehydrated hAM/chorion (EpiFix®)	(i) Cell proliferation assay (ii) Chemotaxis assay (iii) ELISA assay	(i) Dehydrated hAM/chorion extract promoted HMVEC proliferation. (ii) Dehydrated hAM/chorion tissue recruited migration of HUVEC. (iii) Dehydrated hAM/chorion extract increased endogenous production of over 30 angiogenic factors by HMVEC, including GM-CSF, angiogenin, TGF-β3, and HB-EGF Heparin-binding EGF-like growth factor.	(Koob et al., 2014)
hAM	Cytotoxicity assay	Decellularized hAM enhanced the viability of hUC-MSC seeded onto the epithelial surface of hAM.	(Hashemi et al., 2020)

Abbreviations: bFGF: basic fibroblast growth factor, EGF: epidermal growth factor, GM-CSF: granulocyte macrophage colony-stimulating factor, hAM: human amniotic membrane, HB-EGF: Heparin-binding EGF-like growth factor, hMSC: human mesenchymal stromal cells, HMVEC: human microvascular endothelial cells, hUC-MSC: human umbilical cord mesenchymal stromal cells, TGF-1: transforming growth factor 1, TGF-β3: transforming growth factor β3.

(hAMSC) (Konig et al., 2015). The angiogenic properties of PnD were also evaluated by the chorioallantoic membrane (CAM) assay (Edwards et al., 2014; Rameshbabu et al., 2018; Kaushik and Das, 2019). The CAM assay is an intermediate step between *in vitro* and the *in vivo* models. It is minimally invasive to the chick embryo, and it is therefore a potential approach to refinement of animal experimentation (Moreno-Jimenez et al., 2016).

In the context of wound healing, the cell differentiation assay should also be a reasonable method of choice. However, it was not well represented in our dataset, with only 5% of studies investigating the ability of PnD to promote skin cell differentiation *in vitro*. The same is true for the cytotoxicity and viability assays, which would also be useful before the application of the PnD *in vivo* in preclinical and clinical studies.

In general, the PnD treatment showed favorable effects in terms of cutaneous wound healing since it promoted cell proliferation, migration, and differentiation of cells *in vitro* and showed no cytotoxic effects (Table 1, Table 2, Table 3, Table 4, Table 5). In this regard, the functional assays demonstrated considerable potency, since the results from the preclinical studies also show a promoting effect of PnD on cutaneous wound healing (Pichlsberger et al., 2021). Nevertheless, evaluating the potency of the *in vitro* functional assays turned out to be delicate as the PnD tested *in vitro* were often not the same as those applied *in vivo*. For example, in the same study the PnD-derived CM was functionally tested *in vitro*, but whole perinatal cells were applied to the animal wound (Kim et al., 2012a; Edwards et al., 2014; Jin et al., 2016). For the development of more effective PnD therapies, this will need to be considered in future studies.

2.4 Oral wound healing versus cutaneous wound healing

Special PnD, i.e. hAM, chorion and human Amnio-Chorionic Membrane (hACM) have been widely used for wound healing in oral reconstruction (Fenelon et al., 2018; Gulameabasse et al., 2020). For instance, hAM as a scaffold enhanced re-epithelialization of the oral cavity and reduced the contracture effects in moderate-sized defects (Lawson, 1985). The hAM has also been proven as useful biodegradable graft material for clinical vestibuloplasty. One week after the surgical intervention, epithelium started to migrate over the graft area from the margins, and the underlying connective tissue showed the formation of granulation tissue. The hAM completely degenerated after 3 weeks. Three months post intervention, epithelial tissue was restored and completely covered the graft area (Samandari et al., 2004). Measurement of blood flow to grafts used in vestibuloplasty revealed an increased blood flow to hAM grafts, whereas palatal grafts had a reduced blood flow during the same time period. Thus, angiogenesis was induced by hAM within 10–15 days, and the blood flow returned to normal by 30 days after surgery (Guler et al., 1997). These favorable effects of the hAM may be due to growth factors present in the amnion, such as basic Fibroblast Growth Factor (bFGF), Epidermal Growth Factor (EGF), TGFβ and IL-1 (Dadkhah Tehrani et al., 2020).

A corresponding animal study revealed that hAM transplanted on rabbit's gingival wound accelerated the formation of granulation tissue at day 10 by significantly increasing the number of both fibroblasts and blood vessels. Thus, hAM induced rapid epithelialization and both granulation

TABLE 5 Functional tests on perinatal tissue extracts alone or combined with conditioned medium (CM).

Perinatal tissue extracts

PnD	Functional *in vitro* tests	Outcome	Reference
hAM extract	(i) Cell apoptosis assay (ii) Cell proliferation assay (iii) Scratch wound assay	(i) Higher concentrations of hAM extract increased the percentage of apoptotic and necrotic HDF. (ii, iii) hAM extract promoted HDF proliferation and migration.	(Momeni et al., 2018)
Placental laminin	(i) Cell differentiation assay (ii) Cell viability assay (iii) Scratch wound assay (iv) Receptor antagonist assay	(i) Placental laminin purified from hP extract promoted neuronal differentiation of neuronal cell line PC12 (ii) Non-toxic concentration of placental laminin for PC12 cell treatment was determined (0.17 lg/ml). (iii) Placental laminin accelerated migration and motility of mouse embryonic fibroblasts. (iv) Blocking of integrin receptor retarded neurite outgrowth in laminin treated PC12 cells.	(Mukherjee et al., 2020)
a) hAM powder b) hAM powder + AV	(i) Biocompatibility assay (ii) Cell attachment assay (iii) Cell proliferation assay (iv) Scratch wound assay	(i) Heparinized human blood biocompatibility assay showed intact blood cells upon incubation with hAM powder or hAM powder + AV gel. (ii, iii) Media containing hAM powder + AV gel promoted HaCaT and HDF cell attachment and proliferation. (iv) hAM powder + AV significantly accelerated migration of HaCaT.	(Rahman et al., 2019)
Solubilized hAM	(i) Cell proliferation assay (ii) Cell viability assay	(i) hAM-hyaluronic acid hydrogel accelerated proliferation of HDF and keratinocytes compared to controls. (ii) Keratinocytes and HDF remained viable following hAM-hyaluronic acid hydrogel encapsulation.	(Murphy et al., 2017)
hWJ-ECM	(i) Cell proliferation assay (ii) Cytotoxicity assay	(i) The HDF cell line HSF-PI 18 attached to, infiltrated into and proliferated on hWJ-ECM scaffolds. (ii) hWJ-ECM was not cytotoxic.	(Beiki et al., 2017)
hWJ-ECM	(i) Cell differentiation assay (ii) Cell proliferation assay (iii) Cell viability assay (iv) Scratch wound assay	(i) hWJ-ECM promoted differentiation of HDF into myofibroblasts (confirmed by upregulation of α-SMA expression). (ii) hWJ-ECM treatment did not affect cell proliferation or (iii) cell viability of HDF. (iv) hWJ-ECM enhanced HDF migration.	(Bakhtyar et al., 2017)

Perinatal tissue extracts combined with conditioned medium

PnD	Functional *in vitro* tests	Outcome	Reference
a) hP–ECM b) hP-ECM-CM	(i) Cell apoptosis assay (ii) Cytotoxicity assay (iii) CAM Assay (iv) Scratch wound assay	(i) hP-ECM-silk fibroin scaffolds-CM had no detrimental effect on hEK, (ii) provided a non-cytotoxic environment for HDF, hEK and hAMSC to adhere, infiltrate and proliferate, (iii) and promoted vascularization. (iv) Scaffold-CM promoted the migration of HDF and hEK.	(Rameshbabu et al., 2018)

Abbreviations: α-SMA: alpha-smooth muscle actin, **AV**: aloe vera, **HaCaT**: immortalized human keratinocytes, **hAM**: human amniotic membrane, **hAMSC:** human amniotic mesenchymal stromal cells, **HDF:** human dermal fibroblasts, **hEK**: human epidermal keratinocytes, **hP**: human placenta, **hP-ECM**: human placenta extracellular matrix, **hUC-WJ-ECM**: human umbilical cord Wharton´s jelly extracellular matrix.

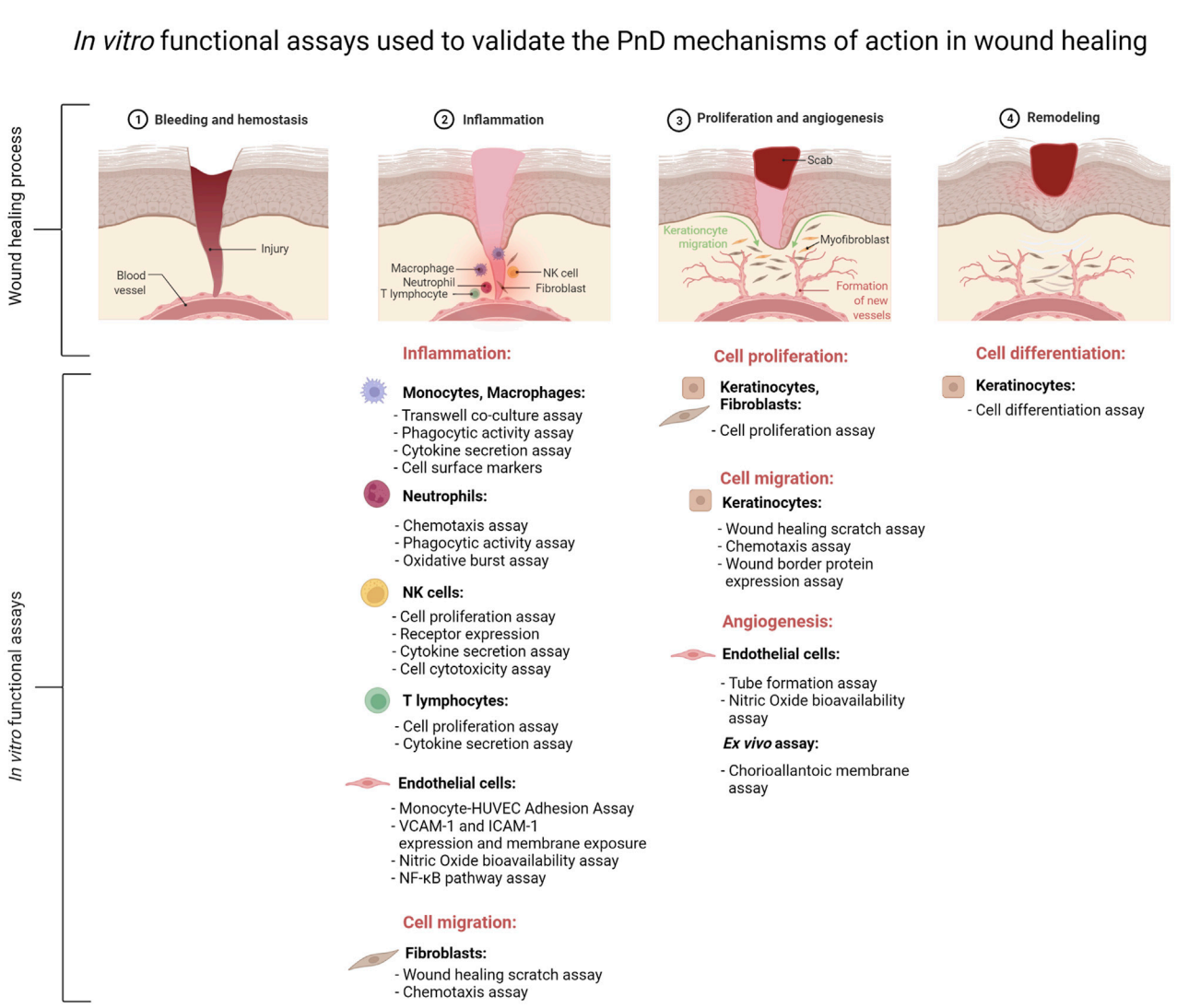

FIGURE 2
Schematic presentation of the major *in vitro* functional assays performed to validate the mechanisms of action of perinatal derivatives (PnD) in the context of inflammation, angiogenesis and remodeling during the complex process of wound healing. The figure was created using Biorender.com.

tissue and collagen formation, and suppressed inflammation i. e., the migration of polymorphonuclear cells at the wounded gingival site (Rinastiti et al., 2006).

In oral wound healing, the anti-adhesive properties of hAM in contact with healthy tissue are useful to prevent tissue adhesion in surgical procedures. The hAM transplant may function as an anatomical barrier towards fibrous tissue proliferation (Samandari et al., 2004; Fenelon et al., 2018), but further models are needed to improve understanding of this mechanism of action.

An interesting aspect in the context of wound healing is that oral wounds mainly heal without scarring. The keratinized *epidermis* of the skin shares some similarities with the oral mucosa, such as the stratified epithelium. In addition, also certain regions of the oral mucosa (gingiva, palate) show signs of keratinization, while the nonkeratinized floor of the mouth and buccal regions do not produce a stratum corneum (Wertz, 2021).

The main difference between skin and the keratinized regions of the oral mucosa is the relatively dry cutaneous surface, which is covered by the secretion products of sweat glands. Hair follicles can be found in most cutaneous regions except the palms and foot soles, and the apical surface is additionally covered by sebum. In contrast, the oral mucosa is constantly moist and well protected by the continuous secretion of mucous glands. The humid milieu may be one of the reasons that the healing of oral mucosal wounds is faster with minimal to no scar formation. There is a smaller inflammatory response with less neutrophils, macrophages, and

T-cell infiltration, and the proliferation and migration rate of keratinocytes from oral mucosa is much more rapid as compared to skin keratinocytes (Turabelidze et al., 2014).

During the healing period of adult skin wounds rapid angiogenesis occurs leading to many more capillaries than in normal tissue. Compared to that, healing wounds of oral mucosa have a reduced angiogenic network but are composed of more mature vessels providing better oxygenation. As inflammatory cells produce a variety of proangiogenic factors, it can be assumed that the selective reduction of inflammation and angiogenesis may help to prevent excessive scarring (Dipietro, 2016).

Covering wounds with various types of dressings may help to keep the wound area in a humid milieu that allows controlled regeneration processes without excessive scarring. Most current *in vitro* assays are performed under fluid conditions, where the cells are exposed to culture medium. Functional assays on cell cultures using air-liquid-interface (ALI) would be helpful to mimic physiologic conditions even more closely.

3 Summary and conclusion

In this review, we addressed studies in which PnD were functionally tested *in vitro* before being applied to pre-clinical or clinical care with respect to inflammation, angiogenesis and wound healing (Figure 2). We have focussed on the types and combinations of PnD and the functional assays used as well as on the outcomes of the *in vitro* assays.

Inflammation is a complex physiological mechanism involving different types of immune cells, protein mediators, and metabolites, making it difficult to study the role of PnD in inflammation *in vitro*. Our analysis indicates that most of the available assays to determine the ability of PnD to control inflammation study the interaction of different types of PnD with a single type of immune cells. These *in vitro* studies are mainly based on transwell co-cultures of PnD with immune cells, or treatment of immune cells with PnD CM, allowing to differentiate between cell-to-cell contact or paracrine signaling, respectively. The following functional assays are the most frequently used for evaluating immune cell activity: cell proliferation assay, cytokine secretion assay, surface markers expression indicative of acquisition of an anti-inflammatory phenotype, cytotoxicity and phagocytosis assay. Oxidative burst capacity is another assay that has been used to validate the anti-inflammatory role of PnD over neutrophils. All specialized phagocytes i.e., neutrophils and macrophages, have the capacity to generate the respiratory burst (Dahlgren et al., 2007), and this assay could be included as an *in vitro* functional test of the anti-inflammatory capacity of PnD over these other phagocytic cells. Moreover, the role of PnD on vascular inflammation can be assessed by means of several functional assays using HUVEC as a valuable *in vitro* model of human vasculature (Pipino et al., 2022).

Among the different functional assays available, the following four assay types are considered as the gold standard for assessing wound healing *in vitro*: the cell proliferation, the scratch wound, the chemotaxis, and the angiogenesis assay. Of note, *in vitro* models with characteristics closer to those cells in chronic wounds are needed to attain all the benefits of the application of PnD to non-healing ulcers (Liarte et al., 2020b). Indeed, while chronic wound fluids are known to be rich in proinflammatory cytokines, such as the anti-proliferative TGFß, it has been shown that AM can inhibit TGFß signaling, restoring keratinocyte proliferation and migration (Ruiz-Canada et al., 2018; Ruiz-Canada et al., 2021). Recently, HaCaT cells had been shown to represent a phenotype better resembling the state of keratinocytes in chronic wounds (Liarte et al., 2020a).

Inflammation, angiogenesis, and wound healing are thoroughly regulated processes that play an important role in tissue regeneration. If the balance of these regulatory mechanisms is disturbed, excessive inflammatory reactions, misguided angiogenesis, delayed wound healing or excessive scarring can occur. A promising therapeutic option is treatment with PnD. To understand the mode of action of PnD, various functional assays are carried out. Furthermore, there is a certain risk that the PnD sample may be of varying quality due to donor variability. Thus, functional assays are also important for checking the quality of the PnD compound prior to preclinical and clinical use.

As the gap between cell culture experiments and a complete organism is difficult to bridge, animal models are needed to resolve questions about toxicology or pharmacology. We strongly suggest that functional *in vitro* testing of PnD is routinely performed before their application to animal models and patients. This helps to minimize animal numbers in animal experimentation in line with the Replacement, Reduction, and Refinement (3R) principles for more ethical use of animals in research (Strech and Dirnagl, 2019) and to ensure the safety and efficacy of the PnD applied to patients.

The present review is in line with the aims of the COST SPRINT Action (CA17116) (Silini et al., 2020) and will contribute to the establishment of guidelines for methods applied to cells and tissues to enable scientifically sound and reproducible research data to promote PnD into clinics.

Author contributions

AF, CP, UJ, SL, FG, MEK, FN, AP, LT and IL-O wrote specific sections of the manuscript. UJ created the figures. IL-O and GE coordinated the work and compiled the manuscript. BG, MP, AP, OP and GE designed the concept of the manuscript. All authors contributed to revising and editing of the manuscript. All authors approved the manuscript in its present form.

Funding

This work contributes to the COST (Cooperation in Science and Technology) Action CA17116 International

Network for Translating Research on Perinatal Derivatives into Therapeutic Approaches (SPRINT), funded by the European Commission. This work was also supported by the Instituto de Salud Carlos III (ISCIII), Ministry of Economy, Industry, and Competitiveness, co-funded by the European Regional Development Fund, grant number PI18/01278 (to AIF), by the Slovenian Research Agency (J7-2,594, to MEK). And by the PON-MISE Sustainable Growth Funding-DD 27/09/2018 (grant 557 number: 21, ex 230, to AP) as well as by MIUR - PON AIM "Attraction and International Mobility" Linea 2 (Attrazione dei ricercatori), profilo 2.1 and Ministero della Sanità Programma di Ricerca Finalizzata 2019 (GR-2019-12369702, to CP).

Acknowledgments

This article contributes to the COST Action CA17116 "International Network for Translating Research on Perinatal Derivatives into Therapeutic Approaches (SPRINT)", supported by COST (European Cooperation in Science and Technology).

Conflict of interest

The authors declare that the research was conducted in the absence of any commercial or financial relationships that could be construed as a potential conflict of interest.

Publisher's note

All claims expressed in this article are solely those of the authors and do not necessarily represent those of their affiliated organizations, or those of the publisher, the editors and the reviewers. Any product that may be evaluated in this article, or claim that may be made by its manufacturer, is not guaranteed or endorsed by the publisher.

References

Abomaray, F. M., Al Jumah, M. A., Kalionis, B., AlAskar, A. S., Al Harthy, S., Jawdat, D., et al. (2015). Human chorionic villous mesenchymal stem cells modify the functions of human dendritic cells, and induce an anti-inflammatory phenotype in CD1+ dendritic cells. *Stem Cell Rev Rep* 11, 423–441. doi:10.1007/s12015-014-9562-8

Abumaree, M. H., Abomaray, F. M., Alshabibi, M. A., AlAskar, A. S., and Kalionis, B. (2017). Immunomodulatory properties of human placental mesenchymal stem/stromal cells. *Placenta* 59, 87–95. doi:10.1016/j.placenta.2017.04.003

Abumaree, M. H., Al Jumah, M. A., Kalionis, B., Jawdat, D., Al Khaldi, A., Abomaray, F. M., et al. (2013). Human placental mesenchymal stem cells (pMSCs) play a role as immune suppressive cells by shifting macrophage differentiation from inflammatory M1 to anti-inflammatory M2 macrophages. *Stem Cell Rev Rep* 9, 620–641. doi:10.1007/s12015-013-9455-2

Abumaree, M. H., Alshehri, N. A., Almotery, A., Al Subayyil, A. M., Bahattab, E., Abomaray, F. M., et al. (2019). Preconditioning human natural killer cells with chorionic villous mesenchymal stem cells stimulates their expression of inflammatory and anti-tumor molecules. *Stem Cell Res. Ther.* 10, 50. doi:10.1186/s13287-019-1153-9

Abumaree, M. H., Bahattab, E., Alsadoun, A., Al Dosaimani, A., Abomaray, F. M., Khatlani, T., et al. (2018). Characterization of the interaction between human decidua parietalis mesenchymal stem/stromal cells and natural killer cells. *Stem Cell Res. Ther.* 9, 102. doi:10.1186/s13287-018-0844-y

Alcaraz, A., Mrowiec, A., Insausti, C. L., Bernabé-García, A., García-Vizcaíno, E. M., López-Martínez, M. C., et al. (2015). Amniotic membrane modifies the genetic program induced by TGFss, stimulating keratinocyte proliferation and migration in chronic wounds. *PLoS One* 10, e0135324. doi:10.1371/journal.pone.0135324

Alipour, R., Motedayyen, H., Sereshki, N., Rafiee, M., Alsahebfosul, F., and Pourazar, A. (2020). Human amniotic epithelial cells affect the functions of neutrophils. *Ijsc* 13, 212–220. doi:10.15283/ijsc19155

Alshabibi, M. A., Khatlani, T., Abomaray, F. M., AlAskar, A. S., Kalionis, B., Messaoudi, S. A., et al. (2018). Human decidua basalis mesenchymal stem/stromal cells protect endothelial cell functions from oxidative stress induced by hydrogen peroxide and monocytes. *Stem Cell Res. Ther.* 9, 275. doi:10.1186/s13287-018-1021-z

Arnaoutova, I., and Kleinman, H. K. (2010). *In vitro* angiogenesis: Endothelial cell tube formation on gelled basement membrane extract. *Nat. Protoc.* 5, 628–635. doi:10.1038/nprot.2010.6

Babatunde, K. A., Wang, X., Hopke, A., Lannes, N., Mantel, P. Y., and Irimia, D. (2021). Chemotaxis and swarming in differentiated HL-60 neutrophil-like cells. *Sci. Rep.* 11, 778. doi:10.1038/s41598-020-78854-6

Bakhtyar, N., Jeschke, M. G., Herer, E., Sheikholeslam, M., and Amini-Nik, S. (2018). Exosomes from acellular Wharton's jelly of the human umbilical cord promotes skin wound healing. *Stem Cell Res. Ther.* 9, 193. doi:10.1186/s13287-018-0921-2

Bakhtyar, N., Jeschke, M. G., Mainville, L., Herer, E., and Amini-Nik, S. (2017). Acellular gelatinous material of human umbilical cord enhances wound healing: A candidate remedy for deficient wound healing. *Front. Physiol.* 8, 200. doi:10.3389/fphys.2017.00200

Beiki, B., Zeynali, B., and Seyedjafari, E. (2017). Fabrication of a three dimensional spongy scaffold using human Wharton's jelly derived extra cellular matrix for wound healing. *Mater. Sci. Eng. C* 78, 627–638. doi:10.1016/j.msec.2017.04.074

Bernabé-García, A., Liarte, S., Moraleda, J. M., Castellanos, G., and Nicolás, F. J. (2017). Amniotic membrane promotes focal adhesion remodeling to stimulate cell migration. *Sci. Rep.* 7, 15262. doi:10.1038/s41598-017-15509-z

Bian, X., Li, B., Yang, J., Ma, K., Sun, M., Zhang, C., et al. (2020). Regenerative and protective effects of dMSC-sEVs on high-glucose-induced senescent fibroblasts by suppressing RAGE pathway and activating Smad pathway. *Stem Cell Res. Ther.* 11, 166. doi:10.1186/s13287-020-01681-z

Boissel, L., Tuncer, H. H., Betancur, M., Wolfberg, A., and Klingemann, H. (2008). Umbilical cord mesenchymal stem cells increase expansion of cord blood natural killer cells. *Biol. Blood Marrow Transplant.* 14, 1031–1038. doi:10.1016/j.bbmt.2008.06.016

Boukamp, P., Petrussevska, R. T., Breitkreutz, D., Hornung, J., Markham, A., and Fusenig, N. E. (1988). Normal keratinization in a spontaneously immortalized aneuploid human keratinocyte cell line. *J. Cell Biol.* 106, 761–771. doi:10.1083/jcb.106.3.761

Brandstadter, J. D., and Yang, Y. (2011). Natural killer cell responses to viral infection. *J. Innate Immun.* 3, 274–279. doi:10.1159/000324176

Bravo, B., Gallego, M. I., Flores, A. I., Bornstein, R., Puente-Bedia, A., Hernández, J., et al. (2016). Restrained Th17 response and myeloid cell infiltration into the central nervous system by human decidua-derived mesenchymal stem cells during experimental autoimmune encephalomyelitis. *Stem Cell Res. Ther.* 7, 43. doi:10.1186/s13287-016-0304-5

Bullard, J. D., Lei, J., Lim, J. J., Massee, M., Fallon, A. M., and Koob, T. J. (2019). Evaluation of dehydrated human umbilical cord biological properties for wound care and soft tissue healing. *J. Biomed. Mat. Res.* 107, 1035–1046. doi:10.1002/jbm.b.34196

Cargnoni, A., Papait, A., Masserdotti, A., Pasotti, A., Stefani, F. R., Silini, A. R., et al. (2021). Extracellular vesicles from perinatal cells for anti-inflammatory therapy. *Front. Bioeng. Biotechnol.* 9, 637737. doi:10.3389/fbioe.2021.637737

Castellanos, G., Bernabé-García, A., Moraleda, J. M., and Nicolás, F. J. (2017). Amniotic membrane application for the healing of chronic wounds and ulcers. *Placenta* 59, 146–153. doi:10.1016/j.placenta.2017.04.005

Chambers, D. C., Enever, D., Ilic, N., Sparks, L., Whitelaw, K., Ayres, J., et al. (2014). A phase 1b study of placenta-derived mesenchymal stromal cells in patients with idiopathic pulmonary fibrosis. *Respirology* 19, 1013–1018. doi:10.1111/resp.12343

Chatterjee, D., Marquardt, N., Tufa, D. M., Beauclair, G., Low, H. Z., Hatlapatka, T., et al. (2014). Role of gamma-secretase in human umbilical-cord derived mesenchymal stem cell mediated suppression of NK cell cytotoxicity. *Cell Commun. Signal* 12, 63. doi:10.1186/s12964-014-0063-9

Colocho, G., Graham, W. P., 3R. D., Greene, A. E., Matheson, D. W., and Lynch, D. (1974). Human amniotic membrane as a physiologic wound dressing. *Arch. Surg.* 109, 370–373. doi:10.1001/archsurg.1974.01360030022006

Croxatto, D., Vacca, P., Canegallo, F., Conte, R., Venturini, P. L., Moretta, L., et al. (2014). Stromal cells from human decidua exert a strong inhibitory effect on NK cell function and dendritic cell differentiation. *PLoS One* 9, e89006. doi:10.1371/journal.pone.0089006

Dadkhah Tehrani, F., Firouzeh, A., Shabani, I., and Shabani, A. (2020). A review on modifications of amniotic membrane for biomedical applications. *Front. Bioeng. Biotechnol.* 8, 606982. doi:10.3389/fbioe.2020.606982

Dahlgren, C., Karlsson, A., and Bylund, J. (2007). Measurement of respiratory burst products generated by professional phagocytes. *Methods Mol. Biol.* 412, 349–363. doi:10.1007/978-1-59745-467-4_23

Dash, B. C., Xu, Z., Lin, L., Koo, A., Ndon, S., Berthiaume, F., et al. (2018). *Stem Cells and Engineered Scaffolds for Regenerative Wound Healing*. Basel): Bioengineering. 5.

De La Torre, P., Pérez-Lorenzoand Flores, A. I. (2018). "Human placenta-derived mesenchymal stromal cells: A review from basic research to clinical applications," in *Stromal cells - structure, function, and therapeutic implications*. Editor M. T. VALARMATHI (London: IntechOpen Limited).

Demidova-Rice, T. N., Durham, J. T., and Herman, I. M. (2012). Wound healing angiogenesis: Innovations and challenges in acute and chronic wound healing. *Adv. Wound Care* 1, 17–22. doi:10.1089/wound.2011.0308

Deng, Q., Huang, S., Wen, J., Jiao, Y., Su, X., Shi, G., et al. (2020). PF-127 hydrogel plus sodium ascorbyl phosphate improves Wharton's jelly mesenchymal stem cell-mediated skin wound healing in mice. *Stem Cell Res. Ther.* 11, 143. doi:10.1186/s13287-020-01638-2

Di Fulvio, P., Pandolfi, A., Formoso, G., Di Silvestre, S., Di Tomo, P., Giardinelli, A., et al. (2014). Features of endothelial dysfunction in umbilical cord vessels of women with gestational diabetes. *Nutr. Metabolism Cardiovasc. Dis.* 24, 1337–1345. doi:10.1016/j.numecd.2014.06.005

Di Pietrantonio, N., Palmerini, C., Pipino, C., Baldassarre, M. P. A., Bologna, G., Mohn, A., et al. (2021). Plasma from obese children increases monocyte-endothelial adhesion and affects intracellular insulin signaling in cultured endothelial cells: Potential role of mTORC1-S6K1. *Biochimica Biophysica Acta (BBA) - Mol. Basis Dis.* 1867, 166076. doi:10.1016/j.bbadis.2021.166076

Di Pietro, N., Baldassarre, M. P. A., Cichelli, A., Pandolfi, A., Formoso, G., and Pipino, C. (2020). Role of polyphenols and carotenoids in endothelial dysfunction: An overview from classic to innovative biomarkers. *Oxid. Med. Cell Longev.* 2020, 6381380. doi:10.1155/2020/6381380

Di Tomo, P., Di Silvestre, S., Cordone, V. G., Giardinelli, A., Faricelli, B., Pipino, C., et al. (2015). *Centella asiatica* and lipoic acid, or a combination thereof, inhibit monocyte adhesion to endothelial cells from umbilical cords of gestational diabetic women. *Nutr. Metabolism Cardiovasc. Dis.* 25, 659–666. doi:10.1016/j.numecd.2015.04.002

Diegelmann, R. F., and Evans, M. C. (2004). Wound healing: An overview of acute, fibrotic and delayed healing. *Front. Biosci.* 9, 283–289. doi:10.2741/1184

DiPietro, L. A. (2016). Angiogenesis and wound repair: When enough is enough. *J. Leukoc. Biol.* 100, 979–984. doi:10.1189/jlb.4mr0316-102r

Du, L., Lv, R., Yang, X., Cheng, S., Ma, T., and Xu, J. (2016). Hypoxic conditioned medium of placenta-derived mesenchymal stem cells protects against scar formation. *Life Sci.* 149, 51–57. doi:10.1016/j.lfs.2016.02.050

Edinger, J., Karasiewicz, K., He, S., Ye, Q., and Hariri, R. (2018). "Placenta-derived mesenchymal stromal cells: Modulation of immunity and inflammation," in *Placenta*. Editor R. G. AHMED (London: IntechOpen Limited). doi:10.5772/intechopen.79728

Edwards, S. S., Zavala, G., Prieto, C. P., Elliott, M., Martínez, S., Egaña, J. T., et al. (2014). Functional analysis reveals angiogenic potential of human mesenchymal stem cells from Wharton's jelly in dermal regeneration. *Angiogenesis* 17, 851–866. doi:10.1007/s10456-014-9432-7

Erkers, T., Nava, S., Yosef, J., Ringdén, O., and Kaipe, H. (2013). Decidual stromal cells promote regulatory T cells and suppress alloreactivity in a cell contact-dependent manner. *Stem Cells Dev.* 22, 2596–2605. doi:10.1089/scd.2013.0079

Fénelon, M., Catros, S., and Fricain, J. C. (2018). What is the benefit of using amniotic membrane in oral surgery? A comprehensive review of clinical studies. *Clin. Oral Invest* 22, 1881–1891. doi:10.1007/s00784-018-2457-3

Fujiwara, N., and Kobayashi, K. (2005). Macrophages in inflammation. *Cdtia* 4, 281–286. doi:10.2174/1568010054022024

Gu, Y. Z., Xue, Q., Chen, Y. J., Yu, G. H., Qing, M. D., Shen, Y., et al. (2013). Different roles of PD-L1 and FasL in immunomodulation mediated by human placenta-derived mesenchymal stem cells. *Hum. Immunol.* 74, 267–276. doi:10.1016/j.humimm.2012.12.011

Gulameabasse, S., Gindraux, F., Catros, S., Fricain, J. C., and Fenelon, M. (2020). Chorion and amnion/chorion membranes in oral and periodontal surgery: A systematic review. *J. Biomed. Mater Res.* 109 (8), 1216–1229. doi:10.1002/jbm.b.34783

Güler, R., Ercan, M. T., Ulutunçel, N., Devrim, H., and Uran, N. (1997). Measurement of blood flow by the 133Xe clearance technique to grafts of amnion used in vestibuloplasty. *Br. J. Oral Maxillofac. Surg.* 35, 280–283. doi:10.1016/s0266-4356(97)90048-6

Han, Y., Sun, T., Han, Y., Lin, L., Liu, C., Liu, J., et al. (2019). Human umbilical cord mesenchymal stem cells implantation accelerates cutaneous wound healing in diabetic rats via the Wnt signaling pathway. *Eur. J. Med. Res.* 24, 10. doi:10.1186/s40001-019-0366-9

Hasegawa, T., Mizoguchi, M., Haruna, K., Mizuno, Y., Muramatsu, S., Suga, Y., et al. (2007). Amnia for intractable skin ulcers with recessive dystrophic epidermolysis bullosa: Report of three cases. *J. Dermatol* 34, 328–332. doi:10.1111/j.1346-8138.2007.00281.x

Hashemi, S. S., Mohammadi, A. A., Kabiri, H., Hashempoor, M. R., Mahmoodi, M., Amini, M., et al. (2019). The healing effect of wharton's jelly stem cells seeded on biological scaffold in chronic skin ulcers: A randomized clinical trial. *J. Cosmet. Dermatol* 18, 1961–1967. doi:10.1111/jocd.12931

Hashemi, S. S., Pourfath, M. R., Derakhshanfar, A., Behzad-Behbahani, A., and Moayedi, J. (2020). The role of labeled cell therapy with and without scaffold in early excision burn wounds in a rat animal model. *Iran. J. Basic Med. Sci.* 23, 673–679. doi:10.22038/ijbms.2020.34324.8156

Hashemian, S. R., Aliannejad, R., Zarrabi, M., Soleimani, M., Vosough, M., Hosseini, S. E., et al. (2021). Mesenchymal stem cells derived from perinatal tissues for treatment of critically ill COVID-19-induced ARDS patients: A case series. *Stem Cell Res. Ther.* 12, 91. doi:10.1186/s13287-021-02165-4

He, L., Tu, H. J., He, W. F., Guo, L. L., Yu, S. X., Li, J., et al. (2015). Lentiviral-mediated overexpression of homeobox A4 by human umbilical cord mesenchymal stem cells repairs full-thickness skin defects. *Mol. Med. Rep.* 11, 3517–3522. doi:10.3892/mmr.2015.3208

He, X., Shu, J., Xu, L., Lu, C., and Lu, A. (2012). Inhibitory effect of Astragalus polysaccharides on lipopolysaccharide-induced TNF-a and IL-1β production in THP-1 cells. *Molecules* 17, 3155–3164. doi:10.3390/molecules17033155

Hu, K., Yang, Y., Tu, Q., Luo, Y., and Ma, R. (2013). Alpinetin inhibits LPS-induced inflammatory mediator response by activating PPAR-γ in THP-1-derived macrophages. *Eur. J. Pharmacol.* 721, 96–102. doi:10.1016/j.ejphar.2013.09.049

Hu, Y., Rao, S. S., Wang, Z. X., Cao, J., Tan, Y. J., Luo, J., et al. (2018). Exosomes from human umbilical cord blood accelerate cutaneous wound healing through miR-21-3p-mediated promotion of angiogenesis and fibroblast function. *Theranostics* 8, 169–184. doi:10.7150/thno.21234

Huang, Q., Yang, Y., Luo, C., Wen, Y., Liu, R., Li, S., et al. (2019). An efficient protocol to generate placental chorionic plate-derived mesenchymal stem cells with superior proliferative and immunomodulatory properties. *Stem Cell Res. Ther.* 10, 301. doi:10.1186/s13287-019-1405-8

Insausti, C. L., Alcaraz, A., García-Vizcaíno, E. M., Mrowiec, A., López-Martínez, M. C., Blanquer, M., et al. (2010). Amniotic membrane induces epithelialization in massive posttraumatic wounds. *Wound Repair Regen.* 18, 368–377. doi:10.1111/j.1524-475x.2010.00604.x

Jin, E., Kim, T. H., Han, S., and Kim, S. W. (2016). Amniotic epithelial cells promote wound healing in mice through high epithelialization and engraftment. *J. Tissue Eng. Regen. Med.* 10, 613–622. doi:10.1002/term.2069

Kaushik, K., and Das, A. (2019). Cycloxygenase-2 inhibition potentiates trans-differentiation of Wharton's jelly-mesenchymal stromal cells into endothelial cells: Transplantation enhances neovascularization-mediated wound repair. *Cytotherapy* 21, 260–273. doi:10.1016/j.jcyt.2019.01.004

Kim, S. W., Zhang, H. Z., Guo, L., Kim, J. M., and Kim, M. H. (2012a). Amniotic mesenchymal stem cells enhance wound healing in diabetic NOD/SCID mice through high angiogenic and engraftment capabilities. *Plos One* 7. doi:10.1371/annotation/f6ebe3d3-ef7c-42ce-86fe-d5a661d7f67f

Kim, S. W., Zhang, H. Z., Guo, L., Kim, J. M., and Kim, M. H. (2012b). Amniotic mesenchymal stem cells enhance wound healing in diabetic NOD/SCID mice through high angiogenic and engraftment capabilities. *PLoS One* 7, e41105. doi:10.1371/journal.pone.0041105

Kim, S. Y., Oh, S. H., Lee, J. H., Suh, M. W., and Park, M. K. (2019). Effects of placenta-derived mesenchymal stem cells on the particulate matter-induced

damages in human middle ear epithelial cells. *Stem Cells Int.* 2019, 4357684. doi:10.1155/2019/4357684

Kim, Y. J., Ahn, H. J., Lee, S. H., Lee, M. H., and Kang, K. S. (2020). Effects of conditioned media from human umbilical cord blood-derived mesenchymal stem cells in the skin immune response. *Biomed. Pharmacother.* 131, 110789. doi:10.1016/j.biopha.2020.110789

Kitala, D., Klama-Baryła, A., Łabuś, W., Ples, M., Misiuga, M., Kraut, M., et al. (2019). Amniotic cells share clusters of differentiation of fibroblasts and keratinocytes, influencing their ability to proliferate and aid in wound healing while impairing their angiogenesis capability. *Eur. J. Pharmacol.* 854, 167–178. doi:10.1016/j.ejphar.2019.02.043

Kleiveland, C. R. (2015). "Peripheral blood mononuclear cells," in *The impact of food bioactives on health:* In vitro *and* ex vivo *models*. Editors K. VERHOECKX, COTTER, P., LOPEZ-EXPOSITO, I., C. KLEIVELAND, T. LEA, A. MACKIE, T. REQUENA, D. SWIATECKA, et al. (Cham. (CH). doi:10.1007/978-3-319-16104-4_15

Kocherova, I., Bryja, A., Mozdziak, P., Angelova Volponi, A., Dyszkiewicz-Konwińska, M., Piotrowska-Kempisty, H., et al. (2019). Human umbilical vein endothelial cells (HUVECs) Co-culture with osteogenic cells: From molecular communication to engineering prevascularised bone grafts. *J. Clin. Med.* 8. doi:10.3390/jcm8101602

König, J., Weiss, G., Rossi, D., Wankhammer, K., Reinisch, A., Kinzer, M., et al. (2015). Placental mesenchymal stromal cells derived from blood vessels or avascular tissues: What is the better choice to support endothelial cell function? *Stem Cells Dev.* 24, 115–131. doi:10.1089/scd.2014.0115

Koob, T. J., Lim, J. J., Massee, M., Zabek, N., Rennert, R., Gurtner, G., et al. (2014). Angiogenic properties of dehydrated human amnion/chorion allografts: Therapeutic potential for soft tissue repair and regeneration. *Vasc. Cell* 6, 10. doi:10.1186/2045-824x-6-10

Koob, T. J., Rennert, R., Zabek, N., Massee, M., Lim, J. J., Temenoff, J. S., et al. (2013). Biological properties of dehydrated human amnion/chorion composite graft: Implications for chronic wound healing. *Int. Wound J.* 10, 493–500. doi:10.1111/iwj.12140

Lawson, V. G. (1985). Oral cavity reconstruction using pectoralis major muscle and amnion. *Archives Otolaryngology - Head Neck Surg.* 111, 230–233. doi:10.1001/archotol.1985.00800060054006

Lee, C. E. (2018). Macrophages and inflammation. *J. Rheum. Dis.* 25, 11–18. doi:10.4078/jrd.2018.25.1.11

Leng, S. X., Mcelhaney, J. E., Walston, J. D., Xie, D., Fedarko, N. S., and Kuchel, G. A. (2008). ELISA and multiplex technologies for cytokine measurement in inflammation and aging research. *J. Gerontol. A Biol. Sci. Med. Sci.* 63, 879–884. doi:10.1093/gerona/63.8.879

Li, H., Niederkorn, J. Y., Neelam, S., Mayhew, E., Word, R. A., Mcculley, J. P., et al. (2005). Immunosuppressive factors secreted by human amniotic epithelial cells. *Invest Ophthalmol. Vis. Sci.* 46, 900–907. doi:10.1167/iovs.04-0495

Li, J., Koike-Soko, C., Sugimoto, J., Yoshida, T., Okabe, M., and Nikaido, T. (2015). Human amnion-derived stem cells have immunosuppressive properties on NK cells and monocytes. *Cell Transpl.* 24, 2065–2076. doi:10.3727/096368914x685230

Li, J. Y., Ren, K. K., Zhang, W. J., Xiao, L., Wu, H. Y., Liu, Q. Y., et al. (2019). Human amniotic mesenchymal stem cells and their paracrine factors promote wound healing by inhibiting heat stress-induced skin cell apoptosis and enhancing their proliferation through activating PI3K/AKT signaling pathway. *Stem Cell Res. Ther.* 10, 247. doi:10.1186/s13287-019-1366-y

Liarte, S., Bernabe-Garcia, A., Armero-Barranco, D., and Nicolas, F. J. (2018). Microscopy based methods for the assessment of epithelial cell migration during *in vitro* wound healing. *J. Vis. Exp.* 1, 56799. doi:10.3791/56799

Liarte, S., Bernabe-Garcia, A., and Nicolas, F. J. (2020a). Human skin keratinocytes on sustained TGF-beta stimulation reveal partial EMT features and weaken growth arrest responses. *Cells* 9, 255. doi:10.3390/cells9010255

Liarte, S., Bernabe-Garcia, A., and Nicolas, F. J. (2020b). Role of TGF-beta in skin chronic wounds: A keratinocyte perspective. *Cells* 9. doi:10.3390/cells9020306

Liu, J., Yan, Z., Yang, F., Huang, Y., Yu, Y., Zhou, L., et al. (2021). Exosomes derived from human umbilical cord mesenchymal stem cells accelerate cutaneous wound healing by enhancing angiogenesis through delivering angiopoietin-2. *Stem Cell Rev. Rep.* 17, 305–317. doi:10.1007/s12015-020-09992-7

Lublin, F. D., Bowen, J. D., Huddlestone, J., Kremenchutzky, M., Carpenter, A., Corboy, J. R., et al. (2014). Human placenta-derived cells (PDA-001) for the treatment of adults with multiple sclerosis: A randomized, placebo-controlled, multiple-dose study. *Mult. Scler. Relat. Disord.* 3, 696–704. doi:10.1016/j.msard.2014.08.002

Ma, H., Jiang, S., DU, L., Liu, J., Xu, X., Lu, X., et al. (2021). Conditioned medium from primary cytotrophoblasts, primary placenta-derived mesenchymal stem cells, or sub-cultured placental tissue promoted HUVEC angiogenesis *in vitro*. *Stem Cell Res. Ther.* 12, 141. doi:10.1186/s13287-021-02192-1

Ma, Y., Liu, X., Long, Y., and Chen, Y. (2022). Emerging therapeutic potential of mesenchymal stem cell-derived extracellular vesicles in chronic respiratory diseases: An overview of recent progress. *Front. Bioeng. Biotechnol.* 10, 845042. doi:10.3389/fbioe.2022.845042

Magatti, M., Caruso, M., DE Munari, S., Vertua, E., De, D., Manuelpillai, U., et al. (2015). Human amniotic membrane-derived mesenchymal and epithelial cells exert different effects on monocyte-derived dendritic cell differentiation and function. *Cell Transpl.* 24 (9), 1733–1752. doi:10.3727/096368914X684033

Magatti, M., DE Munari, S., Vertua, E., Gibelli, L., Wengler, G. S., and Parolini, O. (2008). Human amnion mesenchyme harbors cells with allogeneic T-cell suppression and stimulation capabilities. *Stem Cells* 26, 182–192. doi:10.1634/stemcells.2007-0491

Magatti, M., DE Munari, S., Vertua, E., Nassauto, C., Albertini, A., Wengler, G. S., et al. (2009). Amniotic mesenchymal tissue cells inhibit dendritic cell differentiation of peripheral blood and amnion resident monocytes. *Cell Transpl.* 18, 899–914. doi:10.3727/096368909x471314

Magatti, M., Vertua, E., Cargnoni, A., Silini, A., and Parolini, O. (2018). The immunomodulatory properties of amniotic cells: The two sides of the coin. *Cell Transpl.* 27, 31–44. doi:10.1177/0963689717742819

Mahmood, R., Mehmood, A., Choudhery, M. S., Awan, S. J., Khan, S. N., and Riazuddin, S. (2019). Human neonatal stem cell-derived skin substitute improves healing of severe burn wounds in a rat model. *Cell Biol. Int.* 43, 147–157. doi:10.1002/cbin.11072

Marshall, J. S., Warrington, R., Watson, W., and Kim, H. L. (2018). An introduction to immunology and immunopathology. *Allergy Asthma Clin. Immunol.* 14, 49. doi:10.1186/s13223-018-0278-1

Mcquilling, J. P., Kammer, M., Kimmerling, K. A., and Mowry, K. C. (2019). Characterisation of dehydrated amnion chorion membranes and evaluation of fibroblast and keratinocyte responses *in vitro*. *Int. Wound J.* 16, 827–840. doi:10.1111/iwj.13103

Mebarki, M., Iglicki, N., Marigny, C., Abadie, C., Nicolet, C., Churlaud, G., et al. (2021). Development of a human umbilical cord-derived mesenchymal stromal cell-based advanced therapy medicinal product to treat immune and/or inflammatory diseases. *Stem Cell Res. Ther.* 12, 571. doi:10.1186/s13287-021-02637-7

Medina-Leyte, D. J., Domínguez-Pérez, M., Ingrid Mercado, I., Villarreal-Molina, M. T., and Jacobo-Albavera, L. (2020). Use of human umbilical vein endothelial cells (HUVEC) as a model to study cardiovascular disease. *Appl. Sci.* 10, 938. doi:10.3390/app10030938

Medzhitov, R. (2008). Origin and physiological roles of inflammation. *Nature* 454, 428–435. doi:10.1038/nature07201

Mermet, I., Pottier, N., Sainthillier, J. M., Malugani, C., Cairey-Remonnay, S., Maddens, S., et al. (2007). Use of amniotic membrane transplantation in the treatment of venous leg ulcers. *Wound Repair Regen.* 15, 459–464. doi:10.1111/j.1524-475x.2007.00252.x

Moby, V., Boura, C., Kerdjoudj, H., Voegel, J. C., Marchal, L., Dumas, D., et al. (2007). Poly(styrenesulfonate)/poly(allylamine) multilayers: A route to favor endothelial cell growth on expanded poly(tetrafluoroethylene) vascular grafts. *Biomacromolecules* 8, 2156–2160. doi:10.1021/bm070348n

Moloudizargari, M., Govahi, A., Fallah, M., Rezvanfar, M. A., Asghari, M. H., and Abdollahi, M. (2021). The mechanisms of cellular crosstalk between mesenchymal stem cells and natural killer cells: Therapeutic implications. *J. Cell Physiol.* 236, 2413–2429. doi:10.1002/jcp.30038

Momeni, M., Zarehaghighi, M., Hajimiri, M., Khorasani, G., Dinarvand, R., Nekookar, A., et al. (2018). *In vitro* and *in vivo* investigation of a novel amniotic-based chitosan dressing for wound healing. *Wound Repair Regen.* 26, 87–101. doi:10.1111/wrr.12618

Montanucci, P., DI Pasquali, C., Ferri, I., Pescara, T., Pennoni, I., Siccu, P., et al. (2017). Human umbilical cord Wharton jelly-derived adult mesenchymal stem cells, in biohybrid scaffolds, for experimental skin regeneration. *Stem Cells Int.* 2017, 1472642. doi:10.1155/2017/1472642

Moreno-Jimenez, I., Hulsart-Billstrom, G., Lanham, S. A., Janeczek, A. A., Kontouli, N., Kanczler, J. M., et al. (2016). The chorioallantoic membrane (CAM) assay for the study of human bone regeneration: A refinement animal model for tissue engineering. *Sci. Rep.* 6, 32168. doi:10.1038/srep32168

Mukherjee, C., Saleem, S., Das, S., Biswas, S. C., and Bhattacharyya, D. (2020). Human placental laminin: Role in neuronal differentiation, cell adhesion and proliferation. *J. Biosci.* 45. doi:10.1007/s12038-020-00043-4

Munir, H., Rainger, G. E., Nash, G. B., and Mcgettrick, H. (2015). Analyzing the effects of stromal cells on the recruitment of leukocytes from flow. *J. Vis. Exp.* 1, e52480. doi:10.3791/52480

Murphy, S. V., Skardal, A., Song, L., Sutton, K., Haug, R., Mack, D. L., et al. (2017). Solubilized amnion membrane hyaluronic acid hydrogel accelerates full-thickness wound healing. *Stem Cells Transl. Med.* 6, 2020–2032. doi:10.1002/sctm.17-0053

Nensat, C., Songjang, W., Tohtong, R., Suthiphongchai, T., Phimsen, S., Rattanasinganchan, P., et al. (2021). Porcine placenta extract improves high-glucose-induced angiogenesis impairment. *BMC Complement. Med. Ther.* 21, 66. doi:10.1186/s12906-021-03243-z

Nicolas-Avila, J. A., Adrover, J. M., and Hidalgo, A. (2017). Neutrophils in homeostasis, immunity, and cancer. *Immunity* 46, 15–28. doi:10.1016/j.immuni.2016.12.012

Nowak-Sliwinska, P., Alitalo, K., Allen, E., Anisimov, A., Aplin, A. C., Auerbach, R., et al. (2018). Consensus guidelines for the use and interpretation of angiogenesis assays. *Angiogenesis* 21, 425–532. doi:10.1007/s10456-018-9613-x

Pandolfi, A., and De Filippis, E. A. (2007). Chronic hyperglicemia and nitric oxide bioavailability play a pivotal role in pro-atherogenic vascular modifications. *Genes Nutr.* 2, 195–208. doi:10.1007/s12263-007-0050-5

Paternotte, E., Kerdjoudj, H., Kokten, T., Stoltz, J. F., Kearney-Schwartz, A., Voegel, J. C., et al. (2013). Endothelialized and preconditioned natural umbilical arteries with long term patency open the route for future human uses. *Clin. Hemorheol. Microcirc.* 54, 223–234. doi:10.3233/ch-131728

Pianta, S., Bonassi Signoroni, P., Muradore, I., Rodrigues, M. F., Rossi, D., Silini, A., et al. (2015). Amniotic membrane mesenchymal cells-derived factors skew T cell polarization toward Treg and downregulate Th1 and Th17 cells subsets. *Stem Cell Rev. Rep.* 11, 394–407. doi:10.1007/s12015-014-9558-4

Pichlsberger, M., Jerman, U. D., Obradović, H., Tratnjek, L., Macedo, A. S., Mendes, F., et al. (2021). Systematic review of the application of perinatal derivatives in animal models on cutaneous wound healing. *Front. Bioeng. Biotechnol.* 9. doi:10.3389/fbioe.2021.742858

Pipino, C., Bernabe-Garcia, A., Cappellaci, I., Stelling-Ferez, J., DI Tomo, P., Santalucia, M., et al. (2022). Effect of the human amniotic membrane on the umbilical vein endothelial cells of gestational diabetic mothers: New insight on inflammation and angiogenesis. *Front. Bioeng. Biotechnol.* 10. doi:10.3389/fbioe.2022.854845

Pipino, C., Shah, H., Prudente, S., DI Pietro, N., Zeng, L., Park, K., et al. (2020). Association of the 1q25 diabetes-specific coronary heart disease locus with alterations of the gamma-glutamyl cycle and increased methylglyoxal levels in endothelial cells. *Diabetes* 69, 2206–2216. doi:10.2337/db20-0475

Platchek, M., Lu, Q., Tran, H., and Xie, W. (2020). Comparative analysis of multiple immunoassays for cytokine profiling in drug Discovery. *SLAS Discov.* 25, 1197–1213. doi:10.1177/2472555220954389

Rahman, M. S., Islam, R., Rana, M. M., Spitzhorn, L. S., Rahman, M. S., Adjaye, J., et al. (2019). Characterization of burn wound healing gel prepared from human amniotic membrane and Aloe vera extract. *BMC Complement. Altern. Med.* 19, 115. doi:10.1186/s12906-019-2525-5

Raja, Sivamani, K., Garcia, M. S., and Isseroff, R. R. (2007). Wound re-epithelialization: Modulating keratinocyte migration in wound healing. *Front. Biosci.* 12, 2849–2868. doi:10.2741/2277

Rameshbabu, A. P., Bankoti, K., Datta, S., Subramani, E., Apoorva, A., Ghosh, P., et al. (2018). Silk sponges ornamented with a placenta-derived extracellular matrix augment full-thickness cutaneous wound healing by stimulating neovascularization and cellular migration. *ACS Appl. Mater Interfaces* 10, 16977–16991. doi:10.1021/acsami.7b19007

Riddy, D. M., Goy, E., Delerive, P., Summers, R. J., Sexton, P. M., and Langmead, C. J. (2018). Comparative genotypic and phenotypic analysis of human peripheral blood monocytes and surrogate monocyte-like cell lines commonly used in metabolic disease research. *PLoS One* 13, e0197177. doi:10.1371/journal.pone.0197177

Rinastiti, M., Harijadisantoso, A. L., and Sosroseno, W. (2006). Histological evaluation of rabbit gingival wound healing transplanted with human amniotic membrane. *Int. J. Oral Maxillofac. Surg.* 35, 247–251. doi:10.1016/j.ijom.2005.09.012

Ringden, O., Baygan, A., Remberger, M., Gustafsson, B., Winiarski, J., Khoein, B., et al. (2018). Placenta-derived decidua stromal cells for treatment of severe acute graft-versus-host disease. *Stem Cells Transl. Med.* 7, 325–331. doi:10.1002/sctm.17-0167

Rossi, D., Pianta, S., Magatti, M., Sedlmayr, P., and Parolini, O. (2012). Characterization of the conditioned medium from amniotic membrane cells: Prostaglandins as key effectors of its immunomodulatory activity. *PLoS One* 7, e46956. doi:10.1371/journal.pone.0046956

Ruiz-Canada, C., Bernabe-Garcia, A., Liarte, S., Insausti, C. L., Angosto, D., Moraleda, J. M., et al. (2018). Amniotic membrane stimulates cell migration by modulating transforming growth factor-beta signalling. *J. Tissue Eng. Regen. Med.* 12, 808–820. doi:10.1002/term.2501

Ruiz-Canada, C., Bernabe-Garcia, A., Liarte, S., Rodriguez-Valiente, M., and Nicolas, F. J. (2021). Chronic wound healing by amniotic membrane: TGF-beta and EGF signaling modulation in Re-epithelialization. *Front. Bioeng. Biotechnol.* 9, 689328. doi:10.3389/fbioe.2021.689328

Sabapathy, V., Sundaram, B., Mankuzhy, P., and Kumar, S. (2014). Human Wharton's Jelly Mesenchymal Stem Cells plasticity augments scar-free skin wound healing with hair growth. *PLoS One* 9, e93726. doi:10.1371/journal.pone.0093726

Sabzevari, R., Roushandeh, A. M., Mehdipour, A., Alini, M., and Roudkenar, M. H. (2020). SA/G hydrogel containing hCAP-18/LL-37-engineered WJ-MSCs-derived conditioned medium promoted wound healing in rat model of excision injury. *Life Sci.* 261, 118381. doi:10.1016/j.lfs.2020.118381

Sadeghi, B., Roshandel, E., Pirsalehi, A., Kazemi, S., Sankanian, G., Majidi, M., et al. (2021). Conquering the cytokine storm in COVID-19-induced ARDS using placenta-derived decidua stromal cells. *J. Cell Mol. Med.* 25, 10554–10564. doi:10.1111/jcmm.16986

Samandari, M. H., Yaghmaei, M., Ejlali, M., Moshref, M., and Saffar, A. S. (2004). Use of amnion as a graft material in vestibuloplasty: A preliminary report. *Oral Surg. Oral Med. Oral Pathol. Oral Radiol. Endod.* 97, 574–578. doi:10.1016/j.tripleo.2003.10.031

Shu, J., He, X., Zhang, L., Li, H., Wang, P., and Huang, X. (2015). Human amnion mesenchymal cells inhibit lipopolysaccharide-induced TNF-alpha and IL-1beta production in THP-1 cells. *Biol. Res.* 48, 69. doi:10.1186/s40659-015-0062-3

Silini, A., Parolini, O., Huppertz, B., and Lang, I. (2013). Soluble factors of amnion-derived cells in treatment of inflammatory and fibrotic pathologies. *Curr. Stem Cell Res. Ther.* 8, 6–14. doi:10.2174/1574888x11308010003

Silini, A. R., Cargnoni, A., Magatti, M., Pianta, S., and Parolini, O. (2015). The long path of human placenta, and its derivatives, in regenerative medicine. *Front. Bioeng. Biotechnol.* 3, 162. doi:10.3389/fbioe.2015.00162

Silini, A. R., DI Pietro, R., Lang-Olip, I., Alviano, F., Banerjee, A., Basile, M., et al. (2020). Perinatal derivatives: Where do we stand? A roadmap of the human placenta and consensus for tissue and cell nomenclature. *Front. Bioeng. Biotechnol.* 8, 610544. doi:10.3389/fbioe.2020.610544

Singh, R., Chouhan, U. S., Purohit, S., Gupta, P., Kumar, P., Kumar, A., et al. (2004). Radiation processed amniotic membranes in the treatment of non-healing ulcers of different etiologies. *Cell Tissue Bank.* 5, 129–134. doi:10.1023/b:catb.0000034077.05000.29

Solomon, A., Wajngarten, M., Alviano, F., Anteby, I., Elchalal, U., Pe'Er, J., et al. (2005). Suppression of inflammatory and fibrotic responses in allergic inflammation by the amniotic membrane stromal matrix. *Clin. Exp. Allergy* 35, 941–948. doi:10.1111/j.1365-2222.2005.02285.x

Stojadinovic, A., Carlson, J. W., Schultz, G. S., Davis, T. A., and Elster, E. A. (2008). Topical advances in wound care. *Gynecol. Oncol.* 111, S70–S80. doi:10.1016/j.ygyno.2008.07.042

Strech, D., and Dirnagl, U. (2019). 3Rs missing: Animal research without scientific value is unethical. *BMJ Open Sci.* 3. doi:10.1136/bmjos-2018-000048

Sun, J., Zhang, Y., Song, X., Zhu, J., and Zhu, Q. (2019). The healing effects of conditioned medium derived from mesenchymal stem cells on radiation-induced skin wounds in rats. *Cell Transpl.* 28, 105–115. doi:10.1177/0963689718807410

Sun, Q., Li, F., Li, H., Chen, R. H., Gu, Y. Z., Chen, Y., et al. (2015). Amniotic fluid stem cells provide considerable advantages in epidermal regeneration: B7H4 creates a moderate inflammation microenvironment to promote wound repair. *Sci. Rep.* 5, 11560. doi:10.1038/srep11560

Talwadekar, M. D., Kale, V. P., and Limaye, L. S. (2015). Placenta-derived mesenchymal stem cells possess better immunoregulatory properties compared to their cord-derived counterparts-a paired sample study. *Sci Rep.* 5, 15784. doi:10.1038/srep15784

Thery, C., Witwer, K. W., Aikawa, E., Alcaraz, M. J., Anderson, J. D., Andriantsitohaina, R., et al. (2018). Minimal information for studies of extracellular vesicles 2018 (MISEV2018): A position statement of the international society for extracellular vesicles and update of the MISEV2014 guidelines. *J. Extracell. Vesicles* 7, 1535750. doi:10.1080/20013078.2018.1535750

Torre, P., and Flores, A. I. (2020). Current status and future prospects of perinatal stem cells. *Genes (Basel)* 12, 6. doi:10.3390/genes12010006

Turabelidze, A., Guo, S., Chung, A. Y., Chen, L., Dai, Y., Marucha, P. T., et al. (2014). Intrinsic differences between oral and skin keratinocytes. *PLoS One* 9, e101480. doi:10.1371/journal.pone.0101480

Ucci, M., DI Tomo, P., Tritschler, F., Cordone, V. G. P., Lanuti, P., Bologna, G., et al. (2019). Anti-inflammatory role of carotenoids in endothelial cells derived from umbilical cord of women affected by gestational diabetes mellitus. *Oxid. Med. Cell Longev.* 2019, 8184656. doi:10.1155/2019/8184656

Van Deun, J., Mestdagh, P., Agostinis, P., Akay, O., Anand, S., Anckaert, J., et al.EV-TRACK Consortium. (2017). EV-TRACK: Transparent reporting and

centralizing knowledge in extracellular vesicle research. *Nat. Methods* 14, 228–232. doi:10.1038/nmeth.4185

Vellasamy, S., Sandrasaigaran, P., Vidyadaran, S., Abdullah, M., George, E., and Ramasamy, R. (2013). Mesenchymal stem cells of human placenta and umbilical cord suppress T-cell proliferation at G0 phase of cell cycle. *Cell Biol. Int.* 37, 250–256. doi:10.1002/cbin.10033

Vonbrunn, E., Mueller, M., Pichlsberger, M., Sundl, M., Helmer, A., Wallner, S. A., et al. (2020). Electrospun PCL/PLA scaffolds are more suitable carriers of placental mesenchymal stromal cells than collagen/elastin scaffolds and prevent wound contraction in a mouse model of wound healing. *Front. Bioeng. Biotechnol.* 8, 604123. doi:10.3389/fbioe.2020.604123

Wang, G., Joel, M. D. M., Yuan, J., Wang, J., Cai, X., Ocansey, D. K. W., et al. (2020). Human umbilical cord mesenchymal stem cells alleviate inflammatory bowel disease by inhibiting ERK phosphorylation in neutrophils. *Inflammopharmacology* 28, 603–616. doi:10.1007/s10787-019-00683-5

Wang, H., Chen, L., Liu, Y., Luo, B., Xie, N., Tan, T., et al. (2016a). Implantation of placenta-derived mesenchymal stem cells accelerates murine dermal wound closure through immunomodulation. *Am. J. Transl. Res.* 8, 4912–4921.

Wang, S., Mo, M., Wang, J., Sadia, S., Shi, B., Fu, X., et al. (2018). Platelet-derived growth factor receptor beta identifies mesenchymal stem cells with enhanced engraftment to tissue injury and pro-angiogenic property. *Cell Mol. Life Sci.* 75, 547–561. doi:10.1007/s00018-017-2641-7

Wang, S., Yang, H., Tang, Z., Long, G., and Huang, W. (2016b). Wound dressing model of human umbilical cord mesenchymal stem cells-alginates complex promotes skin wound healing by paracrine signaling. *Stem Cells Int.* 2016, 3269267. doi:10.1155/2016/3269267

Wertz, P. W. (2021). Synopsis of barrier function of skin and oral mucosa-volume 1. *Int. J. Mol. Sci.* 22. doi:10.3390/ijms22179383

Winkler, T., Costa, M. L., Ofir, R., Parolini, O., Geissler, S., Volk, H. D., et al. (2022). Hipgen: A randomized, multicentre phase III study using intramuscular PLacenta-eXpanded stromal cells therapy for recovery following hip fracture arthroplasty : A study design. *Bone Jt. Open* 3, 340–347. doi:10.1302/2633-1462.34.bjo-2021-0156.r1

Yang, C., Wu, M., You, M., Chen, Y., Luo, M., and Chen, Q. (2021). The therapeutic applications of mesenchymal stromal cells from human perinatal tissues in autoimmune diseases. *Stem Cell Res. Ther.* 12, 103. doi:10.1186/s13287-021-02158-3

Yang, J., Chen, Z., Pan, D., Li, H., and Shen, J. (2020). Umbilical cord-derived mesenchymal stem cell-derived exosomes combined pluronic F127 hydrogel promote chronic diabetic wound healing and complete skin regeneration. *Int. J. Nanomedicine* 15, 5911–5926. doi:10.2147/ijn.s249129

Yang, K., Li, D., Wang, M., Xu, Z., Chen, X., Liu, Q., et al. (2019). Exposure to blue light stimulates the proangiogenic capability of exosomes derived from human umbilical cord mesenchymal stem cells. *Stem Cell Res. Ther.* 10, 358. doi:10.1186/s13287-019-1472-x

Yue, C., Guo, Z., Luo, Y., Yuan, J., Wan, X., and Mo, Z. (2020). c-Jun overexpression accelerates wound healing in diabetic rats by human umbilical cord-derived mesenchymal stem cells. *Stem Cells Int.* 2020, 7430968. doi:10.1155/2020/7430968

Zantl, R., and Horn, E. (2011). Chemotaxis of slow migrating mammalian cells analysed by video microscopy. *Methods Mol. Biol.* 769, 191–203. doi:10.1007/978-1-61779-207-6_13

Zhang, B., Shi, Y., Gong, A., Pan, Z., Shi, H., Yang, H., et al. (2016). HucMSC exosome-delivered 14-3-3zeta orchestrates self-control of the wnt response via modulation of YAP during cutaneous regeneration. *Stem Cells* 34, 2485–2500. doi:10.1002/stem.2432

Zhang, B., Wu, X., Zhang, X., Sun, Y., Yan, Y., Shi, H., et al. (2015). Human umbilical cord mesenchymal stem cell exosomes enhance angiogenesis through the Wnt4/beta-catenin pathway. *Stem Cells Transl. Med.* 4, 513–522. doi:10.5966/sctm.2014-0267

Zhang, S., Chen, L., Zhang, G., and Zhang, B. (2020). Umbilical cord-matrix stem cells induce the functional restoration of vascular endothelial cells and enhance skin wound healing in diabetic mice via the polarized macrophages. *Stem Cell Res. Ther.* 11, 39. doi:10.1186/s13287-020-1561-x

Zhao, B., Liu, J. Q., Zheng, Z., Zhang, J., Wang, S. Y., Han, S. C., et al. (2016). Human amniotic epithelial stem cells promote wound healing by facilitating migration and proliferation of keratinocytes via ERK, JNK and AKT signaling pathways. *Cell Tissue Res.* 365, 85–99. doi:10.1007/s00441-016-2366-1

Zhao, G., Liu, F., Liu, Z., Zuo, K., Wang, B., Zhang, Y., et al. (2020). MSC-derived exosomes attenuate cell death through suppressing AIF nucleus translocation and enhance cutaneous wound healing. *Stem Cell Res. Ther.* 11, 174. doi:10.1186/s13287-020-01616-8

Zitti, B., and Bryceson, Y. T. (2018). Natural killer cells in inflammation and autoimmunity. *Cytokine Growth Factor Rev.* 42, 37–46. doi:10.1016/j.cytogfr.2018.08.001

frontiers | Frontiers in Bioengineering and Biotechnology

TYPE Review
PUBLISHED 14 September 2022
DOI 10.3389/fbioe.2022.981061

OPEN ACCESS

EDITED BY
J. Mary Murphy,
National University of Ireland Galway, Ireland

REVIEWED BY
Guido Moll,
Charité Universitätsmedizin Berlin, Germany
Carolina Balbi,
University of Zurich, Switzerland

*CORRESPONDENCE
Bernd Giebel,
bernd.giebel@uk-essen.de

SPECIALTY SECTION
This article was submitted to Tissue Engineering and Regenerative Medicine, a section of the journal Frontiers in Bioengineering and Biotechnology

RECEIVED 29 June 2022
ACCEPTED 12 August 2022
PUBLISHED 14 September 2022

CITATION
Papait A, Silini AR, Gazouli M, Malvicini R, Muraca M, O'Driscoll L, Pacienza N, Toh WS, Yannarelli G, Ponsaerts P, Parolini O, Eissner G, Pozzobon M, Lim SK and Giebel B (2022), Perinatal derivatives: How to best validate their immunomodulatory functions. *Front. Bioeng. Biotechnol.* 10:981061. doi: 10.3389/fbioe.2022.981061

Perinatal derivatives: How to best validate their immunomodulatory functions

Andrea Papait[1,2], Antonietta Rosa Silini[3], Maria Gazouli[4], Ricardo Malvicini[5,6], Maurizio Muraca[5], Lorraine O'Driscoll[7,8,9], Natalia Pacienza[6], Wei Seong Toh[10], Gustavo Yannarelli[6], Peter Ponsaerts[11], Ornella Parolini[1,2], Günther Eissner[12], Michela Pozzobon[5], Sai Kiang Lim[13] and Bernd Giebel[14]*

[1]Department of Life Science and Public Health, Università Cattolica del Sacro Cuore, Rome, Italy, [2]Fondazione Policlinico Universitario "Agostino Gemelli" IRCCS, Rome, Italy, [3]Centro di Ricerca E. Menni, Fondazione Poliambulanza Istituto Ospedaliero, Brescia, Italy, [4]Department of Basic Medical Sciences, Laboratory of Biology, Medical School, National and Kapodistrian University of Athens, Athens, Greece, [5]Department of Women and Children Health, University of Padova, Padova, Italy, [6]Laboratorio de Regulación Génica y Células Madre, Instituto de Medicina Traslacional, Trasplante y Bioingeniería (IMeTTyB), Universidad Favaloro-CONICET, Buenos Aires, Argentina, [7]School of Pharmacy and Pharmaceutical Sciences, Trinity College Dublin, Dublin, Ireland, [8]Trinity Biomedical Sciences Institute, Trinity College Dublin, Dublin, Ireland, [9]Trinity St. James's Cancer Institute, Trinity College Dublin, Dublin, Ireland, [10]Department of Orthopaedic Surgery, Yong Loo Lin School of Medicine, National University of Singapore, Singapore, Singapore, [11]Laboratory of Experimental Hematology, Vaccine and Infectious Disease Institute (Vaxinfectio), University of Antwerp, Antwerp, Belgium, [12]Systems Biology Ireland, School of Medicine, Conway Institute, University College Dublin, Dublin, Ireland, [13]Institute of Medical Biology and Institute of Molecular and Cell Biology, Agency for Science, Technology and Research, Singapore, Singapore, [14]Institute for Transfusion Medicine, University Hospital Essen, University of Duisburg-Essen, Essen, Germany

Perinatal tissues, mainly the placenta and umbilical cord, contain a variety of different somatic stem and progenitor cell types, including those of the hematopoietic system, multipotent mesenchymal stromal cells (MSCs), epithelial cells and amnion epithelial cells. Several of these perinatal derivatives (PnDs), as well as their secreted products, have been reported to exert immunomodulatory therapeutic and regenerative functions in a variety of pre-clinical disease models. Following experience with MSCs and their extracellular vesicle (EV) products, successful clinical translation of PnDs will require robust functional assays that are predictive for the relevant therapeutic potency. Using the examples of T cell and monocyte/macrophage assays, we here discuss several assay relevant parameters for assessing the immunomodulatory activities of PnDs. Furthermore, we highlight the need to correlate the *in vitro* assay results with preclinical or clinical outcomes in order to ensure valid predictions about the *in vivo* potency of therapeutic PnD cells/products in individual disease settings.

KEYWORDS

perinatal derivatives, mesenchymal stromal cells, functional assays, mechanisms of action, extracellular vesicles, exosomes, microvesicles, immunomodulation

Introduction

The first report that cells from perinatal tissues may provide a promising source for novel cellular therapies was published in 2004 (Bailo et al., 2004). In this pioneering study it was shown that mesenchymal stromal cell (MSC)-like human amnion and chorion cells obtained from human term placenta had the capability to suppress lymphocyte responsiveness *in vitro*. Furthermore, these cells could engraft into neonatal pigs and rats without being rejected (Bailo et al., 2004). The broad availability of placental tissues as biological waste products; the ease in isolating and expanding perinatal cells from various regions of the placenta; and the cells' potent immunomodulatory properties, have attracted increasing research interest developing the potential of placental cells and their secretome for treating a variety of diseases, especially those characterized by an inflammatory disbalance (Silini et al., 2020). To harmonize research in the field of perinatal derivatives (PnDs), the First International Workshop on Placenta-derived Stem Cells was held in Brescia, Italy in 2007. In this workshop four major regions of the fetal placenta were discussed as possible sources for therapeutically relevant stem and progenitor cells, namely the amniotic epithelial, the amniotic mesenchymal, the chorionic mesenchymal, and the chorionic trophoblastic tissues (Parolini et al., 2008). Since then, a variety of additional cell types, including endothelial cells, have been also isolated from other perinatal tissues and studied for their therapeutic functions. To harmonize the nomenclature and the criteria for the definition of cells isolated from different perinatal tissues and as an output of the European Union Cooperation in Science and Technology (COST) Action International Network for Translating Research on Perinatal Derivatives into Therapeutic Approaches (SPRINT), we recently published an update on the nomenclature and criteria (Silini et al., 2020). Despite most PnDs, including perinatal cells themselves as well as products obtained from their secretome, have already demonstrated huge therapeutic potential in various preclinical studies, no uniformity and/or standardization in potency testing exists so far. In this manuscript we will highlight the importance of testing the therapeutic potency of PnDs using appropriate functional assays and introduce several of the challenges that need to be considered for translating PnDs into the clinics.

As there is extensive experience with MSC products most commonly obtained from adult material, mainly adult bone marrow and fat tissue (Moll and James. 2019; Ringdén et al., 2022), we first summarize key aspects and challenges of the therapeutic MSC field, and highlight the need for robust assays to test the therapeutic potency of adult MSC and PnD products. In addition to pro-regenerative functions, PnDs like adult MSCs are known for their ability to modulate immune responses. Accordingly, in the second part of this manuscript, using the example of functional assays exploring T cell and monocyte/macrophage activities, we provide various considerations for setting up appropriate functional assays for evaluating the therapeutic potency of MSC and PnD products.

Lessons from the adult MSC field

Although our main focus is PnDs, the challenges identified in clinical translation of MSCs has provided many learning points that are of substantial relevance to the development of envisioned PnD therapies. Thus, for clarity it is appropriate to briefly introduce the MSC field and some of its current limitations.

Historically, non-hematopoietic therapeutic stem cell research began with the discovery of MSCs raised from adult bone marrow cells in the 1960s (Friedenstein et al., 1968), and the demonstration of their multi-lineage potential at the turn of the millennium (Pittenger et al., 1999). Considering their differentiation potential far beyond the mesenchymal lineage (Munoz-Elias et al., 2003; Pittenger and Martin 2004), MSCs quickly emerged as a promising stem cell entity for regenerative approaches, either in the autologous or allogeneic setting. Connected to proposed allogeneic MSCs applications, their interaction with different allogenic immune cells has been studied in detail.

Contrary to the initial expectations, upon administration *in vivo*, allogenic MSCs are not acutely destroyed by the immune system, but display a strong modulating function on various immune cells by suppressing their pro-inflammatory activities and inducing their regulatory, i.e., their tolerogenic, functions (Bartholomew et al., 2002; Di Nicola et al., 2002; Meisel et al., 2004). Consequently, MSCs have been increasingly tested for their immunomodulatory capability in preclinical models, as well as in a number of different clinical studies (Moll and James. 2019; Ringdén et al., 2022). One of the first administrations of MSCs in a patient with inflammatory disbalance was performed by Le Blanc and others when they succesfully treated a steroid refractory Graft-versus-Host Disease (GvHD) patient with adult bone marrow derived MSCs (Le Blanc et al., 2004).

In addition to bone marrow, MSCs have been isolated from various adult tissues, including fat (Moll and James. 2019). They have also been isolated from perinatal tissues, namely placenta, umbilical cord tissue and umbilical cord blood (Silini et al., 2020) and from the human second trimester amniotic fluid (AF-MSCs) (Roubelakis et al., 2007; Roubelakis et al., 2011; Legaki et al., 2016). Irrespective of their origin, MSCs obtained from all tissues share some common features that have been defined as *bona fide* criteria for MSCs by the International Society of Cell and Gene Therapy in 2006 (Dominici et al., 2006). Specifically, they grow as plastic-adherent cells and possess the ability to differentiate to various lineages including osteogenic, adipogenic and chondrogenic lineages. Furthermore, MSCs express characteristic cell surface antigens including CD73, CD90 and CD105 and they lack expression of hematopoietic and

endothelial cell specific antigens including CD14, CD45 and CD34, CD11b and CD79a, or CD19 and HLA-DR (Dominici et al., 2006). Due to their multipotency they were initially defined as mesenchymal stem cells, however, over the years it became clear that despite their multipotency they lack stem cell features and thus, have been renamed in multipotent stromal cells (Caplan 1991; Viswanathan et al., 2019).

To date, MSCs, mainly raised from adult tissues, have been registered in more than 1,400 clinical trials, either in regenerative settings or as immunomodulatory agents (clinicaltrials.gov). As exemplified by the MSC treatment of GvHD patients, many studies including a phase III clinical trial reported therapeutic efficacy of MSC therapies in GvHD patients, while others also including a phase III clinical trial failed to show efficacy (Baron and Storb 2012; Galipeau 2013; Kurtzberg et al., 2020a; Kurtzberg et al., 2020b; Kebriaei et al., 2020). Explaining the current controversy, over the years it has become clear that, despite some common features, MSCs represent a heterogenous cell entity with tissue-specific and intra-individual differences (Phinney et al., 1999; Vogel et al., 2003; Phinney 2012; Radtke et al., 2016).

Although known for several years now, discussions about the impact of this heterogeneity on the clinical outcome of MSC therapies have just begun (Dunn et al., 2021; Galipeau et al., 2021; Krampera and Le Blanc 2021). Among others, the relevance of differences in the expression level of the clotting cascade inducing tissue factor (TF) among MSCs of different origins emerged as a critical discussion point. To this end, placental and fat MSCs express higher levels of TF than BM-MSCs and thus may provide higher thromboembolic complications risks following MSC administration than that of BM-MSCs (Moll et al., 2022). As a consequence of such potential functional differences, regulatory authorities are increasingly requesting clarity on the role of cell heterogeneity and functionality. It is expected that, in the future, such clarity will be sought for other non-hematopoietic stem/progenitor cell products. In this context it is worth highlighting that this issue was critical in the US Food and Drug Administration (FDA) evaluation of the commercial MSC product remestemcel-L, which had shown efficacy in suppressing paediatric acute GvHD when evaluated in a single armed phase III clinical trial (Kurtzberg et al., 2020a; Kurtzberg et al., 2020b). The US FDA opined that as the critical quality attributes (CQAs) did not correlate with clinical effectiveness and/or *in vivo* potency/activity, the clinical effectiveness of individual lots of remestemcel-L being produced from graft material of varying donors was not adequately controlled. Without a proper CQA strategy, substantial functional heterogeneity that often is observed between independent MSC batches, especially when derived from different donors, may not be detectable. Consequently, in October 2020 the US FDA declined the approval of remestemcel-L for the treatment of paediatric acute GvHD in the United States (https://www.fda.gov/media/140988/download). Thus, it is evident that potency assays based on CQAs that are linked to a clearly defined mechanism of action (MoA), and/or CQAs that have a demonstrated relationship with clinical efficacy are critical to the successful translation of cellular products into the clinics.

Similar to MSCs, perinatal MSC products and other PnDs are complex biological products with multimodal *in vivo* activity that are likely to vary in donor dependent manners. Furthermore, such activities are highly affected by cell seeding and expansion conditions, as well as the duration of culture, both in number of passages or the duration between passaging. Thus, it is timely to consider and re-evaluate the reliability of existing functional assays that are frequently used for the characterization of PnDs, especially in view of their ability to link *in vitro* regenerative/immunomodulatory properties with clinical potency.

As such, for cell-based assays it will be important to determine specific PnD attributes that are being measured. If these attributes are involved in a clearly defined therapeutic MoA by the PnD against a specific disease, these attributes could be qualified as CQAs and the assays for these CQAs could be eventually used as potency assays to predict and ensure potency of individual lots of given PnD preparations. Before discussing functional assays for predicting potency in greater detail, basic concepts of the MoA of MSCs and PnDs will be discussed next.

MSCs mediate many therapeutic effects *via* their secretome

Administered MSCs were initially considered to home into affected tissues and to replace lost cell types in regenerative approaches or to modulate immune responses by direct cell-to-cell contacts in inflamed tissues. Upon studying their biodistribution, however, it was recognized that most of systemically administered MSCs embolise the lungs and are rarely recovered in affected tissues (Gao et al., 2001; Schrepfer et al., 2007; Lee et al., 2009). Therefore, it was postulated that MSCs may act in a paracrine, rather than in a cellular manner (Caplan 2017). Indeed, in myocardial infarction models, administration of their conditioned media or encapsulated MSCs induced comparable therapeutic effects to those achieved with systemically applied MSCs (Gnecchi et al., 2005; Gnecchi et al., 2006; Timmers et al., 2007). Thus, it became clear that MSCs mediate tissue repair in many applications through their secretome, particularly EVs (Bruno et al., 2009; Lai et al., 2010). Indeed, EVs have already shown clinical improvement in an acute GvHD patient, in chronic kidney disease patients, in a cochlear implant patient and in many animal models (Kordelas et al., 2014; Nassar et al., 2016; Warnecke et al., 2021). Despite these applications revealed positive effects of the applied MSC-EV products, variable activities and inter-donor heterogeneity among independent MSC-EV products should still be expected.

Indeed, as shown at the example of murine models for GvHD, ischemic stroke and Niemann's Pick Type C, independent MSC-EV preparations can differ in their ability in suppressing respective disease symptoms (Madel et al., 2020; Wang et al., 2020; Van Hoecke et al., 2021). Similarly, with the aim to translate PnDs, including EVs derived thereof, into a clinical setting, it is strongly recommended to establish a suitable potency testing and reliable functional analysis toolbox for PnDs from the outset.

Assays for the assessment of immunomodulatory PnD activities

It is generally assumed that, as for adult MSCs, one of the major PnD associated activities is their capability to modulate immune responses (Börger et al., 2017; Silini et al., 2020). Consequently, their immunomodulatory activities are frequently investigated in various *in vitro* assays, primarily on T cells or on macrophages. To this end, a huge variety of protocols for simple *in vitro* assays and subsequent read-out strategies have been developed. However, not all of these assays monitor the same immunomodulatory activity. Furthermore, not all monitored activities are involved in the mechanism by which cells exert their therapeutic effects for an indicated disease. In fact, in the past, most *in vitro* potency assays have failed to reliably and reproducibly predict the clinical effectiveness of administered MSCs (Galipeau et al., 2016). Thus, it is important that potency assays intended to predict the therapeutic function of a PnD measure the activities that are of direct relevance to the PnD's MoA for a specific disease. Without favoring any specific procedure, we feel it is important to discuss assay relevant parameters and potential caveats of respective assays and potential read-out strategies. Of note, this review is part of a quadrinomial series on functional assays for validation of PnDs, spanning biological functions, such as immunomodulation, anti-inflammation, anti-microbial/anti-cancer, wound healing, angiogenesis and regeneration.

T cell assays

T lymphocytes are the main component of the adaptive immune response and have an extremely high capacity to discriminate between self and non-self. In fact, they express a series of highly polymorphic receptors that allow them to actively respond to antigens presented either by antigen presenting cells or by infected cells. This type of response triggers both CD4 T helper and cytotoxic CD8 T lymphocytes (Mueller et al., 2013; Kumar et al., 2018). Furthermore, both CD4 and CD8 T lymphocytes are capable of developing immunological memory, a feature typical of adaptive immunity (Mueller et al., 2013; Kumar et al., 2018). Coupled to their ability to discriminate between self and non-self, T lymphocytes are the main actors in allograft rejection; they also play a relevant role in autoimmunity (Marino, Paster et al., 2016; Khan and Ghazanfar 2018). However, not all T lymphocytes mediate defense functions, a proportion of them, especially the regulatory T cells mediate tolerogenic functions that are required during the whole course of pregnancy and other developmental and regenerative processes (Weirather et al., 2014; Boothby et al., 2020; Fung et al., 2020; Green et al., 2021). As important as these regulatory T cell functions are, regulatory T cells also promote tumor growth and have been identified as promising targets in anti-tumor therapies (Paluskievicz et al., 2019; Bai et al., 2020; Seed et al., 2021).

Many degenerative and acute diseases including GvHD, ischemic stroke, sepsis and COVID-19 are accompanied by uncontrolled pro-inflammatory reactions, regularly also involving T cell effector responses (Hill 2009; Nakamura et al., 2020). Upon administration of potent PnD or adult MSC products that promote regeneration or improvement of acute disease symptoms, respectively, pathology associated T cell effector responses get suppressed *in vivo* and frequently are converted into regulatory T cell responses (Balza et al., 2016; De Biasi et al., 2021; Strobl et al., 2021). Furthermore, perinatal and adult MSC products can convey immunomodulatory activities in different autoimmune disease models, highlight their ability to reduce Th1/Th17 imbalances and to trigger T cell polarization towards regulatory T cell functions (Sun et al., 2009; Obermajer et al., 2014; Parolini et al., 2014; Tsai et al., 2014; Wang D et al., 2014; Wang H et al., 2014; Wang et al., 2017; Ma et al., 2019).

Coupled to such observations, it is broadly assumed that one of the central MoA attributes of PnD and adult MSC products is their ability to suppress T effector and to induce regulatory T cell functions. Consequently, many groups have started to study impacts of PnD and adult MSC products on T cells in a variety of different T cell assays.

Fundamentally, T cell assays can be categorized by whether they use primary or cell line derived T cells, such as Jurkat cells. Even though the usage of cell lines allows a higher degree of standardization, they regularly contain an array of different genetic mutations some of which can affect the reactivity of respective cells on environmental factors and thus change some of their key functions (Khan and Ghazanfar, 2018). For example, although Jurkat cells are widely used to study T cell receptor (TCR) signaling (Abraham and Weiss, 2004), they in contrast to primary T cells poorly respond to immunomodulatory signals including those of MSC products (Zhang et al., 2017).

Assays using primary T cells can be subdivided in two additional main categories, those which are based on purified T cells (either CD3, CD4, or CD8 T cells) or those which use mixtures of cells, typically peripheral blood mononuclear cells (PBMCs). In virtually all T cell assay variants, T cells are experimentally activated. As a range of different T cell

TABLE 1 Type of stimuli used in T-cell assays.

Population	Stimulation	Observed effect	Reference
human T lymphocytes	phytohemagglutinin (PHA)	PHA as a mitogen induces T lymphocyte proliferation	Ceuppens et al. (1988)
purified resting human T lymphocytes	ionomycin	ionomycin induces the proliferation of T lymphocytes	Chatila et al. (1989)
peripheral blood mononuclear cells (PBMC)	ionomycin + phorbol 12-myristate 13-acetate (PMA)	stimulation of T lymphocyte proliferation	Hou et al., (2018), Lehnert et al. (2014)
Total PBMC/purified T lymphocytes	concanavalin A (ConA)	stimulation of T lymphocyte proliferation	Arneth, (2010), Palacios (1982)
purified T lymphocytes (human and mouse)	lipopolysaccharides (LPS)	stimulation of T lymphocyte proliferation by triggering Toll-like receptor 4 (TLR4)	Zanin-Zhorov et al. (2007)
PBMC/purified T lymphocytes	anti-CD3/anti-CD28 antibodies	T lymphocyte proliferation due to activating antibodies that are typically directed against the T cell surface molecules CD3 and/or CD28	Jiao et al. (2019), Trickett and Kwan (2003)
PBMC (responder) vs. g-irradiated PBMC (stimulator)	mixed lymphocyte reaction (MLR) assay	proliferation of T lymphocytes due to HLA mismatching that triggers the activation of the responder PBMC, while the stimulator gamma-irradiated PBMC do not proliferate	Tomonari (1980), Yang et al. (2009)
PBMC	multidonor mixed lymphocyte reaction (mdMLR) assay	proliferation and activation of T lymphocytes due to HLA mismatching that triggers mutual activation of PBMC of the different donors	Madel et al. (2020), Pachler et al. (2017)

activating stimuli are used, the variety of available T cell assays is further multiplied. Consequently, comparison of the effects of PnD and adult MSC products on T cell proliferation becomes difficult when different stimuli are used. Frequently T cells are activated by the addition of mitogens, such as the lectin phytohemagglutinin (PHA) (Ceuppens et al., 1988), Ionomycin (Chatila et al., 1989; Hou et al., 2018) usually in combination with tumor promoting agents, such as phorbol 12-myristate 13-acetate (PMA) (Lehnert et al., 2014; Hou et al., 2018) or concanavalin A (ConA) (Palacios, 1982; Arneth, 2010); or by pro-inflammatory bacterial products such as lipopolysaccharides (LPS) (Zanin-Zhorov et al., 2007). Another strategy is based on T cell activating antibodies that are typically directed against the T cell surface molecules CD3 and/or CD28 (Trickett and Kwan, 2003; Jiao et al., 2019) (Figure 1A). Furthermore, T cells can be activated by allogenic cells, typically in mixed lymphocyte reaction (MLR) assays (Tomonari, 1980; Yang et al., 2009). Here, T cells of at least one given donor are co-cultured with immune cells of other allogenic donors, or with specific allogenic T cell response-inducing cell line cells. In classical MLR assays, T cell stimulating cells are regularly irradiated to inhibit their own proliferation (Sasazuki et al., 1976) (Figure 1A). However, assays have also been developed in which mononuclear cells, including T cells of multiple donors, have been combined for effective allogenic T cell activation (Pachler et al., 2017; Madel et al., 2020) (Table 1). Additional critical parameters in such assays are the numbers of seeded cells, the cells' seeding densities, the choice of the cell culture containers, the assay duration, and the cell culture media including their supplements, e.g., serum and/or recombinant cytokines.

For the selection of an appropriate T cell assay, it must be considered whether PnD or adult MSC products may act directly or indirectly on T cells. For example, it has been reported that MSC-EVs do not directly act on T cells; rather, they modulate the biology of co-cultured monocytes/macrophages by altering their secretome (Zhang et al., 2014; Zhang B. et al., 2018). Furthermore, dosing should be carefully considered. Ideally physiologically relevant concentrations of PND and adult MSC products should be applied in the functional assays. However, because MSC products may act in a complex cascade with different cellular targets (Gimona et al., 2021), it might be that *in vivo* their therapeutic activities are much more exponentiated than in given *in vitro* assays. Thus, *in vitro* experiments may require higher product doses than related *in vivo* applications.

The mode of activation of T cells is critical for their response to PnD or adult MSC product modulation (Kronsteiner et al., 2011). Mitogens act on several signaling pathways, some of which bypass the direct triggering of TCR and co-stimulatory molecules. This is the case, for example, with ionomycin, which induces intracellular calcium release and subsequent phospholipase C activation, hydrolysis of phosphoinositides and activation of Protein Kinase C (PKC) (Hossain et al., 2007). As mentioned before, ionomycin is usually used in combination with PMA, which is a specific activator of PKC, thus exerting a synergistic action (Lehnert et al., 2014; Hou et al., 2018). In contrast, ConA is an activator of the transcription factors Nuclear Factor of Activated T cells (NFAT), a family of transcription factors that are important in the development and function of the immune system, including TCR engagement (Bemer and Truffa-Bachi, 1996). PHA, can lead to rapid T cell activation by specifically binding to the Alpha-1,6-

TABLE 2 Mechanism of action of the different stimuli and possible readouts.

Population	Experimental procedure	Observed effect	Reference
naive Murine T-Cells	stimulation with ionomycin	Ionomycin induces intracellular calcium release and subsequent phospholipase C activation, hydrolysis of phosphoinositides and activation of Protein Kinase C (PKC)	Hossain et al. (2007)
PBMC	stimulation with PMA	PMA is a specific activator of PKC thus exerting a synergistic action	Hou et al. (2018), Lehnert et al. (2014)
purified mouse T lymphocytes	stimulation with ConA	ConA is an activator of Nuclear Factor of Activated T cells (NFAT), a family of transcription factors that are important in the development and function of the immune system, including TCR engagement	Bemer and Truffa-Bachi (1996)
mouse naive purified T lymphocytes	stimulation with PHA	PHA can lead to rapid T lymphocyte activation by specifically binding to the alpha-1,6-mannosylglycoprotein 6-beta-N-acetylglucosaminyltransferase (Mgat5) receptor expressed on the surface of T lymphocytes, thus triggering different signalling pathways that, in turn, induce the recruitment of TCRs and the activation of T lymphocytes	Demetriou et al. (2001)
purified T lymphocytes	staining with carboxyfluorescein diacetate succinimidyl ester (CFSE) or PKH	the proliferation rate of activated T lymphocytes is typically analysed after staining with fluorescent dyes, e.g. CFSE or PKH dyes, whose intensities decrease after cell division	Tario et al. (2011)
total PBMC/ purified T lymphocytes	evaluation of different activation markers by flow cytometry	cell surface molecules are established as being upregulated on activated T lymphocytes: these include the early activation marker CD69 and late activation markers, such as the IL-2 receptor (CD25) and the intercellular adhesion molecule 1 (ICAM-1; CD54)	Lindsey et al. (2007), Sancho et al. (1999)
PBMC	cytokine evaluation	production and release of cytokines as well as polarisation towards specific subsets indicate a functional change in T lymphocytes as a result of the stimulation received. By using bivalent antibodies, such changes can be monitored using flow cytometry. More frequently, however, the cytokine content in conditioned media is analysed by a conventional cytokine analysis method. Elispot assays, where cells are cultured on a membrane, allow quantification of cells secreting specific cytokines	Bueno et al. (2001)
PBMC/ purified T lymphocytes	analysis of Th subset polarization	PnDs are able to influence the differentiation of purified naïve T lymphocytes stimulated with monoclonal anti-CD3 and/or anti-CD28 antibodies, converting T lymphocyte development under Th1 or Th17 differentiation conditions towards development of CD4+ Th2 T lymphocytes	Liu et al. (2014), Pianta et al. (2015), Krampera et al. (2003)

Mannosylglycoprotein 6-Beta-N-Acetylglucosaminyltransferase (Mgat5) receptor expressed on the surface of T lymphocytes, thus triggering different signalling pathways that, in turn, induce the recruitment of TCRs and the activation of T lymphocytes (Demetriou et al., 2001) (Table 2 and Figure 1A). It has been estimated that the recruitment and clustering of approximately 8,000 TCRs is required to lead to the activation of T lymphocytes. However, it should also be emphasized that this stimulation mode is very different from the physiological activation obtained following stimulation with anti-CD3 and anti-CD28 antibodies or by allogenic stimulation. This number is significantly reduced when stimulation is performed with antibodies against CD3 and CD28 (Viola and Lanzavecchia, 1996). Thus, mitogen activation does not reflect the physiological situation and alters normal T cell functions including their differentiation and maturation capabilities from naïve to effector cells (Duarte et al., 2002; Maus et al., 2002). Consequently, activities recorded by such assays may not reflect the *in vivo* potency of PND and adult MSC products.

A common hallmark of the various type of T cell assays is that the T cells become activated and proliferate within these assays (Iritani et al., 2002; Obst, 2015). Coupled to the activation, T cell gene expression profile and cytokine secretion changes. Activation can also trigger the differentiation of naïve T lymphocytes as well as the polarization of naïve T cells towards different T effector cell subsets (Luckheeram et al., 2012). Different read outs are used to analyse T cell activation and proliferation. The proliferation rate of activated T cells is typically analysed after staining with fluorescent dyes, e.g., carboxyfluorescein diacetate succinimidyl ester (CFSE) or PKH dyes, whose intensities following labelling get mainly reduced by cell divisions (Tario et al., 2011). The fluorescence intensity of labelled cells is regularly monitored by flow cytometry (Figure 1B). Depending on the purpose of the experiment, more complex cell surface analyses can be performed. For example, by using a selection of different antibodies, the resolution of such assays can be increased in order to study cell proliferation of specific T cell subsets. Flow cytometry can be also informative without exploring the proliferation history of respective T cells. For example, activation of T cells results in their cell growth being

accompanied by changes in their light scattering features. Furthermore, a couple of different cell surface molecules are established as being upregulated on activated T cells. These include the early activation marker CD69 (Lindsey et al., 2007) and later activation markers, such as the IL-2 receptor (CD25) and the intercellular adhesion molecule 1 (ICAM-1; CD54) (Sancho et al., 1999) (Table 2 and Figure 1C).

Although T cell proliferation assays or analyses of the T cell activation status are frequently used for studying the impacts of PnD and adult MSC products, the expectation that all therapeutically relevant products result in a suppression of T cell proliferation or in efficient inactivation of T cells might not necessarily be true and, indeed, has been challenged by several groups. For example, it has been shown that following primary activation of CD69 via the canonical NFκB signalling pathway, MSCs can promote its expression in a non-canonical manner. In the absence of MSCs, at a later stage, canonical NFκB signalling apparently contributes to the reduction of CD69 expression. Thus, canonical NFκB signalling plays a dual role, i.e. at the early stage it activates and at a later stage it terminates the expression of CD69. Apparently, the later function can be suppressed by MSCs (Saldanha-Araujo et al., 2012) (Table 2).

Following activation, T cells also change their cytokine secretion. Indeed, the production and release of cytokines as well as polarisation towards specific subsets are indicative for a functional change in T lymphocytes as a result of the stimulation received. By using bivalent antibodies, such changes can be monitored flow cytometrically (Bueno et al., 2001). More frequently, however, the cytokine content in conditioned media is analyzed by a conventional cytokine analysis method. Elispot assays, in which cells are cultured on a membrane, allow quantification of cells secreting specific cytokines. Notably, if T cells are cultured in the presence of other immune cells, changes in the concentration of the cytokines in cell supernatants may also be caused by non-T cells (Table 2).

The variability in performing T cell activation assays is amplified by the PnD and adult MSC products to be tested. If the function of cellular products should be evaluated, cell culture conditions need to be used which are permissive for the cells to be explored and the T cell containing cell fraction. In contrast, EV and other secretome products can be added to T cells cultured under optimal growth conditions.

The activation of T lymphocytes following the use of different stimuli is a fundamental prerequisite to not only trigger proliferation, but also for the differentiation of naïve T lymphocytes and their polarization towards effector subsets. In fact, PnD and adult MSC products have been reported to affect the differentiation of naïve T lymphocytes towards effector and memory subsets (Liu et al., 2014; Pianta et al., 2015). PnDs were also shown to influence the differentiation of purified naïve T lymphocytes, especially, they could convert T cell development under Th1 or Th17 differentiation conditions towards development of $CD4^+$ Th2 T lymphocytes (Krampera et al., 2003; Liu et al., 2014) (Figure 1D). Such impacts on T cell polarization and differentiation can be stimulus dependent, for example MSC secretome products could polarize T cells towards Tregs when stimulated by allogenic antigen presenting cells (APCs), but not if T cells were activated anti-CD3 and anti-CD28 antibodies (Zhang S. et al., 2018) (Table 2 and Figure 1D).

We are aware there are many other parameters that essentially influence the outcome in T cell assays and that would be worthy of discussion, e.g., the co-incubation time of PnD and adult MSC products and T cells. While further refining such assays, there might even be other parameters we are not yet aware of that could essentially affect given readouts.

Monocyte and macrophage assays

Macrophages and their progenitors, the monocytes, are cells of innate immunity and are involved in the maintenance of tissue homeostasis (Wynn and Vannella, 2016). During tissue injury or infection, macrophages are triggered to phagocytose microbes (Wynn and Vannella, 2016), secrete pro-inflammatory factors that initiate inflammation, and recruit other immune cells to the site of injury/infection. As the insult is cleared, macrophages participate in tissue regeneration by secreting anti-inflammatory/tolerogenic factors that facilitate regenerative processes such as angiogenesis and proliferation, critical for tissue repair and regeneration (Wynn and Vannella, 2016). This functional plasticity of the macrophages has been conceptualized as macrophage polarization, with pro-inflammatory macrophages termed classically activated or M1 macrophages, and anti-inflammatory macrophages termed alternatively activated or M2 macrophages (Mills et al., 2000). Moreover, whilst beyond the scope of this review, M2 macrophages show a high complexity and can be divided into four major types based on their roles: M2a, M2b, M2c and M2d (Murray et al., 2014; Xue et al., 2014) (Figure 2B).

Since macrophages play decisive roles in controlling defence or regenerative immune responses and also are involved in the physiopathology of many diseases, they are the cell type of choice for many research groups in evaluating the immunomodulatory capability of therapeutic cells and their products. In this sense, and similar to the T cells, biological assays employing monocytic cell lines or primary cells should be developed to assess and better characterize the effect of PnD or adult MSC products on these immune cells. In this sense, to set up a biological assay, the choice of a cell line or primary cells is crucial, as it is a compromise between translationality and reproducibility. While primary cells may better reflect the MoA of a product *in vivo*, high variability between donors may hinder the development of a standardized assay, while the opposite is true for cell lines.

In terms of cell lines, human THP-1 monocytic and murine RAW 264.7 macrophage cells, and as primary cells, human

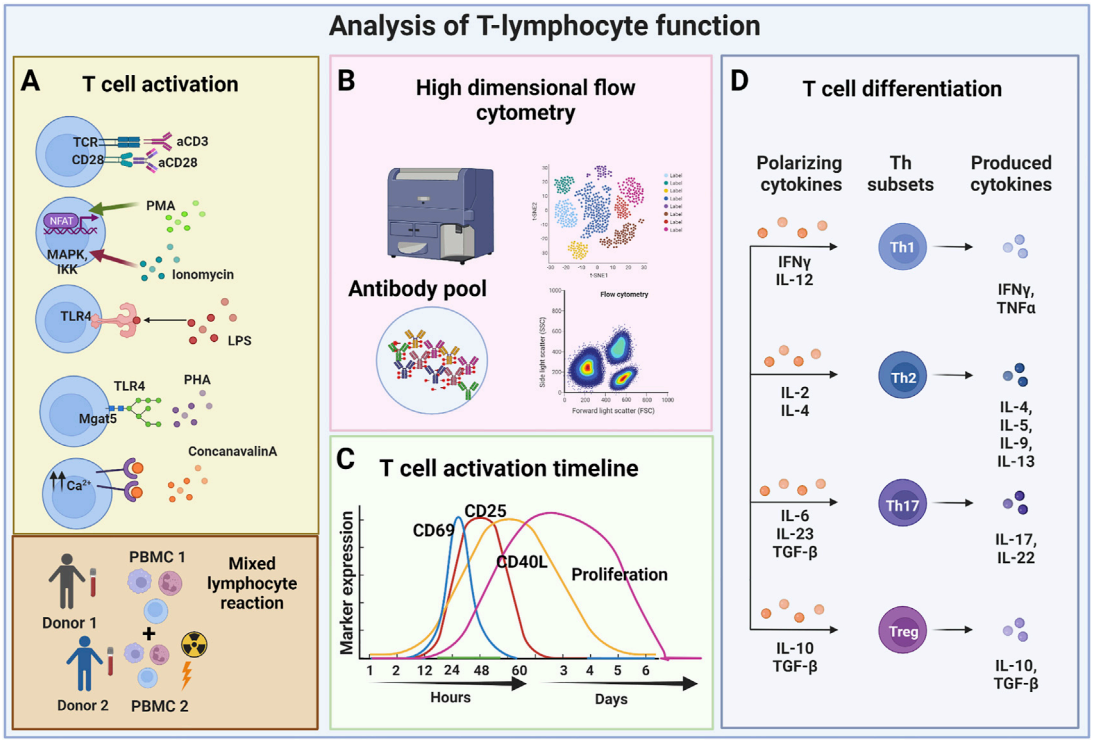

FIGURE 1
Analysis of T-lymphocyte function. **(A)** T lymphocytes can be activated using various stimuli including monoclonal antibodies (stimulation with anti-CD3 anti-CD28), and mitogens, such as PMA frequently used in combination with ionomycin. Other modes of stimulation include the use of lipopolysaccharides that triggers TLR4 activation (thus mimicking the bacterial stimulus), and causing the release of PHA that induces the recruitment of TCRs consequently activating T lymphocytes. Finally, T lymphocytes can also be stimulated by ConA, which causes the release of intracellular Ca^{2+} that triggers the calcium cascade, and by mixed lymphocyte reactions which are based on the allogeneic response determined by HLA mismatching between two different donors. **(B)** Depending on the considered mechanism of action, different readout methods are used. Flow cytometry can perform in-depth immune-phenotype analyses. **(C)** Various markers can be used to analyze T cell activity in given assays, some being selectively expressed at specific timepoints following T cell activation. **(D)** The functional polarization of T lymphocytes can be triggered with different combinations of cytokines towards different CD4 Th subsets or towards different CD8 memory T cell subsets. Cytokine analyses provide important information about resulting T cell functions. (Created with BioRender.com).

peripheral blood monocytes or murine bone marrow-derived monocytes are most frequently used. Primary monocytes can be efficiently differentiated into macrophages (or dendritic cells) using selective cytokine cocktails, typically either containing GM-CSF (+IL-4) or M-CSF. Of note, and highly compromising standardization, most laboratories have their own strategies to prepare, culture and stimulate their monocytic cells or macrophages.

Monocytes and macrophages are most frequently stimulated with interferon (IFN)-γ and LPS to polarize them towards pro-inflammatory M1 macrophages or with IL-4 and IL-13 for obtaining anti-inflammatory M2 macrophages (Figure 2B). In addition, a huge variety of other stimulatory molecules are used for functional activation—including TLR agonists, nucleotide derivatives, glucocorticoids, and antibody-Fc receptor stimulation (Murray et al., 2014). It is however important to note that different polarization programs may be initiated, depending on the stimulus, and macrophages may not polarize solely into M1 or M2 phenotypes (Xue et al., 2014). In order to characterize the macrophage subpopulations, flow cytometric analysis is commonly performed to assess CD80 and CD86 positivity for pro-inflammatory M1 polarisation, and for CD163 or CD206 positivity for anti-inflammatory M2 polarisation. Often, released cytokines are also analysed, with IL-1β and TNF-α considered to be markers of pro-inflammatory M1 macrophage function, and with Arginase (Arg)-1, IL-10, and Retnlα as markers for anti-inflammatory M2 macrophage function (Figures 2C,D).

However, it is noteworthy to mention that many of the murine markers have not been translated to human macrophages and that there are markers that are only present in murine cells while others are only present in human cells (Murray et al., 2014). In this sense, murine macrophages are strong producers of NO in response to LPS stimulation, while human macrophages barely produce NO (Padgett and Pruett, 1992). Moreover, both mouse and human macrophages are able

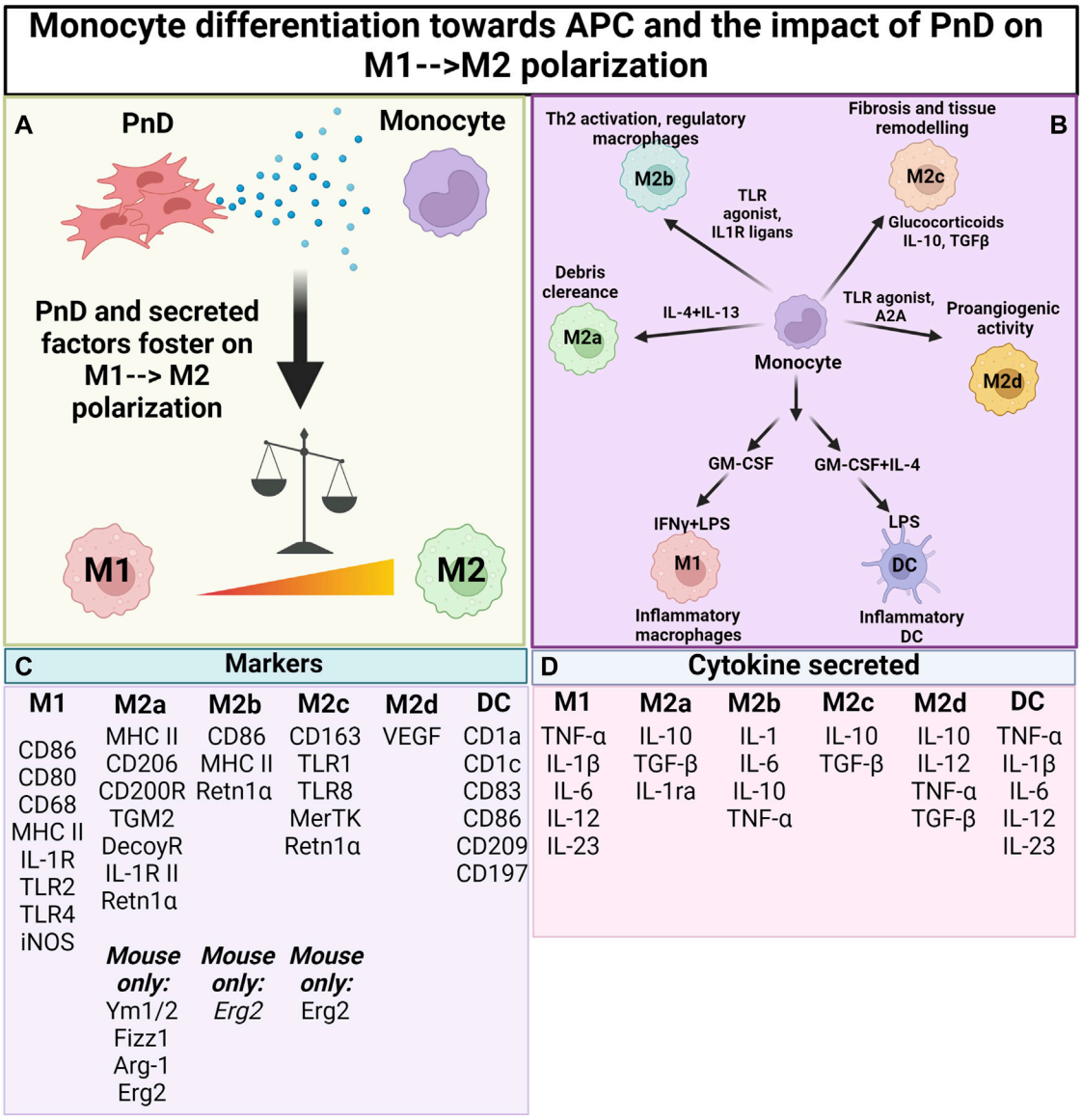

FIGURE 2
Impact of PnD on monocyte differentiation towards antigen presenting cells. **(A)** Perinatal Derivatives (PnD) and their secreted factors impact monocyte differentiation towards antigen presenting cells fostering the acquisition of phenotype and functional features typical of M2 macrophages. **(B)** Depending on the factors present in the microenvironment monocytes can be discriminated into different subsets of M2 macrophages (M2a, M2b, M2c and M2d) each of them being characterized by peculiar functions. **(C)** Summary table for the markers specific for macrophage and DC subsets. **(D)** Summary table for the cytokines released by the different macrophage/DC subsets. (Created with BioRender.com).

to express Arg-1, but only the latter secrete it (de Boniface et al., 2012). To add to the complexity, even though Arg-1 is usually considered to be an M2 marker, M1 macrophages can also express this enzyme and the same is true for IL-6 in mouse cells (Murray et al., 2014). As a consequence, more than one marker should be assessed to define the macrophage subpopulation. When studying human monocytes and macrophages, typically CD206 is used as a cell surface marker protein reflecting M2 type monocytes and macrophages. In mouse, Erg2 has recently been suggested as a reliable marker for flow cytometric analysis (Jablonski et al., 2015). Likewise, one should realize that the most extreme M1 and M2 macrophage polarisation stages that can be obtained in *in vitro* experiments only rarely occur *in vivo*, where polarisation—and subsequent immune function—is highly dependent on tissue/disease-derived environmental cues and on the interaction with other immune cells (Quarta et al., 2020; 2021a) (Figure 2; Table 3).

Previous studies have noted the immunomodulatory capabilities of MSCs and their secreted EV products on enhancing M2 over M1 macrophage polarization facilitate tissue repair (Zhang B. et al., 2018; Willis et al., 2018; Luo et al., 2021; Chuah et al., 2022). In this sense, MSC-EVs have been reported to modulate the macrophage

TABLE 3 Macrophage polarization analysis.

Experimental model	Observed Effects	References
PBMC or purified monocytes	CD80 and CD86 positivity for pro-inflammatory M1 polarisation; CD163 or CD206 positivity for anti-inflammatory M2 polarisation	Murray et al. (2014), Xue et al. (2014)
PBMC or purified monocytes	cytokine analysis where IL-1β and TNF-α are considered to be markers of pro-inflammatory M1 macrophage function, IL-10 is considered a marker of M2 macrophage induction	Murray et al. (2014), Xue et al. (2014)
PBMC or purified monocytes	gene expression analysis for genes canonically expressed by M1 or M2 macrophages like iNOS, Arginase 1, Retn1a	Murray et al. (2014), Xue et al. (2014)
PBMC or purified monocytes	mMurine macrophages are strong producers of NO in response to LPS stimulation, while human macrophages barely produce NO. Both mouse and human macrophages are able to express Arg-1	Padgett and Pruett (1992), de Boniface et al. (2012)
Bone marrow derived macrophages	Erg2 is a new marker for flow cytometry analysis	Jablonski et al. (2015)
RAW 264.7 cells	MSC-EVs have been reported to modulate macrophage phenotypes in several injuries and diseases such as severe asthma	Dong et al. (2021)
Macrophage polarization in a mouse model of bronchopulmonary dysplasia	MSC-EVs have been reported to modulate macrophage phenotypes in several injuries and diseases such as bronchopulmonary dysplasia	Willis et al. (2018)
RAW 264.7 cells	MSC-EVs have been reported to modulate macrophage phenotypes in several injuries and diseases such as skeletal muscle contusion	Luo et al. (2021)
Macrophage polarization in a rat osteochondral defect model	MSC-EVs have been reported to modulate macrophage phenotypes in several injuries and diseases such as cartilage/bone defect	Zhang Chuah et al. (2018)
THP1 cells	MSC-EVs activate TLR4 in a MYD88-dependent pathway through Fibronectin Containing Extra Domain A (FN-EDA)	Zhang et al. (2014b)
RAW 264.7 cells	MSC-EVs inhibit IL-6 secretion in LPS-stimulated macrophages (RAW 264.7 cells)	Pacienza et al. (2019)

phenotypes in several injuries and diseases such as severe asthma (Dong et al., 2021), bronchopulmonary dysplasia (Willis et al., 2018), skeletal muscle contusion (Luo et al., 2021) and cartilage/bone defects (Zhang B. et al., 2018). This implicates the role of macrophages as the therapeutic target of MSCs and their EVs in tissue repair. Consistently, depletion of macrophages abolished the therapeutic effects of MSCs in tissue repair (Luo et al., 2021). Thus, these findings support and should encourage the use of macrophages for the development of *in vitro* cell-based assays to assess the immunomodulatory capabilities also of PnD products, especially in pathologies where this immune cell type plays major roles. Nevertheless, referring to the tissue-dependent context where macrophages reside, most of the currently applied macrophage polarisation studies (and influence of potential modulators thereon) lack a tissue-specific context. For example, it has recently been demonstrated using murine iPSC-derived macrophages—and further confirmed *in vivo*—that both M1 and M2 polarisation is highly influenced by neural environments (Quarta et al., 2019; Quarta et al., 2021b).

Regarding the modulation of monocyte/macrophage polarisation by PnD and adult MSC products, like that of T cell polarisation, the observed effect is dependent on the stimuli applied to the cells. For instance, it was previously reported that MSC-EVs activate TLR4 in a MYD88-dependent pathway in THP-1 cells through Fibronectin Containing Extra Domain A (FN-EDA) being present in the secretome (Zhang et al., 2014). Unlike LPS which activates TLR4 in the same pathway, MSC-EVs did not induce the expression of pro-inflammatory cytokines, but instead induce the expression of anti-inflammatory cytokines, such as IL-10. This phenomenon was reproducible in primary human and mouse monocytes. Therefore, the design and implementation of an *in vitro* macrophage polarization assay with the relevant functional endpoints should allow the exploration of PnD and adult MSC products on macrophage polarization. Considering their impact on macrophages, as one of the key immunomodulatory functions of PnD and adult MSC products, such assays should also enable the search for critical PnD and adult MSC attributes that manifest their therapeutic potency (Figure 2A).

Of note, an *in vitro* assay has recently been established using RAW 264.7 cells for the assessment of anti-inflammatory activities of given MSC-EV products. The assay documents the ability of MSC-EV preparations to inhibit IL-6 secretion in LPS-stimulated macrophages. Interestingly, this RAW 264.7 cell-based assay showed that different MSC-EV batches vary in their macrophage polarisation abilities, and that its activity predictions correlate with their documented *in vivo* functions obtained in a mouse model of LPS-induced systemic inflammation (Pacienza et al., 2019). Furthermore, as with the activation, suppression or polarisation of T cells, developing novel assays in which the downstream effect of polarised macrophages (e.g., by addition of PnD or adult MSC products) is investigated on T cell function is highly advisable. Such studies could help to elucidate cross talks between the innate and adaptive immune systems whose dysregulation can result in the adoption of inflammatory and autoimmune diseases (Figure 2A; Table 3).

How to identify the right assay

Due to the high number of variables and the fact that each disease may require specific therapeutic activities, it is hard to provide any concrete recommendations for a certain assay type. Considering product heterogeneity, it may be best for the establishment and validation of appropriate assays, if products manufactured in the same standardized manner are available that differ in their clinical or preclinical potency to improve symptoms in a given disease model. Assay candidates should provide the same prediction for an assumed MoA as observed *in vivo*. To this end, as elaborated in a recent position paper on potency testing of MSC-EV products (Gimona et al., 2021), it might be that the MoA requires the combined action of different biological activities, the so called MoA attributes. If different MoA attributes are required for defining the therapeutic potency of PnD and adult MSC products, an array matrix consisting of several potency assays may become required for appropriate potency testing of respective drugs (https://www.fda.gov/media/79856/down) (Chinnadurai et al., 2018; Gimona et al., 2021).

When using primary cells as test cell type, donor-to-donor variations in the reactivity of the assay cells, e.g., the T cells and macrophages, need to be considered. Cell lines might be altered so substantially that they do no longer allow monitoring of the given cell activity. Moreover, knowing the pathophysiology of a given disease and the role that each immune cell plays is critical to choose the right cell type to assess the activity of a given PnD and adult MSC product. Having identified an *in vitro* assay reflecting the *in vivo* potency of the PnD or adult MSC products, it needs to be considered whether or not the assay can be qualified as a potency assay. Of note, functional assays providing information about the potency of given PnD or adult MSC products are not automatically potency assays. The term Potency Assay is a regulatory authority term and deciphers an assay which had been standardized and qualified to be very reproducible. As elaborated in a recent white paper (Gimona et al., 2021), a potency assay needs to be designed and to predict the therapeutic effectiveness of the drug substance in accordance with the International Council for Harmonisation of Technical Requirements for Pharmaceuticals for Human Use (ICH) guidelines. Due to the variation of the biology of primary cells, setting up potency assays based on primary cells is very challenging (Gimona et al., 2021). Here, cell lines might be the better choice, providing that they are able to recapitulate the MoA of the PnD or adult MSC products that are required to alleviate the disease. Although still in its infancy, replacement of monocytic cell lines with standardized batches of human iPSC-derived monocytes/macrophages may well become part in future potency assay development. Setting up the appropriate potency assays remains a major challenge in the field of therapeutic development of PnD and adult MSC products. Although the use of animal cells for testing of human therapeutics remains controversial, murine immune cell lines such as the RAW 264.7 cells remain to date widely be used for testing the immunomodulatory potential of MSCs and their products (Zampetaki et al., 2004; Pacienza et al., 2019; Malvicini et al., 2022).

Conclusion

As exemplified by the decision of the US FDA to not provide market approval to remestemcel-L, potency testing of cellular and secretome based drugs, including PnD and adult MSC products, is a central task for the future. Although many functional activities can be read out in available assays, it is necessary to confirm that these activities reflect actual MoA attributes that are required to reduce pathophysiological symptoms in given diseases. A functional assay reflecting such MoA attributes, and thus the potency of PnD and adult MSC products, is not automatically a potency assay. A potency assay has to fulfill several regulatory requirements. We envisage that the establishment of appropriate potency tests will remain a major challenge in the cell and EV-based therapeutic field.

Author contributions

All authors listed have made a substantial, direct, and intellectual contribution to the work and approved it for publication.

Funding

This work contributes to the COST Action CA17116 International Network for Translating Research on Perinatal Derivatives into Therapeutic Approaches (SPRINT), supported by COST (European Cooperation in Science and Technology). This work was partially supported by the European Union's Horizon 2020 research and innovation programme under grant agreement Nos 779293-HIPGEN and 814495-EVPRO, the Italian Ministry of Research and University (MIUR, 5x1000), and Contributi per il funzionamento degli Enti privati che svolgono attivitá di ricerca - C.E.P.R. (2020-2021).

Conflict of interest

The authors declare that the research was conducted in the absence of any commercial or financial relationships that could be construed as a potential conflict of interest.

Publisher's note

All claims expressed in this article are solely those of the authors and do not necessarily represent those of their

affiliated organizations, or those of the publisher, the editors and the reviewers. Any product that may be evaluated in this article, or claim that may be made by its manufacturer, is not guaranteed or endorsed by the publisher.

References

Abraham, R. T., and Weiss, A. (2004). Jurkat T cells and development of the T-cell receptor signalling paradigm. *Nat. Rev. Immunol.* 4 (4), 301–8. doi:10.1038/nri1330

Arneth, B. M. (2010). Measurement of T cell activation after 16-hr *in vitro* stimulation with concanavalin A. *Curr. Protoc. Cytom.* 6, 1–10. doi:10.1002/0471142956.cy0628s51

Bai, F., Zhang, P., Fu, Y., Chen, H., Zhang, M., Huang, Q., et al. (2020). Targeting ANXA1 abrogates Treg-mediated immune suppression in triple-negative breast cancer. *J. Immunother. Cancer* 8 (1), e000169. doi:10.1136/jitc-2019-000169

Bailo, M., Soncini, M., Vertua, E., Signoroni, P. B., Sanzone, S., Lombardi, G., et al. (2004). Engraftment potential of human amnion and chorion cells derived from term placenta. *Transplantation* 78 (10), 1439–1448. doi:10.1097/01.tp.0000144606.84234.49

Balza, E., Piccioli, P., Carta, S., Lavieri, R., Gattorno, M., Semino, C., et al. (2016). Proton pump inhibitors protect mice from acute systemic inflammation and induce long-term cross-tolerance. *Cell. Death Dis.* 7 (7), e2304. doi:10.1038/cddis.2016.218

Baron, F., and Storb, R. (2012). Mesenchymal stromal cells: A new tool against graft-versus-host disease? *Biol. Blood Marrow Transpl.* 18 (6), 822–840. doi:10.1016/j.bbmt.2011.09.003

Bartholomew, A., Sturgeon, C., Siatskas, M., Ferrer, K., McIntosh, K., Patil, S., et al. (2002). Mesenchymal stem cells suppress lymphocyte proliferation *in vitro* and prolong skin graft survival *in vivo*. *Exp. Hematol.* 30 (1), 42–48. doi:10.1016/s0301-472x(01)00769-x

Bemer, V., and Truffa-Bachi, P. (1996). T cell activation by concanavalin A in the presence of cyclosporin A: Immunosuppressor withdrawal induces NFATp translocation and interleukin-2 gene transcription. *Eur. J. Immunol.* 26 (7), 1481–1488. doi:10.1002/eji.1830260712

Boothby, I. C., Cohen, J. N., and Rosenblum, M. D. (2020). Regulatory T cells in skin injury: At the crossroads of tolerance and tissue repair. *Sci. Immunol.* 5 (47), eaaz9631. doi:10.1126/sciimmunol.aaz9631

Börger, V., Bremer, M., Ferrer-Tur, R., Gockeln, L., Stambouli, O., Becic, A., et al. (2017). Mesenchymal stem/stromal cell-derived extracellular vesicles and their potential as novel immunomodulatory therapeutic agents. *Int. J. Mol. Sci.* 18 (7), 1450. doi:10.3390/ijms18071450

Bruno, S., Grange, C., Deregibus, M. C., Calogero, R. A., Saviozzi, S., Collino, F., et al. (2009). Mesenchymal stem cell-derived microvesicles protect against acute tubular injury. *J. Am. Soc. Nephrol.* 20 (5), 1053–1067. doi:10.1681/ASN.2008070798

Bueno, C., Almeida, J., Alguero, M. C., Sánchez, M. L., Vaquero, J. M., Laso, F. J., et al. (2001). Flow cytometric analysis of cytokine production by normal human peripheral blood dendritic cells and monocytes: Comparative analysis of different stimuli, secretion-blocking agents and incubation periods. *Cytometry* 46 (1), 33–40. doi:10.1002/1097-0320(20010215)46:1<33:aid-cyto1035>3.0.co;2-s

Caplan, A. I. (1991). Mesenchymal stem cells. *J. Orthop. Res.* 9 (5), 641–650. doi:10.1002/jor.1100090504

Caplan, A. I. (2017). New MSC: MSCs as pericytes are sentinels and gatekeepers. *J. Orthop. Res.* 35 (6), 1151–1159. doi:10.1002/jor.23560

Ceuppens, J. L., Baroja, M. L., Lorre, K., Van Damme, J., and Billiau, A. (1988). Human T cell activation with phytohemagglutinin. The function of IL-6 as an accessory signal. *J. Immunol.* 141 (11), 3868–3874.

Chatila, T., Silverman, L., Miller, R., and Geha, R. (1989). Mechanisms of T cell activation by the calcium ionophore ionomycin. *J. Immunol.* 143 (4), 1283–1289.

Chinnadurai, R., Rajan, D., Qayed, M., Arafat, D., Garcia, M., Liu, Y., et al. (2018). Potency analysis of mesenchymal stromal cells using a combinatorial assay matrix approach. *Cell. Rep.* 22 (9), 2504–2517. doi:10.1016/j.celrep.2018.02.013

Chuah, S. J., Yong, C. W., Teo, K. Y. W., Chew, J. R. J., Cheow, Y. A., Zhang, S., et al. (2022). Mesenchymal stromal cell-derived small extracellular vesicles modulate macrophage polarization and enhance angio-osteogenesis to promote bone healing. *Genes. Dis.* 9 (4), 841–844. doi:10.1016/j.gendis.2021.11.012

De Biasi, S., Tartaro, D. L., Gibellini, L., Paolini, A., Quong, A., Petes, C., et al. (2021). Endogenous control of inflammation characterizes pregnant women with asymptomatic or paucisymptomatic SARS-CoV-2 infection. *Nat. Commun.* 12 (1), 4677. doi:10.1038/s41467-021-24940-w

de Boniface, J., Mao, Y., Schmidt-Mende, J., Kiessling, R., and Poschke, I. (2012). Expression patterns of the immunomodulatory enzyme arginase 1 in blood, lymph nodes and tumor tissue of early-stage breast cancer patients. *Oncoimmunology* 1 (8), 1305–1312. doi:10.4161/onci.21678

Demetriou, M., Granovsky, M., Quaggin, S., and Dennis, J. W. (2001). Negative regulation of T-cell activation and autoimmunity by Mgat5 N-glycosylation. *Nature* 409 (6821), 733–739. doi:10.1038/35055582

Di Nicola, M., Carlo-Stella, C., Magni, M., Milanesi, M., Longoni, P. D., Matteucci, P., et al. (2002). Human bone marrow stromal cells suppress T-lymphocyte proliferation induced by cellular or nonspecific mitogenic stimuli. *Blood* 99 (10), 3838–3843. doi:10.1182/blood.v99.10.3838

Dominici, M., Le Blanc, K., Mueller, I., Slaper-Cortenbach, I., Marini, F., Krause, D., et al. (2006). Minimal criteria for defining multipotent mesenchymal stromal cells. The International Society for Cellular Therapy position statement. *Cytotherapy* 8 (4), 315–317. doi:10.1080/14653240600855905

Dong, B., Wang, C., Zhang, J., Zhang, J., Gu, Y., Guo, X., et al. (2021). Exosomes from human umbilical cord mesenchymal stem cells attenuate the inflammation of severe steroid-resistant asthma by reshaping macrophage polarization. *Stem Cell. Res. Ther.* 12 (1), 204. doi:10.1186/s13287-021-02244-6

Duarte, R. F., Chen, F. E., Lowdell, M. W., Potter, M. N., Lamana, M. L., Prentice, H. G., et al. (2002). Functional impairment of human T-lymphocytes following PHA-induced expansion and retroviral transduction: Implications for gene therapy. *Gene Ther.* 9 (20), 1359–1368. doi:10.1038/sj.gt.3301807

Dunn, C. M., Kameishi, S., Grainger, D. W., and Okano, T. (2021). Strategies to address mesenchymal stem/stromal cell heterogeneity in immunomodulatory profiles to improve cell-based therapies. *Acta Biomater.* 133, 114–125. doi:10.1016/j.actbio.2021.03.069

Friedenstein, A. J., Petrakova, K. V., Kurolesova, A. I., and Frolova, G. P. (1968). Heterotopic of bone marrow. Analysis of precursor cells for osteogenic and hematopoietic tissues. *Transplantation* 6 (2), 230–247. doi:10.1097/00007890-196803000-00009

Fung, T. H. W., Yang, K. Y., and Lui, K. O. (2020). An emerging role of regulatory T-cells in cardiovascular repair and regeneration. *Theranostics* 10 (20), 8924–8938. doi:10.7150/thno.47118

Galipeau, J., Krampera, M., Barrett, J., Dazzi, F., Deans, R. J., Joost, D. B., et al. (2016). International Society for Cellular Therapy perspective on immune functional assays for mesenchymal stromal cells as potency release criterion for advanced phase clinical trials. *Cytotherapy* 18 (2), 151–159. doi:10.1016/j.jcyt.2015.11.008

Galipeau, J. (2013). The mesenchymal stromal cells dilemma--does a negative phase III trial of random donor mesenchymal stromal cells in steroid-resistant graft-versus-host disease represent a death knell or a bump in the road? *Cytotherapy* 15 (1), 2–8. doi:10.1016/j.jcyt.2012.10.002

Galipeau, Jacques, Krampera, Mauro, Leblanc, Katarina, Nolta, Jan A., Phinney, Donald G., Shi, Yufang, et al. (2021). Mesenchymal stromal cell variables influencing clinical potency: The impact of viability, fitness, route of administration and host predisposition. *Cytotherapy* 23 (5), 368–372. doi:10.1016/j.jcyt.2020.11.007

Gao, J., Dennis, J. E., Muzic, R. F., Lundberg, M., and Caplan, A. I. (2001). The dynamic *in vivo* distribution of bone marrow-derived mesenchymal stem cells after infusion. *Cells Tissues Organs* 169 (1), 12–20. doi:10.1159/000047856

Gimona, M., Brizzi, M. F., Choo, A. B. H., Dominici, M., Davidson, S. M., Grillari, J., et al. (2021). Critical considerations for the development of potency tests for therapeutic applications of mesenchymal stromal cell-derived small extracellular vesicles. *Cytotherapy* 23 (5), 373–380. doi:10.1016/j.jcyt.2021.01.001

Gnecchi, M., He, H., Liang, O. D., Melo, L. G., Morello, F., Mu, H., et al. (2005). Paracrine action accounts for marked protection of ischemic heart by Akt-modified mesenchymal stem cells. *Nat. Med.* 11 (4), 367–368. doi:10.1038/nm0405-367

Gnecchi, M., He, H., Noiseux, N., Liang, O. D., Zhang, L., Morello, F., et al. (2006). Evidence supporting paracrine hypothesis for Akt-modified mesenchymal stem cell-mediated cardiac protection and functional improvement. *FASEB J.* 20 (6), 661–669. doi:10.1096/fj.05-5211com

Green, S., Politis, M., Rallis, K. S., Saenz de Villaverde Cortabarria, A., Efthymiou, A., Mureanu, N., et al. (2021). Regulatory T cells in pregnancy adverse outcomes: A systematic review and meta-analysis. *Front. Immunol.* 12, 737862. doi:10.3389/fimmu.2021.737862

Hill, G. R. (2009). Inflammation and bone marrow transplantation. *Biol. Blood Marrow Transpl.* 15, 139–141. doi:10.1016/j.bbmt.2008.11.008

Hossain, Mohammad, Giver, Cynthia R., and Waller., Ned (2007). Short-term ionomycin exposure activates naive murine T-cells and induces a rapid phenotypic shift to memory T-cell status: Potential for use as a method to reduce GvHD activity of allogeneic T-cells. *Blood* 110 (11), 2182. doi:10.1182/blood.V110.11.2182.2182

Hou, H., Zhou, Y., Yu, J., Mao, L., Bosco, M. J., Wang, J., et al. (2018). Establishment of the reference intervals of lymphocyte function in healthy adults based on IFN-γ secretion assay upon phorbol-12-myristate-13-acetate/ionomycin stimulation. *Front. Immunol.* 9, 172. doi:10.3389/fimmu.2018.00172

Iritani, B. M., Delrow, J., Grandori, C., Gomez, I., Klacking, M., Carlos, L. S., et al. (2002). Modulation of T-lymphocyte development, growth and cell size by the Myc antagonist and transcriptional repressor Mad1. *Embo J.* 21 (18), 4820–4830. doi:10.1093/emboj/cdf492

Jablonski, K. A., Amici, S. A., Webb, L. M., Ruiz-Rosado Jde, D., Popovich, P. G., Partida-Sanchez, S., et al. (2015). Novel markers to delineate murine M1 and M2 macrophages. *PLoS One* 10 (12), e0145342. doi:10.1371/journal.pone.0145342

Jiao, J., Zhao, X., Hou, R., Wang, Y., Chang, W., Liang, N., et al. (2019). Comparison of two commonly used methods for stimulating T cells. *Biotechnol. Lett.* 41 (12), 1361–1371. doi:10.1007/s10529-019-02743-w

Kebriaei, P., Hayes, J., Daly, A., Uberti, J., Marks, D. I., Soiffer, R., et al. (2020). A phase 3 randomized study of remestemcel-L versus placebo added to second-line therapy in patients with steroid-refractory acute graft-versus-host disease. *Biol. Blood Marrow Transpl.* 26 (5), 835–844. doi:10.1016/j.bbmt.2019.08.029

Khan, U., and Ghazanfar, H. (2018). T lymphocytes and autoimmunity. *Int. Rev. Cell. Mol. Biol.* 341, 125–168. doi:10.1016/bs.ircmb.2018.05.008

Kordelas, L., Rebmann, V., Ludwig, A. K., Radtke, S., Ruesing, J., Doeppner, T. R., et al. (2014). MSC-Derived exosomes: A novel tool to treat therapy-refractory graft-versus-host disease. *Leukemia* 28 (4), 970–973. doi:10.1038/leu.2014.41

Krampera, M., Glennie, S., Dyson, J., Scott, D., Laylor, R., Simpson, E., et al. (2003). Bone marrow mesenchymal stem cells inhibit the response of naive and memory antigen-specific T cells to their cognate peptide. *Blood* 101 (9), 3722–3729. doi:10.1182/blood-2002-07-2104

Krampera, M., and Le Blanc, K. (2021). Mesenchymal stromal cells: Putative microenvironmental modulators become cell therapy. *Cell. Stem Cell.* 28 (10), 1708–1725. doi:10.1016/j.stem.2021.09.006

Kronsteiner, B., Wolbank, S., Peterbauer, A., Hackl, C., Redl, H., van Griensven, M., et al. (2011). Human mesenchymal stem cells from adipose tissue and amnion influence T-cells depending on stimulation method and presence of other immune cells. *Stem Cells Dev.* 20 (12), 2115–2126. doi:10.1089/scd.2011.0031

Kumar, B. V., Connors, T. J., and Farber, D. L. (2018). Human T cell development, localization, and function throughout life. *Immunity* 48 (2), 202–213. doi:10.1016/j.immuni.2018.01.007

Kurtzberg, J., Abdel-Azim, H., Carpenter, P., Chaudhury, S., Horn, B., Mahadeo, K., et al. (2020a). A phase 3, single-arm, prospective study of remestemcel-L, *ex vivo* culture-expanded adult human mesenchymal stromal cells for the treatment of pediatric patients who failed to respond to steroid treatment for acute graft-versus-host disease. *Biol. Blood Marrow Transpl.* 26 (5), 845–854. doi:10.1016/j.bbmt.2020.01.018

Kurtzberg, J., Prockop, S., Chaudhury, S., Horn, B., Nemecek, E., Prasad, V., et al. (2020b). Study 275: Updated expanded access program for remestemcel-L in steroid-refractory acute graft-versus-host disease in children. *Biol. Blood Marrow Transpl.* 26 (5), 855–864. doi:10.1016/j.bbmt.2020.01.026

Lai, R. C., Arslan, F., Lee, M. M., Sze, N. S., Choo, A., Chen, T. S., et al. (2010). Exosome secreted by MSC reduces myocardial ischemia/reperfusion injury. *Stem Cell. Res.* 4 (3), 214–222. doi:10.1016/j.scr.2009.12.003

Le Blanc, K., Rasmusson, I., Sundberg, B., Gotherstrom, C., Hassan, M., Uzunel, M., et al. (2004). Treatment of severe acute graft-versus-host disease with third party haploidentical mesenchymal stem cells. *Lancet* 363 (9419), 1439–1441. doi:10.1016/S0140-6736(04)16104-7

Lee, R. H., Pulin, A. A., Seo, M. J., Kota, D. J., Ylostalo, J., Larson, B. L., et al. (2009). Intravenous hMSCs improve myocardial infarction in mice because cells embolized in lung are activated to secrete the anti-inflammatory protein TSG-6. *Cell. Stem Cell.* 5 (1), 54–63. doi:10.1016/j.stem.2009.05.003

Legaki, E., Roubelakis, M. G., Theodoropoulos, G. E., Lazaris, A., Kollia, A., Karamanolis, G., et al. (2016). Therapeutic potential of secreted molecules derived from human amniotic fluid mesenchymal stem/stroma cells in a mice model of colitis. *Stem Cell. Rev. Rep.* 12 (5), 604–612. doi:10.1007/s12015-016-9677-1

Lehnert, C., Weiswange, M., Jeremias, I., Bayer, C., Grunert, M., Debatin, K. M., et al. (2014). TRAIL-receptor costimulation inhibits proximal TCR signaling and suppresses human T cell activation and proliferation. *J. I.* 193 (8), 4021–4031. doi:10.4049/jimmunol.1303242

Lindsey, W. B., Lowdell, M. W., Marti, G. E., Abbasi, F., Zenger, V., King, K. M., et al. (2007). CD69 expression as an index of T-cell function: Assay standardization, validation and use in monitoring immune recovery. *Cytotherapy* 9 (2), 123–132. doi:10.1080/14653240601182838

Liu, W., Morschauser, A., Zhang, X., Lu, X., Gleason, J., He, S., et al. (2014). Human placenta-derived adherent cells induce tolerogenic immune responses. *Clin. Transl. Immunol.* 3 (5), e14. doi:10.1038/cti.2014.5

Luckheeram, R. V., Zhou, R., Verma, A. D., and Xia, B. (2012). $CD4^+$T cells: Differentiation and functions. *Clin. Dev. Immunol.* 2012, 1–12. doi:10.1155/2012/925135

Luo, Z., Lin, J., Sun, Y., Wang, C., and Chen, J. (2021). Bone marrow stromal cell-derived exosomes promote muscle healing following contusion through macrophage polarization. *Stem Cells Dev.* 30 (3), 135–148. doi:10.1089/scd.2020.0167

Ma, D., Xu, K., Zhang, G., Liu, Y., Gao, J., Tian, M., et al. (2019). Immunomodulatory effect of human umbilical cord mesenchymal stem cells on T lymphocytes in rheumatoid arthritis. *Int. Immunopharmacol.* 74, 105687. doi:10.1016/j.intimp.2019.105687

Madel, Rabea Julia, Börger, Verena, Dittrich, Robin, Bremer, Michel, Tobias, Tertel, Babo, Hideo A., et al. (2020). Independent human mesenchymal stromal cell-derived extracellular vesicle preparations differentially affect symptoms in an advanced murine Graft-versus-Host-Disease model. *bioRxiv* 2020, 423658. doi:10.1101/2020.12.21.423658

Malvicini, R., Santa-Cruz, D., De Lazzari, G., Tolomeo, A. M., Sanmartin, C., Muraca, M., et al. (2022). Macrophage bioassay standardization to assess the anti-inflammatory activity of mesenchymal stromal cell-derived small extracellular vesicles. *Cytotherapy*. doi:10.1016/j.jcyt.2022.05.011

Marino, J., Paster, J., and Benichou, G. (2016). Allorecognition by T Lymphocytes and allograft rejection. *Front. Immunol.* 7, 582. doi:10.3389/fimmu.2016.00582

Maus, M. V., Thomas, A. K., Leonard, D. G., Allman, D., Addya, K., Schlienger, K., et al. (2002). *Ex vivo* expansion of polyclonal and antigen-specific cytotoxic T lymphocytes by artificial APCs expressing ligands for the T-cell receptor, CD28 and 4-1BB. *Nat. Biotechnol.* 20 (2), 143–148. doi:10.1038/nbt0202-143

Meisel, R., Zibert, A., Laryea, M., Gobel, U., Daubener, W., and Dilloo, D. (2004). Human bone marrow stromal cells inhibit allogeneic T-cell responses by indoleamine 2, 3-dioxygenase-mediated tryptophan degradation. *Blood* 103 (12), 4619–4621. doi:10.1182/blood-2003-11-3909

Mills, C. D., Kincaid, K., Alt, J. M., Heilman, M. J., and Hill, A. M. (2000). M-1/M-2 macrophages and the Th1/Th2 paradigm. *J. Immunol.* 164 (12), 6166–6173. doi:10.4049/jimmunol.164.12.6166

Moll, G., James, A., Kamhieh-Milz, J., Bieback, K., Ringden, O., Volk, H. D., et al. (2019). Ankrum, julian kamhieh-milz, karen bieback, olle Ringdén, hans-dieter volk, sven geissler, and petra ReinkeIntravascular mesenchymal stromal/stem cell therapy product diversification: Time for new clinical guidelines. *Trends Mol. Med.* 25 (2), 149–163. doi:10.1016/j.molmed.2018.12.006

Moll, G., Ankrum, J. A., Olson, S. D., and Nolta, J. A. (2022). Improved MSC minimal criteria to maximize patient safety: A call to embrace tissue factor and hemocompatibility assessment of MSC products. *Stem Cells Transl. Med.* 11 (1), 2–13. doi:10.1093/stcltm/szab005

Mueller, S. N., Gebhardt, T., Carbone, F. R., and Heath, W. R. (2013). Memory T cell subsets, migration patterns, and tissue residence. *Annu. Rev. Immunol.* 31, 137–161. doi:10.1146/annurev-immunol-032712-095954

Munoz-Elias, G., Woodbury, D., and Black, I. B. (2003). Marrow stromal cells, mitosis, and neuronal differentiation: Stem cell and precursor functions. *Stem Cells* 21 (4), 437–448. doi:10.1634/stemcells.21-4-437

Murray, P. J., Allen, J. E., Biswas, S. K., Fisher, E. A., Gilroy, D. W., Goerdt, S., et al. (2014). Macrophage activation and polarization: Nomenclature and experimental guidelines. *Immunity* 41 (1), 14–20. doi:10.1016/j.immuni.2014.06.008

Nakamura, A., Otani, K., and Shichita, T. (2020). Lipid mediators and sterile inflammation in ischemic stroke. *Int. Immunol.* 32 (11), 719–725. doi:10.1093/intimm/dxaa027

Nassar, W., El-Ansary, M., Sabry, D., Mostafa, M. A., Fayad, T., Kotb, E., et al. (2016). Umbilical cord mesenchymal stem cells derived extracellular vesicles can safely ameliorate the progression of chronic kidney diseases. *Biomater. Res.* 20, 21. doi:10.1186/s40824-016-0068-0

Obermajer, N., Popp, F. C., Soeder, Y., Haarer, J., Geissler, E. K., Schlitt, H. J., et al. (2014). Conversion of Th17 into IL-17a(neg) regulatory T cells: A novel mechanism in prolonged allograft survival promoted by mesenchymal stem cell-supported

minimized immunosuppressive therapy. *J. I.* 193 (10), 4988–4999. doi:10.4049/jimmunol.1401776

Obst, R. (2015). The timing of T cell priming and cycling. *Front. Immunol.* 6, 563. doi:10.3389/fimmu.2015.00563

Pachler, K., Ketterl, N., Desgeorges, A., Dunai, Z. A., Laner-Plamberger, S., Streif, D., et al. (2017). An *in vitro* potency assay for monitoring the immunomodulatory potential of stromal cell-derived extracellular vesicles. *Int. J. Mol. Sci.* 18 (7), 1413. doi:10.3390/ijms18071413

Pacienza, N., Lee, R. H., Bae, E. H., Kim, D. K., Liu, Q., Prockop, D. J., et al. (2019). *In vitro* macrophage assay predicts the *in vivo* anti-inflammatory potential of exosomes from human mesenchymal stromal cells. *Mol. Ther. - Methods & Clin. Dev.* 13, 67–76. doi:10.1016/j.omtm.2018.12.003

Padgett, Eric L., and Pruett, Stephen B. (1992). Evaluation of nitrite production by human monocyte-derived macrophages. *Biochem. Biophysical Res. Commun.* 186 (2), 775–781. doi:10.1016/0006-291X(92)90813-Z

Palacios, R. (1982). Concanavalin A triggers T lymphocytes by directly interacting with their receptors for activation. *J. Immunol.* 128 (1), 337–342.

Paluskievicz, C. M., Cao, X., Abdi, R., Zheng, P., Liu, Y., and Bromberg, J. S. (2019). T regulatory cells and priming the suppressive tumor microenvironment. *Front. Immunol.* 10, 2453. doi:10.3389/fimmu.2019.02453

Parolini, O., Alviano, F., Bagnara, G. P., Bilic, G., Bühring, H. J., Evangelista, M., et al. (2008). Concise review: Isolation and characterization of cells from human term placenta: Outcome of the first international workshop on placenta derived stem cells. *Stem Cells* 26 (2), 300–311. doi:10.1634/stemcells.2007-0594

Parolini, O., Souza-Moreira, L., O'Valle, F., Magatti, M., Hernandez-Cortes, P., Gonzalez-Rey, E., et al. (2014). Therapeutic effect of human amniotic membrane-derived cells on experimental arthritis and other inflammatory disorders. *Arthritis Rheumatol.* 66 (2), 327–339. doi:10.1002/art.38206

Phinney, D. G. (2012). Functional heterogeneity of mesenchymal stem cells: Implications for cell therapy. *J. Cell. Biochem.* 113 (9), 2806–2812. doi:10.1002/jcb.24166

Phinney, D. G., Kopen, G., Righter, W., Webster, S., Tremain, N., and Prockop, D. J. (1999). Donor variation in the growth properties and osteogenic potential of human marrow stromal cells. *J. Cell. Biochem.* 75 (3), 424–436. doi:10.1002/(sici)1097-4644(19991201)75:3<424:aid-jcb8>3.0.co;2-8

Pianta, S., Bonassi Signoroni, P., Muradore, I., Rodrigues, M. F., Rossi, D., Silini, A., et al. (2015). Amniotic membrane mesenchymal cells-derived factors skew T cell polarization toward Treg and downregulate Th1 and Th17 cells subsets. *Stem Cell. Rev. Rep.* 11 (3), 394–407. doi:10.1007/s12015-014-9558-4

Pittenger, M. F., Mackay, A. M., Beck, S. C., Jaiswal, R. K., Douglas, R., Mosca, J. D., et al. (1999). Multilineage potential of adult human mesenchymal stem cells. *Science* 284 (5411), 143–147. doi:10.1126/science.284.5411.143

Pittenger, M. F., and Martin, B. J. (2004). Mesenchymal stem cells and their potential as cardiac therapeutics. *Circ. Res.* 95 (1), 9–20. doi:10.1161/01.RES.0000135902.99383.6f

Quarta, A., Berneman, Z., and Ponsaerts, P. (2021a). Functional consequences of a close encounter between microglia and brain-infiltrating monocytes during CNS pathology and repair. *J. Leukoc. Biol.* 110 (1), 89–106. doi:10.1002/jlb.3ru0820-536r

Quarta, A., Berneman, Z., and Ponsaerts, P. (2020). Neuroprotective modulation of microglia effector functions following priming with interleukin 4 and 13: Current limitations in understanding their mode-of-action. *Brain Behav. Immun.* 88, 856–866. doi:10.1016/j.bbi.2020.03.023

Quarta, A., Le Blon, D., D'Aes, T., Pieters, Z., Hamzei Taj, S., Miró-Mur, F., et al. (2019). Murine iPSC-derived microglia and macrophage cell culture models recapitulate distinct phenotypical and functional properties of classical and alternative neuro-immune polarisation. *Brain Behav. Immun.* 82, 406–421. doi:10.1016/j.bbi.2019.09.009

Quarta, A., Meese, T., Pieters, Z., Van Breedam, E., Le Blon, D., Van Broeckhoven, J., et al. (2021b). Murine induced pluripotent stem cell-derived neuroimmune cell culture models emphasize opposite immune-effector functions of interleukin 13-primed microglia and macrophages in terms of neuroimmune toxicity. *Glia* 69 (2), 326–345. doi:10.1002/glia.23899

Radtke, S., Gorgens, A., Liu, B., Horn, P. A., and Giebel, B. (2016). Human mesenchymal and murine stromal cells support human lympho-myeloid progenitor expansion but not maintenance of multipotent haematopoietic stem and progenitor cells. *Cell. Cycle* 15 (4), 540–545. doi:10.1080/15384101.2015.1128591

Ringdén, O., Moll, G., Gustafsson, B., and Sadeghi, B. (2022). Mesenchymal stromal cells for enhancing hematopoietic engraftment and treatment of graft-versus-host disease, hemorrhages and acute respiratory distress syndrome. *Front. Immunol.* 13, 839844. doi:10.3389/fimmu.2022.839844

Roubelakis, M. G., Bitsika, V., Zagoura, D., Trohatou, O., Pappa, K. I., Makridakis, M., et al. (2011). *In vitro* and *in vivo* properties of distinct populations of amniotic fluid mesenchymal progenitor cells. *J. Cell. Mol. Med.* 15 (9), 1896–1913. doi:10.1111/j.1582-4934.2010.01180.x

Roubelakis, M. G., Pappa, K. I., Bitsika, V., Zagoura, D., Vlahou, A., Papadaki, H. A., et al. (2007). Molecular and proteomic characterization of human mesenchymal stem cells derived from amniotic fluid: Comparison to bone marrow mesenchymal stem cells. *Stem Cells Dev.* 16 (6), 931–952. doi:10.1089/scd.2007.0036

Saldanha-Araujo, F., Haddad, R., Kelen, C., Malmegrim de Farias, R., Alessandra de Paula Alves SouzaPalma, Patrícia V., et al. (2012). Mesenchymal stem cells promote the sustained expression of CD69 on activated T lymphocytes: Roles of canonical and non-canonical NF-κB signalling. *J. Cell. Mol. Med.* 16 (6), 1232–1244. doi:10.1111/j.1582-4934.2011.01391.x

Sancho, D., Yáñez-Mó, M., Tejedor, R., and Sánchez-Madrid, F. (1999). Activation of peripheral blood T cells by interaction and migration through endothelium: Role of lymphocyte function antigen-1/intercellular adhesion molecule-1 and interleukin-15. *Blood* 93 (3), 886–896. doi:10.1182/blood.v93.3.886.403k10_886_896

Sasazuki, T., McMichael, A., Radvany, R., Payne, R., and McDevitt, H. (1976). Use of high dose X-irradiation to block back stimulation in the MLC reaction. *Tissue Antigens* 7 (2), 91–96. doi:10.1111/j.1399-0039.1976.tb01037.x

Schrepfer, S., Deuse, T., Reichenspurner, H., Fischbein, M. P., Robbins, R. C., and Pelletier, M. P. (2007). Stem cell transplantation: The lung barrier. *Transpl. Proc.* 39 (2), 573–576. doi:10.1016/j.transproceed.2006.12.019

Seed, R. I., Kobayashi, K., Ito, S., Takasaka, N., Cormier, A., Jespersen, J. M., et al. (2021). A tumor-specific mechanism of T(reg) enrichment mediated by the integrin αvβ8. *Sci. Immunol.* 6 (57), eabf0558. doi:10.1126/sciimmunol.abf0558

Silini, A. R., Di Pietro, R., Lang-Olip, I., Alviano, F., Banerjee, A., Basile, M., et al. (2020). Perinatal derivatives: Where do we stand? A roadmap of the human placenta and consensus for tissue and cell nomenclature. *Front. Bioeng. Biotechnol.* 8, 610544. doi:10.3389/fbioe.2020.610544

Strobl, J., Gail, L. M., Kleissl, L., Pandey, R. V., Smejkal, V., Huber, J., et al. (2021). Human resident memory T cells exit the skin and mediate systemic Th2-driven inflammation. *J. Exp. Med.* 218 (11), e20210417. doi:10.1084/jem.20210417

Sun, L., Akiyama, K., Zhang, H., Yamaza, T., Hou, Y., Zhao, S., et al. (2009). Mesenchymal stem cell transplantation reverses multiorgan dysfunction in systemic lupus erythematosus mice and humans. *Stem Cells* 27 (6), 1421–1432. doi:10.1002/stem.68

Tario, J. D., Jr., Muirhead, K. A., Pan, D., Munson, M. E., and Wallace, P. K. (2011). Tracking immune cell proliferation and cytotoxic potential using flow cytometry. *Methods Mol. Biol.* 699, 119–164. doi:10.1007/978-1-61737-950-5_7

Timmers, L., Lim, S. K., Arslan, F., Armstrong, J. S., Hoefer, I. E., Doevendans, P. A., et al. (2007). Reduction of myocardial infarct size by human mesenchymal stem cell conditioned medium. *Stem Cell. Res.* 1 (2), 129–137. doi:10.1016/j.scr.2008.02.002

Tomonari, K. (1980). Cytotoxic T cells generated in the autologous mixed lymphocyte reaction. I. Primary autologous mixed lymphocyte reaction. *J. Immunol.* 124 (3), 1111–1121.

Trickett, A., and Kwan, Y. L. (2003). T cell stimulation and expansion using anti-CD3/CD28 beads. *J. Immunol. Methods* 275 (1-2), 251–255. doi:10.1016/s0022-1759(03)00010-3

Tsai, P. J., Wang, H. S., Lin, G. J., Chou, S. C., Chu, T. H., Chuan, W. T., et al. (2014). Undifferentiated Wharton?s jelly mesenchymal stem cell transplantation induces insulin-producing cell differentiation and suppression of T cell-mediated autoimmunity in non-obese diabetic mice. *Cell. Transpl.* 24, 1555–1570. doi:10.3727/096368914X683016

Van Hoecke, L., Caroline Van, C., Verena, B., Arnout, B., Jonas, C., Imschoot, G. V., et al. (2021). Anti-inflammatory mesenchymal stromal cell-derived extracellular vesicles improve pathology in niemann–pick type C disease. *Biomedicines* 9 (12), 1864. doi:10.3390/biomedicines9121864

Viola, A., and Lanzavecchia, A. (1996). T cell activation determined by T cell receptor number and tunable thresholds. *Science* 273 (5271), 104–106. doi:10.1126/science.273.5271.104

Viswanathan, S., Shi, Y., Galipeau, J., Krampera, M., Leblanc, K., Martin, I., et al. (2019). Mesenchymal stem versus stromal cells: International society for cell & gene therapy (ISCT®) mesenchymal stromal cell committee position statement on nomenclature. *Cytotherapy* 21 (10), 1019–1024. doi:10.1016/j.jcyt.2019.08.002

Vogel, W., Grunebach, F., Messam, C. A., Kanz, L., Brugger, W., and Buhring, H. J. (2003). Heterogeneity among human bone marrow-derived mesenchymal stem cells and neural progenitor cells. *Haematologica* 88 (2), 126–133.

Wang, C., Borger, V., Sardari, M., Murke, F., Skuljec, J., Pul, R., et al. (2020). Mesenchymal stromal cell-derived small extracellular vesicles induce ischemic

neuroprotection by modulating leukocytes and specifically neutrophils. *Stroke* 51 (6), 1825–1834. doi:10.1161/STROKEAHA.119.028012

Wang, D., Feng, X., Lu, L., Konkel, J. E., Zhang, H., Chen, Z., et al. (2014). A CD8 T cell/indoleamine 2, 3-dioxygenase axis is required for mesenchymal stem cell suppression of human systemic lupus erythematosus. *Arthritis Rheumatol.* 66 (8), 2234–2245. doi:10.1002/art.38674

Wang, D., Huang, S., Yuan, X., Liang, J., Xu, R., Yao, G., et al. (2017). The regulation of the Treg/Th17 balance by mesenchymal stem cells in human systemic lupus erythematosus. *Cell. Mol. Immunol.* 14 (5), 423–431. doi:10.1038/cmi.2015.89

Wang, H., Qiu, X., Ni, P., Qiu, X., Lin, X., Wu, W., et al. (2014). Immunological characteristics of human umbilical cord mesenchymal stem cells and the therapeutic effects of their transplantion on hyperglycemia in diabetic rats. *Int. J. Mol. Med.* 33 (2), 263–270. doi:10.3892/ijmm.2013.1572

Warnecke, A., Prenzler, N., Harre, J., Kohl, U., Gartner, L., Lenarz, T., et al. (2021). First-in-human intracochlear application of human stromal cell-derived extracellular vesicles. *J. Extracell. Vesicles* 10 (8), e12094. doi:10.1002/jev2.12094

Weirather, J., Hofmann, U. D., Beyersdorf, N., Ramos, G. C., Vogel, B., Frey, A., et al. (2014). Foxp3+ CD4+ T cells improve healing after myocardial infarction by modulating monocyte/macrophage differentiation. *Circ. Res.* 115 (1), 55–67. doi:10.1161/circresaha.115.303895

Willis, G. R., Fernandez-Gonzalez, A., Anastas, J., Vitali, S. H., Liu, X., Ericsson, M., et al. (2018). Mesenchymal stromal cell exosomes ameliorate experimental bronchopulmonary dysplasia and restore lung function through macrophage immunomodulation. *Am. J. Respir. Crit. Care Med.* 197 (1), 104–116. doi:10.1164/rccm.201705-0925OC

Wynn, T. A., and Vannella, K. M. (2016). Macrophages in tissue repair, regeneration, and fibrosis. *Immunity* 44 (3), 450–462. doi:10.1016/j.immuni.2016.02.015

Xue, J., Schmidt, S. V., Sander, J., Draffehn, A., Krebs, W., Quester, I., et al. (2014). Transcriptome-based network analysis reveals a spectrum model of human macrophage activation. *Immunity* 40 (2), 274–288. doi:10.1016/j.immuni.2014.01.006

Yang, S. H., Park, M. J., Yoon, I. H., Kim, S. Y., Hong, S. H., Shin, J. Y., et al. (2009). Soluble mediators from mesenchymal stem cells suppress T cell proliferation by inducing IL-10. *Exp. Mol. Med.* 41 (5), 315–324. doi:10.3858/emm.2009.41.5.035

Zampetaki, A., Mitsialis, S. A., Pfeilschifter, J., and Kourembanas, S. (2004). Hypoxia induces macrophage inflammatory protein-2 (MIP-2) gene expression in murine macrophages via NF-κB: The prominent role of p42/p44 and PI3 kinase pathways. *FASEB J.* 18 (10), 1090–1092. doi:10.1096/fj.03-0991fje

Zanin-Zhorov, A., Tal-Lapidot, G., Cahalon, L., Cohen-Sfady, M., Pevsner-Fischer, M., Lider, O., et al. (2007). Cutting edge: T cells respond to lipopolysaccharide innately via TLR4 signaling. *J. Immunol.* 179 (1), 41–44. doi:10.4049/jimmunol.179.1.41

Zhang, B., Yeo, R. W. Y., Lai, R. C., Sim, E. W. K., Chin, K. C., and Lim, S. K. (2018a). Mesenchymal stromal cell exosome-enhanced regulatory T-cell production through an antigen-presenting cell-mediated pathway. *Cytotherapy* 20 (5), 687–696. doi:10.1016/j.jcyt.2018.02.372

Zhang, B., Yin, Y., Lai, R. C., Tan, S. S., Choo, A. B., and Lim, S. K. (2014). Mesenchymal stem cells secrete immunologically active exosomes. *Stem cells Dev.* 23 (11), 1233–1244. doi:10.1089/scd.2013.0479

Zhang, C., Yang, S. J., Wen, Q., Zhong, J. F., Chen, X. L., Stucky, A., et al. (2017). Human-derived normal mesenchymal stem/stromal cells in anticancer therapies. *J. Cancer* 8 (1), 85–96. doi:10.7150/jca.16792

Zhang, S., Chuah, S. J., Lai, R. C., Hui, J. H. P., Lim, S. K., and Toh, W. S. (2018b). MSC exosomes mediate cartilage repair by enhancing proliferation, attenuating apoptosis and modulating immune reactivity. *Biomaterials* 156, 16–27. doi:10.1016/j.biomaterials.2017.11.028

frontiers | Frontiers in Bioengineering and Biotechnology

TYPE Review
PUBLISHED 03 October 2022
DOI 10.3389/fbioe.2022.961987

OPEN ACCESS

EDITED BY
Vahid Serpooshan,
Emory University, United States

REVIEWED BY
Angliana Chouw,
PT Prodia Stem Cell Indonesia, Indonesia
Ramesh Bhonde,
Dr. D.Y. Patil Vidyapeeth, India

*CORRESPONDENCE
Michela Pozzobon,
m.pozzobon@irpcds.org,
michela.pozzobon@unipd.it
Peter Ponsaerts,
peter.ponsaerts@uantwerpen.be

SPECIALTY SECTION
This article was submitted to Tissue Engineering and Regenerative Medicine, a section of the journal Frontiers in Bioengineering and Biotechnology

RECEIVED 05 June 2022
ACCEPTED 01 July 2022
PUBLISHED 03 October 2022

CITATION
Pozzobon M, D'Agostino S, Roubelakis MG, Cargnoni A, Gramignoli R, Wolbank S, Gindraux F, Bollini S, Kerdjoudj H, Fenelon M, Di Pietro R, Basile M, Borutinskaitė V, Piva R, Schoeberlein A, Eissner G, Giebel B and Ponsaerts P (2022), General consensus on multimodal functions and validation analysis of perinatal derivatives for regenerative medicine applications. *Front. Bioeng. Biotechnol.* 10:961987. doi: 10.3389/fbioe.2022.961987

General consensus on multimodal functions and validation analysis of perinatal derivatives for regenerative medicine applications

Michela Pozzobon[1]*, Stefania D'Agostino[1], Maria G. Roubelakis[2], Anna Cargnoni[3], Roberto Gramignoli[4], Susanne Wolbank[5], Florelle Gindraux[6], Sveva Bollini[7], Halima Kerdjoudj[8], Mathilde Fenelon[9], Roberta Di Pietro[10], Mariangela Basile[10], Veronika Borutinskaitė[11], Roberta Piva[12], Andreina Schoeberlein[13], Guenther Eissner[14], Bernd Giebel[15] and Peter Ponsaerts[16]*

[1]Department of Women's and Children's Health, University of Padova, Padova, Italy, [2]Laboratory of Biology, Medical School of Athens, National and Kapodistrian University of Athens, Athens, Greece, [3]Centro di Ricerca E. Menni, Fondazione Poliambulanza Istituto Ospedaliero, Brescia, Italy, [4]Department of Laboratory Medicine, Division of Pathology, Karolinska Institutet, Stockholm, Sweden, [5]Ludwig Boltzmann Institute for Experimental and Clinical Traumatology, The Research Center in Cooperation with AUVA Trauma Research Center, Austrian Cluster for Tissue Regeneration, Vienna, Austria, [6]Service de Chirurgie Orthopédique, Traumatologique et plastique, CHU Besançon, Laboratoire de Nanomédecine, Imagerie, Thérapeutique EA 4662, University Bourgogne Franche-Comté, Besançon, France, [7]Department of Experimental Medicine (DIMES), School of Medical and Pharmaceutical Sciences, University of Genova, Genova, Italy, [8]University of Reims Champagne Ardenne, EA 4691 BIOS "Biomatériaux et Inflammation en Site Osseux", UFR d'Odontologie, Reims, France, [9]University of Bordeaux, INSERM, BIOTIS, U1026, Bordeaux, France, [10]Department of Medicine and Ageing Sciences, Section of Biomorphology, G. d'Annunzio University of Chieti-Pescara, Chieti, Italy, [11]Department of Molecular Cell Biology, Institute of Biochemistry, Vilnius University, Vilnius, Lithuania, [12]Department of Neuroscience and Rehabilitation, University of Ferrara, Ferrara, Italy, [13]Department of Obstetrics and Feto-maternal Medicine, Inselspital, Bern University Hospital, Department for BioMedical Research (DBMR), University of Bern, Bern, Switzerland, [14]Systems Biology Ireland, School of Medicine, Conway Institute, University College Dublin, Dublin, Ireland, [15]Institute for Transfusion Medicine, University Hospital Essen, University of Duisburg-Essen, Essen, Germany, [16]Laboratory of Experimental Hematology, Vaccine and Infectious Disease Institute (Vaxinfectio), University of Antwerp, Antwerp, Belgium

Perinatal tissues, such as placenta and umbilical cord contain a variety of somatic stem cell types, spanning from the largely used hematopoietic stem and progenitor cells to the most recently described broadly multipotent epithelial and stromal cells. As perinatal derivatives (PnD), several of these cell types and related products provide an interesting regenerative potential for a variety of diseases. Within COST SPRINT Action, we continue our review series, revising and summarizing the modalities of action and proposed medical approaches using PnD products: cells, secretome, extracellular vesicles, and decellularized tissues. Focusing on the brain, bone, skeletal muscle, heart, intestinal, liver, and lung pathologies, we discuss the importance of potency testing in validating PnD therapeutics, and critically evaluate the concept of PnD application in the field of tissue regeneration. Hereby we aim to shed light on the

actual therapeutic properties of PnD, with an open eye for future clinical application. This review is part of a quadrinomial series on functional/potency assays for validation of PnD, spanning biological functions, such as immunomodulation, anti-microbial/anti-cancer, anti-inflammation, wound healing, angiogenesis, and regeneration.

KEYWORDS

perinatal derivatives, amniotic membrane and fluid stem cells, extracellular vesicles, tissue regeneration, regenerative medicine

1 Introduction

Stem and progenitor cells, including their cellular and acellular derivatives, are increasingly applied as therapeutic agents for a variety of pathologies, not only in preclinical animal studies but—more importantly—in human clinical trials also. However, the field of regenerative medicine for non-hematopoietic diseases has evolved over the past 20 years from direct cell replacement to trophic support exerted by administered cell populations or their derivatives in order to induce tissue repair (i.e., improve the functionality of damaged/diseased cells/tissues) and/or regeneration (i.e., stimulate the growth of new cells replacing diseased cells/tissues). Nevertheless, many questions remain regarding the type of stem cell (product) needed, the minimal criteria such a product needs to comply with, and appropriate guidelines for determining the success of an applied therapeutic intervention, both in preclinical animal studies and human clinical trials. While this field has been dominated by studies using tissue and cell products obtained from adult stem cell sources, and besides pluripotent stem cell derivatives (embryonic stem/induced pluripotent stem cells, ES/iPSC), emerging alternatives can be found in perinatal tissues. Due to their naïvity and easy access, perinatal tissues and cells collected during pregnancy (AFS) and at full-term pregnancy, here referred to as Perinatal Derivatives (PnD), may provide important advantages over adult stem cell products, especially for non-hematopoietic (stem) cell products. The main non-hematopoietic PnD currently used in pre-clinical and clinical applications are amniotic fluid/tissue and cells isolated from the placenta, including the amniotic membrane and the umbilical cord. For a detailed description and correct nomenclature of the different perinatal cell types of therapeutic interest, we refer to a recent SPRINT-COST supported review manuscript by Silini and colleagues, in which a proposed consensus nomenclature for human perinatal tissues and cells has been published (Silini et al., 2020). Here we will further elaborate on the most frequently studied PnD, their phenotypic characteristics, and suggested therapeutic efficacy in different pathologies, including various tools to determine their potency, by means of functional assays and before (and after) administration. A general overview of the manuscript organization is provided in Figure 1.

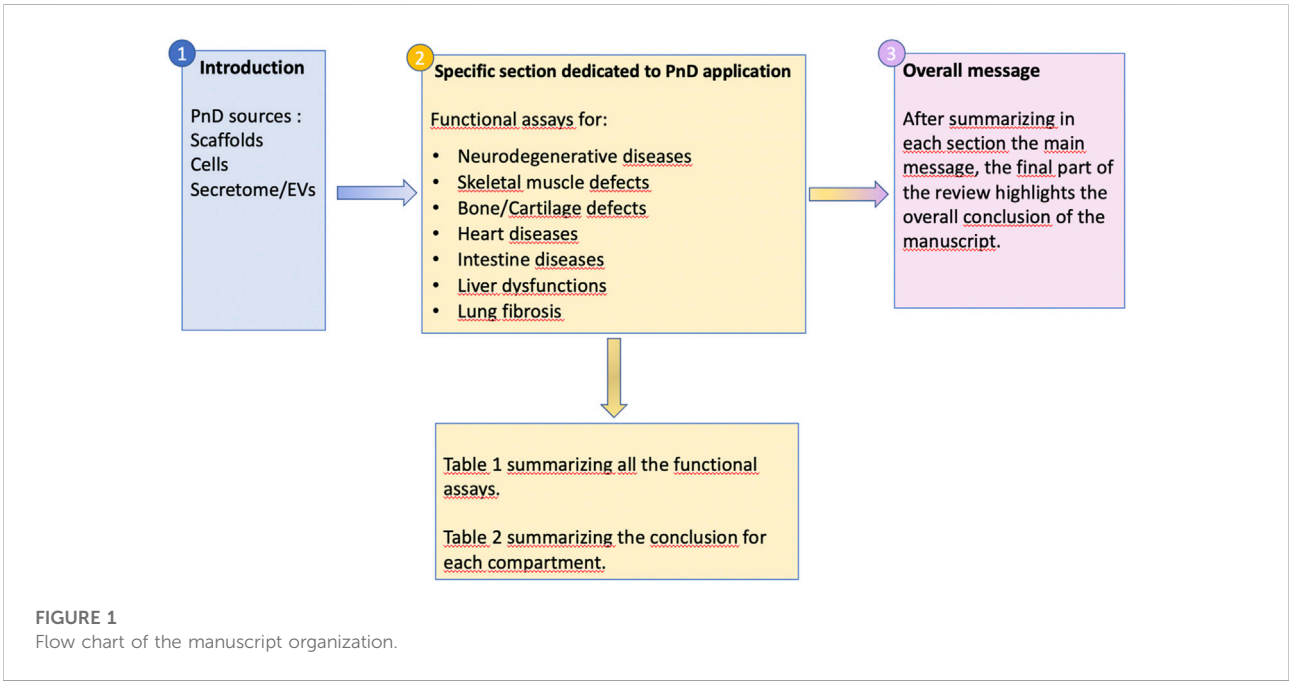

FIGURE 1
Flow chart of the manuscript organization.

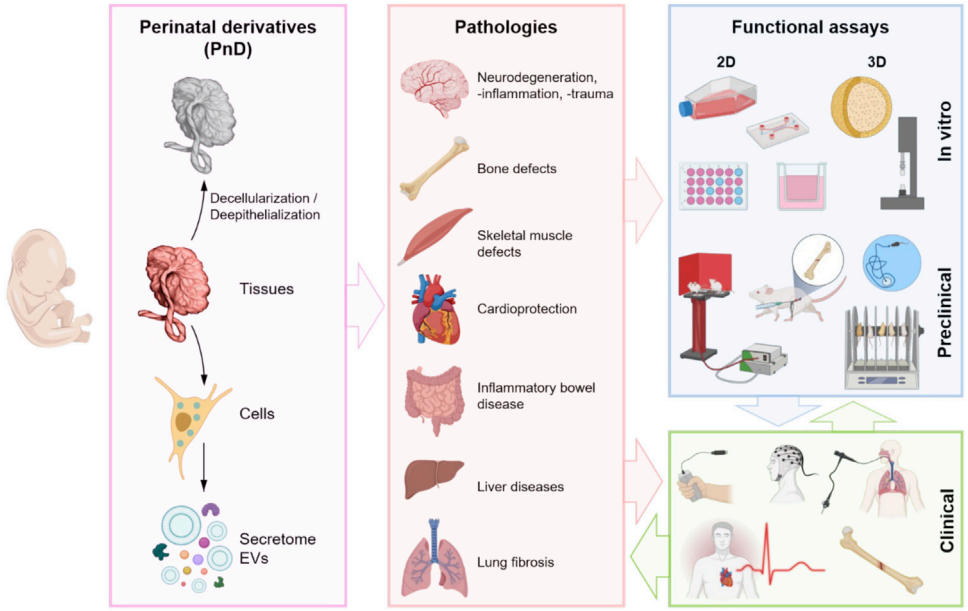

FIGURE 2
Schematic representation of the use of different PnD (tissues, cells, and paracrine derivatives—secretome (whole soluble factors including EVs) and isolated EVs), their application in different diseased organs and the functional assays. Created with BioRender.com.

More specifically, with this manuscript, a team composed of experts and pioneers in using PnD products in clinical and veterinarian treatments, afferent to the COST SPRINT Action (CA17116), aimed to offer a guide on when and how it may be advantageous to the employment of placenta-derived cells or scaffolds. We will consider the applications of different sources of PnD with a focus on the functional/potency assays for the regeneration of different affected organs (Figure 2).

Based on the unique ontogenetical and biological properties that characterize perinatal cells, different cells, spanning from infiltrating (maternal) immune cells to endothelial, epithelial, or mesenchymal stromal cells (MSC), have been isolated and studied during the last decades (Silini et al., 2020). These multipotent stem cells have been offering new, promising experimental applications for regenerative medicine and tissue engineering approaches. With its immunologically-privileged status (Zhang et al., 2017a), the PnD lends credence to its use as an allograft scaffold in tissue regenerative medicine. However, to widen a safe application, different strategies of nuclei depletion (decellularization or de-epithelization process) have been assessed to give rise to decellularized PnD (Gilbert et al., 2006; Crapo et al., 2011). After checking the quality of the decellularization process following standardized procedures of nuclei and DNA quantification (Gilbert et al., 2006; Crapo et al., 2011), naturally derived scaffolds, as from PnD, are thought to be an ideal and safe system to deliver chemokines and growth factors, to provide adequate structural and biomechanical microarchitecture in the damaged microenvironment (Jadalannagari et al., 2017; Dubus et al., 2022), with attention to avoid foreign body reaction and formation of the fibrous capsule (Keane et al., 2012; Hussein et al., 2016).

The development of a validation system designed according to international reference standards is an ambitious goal whose achievement still requires considerable effort toward the 1) cell-based strategies and 2) the cell-free strategies. Regarding the first, the efficacy of decellularized PnD (dP) combined with cells requires the employment of a conventional functional assay aimed at measuring the biochemical and mechanical properties of the dP on cell growth, differentiation, and functionality. In this scenario, the dP may act both as 1) a stem/progenitor-cell-like niche with key elements to control the regulation of stem cell fate and function, or 2) a platform for mature cells with the signals needed to initiate and maintain the differentiation of tissue-specific lineages and to support the cell repopulation after implantation. This approach relies on the ability of dP to promote the growth of cells with the enhanced potential to regenerate tissue damaged by injury, disease, or aging. This is the case of decellularized amniotic membrane (AM) and ultra-thin AM (Zhang et al., 2016) or Wharton's jelly (Penolazzi et al., 2020; Dubus et al., 2022; Penolazzi et al., 2022) which have been produced as a suitable scaffold for the *ex vivo* expansion and delivery of stem and progenitor cells.

Regarding the cell-free strategies, the use of *in vivo* biological assays will allow testing the efficacy of dP extracellular matrix (dP-ECM) as a cell-free scaffold to produce a good regeneration guide.

TABLE 1 Overview of the functional assays for the different compartments analyzed in the present manuscript.

Source of PnD	Functional assay			Pathology/ model	References
	In vitro	*In vivo*/preclinic	Clinic		
hUC-WJ-MSC from term or preterm birth	Proliferation capacity Protein composition of secretome Iinflammatory/anti-inflammatory factors Adhesion molecules Neuroprotective effect on oxidative stress Stimulation of neurite outgrowth Metabolic activity under serum starvation Expression of functional genes Glial differentiation of neural progenitors Oligodendrocyte lineage markers gene expression			Spinal cord injury, Parkinson's disease, Alzheimer's disease, Perinatal brain injury	Petrenko et al. (2020), Oppliger et al. (2017)
hUC-WJ-MSC-EVs	Immunocytochemistry and expression of oligodendrocyte lineage markers miRNA cargo analysis Inflammatory-related gene and protein expression and cytokine secretion sEV uptake: confocal microscopy, flow cytometry			Perinatal brain injury	Joerger-Messerli et al. (2021), Thomi et al. (2019)
Amnion muscle combined graft (AMCG)		Grasping tests. Scar formation toluidine blue staining		Rat's median nerve defect	Marchesini et al. (2018)
hAM			Muscle Testing of Lister Jamar test Classification of Sakellarides Quick-DASH evaluation questionnaire	Loss of substance of the median nerve	Riccio et al. (2014)
hAM+ hUC-WJ-MSC			Modified Medical Research Council classification (MRCC) Electromyogram (EMG)	Radial nerve injury	Li et al. (2013)
hAEC		Stress relaxation tests		Injured brachial plexus nerve in rabbit	Jin et al. (2015)
Decellularized WJ	DNA quantification DAPI staining and visualization Histological staining Growth factor release MALDI TOFF proteomic assay	Direct and indirect cytotoxicity evaluation after subcutaneous implantation (ISO/EN 10993 part 5-6 guidelines)		Bone/Cartilage regeneration	Hussein et al. (2016)
hAM	Silver nitrate, Von Kossa and Alizarin red stainings Immunohistochemistry for osteogenesis Energy dispersive X-ray (EDX)	2D or 3D-Radiography Histology Immunohistochemistry to evaluate bone formation		*In vitro* and *in vivo* osteogenic potential	Lindenmair et al. (2010), Gualdi et al. (2019), Fenelon et al. (2021), F enelon et al. (2020)

(Continued on following page)

TABLE 1 (*Continued*) Overview of the functional assays for the different compartments analyzed in the present manuscript.

Source of PnD	Functional assay			Pathology/ model	References
	In vitro	*In vivo*/preclinic	Clinic		
	X-ray diffraction (XRD)				
	Metabolic activity assay				
hUC-WJ-MSC + muscle scaffold	Histological staining for quantification of fibrous area	Evaluation of maximal isometric contractile force		Volumetric muscle loss	Qiu et al. (2018), Hadipour et al. (2021); Izadi et al. (2021), Magarotto et al. (2021)
hUC-WJ-MSC-EVs + muscle scaffold	Quantification of centrally located myofibers or cross section area				
Decellularized hAM	Immunofluorescence staining for regenerating muscle, nerve, blood vessels markers				
	Immunofluorescence and flow cytometry for M2 macrophage polarization				
hAM	Live imaging and cell tracking to study cell motility			Muscle injury (3D model)	Hasmad et al. (2018), Hadipour et al. (2021)
	Measuring of fibers angle for alignment detection				
hUC-MSC	Histological staining for quantification of fibrous area	Gait/walk analysis		Chemical muscle damage Unilateral hindlimb ischemia	Su et al. (2019), Arutyunyan et al. (2019)
	Hystomorophometric analysis				
	Immunofluorescence staining for regenerating blood vessels				
	Immunofluorescence and cytometry for M2 macrophage polarization				
hUC-WJ-MSC,	Immunofluorescence staining for regenerating muscle markers	Grip analysis		Duchenne Muscular Dystrophy	Mishra et al. (2020), Park et al. (2021), Bier et al. (2018)
hUC-WJ-MSC-EVs	Histological staining for quantification of fibrous area				
	Transcriptome analysis for myogenic markers or miRNA				
hUC-WJ-MSC	Immunofluorescence staining for regenerating muscle markers			Sarcopenia	Wang et al. (2018)
	Apoptosis detection				
hUC-WJ-MSC-EVs	Immunofluorescence staining for regenerating nerve markers	Gait/walk analysis		Sciatic nerve resection	Ma et al. (2019)
	Hystomorophometric analysis				
hAFSC-CM	Cell viability assay			Myocardial ischemic injury	Balbi et al. (2019a)
	Assessment of Ca2+ transients				
	Capillary network formation assay				
hAFSC-CM	*Ex-vivo* histological evaluation of fibrosis and scarring on murine myocardial tissue sections	*In vivo* cardiac function analysis by ultrasounds		Myocardial ischemic injury	Balbi et al. (2019b)
hAFSC-EVs	*Ex-vivo* Immunofluorescence for inflammatory cells (MPO) and TUNEL assay for cardiomyocyte apoptosis (cardiac troponin I)				
	Ex-vivo Immunofluorescence for neoangiogenesis and				

(Continued on following page)

TABLE 1 (*Continued*) Overview of the functional assays for the different compartments analyzed in the present manuscript.

Source of PnD	Functional assay			Pathology/ model	References
	In vitro	*In vivo*/preclinic	Clinic		
	activation of epicardial progenitor cells				
hAFSC-EVs	Cell viability assay			Myocardial ischemic injury	Takov et al. (2020)
	Modified Boyden's chamber assay on HUVEC				
	WB analysis of PI3K signaling				
	Proteome profiler human phospho-kinase array on HUVEC				
	Ex-vivo TTC staining of tissue sections				
hAFSC-CM	Cell viability assay	*In vitro* blocking experiments using anti-Il6 and anti-Cxcl1 antibodies and PI3K inhibitor on murine neonatal cardiomyocytes exposed to doxorubicin		Mouse neonatal cardiomyocytes or murine cardiac tissues exposed to doxorubicin. Doxorubicin-induced cardiotoxicity	Lazzarini et al. (2016)
	Immunocytochemistry for prosenescent and apoptotic marker	*In vivo* cardiac function analysis by ultrasounds			
	Immunostaining for DNA damage				
	RNA microarray				
	Real time qRT-PCR				
	WB analysis				
	MitoTracker Deep Red staining				
	Oxidative phosphorylation activity				
	Ex-vivo biochemical evaluation of mithocondrial metabolism				
hUC-MSC	Cell viability, TUNEL and ApopTag assay	*In vivo* cardiac function analysis by ultrasounds		Myocardial ischemia/ reperfusion injury	Danieli et al. (2015), Santos Nascimento et al. (2014)
hAMSC-CM	WB analysis				
	Boyden chamber assay on endothelial progenitors				
	Angiogenic assay on Matrigel on endothelial progenitor cells				
	Ex-vivo TTC staining				
	Ex-vivo histological analysis of fibrosis and infarct size				
	Ex-vivo immunostaining for angiogenesis				
hUC-MSC-EVs	*Ex-vivo* real time qRT-PCR	*In vivo* cardiac function analysis by ultrasounds		Myocardial ischemic injury	Huang et al. (2020)
	Ex-vivo ELISA	*In vitro* functional evaluation of mechanism of action by SOX6 knockdown and miR-19 inhibition			
	Ex-vivo histological evaluation of myocardial injury and cell apoptosis				
	Ex-vivo TTC staining				
	Cell viability assay				
	Evaluation of ROS production				

(Continued on following page)

TABLE 1 (*Continued*) Overview of the functional assays for the different compartments analyzed in the present manuscript.

Source of PnD	Functional assay			Pathology/ model	References
	In vitro	*In vivo*/preclinic	Clinic		
	WB analysis				
hUC-MSC		Evaluation of weight loss, intestinal mucosal injury, colon shortening, and reduced clinical disease phenotype. Evaluation of intestinal tight junctions, autophagy markers and VEGF signal at the injured site	Decreased IBD activity index, enhance healing process	DSS murine model. Fistula	Banerjee et al. (2015), Panhua et al. (2019), Wang et al. (2020), Hossein-khannazer et al. (2021)
hUC-MSC-EVs		Evaluation of restored mucosal barrier repair with inteleukin and TNFa signaling analysis		DSS murine model	Mao et al. (2017b), Tolomeo et al. (2021), Yang et al. (2021)
MSC isolated from AF and chorionic plate		Detection of anti-inflammatory interleukins induced liver recovery.		CCl_4-injured NOD/ SCID mice	Zagoura et al. (2012), Peng et al. (2014)
MSC isolated from chorionic plate		Evaluation of the expression levels of α-smooth muscle actin (α-SMA) and Col I		CCl_4-injured rat	Lee et al. (2010)
hAEC	Evaluation of CYP3A4 activity and inducibility, albumin secretion, ammonia metabolism, the ability to efflux rhodamine or store bile acids, lipids or glycogen. Production of multicellular organoids with hepatic function in coculture with HUVEC and MSC			Liver organoid. *In vitro* 3D culture model of hepatocytes	Furuya et al. (2019), Pettinato et al. (2019), Ramachandran et al. (2015)
hAM stromal extract	Western Blot analysis. Detection of proliferating cells			*In vitro* model of myofibroblasts culture	Li et al. (2008)
hAEC	Proliferation assay. Immunostaining for the assessment of transformation of fibroblasts to myofibroblasts. Colorimetric assay for collagen. Gene expressions of TGF-β, PDGF-α, and PDGF-β by real-time PCR. Matrix Metalloproteinase (MMP-2 and MMP-9) Activity Assay in culture supernatants (by gelatin zymography)	Hystomorophometric analysis. Quantification of collagen. Immunofluorescence lung area fraction occupied by CD45-positive cells, macrophages and neutrophils. Gene expression. Pro-inflammatory cytokines analysis. Protein zymography		*In vitro* model of primary mouse lung fibroblasts culture. Bleomycin-induced lung fibrosis model	Vosdoganes et al. (2013), Murphy et al. (2011), Vosdoganes et al. (2013), Tan et al. (2014), Tan et al. (2015), Moodley et al. (2010)
hAEC-CM hAEC-Exo	Chemotactic Macrophage Migration Assay. Colorimetric assay for collagen. Immunofluorescence staining			*In vitro* model of primary mouse lung macrophages culture. *In vitro* model of human lung fibroblasts culture/ bleomycin-induced lung fibrosis model	Murphy et al. (2012)
hAMSC		Hystomorophometric analysis. Immunostaining and gene expression of inflammatory mediators and ECM proteins. Flow-cytometry of bronchoalveolar lavage		Bleomycin-induced lung fibrosis model	Carg noni et al. (2020), Moodley et al. (2013)

(Continued on following page)

TABLE 1 (*Continued*) Overview of the functional assays for the different compartments analyzed in the present manuscript.

Source of PnD	Functional assay			Pathology/ model	References
	In vitro	*In vivo*/preclinic	Clinic		
hAMSC-CM		Lung expression of inflammatory mediators by Cytometric Bead Array. Lung PGE2 levels by EIA assay		Bleomycin-induced lung fibrosis model	Cargnoni et al. (2014)
Human Fetal Membrane-Derived Cell (hAEC+hAMSC+hCMSC)		Hagood's score. Collagen deposition analysis. Hystology on inflammatory cell infiltrations		Bleomycin-induced lung fibrosis model	Cargnoni et al. (2009)
hUC-MSC		Histopathological analysis. Ashcroft's score. Colorimetric quantification of collagen. Gene expression by quantitative real-time PCR. Immunofluorescence staining	28-day mortality. Clinical symptom improvement Hematologic indicators Lung imaging changes. Length of hospitalization PaO2/ FiO2 ratio. Dynamics of cytokines, and IgG and IgM anti-SARS-CoV-2 antibodies	Bleomycin-induced lung fibrosis model. Severe COVID-19 moderate and severe COVID-19. Acute respiratory distress syndrome (ARDS) in COVID-19	Moroncini et al. (2018), Shu et al. (2020), Lanzoni et al. (2021)

Neurodegeneration, -inflammation, -trauma; Bone defects/cartilage; Skeletal muscle defects; Heart diseases; Inflammatory bowel disease; Liver disease; Lung fibrosis.

A wide variety of clinical applications, after biocompatibility evaluation by subcutaneous implantation tests according to ISO/EN 10993 part 6 guidelines, have been reported for human amniotic membrane (hAM) / human amnio-chorionic membrane (hACM (Fenelon et al., 2019; Fénelon et al., 2021). *In vitro* cytocompatibility was assessed by extract cytotoxicity assay and contact cytotoxic assay according to the ISO/EN 10993 part 5 guideline.

Multicellular potency has been found critical in preclinical/clinical transplantation as much as PnD paracrine effects, subsidiary to support engraftment and long-term survival for donor cells.

It has been largely described as dP or perinatal cells have constitutive angiogenic and anti-inflammatory properties (C hoi et al., 2012) carried out by release mediators such as transforming growth factor beta 1 (TGF- β1), basic fibroblast growth factor (bFGF), epidermal growth factor (EGF), platelet-derived growth factor (PDGF), insulin-like growth factor 1 (IGF-1), vascular endothelial growth factor (VEGF), anti-inflammatory cytokines (i.e. interleukin (IL)-10), antimicrobial peptides (β-defensins, elafin), and tissue inhibitor of metalloproteinases (TIMP-1, 2, 3 and 4) (Hao et al., 2000; Mao et al., 2017a).

A remarkable property of natural scaffolds and more consistent in progenitor/stem cells is to secrete extracellular vesicles (EVs) commonly distinguished as: 1) macrovesicles (MVs) and 2) exosomes (Rani et al., 2015) vehiculating immunomodulatory or anti-inflammatory molecules in the form of miRNA, mRNA, proteins characteristic of cells of origin (Chen et al., 2010; Rani et al., 2015). Moreover, EVs may have a superior safety profile as compared to the cells they derived from since they do not replicate (Reis et al., 2016) nor cause microvascular embolism (Xiong et al., 2017) and can be stored without losing their properties (Wen et al., 2016). Thus, extensive research is currently underway to establish the potential use of mesenchymal stromal cells extracellular vesicles (MSC-EVs) for cell-free therapeutic applications in diseases, such as cardiovascular diseases (Fleury et al., 2014), liver failure (Maji et al., 2017), and respiratory diseases (Abreu et al., 2016). In addition, animal model-based studies suggest that exosome-sized or small EVs (sEVs), compared to their parental cells, may represent a novel cell-free medicinal product that is effective and can be safely stored without loss of function, as an alternative to cell-based therapies (El Andaloussi et al., 2013; Masyuk et al., 2013).

The role of PnD has been considered paramount in specific environments where support or corrective effects are needed, such as neurodegenerative diseases, skeletal muscle and bone repair, cardioprotection, intestine inflammation, and liver and lung chronic or congenital disorders. The use of either tissue patches, depleted from cells (decellularized hAM or umbilical cord), or perinatal cells/EVs have been validated in preclinical models and translated to the clinic (Figure 2). During the past year, our team composed of international experts on PnD technologies revised and compared existing standardized procedures validated to produce PnD medical products. The present work compiles minimum requirements and provides an overview of the minimal measures needed to translate PnD therapies to the clinic. Being supportive, Table 1 summarizes

the applications of functional/potency assays of PnD in research and the clinic (also see Table 1 for more details).

Crucial aspects of qualification and functional characterization of the final products will be described and discussed. Within the next paragraphs, we aim to bring to light the standardized procedures used to produce a specific regenerative effect. Table 2 provides an overall conclusion for each of the compartments discussed below.

2 Specific sections dedicated to PnD applications

2.1 Role of perinatal derivatives in treatment of neurodegenerative diseases

Novel treatment suggestions for neurodegenerative disorders applying cell or cell-derived products, including those from perinatal sources, primarily rely on the beneficial paracrine effects of the applied products. Although PnD have been shown to display trans-differentiation capacity into neural-like cells *in vitro*, or shown to home to the regions of interest upon transplantation, their differentiation capacity into neural cell types and the replacement of damaged neural cells *in vivo* following grafting plays only a minor (if after all) contribution to the beneficial effect PnD can display as a treatment modality for neurodegenerative disorders. More likely, as neurodegeneration is often accompanied by out-of-balance neuroinflammation, PnD interventions aid in resolving chronic inflammatory processes, induction of neuroprotection by the release of neurotrophic factors, and by stimulation of endogenous neurogenesis, with all three contributing to a successful neuro-regenerative potential (Volkman and Offen, 2017).

2.1.1 Functional assays to demonstrate a neuroprotective effect of perinatal derivatives on neural stem/progenitor cells and neuronal cells after oxidative stress

Oxidative stress following acute or chronic hypoxic-ischemic insults, such as ischemic stroke, hemorrhagic stroke, or hypoxic-ischemic encephalopathy, is a common hallmark of many neurodegenerative diseases. A number of assays have been developed to assess the potential of PnD to reduce or resolve stress responses during/after an ischemic insult. Hereto, neural stem (NSC) or progenitor cells (NPC), neuronal primary cells, or cell lines (such as the mouse neuroblastoma cell line Neuro 2a) are exposed to conditions mimicking a hypoxic-ischemic insult, such as oxygen-glucose deprivation (OGD), possibly followed by reoxygenation or the exposure to H_2O_2 (Petrenko et al., 2020). Different types of PnD may then be added in direct or in indirect co-culture (transwell culture system) with the neural cells. Alternatively, the neural cells' culture medium can be supplemented or replaced with a conditioned medium containing the PnD's secretome (fractions). Since NSC/NPC have the potential to differentiate into all neural cell types, the effects of the PnD treatment on the cell fate specification and differentiation can be assessed by measuring the expression of cell type-specific markers along with the documentation of nuclear and cytoplasmic morphological changes in cells undergoing differentiation. With neuronal cell death being a hallmark of hypoxic-ischemic insults, in the first instance changes in neuronal apoptotic and necrotic outcome measures, such as standard viability assays as well as DNA fragmentation or the expression of molecules associated with apoptotic pathways (e.g., caspases), are valid indicators of the neuroprotective potential of PnD. Depending on the disease model, more specific assays such as the effect of PnD on neurite outgrowth (measured as the total area of neurites) of dorsal root ganglion (Petrenko et al., 2020) or other neurons will complement these outcome measures.

2.1.2 Functional assays to demonstrate a pro-myelination effect of perinatal derivatives on oligodendrocyte (progenitor) cells

Myelination of neuronal axons is a prerequisite for the efficient transmission of electrical signals in the central nervous system (CNS). Many neurodevelopmental or degenerative disorders disrupt myelination or myelin homeostasis. Oligodendrocytes in the CNS and Schwann cells in the peripheral nervous system (PNS) are the cells that build the myelin sheath enwrapping the axons. Oligodendrocytes differentiate from NSC/NPC into oligodendrocyte progenitor cells (OPC), differentiation-committed precursors, newly formed oligodendrocytes, myelin-forming oligodendrocytes, and finally mature oligodendrocytes. This oligodendrocyte fate specification is used to model the potential of PnD to support processes involved in myelination. Hereto, NSC/NPC are directly or indirectly co-cultured with PnD or the culture medium supplemented with a conditioned medium derived from PnD cultures. Differentiation into the different stages of oligodendrocyte development is observed by morphological changes and the expression of stage-specific proteins such as chondroitin sulfate proteoglycan 4 (CSPG4) and platelet-derived growth factor receptor alpha (PDGFRA), markers of oligodendrocyte progenitor cells, galactosylceramidase (GALC), a marker of immature oligodendrocytes, or the mature oligodendroglial marker myelin basic protein (MBP) (Oppliger et al., 2017). Improvement of damage or developmental arrest can also be assessed by co-culturing PnD or administering their secretome to oligodendrocyte cell lines (e.g., MO3.13, (Joerger-Messerli et al., 2021)) or primary OPC after lipopolysaccharide (LPS)- and/or OGD-mediated injury.

2.1.3 Functional assays to demonstrate anti-inflammatory effects of perinatal derivatives on microglia and astrocytes

Microglia are the resident immune cells of the CNS and act as scavengers to remove damaged cells or pathogens. Under pathological conditions, microglia react to danger or pathogen-associated molecular patterns (DAMP/PAMP), proliferate, migrate, undergo morphological changes, and secrete inflammatory molecules such as cytokines, chemokines, and neurotoxic factors. This stimulation can be mimicked *in vitro* by the exposure of primary microglia (Stansley et al., 2012), mixed glial cells (Thomi et al., 2019), immortalized (Stansley et al., 2012; Thomi et al., 2019; Spinelli et al., 2020), or iPSC-derived (Hasselmann and Blurton-Jones, 2020) microglial cell lines to LPS or a combination of interferon-gamma and tumor necrosis factor-alpha (IFNγ+TNFα) (Lively and Schlichter, 2018), with or without hypoxia. Indirect co-cultures with the microglial cells in the bottom and the PnD in transwells, or the addition of PnD-conditioned medium to microglial cells are used to examine the PnD immunoregulatory effects on microglial activation by measuring microglial proliferation, the expression or secretion of inflammatory molecules and by documenting morphological changes (Cao et al., 2019). Alternatively, organotypic brain explant models allow for stimulating glial cells in their niche and the context of pathological cell interactions (Holloway et al., 2021). Furthermore, the recent development of neuro-immune competent organoid models may even shed further light on the diffusion properties of PnD-derived therapeutic actors within a brain-like environment.

Astrocyte activation is a second important hallmark in many neuroinflammatory and degenerative diseases. Primary astrocytes or glial cell cultures enriched in astrocytes (Gorina et al., 2009) can be activated by the treatment with LPS (Roboon et al., 2021) or by OGD (ischemia-reperfusion (Wu et al., 2021)) or H_2O_2 (Wen et al., 2021) in indirect (transwell) co-culture systems. Outcome measures include the production of reactive oxygen species (ROS), the upregulation of the intermediate filament proteins glial fibrillary acidic protein (GFAP) and vimentin, and the presence of complement $C3^+$ astrocytes or reactive astrocyte-induced neuronal cell death (Liddelow et al., 2017).

2.1.4 Functional assays to demonstrate the influence of perinatal derivatives on blood-brain barrier integrity

CNS injury or hypoxic-ischemic and inflammatory insults are accompanied by an increase in the blood-brain barrier (BBB) permeability, resulting in the extravasation of proteins and uncontrolled immune cell trafficking (Cecchelli et al., 2014). Advanced *in vitro* BBB models include brain microvessel endothelial cells, pericytes, and astrocytes (Jamieson et al., 2019) grown in transwell cell cultures or microfluidic devices (Campisi et al., 2018). Small molecule tracers, such as the fluorescent FITC-dextran (Campisi et al., 2018), are added into the upper chamber or outer compartment and are used to monitor the permeability of the BBB model upon stimulation with inflammatory molecules such as TNFα (Chen et al., 2016). The influence on BBB permeability by PnD secretomes can be tested by adding a PnD-conditioned medium to the culture system. Additionally, readout systems include the expression of adhesion molecules and tight junction proteins on the endothelial cells that are involved in the rolling, tethering, and extravasation of peripheral immune cells from the bloodstream to the brain. Transendothelial electric resistance (TEER) is used to measure the integrity of tight junctions in transwell BBB culture models (Srinivasan et al., 2015).

2.1.5 Functional assays to demonstrate the influence of perinatal derivatives on peripheral nerve repair

hAM has been evaluated as nerve wraps or conduits for the repair of peripheral nerve injuries *in vitro* in human and pre-clinical models (Wolfe et al., 2022) and humans (Fénelon et al., 20212021). hAM alone or associated with adult or perinatal cells (Fénelon et al., 2021), such as allogeneic hUC-MSC (Li et al., 2013), has been evaluated. In animal models, allogeneic hUC-MSC alone or coupled to additional scaffolds like PCL polycaprolactone (PCL) or chitosan were delivered at the site of injury (Bojanic et al., 2020), supplemented with systemic erythropoietin injection (Ülger et al., 2021).

In addition, human amniotic membrane epithelial cells (hAEC) (Jin et al., 2015), hAMSC (Chen et al., 2022), hAF stem cells (Su et al., 2018), or hUC-MSC (Bojanic et al., 2020) have been tested alone or coupled to additional scaffolds like PCL or chitosan or embedded in fibrin hydrogel-containing polylactate (PLA) nerve conduits (Su et al., 2018). For sciatic nerve injury models, Schwann cell proliferation and migration were used as *in vitro* assays (Chen et al., 2022). Non-invasive, conventional magnetic resonance imaging (MRI) coupled to a diffusion tensor MRI (DTI)-based fiber tractography assay has been used in the minipig model to follow the repair of sciatic nerve injury after hAF stem cell grafting (Su et al., 2018). Stress relaxation and creep testing were performed to assess the viscoelastic behavior of strained brachial plexus samples, and grooming behavior was scored as an indicator of forepaw motor function in a rabbit model (Jin et al., 2015).

Animal studies and clinical trials have highlighted their role in preventing the recurrence of perineural adhesions, reducing extra- and intra-neural fibrosis, accelerating nerve repair/regeneration, and improving nerve function (Lemke et al., 2018; Bour geois et al., 2019; Fénelon et al., 2021; Mirzayan et al., 2021). Different types of nerve injuries, including those affecting lower or upper extremity and thorax were assessed for: gap, transection, neurotmesis, crush, epineurectomy, induction of chemical fibrosis, and partial transection.

Histological (HE, Toluidine Blue, Oil Red O staining) or immunohistological analysis have allowed qualitative/stereological analysis of the gross morphology or microstructure of: **1)** nerve parameters such as axon regeneration—increase of axon size—number—diameter—density, axonal migration, myelin sheath thickness or nerve fiber diameter; **2)** muscle mass innervated by the transected then repaired nerve and **3)** muscle atrophy attenuation (Bour geois et al., 2019; Bojanic et al., 2020; Ülger et al., 2021; Wolfe et al., 2022). Retrograde axonal transport was estimated through fluorogold-labeled neuron counts after hUC-MSC grafting (Bojanic et al., 2020).

Neuromorphometry employs transmission electron microscopy or high-resolution light microscopy in which the number of myelinated fibers, the total number of nerve fibers, axon diameter, myelin thickness, G-ratio, and N-ratio were the most commonly reported outcomes (Marchesini et al., 2018; Wolfe et al., 2022).

In a rat scarring model for recurrent adhesions in the peripheral sciatic nerve, a vital hAM has been demonstrated to prevent adhesion, improve the level of extra- and intra-neural fibrosis, and support nerve regeneration, and also reflected in the sciatic functional index (Lemke et al., 2018).

Functional motor assessments included various types of static or dynamic gait analysis, strength measurements, or analysis of other specific behavior (Su et al., 2018; Bour geois et al., 2019; Ülger et al., 2021; Wolfe et al., 2022). The sciatic functional index (SFI) is an index of the functional condition of rat sciatic nerve based on measurements made from walking tracks (Ülger et al., 2021). Functional sensory outcomes measures also included withdrawal latency reflex (WRL) tests, tactile tests, or heat cutaneous allodynia (Wolfe et al., 2022).

Electrophysiological tests were performed in the pre-clinical model using a bipolar stimulating electrode placed under the nerve proximal to the hAM graft. Recordings were conducted using superficial electrodes and performed with an electromyogram (EMG). The peak amplitude of the compound muscle action potential (CMAP), CMAP latency of onset, and nerve conduction velocity (NCV) values were calculated (Su et al., 2018; Bour geois et al., 2019; Wolfe et al., 2022).

In humans, non-invasive ultrasound was used to determine neuroma formation and nerve regeneration determined based on EMG (Li et al., 2013).

After hAM grafting, sometimes associated with the hUC-MSC application, sensory and motor function restoration was evaluated based on the Modified Medical Research Council classification (MRCC), categorizing superficial cutaneous pain and tactile sensibility (Li et al., 2013). Additional tests include the Lister test for the intrinsic muscles of the hand, grip power and pinch strength measurements, and Jamar or Sakellarides tests (Riccio et al., 2014).

Finally, satisfaction of patients was assessed by means of the pain disappearance and the Quick Disabilities of the Arm, Shoulder, and Hand (Quick DASH) which evaluates 30 items that measure: 1) physical abilities (21 items); 2) severity of symptoms (5 items), and 3) social skills or roles (4 items) (Marchesini et al., 2018).

2.1.6 Conclusion

The advantage of CNS *in vitro* cell culture systems, compared to animal models, is the relative ease of use, their potential for standardization, and the comparatively short interval from the models' onset to the collection of data. Unfortunately, these assays either alone or in combination are not uniformly used throughout various studies evaluating novel therapeutic strategies for CNS disorders. Therefore, this field may majorly benefit from defining a standardized approach to select a number of appropriate elementary *in vitro* assays for which PnD should pass before proceeding to animal studies and/or human clinical trials. Furthermore, in line with the view of *in vitro* models contributing to the 3R principles in animal experimentation, the development of 3D models and organoids for *in vitro* CNS research may be a major step forward toward clinically meaningful readouts. Once established, this may increase the predictivity of therapeutic success of various PnD.

2.2 Role of perinatal derivatives in treatment of the skeletal-muscle injury

The most challenging aspect of skeletal muscle regeneration is the need for reconstruction of muscle fiber architecture in order to restore tensile force and function. With this in mind, various kinds of supportive scaffolds have been employed for tissue engineering purposes, to guarantee correct myoblast alignment and to induce their fusion. Several approaches already involved the use of scaffolds of natural origins like decellularized PnD to drive myofiber production in damaged muscle.

2.2.1 Functional assays to demonstrate the influence of perinatal derivatives-derived scaffolds on skeletal muscle repair

Experimentally, decellularized scaffolds produced from human amniotic membrane have been proven effective in muscle repair and force regain when combined with training in a rat volumetric muscle loss (VML) model (Izadi et al., 2021). This approach furthermore led to a significant increase in the number of the newly formed centrally nucleated myofibers compared to untreated muscles, an important parameter often evaluated in such models because it is directly correlated to the fusion of myoblasts occurring during muscle regeneration (Wang et al., 2018; Hadipour et al., 2021; Izadi et al., 2021; Magarotto et al., 2021). Moreover, tissue regeneration after scaffold implantation was not only visible by histological methods, but at a functional level. Here electrophysiological methods allowed to demonstrate increased isometric contraction force of the muscle after nerve stimulation (Qiu et al., 2018; Izadi et al., 2021;

Magarotto et al., 2021). In an alternative approach, the peculiar tissue architecture was reproduced in artificial implantable scaffolds with the addition of electrospun fibers of polymers like poly(lactic-co-glycolic acid) PLGA or PCL onto the decellularized amniotic membrane. This guaranteed optimal mechanical properties (strength and elasticity) and cell orientation, as evaluated by measuring the angle of the generated fibers or with live imaging techniques to track cell motility (Hasmad et al., 2018). Furthermore, stem cell differentiation was favored toward a myogenic phenotype, defined by the expression of regenerating muscle markers like MyoD, MyoG, Mhc (Hadipour et al., 2021; Izadi et al., 2021; Magarotto et al., 2021; Park et al., 2021).

2.2.2 Functional assays to demonstrate the influence of perinatal derivatives on skeletal muscle repair

The employment of a scaffold is often not sufficient for complete regeneration in case of extensive tissue damage. In this situation, an effective approach is the administration of cell types that show myogenic potential (Mishra et al., 2020) or are active in the crosstalk with the other cell types that reside in the muscle niche. UC-MSC are active in muscle repair thanks to the interaction with the inflammatory compartment, which triggers and supports regenerative mechanisms. Importantly, they are not only involved in the production of myogenic miRNAs (Mishra et al., 2020; Sun and Karaoz, 2020; Park et al., 2021), but they are also capable to 1) promote macrophage polarization toward an M2 pro-regenerative phenotype, as characterized by the expression of both CD68 and CD206 (Qiu et al., 2018; Arutyunyan et al., 2019), and 2) reduce neutrophil-mediated acute inflammation, indicated by reduced infiltration of $Ly6G^{+}$ cells at the site of injury (Su et al., 2019). Mechanistically, MSC were found to reduce chronic inflammation in sarcopenia through TNFα and IL-6 downregulation (reducing M1-oriented pro-inflammatory signals) and IL-4 and IL-10 upregulation (stimulating M2-oriented anti-inflammatory signals (Wang et al., 2018). For their immunomodulatory and antifibrotic properties, they were also proposed for the treatment of Duchenne's Muscular Dystrophy (Sun and Karaoz, 2020; Park et al., 2021). Moving from cell-based interventions to acellular therapeutics, similar immunomodulatory and/or anti-fibrotic effects were also exerted by their secretome. The mechanism of action of MSC-EVs in muscle regeneration is still under investigation. However, evidence exists that they can modulate the inflammatory response and direct it toward regeneration with the reduction of fibrosis, a parameter quantified by the histological analysis of collagen deposition in the regenerating tissue (Bier et al., 2018; Magarotto et al., 2021). MSC-EVs also act on neuromuscular junctions, repairing axons and restoring nerve physiology (Ma et al., 2019; Magarotto et al., 2021), which is paramount for muscle function, evaluated *in vivo* by grip or gait analysis (Ma et al., 2019; Su et al., 2019).

2.2.3 Conclusion

The multifaceted properties of PnD derivatives are attracting scientific interest for the development of new therapeutic applications in the regenerative medicine field of muscle regeneration. Besides the structural and mechanical support, it appears evident that the paracrine factors released by MSC such as the EVs are the executive of the mechanism of action of PnD in skeletal muscle repair. However, this complex aspect is still under investigation.

When skeletal tissues are damaged, natural scaffolds with their own growth factors and cytokines but also adjuvanted with MSC and EVs stimulate a favorable microenvironment. The promoted regeneration by the induction of pleiotropic effects such as, among others, immune-modulating and pro angiogenic can be validated *in vivo*. In this paragraph indeed, we underlined that *in vivo* functional assays are the best way to prove the PnD derivatives effects.

2.3 Role of perinatal derivatives for bone repair

Bone tissue engineering has emerged as an interdisciplinary strategy combining biomaterials, cells, and/or biologically active molecules, aiming to reconstruct injured or lost bone. PnD and in particular, perinatal tissues and derived cells have been used for that purpose. Orthopedic surgeons successfully apply cryopreserved or decellularized and lyophilized bone allografts. Thus, de-epithelialized or decellularization and/or lyophilization have been used accordingly for perinatal tissues to improve their storage, their biocompatibility, and their capacities to act as a scaffold.

2.3.1 Functional assays to demonstrate the osteogenic potential of the amniotic membrane

Both human amniotic membrane MSC (AMSC) and hAECs display *in vitro* and *in vivo* osteogenic differentiation potential (Kmiecik et al., 2015). It was reported that under osteogenic conditions *in vitro*, intact hAM became mineralized and expressed markers of early and late osteoblastic differentiation, as demonstrated by a significant rise in calcium contents, induction of alkaline phosphatase (AP) activity, RUNX2, AP, BMP-2, and BMP-4 mRNA expression and osteocalcin staining colocalizing with von Kossa/alizarin red staining (Lindenmair et al., 2010).

Similarly, anti-collagen I immunohistochemistry was carried out on intact osteodifferentiated hAM to highlight osteoblastic differentiation potential (Gualdi et al., 2019). Furthermore, Energy dispersive X-ray (EDX) and X-ray diffraction (XRD) were used as a novel approach to qualify the mineralization of amniotic cells in intact

osteodifferentiated hAM and derived amniotic cells (Gualdi et al., 2019). Here, it was reported that, in osteogenic conditions, hAEC had a mesenchymal phenotype with osteocyte function, and even native synthesis of hydroxyapatite, focusing osteogenic potential mainly in this epithelial layer. The whole hAM is characterized using silver nitrate and Alizarin red which are typically used to label the mineralization of isolated cells. Both assays would be easy to implement in a tissue bank.

2.3.2 Functional assays to demonstrate the potential of perinatal derivatives in bone repair

In vitro, the ability of fresh and preserved AM to act as a scaffold upon which adult human bone marrow MSC (hBMSC) can proliferate and differentiate into osteogenic lineage has been assessed using metabolic activity assays, alkaline phosphatase staining, and alizarin red quantification (Fenelon et al., 2019; F enelon et al., 2020). *In vivo*, the efficiency of hUC-MSC to promote bone regeneration can be assessed using ectopic or orthotopic models to evaluate their osteoinductive and/or osteoconductive properties. Representative 2D or 3D-radiography followed by histology (Masson's trichrome and HES staining) are the most commonly performed analysis to evaluate bone regeneration in animal models (Etchebarne et al., 2021; Fenelon et al., 2021). Immunohistochemistry (type I collagen, osteocalcin, AP) brings additional information (Laurent et al., 2017). As an example, it has been investigated the *in vitro* and *in vivo* bone regenerative performance of hUC-MSC and Arginyl-glycyl-aspartic acid (RGD) modified macroporous calcium phosphate cements (CPC). Similarly, it has been observed high expressions of osteogenic specific genes on CPC seeded with hUC-MSC. After implantation for 24 weeks in the rat calvaria bone defect model, the newly formed bone tissue exhibited a higher bone mineral density, new bone amount, and vessel density versus CPC control group (Chen et al., 2013). These observations are in agreement with a study combining blood umbilical cord-derived stem cells with a partially demineralized bone matrix (Liu et al., 2010). Calcium phosphate synthetic bone substitutes (Barboni et al., 2013) and magnesium-enriched hydroxyapatite (MgHA)/collagen-based scaffold (Riccio et al., 2012) were also combined with ovine amniotic fluid PnD. Implanted in an ovine maxillary sinus augmentation model, this study demonstrated a reduced fibrotic reaction, a limited inflammatory response, and an accelerated process of angiogenesis for Sinus explants derived from the PnD-scaffold group compared with the control group (without PnD) (Riccio et al., 2012; Barboni et al., 2013).

Bone develops through a tightly regulated process leading to a hierarchically ordered three-dimensional structure, described in the literature as a bone nodule (Mechiche Alami et al., 2016). UC-WJ-MSC are able to form these 3D structures *in vitro* (Rammal et al., 2017). However, the nodule density of around 9 ± 2 nodules in the cultured area suggests a low commitment of UC-WJ-MSC into osteoprogenitor cells (Rammal et al., 2019). These observations are consistent with other studies highlighting a very low yield of UC-WJ-MSC able to differentiate into osteoblastic lineage (Jin and Lee, 2018; Golchin and Farahany, 2019). Once injected into damaged tissue, UC-WJ-MSC showed a relatively poor rate of cell engraftment and engrafted ones are rather to be short-lived (Wang et al., 2014). The low rate of cell differentiation is in favor of a paracrine mechanism. Despite the small fraction of committed cells, the osteoinductive (i.e., able to induce cell differentiation without adding chemical inductors) scaffold decreased the production of IL-1β, IL-6, and IL-8 inflammatory mediators and increased the release of b-FGF, VEGF angiogenic growth factors by cells in comparison with the inert scaffold. Furthermore, this paracrine action of PnD's cells enhanced the migration of endothelial cells, the neutrophil diapedesis via ICAM1 up-regulation and the osteogenic potential of endothelial cells (e.g. overproduction of BMP-2) (Rammal et al., 2019).

2.3.3 Clinical assays to demonstrate the influence of PnD on bone repair

Usually, in the clinic, bone union and failure were assessed every 6 months during the first year as follows: first X-ray (or Computed Tomography (CT) scan if doubt) showing 3 of 4 continuous cortices (united) (Moris et al., 2016). Clinically, healing is assessed by the absence of pain and absence of mobility at the fracture site and, in the case of the lower limb, weight-bearing (Gindraux et al., 2020). Some patients could also benefit from the Position–Emission Tomography. In bone repair, osseous biopsies for histological or immuno-histochemistry analysis are often too invasive and usually not performed. When used for example to evaluate the benefit of a specific treatment, markers are comparable to those used *in vivo* (Etchebarne et al., 2021).

2.3.4 Conclusion

In conclusion, for bone regenerative approaches, PnD have been considered in different formats. Although PnD may contribute to bone formation directly, their major value may rely rather on their paracrine activity. The amniotic membrane may act as a collagenous niche for tissue deposition and ingrowth. In consequence, *in vitro* functional assays identifying activities such as immunomodulation, proangiogenic and trophic factor release may represent suitable surrogates for these properties.

2.4 Potential role of perinatal derivatives in cardioprotection

Cardiovascular disease and heart failure represent major social and economic burdens as being the leading cause of mortality and morbidity worldwide, with ischemic myocardial infarction the most common event underlying the development of cardiac dysfunction and heart failure (Segers and Lee, 2008; Roger, 2013). When facing prolonged ischemia, the adult mammalian heart can only activate a defective repair mechanism aiming at replacing

cardiomyocytes lost during the hypoxic injury with a non-contractile fibrotic collagen scar, leading over time to the detrimental remodeling of the left ventricle, with progression toward myocardial dysfunction and heart failure (Madonna et al., 2016). Despite the remarkable progress achieved by pharmacological and interventional cardiology in the last 20 years, heart transplantation still represents the ultimate therapeutic option for heart failure. Therefore, preclinical research in cardiac regenerative medicine has been recently developed to define innovative therapeutic strategies to enhance cardiac repair mechanisms.

2.4.1 Emerging regenerative approaches for heart repair

Bona fide myocardial regeneration can only be obtained by structural and functional reconstitution of compromised/lost cardiomyocytes following injury, via the active renewal of surviving resident ones (Eschenhagen et al., 2017). Such regenerative mechanisms have been extensively described in lower vertebrates. Notably, the neonatal rodent heart has recently been shown to promote proficient myocardial renewal as well, although this response is strictly limited to the very first week after birth, with a clear transition to fibrosis and defective repair soon afterward (Foglia and Poss, 2016). True cardiac regeneration and active myocardial renewal are thus very challenging to be accomplished in the mammalian adult heart; therefore, increasing efforts have recently been focused on optimizing endogenous mechanisms of cardiac repair. These directions focus on enhancing cardio-protection and supporting local angiogenesis, in order to preserve as much viable myocardium as possible during injury/disease. In such a perspective, high expectations have been allocated to paracrine effects from stem/progenitor cells and MSC for cardiac repair (Gnecchi et al., 2012; Hodgkinson et al., 2016; Bollini et al., 2018; Menasché, 2018; Balbi et al., 2020; Magh in et al., 2020). Indeed, the secretome isolated from MSC of different PnD origin has widely been investigated in preclinical cell-free strategies for implementing endogenous myocardial repair as tentative proof-of-principle for future therapy. As a matter of fact, endogenous cardiac repair should be promptly targeted during the early phase following acute heart injury (i.e., following myocardial infarction, at time of reperfusion) or improved by additional therapy in case of off-target cardiotoxic effects due to chronic pharmacological treatment (i.e., chemotherapy).

2.4.2 Functional assays to validate perinatal derivatives in cardioprotection/repair

In vitro cardioprotective and pro-angiogenic assays are broadly used to define the paracrine effects of stem/progenitor cell secretomes on supporting cardiomyocyte survival and triggering new vessel development. The *in vitro* mimicking of the altered/injured myocardial conditions can be obtained by exposing cardiomyocytes to severe stress/damage to assess their apoptosis and necrosis, as it has been previously and comprehensively shown (Lazzarini et al., 2016; Balbi et al., 2019a; Balbi et al., 2019b; Takov et al., 2020).

Cardioprotection is usually assessed by evaluating the level of intracellular ROS and metabolism impairment, along with activation of apoptotic pathways and DNA fragmentation in target cardiac cells undergoing hypoxic and/or oxidative stress insult/injury. Cardiomyocyte cell viability is usually evaluated by annexin V and propidium iodide (AnnV/PI) staining, and by MTT/MTS and lactate dehydrogenase activity assay, thus measuring metabolic activity. Angiogenic analyses are generally based on evaluating endothelial progenitor or endothelial-like cell migration and capacity to form tube structures and capillary configurations on Matrigel, following specific stimuli.

The cardio-active and pro-vasculogenic potential of different secretome formulations (the total cell-conditioned medium or its separated and concentrated EV subfraction) from human PnD (i.e., AM-derived progenitors, amniotic fluid stem cells, and umbilical cord stromal mesenchymal cells) have been intensely scrutinized in the last years. The human amniotic fluid progenitor cell secretome and EVs separated and concentrated from that have been recently described to counteract cell death and premature senescence in rodent cardiomyocytes exposed to severe hypoxic stress and cardiotoxic exposure to doxorubicin *in vitro*; likewise, human endothelial colony-forming cells (ECFC) and human umbilical vein endothelial cells (HUVEC) have been shown to respond to the secretome paracrine stimulation by improving their migratory and formation of capillary-like structure *in vitro* (Lazzarini et al., 2016; Balbi et al., 2019a; Balbi et al., 2019b; Takov et al., 2020). Similar promising cardioprotective results have also been obtained with a human amniotic membrane MSC-conditioned medium on the rat embryonic cardiomyoblast-like H9c2 cell line in a model of hypoxia and reoxygenation injury *in vitro* (Danieli et al., 2015). The therapeutic paracrine relevance of human PnD has further been reported in a study demonstrating that human amniotic membrane proteins (AMPs) extracted from the amniotic membrane can antagonize doxorubicin-elicited detrimental effects on H9c2 via the inhibition of oxidative stress and apoptosis. The whole secretome of independent formulation of human umbilical cord mesenchymal stromal cells (UC-MSC), and the EVs obtained from it, has been also proven to be effective in preserving rodent cardiomyocyte cell lines from apoptosis, while stimulating the pro-angiogenic potential HUVEC (Santos Nascimento et al., 2014; Huang et al., 2020).

2.4.3 Conclusion

The majority of studies, reporting *in vivo* validation of PnD therapeutic efficacy (by assessing cardiac function via ultrasound analysis in preclinical animal models of myocardial injury, as extensively reviewed and discussed elsewhere (Magh in et al., 2020)), are to a certain degree supplemented with *in vitro* data describing cardioprotective effects. Some mechanistic studies have been reported, showing

as human amniotic fluid stem cell secretome may preserve doxorubicin-stressed murine primary neonatal cardiomyocytes by activating the PI3K/Akt signaling cascade, and by upregulating the NF-κB controlled genes, Il6 and Cxcl1 (Lazzarini et al., 2016). Moreover, human umbilical cord MSC-EVs have been shown to exert beneficial effects as mediating the horizontal transfer of miR-19a, targeting Sox6 in hypoxic H9c2 cells *in vitro*; such candidate mechanism of action was further assessed by means of Sox6 knockdown together with miR-19a inhibition within MSC-EVs (Huang et al., 2020). In conclusion, while most of the studies published so far have reported beneficial effects by using different PnD, consensus on a uniform method for standardized dosing and protocol of administration has not been reached yet.

2.5 Potential role of perinatal derivatives in bowel inflammation/intestinal regeneration

Inflammatory Bowel Diseases (IBD) such as Ulcerative Colitis and Crohn's Disease are chronic inflammatory diseases of unknown etiology. The majority of patients are diagnosed early in life and the incidence is increasing; therefore, the effect of IBD on healthcare systems will rise exponentially.

In the last decade, numerous studies demonstrated as perinatal cells can modulate the activity of inflammatory cells such as macrophages, T and B lymphocytes. The easy cell availability and lack of ethical concerns yield PnD a promising tool in regenerative medicine (Zhang et al., 2017a).

The factors involved in the immunomodulatory actions of perinatal cells have not been fully identified but have been suggested to rise from factors secreted either as soluble proteins (secretome) or entrapped in EVs. Perinatal-derived EVs contribute to modulating the immune response in inflammatory bowel diseases (IBD) by directly targeting different elements of the inflammatory microenvironment, ultimately leading to the repair and regeneration of damaged tissues (Tolomeo et al., 2021).

2.5.1 Functional assays to support perinatal derivatives in modulating inflammatory bowel diseases

The efficiency of MSC derived from PnD as well as their secretome (conditioned media or purified EVs) have been tested in chemically-induced experimental colitis mouse models, suggesting as a new and innovative approach for IBD cell-based therapy.

Initial studies have shown that UC-MSC modulate dextran sulfate sodium (DSS) induced acute colitis in NOD.CB17-Prkdc scid/J immunodeficient mice (Banerjee et al., 2015). Recently, human UC-MSC effectively alleviated weight loss, intestinal mucosal injury, colon shortening, and reduced clinical disease phenotype in the DSS-induced mouse IBD model by inhibiting ERK phosphorylation in neutrophils (Wang et al., 2020). In a similar experimental approach, both efficacy and mechanism of action of UC-MSC were further evaluated in acute and chronic mouse models of IBD, established by using a DSS solution. Findings of this study indicated an enhanced expression of the intestinal tight junction protein occludin, downregulation of the expression of the autophagy marker LC3A/B in colon tissue, and upregulated the expression of VEGF-A and VEGFR-1 at the injured site (Panhua et al., 2019). In addition, in a DSS-induced colitis model UC-MSC, when administered with MIS416, a novel microparticle that activates NOD2 and TLR9 signaling was found to improve the pathological phenotype by systemically regulating the immune response, (Lee et al., 2018). In this context, treatment with hAFSC resulted in preventing colon shortening after induction of colitis and dramatically ameliorated the body weight loss induced by the DSS treatment

Similar results were obtained when UC-MSC were administered in a trinitrobenzene sulfonate (TNBS)-induced mouse model of colitis (Liang et al., 2011). More specifically, the administration of UC-MSC reduced the severity of TNBS-induced colitis in mice by increasing anti-inflammatory responses in colons of mice, such as the production of IL-10 and reduced production of inflammatory cytokines (Kim et al., 2013). Moreover, preconditioning of UC-MSC with polyribocytidylic acid enhanced the therapeutic effects of UC-MSC in TNBS-induced colitis (Qiu et al., 2017).

Notably, a number of studies showed as AF-MSC and UC-MSC-derived secreted molecules had a significant therapeutic effect, suggesting a paracrine anti-inflammatory mode of action. Indeed, secretome studies on AF-MSC indicated the presence of anti-inflammatory molecules such as interleukins IL-10, IL-1ra, IL-13, and IL-27; and angiogenic factors like angiopoietin-1, PD-ECGF, uPA that can contribute to the functional improvement of DSS-induced colitis in immunodeficient colitis mouse model phenotype (Legaki et al., 2016). Similarly, intraperitoneal injection of MSC extracts in the DSS-C57BL/6 mouse model reduced colitis, disease activity index, histological colitis scores, and increased body weight (Song et al., 2017). EV-based strategies, including UC-MSC-EVs exerted profound effects on alleviating DSS-induced IBD through the modulation of IL-7 expression in macrophages (Mao et al., 2017b) and induction of MUC2 expression (Tolomeo et al., 2021). Furthermore, recent studies indicated that UC-MSC-EV samples containing miRNA-378a inhibited NLR family pyrin domain containing 3 (NLRP3) inflammasomes and abrogated cell pyroptosis, (Cai et al., 2021) and also restored mucosal barrier repair and intestinal immune

homeostasis via TNF-α stimulated gene 6 (Tsg6), to protect against DSS-induced colitis (Yang et al., 2021).

2.5.2 Functional assays to demonstrate the influence of perinatal derivatives in clinic for inflammatory bowel diseases

Experimental approaches have been translated into clinical settings by using stem cell-based therapies for IBDs. Recent data showed that local administration of autologous MSC into perianal fistula leads to an enhanced healing process, promoted fistula relief, and ameliorated clinical complications (Hossein-khannazer et al., 2021).

Interestingly, administration of perinatal MSC to patients with Crohn's disease was proved safe and well-tolerated, generating decreased Crohn's disease activity index score and complete remission. Similarly, the application of allogeneic UC-MSC exhibited safety, feasibility, limited or no adverse effects, and led to the improvement of clinical symptoms. However, no significant changes in the levels of inflammatory cytokines in blood serum were detected (Hossein-khannazer et al., 2021; Vieujean et al., 2022).

2.5.3 Conclusion

Overall, cell-based therapy in IBDs demonstrated that MSC are safe and beneficial following anti-inflammatory activity. However, cell-free products (EVs or secretomes in general) may represent an ideal source of anti-inflammatory agents, solving the problem of cell safety and toxicity (Villa et al., 2019; Herrmann et al., 2021). Notwithstanding, additional studies are ongoing to optimize and standardize preparation, administration, and dosage. Accordingly, the development of functional assays to validate PnD products is a prospective direction to modulate microbial structure or intestinal homeostasis.

2.6 Potential role of perinatal derivatives in liver regeneration

Liver dysfunction comprises heterogeneous malfunctions that could potentially lead to acute or chronic liver disease, such as fulminant hepatitis or acute liver disease, advanced fibrosis/cirrhosis, congenital metabolic disorders, or fatty liver disease (Psaraki et al., 2021). Liver transplantation is the gold-standard therapy for many of the afore disorders, limited by organ shortage and the need for a lifelong immunosuppressive regimen. Recent refinements and preclinical/clinical studies have validated alternative approaches where fetal or neonatal liver cells have been infused in patients with chronic or congenital liver disorders (Gramignoli et al., 2015; Bluhme et al., 2022).

Despite innate proliferative capacities, these progenitor cells have shown limited metabolic and synthetic strength, with reduced clinical outcomes. Furthermore, the limited availability of adult human hepatocytes for clinical treatments, in addition to the immunosuppressant regiment required to sustain cellular long-term engraftment have encouraged the use of different cell sources. Over the past years, several groups and companies have been proposing stem cells as an alternative solution, bounded by genetic and epigenetic instabilities, and limited by hepatic maturation level (Bluhme et al., 2022). The additional negative caveat is represented by the chronic inflammatory milieu in response to allograft, which may favor the oncogenic transformation of transplanted cells. Immune-privileged cells such as perinatal stem cells have attracted attention in preclinical studies. Cells isolated from AM have satisfied safety and efficacy requirements, overcoming all the aforementioned risks, and reverting life-threatening acute and congenital liver diseases. Encouraged by lack of tumorigenicity and multipotency potential, hAEC have been transplanted and corrected inborn errors of metabolism such as maple syrup urine disease (MSUD) (Skvorak et al., 2013a; Skvorak et al., 2013b). Phenylketonuria (Strom et al., 2013), and another liver-based disease, is associated with end-stage renal pathologies (atypical hemolytic uraemic syndrome) (Casiraghi et al., 2021). Preclinical analysis revealed correction or normalization in amino acid and neurotransmitter imbalances in human perinatal treated animals, to a superior level reached by syngeneic murine hepatocytes. And the lack of immuno-recognition in xenogenic settings raised attention to the immune-evasive capacity amniotic cells have, rather than an immuno-privileged phenotype.

Allogeneic perinatal cells have been infused to rescue livers in acute failure, supporting parenchymal cell survival and hepatic functions, highlighting remarkable engraftment and anti-inflammatory effects. Both MSC isolated from amniotic fluid and chorionic plate have proved their potential in rescuing intoxicated livers (Lee et al., 2010; Zagoura et al., 2012; Peng et al., 2014).

Xenotransplantation of perinatal cells into immune-competent animals has proved long-term acceptance without the administration of immunosuppressive drugs and resulted in hepatoprotection and regulation of the inflammatory process (Milosavljevic et al., 2017; Shi et al., 2017). However, in clinical situations, liver treatments by allogeneic cells have been proved to require immediate availability (in fulminant hepatitis) and a high number of cells (up to 2×10^8 cells per kg of body weight in metabolic disorders) (Gramignoli et al., 2015). Such challenges have been frequently hampered by limited engraftment capacity by donor cells, as well as lack of selective advantage. Recent clinical trials have tested the supportive role offered by UC-MSC to allogeneic human hepatocytes for the treatment of liver disease (Iansante et al., 2018). Different reports highlighted as injection of UC-WJ-MSC in patients with chronic liver disorders or steatohepatitis ameliorate transaminase levels and lipid profile,

reduces bilirubin and hyperglycemic profile, resulting in improved MELD score and overall survival (see (Shahrbaf et al., 2022) for revision of such clinical studies). Beneficial clinical support offered by perinatal cells has been ascribed to repeated infusion rather than one single infusion (Jia et al., 2020), in line with results offered by 3 decades of hepatocyte transplantation (Gramignoli et al., 2015). Another source of perinatal MSC, amniotic membrane, has been described as instrumental to attenuate Kupffer autophagy and prevent Stellate activation (Shahrbaf et al., 2022). Recently, it has been reported the therapeutic effects of intact AMSC and secreted factors in reversing sclerosing cholangitis (Sugiura et al., 2018). The pro-regenerative effect offered by perinatal MSC in advanced fibrotic/cirrhotic conditions has been ascribed to ECM remodeling factors, such as secreted MMPs (Fu et al., 2018), or angiogenic and hepatogenic mediators (Ding et al., 2018; Hoffmann et al., 2020). Indeed, perinatal cells actively interact and crosstalk with (innate and adaptive) immune cells or support hepatic regeneration not only by cell-to-cell interactions but also through paracrine mediators. Several studies suggest as perinatal therapies, adequate for patients with liver diseases exacerbated by deranged inflammation, will most likely benefit from PnD secretome rather than cellular hepatic maturation (Nagaishi et al., 2014; Liu et al., 2015; Trohatou and Ro ubelakis, 2017). The clinical efficacy of CP-MSC or AF-MSC injections has been described in relation to secreted anti-inflammatory (i.e., TGF-β1 and IL-10) or anti-fibrotic (i.e., MMP-2 and MMP-9) mediators (Shahrbaf et al., 2022). But soluble mediators are characterized by shorter half-life and limited paracrine distribution compared to active molecules (surface-bound or miRNA) embedded in EVs.

2.6.1 Hepato-specific functional assays to validate perinatal derivatives in liver disease

In the majority of the published reports, the cell viability test has been the sole evaluation for donor quality before infusion. Viability quantification has been routinely offered and used to validate cell transplantation procedures. Regulatory Agencies, such as FDA or EMA, mandate parameters such as product sterility, cell viability, and identity to be included to validate cellular biopharmaceutical products. PnD products are not relieved by such qualifications. While product sterility (bacteria- or mycoplasma-free) is quite a standardized procedure, routinely performed in every manufacturing site, currently, no consensus on the level of viability for the cell product is widely accepted. In many phase II trials, MSC viability between 70% and 90% is commonly required (Matthay et al., 2019), while primary liver cell preparation cannot be inferior to 60% in viability to allow injection in patients (Gramignoli et al., 2015). Furthermore, cell viability is seldom performed to determine the percentage of viable cells versus death (necrotic) cells, with additional detection of cells in the early stages of the cell death cascade (i.e., apoptosis).

The International committee described epithelial cells isolated from the fetal side of the amniotic membrane as positive for CD49f and CD326 (ISCT committee; (Dominici et al., 2006)) and published a position paper recommending the inclusion of functional assays to couple with identity validation for therapeutic cell products (Viswanathan et al., 2019). Nevertheless, current biosynthetic analysis or quantification of secreted anti-inflammatory/anti-fibrotic mediators can be instrumental only for a therapeutic approach where no stem cell maturation/transdifferentiation is required. Hepato-specific phase I and II activities, bile acid transporters, and urea cycle enzymes are critical to determining long/term correction of congenital liver disorders. In hepatocyte transplant programs, such a multiparametric functional analysis is commonly the minimum criteria in order to confirm cell function (Donato et al., 2008; Bluhme et al., 2022).

Between perinatal cells, hAEC have attracted particular attention for their hepatocyte-like features and can acquire hepatic functions upon transplantation. Epithelial cells released by the amniotic membrane have been proved to secrete low levels of albumin, and upon engraftment in liver parenchyma mature into functional hepatocyte-like cells expressing Cytochrome P450 (CYP) enzymes (as CYP3A4) or secreting proteinases (as A1AT) (Takashima et al., 2004). *Ex vivo* maturation of stem or progenitor cells into a functional hepatic phenotype is still debated. During the past years, revisional studies elegantly proved as the generation of hepatocyte-like cells starting from somatic or perinatal MSC was not a direct consequence of trans-differentiation into endoderm-like cells, but rather resulting from the fusion between donor cells and recipient's hepatocytes (Camargo et al., 2004; Willenbring et al., 2004). Differently, epithelial cells isolated from the amniotic membrane have been proved capable to mature into functional, adult parenchymal cells upon being implanted in the liver, precluding any fusion event between donor and recipient cells (Marongiu et al., 2015). Such hepatic maturation has only been partially achieved in 2D culture (M iki et al., 2005; Marongiu et al., 2011; Fanti et al., 2017; Maymó et al., 2018; Passaretta et al., 2020).

Metabolic activities in human hepatocytes or stem cell-derived hepatocyte-like cells can be assessed by incubation with drugs or chemical substrates and analyzed with unexpensive and widely available lab equipment (such as spectrophotometers) (Kim et al., 2005; Gramignoli et al., 2012). Release criteria and a battery of potency assays have been developed and described, where up to eleven different hepatic functions can be simultaneously measured to validate donor cells transplanted to offer support or replace liver cells (Gramignoli et al., 2013; Gramignoli et al., 2014). Indeed, in order to validate multi-functional cells, such as liver cells, a matrix of functional assays has been recommended to support injection of multipotent PnD cells and confirm maturation capacity into periportal or centro-lobular hepatocytes and cholangiocytes. Bio-synthetic and metabolic activities have been frequently coupled with selective transcriptome analysis. Hepatic maturation can be monitored by transcriptomic assays specifically designed to

validate stem/progenitor cell transplantations and match patients' needs (Zabulica et al., 2019).

2.6.2 Liver organoid as novel perinatal derivatives maturation potency assay for liver disease

The therapeutic potential of liver organoids represents an alternative of functional and expandable cells for transplantation, exceeding the current limitations (Prior et al., 2019). Liver organoids have been recently established from different cell sources among which hAEC have currently gained particular attention.

Some authors demonstrated that the combination of different cell types (endothelial, mesenchymal) in a 3D culture system may promote and enhance stem cell differentiation, physiological function, and proliferation ability, providing a tissue engineering strategy, referred to as "building blocks", for larger tissue constructs (Takebe et al., 2013; Laschke and Menger, 2017; Nie et al., 2018; Lebreton et al., 2019). Recently, multicellular organoids have been generated with hepatic features and functions by combining hAEC with HUVEC and MSC (Furuya et al., 2019). Besides obtaining functional organoids, they evaluated cellular differentiation within organoids through a bioinformatics approach demonstrating a higher level of cell differentiation in comparison with 2D cell cultures.

Additional studies have been conducted to evaluate liver organoids for hepato-specific gene expression and functions, such as CYP3A4 activity and inducibility, albumin secretion, ammonia and metabolism, the ability to efflux rhodamine or store bile acids, lipids, or glycogen (Ramachandran et al., 2015; Pettinato et al., 2019; Wu et al., 2019).

Based on these results, liver organoids could represent a novel *in vitro* model to study novel therapeutic interventions, but may become important an alternative strategy to organ transplantation for liver failure (Furuya et al., 2019). However, implantation strategies and high engraftment efficiency are crucial to rescue metabolic defects. The percentage of organoid engraftment reported is extremely low (1%) (Huch et al., 2013) and restoring enzyme or protein deficiency requires several billion proficient cells, quantified in approx. 5–10% of total liver mass according to missing enzyme (Gramignoli et al., 2015). It has been reported as liver organoids can mimic structures and genetic signatures, although their biomedical use on a large scale is currently limited to the lack in control of cell size, shape, and composition (Rossi et al., 2018). In this regard, it appears crucial to optimize long-term cultures and differentiation characteristics of liver organoids aimed at generating a tissue architecture closer to the *in vivo* conditions (Ramachandran et al., 2015). *In vitro* refinements as well as *in vivo* validation are in progress.

2.6.3 Conclusion

The liver, with its unique regenerative capacity and plethora of functions critical for life, is most likely one of the organs that can largely benefit from PnD supportive strategies to enhance regeneration rather than organ replacement.

Cell-based therapies have proved safety and efficacy for liver regeneration or inborn errors of metabolism correction. However, a reliable, stable source of functional hepatocyte-like cells is still pending to offer such a strategy to millions of patients with congenital or chronic liver disease. Perinatal cells such as MSC or hAEC have been recognized with constitutive and robust anti-inflammatory and anti-fibrotic properties, qualifying these PnD as suitable bioproducts for inflammatory conditions such as hepatitis, fibrosis, and cirrhosis. However, to correct enzymatic defects, a large amount of proficient and metabolic active cells is needed. Convincing evidence in support of the maturation of epithelial cells isolated from AM is encouraging. Moving from the fact that hAEC originates from epiblast during the second week of embryo development and display the presence of early-phase hepatic markers, such PnD product is motivating translation into phase I and II clinical trials. Conversely, transdifferentiation of MSC into functional hepatocyte-like cells has raised more concerns than solid evidence and will most likely restrict their use to paracrine effects or secretome approaches in the near future.

Major challenge in many published studies is validating progenitor/stem cell maturation into functional hepatocytes. Transcriptomic analysis has represented an easy and relatively cheap method to initially test PnD, but such analysis needs to be coupled with real metabolic activity and performed in direct comparison with primary human hepatocytes.

The involvement of metabolic enzymes characteristic of mature, functional somatic cells and the current lack of standardized and reproducible protocols able to induce hepatic maturation on any progenitor or stem cell *in vitro* to a level that corresponds to postnatal liver cells (Zabulica et al., 2019) makes hepatic potency assay refinement even more complex than any other organ, where immunomodulation or inflammatory governance is the sole or major goals.

Finally, concerning the liver organoid approach, whilst many 3D liver models are described as organoids, not all of them are equally organotypic since in most cases they are aggregates of a single cell type or mixed cell types rather than containing both parenchymal and non-parenchymal cells of the liver necessary for modeling inflammation and liver disease. Although this approach still needs further validation *in vitro* and *in vivo*, to circumvent the issue of angiogenesis, innervation or survival of encapsulated hepatocytes, PnD-derived organoids deserve much attention in comparison both with iPSC-derived organoids, which imply the risk to develop teratomas and with adult stem cells-derived

organoids which show a lack of heterogeneity in the starting population.

2.7 Potential role of perinatal derivatives on lung fibrosis

Idiopathic pulmonary fibrosis (IPF) is a progressive, fatal, chronic interstitial lung disease characterized by aberrant extracellular matrix deposition leading to loss of normal lung architecture and respiratory capacity. In Europe and North America, IPF has an incidence of 3–9 cases per 100,000 people and is increasing worldwide (Scelfo et al., 2017).

Although IPF etiology remains unknown, it is generally considered a dysregulated wound healing process mediated by resident fibroblasts and recruited fibrocytes which are activated to myofibroblasts (the latter of which are mostly responsible for extracellular matrix production) by repetitive alveolar injuries (induced for example by environmental exposures, smoking, viral infections and by genetic predispositions). However, more recent findings evidenced the contribution of diverse immune cell types, belonging to both innate (neutrophils, monocytes, macrophages) and adaptative (T and B lymphocytes) immune systems, in the initiation and progression of fibrotic lesion in IPF patients (Desai et al., 2018; Heukels et al., 2019).

In this context, PnD have been applied in lung fibrosis models with the purpose either to counteract the proliferation and collagen production of lung myofibroblasts and also to modulate the inflammatory response involved in fibrosis initiation and progression.

2.7.1 Lung-specific functional assays to validate perinatal derivatives in lung fibrosis

Due to the multiple cellular actors involved in the pathogenesis of IPF and the consequent implication of different pathways contributing either to fibrogenesis and fibrolysis, *in vitro* models of fibrosis do not resemble the complex conditions of *in vivo* fibrotic tissues. The general *in vitro* approach is to analyze the effects of PnD on *in vitro* models of inflammation-independent fibrosis, for example, the assessment of their direct effects on the proliferation, collagen production, and the secretion of profibrotic cytokines (e.g., TGF-β, PDGF-a, and PDGF-b), of lung fibroblasts activated to myofibroblasts with TGF-β (Li et al., 2008; Vosdoganes et al., 2013).

Recently, 3D *in vitro* lung models have been developed in the effort to reproduce the cellular and functional complexity of pulmonary tissue and possibly recapitulate the cellular and structural alterations present in the lungs of patients with IPF. Lung organoids have been developed by combining collagen-functionalized alginate beads and induced pluripotent stem cell (iPSC) derived from human lung fibroblasts in a rotational bioreactor (Wilkinson et al., 2017). To generate a model of progressive scarring, as found in IPF patients, organoids have been treated with exogenous TGF-β1 and observed increased expression of collagen 1, α-SMA, and the emergence of fibroblastic foci confirming the possibility to model lung fibrosis *in vitro*.

Lung spheroids (called pulmospheres) have been developed using cells and extracellular matrix components isolated from lung biopsies obtained from IPF patients (Surolia et al., 2017) and they have been applied to evaluate the responsiveness of individual patients to antifibrotic drugs.

The limitations of the *in vitro* lung disease modeling make it so that studies focused on establishing the potential anti-fibrotic effects of PnD have been performed on animal models evaluating a series of cellular/humoral/tissue parameters. Specifically, PnDs, and mainly hAEC and hAMSC, have been administered in animals with bleomycin-induced pulmonary fibrosis to evaluate either their ability to reduce lung inflammation and their potential to slow down the progression and even to reverse the fibrotic lesion.

In these studies, the anti-inflammatory ability of PnD was evaluated in terms of reduction of inflammation and immune cell infiltration in lung parenchyma and broncho-alveolar lavage. Specifically, these were observed as: 1) a reduction of neutrophils (Cargnoni et al., 2009; Murphy et al., 2011) and macrophages in the lungs (Tan et al., 2014); 2) increased lung levels of regulatory T cells (Treg), able to suppress T cell activation (Tan et al., 2015); 3) promotion of macrophage polarization toward an anti-inflammatory phenotype (M2 macrophages) (Murphy et al., 2012; Tan et al., 2014; Tan et al., 2018); 4) reduction of lung levels of proinflammatory cytokines (MCP-1, TNF-a, IL-1, IL-6) (Moodley et al., 2010; Murphy et al., 2011) and chemokines (CXCL12, CXCL13, BAFF (Carg noni et al., 2020)); 5) increase of tissue levels of cytokines and molecules with anti-inflammatory activities, such as IL-10 (Carg noni et al., 2020) and TSG-6 (Moodley et al., 2013); 6) reduction in the number and in the maturation ability of B cells recruited in lung parenchyma (Carg noni et al., 2020); and 7) reduction in the number and size of Tertiary Lymphoid Organs (TLO) (Carg noni et al., 2020), T and B cell aggregates found in the lungs of IPF patients and that correlate with inflammation chronicization and severity of lung fibrotic lesions (Todd et al., 2013).

Associated and possibly mediated by the ability to counteract the inflammatory response and the chronicization of lung inflammatory processes, PnD (hAEC and hAMSC) exhibited the ability to interfere with the progression of lung fibrotic lesions. Lung fibrosis has been evaluated through the assessment of parameters/factors involved either in fibrogenesis or in fibrolysis. Indeed, it has been observed that PnD decreases lung levels of TGF-β1 (Moodley et al., 2010), a pro-fibrotic growth factor with a crucial role in triggering the activation of lung fibroblasts to myofibroblasts (α-SMA positive cells) (Murphy et al., 2012; Vosdoganes et al., 2013; Carg noni et al., 2020) and lung accumulation of collagen and fibronectin (Vosdoganes et al., 2013; Carg noni et al., 2020). Instead, PnD appears to promote fibrolysis by increasing lung levels of MMPs and by decreasing their inhibitors TIMPs (Moodley et al., 2010).

TABLE 2 Conclusion at a glance.

Conclusion at a glance for each analyzed compartment	
Neuronal	*in vitro* assays are not uniformly used to evaluate novel therapeutic strategies for CNS disorders, limiting uniform conclusions.
	3D models and organoids for *in vitro* CNS research may be a major step forward towards clinically meaningful readouts
Muscle	*in vitro* analysis on paracrine factors released by MSC have been proposed as executive of the mode of action for PnDs in skeletal muscle repair.
	pleiotropic effects can be validated *in vivo*.
Bone	*in vitro* functional assays identified activities such as immunomodulation, proangiogenic and trophic factor release after employment of AM
Heart	*in vitro* assays describe cardioprotective effects.
	in vivo validation of PnD therapeutic efficacy (by assessing cardiac function via ultrasound analysis)
Intestine	*in vivo* animal models to validate PnD products is a prospective direction to modulate microbial structure or intestinal homeostasis.
Liver	transcriptomic analysis coupled with metabolic activity are required to validate progenitor/stem cell maturation into functional hepatocytes.
	3D PnD-derived organoids are innovative, instrumental tools to study angiogenesis, innervation and to improve survival of encapsulated hepatocytes
Lung.	limitations of the *in vitro* 3D lung models to recapitulate all disease features
	in vivo models evidenced the anti-inflammatory and anti-fibrotic actions of PnD (cells, secretome and EVs) encouraging application in clinical studies

UC-MSC, similar to hAEC and hAMSC, were recently reported to reduce collagen deposition and lung IL-6 expression in bleomycin-challenged mice when administered twice (24 h and 7 days post-bleomycin) (Moroncini et al., 2018). However, differently from the other PnD, hUC-MSC treatment reduced lung levels of M2 macrophages.

It must be underlined that the anti-inflammatory and anti-fibrotic effects of perinatal cells were observed regardless of any significant engraftment of these cells in the injured lung after administration (Cargnoni et al., 2009; Murphy et al., 2011), suggesting that secreted factors, rather than cells per sé, act via a paracrine mechanism on host cells. Indeed, both conditioned medium generated from the *in vitro* culture of hAMSC (hAMSC-CM) and EVs from hAEC (hAEC-EVs), have been shown to exert beneficial actions in a bleomycin-induced lung fibrosis model. The treatment with hAMSC-CM preserved blood gas parameters of bleomycin-challenged mice and reduced lung levels of pro-inflammatory and pro-fibrotic cytokines (IL-6, TNF-α, MIP-1α, MCP-1 TGF-β) associated with reduced lung macrophage levels (Cargnoni et al., 2014). Intranasal instillation of hAEC-Exo administered early, on day 1 post bleomycin challenge, reduced lung inflammation while treatment on day 7 improved tissue-to-airspace ratio and reduced fibrosis (Tan et al., 2018).

2.7.2 Conclusion

The experimental evidence supporting the anti-inflammatory and anti-fibrotic actions of PnD (cells and derived secretome and EV) has encouraged their application in clinical studies. In particular, placental stromal cells (Chambers et al., 2014) and hUC-MSC (Zhang et al., 2017b) were transplanted in IPF patients with null/mild side effects. More recently, to limit the immunopathogenic effects of cytokine storm, hUC-MSC were used, in combination with the standard optimal care, to treat COVID-19 patients with ARDS (Meng et al., 2020; Shu et al., 2020). The studies performed until now indicated that PnD administration is feasible and safe (Lanzoni et al., 2021), however, clinical trials with a large population of patients are needed to demonstrate the potential efficacy of PnD in human diseases.

3 Overall message

The use of PnD in regenerative medicine covers the employment of scaffolds after decellularization or de-epithelization, stem cells, and secretome including EVs. Recent preclinical and clinical results propose PnD derivatives as safe and effective biological products, whereas their therapeutic application and effectiveness remain challenged. Potency assays are designed to certify the mechanism of action of starting material, pre- or post-commitment.

Any PnD technology is required to satisfy strict release criteria, based on the quality of cell products as well as potency measurements validating specific capacity. Unlike conventional release criteria based on static marker qualification (immune-cytological analysis), specific potency assays are less standardized and cannot be performed on donor cells inefficiently or partially committed over a specific phenotype.

Multiple factors influence treatment outcomes and the proposed potency assays aim to mark a new path to standardize PnD application. This manuscript aimed at offering a guide on when and how it may be advantageous for the employment of placenta-derived cells or scaffolds. The described potency assays can serve as the first tool to standardize PnD derivation and usage, and the second instance may contribute to match recipients' needs with donor characteristics. We are aware that standardization in manufacturing and qualification represents the main limitations hampering a more intensive and extensive use of PnD in clinical trials, so far. A current lack of consensus in the scientific community has limited PnD use in clinical settings, although such derivatives have been reported well-tolerated and refractory to the host's

immunorecognition and rejection. To establish and predict PnD functionality, COST working group of experts has been actively recruited and worked to establish a clear set of laboratory tests that can be conducted in every research or transplant centers, using common laboratory equipment and fulfilling regulatory agencies' requirements. Different validation analyses will likely require both *in vitro* 2D/3D tests to refine activity and modalities, correlated by *in vivo* validations using human-related animal models. As result, we can envision in the near future, a guide compiled by the international community that will standardize the assays, detail advantages and disadvantages, and tailor the implementation of PnD according to patient's needs. Any ethical or religious issues have been depicted during the past years, since perinatal cells and tissue are commonly considered waste material (at least in the vast majority of medical centers) and may represent a new perspective in regenerative and interventional medicine, upon standardization and validation of the afore processes.

Data availability statement

The original contributions presented in the study are included in the article/Supplementary Material, and further inquiries can be directed to the corresponding authors.

Author contributions

SD, MR, AC, RG, SW, FG, SB, HK, MF, RD, MB, VB, RDP, AS, MP, wrote the specific parts of the manuscript and the table. AS draw the figure. MP, PP, coordinated the work and compiled the manuscript. All authors contributed to revising and editing the manuscript and approved the manuscript.

Funding

This work contributes to the COST Action CA17116 International Network for Translating Research on Perinatal Derivatives into Therapeutic Approaches (SPRINT), supported by COST (European Cooperation in Science and Technology). SDA is supported by the Grant 27/01, Foundation Institute of Pediatric Research Città della Speranza, Italy, PI: MP.

Conflict of interest

The authors declare that the research was conducted in the absence of any commercial or financial relationships that could be construed as a potential conflict of interest.

Publisher's note

All claims expressed in this article are solely those of the authors and do not necessarily represent those of their affiliated organizations, or those of the publisher, the editors and the reviewers. Any product that may be evaluated in this article, or claim that may be made by its manufacturer, is not guaranteed or endorsed by the publisher.

References

Abreu, S. C., Weiss, D. J., and Rocco, P. R. M. (2016). Extracellular vesicles derived from mesenchymal stromal cells: A therapeutic option in respiratory diseases? *Stem Cell Res. Ther.* 7 (1), 53. doi:10.1186/s13287-016-0317-0

Arutyunyan, I., Fatkhudinov, T., Elchaninov, A., Vasyukova, O., Makarov, A., Usman, N., et al. (2019). Umbilical cord-derived mesenchymal stromal/stem cells enhance recovery of surgically induced skeletal muscle ischemia in a rat model. *Histol. Histopathol.* 34 (5), 513–523. doi:10.14670/HH-18-057

Balbi, C., Costa, A., Barile, L., and Bollini, S. (2020). Message in a bottle: Upgrading cardiac repair into rejuvenation. *Cells* 9 (3), 724. doi:10.3390/cells9030724

Balbi, C., Lodder, K., Costa, A., Moimas, S., Moccia, F., van Herwaarden, T., et al. (2019). Reactivating endogenous mechanisms of cardiac regeneration via paracrine boosting using the human amniotic fluid stem cell secretome. *Int. J. Cardiol.* 287, 87–95. doi:10.1016/j.ijcard.2019.04.011

Balbi, C., Lodder, K., Costa, A., Moimas, S., Moccia, F., van Herwaarden, T., et al. (2019). Supporting data on *in vitro* cardioprotective and proliferative paracrine effects by the human amniotic fluid stem cell secretome. *Data Brief.* 25, 104324. doi:10.1016/j.dib.2019.104324

Banerjee, A., Bizzaro, D., Burra, P., Di Liddo, R., Pathak, S., Arcidiacono, D., et al. (2015). Umbilical cord mesenchymal stem cells modulate dextran sulfate sodium induced acute colitis in immunodeficient mice. *Stem Cell Res. Ther.* 6 (1), 79. doi:10.1186/s13287-015-0073-6

Barboni, B., Mangano, C., Valbonetti, L., Marruchella, G., Berardinelli, P., Martelli, A., et al. (2013). Synthetic bone substitute engineered with amniotic epithelial cells enhances bone regeneration after maxillary sinus augmentation. *PLoS One* 8 (5), e63256. doi:10.1371/journal.pone.0063256

Bier, A., Berenstein, P., Kronfeld, N., Morgoulis, D., Ziv-Av, A., Goldstein, H., et al. (2018). Placenta-derived mesenchymal stromal cells and their exosomes exert therapeutic effects in Duchenne muscular dystrophy. *Biomaterials* 174, 67–78. doi:10.1016/j.biomaterials.2018.04.055

Bluhme, E., Henckel, E., Gramignoli, R., Kjellin, T., Hammarstedt, C., Nowak, G., et al. (2022). Procurement and evaluation of hepatocytes for transplantation from neonatal donors after circulatory death. *Cell Transpl.* 31, 096368972110699. doi:10.1177/09636897211069900

Bojanic, C., To, K., Zhang, B., Mak, C., and Khan, W. S. (2020). Human umbilical cord derived mesenchymal stem cells in peripheral nerve regeneration. *World J. Stem Cells* 12 (4), 288–302. doi:10.4252/wjsc.v12.i4.288

Bollini, S., Smits, A. M., Balbi, C., Lazzarini, E., and Ameri, P. (2018). Triggering endogenous cardiac repair and regeneration via extracellular vesicle-mediated communication. *Front. Physiol.* 9, 1497. doi:10.3389/fphys.2018.01497

Bourgeois, M., Loisel, F., Obert, L., Pluvy, I., and Gindraux, F. (2019). Can the amniotic membrane be used to treat peripheral nerve defects? A review of literature. *Hand Surg. Rehabil.* 38 (4), 223–232. doi:10.1016/j.hansur.2019.05.006

Choi, J. S., Kim, J. D., Yoon, H. S., and Cho, Y. W. (2012). Full-thickness skin wound healing using human placenta-derived extracellular matrix containing bioactive molecules. *Tissue Eng. Part A* 19 (3–4), 329–339. doi:10.1089/ten.tea.2011.0738

Cai, X., Zhangyu, Z., Yuantao, J., Ocansey, D. K. W., Tu, Q., Zhang, X., et al. (2021). hucMSC-derived exosomes attenuate colitis by regulating macrophage pyroptosis via the miR-378a-5p/NLRP3 axis. *Stem Cell Res. Ther.* 12 (1), 416. doi:10.1186/s13287-021-02492-6

Camargo, F. D., Finegold, M., and Goodell, M. A. (2004). Hematopoietic myelomonocytic cells are the major source of hepatocyte fusion partners. *J. Clin. Invest.* 113 (9), 1266–1270. doi:10.1172/jci21301

Campisi, M., Shin, Y., Osaki, T., Hajal, C., Chiono, V., Kamm, R. D., et al. (2018). 3D self-organized microvascular model of the human blood-brain barrier with endothelial cells, pericytes and astrocytes. *Biomaterials* 180, 117–129. doi:10.1016/j.biomaterials.2018.07.014

Cao, D., Qiao, H., He, D., Qin, X., Zhang, Q., Zhou, Y., et al. (2019). Mesenchymal stem cells inhibited the inflammation and oxidative stress in LPS-activated microglial cells through AMPK pathway. *J. Neural Transm. (Vienna).* 126 (12), 1589–1597. doi:10.1007/s00702-019-02102-z

Cargnoni, A., Romele, P., Bonassi Signoroni, P., Farigu, S., Magatti, M., Vertua, E., et al. (2020). Amniotic MSCs reduce pulmonary fibrosis by hampering lung B-cell recruitment, retention, and maturation. *Stem Cells Transl. Med.* 9 (9), 1023–1035. doi:10.1002/sctm.20-0068

Cargnoni, A., Gibelli, L., Tosini, A., Signoroni, P. B., Nassuato, C., Arienti, D., et al. (2009). Transplantation of allogeneic and xenogeneic placenta-derived cells reduces bleomycin-induced lung fibrosis. *Cell Transpl.* 18 (4), 405–422. doi:10.3727/096368909788809857

Cargnoni, A., Piccinelli, E. C., Ressel, L., Rossi, D., Magatti, M., Toschi, I., et al. (2014). Conditioned medium from amniotic membrane-derived cells prevents lung fibrosis and preserves blood gas exchanges in bleomycin-injured mice-specificity of the effects and insights into possible mechanisms. *Cytotherapy* 16 (1), 17–32. doi:10.1016/j.jcyt.2013.07.002

Casiraghi, F., Ordonez, P. Y. R., Azzollini, N., Todeschini, M., Rottoli, D., Donadelli, R., et al. (2021). Amnion epithelial cells are an effective source of factor H and prevent kidney complement deposition in factor H-deficient mice. *Stem Cell Res. Ther.* 12 (1), 332. doi:10.1186/s13287-021-02386-7

Cecchelli, R., Aday, S., Sevin, E., Almeida, C., Culot, M., Dehouck, L., et al. (2014). A stable and reproducible human blood-brain barrier model derived from hematopoietic stem cells. *PLoS One* 9 (6), e99733. doi:10.1371/journal.pone.0099733

Chambers, D. C., Enever, D., Ilic, N., Sparks, L., Whitelaw, K., Ayres, J., et al. (2014). A phase 1b study of placenta-derived mesenchymal stromal cells in patients with idiopathic pulmonary fibrosis. *Respirology* 19 (7), 1013–1018. doi:10.1111/resp.12343

Chen, C. C., Liu, L., Ma, F., Wong, C. W., Guo, X. E., Chacko, J. V., et al. (2016). Elucidation of exosome migration across the blood–brain barrier model *in vitro*. *Cell. Mol. Bioeng.* 9 (4), 509–529. doi:10.1007/s12195-016-0458-3

Chen, T. S., Lai, R. C., Lee, M. M., Choo, A. B. H., Lee, C. N., Lim, S. K., et al. (2010). Mesenchymal stem cell secretes microparticles enriched in pre-microRNAs. *Nucleic Acids Res.* 38 (1), 215–224. doi:10.1093/nar/gkp857

Chen, W., Chang, S., Yang, C., Zhou, J., Zhang, H., Nie, K., et al. (2022). Schwann cell-like cells derived from human amniotic mesenchymal stem cells promote sciatic nerve repair through an exosome-induced SOX2/FN1 pathway *in vitro*. *Int. J. Mol. Med.* 49 (6), 80. doi:10.3892/ijmm.2022.5136

Chen, W., Liu, J., Manuchehrabadi, N., Weir, M. D., Zhu, Z., Xu, H. H. K., et al. (2013). Umbilical cord and bone marrow mesenchymal stem cell seeding on macroporous calcium phosphate for bone regeneration in rat cranial defects. *Biomaterials* 34 (38), 9917–9925. doi:10.1016/j.biomaterials.2013.09.002

Crapo, P. M., Gilbert, T. W., and Badylak, D. V. M. (2011). An overview of tissue and whole organ decellularization processes. *Biomaterials* 32 (12), 3233–3243. doi:10.1016/j.biomaterials.2011.01.057

Danieli, P., Malpasso, G., Ciuffreda, M. C., Cervio, E., Calvillo, L., Copes, F., et al. (2015). Conditioned medium from human amniotic mesenchymal stromal cells limits infarct size and enhances angiogenesis. *Stem Cells Transl. Med.* 4 (5), 448–458. doi:10.5966/sctm.2014-0253

Desai, O., Winkler, J., Minasyan, M., and Herzog, E. L. (2018). The role of immune and inflammatory cells in idiopathic pulmonary fibrosis. *Front. Med.* 5, 43. doi:10.3389/fmed.2018.00043

Ding, C., Zou, Q., Wang, F., Wu, H., Chen, R., Lv, J., et al. (2018). Human amniotic mesenchymal stem cells improve ovarian function in natural aging through secreting hepatocyte growth factor and epidermal growth factor. *Stem Cell Res. Ther.* 9 (1), 55. doi:10.1186/s13287-018-0781-9

Dominici, M., Le Blanc, K., Mueller, I., Slaper-Cortenbach, I., Marini, F. C., Krause, D. S., et al. (2006). Minimal criteria for defining multipotent mesenchymal stromal cells. The International Society for Cellular Therapy position statement. *Cytotherapy* 8 (4), 315–317. doi:10.1080/14653240600855905

Donato, M. T., Lahoz, A., Montero, S., Bonora, A., Pareja, E., Mir, J., et al. (2008). Functional assessment of the quality of human hepatocyte preparations for cell transplantation. *Cell Transpl.* 17 (10–11), 1211–1219. doi:10.3727/096368908787236620

Dubus, M., Scomazzon, L., Chevrier, J., Ledouble, C., Baldit, A., Braux, J., et al. (2022). Antibacterial and immunomodulatory properties of acellular wharton's jelly matrix. *Biomedicines* 10 (2), 227. doi:10.3390/biomedicines10020227

El Andaloussi, S., Mäger, I., Breakefield, X. O., and Wood, M. J. A. (2013). Extracellular vesicles: Biology and emerging therapeutic opportunities. *Nat. Rev. Drug Discov.* 12 (5), 347–357. doi:10.1038/nrd3978

Eschenhagen, T., Bolli, R., Braun, T., Field, L. J., Fleischmann, B. K., Frisén, J., et al. (2017). Cardiomyocyte regeneration. *Circulation* 136 (7), 680–686. doi:10.1161/circulationaha.117.029343

Etchebarne, M., Fricain, J-C., Kerdjoudj, H., Di Pietro, R., Wolbank, S., Gindraux, F., et al. (2021). Use of amniotic membrane and its derived products for bone regeneration: A systematic review. *Front. Bioeng. Biotechnol.* 9, 661332. doi:10.3389/fbioe.2021.661332

Fenelon, M., Etchebarne, M., Siadous, R., Grémare, A., Durand, M., Sentilhes, L., et al. (2020). Assessment of fresh and preserved amniotic membrane for guided bone regeneration in mice. *J. Biomed. Mater. Res. A* 108 (10), 2044–2056. doi:10.1002/jbm.a.36964

Fanti, M., Gramignoli, R., Serra, M., Cadoni, E., Strom, S. C., Marongiu, F., et al. (2017). Differentiation of amniotic epithelial cells into various liver cell types and potential therapeutic applications. *Placenta* 59, 139–145. doi:10.1016/j.placenta.2017.03.020

Fenelon, M., B Maurel, D., Siadous, R., Gremare, A., Delmond, S., Durand, M., et al. (2019). Comparison of the impact of preservation methods on amniotic membrane properties for tissue engineering applications. *Mater Sci. Eng. C Mater Biol. Appl.* 104, 109903. doi:10.1016/j.msec.2019.109903

Fénelon, M., Catros, S., Meyer, C., Fricain, J. C., Obert, L., Auber, F., et al. (2021). Applications of human amniotic membrane for tissue engineering. *Membr. (Basel)* 11 (6), 387. doi:10.3390/membranes11060387

Fénelon, M., Catros, S., Meyer, C., Fricain, J. C., Obert, L., Auber, F., et al. (20212021). Applications of human amniotic membrane for tissue engineering. *Membr. (Basel).* 1111 (6), 387. doi:10.3390/membranes11060387

Fenelon, M., Etchebarne, M., Siadous, R., Grémare, A., Durand, M., Sentilhes, L., et al. (2021). Comparison of amniotic membrane versus the induced membrane for bone regeneration in long bone segmental defects using calcium phosphate cement loaded with BMP-2. *Mater. Sci. Eng. C* 124, 112032. doi:10.1016/j.msec.2021.112032

Fleury, A., Martinez, M. C., and Le Lay, S. (2014). Extracellular vesicles as therapeutic tools in cardiovascular diseases. *Front. Immunol.* 5, 370. doi:10.3389/fimmu.2014.00370

Foglia, M. J., and Poss, K. D. (2016). Building and re-building the heart by cardiomyocyte proliferation. *Development* 143 (5), 729–740. doi:10.1242/dev.132910

Fu, Q., Ohnishi, S., and Sakamoto, N. (2018). Conditioned medium from human amnion-derived mesenchymal stem cells regulates activation of primary hepatic stellate cells. *Stem Cells Int.* 2018, 1–11. doi:10.1155/2018/4898152

Furuya, K., Zheng, Y. W., Sako, D., Iwasaki, K., Zheng, D. X., Ge, J. Y., et al. (2019). Enhanced hepatic differentiation in the subpopulation of human amniotic stem cells under 3D multicellular microenvironment. *World J. Stem Cells* 11 (9), 705–721. doi:10.4252/wjsc.v11.i9.705

Gilbert, T. W., Sellaro, T. L., and Badylak, S. F. (2006). Decellularization of tissues and organs. *Biomaterials* 27 (19), 3675–3683. doi:10.1016/j.biomaterials.2006.02.014

Gindraux, F., Loisel, F., Bourgeois, M., Oudina, K., Melin, M., de Billy, B., et al. (2020). Induced membrane maintains its osteogenic properties even when the second stage of Masquelet's technique is performed later. *Eur. J. Trauma Emerg. Surg.* 46 (2), 301–312. doi:10.1007/s00068-019-01184-4

Gnecchi, M., Danieli, P., and Cervio, E. (2012). Mesenchymal stem cell therapy for heart disease. *Vasc. Pharmacol.* 57 (1), 48–55. doi:10.1016/j.vph.2012.04.002

Golchin, A., and Farahany, T. Z. (2019). Biological products: Cellular therapy and FDA approved products. *Stem Cell Rev. Rep.* 15 (2), 166–175. doi:10.1007/s12015-018-9866-1

Gorina, R., Santalucia, T., Petegnief, V., Ejarque-Ortiz, A., Saura, J., Planas, A. M., et al. (2009). Astrocytes are very sensitive to develop innate immune responses to lipid-carried short interfering RNA. *Glia* 57 (1), 93–107. doi:10.1002/glia.20738

Gramignoli, R., Green, M. L., Tahan, V., Dorko, K., Skvorak, K. J., Marongiu, F., et al. (2012). Development and application of purified tissue dissociation enzyme mixtures for human hepatocyte isolation. *Cell Transpl.* 21 (6), 1245–1260. doi:10.3727/096368911x600939

Gramignoli, R., Tahan, V., Dorko, K., Skvorak, K. J., Hansel, M. C., Zhao, W., et al. (2013). New potential cell source for hepatocyte transplantation: Discarded livers

from metabolic disease liver transplants. *Stem Cell Res.* 11 (1), 563–573. doi:10.1016/j.scr.2013.03.002

Gramignoli, R., Tahan, V., Dorko, K., Venkataramanan, R., Fox, I. J., Ellis, E. C. S., et al. (2014). Rapid and sensitive assessment of human hepatocyte functions. *Cell Transpl.* 23 (12), 1545–1556. doi:10.3727/096368914x680064

Gramignoli, R., Vosough, M., Kannisto, K., Srinivasan, R. C., and Strom, S. C. (2015). Clinical hepatocyte transplantation: Practical limits and possible solutions. *Eur. Surg. Res.* 54 (3–4), 162–177. doi:10.1159/000369552

Gualdi, T., Laurent, R., Moutarlier, V., Fenelon, M., Nallet, A., Pouthier, F., et al. (2019). *In vitro* osteodifferentiation of intact human amniotic membrane is not beneficial in the context of bone repair. *Cell Tissue Bank.* 20 (3), 435–446. doi:10.1007/s10561-019-09778-3

Hadipour, A., Bayati, V., Rashno, M., and Orazizadeh, M. (2021). Aligned poly(ε-caprolactone) nanofibers superimposed on decellularized human amniotic membrane promoted myogenic differentiation of adipose derived stem cells. *Cell J.* 23 (6), 603–611. doi:10.22074/cellj.2021.7261

Hao, Y., Ma, D. H. K., Hwang, D. G., Kim, W. S., and Zhang, F. (2000). Identification of antiangiogenic and antiinflammatory proteins in human amniotic membrane. *Cornea* 19 (3), 348–352. doi:10.1097/00003226-200005000-00018

Hasmad, H., Yusof, M. R., Mohd Razi, Z. R., Idrus, R. B., and Chowdhury, S. R. (2018). Human amniotic membrane with aligned electrospun fiber as scaffold for aligned tissue regeneration. *Tissue Eng. Part C. Methods* 24 (6), 368–378. doi:10.1089/ten.tec.2017.0447

Hasselmann, J., and Blurton-Jones, M. (2020). Human iPSC-derived microglia: A growing toolset to study the brain's innate immune cells. *Glia* 68 (4), 721–739. doi:10.1002/glia.23781

Herrmann, I. K., Wood, M. J. A., and Fuhrmann, G. (2021). Extracellular vesicles as a next-generation drug delivery platform. *Nat. Nanotechnol.* 16 (7), 748–759. doi:10.1038/s41565-021-00931-2

Heukels, P., Moor, C. C., von der Thüsen, J. H., Wijsenbeek, M. S., and Kool, M. (2019). Inflammation and immunity in IPF pathogenesis and treatment. *Respir. Med. X.* 147, 79–91. doi:10.1016/j.rmed.2018.12.015

Hodgkinson, C. P., Bareja, A., Gomez, J. A., and Dzau, V. J. (2016). Emerging concepts in paracrine mechanisms in regenerative cardiovascular medicine and biology. *Circ. Res.* 118 (1), 95–107. doi:10.1161/circresaha.115.305373

Hoffmann, K., Nagel, A. J., Tanabe, K., Fuchs, J., Dehlke, K., Ghamarnejad, O., et al. (2020). Markers of liver regeneration—the role of growth factors and cytokines: A systematic review. *BMC Surg.* 20 (1), 31. doi:10.1186/s12893-019-0664-8

Holloway, R. K., Ireland, G., Sullivan, G., Becher, J. C., Smith, C., Boardman, J. P., et al. (2021). Microglial inflammasome activation drives developmental white matter injury. *Glia* 69 (5), 1268–1280. doi:10.1002/glia.23963

Hossein-khannazer, N., Torabi, S., Hosseinzadeh, R., Shahrokh, S., Asadzadeh Aghdaei, H., Memarnejadian, A., et al. (2021). Novel cell-based therapies in inflammatory bowel diseases: The established concept, promising results. *Hum. Cell* 34 (5), 1289–1300. doi:10.1007/s13577-021-00560-w

Huang, L., Yang, L., Ding, Y., Jiang, X., Xia, Z., You, Z., et al. (2020). Human umbilical cord mesenchymal stem cells-derived exosomes transfers microRNA-19a to protect cardiomyocytes from acute myocardial infarction by targeting SOX6. *Cell Cycle* 19 (3), 339–353. doi:10.1080/15384101.2019.1711305

Huch, M., Dorrell, C., Boj, S. F., Van Es, J. H., Li, V. S. W., Van De Wetering, M., et al. (2013). *In vitro* expansion of single Lgr5 + liver stem cells induced by Wnt-driven regeneration. *Nature* 494 (7436), 247–250. doi:10.1038/nature11826

Hussein, K. H., Park, K. M., Kang, K. S., and Woo, H. M. (2016). Biocompatibility evaluation of tissue-engineered decellularized scaffolds for biomedical application. *Mater. Sci. Eng. C* 67, 766–778. doi:10.1016/j.msec.2016.05.068

Iansante, V., Mitry, R. R., Filippi, C., Fitzpatrick, E., and Dhawan, A. (2018). Human hepatocyte transplantation for liver disease: Current status and future perspectives. *Pediatr. Res.* 83 (1), 232–240. doi:10.1038/pr.2017.284

Izadi, M. R., Habibi, A., Khodabandeh, Z., and Nikbakht, M. (2021). Synergistic effect of high-intensity interval training and stem cell transplantation with amniotic membrane scaffold on repair and rehabilitation after volumetric muscle loss injury. *Cell Tissue Res.* 383 (2), 765–779. doi:10.1007/s00441-020-03304-8

Jadalannagari, S., Converse, G., McFall, C., Buse, E., Filla, M., Villar, M. T., et al. (2017). Decellularized Wharton's Jelly from human umbilical cord as a novel 3D scaffolding material for tissue engineering applications. *PLoS One* 12 (2), e0172098. doi:10.1371/journal.pone.0172098

Jamieson, J. J., Linville, R. M., Ding, Y. Y., Gerecht, S., and Searson, P. C. (2019). Role of iPSC-derived pericytes on barrier function of iPSC-derived brain microvascular endothelial cells in 2D and 3D. *Fluids Barriers CNS* 16 (1), 15. doi:10.1186/s12987-019-0136-7

Jia, Y., Shu, X., Yang, X., Sun, H., Cao, H., Cao, H., et al. (2020). Enhanced therapeutic effects of umbilical cord mesenchymal stem cells after prolonged treatment for HBV-related liver failure and liver cirrhosis. *Stem Cell Res. Ther.* 11 (1), 277. doi:10.1186/s13287-020-01787-4

Jin, H., Yang, Q., Ji, F., Zhang, Y., Zhao, Y., Luo, M., et al. (2015). Human amniotic epithelial cell transplantation for the repair of injured brachial plexus nerve: Evaluation of nerve viscoelastic properties. *Neural Regen. Res.* 10 (2), 260. doi:10.4103/1673-5374.152380

Jin, Y. Z., and Lee, J. H. (2018). Mesenchymal stem cell therapy for bone regeneration. *Clin. Orthop. Surg.* 10 (3), 271. doi:10.4055/cios.2018.10.3.271

Joerger-Messerli, M. S., Thomi, G., Haesler, V., Keller, I., Renz, P., Surbek, D. V., et al. (2021). Human wharton's jelly mesenchymal stromal cell-derived small extracellular vesicles drive oligodendroglial maturation by restraining MAPK/ERK and notch signaling pathways. *Front. Cell Dev. Biol.* 9, 622539. doi:10.3389/fcell.2021.622539

Keane, T. J., Londono, R., Turner, N. J., and Badylak, S. F. (2012). Consequences of ineffective decellularization of biologic scaffolds on the host response. *Biomaterials* 33 (6), 1771–1781. doi:10.1016/j.biomaterials.2011.10.054

Kim, H., Shin, T., Lee, B., Yu, K., Seo, Y., Lee, S., et al. (2013). Human umbilical cord blood mesenchymal stem cells reduce colitis in mice by activating NOD2 signaling to COX2. *Gastroenterology* 145 (6), 1392–1403.e8. e8. doi:10.1053/j.gastro.2013.08.033

Kim, M. J., Kim, H., Cha, I. J., Park, J. S., Shon, J. H., Liu, K. H., et al. (2005). High-throughput screening of inhibitory potential of nine cytochrome P450 enzymes *in vitro* using liquid chromatography/tandem mass spectrometry. *Rapid Commun. Mass Spectrom.* 19 (18), 2651–2658. doi:10.1002/rcm.2110

Kmiecik, G., Spoldi, V., Silini, A., and Parolini, O. (2015). Current view on osteogenic differentiation potential of mesenchymal stromal cells derived from placental tissues. *Stem Cell Rev. Rep.* 11 (4), 570–585. doi:10.1007/s12015-014-9569-1

Lanzoni, G., Linetsky, E., Correa, D., Messinger Cayetano, S., Alvarez, R. A., Kouroupis, D., et al. (2021). Umbilical cord mesenchymal stem cells for COVID-19 acute respiratory distress syndrome: A double-blind, phase 1/2a, randomized controlled trial. *Stem Cells Transl. Med.* 10 (5), 660–673. doi:10.1002/sctm.20-0472

Laschke, M. W., and Menger, M. D. (2017). Life is 3D: Boosting spheroid function for tissue engineering. *Trends Biotechnol.* 35 (2), 133–144. doi:10.1016/j.tibtech.2016.08.004

Laurent, R., Nallet, A., de Billy, B., Obert, L., Nicod, L., Meyer, C., et al. (2017). Fresh and *in vitro* osteodifferentiated human amniotic membrane, alone or associated with an additional scaffold, does not induce ectopic bone formation in Balb/c mice. *Cell Tissue Bank.* 18 (1), 17–25. doi:10.1007/s10561-016-9605-2

Lazzarini, E., Balbi, C., Altieri, P., Pfeffer, U., Gambini, E., Canepa, M., et al. (2016). The human amniotic fluid stem cell secretome effectively counteracts doxorubicin-induced cardiotoxicity. *Sci. Rep.* 21, 29994. doi:10.1038/srep29994

Lebreton, F., Lavallard, V., Bellofatto, K., Bonnet, R., Wassmer, C. H., Perez, L., et al. (2019). Insulin-producing organoids engineered from islet and amniotic epithelial cells to treat diabetes. *Nat. Commun.* 10 (1), 4491. doi:10.1038/s41467-019-12472-3

Lee, B. C., Shin, N., Lee, J. Y., Kang, I., Kim, J. J., Lee, S. E., et al. (2018). MIS416 enhances therapeutic functions of human umbilical cord blood-derived mesenchymal stem cells against experimental colitis by modulating systemic immune milieu. *Front. Immunol.* 9, 1078. doi:10.3389/fimmu.2018.01078

Lee, M. J., Jung, J., Na, K. H., Moon, J. S., Lee, H. J., Kim, J. H., et al. (2010). Anti-fibrotic effect of chorionic plate-derived mesenchymal stem cells isolated from human placenta in a rat model of CCl4-injured liver: Potential application to the treatment of hepatic diseases. *J. Cell. Biochem.* 111 (6), 1453–1463. doi:10.1002/jcb.22873

Legaki, E., Roubelakis, M. G., Theodoropoulos, G. E., Lazaris, A., Kollia, A., Karamanolis, G., et al. (2016). Therapeutic potential of secreted molecules derived from human amniotic fluid mesenchymal stem/stroma cells in a mice model of colitis. *Stem Cell Rev. Rep.* 12 (5), 604–612. doi:10.1007/s12015-016-9677-1

Lemke, A., Ferguson, J., Gross, K., Penzenstadler, C., Bradl, M., Mayer, R. L., et al. (2018). Transplantation of human amnion prevents recurring adhesions and

ameliorates fibrosis in a rat model of sciatic nerve scarring. *Acta Biomater.* 66, 335–349. doi:10.1016/j.actbio.2017.11.042

Li, W., He, H., Chen, Y. T., Hayashida, Y., and Tseng, S. C. G. (2008). Reversal of myofibroblasts by amniotic membrane stromal extract. *J. Cell. Physiol.* 215 (3), 657–664. doi:10.1002/jcp.21345

Li, Z., Qin, H., Feng, Z., Liu, W., Zhou, Y., Yang, L., et al. (2013). Human umbilical cord mesenchymal stem cell-loaded amniotic membrane for the repair of radial nerve injury. *Neural Regen. Res.* 8 (36), 3441–3448. doi:10.3969/j.issn.1673-5374.2013.36.010

Liang, L., Dong, C., Chen, X., Fang, Z., Xu, J., Liu, M., et al. (2011). Human umbilical cord mesenchymal stem cells ameliorate mice trinitrobenzene sulfonic acid (TNBS)-induced colitis. *Cell Transpl.* 20 (9), 1395–1408. doi:10.3727/096368910x557245

Liddelow, S. A., Guttenplan, K. A., Clarke, L. E., Bennett, F. C., Bohlen, C. J., Schirmer, L., et al. (2017). Neurotoxic reactive astrocytes are induced by activated microglia. *Nature* 541 (7638), 481–487. doi:10.1038/nature21029

Lindenmair, A., Wolbank, S., Stadler, G., Meinl, A., Peterbauer-Scherb, A., Eibl, J., et al. (2010). Osteogenic differentiation of intact human amniotic membrane. *Biomaterials* 31 (33), 8659–8665. doi:10.1016/j.biomaterials.2010.07.090

Liu, G., Li, Y., Sun, J., Zhou, H., Zhang, W., Cui, L., et al. (2010). *In vitro* and *in vivo* evaluation of osteogenesis of human umbilical cord blood-derived mesenchymal stem cells on partially demineralized bone matrix. *Tissue Eng. Part A* 16 (3), 971–982. doi:10.1089/ten.tea.2009.0516

Liu, W. H., Song, F. Q., Ren, L. N., Guo, W. Q., Wang, T., Feng, Y. X., et al. (2015). The multiple functional roles of mesenchymal stem cells in participating in treating liver diseases. *J. Cell. Mol. Med.* 19 (3), 511–520. doi:10.1111/jcmm.12482

Lively, S., and Schlichter, L. C. (2018). Microglia responses to pro-inflammatory stimuli (LPS, IFNγ+TNFα) and reprogramming by resolving cytokines (IL-4, IL-10). *Front. Cell. Neurosci.* 12, 215. doi:10.3389/fncel.2018.00215

Miki, T., Lehmann, T., Cai, H., Stolz, D. B., and Strom, S. C. (2005). Stem cell characteristics of amniotic epithelial cells. *Stem Cells* 23 (10), 1549–1559. doi:10.1634/stemcells.2004-0357

Ma, Y., Dong, L., Zhou, D., Li, L., Zhang, W., Zhen, Y., et al. (2019). Extracellular vesicles from human umbilical cord mesenchymal stem cells improve nerve regeneration after sciatic nerve transection in rats. *J. Cell. Mol. Med.* 23 (4), 2822–2835. doi:10.1111/jcmm.14190

Madonna, R., Van Laake, L. W., Davidson, S. M., Engel, F. B., Hausenloy, D. J., Lecour, S., et al. (2016). Position paper of the European society of cardiology working group cellular biology of the heart: Cell-based therapies for myocardial repair and regeneration in ischemic heart disease and heart failure. *Eur. Heart J.* 37 (23), 1789–1798. doi:10.1093/eurheartj/ehw113

Magarotto, F., Sgrò, A., Dorigo Hochuli, A. H., Andreetta, M., Grassi, M., Saggioro, M., et al. (2021). Muscle functional recovery is driven by extracellular vesicles combined with muscle extracellular matrix in a volumetric muscle loss murine model. *Biomaterials* 269, 120653. doi:10.1016/j.biomaterials.2021.120653

Maghin, E., Garbati, P., Quarto, R., Piccoli, M., and Bollini, S. (2020). Young at heart: Combining strategies to rejuvenate endogenous mechanisms of cardiac repair. *Front. Bioeng. Biotechnol.* 13, 447. doi:10.3389/fbioe.2020.00447

Maji, S., Matsuda, A., Yan, I. K., Parasramka, M., and Patel, T. (2017). Extracellular vesicles in liver diseases. *Am. J. Physiology-Gastrointestinal Liver Physiology* 312 (3), G194–G200. doi:10.1152/ajpgi.00216.2016

Mao, F., Wu, Y., Tang, X., Kang, J., Zhang, B., Yan, Y., et al. (2017). Exosomes derived from human umbilical cord mesenchymal stem cells relieve inflammatory bowel disease in mice. *Biomed. Res. Int.* 2017, 1–12. doi:10.1155/2017/5356760

Mao, Y., Hoffman, T., Singh-Varma, A., Duan-Arnold, Y., Moorman, M., Danilkovitch, A., et al. (2017). Antimicrobial peptides secreted from human cryopreserved viable amniotic membrane contribute to its antibacterial activity. *Sci. Rep.* 7 (1), 13722. doi:10.1038/s41598-017-13310-6

Marchesini, A., Raimondo, S., Zingaretti, N., Riccio, V., Battiston, B., Provinciali, M., et al. (2018). The amnion muscle combined graft (AMCG) conduits in nerves repair: An anatomical and experimental study on a rat model. *J. Mater. Sci. Mater. Med.* 29 (8), 120. doi:10.1007/s10856-018-6126-5

Marongiu, F., Gramignoli, R., Dorko, K., Miki, T., Ranade, A. R., Paola Serra, M., et al. (2011). Hepatic differentiation of amniotic epithelial cells. *Hepatology* 53 (5), 1719–1729. doi:10.1002/hep.24255

Marongiu, M., Serra, M. P., Contini, A., Sini, M., Strom, S. C., Laconi, E., et al. (2015). Rat-derived amniotic epithelial cells differentiate into mature hepatocytes *in vivo* with no evidence of cell fusion. *Stem Cells Dev.* 24 (12), 1429–1435. doi:10.1089/scd.2014.0532

Masyuk, A. I., Masyuk, T. V., and Larusso, N. F. (2013). Exosomes in the pathogenesis, diagnostics and therapeutics of liver diseases. *J. Hepatology* 59 (3), 621–625. doi:10.1016/j.jhep.2013.03.028

Matthay, M. A., Calfee, C. S., Zhuo, H., Thompson, B. T., Wilson, J. G., Levitt, J. E., et al. (2019). Treatment with allogeneic mesenchymal stromal cells for moderate to severe acute respiratory distress syndrome (START study): A randomised phase 2a safety trial. *Lancet Respir. Med.* 7 (2), 154–162. doi:10.1016/s2213-2600(18)30418-1

Maymó, J. L., Riedel, R., Pérez-Pérez, A., Magatti, M., Maskin, B., Dueñas, J. L., et al. (2018). Proliferation and survival of human amniotic epithelial cells during their hepatic differentiation. *PLoS One* 13 (1), e0191489. doi:10.1371/journal.pone.0191489

Mechiche Alami, S., Gangloff, S. C., Laurent-Maquin, D., Wang, Y., and Kerdjoudj, H. (2016). Concise review: *In vitro* formation of bone-like nodules sheds light on the application of stem cells for bone regeneration. *Stem Cells Transl. Med.* 5 (11), 1587–1593. doi:10.5966/sctm.2015-0413

Menasché, P. (2018). Cell therapy trials for heart regeneration — Lessons learned and future directions. *Nat. Rev. Cardiol.* 15 (11), 659–671. doi:10.1038/s41569-018-0013-0

Meng, F., Xu, R., Wang, S., Xu, Z., Zhang, C., Li, Y., et al. (2020). Human umbilical cord-derived mesenchymal stem cell therapy in patients with COVID-19: A phase 1 clinical trial. *Signal Transduct. Target. Ther.* 5 (1), 172. doi:10.1038/s41392-020-00286-5

Milosavljevic, N., Gazdic, M., Simovic Markovic, B., Arsenijevic, A., Nurkovic, J., Dolicanin, Z., et al. (2017). Mesenchymal stem cells attenuate acute liver injury by altering ratio between interleukin 17 producing and regulatory natural killer T cells. *Liver Transpl.* 23 (8), 1040–1050. doi:10.1002/lt.24784

Mirzayan, R., Syed, S. P., and Shean, C. J. (2021). Dissection of an ulnar nerve previously transposed and wrapped with human amniotic membrane: A report of 3 cases. *JBJS Case Connect.* 11 (3). doi:10.2106/jbjs.cc.21.00066

Mishra, S., Sevak, J. K., Das, A., Arimbasseri, G. A., Bhatnagar, S., Gopinath, S. D., et al. (2020). Umbilical cord tissue is a robust source for mesenchymal stem cells with enhanced myogenic differentiation potential compared to cord blood. *Sci. Rep.* 10 (1), 18978. doi:10.1038/s41598-020-75102-9

Moodley, Y., Ilancheran, S., Samuel, C., Vaghjiani, V., Atienza, D., Williams, E. D., et al. (2010). Human amnion epithelial cell transplantation abrogates lung fibrosis and augments repair. *Am. J. Respir. Crit. Care Med.* 182 (5), 643–651. doi:10.1164/rccm.201001-0014oc

Moodley, Y., Vaghjiani, V., Chan, J., Baltic, S., Ryan, M., Tchongue, J., et al. (2013). Anti-inflammatory effects of adult stem cells in sustained lung injury: A comparative study. *PLoS One* 8 (8), e69299. doi:10.1371/journal.pone.0069299

Moris, V., Loisel, F., Cheval, D., See, L. A., Tchurukdichian, A., Pluvy, I., et al. (2016). Functional and radiographic evaluation of the treatment of traumatic bone loss of the hand using the Masquelet technique. *Hand Surg. Rehabil.* 35 (2), 114–121. doi:10.1016/j.hansur.2015.11.002

Moroncini, G., Paolini, C., Orlando, F., Capelli, C., Grieco, A., Tonnini, C., et al. (2018). Mesenchymal stromal cells from human umbilical cord prevent the development of lung fibrosis in immunocompetent mice. *PLoS One* 13 (6), e0196048. doi:10.1371/journal.pone.0196048

Murphy, S., Lim, R., Dickinson, H., Acharya, R., Rosli, S., Jenkin, G., et al. (2011). Human amnion epithelial cells prevent bleomycin-induced lung injury and preserve lung function. *Cell Transpl.* 20 (6), 909–924. doi:10.3727/096368910x543385

Murphy, S. V., Shiyun, S. C., Tan, J. L., Chan, S., Jenkin, G., Wallace, E. M., et al. (2012). Human amnion epithelial cells do not abrogate pulmonary fibrosis in mice with impaired macrophage function. *Cell Transpl.* 21 (7), 1477–1492. doi:10.3727/096368911x601028

Nagaishi, K., Ataka, K., Echizen, E., Arimura, Y., and Fujimiya, M. (2014). Mesenchymal stem cell therapy ameliorates diabetic hepatocyte damage in mice by inhibiting infiltration of bone marrow-derived cells. *Hepatology* 59 (5), 1816–1829. doi:10.1002/hep.26975

Nie, Y. Z., Zheng, Y. W., Miyakawa, K., Murata, S., Zhang, R. R., Sekine, K., et al. (2018). Recapitulation of Hepatitis B virus–host interactions in liver organoids from human induced pluripotent stem cells. *EBioMedicine* 35, 114–123. doi:10.1016/j.ebiom.2018.08.014

Oppliger, B., Joerger-Messerli, M. S., Simillion, C., Mueller, M., Surbek, D. V., Schoeberlein, A., et al. (2017). Mesenchymal stromal cells from umbilical cord Wharton's jelly trigger oligodendroglial differentiation in neural

progenitor cells through cell-to-cell contact. *Cytotherapy* 19 (7), 829–838. doi:10.1016/j.jcyt.2017.03.075

Panhua, X., qing, Li Q., Zhuqing, X., Li, Z., Cai, X., Qing, P R., et al. (2019). Mechanism and therapeutic effect of umbilical cord mesenchymal stem cells in inflammatory bowel disease. *Sci. Rep.* 9 (1), 17646. doi:10.1038/s41598-019-54194-y

Park, S. E., Jeong, J. Bin, Oh, S. J., Kim, S. J., Kim, H., Choi, A., et al. (2021). Wharton's jelly-derived mesenchymal stem cells reduce fibrosis in a mouse model of duchenne muscular dystrophy by upregulating microRNA 499. *Biomedicines* 9 (9), 1089. doi:10.3390/biomedicines9091089

Passaretta, F., Bosco, D., Centurione, L., Centurione, M. A., Marongiu, F., Di Pietro, R., et al. (2020). Differential response to hepatic differentiation stimuli of amniotic epithelial cells isolated from four regions of the amniotic membrane. *J. Cell. Mol. Med.* 24 (7), 4350–4355. doi:10.1111/jcmm.14928

Peng, S. Y., Chou, C. J., Cheng, P. J., Ko, I. C., Kao, Y. J., Chen, Y. H., et al. (2014). Therapeutic potential of amniotic-fluid-derived stem cells on liver fibrosis model in mice. *Taiwan. J. Obstet. Gynecol.* 53 (2), 151–157. doi:10.1016/j.tjog.2014.04.005

Penolazzi, L., Lambertini, E., D'Agostino, S., Pozzobon, M., Notarangelo, M. P., Greco, P., et al. (2022). Decellularized extracellular matrix-based scaffold and hypoxic priming: A promising combination to improve the phenotype of degenerate intervertebral disc cells. *Life Sci.* 301, 120623. doi:10.1016/j.lfs.2022.120623

Penolazzi, L., Pozzobon, M., Bergamin, L. S., D'Agostino, S., Francescato, R., Bonaccorsi, G., et al. (2020). Extracellular matrix from decellularized wharton's jelly improves the behavior of cells from degenerated intervertebral disc. *Front. Bioeng. Biotechnol.* 27, 262. doi:10.3389/fbioe.2020.00262

Petrenko, Y., Vackova, I., Kekulova, K., Chudickova, M., Koci, Z., Turnovcova, K., et al. (2020). A comparative analysis of multipotent mesenchymal stromal cells derived from different sources, with a focus on neuroregenerative potential. *Sci. Rep.* 10 (1), 4290. doi:10.1038/s41598-020-61167-z

Pettinato, G., Lehoux, S., Ramanathan, R., Salem, M. M., He, L. X., Muse, O., et al. (2019). Generation of fully functional hepatocyte-like organoids from human induced pluripotent stem cells mixed with Endothelial Cells. *Sci. Rep.* 9 (1), 8920. doi:10.1038/s41598-019-45514-3

Prior, N., Inacio, P., and Huch, M. (2019). Liver organoids: From basic research to therapeutic applications. *Gut* 68 (12), 2228–2237. doi:10.1136/gutjnl-2019-319256

Psaraki, A., Ntari, L., Karakostas, C., Korrou-Karava, D., and Roubelakis, M. G. (2021). Extracellular vesicles derived from mesenchymal stem/stromal cells: The regenerative impact in liver diseases. *Hepatology* 75, 1590–1603. doi:10.1002/hep.32129

Qiu, X., Liu, S., Zhang, H., Zhu, B., Su, Y., Zheng, C., et al. (2018). Mesenchymal stem cells and extracellular matrix scaffold promote muscle regeneration by synergistically regulating macrophage polarization toward the M2 phenotype. *Stem Cell Res. Ther.* 9 (1), 88. doi:10.1186/s13287-018-0821-5

Qiu, Y., Guo, J., Mao, R., Chao, K., Chen, B., He, Y., et al. (2017). TLR3 preconditioning enhances the therapeutic efficacy of umbilical cord mesenchymal stem cells in TNBS-induced colitis via the TLR3-Jagged-1-Notch-1 pathway. *Mucosal Immunol.* 10 (3), 727–742. doi:10.1038/mi.2016.78

Ramachandran, S. D., Schirmer, K., Münst, B., Heinz, S., Ghafoory, S., Wölfl, S., et al. (2015). *In vitro* generation of functional liver organoid-like structures using adult human cells. *PLoS One* 10 (10), e0139345. doi:10.1371/journal.pone.0139345

Rammal, H., Dubus, M., Aubert, L., Reffuveille, F., Laurent-Maquin, D., Terryn, C., et al. (2017). Bioinspired nanofeatured substrates: Suitable environment for bone regeneration. *ACS Appl. Mater. Interfaces* 9 (14), 12791–12801. doi:10.1021/acsami.7b01665

Rammal, H., Entz, L., Dubus, M., Moniot, A., Bercu, N. B., Sergheraert, J., et al. (2019). Osteoinductive material to fine-tune paracrine crosstalk of mesenchymal stem cells with endothelial cells and osteoblasts. *Front. Bioeng. Biotechnol.* 9, 256. doi:10.3389/fbioe.2019.00256

Rani, S., Ryan, A. E., Griffin, M. D., and Ritter, T. (2015). Mesenchymal stem cell-derived extracellular vesicles: Toward cell-free therapeutic applications. *Mol. Ther.* 23 (5), 812–823. doi:10.1038/mt.2015.44

Reis, M., Ogonek, J., Qesari, M., Borges, N. M., Nicholson, L., Preußner, L., et al. (2016). Recent developments in cellular immunotherapy for HSCT-associated complications. *Front. Immunol.* 7, 500. doi:10.3389/fimmu.2016.00500

Riccio, M., Maraldi, T., Pisciotta, A., La Sala, G. B., Ferrari, A., Bruzzesi, G., et al. (2012). Fibroin scaffold repairs critical-size bone defects *in vivo* supported by human amniotic fluid and dental pulp stem cells. *Tissue Eng. Part A* 18 (9–10), 1006–1013. doi:10.1089/ten.tea.2011.0542

Riccio, M., Pangrazi, P. P., Parodi, P. C., Vaienti, L., Marchesini, A., Neuendorf, A. D., et al. (2014). The amnion muscle combined graft (amcg) conduits: A new alternative in the repair of wide substance loss of peripheral nerves. *Microsurgery* 34 (8), 616–622. doi:10.1002/micr.22306

Roboon, J., Hattori, T., Ishii, H., Takarada-Iemata, M., Nguyen, D. T., Heer, C. D., et al. (2021). Inhibition of CD38 and supplementation of nicotinamide riboside ameliorate lipopolysaccharide-induced microglial and astrocytic neuroinflammation by increasing NAD+. *J. Neurochem.* 158 (2), 311–327. doi:10.1111/jnc.15367

Roger, V. L. (2013). Epidemiology of heart failure. *Circ. Res.* 113 (6), 646–659. doi:10.1161/circresaha.113.300268

Rossi, G., Manfrin, A., and Lutolf, M. P. (2018). Progress and potential in organoid research. *Nat. Rev. Genet.* 19 (11), 671–687. doi:10.1038/s41576-018-0051-9

Santos Nascimento, D., Mosqueira, D., Sousa, L. M., Teixeira, M., Filipe, M., Resende, T. P., et al. (2014). Human umbilical cord tissue-derived mesenchymal stromal cells attenuate remodeling after myocardial infarction by proangiogenic, antiapoptotic, and endogenous cell-activation mechanisms. *Stem Cell Res. Ther.* 5 (1), 5. doi:10.1186/scrt394

Scelfo, C., Caminati, A., and Harari, S. (2017). Recent advances in managing idiopathic pulmonary fibrosis. *F1000Res.* 276, 2052. doi:10.12688/f1000research.10720.1

Segers, V. F. M., and Lee, R. T. (2008). Stem-cell therapy for cardiac disease. *Nature* 451 (7181), 937–942. doi:10.1038/nature06800

Shahrbaf, M. A., Nouri, M., Zarrabi, M., Gramignoli, R., and Vosough, M. (2022). Extraembryonic mesenchymal stromal/stem cells in liver diseases: A critical revision of promising advanced therapy medicinal products. *Cells* 11 (7), 1074. doi:10.3390/cells11071074

Shi, M., Liu, Z., Wang, Y., Xu, R., Sun, Y., Zhang, M., et al. (2017). A pilot study of mesenchymal stem cell therapy for acute liver allograft rejection. *Stem Cells Transl. Med.* 6 (12), 2053–2061. doi:10.1002/sctm.17-0134

Shu, L., Niu, C., Li, R., Huang, T., Wang, Y., Huang, M., et al. (2020). Treatment of severe COVID-19 with human umbilical cord mesenchymal stem cells. *Stem Cell Res. Ther.* 11 (1), 361. doi:10.1186/s13287-020-01875-5

Silini, A. R., Di Pietro, R., Lang-Olip, I., Alviano, F., Banerjee, A., Basile, M., et al. (2020). Perinatal derivatives: Where do we stand? A roadmap of the human placenta and consensus for tissue and cell nomenclature. *Front. Bioeng. Biotechnol.* 8, 1438. doi:10.3389/fbioe.2020.610544

Skvorak, K. J., Dorko, K., Marongiu, F., Tahan, V., Hansel, M. C., Gramignoli, R., et al. (2013). Improved amino acid, bioenergetic metabolite and neurotransmitter profiles following human amnion epithelial cell transplant in intermediate maple syrup urine disease mice. *Mol. Genet. Metab.* 109 (2), 132–138. doi:10.1016/j.ymgme.2013.02.011

Skvorak, K. J., Dorko, K., Marongiu, F., Tahan, V., Hansel, M. C., Gramignoli, R., et al. (2013). Placental stem cell correction of murine intermediate maple syrup urine disease. *Hepatology* 57 (3), 1017–1023. doi:10.1002/hep.26150

Song, J. Y., Kang, H. J., Hong, J. S., Kim, C. J., Shim, J. Y., Lee, C. W., et al. (2017). Umbilical cord-derived mesenchymal stem cell extracts reduce colitis in mice by re-polarizing intestinal macrophages. *Sci. Rep.* 7 (1), 9412. doi:10.1038/s41598-017-09827-5

Spinelli, M., Boucard, C., Nicuolo, F. D, Haesler, V., Castellani, R., Pontecorvi, A., et al. (2020). Synthetic PreImplantation Factor (sPIF) reduces inflammation and prevents preterm birth. *PLoS One* 15 (6), e0232493. doi:10.1371/journal.pone.0232493

Srinivasan, B., Kolli, A. R., Esch, M. B., Abaci, H. E., Shuler, M. L., Hickman, J. J., et al. (2015). TEER measurement techniques for *in vitro* barrier model systems. *SLAS Technol.* 20 (2), 107–126. doi:10.1177/2211068214561025

Stansley, B., Post, J., and Hensley, K. (2012). A comparative review of cell culture systems for the study of microglial biology in Alzheimer's disease. *J. Neuroinflammation* 9 (1), 115. doi:10.1186/1742-2094-9-115

Strom, S. C., Skvorak, K., Gramignoli, R., Marongiu, F., and Miki, T. (2013). Translation of amnion stem cells to the clinic. *Stem Cells Dev.* 22 (1), 96–102. doi:10.1089/scd.2013.0391

Su, C. F., Chang, L. H., Kao, C. Y., Lee, D. C., Cho, K. H., Kuo, L. W., et al. (2018). Application of amniotic fluid stem cells in repairing sciatic nerve injury in minipigs. *Brain Res.* 1678, 397–406. doi:10.1016/j.brainres.2017.11.010

Su, W. H., Wang, C. J., Fu, H. C., Sheng, C. M., Tsai, C. C., Cheng, J. H., et al. (2019). Human umbilical cord mesenchymal stem cells extricate bupivacaine-impaired skeletal muscle function via mitigating neutrophil-mediated acute inflammation and protecting against fibrosis. *Int. J. Mol. Sci.* 20 (17), 4312. doi:10.3390/ijms20174312

Sugiura, R., Ohnishi, S., Ohara, M., Ishikawa, M., Miyamoto, S., Onishi, R., et al. (2018). Effects of human amnion-derived mesenchymal stem cells and conditioned medium in rats with sclerosing cholangitis. *Am. J. Transl. Res.* 10 (7), 2102–2114.

Sun, E., and Karaoz, E. (2020). Can wharton jelly derived or adipose tissue derived mesenchymal stem cell can be a treatment option for duchenne muscular dystrophy? Answers as transcriptomic aspect. *Am. J. Stem Cells* 9 (4), 57–67.

Surolia, R., Li, F. J., Wang, Z., Li, H., Liu, G., Zhou, Y., et al. (2017). 3D pulmospheres serve as a personalized and predictive multicellular model for assessment of antifibrotic drugs. *JCI Insight* 2 (2), 94088. doi:10.1172/jci.insight.94088

Takashima, S., Ise, H., Zhao, P., Akaike, T., and Nikaido, T. (2004). Human amniotic epithelial cells possess hepatocyte-like characteristics and functions. *Cell Struct. Funct.* 29 (3), 73–84. doi:10.1247/csf.29.73

Takebe, T., Sekine, K., Enomura, M., Koike, H., Kimura, M., Ogaeri, T., et al. (2013). Vascularized and functional human liver from an iPSC-derived organ bud transplant. *Nature* 499 (7459), 481–484. doi:10.1038/nature12271

Takov, K., He, Z., Johnston, H. E., Timms, J. F., Guillot, P. V., Yellon, D. M., et al. (2020). Small extracellular vesicles secreted from human amniotic fluid mesenchymal stromal cells possess cardioprotective and promigratory potential. *Basic Res. Cardiol.* 115 (3), 26. doi:10.1007/s00395-020-0785-3

Tan, J. L., Chan, S. T., Lo, C. Y., Deane, J. A., McDonald, C. A., Bernard, C. C. A., et al. (2015). Amnion cell-mediated immune modulation following bleomycin challenge: Controlling the regulatory T cell response. *Stem Cell Res. Ther.* 6 (1), 8. doi:10.1186/scrt542

Tan, J. L., Chan, S. T., Wallace, E. M., and Lim, R. (2014). Human amnion epithelial cells mediate lung repair by directly modulating macrophage recruitment and polarization. *Cell Transpl.* 23 (3), 319–328. doi:10.3727/096368912x661409

Tan, J. L., Lau, S. N., Leaw, B., Nguyen, H. P. T., Salamonsen, L. A., Saad, M. I., et al. (2018). Amnion epithelial cell-derived exosomes restrict lung injury and enhance endogenous lung repair. *Stem Cells Transl. Med.* 7 (2), 180–196. doi:10.1002/sctm.17-0185

Thomi, G., Surbek, D., Haesler, V., Joerger-Messerli, M., and Schoeberlein, A. (2019). Exosomes derived from umbilical cord mesenchymal stem cells reduce microglia-mediated neuroinflammation in perinatal brain injury. *Stem Cell Res. Ther.* 10 (1), 105. doi:10.1186/s13287-019-1207-z

Todd, N. W., Scheraga, R. G., Galvin, J. R., Iacono, A. T., Britt, E. J., Luzina, I. G., et al. (2013). Lymphocyte aggregates persist and accumulate in the lungs of patients with idiopathic pulmonary fibrosis. *J. Inflamm. Res.* 6 (1), 63–70. doi:10.2147/jir.s40673

Tolomeo, A. M., Castagliuolo, I., Piccoli, M., Grassi, M., Magarotto, F., De Lazzari, G., et al. (2021). Extracellular vesicles secreted by mesenchymal stromal cells exert opposite effects to their cells of origin in murine sodium dextran sulfate-induced colitis. *Front. Immunol.* 13, 627605. doi:10.3389/fimmu.2021.627605

Trohatou, O., and Roubelakis, M. G. (2017). Mesenchymal stem/stromal cells in regenerative medicine: Past, present, and future. *Cell. Reprogr.* 19 (4), 217–224. doi:10.1089/cell.2016.0062

Ülger, M., Sezer, G., Özyazgan, İ., Özocak, H., Yay, A., Balcıoğlu, E., et al. (2021). The effect of erythropoietin and umbilical cord-derived mesenchymal stem cells on nerve regeneration in rats with sciatic nerve injury. *J. Chem. Neuroanat.* 114, 101958. doi:10.1016/j.jchemneu.2021.101958

Vieujean, S., Loly, J. P., Boutaffala, L., Meunier, P., Reenaers, C., Briquet, A., et al. (2022). Mesenchymal stem cell injection in Crohn's disease strictures: A phase I-ii clinical study. *J. Crohn's. Colitis* 16 (3), 506–510. doi:10.1093/ecco-jcc/jjab154

Villa, F., Quarto, R., and Tasso, R. (2019). Extracellular vesicles as natural, safe and efficient drug delivery systems. *Pharmaceutics* 11 (11), 557. doi:10.3390/pharmaceutics11110557

Viswanathan, S., Shi, Y., Galipeau, J., Krampera, M., Leblanc, K., Martin, I., et al. (2019). Mesenchymal stem versus stromal cells: International society for cell & gene therapy (ISCT®) mesenchymal stromal cell committee position statement on nomenclature. *Cytotherapy* 21 (10), 1019–1024. doi:10.1016/j.jcyt.2019.08.002

Volkman, R., and Offen, D. (2017). Concise review: Mesenchymal stem cells in neurodegenerative diseases. *Stem Cells* 35 (8), 1867–1880. doi:10.1002/stem.2651

Vosdoganes, P., Wallace, E. M., Chan, S. T., Acharya, R., Moss, T. J. M., Lim, R., et al. (2013). Human amnion epithelial cells repair established lung injury. *Cell Transpl.* 22 (8), 1337–1349. doi:10.3727/096368912x657657

Wang, G., Joel, M. D. M., Yuan, J., Wang, J., Cai, X., Ocansey, D. K. W., et al. (2020). Human umbilical cord mesenchymal stem cells alleviate inflammatory bowel disease by inhibiting ERK phosphorylation in neutrophils. *Inflammopharmacology* 28 (2), 603–616. doi:10.1007/s10787-019-00683-5

Wang, Q. Q., Jing, X. M., Bi, Y. Z., Cao, X. F., Wang, Y. Z., Li, Y. X., et al. (2018). Human umbilical cord wharton's jelly derived mesenchymal stromal cells may attenuate sarcopenia in aged mice induced by hindlimb suspension. *Med. Sci. Monit.* 24, 9272–9281. doi:10.12659/msm.913362

Wang, Y., Chen, X., Cao, W., and Shi, Y. (2014). Plasticity of mesenchymal stem cells in immunomodulation: Pathological and therapeutic implications. *Nat. Immunol.* 15 (11), 1009–1016. doi:10.1038/ni.3002

Wen, S., Dooner, M., Cheng, Y., Papa, E., Del Tatto, M., Pereira, M., et al. (2016). Mesenchymal stromal cell-derived extracellular vesicles rescue radiation damage to murine marrow hematopoietic cells. *Leukemia* 30 (11), 2221–2231. doi:10.1038/leu.2016.107

Wen, S. J., Zheng, X. M., Liu, L. F., Li, N. N., Mao, H. A., Huang, L., et al. (2021). Effects of primary microglia and astrocytes on neural stem cells in *in vitro* and *in vivo* models of ischemic stroke. *Neural Regen. Res.* 16 (9), 1677–1685. doi:10.4103/1673-5374.306093

Wilkinson, D. C., Alva-Ornelas, J. A., Sucre, J. M. S., Vijayaraj, P., Durra, A., Richardson, W., et al. (2017). Development of a three-dimensional bioengineering technology to generate lung tissue for personalized disease modeling. *Stem Cells Transl. Med.* 6 (2), 622–633. doi:10.5966/sctm.2016-0192

Willenbring, H., Bailey, A. S., Foster, M., Akkari, Y., Dorrell, C., Olson, S., et al. (2004). Myelomonocytic cells are sufficient for therapeutic cell fusion in liver. *Nat. Med.* 10 (7), 744–748. doi:10.1038/nm1062

Wolfe, E. M., Mathis, S. A., Ovadia, S. A., and Panthaki, Z. J. (2022). Comparison of collagen and human amniotic membrane nerve wraps and conduits for peripheral nerve repair in preclinical models: A systematic review of the literature. *J. Reconstr. Microsurg.* 2022. doi:10.1055/s-0041-1732432

Wu, F., Wu, D., Ren, Y., Huang, Y., Feng, B., Zhao, N., et al. (2019). Generation of hepatobiliary organoids from human induced pluripotent stem cells. *J. Hepatology* 70 (6), 1145–1158. doi:10.1016/j.jhep.2018.12.028

Wu, X. M., Qian, C., Jiang, F., Bao, Y. X., Qian, Z. M., Ke, Y., et al. (2021). The involvement of nuclear factor-κB in astroprotection against ischemia-reperfusion injury by ischemia-preconditioned neurons. *J. Cell. Physiol.* 236 (6), 4515–4527. doi:10.1002/jcp.30168

Xiong, Y., Mahmood, A., and Chopp, M. (2017). Emerging potential of exosomes for treatment of traumatic brain injury. *Neural Regen. Res.* 12 (1), 19. doi:10.4103/1673-5374.198966

Yang, S., Liang, X., Song, J., Li, C., Liu, A., Luo, Y., et al. (2021). A novel therapeutic approach for inflammatory bowel disease by exosomes derived from human umbilical cord mesenchymal stem cells to repair intestinal barrier via TSG-6. *Stem Cell Res. Ther.* 12 (1), 315. doi:10.1186/s13287-021-02404-8

Zabulica, M., Srinivasan, R. C., Vosough, M., Hammarstedt, C., Wu, T., Gramignoli, R., et al. (2019). Guide to the assessment of mature liver gene expression in stem cell-derived hepatocytes. *Stem Cells Dev.* 28 (14), 907–919. doi:10.1089/scd.2019.0064

Zagoura, D. S., Roubelakis, M. G., Bitsika, V., Trohatou, O., Pappa, K. I., Kapelouzou, A., et al. (2012). Therapeutic potential of a distinct population of human amniotic fluid mesenchymal stem cells and their secreted molecules in mice with acute hepatic failure. *Gut* 61 (6), 894–906. doi:10.1136/gutjnl-2011-300908

Zhang, C., Yin, X., Zhang, J., Ao, Q., Gu, Y., Liu, Y., et al. (2017). Clinical observation of umbilical cord mesenchymal stem cell treatment of severe idiopathic pulmonary fibrosis: A case report. *Exp. Ther. Med.* 13 (5), 1922–1926. doi:10.3892/etm.2017.4222

Zhang, L, Zou, D, Li, S, Wang, J, Qu, Y, Ou, S, et al. (2016). An Ultra-thin Amniotic Membrane as Carrier in corneal epithelium Tissue-Engineering. *Sci. Rep.* 6 (1), 21021. doi:10.1038/srep21021

Zhang, X, Zhivaki, D, and Lo-Man, R (2017). Unique aspects of the perinatal immune system. *Nat. Rev. Immunol.* 17 (8), 495–507. doi:10.1038/nri.2017.54

Glossary

α-SMA α- smooth muscle actin
AMP amniotic membrane protein
AMSC amniotic membrane mesenchymal stromal cells
AnnV/PI annexin V and propidium iodide
AP alkaline phosphatase
BBB blood-brain barrier
bFGF basic fibroblast growth factor
CD Crohn's disease
CM conditioned medium
CMAP compound muscle action potential
CNS central nervous system
CPC calcium phosphate cements
CT computed tomography
DAMP danger-associated molecular patterns
dP decellularized perinatal derivative
dP-ECM dP extracellular matrix
DSS dextran sulfate sodium;
ECFC endothelial colony-forming cells
EDX energy dispersive X-ray
EGF epidermal growth factor
EMG electromyologram
EPT extensor postural thrust
ES embryonic stem cells
EV extracellular vesicles
GFAP glial fibrillary acidic protein
GT grasping test
hACM human amnio-chorionic membrane
hAEC amniotic membrane epithelial cells
hAEC-Exo exosomes from hAEC
hAFSC amniotic fluid stem cells
hAF-MSC amniotic fluid mesenchymal stromal cells
hAM human AM
hAMSC-CM human amniotic membrane mesenchymal stromal cells conditioned medium
hBMSC human bone marrow mesenchymal stromal cells
HE hematoxylin and eosin;
HUVEC human umbilical vein endothelial cells
IBD inflammatory bowel diseases
IFNγ interferon-gamma
IGF insulin-like growth factor
IL interleukin
iPSC induced pluripotent stem cells
IPF Idiopathic pulmonary fibrosis
LPS lipopolysaccharide
MgHA magnesium-enriched hydroxyapatite
MMP metalloproteinase
MSC mesenchymal stromal cells
MSCEVs MSC- derived extracellular vesicles
MSCMVs MSC-derived microvesicles
MSUD maple syrup urine disease
MVs microvesicles
NCV nerve conduction velocity
NLRP3 NLR family pyrin domain containing 3
NPC progenitor cells
NSC neural stem cells
OGD oxygen-glucose deprivation
OPC oligodendrocyte progenitor cells
PAMP pathogen-associated molecular patterns
PCL: polycaprolactone
PDGF platelet-derived growth factor;
PLA polylactate
PLGA poly(lactic-co-glycolic acid)
PnD perinatal derivatives
PNS peripheral nervous system
ROS reactive oxygen species
RGD Arginyl-glycyl-aspartic acid
SFI sciatic functional index
TEER Trans endothelial electric resistance
TGF- β1 transforming growth factor beta 1
TIMP tissue inhibitor of metalloproteinases
TNBS trinitrobenzene sulfonate;
TNFα tumor necrosis factor-alpha
UC-MSC umbilical cord mesenchymal stromal cells
UC-WJ-MSC Umbilical cord Wharton's jelly mesenchymal stromal cells
VEGF vascular endothelial growth factor
VML volumetric muscle loss
WRL withdrawal reflex latency
XRD X-ray diffraction.

frontiers | Frontiers in Bioengineering and Biotechnology

TYPE Original Research
PUBLISHED 11 October 2022
DOI 10.3389/fbioe.2022.977590

OPEN ACCESS

EDITED BY
Peter Ponsaerts,
University of Antwerp, Belgium

REVIEWED BY
Guido Moll,
Charité Universitätsmedizin Berlin, Germany
Zongjin Li,
Nankai University, China

*CORRESPONDENCE
Florelle Gindraux,
fgindraux@chu-besancon.fr
Nicola Hofmann,
nicola.hofmann@gewebenetzwerk.de ;
Xavier Lafarge,
Xavier.Lafarge@efs.sante.fr
Francisco J. Nicolás,
franciscoj.nicolas2@carm.es

†These authors have contributed equally to this work

SPECIALTY SECTION
This article was submitted to Tissue Engineering and Regenerative Medicine, a section of the journal Frontiers in Bioengineering and Biotechnology

RECEIVED 24 June 2022
ACCEPTED 04 August 2022
PUBLISHED 11 October 2022

CITATION
Gindraux F, Hofmann N, Agudo-Barriuso M, Antica M, Couto PS, Dubus M, Forostyak S, Girandon L, Gramignoli R, Jurga M, Liarte S, Navakauskiene R, Shablii V, Lafarge X and Nicolás FJ (2022), Perinatal derivatives application: Identifying possibilities for clinical use. *Front. Bioeng. Biotechnol.* 10:977590. doi: 10.3389/fbioe.2022.977590

Perinatal derivatives application: Identifying possibilities for clinical use

Florelle Gindraux[1,2*†], Nicola Hofmann[3*†], Marta Agudo-Barriuso[4], Mariastefania Antica[5], Pedro Silva Couto[6], Marie Dubus[7], Serhiy Forostyak[8,9], Lenart Girandon[10], Roberto Gramignoli[11], Marcin Jurga[12], Sergio Liarte[13], Ruta Navakauskiene[14], Volodymyr Shablii[15,16], Xavier Lafarge[17*†] and Francisco J. Nicolás[13*†]

[1]Service de Chirurgie Orthopédique, Traumatologique et Plastique, CHU- Besançon, France, [2]Laboratoire de Nanomédecine, Imagerie, Thérapeutique, Université Bourgogne Franche-Comté, Besançon, France, [3]German Society for Tissue Transplantation (DGFG) gGmbH, Hannover, Germany, [4]Experimental Ophthalmology Group, University of Murcia and Instituto Murciano de Investigación Biosanitaria (IMIB), Campus Ciencias de la Salud, Murcia, Spain, [5]Division of Molecular Biology, Rudjer Boskovic Institute, Zagreb, Croatia, [6]Department of Biochemical Engineering, Advanced Centre for Biochemical Engineering, University College London, London, United Kingdom, [7]Biomatériaux et Inflammation en Site Osseux (BIOS) EA 4691, Université de Reims Champagne Ardenne, Reims, France, [8]PrimeCell Bioscience, Ostrava, Czech Republic, [9]Department of Burns and Plastic Surgery, Faculty of Medicine, Institution Shared With University Hospital Brno, Masaryk University, Brno, Czechia, [10]Educell ltd, Trzin, Slovenia, [11]Department of Laboratory Medicine, Division of Pathology, Karolinska Institutet, Stockholm, Sweden, [12]EXO Biologics (NV), Liege, Belgium, [13]Regeneration, Molecular Oncology and TGFβ, IMIB-Arrixaca, Murcia, Spain, [14]Department of Molecular Cell Biology, Institute of Biochemistry, Life Sciences Center, Vilnius University, Vilnius, Lithuania, [15]Laboratory of Biosynthesis of Nucleic Acids, Institute of Molecular Biology and Genetics, Department of Functional Genomics, National Academy of Science, Kyiv, Ukraine, [16]Placenta Stem Cell Laboratory, Cryobank, Institute of Cell Therapy, Kyiv, Ukraine, [17]Établissement Français du Sang Nouvelle-Aquitaine, France/INSERM U1035, Université de Bordeaux, Biothérapie des Maladies Génétiques Inflammatoires et Cancers (BMGIC), Bordeaux, France

Perinatal derivatives are drawing growing interest among the scientific community as an unrestricted source of multipotent stromal cells, stem cells, cellular soluble mediators, and biological matrices. They are useful for the treatment of diseases that currently have limited or no effective therapeutic options by means of developing regenerative approaches. In this paper, to generate a complete view of the state of the art, a comprehensive 10-years compilation of clinical-trial data with the common denominator of PnD usage has been discussed, including commercialized products. A set of criteria was delineated to challenge the 10-years compilation of clinical trials data. We focused our attention on several aspects including, but not limited to, treated disorders, minimal or substantial manipulation, route of administration, dosage, and frequency of application. Interestingly, a clear correlation of PnD products was observed within conditions, way of administration or dosage, suggesting there is a consolidated clinical practice approach for the use of PnD in medicine. No regulatory aspects could be read from the database since this information is not mandatory for registration. The database will be publicly available for consultation. In summary, the main aims of this position paper are to show possibilities for clinical application of PnD and propose an approach for clinical trial preparation and registration in a uniform and standardized way. For this purpose, a questionnaire was created compiling different sections that are

relevant when starting a new clinical trial using PnD. More importantly, we want to bring the attention of the medical community to the perinatal products as a consolidated and efficient alternative for their use as a new standard of care in the clinical practice.

KEYWORDS

clinical trials, perinatal derivatives, ICD-10 = international classification of diseases, questionnaire for PnD use in human conditions, amniotic membrane

1 Introduction

The scientific community is experiencing a particularly growing interest for the medical use of perinatal products. During the last 3 decades, an exponential amount of reports described the use of human perinatal tissues and cells in a plethora of preclinical settings, supporting their implementation into regenerative and interventional approaches (Figure 1A). This is based on the unique characteristics and features shown by perinatal derivatives largely ascribed to their origin and physiological role, supporting proper foetal development during gestation and providing protection against deleterious maternal immune-recognition (Figure 1B).

Perinatal derivatives (PnD) include fetal and maternal tissues (e.g. human amniotic membrane [hAM]), multipotent stromal cells (MSC) and stem cells embedded in different parts of the placenta or human umbilical cord (hUC). Also, tissue/cellular extracts or secreted mediators such as extracellular vesicles (EVs) represent promising candidates in regenerative medicine, once validated and proved safe and effective in registered clinical trials (Silini et al., 2015; Silini et al., 2017; Torre and Flores, 2020) (Figure 1C).

Among PnD, hAM has a long history of clinical use. For almost one hundred years hAM tissue has been applied in the treatment of skin injuries, in periodontics, orthopedics, the management of female reproductive tract lesions and, particularly, for the assessment of injury on ocular surfaces (Ashworth et al., 1986; Silini et al., 2017; Murri et al., 2018; Sittadjody et al., 2021). Due to the extensive knowledge available on the clinical application of hAM, the commercial use of the matrix is also already established or approved for use by many national authorities.

As the pinnacle of the current state of the art for its more common use both, hAM and hAM extracts, have been successfully shown to promote corneal healing. In a recent development it was demonstrated how the application of hAM along with hAM extract eye drops (AMEED) can synergistically promote stability of the ocular surface and regeneration of corneal epithelium after chemical burns. Notably, this treatment showed to be devoid of undesired effects like causing persistent epithelial defect (conjunctivitis and vascularization of the cornea) or inflammation, conditions that usually appear when resorting to traditional treatments with antibiotics or corticosteroid drops (Murri et al., 2018). The aforementioned combined treatment constitutes a good example on how PnD provide resourceful clinical options for the management of difficult entities in comparison to conventional treatments. Nevertheless, AMEED is only available in Italy, Spain, United States and other markets currently without US-FDA regulation.

Beyond hAM and its extracts, PnD cells are lately receiving particular attention for their broad differentiation potential and tolerogenicity. Among naturally occurring stem cells, PnD are regarded with the greatest potential for cell therapy and regenerative medicine, as cells derived from the placenta do possess unique plasticity and differentiation properties (Bailo et al., 2004; Silini et al., 2020). As per their obtention, only in the last couple of decades new methods of isolation have been tested and improved to purify stem cells derived from different placental regions, human amniotic fluid (hAF), hAM, chorion, hUC (including Wharton's jelly [WJ]) and cord blood. From these origins, placenta and cord blood have been more intensely examined. The placenta is a known rich source of both stem and stromal cells with demonstrated therapeutic potential in a variety of disease models; being relatively easy to isolate and showing a stable behaviour *in vitro* (Caprnda et al., 2017; Torre and Flores, 2020). Similarly, clinical trial evaluation of safety, efficacy and therapeutic potency of PnD stem cells from other origins in various diseases is increasing.

Contrary to the wide and old routine use of hAM, therapies using cells and EVs have yet to prove their suitability and safety. There has been an increasing diversification of MSC products in the past decade, with preferential use of BM-MSCs until 2008, but increasing diversification since then with now equal use of BM, PT (perinatal tissues), and AT (adipose tissues)-derived cells, with a strong trend for PnD to become the most popular source in the past 2 years. Whereas Meta-analysis has demonstrated that bone marrow MSC infusion is safe (Moll et al., 2019), MSC products from different sources are not investigated enough. With the introduction of the new hemocompatibility characteristic (Moll et al., 2020; Moll et al., 2022) a tool is available with which the safety of the systemic intravascular administration of MSC/EV-products can be examined. Therapies derived from PnD cells and tissues might become advanced therapy medicinal products (ATMP), and EVs biological products through their medical use. The ATMP category englobes products based in recombinant nucleic acids

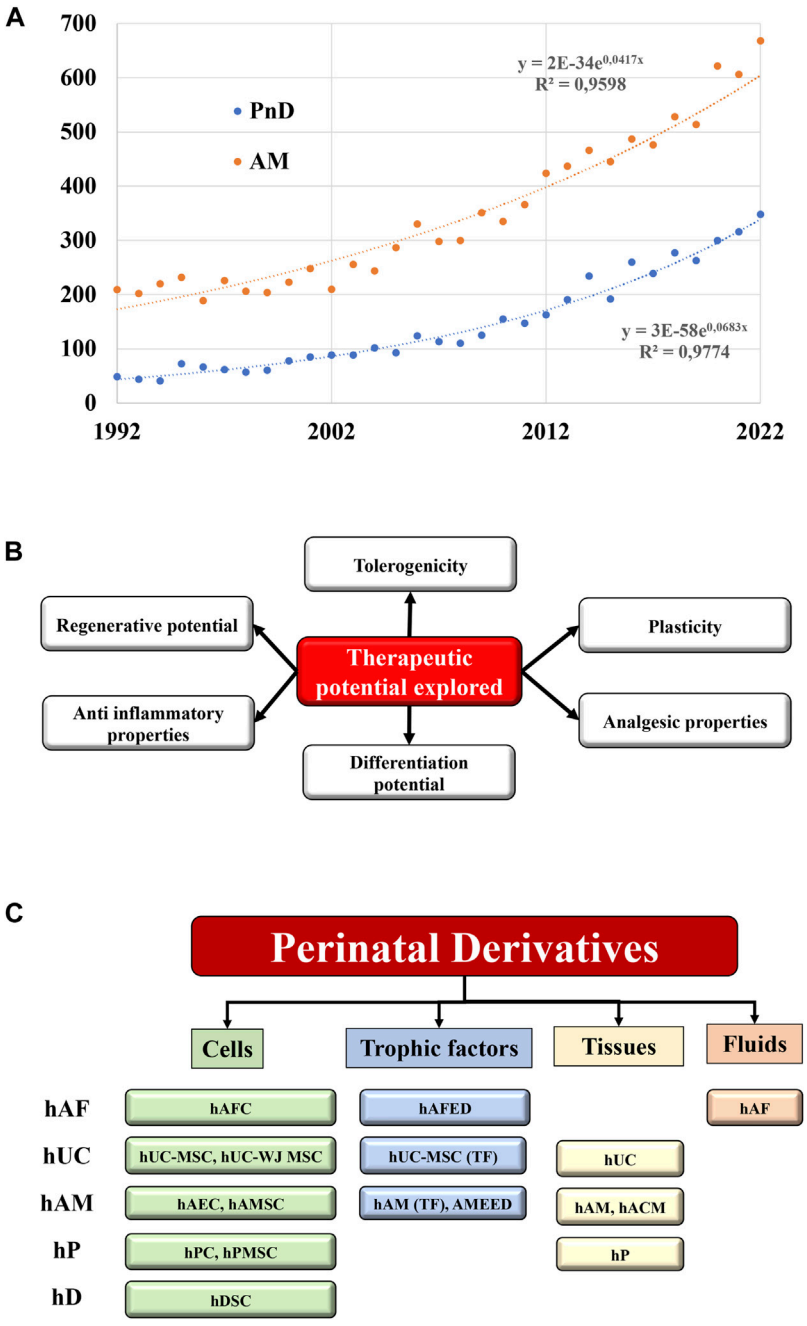

FIGURE 1
State of the art of the Perinatal derivatives. **(A)** Represents the exponential increase within the last 3 decades of the annual number of references indexed in pubmed.gov site with the keywords "perinatal derivatives" and "amniotic membrane". The numbers of references doubled every 10 years for the PnD, and every 17 years for the amniotic membranes. **(B)** Therapeutic potential of PnD. **(C)** Different types of PnD utilized in the clinical trials (cells, trophic factors, tissues, fluids) according the different sources of PnD. Abbreviations: hP: human placenta; hUC: human umbilical cord; hAM: human amniotic membrane; hAF: human amniotic fluid; hD: human decidua; TF: trophic factors; hPC: human placental cells; hPMSC: human placental mesenchymal stromal cells; WJ: Wharton's jelly; MSC: mesenchymal stromal cells; hACM: amnio-chorionic membrane; hAEC: human amniotic epithelial cells; hAMC: human amniotic membrane cells; AMEED: amniotic membrane extract eye drops; hAFC: human amniotic fluid cells; hAFED: human amniotic fluid eye drops; hDSC: human decidua stromal cells.

and/or engineered cells and/or tissues. Within ATMP, PnD mainly fall into two sub-lists, somatic cell therapy medicinal products and tissue-engineered products (Iglesias-Lopez et al., 2019). The requirements for these applications are correspondingly much higher, and more clinical investigation via clinical trials is necessary.

Yet, although the evidence of PnD usefulness exists and the interest in the field is obvious, no clear guidelines can be found as how to compare the diversity of PnD origins and applications through clinical trials. Since research in this field is growing such guidelines are essential and defining criteria for clinical use of PnD should be improved. In this study, the current state of PnD and PnD stem cells knowledge in clinical trials was analyzed, in an effort to discriminate different valuable research areas.

A database of clinical trials using PnD tissues, PnD stem cells as well as trophic factors (TF) was created and it is discussed. Moreover, this analysis allowed to create a questionnaire which will be useful to define key clinical trial information significant for the development of PnD products.

1.1 Registered clinical trials with perinatal derivatives

By definition, a clinical trial constitutes a research study performed following a clinical setting with the specific intent to evaluate the effects of novel health-related interventions in humans. Such prospective biomedical or behavioral research studies, involving healthy human participants and/or selected groups of patients, are designed to address specific therapeutical issues moving from safety and efficacy to management refinement and market assessment. They are regularly conducted based on previous approval by local ethic committees and health authorities. Such stakeholders are responsible for carefully balancing the risk to benefit ratio of the proposed intervention, and for vetting the initiative when the benefit does not justify the risk. Depending on the product type and development stage, researchers initially enroll volunteers or patients into small pilot research and subsequently conduct progressively larger scale comparative studies. In consequence, clinical trials are commonly subdivided into four different phases: *Phase I* studies, also referred as Early Phase or as "first-in-human" studies if a new substance is tested for the first time, imply testing a new drug into a small group (n = 10–15) of healthy volunteers for safety and administration protocol evaluation; *Phase II* clinical trials aim to evaluate the biological activity or clinical effect of the treatment on a sizable group of patients (n = 50–300), allowing for additional analysis for setting optimal or even tailoring therapeutic conditions according to patients genetic background and metabolic rate to minimise non-desired effects; *Phase III* studies usually consist in a randomized controlled multicenter trial on a large patient cohort (n = 300–3,000 subjects), where efficacy of the new intervention is assessed in comparison to treatments regarded "gold standard"; *Phase IV* constitutes the latest stage and is commonly referred as post-marketing surveillance because involves continuous safety surveillance from official market clearance to detect and confirm any rare or long-term adverse effects over the patient population (n > 1,000–10,000).

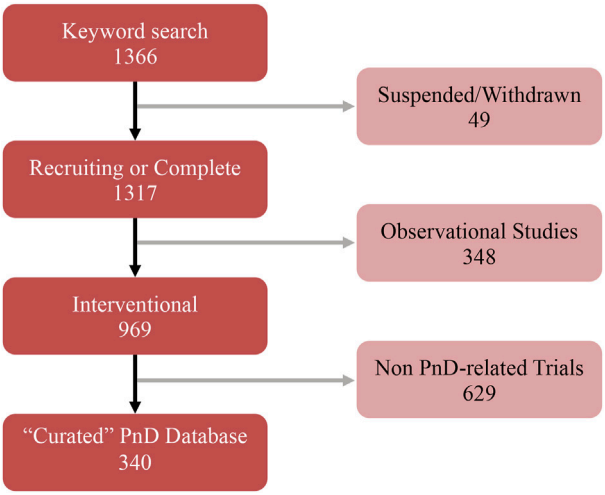

FIGURE 2
Summary of the several curation steps applied to the keyword search of PnD-related clinical trials.

As it will be discussed in detail, during the last 10 years numerous clinical trials including PnD for the treatment of a plethora of medical conditions have been registered. Although spanning across all four trial phases, some already finished and many currently ongoing, the bulk of them are Phase I clinical trials.

2 Materials and methods

As part of our COST Action (CA17116; https://www.sprint-cost.org/) we created a questionnaire exclusively regarding the use of perinatal cells to have a distinct compilation of the different items required to properly know how a clinical trial has been designed and conducted. At the same time, we realized the lack of important information related to certain data significant to understand and replicate the procedures. Therefore, we inserted into the questionnaire information that should be included as standard into clinical studies when they are reported to the public databases. We have included this document as **Annex 1** with the following sections:

- Perinatal derived product/indication
- Clinical trial information
- Manufacturing (from PubMed and other resources)

This study is focused on analyzing and commenting data obtained from the United States Clinical Trial Registration Portal (clinicaltrials.gov) for 10-year period from 01/01/2011 to 07/10/

2020. To successfully gather all PnD-related clinical trials in the database, the following search-terms were used ("cell" OR "tissue" OR "secretome" OR "scaffold" OR "fluid" OR "vesicle") AND ("placenta" OR "amnion" OR "chorion" OR "umbilical cord" OR "amniotic" OR "decidua" OR "villi"). Cord blood was not taken into account in this study, because of the very wide use made of it as a source of hematopoietic stem cells. Additionally, given the focus of this review in PnD other than cord blood, this word was excluded from the search criteria.

The search was focused exclusively on interventional clinical trials using human PnD, excluding cases where the studies had been suspended or withdrawn (Figure 2). From the keyword-based search, a total of 1,366 clinical trials were identified. After removing studies with the status of "unavailable", "no longer available", "suspended" or "withdrawn", 1,317 clinical trials remained. Then, all observational studies were also removed from the listing, which led to a list of 969 clinical trials. Given that clinicaltrials.gov included all clinical trials registered within the stipulated time frame, a manual curation step was performed with the aim to classify PnD clinical trials according to the use of either "cell", "secretome" or "scaffold" forms. For this purpose, 14 reviewers were assessing the different clinical trials (969) to decide which of them were fulfilling the proposed criteria. After this manual curation step, a short-list comprising 340 clinical trials using PnD in an interventional fashion was established (Figure 2; **Annex 2**). For each clinical trial in the database, the following parameters were collected: NCT number, secondary ID, location, status, phase, condition (based on ICD10 classification), gender, age, enrolment, dosage, route of administration, type of therapy (allogenic or autologous) and type of PnD used. Following criteria by Silini et al., 2020, products where some cells were seeded onto a pre-existing tissue (i.e. hAM), biological matrix (i.e. collagen) or into a polymer gel, were defined as "combined" products; when a tissue/material (i.e. bone substitute or others) was combined to a perinatal tissue (i.e. hAM), this was considered an "association". For readers reference, Nucell® represents a good example of combined products as is constituted of hAFC combined with hAM. Inconsistencies in the number of trials analyzed in the evaluation of different parameters arise from the facts that several PnD are investigated in one study and, at the same time, different indications or different nomenclatures were used in the description. In addition, not all trials had information for all considered criteria.

TABLE 1 PnD classification and number of clinical trials according to PnD and their perinatal origin.

Origin	Type	PnD	Nr. clinical trials
hP	Tissue	hP	2
	Cells	hPC	5
		hPMSC	12
	TF	—	—
hUC	Tissue	hUC	11
	Cells	hUC-WJ-MSC	9
		hUC-MSC	200
	TF	hUC-MSC (TF)	3
hAM	Tissue	hACM	18
		hAM	60
	Cells	hAEC	9
		hAMSC	1
	TF	hAMC (TF)	1
		AMEED	2
hAF	Fluid	hAF	13
	Cells	hAFC	7
	TF	hAFED	1
hD	Tissue	—	—
	Cells	hDSC	5
	TF	—	—

Abbreviations: hP: human placenta; hUC: human umbilical cord; hAM: human amniotic membrane; hAF: human amniotic fluid; hD: human decidua; TF: trophic factors; hPC: human placental cells; hPMSC: human placental mesenchymal stromal cells; WJ: Wharton's jelly; MSC: mesenchymal stromal cells; hACM: amnio-chorionic membrane; hAEC: human amniotic epithelial cells; hAMC: human amniotic membrane cells; AMEED: amniotic membrane extract eye drops; hAFC: human amniotic fluid cells; hAFED: human amniotic fluid eye drops; hDSC: human decidua stromal cells. Note: due to the fact that some trials included more than one PnD the total number of studies is more than the analyzed ones (n = 359 versus 340).

3 Results and discussion

3.1 Part I: Clinical data base analysis

3.1.1 PnD classification: Categories and origin

Denomination for distinct PnD used in clinical trials within the curated short-list was harmonized applying the proposed consensus nomenclature for human perinatal tissues and cells (Silini et al., 2020). In brief, PnD were classified according to their perinatal origin (human placenta [hP], human umbilical cord [hUC], human amniotic membrane [hAM], human amniotic fluid [hAF] and human decidua [hD]); and according to their final presentation (tissue, cells or TF). Note that TF category regroups conditioned media from cells and/or tissues, and contains also fluid eye drops such as amniotic membrane extract eye drops (AMEED) or human amniotic fluid eye drops (hAFED). Although trophic factors (TF) could have been categorized as secretome, we preferred to stick to the term TF as it was the word found in the clinical trial categories and not secretome. We also considered that keeping TF would facilitate the search of the database to future readers. The harmonized denominations found for PnD in the clinical studies are indexed and classified in Table 1, together with the number of clinical trials testing each PnD.

In general, most clinical trials concentrate on applying hUC-MSC (n = 200) followed by hAM (n = 60), and just the remaining

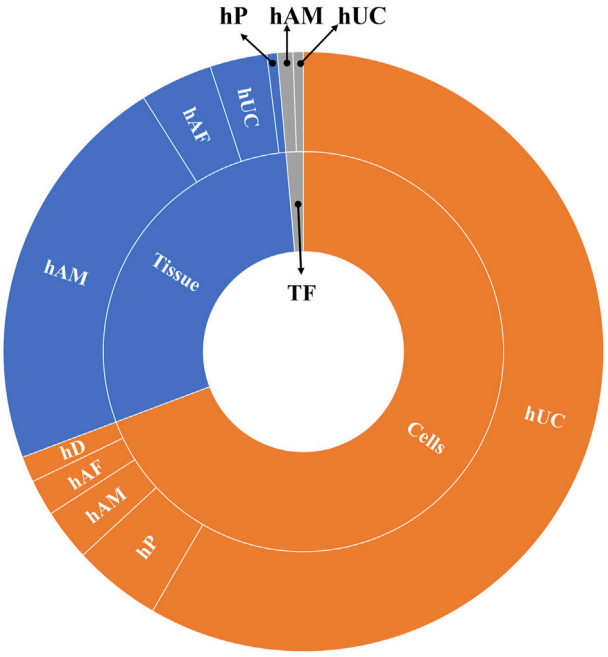

FIGURE 3
Different uses of cells and tissues in the selected clinical trials analyzed. Abbreviations: hP: human placenta; hUC: human umbilical cord; hAM: human amniotic membrane; hAF: human amniotic fluid; hD: human decidua; TF: trophic factors; hACM: amnio-chorionic membrane.

ones are using other multiples sources (n = 80) (Figure 3). Regarding the product presentation, we found again quite homogeneity, as the majority of clinical trials were conducted using cells (n = 248) and/or tissue (n = 104), while just a few (n = 7) involved TF. It is worth noting that all of the clinical trials were conducted using allogenic PnD. However, it should be pointed out that autologous cells from different origins were sometimes combined to PnD (Table 2).

3.1.2 PnD combined products

According to the above given data, from a total of 46 clinical trials implementing combined products, again, we found applied PnD were primarily composed by hUC-MSC (n = 22) and secondly by hAM (n = 14). Few remaining combined products associated several PnD, including hAM/hAFC (n = 3), hACM (n = 2), hUC-WJ-MSC (n = 2), hPMSC (n = 1), hAEC (n = 1) and AMEED (n = 1).

Interestingly, certain PnD combinations (hAM, hAM + hAFC and hACM) were preferably associated to bone substitutes ([n = 8], Table 2). In other conditions, we found a great diversity of PnD combined to multiple substrates/scaffolds and/or other biological components (gels, natural membranes, tissues, conduct-gels, glue, etc.); or along with additional cells (limbal epithelial cells, other stem/stromal cells, bone marrow [BM]-MSC, fibroblasts, etc.).

3.2 Part II: Clinical trials

3.2.1 clinical trial phases

For Phase I, a total of 20 studies are listed ongoing using tissues isolated from different part of the placenta (mainly hAM but also hACM) and hAF, while 177 are the early phase/Ph.1 studies where human PnD cells have been isolated and later infused in (almost exclusive allogeneic) settings. The largest PnD product currently on test is MSC isolated from hUC (commonly defined as hWJ-MSC), used in 151 registered clinical trials. Few early phase studies are ongoing testing cells isolated from hAM (n = 9) or decidua tissue (n = 5), or from a specific or combined section of the placenta (n = 12). In the last decade there has been an increasing number of safety studies for PnD cell-based products, where safety has been the primary target, sometimes involving Phase 2 characteristic analysis as multiple ascending doses, starting from subtherapeutic to high dose of drug. Such preliminary phase is commonly conducted in a single medical center, where the subject can be monitored for tolerability, pharmaco-vigilance/-kinetic/-dynamics of the PnD product. For Phase II, PnD tissue products have been undergoing evaluation in seven registered clinical trials, while 40 studies aimed to evaluated PnD cells (where hUC-MSC represents 90% of the tested PnD products). Phase III trials are expensive, time-consuming and difficult to design. They are usually run by small biotech companies or medical centers and during the last decade only four trials have been registered using hUC-MSC and five studies using other PnD tissue products. For Phase IV, currently just eight hAM or hACM are under final evaluation, while only one bio-pharma technology involving hUC-MSC is included in this phase.

3.2.1.1 Clinical trial classification according to ICD-10 medical fields

Additionally to the technical assessment on PnD characteristics, clinical trials were also analyzed and sorted by the medical field of application, according to the International Statistical Classification of Diseases and Related Health Problems 10th Revision (ICD-10). Thus, all indications were clustered into ICD-10 chapters, each of them corresponding to a specific medical field.

3.2.1.1.1 ICD-10 limitations and shortcomings management

Even though ICD-10 is a thorough and detailed classification intended for delimiting practice according to the causes of disease, discrepancies appeared between ICD-10 classification and common medical terminology, as used in multiple review articles (Silini et al., 2015; Torre and Flores, 2020; Fenelon et al., 2021; Nejad et al., 2021; Elkhenany et al., 2022). Therefore, some adjustments were done to ease the discussion of the results. The first deviation from ICD-10 was made when clinical trials for some of the medical indications (21 clinical trials, 7% of all clinical trials) could not be easily classified solely in one ICD-10 chapter. To avoid

TABLE 2 Number of clinical trials with combined cells or scaffolds.

Type of PnD	Combined with	Number of trials
Tissue	Bone substitute	8
	Gel	2
	Glue	1
	Limbal (epithelial) stem cells	4
	BM-MSC	3
	Fibroblasts	1
Cells	Gel	8
	Natural membrane	5
	Tissue	3
	Conduct	1
	Cells from cord blood (CB-MNC, UCB-HSC, USC-MSC)	5
	Cells from bone marrow (BM-MNC, BM-MSC)	2
	AD-MSC	1
	Limbal (epithelial) stem cells	1

Tissue (skin graft, hAM); Bone substitute (demineralized freeze-dried bone and mineralized freeze-dried bone allograft, hydroxyapatite, demineralized [freeze-dried] bone Matrix, bone autograft); Natural membrane (epicardial extra cellular matrix, collagen); Conduct: collagen (NeuroRegen Scaffold™); Gel (injectable collagen/injectable; Collagen Scaffold™, fibrin, PRP, plasma-derived biomaterial, hyaluronic acid). Abbreviations: BM MSC: BM, mesenchymal stromal cells; CB MNC: cord blood mononuclear cells; UCB HSC: UC, blood hematopoietic stem cells; BM MNC: BM, mononuclear cells; UCB MSC: UC, blood MSC; AD-MSC: adipose tissue-derived MSC; PRP: platelet rich plasma.

duplications, these 21 cases were included into their main, most relevant, ICD-10.

More than half of the clinical trials in this category (57%) belonged to different forms of wound healing fields (and thus discussed in Diseases of the skin and subcutaneous tissue). The second deviation from ICD-10 occurred when it was found that the clinical trials using PnD for COVID-19 were classified into "respiratory system", despite ICD-10 classification into "special purposes". This could be a consequence of the ICD-10 being issued in 2019 when COVID-19 was still not a common reality. The first impression was to include it into "Certain infectious and parasitic diseases", which would clearly be scientifically sound being it a viral disease. However, finally it was decided to keep those in the "respiratory system disease" due to the fact that most COVID-19 patients developed an acute respiratory distress syndrome (ARDS), which constitutes a respiratory condition. In that sense, the vast majority of clinical trials using PnD for the treatment of COVID-19 were not intended for infection mitigation but for improving lung function and prevention of inflammation associated with ARDS. Moreover, despite deviations from ICD-10, we believe that this decision to not include clinical trials for PnD over COVID-19 into the "special purposes" category seems adequate due to the global impact of this disease involving respiratory complications in recent times.

3.2.1.2 Clinical trials distribution according to ICD-10

The whole 340 short-listed clinical trials were grouped into ICD-10 categories (Figure 4). Medical fields with less than 10 clinical trials were grouped into "medical fields with low number of clinical trials".

3.2.1.3 Clinical trial activity assessment according to medical fields

3.2.1.3.1 Diseases of the musculoskeletal system and connective tissue

The most active medical field with regards to clinical trials using PnD is Diseases of the musculoskeletal system and connective tissue (ICD-10 chapter XIII), grouping 18% (n = 61) of all short-listed clinical trials. It is worth noting that the majority of clinical trials in chapter XIII fall into two main subdivisions: joint regeneration (n = 23) and rheumatological autoimmune diseases (n = 17).

3.2.1.3.2 Diseases of the skin and subcutaneous tissue

Interestingly enough, in the initial analysis, wound healing and other diseases of the skin and subcutaneous tissue (ICD-10 chapter XII) did not show much activity, even though there are many commercialized products using PnD. The reason for that, as partially explained above, was that as for ICD-10, the wound healing field is mainly present in Chapter XII (n = 20), but is also divided into other chapters, such as IV, XIII, XIV, XVII, XIX (n = 23), altogether representing 13% (n = 43) of all short-listed clinical trials. It is worth highlighting that ICD-10 clearly distinguishes between different causes of wounds (i.e. burns belong to different ICD-10 than diabetic foot ulcers). However, the etiology of the wound does not affect how the wound is treated, as those are usually treated in a similar way independently of the origin. Thus, we have combined all those trials as "diseases of the skin and subcutaneous tissue". Within this category, the medical indication with the most ongoing clinical trials is diabetic foot ulcers (n = 22). The other significant medical indication is burns (n = 4).

3.2.1.3.3 Diseases of the respiratory system including COVID-19

Diseases of the respiratory system (ICD-10 chapter X + COVID-19) account for 9% (n = 31) of all clinical trials with PnD. In this field, COVID-19 is by far the most addressed condition (n = 18), followed by idiopathic pulmonary fibrosis (n = 2), chronic obstructive pulmonary disease (n = 2) and bronchopleural fistula (n = 2).

3.2.1.3.4 Diseases of the digestive system

This medical field (ICD-10 chapter XI) accounts for 9% (n = 31) of all clinical trials using PnD. Within this category, the far most clinical trials are active for liver cirrhosis (n = 13), followed by periodontal diseases (n = 7) and Crohn's disease (n = 3).

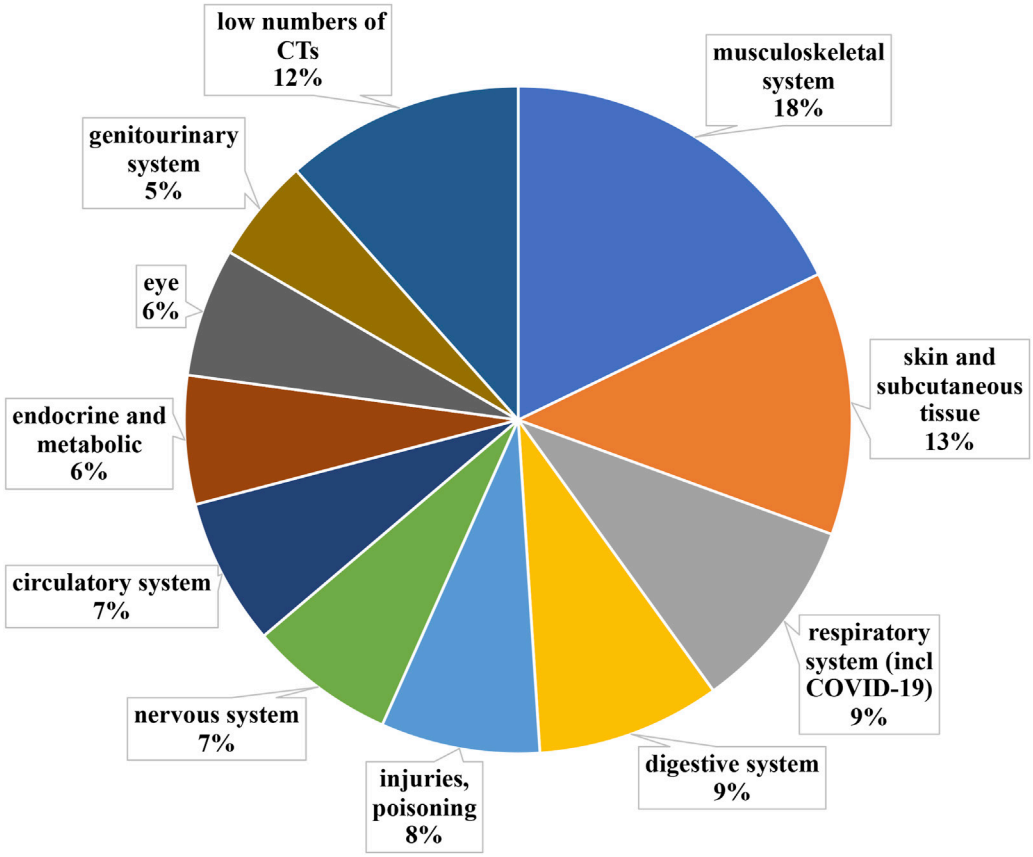

FIGURE 4
Grouping according to medical fields ICD-10 classification of clinical trials implementing PnD. Medical fields with less than 10 clinical trials were grouped into "medical fields with low number of clinical trials". The clinical trials using PnD for COVID-19 were classified as a respiratory system disease despite ICD-10 classification into "special purposes".

3.2.1.3.5 Injury, poisoning and certain other consequences of external causes

The next most active medical field was injury, poisoning and certain other consequences of external causes (ICD-10 chapter XIX), grouping 8% (n = 27) of all shortlisted clinical trials. In this case, the medical indications were more diverse, yet, we found two main medical indications being acute Graft-Versus-Host Disease (aGvHD, n = 8) and spinal cord injury (n = 7).

3.2.1.3.6 Diseases of the nervous system

This medical field (ICD-10 chapter VI) accounted for 7% (n = 24) of all shortlisted clinical trials. Inside this field, the main categories were cerebral palsy (n = 5) and Duchenne's muscular dystrophy (n = 4). One clinical trial was found to be active for each of the next three medical indications: spinocerebellar ataxia, Parkinson's disease and Alzheimer's disease.

3.2.1.3.7 Diseases of the circulatory system

Surprisingly, despite being a major mortality cause, diseases of the circulatory system (ICD-10 chapter IX) accounted just for 7% (n = 24) of all shortlisted clinical trials. Within the field, four medical indications had a similar activity for clinical trials: ischaemic stroke (n = 5), myocardial infarction (n = 4), cerebral infarction (n = 4) and cardiomiopathy (n = 3).

3.2.1.3.8 Multiple medical fields

Clinical trials for some of the medical indications (n = 21) could not be classified solely in one ICD-10 chapter and thus were classified "multiple". However, more than half of the clinical trials in this field (n = 11) fall within the wound healing category, thus will be discussed in diseases of the skin and subcutaneous tissue.

3.2.1.4 Preferred PnD indications according to ICD-10

Additional analysis aimed at understanding which PnD products are prefererably indicated for each medical field identified according to ICD-10 (Table 3). Consistently with other analysis in this work, hUC-MSC and hAM accumulated the bulk of references, 209 and 63 respectively (Table 3; Figures 5A, B). Note: as some studies refer to more than one ICD-10

TABLE 3 PnD vs. ICD-10.

ICD-10		Cells									Tissue				Fluid	
	General condition description	HUC-MSC	hAMC	hPC	hDSC	hAEC	hPMSC	hUC-WJ-MSC	hAFC	hAMSC	hACM	hAM	hUC	hP	hAF	Total
I	Infectious and parasitic	1	1	—	—	—	—	—	—	—	—	—	—	—	—	2
II	Neoplasms	1	—	1	—	—	—	—	—	—	—	1	1	—	—	4
III	Blood and immune	4	—	1	—	—	—	—	—	—	—	—	—	—	—	5
IV	Endocrine, nutritional and metabolic	19	—	1	—	2	2	1	—	—	1	1	1	—	—	28
V	Mental and behavioural	7	—	—	—	—	—	—	—	—	—	—	—	—	—	7
VI	Nervous system	22	—	—	—	2	—	—	—	—	—	—	—	—	—	24
VII	Eye and adnexa	6	—	—	—	—	—	—	—	—	—	13	—	—	1	21
VIII	Ear and mastoid process	—	—	—	—	—	—	—	—	—	—	2	—	—	—	2
IX	Circulatory system	19	3	2	—	—	1	3	—	—	1		1	—	—	30
X	Respiratory system	11	—	—	—	1	1	1	—	—	—	—	—	—	—	14
XI	Digestive system	20	1	1	—	—	—	—	—	—	4	5	—	—	—	31
XII	Skin and subcutaneous	9	—	—	—	—	1			—	7	10	5		2	34
XIII	Musculoskeletal and connective	31	—	—	—	1	2	1	7	1	3	13	1	1	7	68
XIV	Genitourinary	11	—		1	2	2	—	—	1	—	5	—	—	—	22
XV	Pregnancy, childbirth and puerperium		—	—	—	—	—	—	—	—	—	—	—	—	—	0
XVI	Conditions perinatal period	9	—	—	—	—	—	—	—	—	—	—	—	—	—	9
XVII	Congenital malformations	2	—	—	—	—	—	—	—	—	—	4	1	—	—	7
XVIII	Abnormal clinical	1	—	—	—	—	—	—	—	—	—	—	—	—	—	1
XIX	Injury, poisoning and external causes	19	—	—	4	1	—	1	—	—	4	9	1	—	2	41
XX	External causes of morbidity and mortality	2	—	—	—	—	1	—	—	—	—	—	—	—	—	3
XXI	Factors influencing health status	1	—	—	—	—	—	—	—	—	—	—	—	—	—	1
XXII	Codes special purposes	14	—	—	—	—	2	1	—	—	—	—	—	—	3	20
	TOTAL	209	5	6	5	9	12	9	7	2	20	63	11	1	15	374

Note that number of clinical trials in hUC-MSC, hAMC, hAM, hAF, categories includes TF, AMEED, or hAFED, cases (N = 3, 1, two and one respectively).

10.3389/fbioe.2022.977590

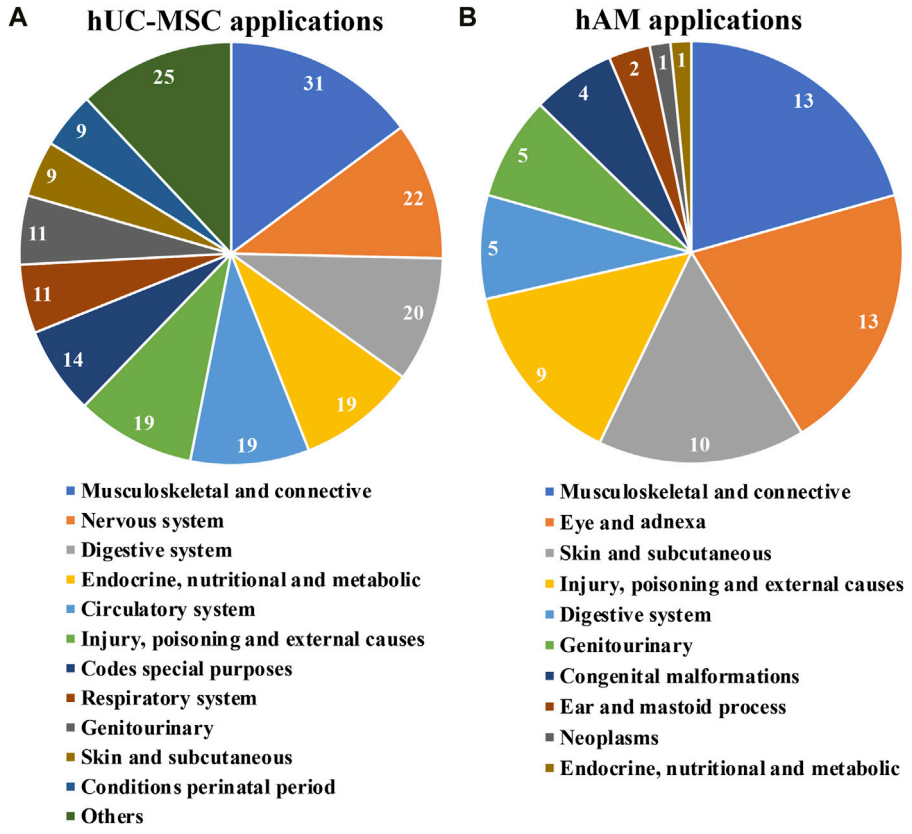

FIGURE 5
Applications for hUC-MSC **(A)** and for hAM **(B)**; grouping according to medical fields ICD-10 classification of clinical trials implementing hUC-MSC and for hAM respectively.

category, the total number of studies with the corresponding PnD reported here differs from the stated number of studies analyzed with the individual PnD. Also, in a very few studies, two different PnD were used contributing also to the discrepancy. The cases with hAM included two applications with AMEED, and the different trofic factor trials were included in their corresponding cell or tissue of origin categories.

For the case of hUC-MSC, clinical trials under assessment span across 21 distinct medical fields (Figure 5A). Interestingly, just nine indications englobed almost 80% of the studies, all of them with at least 11 registered trials so far. This fact would highlight, in a generic manner, the interest of the scientific community in such products. Moreover, "musculoskeletal and connective", "nervous system" and "digestive system", had each of them more than 20 trials. Consequently, in these cases, a swift development in the field is to be expected.

Again, a group of only five fields encompassed most of the trials recorded using hAM (Figure 5B). Interestingly, "musculoskeletal and connective tissue", "skin and subcutaneous tissue" and "injury, poisoning and external causes" show comparable numbers to "eye and adnexa", probably because the effectiveness of these products recognized for a very long time in these indications has required comparatively fewer clinical trials in the last 10 years. In addition, less expected indications such as "digestive system" and "genito-urinary" had five registered trials, suggesting future progresses in these fields.

3.2.2 Gender consideration

Regarding the gender of patients, clinical trials were mainly conducted on both genders. Nevertheless, there were several cases in clinical trials when PnD had been used only on female because of gynecological indications hAM (n = 5), hUC-MSC (n = 10) and hAEC (n = 4), or only in men because of chronic ischemic cardiomyopathy (hUC-MSC, n = 1 because this gender is more affected than women in these particular condition), prostate cancer (hUC-MSC, n = 1), erectile dysfunction (hUC-MSC, n = 1 and hPMSC, n = 1) or Duchenne muscular dystrophy (hUC-MSC, n = 3).

3.2.3 Age

The evaluation of either the use of cells or tissue in clinical trials clearly show a preferential design of clinical trials for adults or aged people (Figure 6), what is not surprising about regenerative medicine products. Clinical trials specifically designed for children did represent less than 10 percent of the total of analyzed clinical trials. hUC-MSC and hAM were predominant in both children and adults, but specific pathologies were explored in children. As there were only six clinical trials using TF, hAFED or AMEED we did not include them in the analysis. Of these, five were conducted in adults and one in children from 6 months to 3 years old.

3.2.4 PnD manipulation and route of administration

Information available regarding PnD manipulation [according to Annex I to Regulation (EC) No 1394/2007] is often not sufficiently explained in our database clinical trials. Therefore, it is difficult to determine whether the tissue is manipulated or not. Of course, procedures are variable depending on the PnD used. Moreover, for a given tissue the manipulation can differ very much undoubtedly adding an additional variable in the assessment of the therapeutic efficacy on the patient. As an example, this is particularly true for the case of the fetal membranes (hAM, hACM) originating from the placenta which can be decellularized, cryopreserved, devitalized, dehydrated or lyophilized, and sometimes irradiated.

Likewise, the protocols for the preparation of MSC and hDSC are not described, or do not always refer to a precise bibliography. Only the tissue of origin is usually mentioned (placenta, Wharton's jelly or hUC). Modalities of isolation, expansion and mode of use of cells (fresh or thawed) should be specified in the future. Of note, hAF was always used after filtration and cryopreservation or lyophilization (Table 4).

3.2.5 PnD route of administration and place of application versus ICD-10

For the analysis of PnD routes and frequency of administration we decided to analyze independently the main presentation types.

Cell-based products were the most frequently used in clinical trials implementing PnD (n = 248 out of 340, 72.6%). A systemic approach was used in 57.5% cases, while local administration were used in 38.1% and in two clinical trials (0.8%) cells were injected locally and systemically in a simultaneous manner (Figure 7).

From PnD cell products, MSC were the most frequently used (93.5%). Perinatal MSC in most cases were used systemically (60.6%) and locally in the rest of cases (34.2%). Systemic administration of perinatal MSC were used preferentially in the following groups, "Endocrine, nutritional and metabolic diseases", "Mental and behavioural disorders", "Diseases of the nervous system", "Diseases of the circulatory system", "Diseases of the digestive system", "Certain conditions originating in the perinatal period" and diseases related to COVID-19 (ARDS, MIS-C) according to ICD-10 classification. In contrast, perinatal MSC were administrated locally more frequently than systemically for the treatment of "Diseases of the eye and adnexa" and "Diseases of the musculoskeletal system and connective tissue" and "Diseases of the genitourinary system" (Figure 7). Note that hAEC were used only in 3.6% of clinical trials utilizing PnD. In contrast to MSC, hAEC-based products were administrated locally except for two out of 10 trials where administration was systemic.

AF-derived cell products were always combined products and included at least hAM and hAF components. They were represented by two commercial products NuCel® and ReNu® (both Organogenesis Inc, United States) which were tested for the treatment of orthopedic diseases (Diseases of the musculoskeletal system and connective tissue). Nucel® was injected into intervertebral disc (n = 3) and for cervical spine fusion (n = 1). On its side, ReNu® was tested for treatment of knee and hip osteo-artritis by intraarticular injection.

Clinical trials implementing hAM also constituted a significant part (22.6%) of clinical trials utilizing PnD. Due to their characteristics, all hAM products are applied locally. The main fields of applications were dermatology, oral surgery and ophthalmology. hAM-based products were most frequently used to treat wounds, burns and ligaments, to avoid scarring after massive surgery and in dentistry and were classified according to ICD-10 as "Diseases of the skin and subcutaneous tissue", "Diseases of the eye and adnexa", "Diseases of the musculoskeletal system and connective tissue", "Injury, poisoning and certain other consequences of external causes" "Diseases of the digestive system" (Supplemental Table S1).

For the case of trials implementing TF, those were mostly administrated locally (n = 16). We found that systemic administration was used just in clinical trials related to ARDS secondary to COVID-19 (Table 5).

3.2.6 PnD dose and frequency of treatment according to ICD-10

For this section, a subset of clinical trials was analyzed based on the use of PnD MSC, including: hDSC, hUC-WJ-MSC, hAMSC, hPMSC and hUC-MSC. This criterium was favoured in order to ascertain appropriate comparison regarding use in several conditions at different dosages and frequencies. Out of the shortlisted clinical trials, 248 used cells of any nature. Among them, trials using MSC of the described nature amounted up to 225.

Having an internal reference for the proper assessment of regenerative results when comparing patient to patient, independently of health provider or the nature of disease, remains crucial. So, to serve this purpose, we selected trials

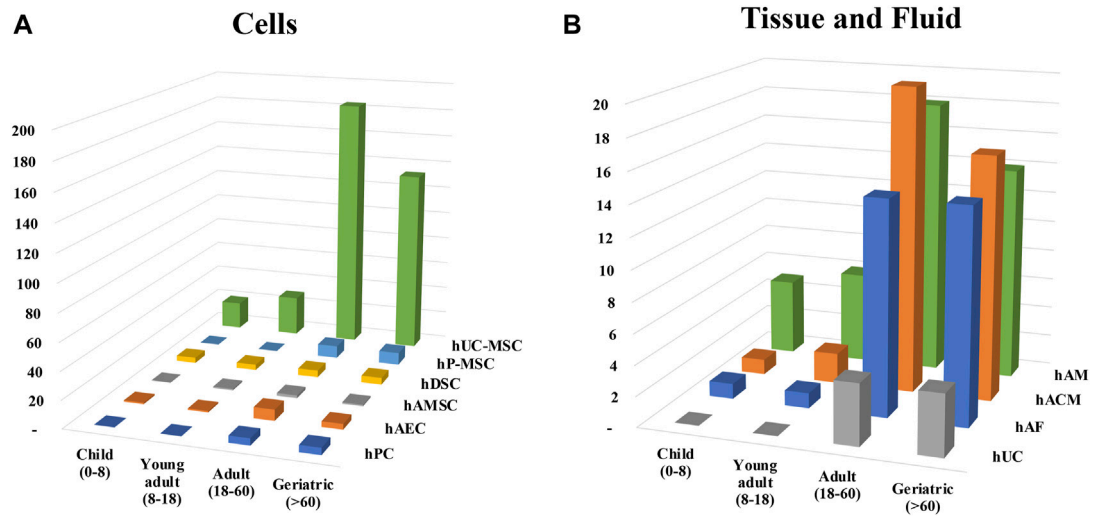

FIGURE 6
Distribution of clinical trials according to age groups. Clinical trials were classified in **(A)** cells or **(B)** tissue and fluid and the different age group were assigned. Patients were divided and named in four groups depending on the range of age: children (0–8 years), young adults (8–18 years), adult (18–60 years) and geriatric (60 and over).

that were referred to the total body weight (BW) of the patient (kg). Of the 225 clinical trials involving MSC, only 83 had been using mass body as a reference. For the rest of the clinical trials, there was no relative reference, and only three had a surface of the lesion reference. Besides, for 19 of the trials we could refer to a given volume of treatment but without further reference on the BW. Worth noting, just in two trials the reference for treatment performance was assigned to the volume or surface of the lesion (keloids and cartilage defects respectively).

Surprisingly, an appreciable number of clinical trials did not indicate the cell dose or numbers (n = 80), although they reflected the administration frequency (n = 35). This fact increases uncertainty and inconsistency for treatment developments. Yet, when trials were reporting the dosage of the treatment, the frequency of treatment was also given in most cases (90%).

We tried to combine the data of frequency and dosage in our analysis. Because some trials were using different doses, then they were considered independent trials in relation to frequency. When different number of frequencies were considered in a single clinical trial, the highest frequency was used for calculations. In order to understand better, and be able to compare between clinical trials, we established four dose ranges: below one million, between 1 and 10 millions, 10 to 100 millions, or above 100 million cells per kg BW (Table 6).

Our analysis showed that the most frequent treatment was an unique dose (frequency 1) of 1–10 million cells/kg BW (25% of trials) which in almost in half of the cases was aimed to treat pulmonary-related conditions. Forty per cent of the remaining trials used the same cell dose applied two, three or four times. The number of cases for the other doses was so low that we could not have any clear conclusion about the preferred usage of frequencies at those doses.

3.2.6.1 PnD cells administration dose according to ICD-10

Understanding whether the treatment of some human conditions prefer a given dose of PnD cells compared to others might be valuable for future research. To ascertain this, we analyzed the dose use for treatment of the different groups of human conditions. To have a comparable measure, following the previously mentioned criteria, we compared doses referred to the total BW of enrolled patients (Table 7).

From the clinical trials providing information about cell doses, the analysis shows how all conditions had a preference for using cells in a range of 1–10 million/kg, (Table 6). Most of the clinical trials analyzed in this group used systemic delivery. Interestingly, certain condition groups were related to treatments below one million cells, amounting for more than 10% of the trials in that category (ICD-10 groups: III, IV, VI, IX, XI, XIX and XXII). Conditions using cells above 10 million/kg BW were ICD-10 groups: III, IX, XI, XVI and XXII. Half of the human conditions groups were using cells only ranging 1 to 10 million cells per kg of BW. The analysis of data from clinical trials that only offered the absolute number of cells (not related to BW) showed a similar order of magnitude per treatment (Supplemental Table S2). Unfortunately, further analysis on absolute amounts and the non-referred units was unpracticable, as in most of the trials the information about doses was not provided.

TABLE 4 Distribution of different manipulation and corresponding route of administration among PnD.

Type	PnD	Manipulation	Route of Administration
Cell products (247)	hDSC (5)	Cryopreservation (2)	Sytemic (2)
		n.a. (3)	Sytemic (3)
	hAEC (9)	n.a. (9)	Local (7)
			Sytemic (1)
			Sytemic, Local (1)
	hAFC (7)	Cryopreservation (4) [NuCel®]	Local (4)
		Micronisation and Cryopreservation (3) [ReNu®]	Local (3)
	NK derived from hP (1)	Cell isolation, Expansion (1)	Systemic (1)
	hMSC (224)	Cell isolation (5)	Local (2)
			Systemic (3)
		Cell isolation, Expansion (36)	Local (11)
			Systemic (21)
			Systemic, Local (1)
			n.a. (3)
		Cell isolation, Expansion, Cryopreservation (7)	Systemic (5)
			Local (2)
		Cell isolation, Expansion, Cryopreservation or native (1)	Local (1)
		Cell isolation, Expansion, Selection (1)	Systemic (1)
		Cryopreservation (4)	Systemic (3)
			Local (1)
		Expansion (1)	Systemic (1)
		Cell isolation and Differenciation (1)	Systemic + Local (1)
		Loading on scaffold (3)	Local (3)
		n.a. (165)	Local (56)
			Systemic (96)
			Systemic, Local (2)
			n.a. (11)
Trophic factors/hAF (20)	hAFED (1) AMEED (2) hAMC (TF) (1) hUC-MSC (TF) (3) hAF (13)	Extraction (1)	Local (1)
		Micronization, Dehydration (1)	n.a. (1)
		Cryopreservation (1)	Local (1)
		Decellularisation (1)	Local (1)
		Extraction of exosome particles (1)	Systemic (1)
		Filtration (1)	Systemic (1)
		Lyophilisation (1)	Local (1)
		Purification, Decellularisation (1)	Systemic (1)
		Cell isolation, Expansion (1)	Local (1)
		n.a. (11)	Local (10)
			n.a. (1)
Tissue products (86)	hACM (18) hAM (59)	Micronization and cryopreservation (3)	Local (3)
		Dehydration, Sterilization (1)	Local (1)
		Dehydration (16)	Local (16)
		AM as scaffold for other cells or collagen (3)	Local (3)
		Decellularisation, Dehydration (2)	Local (2)
		Cryopreservation (9)	Local (9)
		Devitalization, Cryopreservation (2)	Local (2)
		Dehydration, Irradiation (1)	Local (1)
		Irradiation (2)	Local (2)
		Lyophilisation and Irradiation (1)	Local (1)
		None (fresh) (2)	Local (2)

(Continued on following page)

TABLE 4 (*Continued*) Distribution of different manipulation and corresponding route of administration among PnD.

Type	PnD	Manipulation	Route of Administration
		n.a. (35)	Local (35)
	hUC (9)	Cryopreservation (8)	Local (8)
		Devitalization, Cryopreservation (1)	Local (1)

All numbers in brackets indicate the number of clinical studies for that situation.
n.a. = not available.

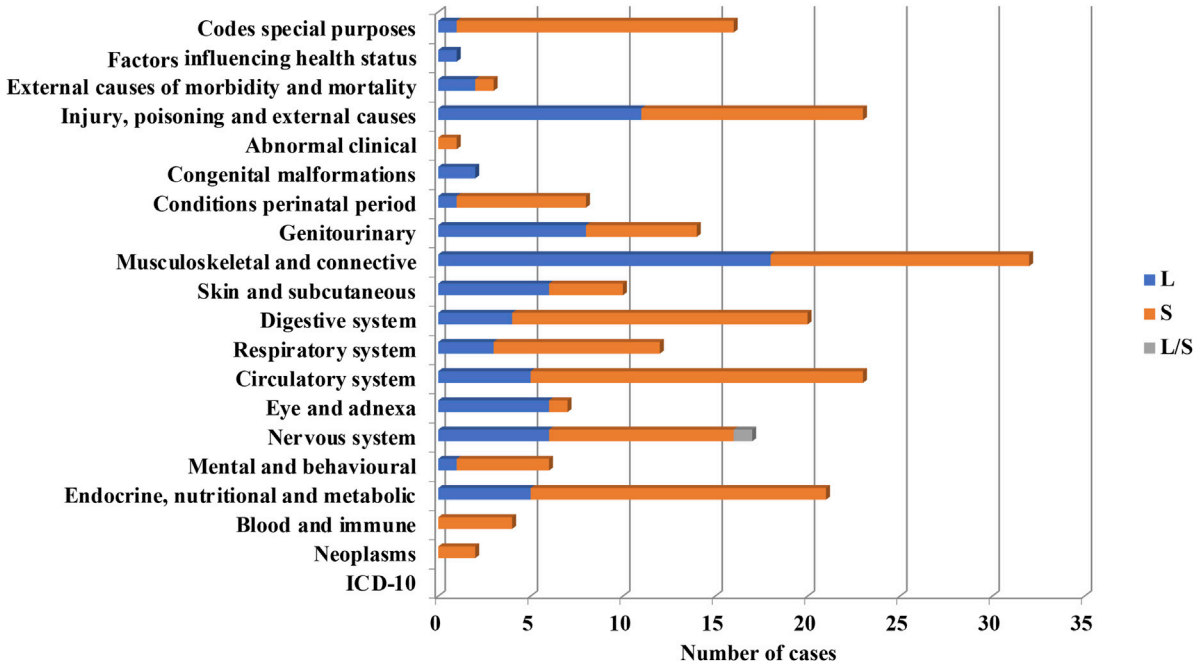

FIGURE 7
Systemic (S) or local (L) use of PnD cell products for the indication of different ICD-10.

3.2.6.2 PnD cell dose according to route of administration

Understanding limitations imposed by the administration route might also be valuable for future research design (Figure 8). The total number of clinical trials using "systemic" administration was 49, while the total number of clinical trials using "local" was 22.

The analysis indicates a preferential usage of the medium cell doses up to 10^7 for systemic administrations. In local administrations, the higher doses used were up to 10^8 cells. Of note, doses in systemic administrations were presented per kg BW. Clinical trials with local administrations did not indicate, with few exception, whether the dosage is designated per kg BW or total infused cells. Yet, it seems fair to assume that most of the local indications are referring to total cell number delivered locally regardless of patient's BW.

In the case of local administration, just five registered clinical trials indicated the dosage per kg of BW. In 4 cases, a medium cell dose up to 10^7 cells per kg BW was used. In 2 cases, higher doses were specified (one study used medium and high doses). This would confirm a trend for higher local doses when comparing to systemic administrations indicated per kg BW.

Considering that most clinical trials were focused on adult patients, the total number of cells infused systemically would be similar when comparing to local administrations. Exceptionally, in the clinical study NCT03645525, on the pediatric condition bronchopulmonary dysplasia, up to 20 million cells were instilled per kg BW directly into lungs of extreme preterm new-born children with an average body-weight of 1 kg.

3.2.7 Enrollment

Enrollment represents the number of participants in a clinical study. However, in "clinicaltrials.gov" website, this

TABLE 5 Distribution of different routes of administration of TF.

Route of administration	Nr of clinical trials	Percent
Local	16	76.2
Systemic	3	14.3
N.a.	2	9.5
Total	21	100.0

TABLE 6 Dose of PnD MSC and frequency of treatment used in clinical trials referring to BW of the patient.

		Frequency						
		1	2	3	4	5	>5	TOTAL
Dose	<1M	4.4	0.0	5.6	4.4	0.0	3.3	17.8
	1M-10M	25.6	13.3	15.6	11.1	2.2	6.7	74.4
	10M-100M	2.2	0.0	1.1	1.1	0.0	1.1	5.6
	>100M	0.0	0.0	1.1	1.1	0.0	0.0	2.2
	TOTAL	32.2	13.3	23.3	17.8	2.2	11.1	100.0

information is not always available. Indeed, for most of the studies registered, the only information available usually indicated the "estimated enrollment", i.e. the target number of participants that the researchers needed for the study. Although estimated enrollment is always present, the information regarding the effective number of participants involved was rarely existent and the "recruitment status" being most of the time not updated ("unknown"). Therefore, no conclusion can be made about the enrollment for these clinical studies. However, it should be highlighted that updates should be made, for instance every 6 months, stating the actual number of participants and the recruitment status (few studies stated the "actual enrollment").

3.2.8 To-be-commercialized products in clinical trials

80 of the 340 clinical interventional trials were conducted on already available commercial products or when a market approval seems to be at least aimed for (to-be-commercialized). From those, 30 clinical trials have used cell products (hUC-MSC, hPC, hPMSC, hUC-WJ-MSC) that already have a registered name, however as far as we know none of them has been approved by any official body to date. In parallel, 48 studies have applied tissue products, mainly as a matrix, and exclusively corresponded to preparation of hAM, hACM or chorion membrane, all commercially obtainable. hAF has been tested in only two studies. Finally, in 14 clinical trials, cells and matrix were used in combination. Of these 78 trials, 52 were registered in the United States, the country where the majority of the manufacturers of these products are located. In Supplemental Table S3-S5, the different commercialized products are listed.

3.2.9 Geographic location of clinical trials

Data shown in Figure 9, give an overview of the distribution of clinical trials conducted or registered and implementing PnD. It is striking that of the 340 identified studies, 144 are located in China and thus a total of more than 50% of all clinical studies in Asia. With 94 studies in the United States, almost another third are conducted in North America. Surprisingly, only 8% of the studies registered are in Europe. While the majority of the indicated studies in China are designed with cells (MSC of various origins), research in the United States is conducted in roughly equal parts on cells, tissue as matrix, extracts and combined PnD.

Our research has shown that interest in the clinical use of PnD is steadily increasing. With this development, the question of regulation of donation, production and distribution is becoming more important at the same time. Among the information available, no details were found on regulatory aspects related to the clinical trials. When using PnD in the form of the tissues such as hAM, hACM, chorion membrane or hUC, which serve as a matrix in clinical therapy, several commercially available products can already be found. The preparation of these tissues has been in common use for decades and is therefore also accepted by national authorities for use. Further preparations may also be authorized for distribution relatively easily from national authorities in the individual countries, if the use does not take place only under local supervision anyway.

However, the newer, promising therapeutic options with the diverse cells isolated from birth-associated tissues, require much more extensive regulatory measures because they will probably be predominantly classified as ATMP. In Europe, these therapies will only find their way into the clinic if they have first been evaluated and approved via the European Medicines Agency (EMA) through the EU centralized procedure (Flory and Reinhardt, 2013; Celis et al., 2015; Salmikangas et al., 2015; Goula et al., 2020; Nejad et al., 2021).

4 Conclusion

Here we proposed to depict the clinical trials using PnD registered on the clinical trial website (https://www.clinicaltrials.gov). To our knowledge, this is the first article that precisely describes these trials over a period of 10 years. It allows to have a synthetic view on the efforts of the scientific community to evaluate the therapeutic potential of these products, although it should be noted that of course we do not have to date exhaustive and reliable data concerning their actual efficacy in every trial. Consequently, our intention is

10.3389/fbioe.2022.977590

TABLE 7 Use of cell dose in different groups of medical conditions. The number of cells are referred to kg of BW of the patient.

ICD-10	ICD-10 (General name of condition)	<1M	1M-10M	10M-100M	>10M
I	Infectious and parasitic	—	—	—	—
II	Neoplasms	—	—	—	—
III	Blood and immune	2	3	1	—
IV	Endocrine, nutritional and metabolic	1	7	—	—
V	Mental and behavioural	—	2	—	—
VI	Nervous system	2	1	—	1
VII	Eye and adnexa	—	—	—	—
VIII	Ear and mastoid process	—	—	—	—
IX	Circulatory system	1	5	1	—
X	Respiratory system	—	5	—	—
XI	Digestive system	3	8	1	—
XII	Skin and subcutaneous	—	4	—	—
XIII	Musculoskeletal and connective	1	8	—	—
XIV	Genitourinary	—	2	—	—
XV	Pregnancy, childbirth and puerperium	—	—	—	—
XVI	Conditions perinatal period	—	7	2	—
XVII	Congenital malformations	—	1	—	—
XVIII	Abnormal clinical	—	1	—	—
XIX	Injury, poisoning and external causes	2	12	—	—
XX	External causes of morbidity and mortality	—	2	—	—
XXI	Factores influencing health status	—	1	—	—
XXII	Codes special purposes	3	7	1	1
	TOTAL CASES	15	76	6	2

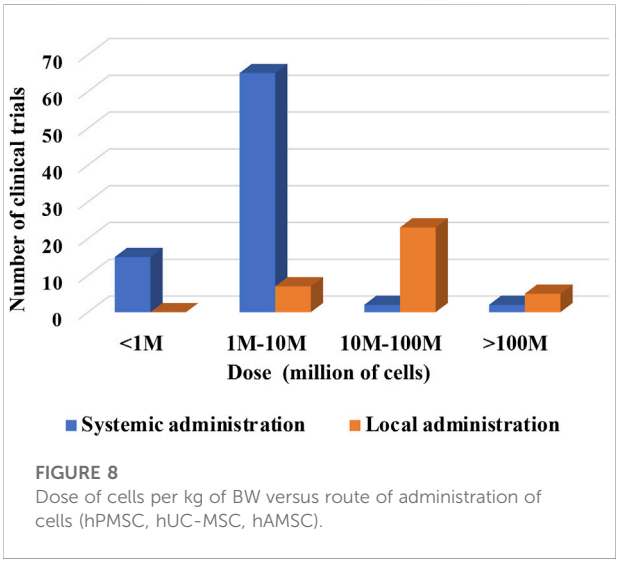

FIGURE 8
Dose of cells per kg of BW versus route of administration of cells (hPMSC, hUC-MSC, hAMSC).

not to endorse any efficacy of the proposed treatments, but to throw light on the attempts to evaluate these therapies in different indications.

Nevertheless, PnD have already demonstrated their suitability for promising therapies. Our results indicate that the PnD that have been tested are very varied and are represented by cells, tissues or TF (including the amniotic fluid itself). None were a gene therapy product, but one can imagine that in the future cellular or tissue PnD could also constitute raw materials easily available and usable to prepare genetically modified products. The indications are also very diverse, although some have been explored more often (e.g. musculoskeletal and connective tissues). Due to the diversity of indications, we have chosen to group them according to ICD-10, even if this classification has its limits and includes pathologies that can be very different.

PnD tested in the clinical trials displayed striking differences in their relative frequencies; one can easily speculate that it is due to different "product life cycles". For instance, in accordance with the fact that hAM was the first PnD to show their therapeutic efficacy in regenerative medicine, we can still find them very represented in the clinical trials recorded over the period considered. This undoubtedly reflects the need to extend the use of hAM to

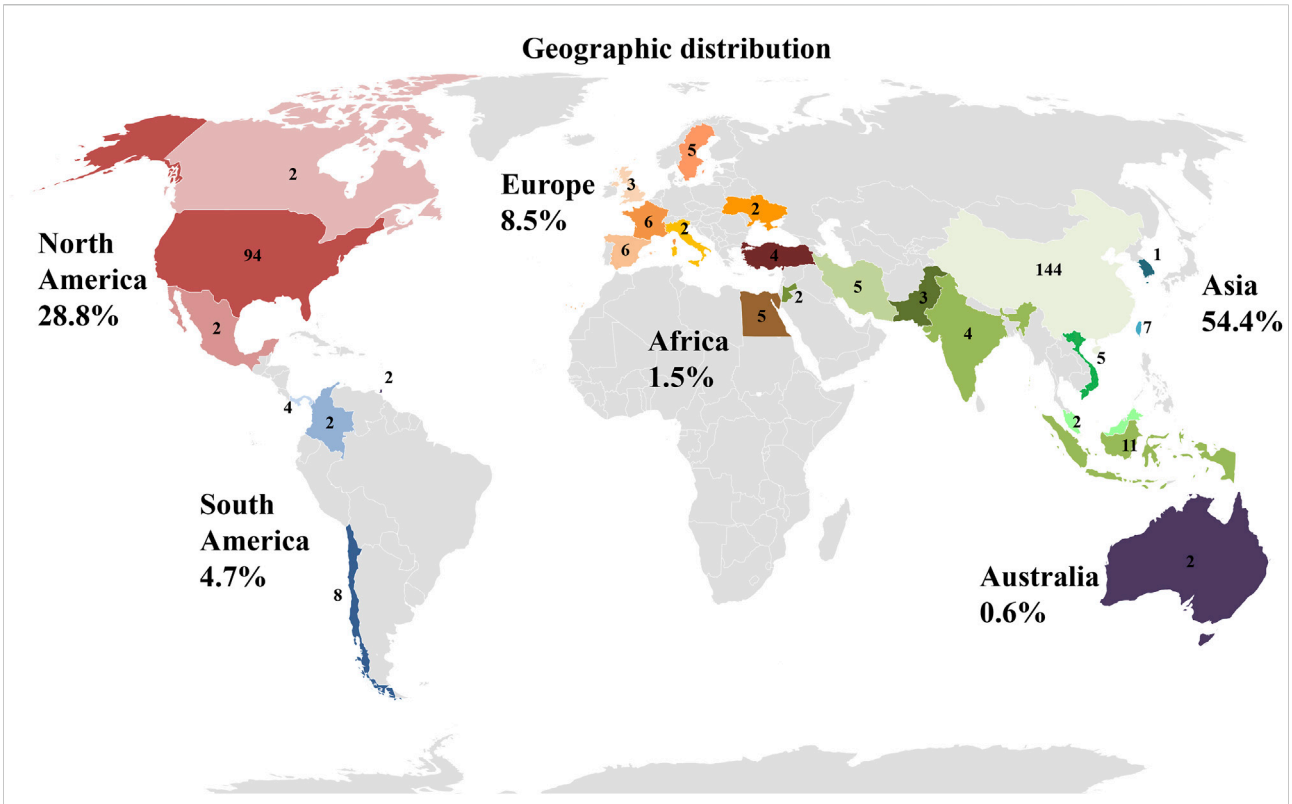

FIGURE 9
Location of clinical trials with PnD. The number of studies per country is indicated. In addition, the individual countries are grouped into geographical regions. Red colors stand for North America, blue for South America, orange for Europe, brown for Africa, green for Asia and purple for Australia. The number indicates percentage of clinical trials with PnD on the different continents in the period under review.

indications other than those accepted until now by the national regulatory authorities, most often limited to ophthalmology, and this despite an abundant literature on these applications. As proof, the eye and its adnexa represented only 20% of the indications tested in the clinical trials for hAM. The extension of these indications can only be encouraged if these protocols confirm therapeutic efficacy, because the absence of ATMP status for hAM allows the easy preparation and availability of these products. At the same time, the issue of the cost and the financial coverage of these new therapeutic approaches should also be facilitated by the national authorities, so as to make them truly accessible to patients.

Interestingly, hUC-MSC actually represented the first product tested (more than half the trials). This reflects the enormous hope that MSC have held due to their multipotency and their relative ease of preparation, and despite their heavier regulatory status as ATMP. In fact, these cells have played a large part in the recent development of regenerative medicine. Since then, issues about ploidy and their thrombotic potential have nevertheless weighed this enthusiasm. In particular for the systemic intravascular administration of MSC/EV-products, the expression of highly procoagulant tissue factor (TF/CD142) and hemocompatibility aspects are of crucial relevance for their safety profiles in patients, which is of particular importance for some PnD products (e.g. DSCs) due to their intrinsically high expression of TF/CD142 in the placenta, to counteract bleeding. This is important for the appropriate mode of delivery (e.g. systemic infusion vs tissue injection or ectopic use) (Moll et al., 2015; Ringden et al., 2022). One can imagine that the organization of these clinical trials in very diverse indications was necessary to define the pathologies likely to respond to these treatments.

Concordantly, combined products used mainly these flagship products, in combination to multiple substrates/scaffolds and/or other biological components/cells, including possibly another PnD. Indeed, hAM was more frequently associated to bone substitute for needs of the condition (orthopedic, maxillo-facial and oral surgeries). On the contrary, PnD cells were combined with gels to facilitate their local administration. However, the majority of the PnD were used alone. While tissue engineering has shown a wide interest and is largely developed in experimental research from PnD, in clinic, hAM was poorly used as scaffold for cells seeding (n = 8); PnD cells

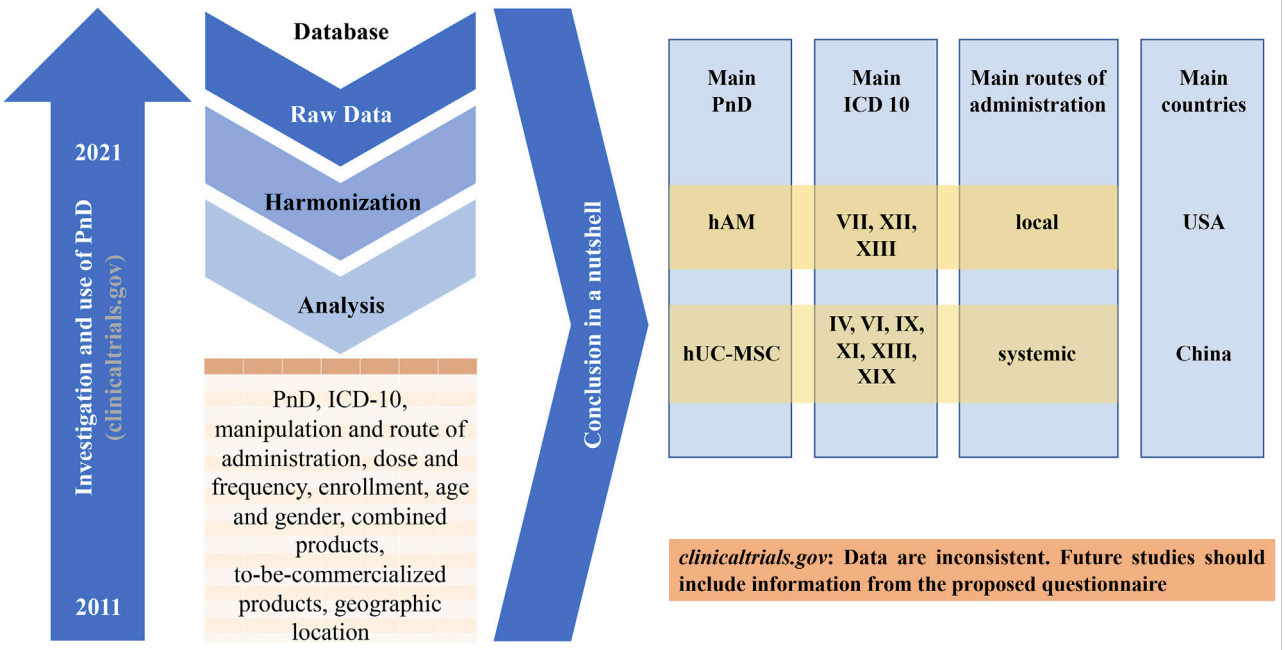

FIGURE 10
Graphical abstract of the study. The United States Clinical Trial Registration Portal (clinicaltrials.gov) was searched for 10-year period from 01/01/2011 to 07/10/2020 with different search-terms. From the keyword-based search, a number of clinical trials were identified. After removing studies for curing, the remaining 340 trials were analyzed. The main conclusions are shown and a more detailed registry is proposed.

slightly more exploited (n = 17). This combination of products seems profitable for future marketing.

All of the other PnD, which are diverse, accounted for only 23% of clinical trials. They can be considered as "emerging" products, which will certainly require more time to prove their effectiveness compared to standard treatments and to reach the patient's bedside.

Moreover, most of PnD were tested in Phase I clinical trials; it echoes the very great diversity of products and indications, and shows that the investigation of the therapeutic potential of PnD is carried out in all directions and still is in an initial pioneering phase, even if some commercial products already exist, in particular in the United States. Therefore, while some protocols will not show positive results, some others may be the source of marketed products constituting a breakthrough for certain indications.

During this study, we observed that the clinical trial website (https://www.clinicaltrials.gov) is mainly built for administrative purpose. Researchers and investigators have difficulties to find relevant informations. There is no uniform specifications as to what informations must be available for the entry. For example, the final number of included patients, the dose used and the type of manipulation of the PnD are often missing. Furthermore, there is usually no conclusive assessment even for studies that have been completed for some time and Publication DOI are very often absent. Frequently, a product name is used suggesting a market approval even if the PnD is neither yet approved nor commercially available. Conversely, it is not always stated if the PnD is already available for purchase. Regulatory aspects are also not addressed. However, all this information would be important in order to be able to assess the success of a study and thus enable the way into clinical practice. Therefore, the authors recommend that all informations from the questionnaire created in this work should also be made available in the future when entering it into the database of the clinical trial website (Figure 10).

Finally, in order to guarantee the safety and quality of these upcoming products for the recipients, further requirements will arise in the future. This concerns all relevant areas from tissue donation to processing and distribution. The development of processing protocols and the establishment of storage facilities in cell and tissue banks are necessary steps on the way to the new therapies. It will be essential to develop standards for this that also comply with legal requirements. From this point of view, it is striking to note that around 70% of the clinical trials were launched by China and the United States; therefore European Countries, Canada and India have lagged considerably behind in the evaluation of these products. In this context, it would be desirable if the regulation on clinical use and especially on commercial use were harmonized. Since the majority of studies with cells have so far been conducted in China, while the largest number of studies with hAM have been conducted in the United States, this will be a particular challenge.

Data availability statement

The original contributions presented in the study are included in the article/Supplementary Material, further inquiries can be directed to the corresponding authors.

Ethics statement

Ethical review and approval was not required for the study on human participants in accordance with the local legislation and institutional requirements. Written informed consent for participation was not required for this study in accordance with the national legislation and the institutional requirements.

Author contributions

FG, NH, XL, and FJN designed the study and wrote the manuscript. MA-B, MA, MD, RG, SL, RN, and VS assisted the redaction and revised all the versions of the manuscript. PC created the database. All authors worked on the database and analyzed the data. All authors contributed to overall manuscript revision, reading, and approved the submitted version.

Funding

This work contributes to the COST Action CA17116 International Network for Translating Research on Perinatal Derivatives into Therapeutic Approaches (SPRINT), supported by COST (European Cooperation in Science and Technology). The Croatian Science Foundation Grant IP-2020-02-2431 and CERRM EU Grant Agreement KK01.1.1.01.0008. Instituto de Salud Carlos III, Fondo de Investigaciones Sanitarias, Plan Estatal I + D + I, and Instituto de Salud Carlos III-Subdirección General de Evaluación y Fomento de la Investigación (grant nos: PI17/02164 and PI21/01339) https://www.isciii.es. Fondos FEDER (EDRF) "Una manera de hacer Europa" A way of making Europe.

Acknowledgments

All the authors are indebted to the different institutions all over Europe that support their research and our cooperation. We thank other members of our COST action (COST Action CA17116) for encouragement and fruitful discussion.

Conflict of interest

Author SF is employed by PrimeCell Bioscience, 70800 Ostrava, Czech Republic Author LG is employed by Educell ltd., 1,236 Trzin, Slovenia. Author MJ is employed by EXO Biologics (NV), Liege, Belgium. Author VS is employed by Placenta Stem Cell Laboratory, Cryobank, Institute of Cell Therapy, Kyiv, Ukraine.

The remaining authors declare that the research was conducted in the absence of any commercial or financial relationships that could be construed as a potential conflict of interest.

The handling editor PP declared a past co-authorship with the authors FG and RG.

Publisher's note

All claims expressed in this article are solely those of the authors and do not necessarily represent those of their affiliated organizations, or those of the publisher, the editors and the reviewers. Any product that may be evaluated in this article, or claim that may be made by its manufacturer, is not guaranteed or endorsed by the publisher.

Supplementary material

The Supplementary Material for this article can be found online at: https://www.frontiersin.org/articles/10.3389/fbioe.2022.977590/full#supplementary-material

References

Ashworth, M. F., Morton, K. E., Dewhurst, J., Lilford, R. J., and Bates, R. G. (1986). Vaginoplasty using amnion. *Obstet. Gynecol.* 67 (3), 443–446.

Bailo, M., Soncini, M., Vertua, E., Signoroni, P. B., Sanzone, S., Lombardi, G., et al. (2004). Engraftment potential of human amnion and chorion cells derived from term placenta. *Transplantation* 78 (10), 1439–1448. doi:10.1097/01.tp.0000144606.84234.49

Caprnda, M., Kubatka, P., Gazdikova, K., Gasparova, I., Valentova, V., Stollarova, N., et al. (2017). Immunomodulatory effects of stem cells: Therapeutic option for neurodegenerative disorders. *Biomed. Pharmacother.* 91, 60–69. doi:10.1016/j.biopha.2017.04.034

Celis, P., Ferry, N., Hystad, M., Schussler-Lenz, M., Doevendans, P. A., Flory, E., et al. (2015). Advanced therapy medicinal products: How to bring cell-based medicinal products successfully to the market - report from the CAT-DGTI-GSCN workshop at the DGTI annual meeting 2014. *Transfus. Med. Hemother.* 42 (3), 194–199. doi:10.1159/000382107

Elkhenany, H., El-Derby, A., Abd Elkodous, M., Salah, R. A., Lotfy, A., and El-Badri, N. (2022). Applications of the amniotic membrane in tissue engineering and regeneration: The hundred-year challenge. *Stem Cell Res. Ther.* 13 (1), 8. doi:10.1186/s13287-021-02684-0

Fenelon, M., Catros, S., Meyer, C., Fricain, J. C., Obert, L., Auber, F., et al. (2021). Applications of human amniotic membrane for tissue engineering. *Membr. (Basel)* 11 (6), 387. doi:10.3390/membranes11060387

Flory, E., and Reinhardt, J. (2013). European regulatory tools for advanced therapy medicinal products. *Transfus. Med. Hemother.* 40 (6), 409–412. doi:10.1159/000356364

Goula, A., Gkioka, V., Michalopoulos, E., Katsimpoulas, M., Noutsias, M., Sarri, E. F., et al. (2020). Advanced therapy medicinal products challenges and perspectives in regenerative medicine. *J. Clin. Med. Res.* 12 (12), 780–786. doi:10.14740/jocmr3964

Iglesias-Lopez, C., Agusti, A., Obach, M., and Vallano, A. (2019). Regulatory framework for advanced therapy medicinal products in Europe and United States. *Front. Pharmacol.* 10, 921. doi:10.3389/fphar.2019.00921

Moll, G., Ankrum, J. A., Kamhieh-Milz, J., Bieback, K., Ringden, O., Volk, H. D., et al. (2019). Intravascular mesenchymal stromal/stem cell therapy product diversification: Time for new clinical guidelines. *Trends Mol. Med.* 25 (2), 149–163. doi:10.1016/j.molmed.2018.12.006

Moll, G., Ankrum, J. A., Olson, S. D., and Nolta, J. A. (2022). Improved MSC minimal criteria to maximize patient safety: A call to embrace tissue factor and hemocompatibility assessment of MSC products. *Stem Cells Transl. Med.* 11 (1), 2–13. doi:10.1093/stcltm/szab005

Moll, G., Drzeniek, N., Kamhieh-Milz, J., Geissler, S., Volk, H. D., and Reinke, P. (2020). MSC therapies for COVID-19: Importance of patient coagulopathy, thromboprophylaxis, cell product quality and mode of delivery for treatment safety and efficacy. *Front. Immunol.* 11, 1091. doi:10.3389/fimmu.2020.01091

Moll, G., Ignatowicz, L., Catar, R., Luecht, C., Sadeghi, B., Hamad, O., et al. (2015). Different procoagulant activity of therapeutic mesenchymal stromal cells derived from bone marrow and placental decidua. *Stem Cells Dev.* 24 (19), 2269–2279. doi:10.1089/scd.2015.0120

Murri, M. S., Moshirfar, M., Birdsong, O. C., Ronquillo, Y. C., Ding, Y., and Hoopes, P. C. (2018). Amniotic membrane extract and eye drops: A review of literature and clinical application. *Clin. Ophthalmol.* 12, 1105–1112. doi:10.2147/OPTH.S165553

Nejad, A. R., Hamidieh, A. A., Amirkhani, M. A., and Sisakht, M. M. (2021). Update review on five top clinical applications of human amniotic membrane in regenerative medicine. *Placenta* 103, 104–119. doi:10.1016/j.placenta.2020.10.026

Ringden, O., Moll, G., Gustafsson, B., and Sadeghi, B. (2022). Mesenchymal stromal cells for enhancing hematopoietic engraftment and treatment of graft-versus-host disease, hemorrhages and acute respiratory distress syndrome. *Front. Immunol.* 13, 839844. doi:10.3389/fimmu.2022.839844

Salmikangas, P., Schuessler-Lenz, M., Ruiz, S., Celis, P., Reischl, I., Menezes-Ferreira, M., et al. (2015). Marketing regulatory oversight of advanced therapy medicinal products (ATMPs) in Europe: The EMA/CAT perspective. *Adv. Exp. Med. Biol.* 871, 103–130. doi:10.1007/978-3-319-18618-4_6

Silini, A. R., Cargnoni, A., Magatti, M., Pianta, S., and Parolini, O. (2015). The long path of human placenta, and its derivatives, in regenerative medicine. *Front. Bioeng. Biotechnol.* 3, 162. doi:10.3389/fbioe.2015.00162

Silini, A. R., Di Pietro, R., Lang-Olip, I., Alviano, F., Banerjee, A., Basile, M., et al. (2020). Perinatal derivatives: Where do we stand? A roadmap of the human placenta and consensus for tissue and cell nomenclature. *Front. Bioeng. Biotechnol.* 8, 610544. doi:10.3389/fbioe.2020.610544

Silini, A. R., Magatti, M., Cargnoni, A., and Parolini, O. (2017). Is immune modulation the mechanism underlying the beneficial effects of amniotic cells and their derivatives in regenerative medicine? *Cell Transpl.* 26 (4), 531–539. doi:10.3727/096368916X693699

Sittadjody, S., Criswell, T., Jackson, J. D., Atala, A., and Yoo, J. J. (2021). Regenerative medicine approaches in bioengineering female reproductive tissues. *Reprod. Sci.* 28 (6), 1573–1595. doi:10.1007/s43032-021-00548-9

Torre, P., and Flores, A. I. (2020). Current status and future prospects of perinatal stem cells. *Genes (Basel)* 12 (1), 6. doi:10.3390/genes12010006

frontiers | Frontiers in Bioengineering and Biotechnology

TYPE Review
PUBLISHED 13 October 2022
DOI 10.3389/fbioe.2022.958669

OPEN ACCESS

EDITED BY
Karthikeyan Narayanan,
Rensselaer Polytechnic Institute,
United States

REVIEWED BY
Amudha Ganapathy,
University of Illinois at Chicago,
United States
Fausto Cremonesi,
University of Milan, Italy
Francesco Alviano,
University of Bologna, Italy

*CORRESPONDENCE
Mateja Erdani Kreft,
mateja.erdani@mf.uni-lj.si

†These authors have contributed equally to this work and share first authorship

SPECIALTY SECTION
This article was submitted to Tissue Engineering and Regenerative Medicine, a section of the journal Frontiers in Bioengineering and Biotechnology

RECEIVED 31 May 2022
ACCEPTED 26 September 2022
PUBLISHED 13 October 2022

CITATION
Silini AR, Ramuta TŽ, Pires AS, Banerjee A, Dubus M, Gindraux F, Kerdjoudj H, Maciulatis J, Weidinger A, Wolbank S, Eissner G, Giebel B, Pozzobon M, Parolini O and Kreft ME (2022), Methods and criteria for validating the multimodal functions of perinatal derivatives when used in oncological and antimicrobial applications. *Front. Bioeng. Biotechnol.* 10:958669. doi: 10.3389/fbioe.2022.958669

Methods and criteria for validating the multimodal functions of perinatal derivatives when used in oncological and antimicrobial applications

Antonietta R. Silini[1†], Taja Železnik Ramuta[2†], Ana Salomé Pires[3,4,5], Asmita Banerjee[6], Marie Dubus[7], Florelle Gindraux[8], Halima Kerdjoudj[7], Justinas Maciulatis[9], Adelheid Weidinger[6], Susanne Wolbank[6], Günther Eissner[10], Bernd Giebel[11], Michela Pozzobon[12], Ornella Parolini[13,14] and Mateja Erdani Kreft[2*]

[1]Centro di Ricerca E. Menni, Fondazione Poliambulanza Istituto Ospedaliero, Brescia, Italy, [2]Faculty of Medicine, Institute of Cell Biology, University of Ljubljana, Ljubljana, Slovenia, [3]Faculty of Medicine, Coimbra Institute for Clinical and Biomedical Research (iCBR) Area of Environment, Genetics and Oncobiology (CIMAGO), Institute of Biophysics, University of Coimbra, Coimbra, Portugal, [4]Center for Innovative Biomedicine and Biotechnology (CIBB), University of Coimbra, Coimbra, Portugal, [5]Clinical Academic Center of Coimbra (CACC), Coimbra, Portugal, [6]Ludwig Boltzmann Institute for Traumatology, The Research Center in Cooperation with AUVA, Austrian Cluster for Tissue Regeneration, Vienna, Austria, [7]Université de Reims Champagne Ardenne, EA 4691 Biomatériaux et Inflammation en Site Osseux (BIOS), Reims, France, [8]Service de Chirurgie Orthopédique, Traumatologique et Plastique, CHU Besançon and Laboratoire de Nanomédecine, Imagerie, Thérapeutique EA 4662, Université Bourgogne Franche-Comté, Besançon, France, [9]The Institute of Physiology and Pharmacology, Medical Academy, Lithuanian University of Health Sciences, Kaunas, Lithuania, [10]Systems Biology Ireland, UCD School of Medicine, University College Dublin, Dublin, Ireland, [11]Institute for Transfusion Medicine, University Hospital Essen, University of Duisburg-Essen, Essen, Germany, [12]Stem Cells and Regenerative Medicine Lab, Department of Women's and Children's Health, University of Padova, Fondazione Istituto di Ricerca Pediatrica Città Della Speranza, Padoa, Italy, [13]Department of Life Science and Public Health, Università Cattolica Del Sacro Cuore, Rome, Italy, [14]Fondazione Policlinico Universitario "Agostino Gemelli" IRCCS, Rome, Italy

Perinatal derivatives or PnDs refer to tissues, cells and secretomes from perinatal, or birth-associated tissues. In the past 2 decades PnDs have been highly investigated for their multimodal mechanisms of action that have been exploited in various disease settings, including in different cancers and infections. Indeed, there is growing evidence that PnDs possess anticancer and antimicrobial activities, but an urgent issue that needs to be addressed is the reproducible evaluation of efficacy, both *in vitro* and *in vivo*. Herein we present the most commonly used functional assays for the assessment of antitumor and antimicrobial properties of PnDs, and we discuss their advantages and disadvantages in assessing the functionality. This review is part of a quadrinomial series on functional assays for the validation of PnDs spanning biological functions such as immunomodulation, anticancer and antimicrobial, wound healing, and regeneration.

KEYWORDS

perinatal derivatives, biological assays, functional assays, potency assays, mechanisms of action, pharmacologic actions, cancer, infections

1 Introduction

Perinatal derivatives or PnDs (that include tissues and cells and secretomes from perinatal, or birth-associated tissues), and especially mesenchymal stromal cells (MSC) from perinatal tissues, have been mostly exploited for their applications in regenerative medicine, substantiated by their ability to modulate immune responses and/or to act in a pro-regenerative manner by promoting progenitor/stem cell differentiation (Silini et al., 2017; Silini et al., 2019). What has been largely unexplored is the applications of PnDs in other sectors, such as in oncology.

As a matter of fact, PnDs have only recently been investigated *in vitro* and *in vivo* for their potential as antitumor therapies. In this context, PnDs have been shown to act multimodally through complex mechanisms of action (MoA), and to target various hallmarks of cancer that capture essential features of tumorigenesis, such as sustaining proliferative signaling, evading growth suppressors, resisting cell death, enabling replicative immortality, inducing angiogenesis, activating invasion and metastasis, reprogramming cellular metabolism, avoiding immune destruction, tumor-promoting inflammation, genome instability, and deregulating cellular metabolism (Hanahan and Weinberg 2011). Treatments that shift the focus to the systemic level and that target the hallmarks of cancer are urgently needed and highly relevant.

In the context of cancer, PnDs have been reported to play opposing roles. Herein we will discuss these studies along with the *in vitro* and *in vivo* assays implemented to obtain a clearer understanding of the potential applications of PnDs as an antitumor treatment.

In addition to the potential applications of PnDs in oncology, several PnDs have been shown to possess antimicrobial properties (King et al., 2007a; Klaffenbach et al., 2011; Ramuta et al., 2021a), which is highly relevant in the field of oncology. As a matter of fact, in the last decade, growing evidence has emerged demonstrating that microbiota and microbial pathogens have immense effect on cancer development and treatment (Bhatt et al., 2017; Raza et al., 2019; Jain et al., 2021). While in 15–20% of cancer cases microbial pathogens drive tumorigenesis, even a larger part of malignancies is associated with the altered composition of commensal microbiota (Bhatt et al., 2017). Furthermore, bacteria are also able to affect the efficacy of chemotherapeutic drugs, either by inhibiting or enhancing their effect (Lehouritis et al., 2015; Roy and Trinchieri 2017). Namely, the microbiota and pathogens may affect the pharmacokinetics, antitumor activity and drug toxicity of chemotherapeutic agents by 1) changing the chemical structure of the drug (biotransformation) (Haiser and Turnbaugh 2012; Wilson and Nicholson 2017), 2) decreasing the absorption of certain drugs (Carmody and Turnbaugh 2014), or even indirectly by 3) affecting the host's gene expression and physiology (e.g., of the local mucosal barrier), which results in altered metabolism of drugs (Björkholm et al., 2009; Selwyn et al., 2015; Selwyn et al., 2016; Roy and Trinchieri 2017).

Thus, herein both the anticancer and antimicrobial properties will be discussed alongside one another to provide a better understanding of the potential applications of PnDs as therapeutic strategies in these fields. We briefly summarize the results obtained using PnDs and then focus on the most frequently used functional assays for analyzing the antitumor and antimicrobial effects of PnDs in order to potentially provide insight into the future development of new functional and/or potency assays.

This review is part of a series of contributions from the COST Action (CA17116) entitled "International Network for Translating Research on Perinatal Derivatives into Therapeutic Approaches-SPRINT". This Action is broadly aimed at establishing consensus for different aspects of PnDs research. The aim of this review is to provide inputs for the development of functional and potency assays that can be used to test PnDs before their oncological and antimicrobial application.

2 The effects of perinatal derivatives on the hallmarks of cancer

In this section we summarize the most frequently used *in vitro* and *in vivo* assays for analyzing the effects of PnDs on several hallmarks of cancer such as cell proliferation and metabolism, cell death and apoptosis, cell migration and invasion, angiogenesis, and metastasis.

2.1 Investigating perinatal derivatives actions on tumor cell proliferation

One of the most widely analyzed hallmark of tumor cells is proliferation. Indeed, *in vitro* PnDs have been shown to mostly exert antiproliferative effects on tumor cells (Gauthaman et al., 2012; Magatti et al., 2012; Liu et al., 2013; Hendijani et al., 2015; Kalamegam et al., 2019; Ramuta et al., 2020a), but it has also been shown that they may induce tumor cell proliferation (Kim et al., 2015; Li et al., 2015).

Several assays are used to assess the effect of PnDs on tumor cell proliferation. The investigation of DNA synthesis analyzes the effects of PnDs on tumor cell proliferation. Incorporation of radiolabeled DNA precursor 3H-thymidine (Ayuzawa et al.,

2009; Magatti et al., 2012; Marleau et al., 2012; Yuan et al., 2013; Riedel et al., 2019; Ramuta et al., 2020b) into new strands of chromosomal DNA or more recent analogs, BrdU (bromoeoxyuridin) (Tian et al., 2010; Gauthaman et al., 2012; Han et al., 2014; Hendijani et al., 2015) and EdU (5-ethynyl-2 deoxyuridine) (Wang M et al., 2015; Janev et al., 2021), have been widely used to assess *de novo* DNA synthesis. 3H-thymidine detection requires radioactive labeling followed by detection with a scintillation beta-counter, while BrdU can be easily detected by antibodies followed by flow cytometry or by immunohistochemistry. BrdU is mutagenic and can alter the cell cycle, thus adequate controls should be implemented. In contrast to BrdU, the newer analog EdU does not require DNA denaturation by exposing cells to HCl, heat or DNAse, and its detection is rapid and highly sensitive. BrdU and EdU are considered reliable assays for a direct index of proliferation. Other analyses implemented for the analysis of tumor cell proliferation are Ki67 cell immunolabelling (Lin et al., 2014; Riedel et al., 2019), and other assays aimed at investigating genes or proteins involved in cell cycle progression, such as cyclins (Magatti, De Munari et al., 2012; Riedel, Pérez-Pérez et al., 2019).

The colony forming unit (CFU) assay analyzes the consequences of external stress signals on the cell's ability to proliferate and form a colony. This assay has been widely used to test the effect of PnDs (Ayuzawa et al., 2009; Liu et al., 2013; Ciavarella et al., 2015; Li et al., 2015; Wang M et al., 2015; Wang W et al., 2015) and is especially useful to assess long-term effects. This method is however time consuming with extended incubation times, plus colony formation ability differs between cells. The traditional assay requires weeks for completion and usually does not allow cell retrieval; however, this can be circumvented by the use of fluorescent dyes allowing quantitative, high throughput colony counting and by the use of specialized agars that allow cell suspension and growth. The assay can also be used to predict tumorigenicity *in vivo*.

In vivo objective assessment of tumor growth is a crucial tool for the advancement of cancer therapies. *In vivo*, PnDs have been shown to both inhibit (Ayuzawa et al., 2009; Wu et al., 2013) and induce (Yang C. et al., 2014; Wang M et al., 2015; Svitina et al., 2018) tumor growth. These contradictory results could be due to several variations, either given by the PnDs used (e.g., tissues, cells, secretomes, homogenates), by the tumor model (e.g., tumor cells, rodent model and strain), by the different treatment regimens (e.g., administration route, dosage), or by the method used to monitor tumor progression (e.g., caliper measurements, imaging).

Monitoring tumor progression after PnDs treatment has been performed through the measurement of tumor diameters (Du et al., 2014; Ma et al., 2015; Bu et al., 2017; Yuan L et al., 2019) (or volumes deduced from diameters) or tumor weight, but also through more sophisticated *in vivo* optical imaging techniques (Di et al., 2014; Leng et al., 2014; Ciavarella et al., 2015; Caffario et al., 2017; Zhang et al., 2017; Yuan Z et al., 2019; Chetty et al., 2020), which include fluorescence and bioluminescence studies. Although traditional caliper measurement is a simple and low-cost method, its major disadvantages include variability of tumor size measurements and tumoral heterogeneity. In contrast, optical imaging is a more accurate, sensitive and specific technique for tumor imaging, allowing the detection of microscopic tumors. The main limitation of optical imaging is the need of tumor cells to express a reporter gene (Puaux et al., 2011). Cell proliferation is often used as a measure of tumor response, with immunohistochemistry being the most widely used *in vivo* technique.

2.2 Investigating perinatal derivatives actions on tumor cell metabolism

Altered cell metabolism is another feature of tumor cells, and proliferating tumor cells hijack their metabolism to fuel continuous growth. Cell metabolism is commonly measured through the reduction of substrates to a final product by intracellular enzyme activity in living cells can be assessed by colorimetric assays. The degree of color change is not directly proportional to the number of viable cells, but rather to enzyme activity. This method permits only a moderately robust measurement of viability; however, the ease of use and potential for high throughput analysis in multiwell plates has made it very popular. The most frequently used tetrazolium compound (MTT) is reduced to formazan (Li et al., 2011; Chao et al., 2012; Gauthaman et al., 2012; Kang et al., 2012; Liu et al., 2013; Lin et al., 2014; Niknejad et al., 2014; Rolfo et al., 2014; Bonomi et al., 2015; Lang et al., 2015; Li et al., 2015; Kamalabadi-Farahani et al., 2018; Mandal et al., 2019; Riedel et al., 2019). A less toxic alternative, Cell Counting Kit-8 (CCK-8) (Wu et al., 2013; Yan et al., 2013; Yang C. et al., 2014; Kim et al., 2015; Di Germanio et al., 2016), has also been used, with a detection sensitivity higher than tetrazolium salts such as MTT or MTS(Wang W et al., 2015). Tumor cell oxidative stress, using superoxide dismutase, intracellular accumulation of reactive oxygen species (ROS), glutathione peroxidase, hydrogen peroxide and lipid peroxidation assays have also been investigated after PnDs treatment (Lin et al., 2014).

2.3 Investigating perinatal derivatives actions on tumor cell death and apoptosis

Similar to their effects on tumor cell proliferation PnDs have been shown to have dual effects on tumor cell death and apoptosis, by either promoting (Chen et al., 2012; Jiao et al., 2012; Del Fattore et al., 2015; Kalamegam et al., 2018) or inhibiting (Niknejad et al., 2014) these processes.

There are several assays used to assess the effect of PnDs on tumor cell death. For example, annexin V/PI assay and flow cytometry are the most popular approaches for detection of apoptosis in tumor cells after PnDs treatment (Gauthaman et al., 2012; Wu et al., 2013; Yang X. et al., 2014; Niknejad et al., 2014; Mamede et al., 2015; Lin et al., 2016; Paris et al., 2016; Shen et al., 2016; Lin H et al., 2017; Chai et al., 2018; Jiao et al., 2018; Yuan et al., 2018; Khalil et al., 2019; Rezaei-Tazangi et al., 2020; Silva et al., 2020). The TUNEL assay (Wu et al., 2013; Niknejad et al., 2014) detects DNA fragmentation in apoptotic cells *in vitro*. After staining, cells can be analyzed by light or fluorescent microscopy. TUNEL staining is fast, accurate and sensitive but fails in discriminating the different types of cell death. The assay can also be used to assess the effect of PnDs on tumor cell death *ex vivo*. Detection of apoptosis regulators, such as caspases (Wu et al., 2013; Yang C. et al., 2014; Niknejad et al., 2014; Mamede et al., 2015; Lin et al., 2016; Kalamegam et al., 2018; Mandal et al., 2019; Rezaei-Tazangi et al., 2020), cytochrome c, Bcl-2, Bax, Fas, FasL, Danger Associated Molecular Proteins (DAMPs), CRT, Hsp90 and Hsp70, etc. Can be detected at the protein and/or mRNA level using flow cytometry, multi-detection plate reader (Mamede et al., 2015), immunoblot (Dzobo et al., 2016; Shen et al., 2016; Yuan et al., 2018), immunohistochemistry, immunofluorescence (Dzobo et al., 2016; Lin H et al., 2017), and RT-PCR (Yang X. et al., 2014). As further progress is made in understanding the mechanisms of cell death, more accurate and precise interpretations of the results of these tests will be possible.

Cell death induced by PnDs in animal models has been mainly analyzed by *in situ* detection of apoptosis as mentioned previously regarding the *in vitro* assays (Dong et al., 2018; Kamalabadi-Farahani et al., 2018; Chen et al., 2019; Fan et al., 2020). An alternative approach is the *in vivo* imaging of apoptosis, using radiolabeled forms of annexin V for positron emission tomography (PET) and single photon emission computed tomography (SPECT) (Iravani and Hicks 2020).

Mitochondria play a key role in response to cellular stress and injury. For this reason, the evaluation of mitochondrial membrane potential (MMP) (Mamede et al., 2015; Lin et al., 2016) could also be used as the marker of cell death. However, the interpretation should be carefully and critically performed. Measurement of mitochondrial activity could not only serve as an alternative to cell viability assays, but also provide distinct information on the metabolic state, and therefore the quality of a cell. For the application of therapeutic cells, knowledge on the mode of energy production can be important. Mitochondrial activity can be determined by quantification of the activity of single complexes such as complex I by measuring the light absorbance of nicotinamide adenine dinucleotide (NADH), the electron donor for complex I, at 340 nm (Nelson and Cox 2004). The downside of this method is that it does not provide any information on the coupling state of the electron transfer system, and therefore, also not on the production level of adenosine triphosphate (ATP). Activity of the entire electron transfer system can be determined, for example, with a Clark electrode-based measurement (Hütter et al., 2006). With this method, the oxygen concentration of a solution is measured as oxygen is reduced at the cathode. The resulting current is directly proportional to the oxygen concentration of the solution (Gnaiger 2008). The advantage of this method is that distinct respiration states can be determined (Gnaiger 2008). By addition of specific substrates and inhibitors, total oxygen consumption (routine respiration) can be distinguished from oxygen consumption with ATP production (oxidative phosphorylation) and oxygen consumption without ATP production (LEAK) (Gnaiger 2008). With this method, mitochondrial respiration can be measured in tissue, tissue homogenate, cells and isolated mitochondria. To our knowledge, there are no studies that have evaluated the effects of PnD on tumor MMP, however, such measurements have successfully been performed in human amniotic membrane tissue (Banerjee et al., 2015; Poženel et al., 2019), isolated human amniotic membrane epithelial cells (Banerjee et al., 2018a), and human amniotic membrane derived MSC (Banerjee et al., 2018a; Banerjee et al., 2018b). In addition to the mitochondrial respiration assay, mitochondrial status can also be monitored with the membrane permeable dye JC-1. JC-1 is a fluorescent cationic carbocyanine dye that exhibits potential-dependent accumulation in mitochondria, forming J-aggregates and diffuses across mitochondria upon depolarisation to form a monomeric state (Sivandzade et al., 2019). Currently, to our knowledge, there is only one study that has investigated the function of amniotic membrane proteins (AMPs) extracted from hAM against hypoxia-induced H9c2 cardiomyoblast cells (Faridvand et al., 2019). AMPs have potent cardioprotective effects in H9c2 cells by inhibiting the Ca2+ overload and the mitochondrial membrane potential dysfunction during hypoxia (Faridvand et al., 2019). Furthermore, there are few studies that evaluated mitochondrial membrane potential in placental trophoblast cells from patients with preeclampsia (Zhang et al., 2022). The anticancer effect of PnDs have not yet been evaluated with the mitochondrial dye JC-1.

In this section, we presented an overview of the most common functional assays that have been used for evaluating the pro-cell death/proapoptotic activity of PnDs. Each assay has its advantages and an understanding of strengths and limitations can allow for the selection of the optimal assay based on a specific need. No matter how appropriate and well accepted the assay is, it is recommended that a second assay using a different principle should be used to confirm the detection of cell-death. In the future, we should also have in mind that intact efferocytosis, i.e. the clearance of apoptotic cells, can promote cancer disease (Vaught et al., 2015). It is therefore important that both processes, apoptosis and efferocytosis are fine-tuned in specific tumor microenvironments. Hence, the novel functional assays for analyzing the influence of PnD on efferocytosis-mediated

regulation of the tumor microenvironment needs to be developed/used.

2.4 Investigating perinatal derivatives actions on tumor cell migration and invasion

PnDs have been reported to both inhibit (Fong et al., 2011; Gauthaman et al., 2012; Kalamegam et al., 2018; Li et al., 2019) and induce (Kim et al., 2015; Li et al., 2015) tumor cell migration.

The spread of neoplastic disease has been described as a sequential multi-step process, termed the invasion-metastatic cascade (Martin and Jiang 2009). During migration and invasion, cells squeeze through tight interstitial spaces, which includes cellular and nuclear deformation caused by the confining microenvironment (Kramer et al., 2013). Overall, during the metastatic cascade, changes in cell-cell and cell-matrix adhesion are of paramount importance and lead to the formation of secondary tumors in distant organs and are largely responsible for the mortality and morbidity of cancer (Martin et al., 2013). There are several commonly used *in vitro* assays to investigate the effects of PnDs on tumor cell migration and invasion potential. Transwell migration and invasion assay (Boyden chamber) is the most frequently used approach. In this assay, a double chamber is filled with two media, one with an attractant (like FBS) to trigger chemotaxis. Cells are seeded in the upper well and migrate vertically between the chambers through a porous membrane (Menyhárt et al., 2016). Migrated cells can be visualized by cytological dyes or stained fluorescent and then assessed by flow cytometry, light or fluorescence microscopy, or lysed and assessed by a plate reader, usually following treatment with MTT reagent (Gauthaman et al., 2012; Kim et al., 2015; Li et al., 2015; Kalamegam et al., 2018; Yuan et al., 2018; Mandal et al., 2019; Silva et al., 2020). By coating the porous filter with ECM components like type I collagen or a basement membrane-like matrix (Matrigel (So et al., 2015; Bu et al., 2017; Meng et al., 2019)) or reduced growth factor matrix (Touboul et al., 2013), invasive cells can be detected by their ability to degrade the matrix and move through the membrane to the bottom well. Parallel measurements with ECM-coated and non-coated assays allow one to calculate an "invasive index": the rate of invasiveness versus migration (Marshall 2011), however this approach is currently missing in *vitro* assays investigating migration and invasion potential of PnDs. The most frequently used method due to its easy setup is the transwell migration assay. More sophisticated migration assays using microfluidic migration devices overcome the limitations of traditional migration assays and promote a stable diffusion-generated concentration gradient that is consistently linear and lasts for more than 48 h. These devices are usually plastic with high optical qualities similar to those of glass, and are specially designed for video microscopy assays. At specific time intervals, images of the observation area can be acquired, allowing real-time monitoring and quantitative measurements of cell migration and thus could also be used in investigating PnDs actions on cancer cell migration and invasion.

Investigation into the effect of PnDs on the invasive potential of cancer cells has been also performed using intact or decellularized human amniotic membrane or amniochorionic membrane. These were used in some studies as a natural 3D scaffold to evaluate tumor cell metastatic and invasion potential in 3D conditions (Ganjibakhsh et al., 2019) or direct influence of PnDs on metastatic and invasion behavior of tumor cells (Touboul et al., 2013; Ramuta T. Z. et al., 2020).

2.5 Investigating perinatal derivatives actions on the tumor vasculature and angiogenesis

PnDs have been widely reported to produce angiogenic factors and induce angiogenesis (Bajetto et al., 2017; Dabrowski et al., 2017; Komaki et al., 2017; Wu et al., 2022), yet some studies have described antiangiogenic effects (Faraj, Stewart et al., 2015), and PnD preparation seems to be a critical point that can influence this feature (Wolbank et al., 2009).

Quantitative real time polymerase chain reaction is often performed to detect and quantify the relative expression levels of angiogenic genes, such as VEGF (Lin D et al., 2017; Mandal et al., 2019), ANG (Mandal et al., 2019; Yuan L et al., 2019), PDGF (Yuan Z et al., 2019), FGF-2 (Subramanian et al., 2012), etc. However, this method is time and resource consuming, requires subsequent post-PCR analysis and may provide only limited information on gene expression that must be followed with immunoblot or ELISA. Indeed, the latter have been widely used to detect known angiogenesis activators by immunoblot or ELISA (Table 1). However, Western blot can produce false-positive/negative results in the sample of interest and requires a larger amount of starting material. Immunophenotypic analysis to measure the expression of major angiogenic proteins, such as VEGF (Borghesi et al., 2020) can be performed with flow cytometry. Despite its ability to identify small populations and quantify the intensity of fluorescence, it still requires complex instrumentation, and highly trained technical staff to manage microfluidics, laser calibration and cleaning, as well as ample experience with the relevant software. In addition, direct and indirect immunocytochemistry (ICCH) can visualize and localize the target VEGF protein expression at a cell compartment level (Subramanian et al., 2012). Indirect ICCH can, however, be more laborious and time-consuming, with the additional risk of non-specific binding of the secondary antibody.

Monitoring the proliferation of human umbilical vein endothelial cells (HUVECs) is often used to evaluate the developing tumor vasculature. These assays have been used to estimate antiangiogenic properties of PnDs in the context of early tumor pre-vasculature. CCK8 (Yuan L et al., 2019) assay offer

TABLE 1 Angiogenesis activators produced by PnDs.

Activator	PnDs
VEGF	Placenta-based somatic stem cells (Zhang et al., 2015)
	Placental-derived adherent stromal cells (Allen et al., 2018)
	Umbilical cord MSCs (Bajetto et al., 2017; Lin D et al., 2017; Ciavarella et al., 2015)
	Wharton jelly MSCs (Kalamegam et al., 2019; Mandal et al., 2019; Subramanian et al., 2012) Umbilical cord MSCs (Dabrowski FA et al., 2017); Amniotic membrane MSCs (Dabrowski FA et al., 2017)
FGFS	Umbilical cord MSCs (Ciavarella et al., 2015)
	Wharton jelly stem cells (Kalamegam et al., 2019)
MMPs	Placenta derived MSCs (Choi et al., 2016)
	Placental-derived adherent stromal cells (Allen et al., 2018)
TIMPs	Umbilical cord MSCs (Ciavarella et al., 2015)
	Human amniotic membrane (Modaresifar et al., 2017)
ANG	Umbilical cord MSCs (Bajetto et al., 2017)
EGF	Umbilical cord MSCs (Ciavarella et al., 2015; Dabrowski FA et al., 2017); Amniotic membrane MSCs (Dabrowski FA et al., 2017)

reproducible and easy setups and provide quantifiable data on the inhibition of endothelial cell proliferation. Alternative methods, such as Trypan blue analysis (Chen et al., 2012) might be more difficult to reproduce and validate. Monitoring of electrical impedance changes (Grzywocz et al., 2018) caused by the proliferation of HUVECs could be enabled by real-time systems. In addition, the digital endothelial tube formation assay-derived images could potentially enable the calculation of digital angiogenic indices (Alshareeda et al., 2018), covering the numerical values of tube morphometry, such as extremities, number of segments, branches and the length of tubes.

To evaluate angiogenesis *in vitro*, the rat aorta ring assay (Modaresifar et al., 2017) can be performed with PnDs. In this assay, aorta rings are dissected from the descending thoracic aorta, rinsed, and cut into circular sections of several millimeters thick. These sections are put on cultured cells and the angiogenic potential is determined by microscopically visualizing endothelial cell sprouting, polarization, and outgrowth to the periphery. This test enables evaluation of angiogenic and antiangiogenic effects of PnDs and is more representative of *in vivo* angiogenesis than two dimensional assays.

3 Antimicrobial effects of perinatal derivatives

One of the most intriguing characteristics of PnDs is their direct and indirect antimicrobial properties, which have therapeutic potential. PnDs have been shown to possess antimicrobial activity against various microorganisms in planktonic form and also in complex microenvironments. While the precise nature of antimicrobial action of PnDs is not well understood, it is clear that more than one mechanism working simultaneously to inhibit microbe growth and endotoxin activity, contributes to this activity (Magatti, Vertua et al., 2017). Antimicrobial properties of PnDs have been investigated in bacteria (Talmi et al., 1991; Mao et al., 2016; Mao et al., 2017; Tehrani et al., 2017; Mao et al., 2018; Ashraf et al., 2019; Palanker et al., 2019; Šket et al., 2019; Ramuta et al., 2020a), fungi (Wang, Xie et al., 2012), bacteria-infected cell cultures (Ramuta et al., 2021b) and rat *in vivo* models (Robson and Krizek 1973; Yadav et al., 2017). Antimicrobial peptides, such as α and β defensins, human cathelicidin LL37, lipocalin, elafin and secretory leukocyte protease inhibitor (SLPI), have been identified in various PnDs (King et al., 2007a; King et al., 2007b; Ramuta T.Ž. et al., 2021; Dubus et al., 2022). Furthermore, it was shown that histones H2A and H2B could also exert an antimicrobial action as a endotoxin-neutralizing barrier (Kim et al., 2002). Moreover, it was reported that hemoglobin-derived peptides purified from a human placenta exhibited antimicrobial activity. These peptides inhibited the growth of Gram-positive and Gram-negative bacteria and yeasts in micromolar concentrations, as well they reduced endotoxin activity by binding to LPS (Liepke et al., 2003; Dubus et al., 2022). In case of decellularized Wharton's jelly tissue, the mass spectrometry analysis showed the release of antimicrobial molecules involved in the innate immune response but also some molecules involved in bacterial agglutination such as fibrinogen beta chain and Fibulin 1 (Dubus et al., 2022). These molecules are thought to exert a bacteriostatic effect on both Gram-positive and Gram-negative strain. In this section, we offer an overview of the most common *in vitro* and *in vivo* functional assays that have been used for evaluating the antimicrobial activity of PnDs against bacteria and fungi.

The gold standards for antimicrobial susceptibility testing have been set by the Clinical and Laboratory Standards Institute, however, due to the versatility of PnDs, the following assays do not strictly follow the standard protocols, as they had to be adapted to enable the analysis of various PnDs-derived preparations in bacterial suspensions.

3.1 Investigating the antimicrobial effects of perinatal derivatives in bacterial suspension

A broth (micro)dilution assay is a simple and inexpensive method which is consequently often used to test the susceptibility of bacterial isolates to various antimicrobials. PnDs (often at various dilutions) are added to liquid broth media, which are then inoculated with bacterial suspensions. Following incubation (the length of which can vary from a couple of hours to several days), bacterial growth is evaluated based on turbidity by using visual or spectrophotometric methods (Jorgensen and Ferraro 2009; Sung et al., 2016; Šket et al., 2019; Dubus et al., 2020; El-Mahdy et al., 2021). Furthermore, bacterial growth can be also quantified by plating serial dilutions of bacterial suspensions incubated with the antimicrobial agent and counting the colony forming units (CFU) (Thadepalli et al., 1977; Mao et al., 2017; Šket et al., 2019). The broth microdilution method is often used to determine the minimum inhibitory concentration (Wiegand et al., 2008; Kim et al., 2012; Yadav et al., 2017) of an antimicrobial agent, which is the lowest concentration that will inhibit the visible growth of a microorganism after overnight incubation. The advantages of using the broth (micro)dilution test are the generation of a quantitative result and high reproducibility, while the main shortcoming is that it is less sensitive and more time-consuming (Jorgensen and Ferraro 2009) than some of the other functional assays for determination of the antimicrobial effects of PnDs. Furthermore, the presence of dead bacteria in the presence of PnDs cannot be determined.

A similar method is a disk diffusion assay. Namely, a bacterial inoculum is plated onto the surface of the agar plate and subsequently PnDs (often at various dilutions) are applied to the inoculated agar surface. After incubation of the agar plates the inhibition zones around the site of application of the PnDs antimicrobials are measured (Talmi et al., 1991; Kjaergaard et al., 2001; Jorgensen and Ferraro 2009; Tehrani et al., 2013; Tehrani et al., 2017; Šket et al., 2019; Ramuta et al., 2020b; Ramuta T.Ž. et al., 2021). The shortcoming of this method is its inability to precisely determine the minimum inhibitory concentration of the antimicrobial agent.

3.2 Investigating the antimicrobial effects of perinatal derivatives in complex (micro)environments

The antimicrobial properties of PnDs have been evaluated in complex (micro)environments, such as biofilms and bacteria-infected epithelia. The effect of PnDs on biofilms has been evaluated by the biofilm formation assay (Dubus et al., 2020; El-Mahdy et al., 2021). The antiadhesive and antifouling properties of PnDs such as Wharton's jelly were mainly attributed the presence of hyaluronic acid and its composites (Drago et al., 2014; Marcuzzo et al., 2017). Biofilm is defined as a bacterial community which is metabolically heterogeneous and embedded in a self-produced extracellular matrix, causing a critical virulence factor responsible for treatment failure and chronicity in medical device-related infections. The (micro)plates are inoculated with fresh bacterial cell suspensions and subsequently the PnDs are added. The biofilms are grown for several hours to days. After staining with crystal violet, the effect of the PnDs on biofilm is quantified spectrophotometrically. This is an inexpensive and easy method which can directly evaluate the biofilm formation on several surfaces (i.e., titanium alloys, calcium phosphate, polymers, etc). However, there are a few shortcomings of the biofilm formation assay. Firstly, it is not possible to distinguish whether the antimicrobial effect can be attributed to killing of planktonic bacteria before the biofilm forms or to the specific antibiofilm effects, because the antimicrobial agent is added to the bacterial suspension before the biofilm is formed. Furthermore, the crystal violet stains the whole biomass (bacteria and exopolymers) and not only the living bacteria, hence it is not possible to determine the ratio of alive vs. dead bacteria in the biofilm (Haney et al., 2018). To get comprehensive insight into how PnDs affect biofilms, additional experiments should be performed also on pre-formed biofilms (Segev-Zarko and Shai 2017). To determine the metabolically active cells in the biofilm, resazurin staining (Yadav et al., 2017) is used. To evaluate the viability of the cells, forming the biofilm, the live/dead bacterial viability kit (El-Mahdy et al., 2021; Dubus et al., 2022) is used. To evaluate the morphology of the biofilm, most frequently confocal microscopy or scanning electron microscopy are used (Yadav et al., 2017; Mao et al., 2018; El-Mahdy et al., 2021).

To evaluate the antimicrobial effect of PnDs in bacteria-infected epithelia, the following cellular *in vitro* models have been established. Cells are grown to confluence using antibiotic-free medium and then inoculated with bacteria. The number of viable bacteria in culture medium are quantified by plating serial dilutions of bacterial suspensions and counting the CFU (Josse et al., 2014; Sung et al., 2016; Dubus et al., 2020; Ramuta et al., 2021a; El-Mahdy et al., 2021). Next, the permeabilization agent is used to release the intracellular bacteria, which are then quantified by plating serial dilutions of bacterial suspensions and counting the CFU. (Josse et al., 2014; Dubus et al., 2020; El-Mahdy et al., 2021). Moreover, the effect of bacteria and PnDs on eukaryotic cells are evaluated by quantifying the number and viability of eukaryotic cells and also the intracellular localization of bacteria is assessed by using various methods of light, confocal and electron microscopy (Josse et al., 2014; Ramuta et al., 2021b; El-Mahdy et al., 2021). To gain better understanding of the effect of PnDs in bacteria-infected

TABLE 2 Summary of assays used to detect antitumor and antimicrobial effects of PnDs.

Anti-microbial effects	Functional assays		References
Tumor cell proliferation and metabolism	Incorporation of radiolabeled DNA precursor 3H-thymidine into the new strands of chromosomal DNA		Ayuzawa et al. (2009) Magatti et al. (2012) Marleau et al. (2012) Yuan et al. (2013) Riedel et al. (2019) Ramuta et al. (2020c)
	Incorporation of a synthetic nucleoside analog BrdU or EdU into the new strands of chromosomal DNA		Tian et al. (2010) Gauthaman et al. (2012) Han et al. (2014) Hendijani et al. (2015) Wang M et al. (2015) Janev et al. (2021)
	Immunolabeling of cell cycle-related proteins (e.g., Ki67, cyclins)		Lin et al. (2014) Riedel et al. (2019) Magatti et al. (2012)
	Colony forming unit (CFU) assay		Ayuzawa et al. (2009) Liu et al. (2013) Ciavarella et al. (2015) Li et al. (2015) Wang M et al. (2015) Wang W et al. (2015)
	Colorimetric assays for metabolism analysis	MTT assay	Li et al. (2011) Chao et al. (2012) Gauthaman et al. (2012) Kang et al. (2012) Liu et al. (2013) Lin et al. (2014) Niknejad et al. (2014) Rolfo et al. (2014) Bonomi et al. (2015) Lang et al. (2015) Li et al. (2015) Kamalabadi-Farahani et al. (2018) Mandal et al. (2019) Riedel et al. (2019)
		Cell Counting Kit-8	Wu et al. (2013) Yan et al. (2013) Yang et al. (2014a) Kim et al. (2015) Di Germanio et al. (2016)
	Annexin V/PI assay and flow cytometry		Gauthaman et al. (2012) Wu et al. (2013) Niknejad et al. (2014) Yang et al. (2014b) Mamede et al. (2015) Lin et al. (2016) Paris et al. (2016) Shen et al. (2016) Lin D et al. (2017) Chai et al. (2018) Jiao et al. (2018) Yuan et al. (2018) Khalil et al. (2019) Rezaei-Tazangi et al. (2020) Silva et al. (2020)
Tumor cell death	TUNEL assay		Wu et al. (2013) Niknejad et al. (2014)
	Detection of apoptosis regulators (e.g., caspases, Bcl-2, DAMPs)	Flow cytometry Multi-detection plate reader	Rezaei-Tazangi et al. (2020) Wu et al. (2013) Lin et al. (2016) Kalamegam et al. (2018) Mandal et al. (2019)

(Continued on following page)

TABLE 2 (*Continued*) Summary of assays used to detect antitumor and antimicrobial effects of PnDs.

Anti-microbial effects	Functional assays		References
		Immunoblot	Mamede et al. (2015) Dzobo et al. (2016) Shen et al. (2016) Yuan et al. (2018)
		Immunohistochemistry, Immunofluorescence RT-PCR	Dzobo et al. (2016) Lin H et al. (2017) Yang et al. (2014a)
	Evaluation of mitochondrial membrane potential (MMP)		Mamede et al. (2015) Lin et al. (2016)
	Evaluation of the mitochondrial status by membrane permeable dye JC-1		Faridvand et al. (2019)
	Evaluation of the activity of the entire electron transfer system		Banerjee et al. (2015) Poženel et al. (2019) Banerjee et al. (2018b)
Tumor cell migration and invasion potential	Transwell migration and invasion assay (Boyden chamber)		Gauthaman et al. (2012) Kim et al. (2015) Li et al. (2015) Kalamegam et al. (2018) Yuan et al. (2018) Mandal et al. (2019) Silva et al. (2020)
	Evaluation of the metastatic and invasion potential of cancer cells on intact or decellularized human amniotic membrane- or amniochorionic membrane-derived scaffolds		Ganjibakhsh et al. (2019) Touboul et al. (2013) Ramuta et al. (2020a)
Angiogenesis	Quantitative RT-PCR for detection of angiogenic genes (e.g., VEGF, ANG, PDGF)		Lin D et al. (2017) Mandal et al. (2019) Yuan L et al. (2019) Subramanian et al. (2012)
	Immunodetection of factors affecting tumor cell angiogenesis	Immunoblot, ELISA	Zhang et al. (2015) Allen et al. (2018) Bajetto et al. (2017) Lin H et al. (2017) Ciavarella et al. (2015) Kalamegam et al. (2019) Mandal et al. (2019) Subramanian et al. (2012) Choi et al. (2016) Modaresifar et al. (2017) Bajetto et al. (2017)
		Flow cytometry Immunocytochemistry	Dabrowski FA et al. (2017) Borghesi et al. (2020) Subramanian et al. (2012)
	Monitoring proliferation of human umbilical vein endothelial cells	Cell Counting Kit-8 Trypan blue assay Monitoring of electrical impedance changes	Yuan Z et al. (2019) Chen et al. (2012) Grzywocz et al. (2018)
In vivo assessment of tumor response	Rat aorta ring assay Measurements of tumor diameters		Modaresifar et al. (2017) Du et al. (2014) Ma et al. (2015) Bu et al. (2017) Yuan L et al. (2019)
	Optical imaging techniques		Di et al. (2014) Leng et al. (2014) Ciavarella et al. (2015) Cafforio et al. (2017)

(Continued on following page)

TABLE 2 (*Continued*) Summary of assays used to detect antitumor and antimicrobial effects of PnDs.

Anti-microbial effects	Functional assays	References
		Zhang et al. (2017) Yuan Z et al. (2019) Chetty et al. (2020)
Bacterial growth	Broth (micro)dilution assay	Jorgensen and Ferraro (2009) Sung et al. (2016) Dubus et al. (2020) El-Mahdy et al. (2021) Thadepalli et al. (1977) Mao et al. (2017) Šket et al. (2019) Wiegand et al. (2008) Kim et al. (2012) Yadav et al. (2017)
	Disk diffusion assay	Kjaergaard et al. (2001) Talmi et al. (1991) Jorgensen and Ferraro, (2009) Tehrani et al. (2013) Tehrani et al. (2017) Šket et al. (2019) Ramuta et al. (2021a) Ramuta et al. (2020b)
Evaluation of biofilms	Biofilm formation assay	Dubus et al. (2020) El-Mahdy et al. (2021)
	Determination of metabolically active cells by resazurin staining Live/dead bacterial viability	Yadav et al. (2017) El-Mahdy et al. (2021) Dubus et al. (2022)
	Morphology evaluation by light and electron microscopy	Yadav et al. (2017) Mao, et al. (2018) El-Mahdy et al. (2021)
Evaluation of antimicrobial activity in a complex (cellular) microenvironment		Josse et al. (2014) Sung et al. (2016) Dubus et al. (2020) El-Mahdy et al. (2021) Ramuta et al. (2021c)

epithelia, special attention must be given to establishment of physiologically-relevant *in vitro* models. For example, a multilayered biomimetic porcine urothelial model that has been shown to react differently to pathogenic vs. non-pathogenic *E. coli* strains has been used for evaluating the antimicrobial properties of PnDs (Ramuta T.Ž. et al., 2021; Predojević et al., 2022). Similar complex *in vitro* models have been established to study the host-pathogen interactions in the airway mucosa (Marrazzo et al., 2016; Hasan et al., 2018), intestine (Pearce et al., 2018; García-Díaz et al., 2022) and skin (Bolle et al., 2020), but have not yet been used for evaluation of PnDs.

The antimicrobial properties of PnDs have also been evaluated *in vivo* using several different methods. These studies have assessed the antimicrobial activity by quantifying bacteria in the spleen or blood or indirectly by measuring antimicrobial cytokines. For example, PnDs have been shown to protect against experimental sepsis (murine cecal ligation and puncture model of sepsis) (Parolini et al., 2014; Laroye et al., 2019) and *E. coli*-induced acute lung injury (Sung et al., 2016).

Conclusion

PnDs have demonstrated contradictory effects in the field of oncology. Various factors that include the specific PnD tissue of origin, the type and size of tumor, the PnD injection route, the treatment regimen and interactions with the host appear to play a role in determining whether PnD exert pro-tumorigenic or antitumorigenic properties. To facilitate the translation of PnDs towards the clinic, it is crucial to standardize procedures for evaluating the properties of PnDs and to define the criteria that distinguish each PnDs as suitable for clinical use. PnDs-derived preparations are a very versatile group, ranging from cells and their conditioned media to tissue-derived scaffolds. This must be taken into account when selecting methods and defining criteria for validating the multimodal functions of PnDs to be used in oncological and antimicrobial applications. Another challenge is the development of assays that can efficiently and reproducibly measure the anticancer and antimicrobial properties of PnDs in *vitro* and *in vivo* models of cancer and infection.

In summary, there is a growing awareness that PnDs possess precisely tuned anticancer and antimicrobial activities. In this review, we

therefore present the most commonly used functional assays (Table 2) with their advantages and disadvantages in assessing the anticancer and antimicrobial functionality of PnDs. This must be considered in future research and in the development of more effective PnDs therapies.

Author contributions

All authors contributed to manuscript preparation and revision. AS, TZR, and MEK coordinated the work and compiled the manuscript.

Funding

This work was supported by: COST Action CA17116 International Network for Translating Research on Perinatal Derivatives into Therapeutic Approaches (SPRINT), supported by COST (European Cooperation in Science and Technology), the French Ministry of Health (PHRCI-2020), the Slovenian Research Agency (J7-2594, P3-0108), Italian Ministry of Research and University (MIUR, 5x1000) and the "Fondazione Alessandra Bono Onlus".

Conflict of interest

The authors declare that the research was conducted in the absence of any commercial or financial relationships that could be construed as a potential conflict of interest.

Publisher's note

All claims expressed in this article are solely those of the authors and do not necessarily represent those of their affiliated organizations, or those of the publisher, the editors and the reviewers. Any product that may be evaluated in this article, or claim that may be made by its manufacturer, is not guaranteed or endorsed by the publisher.

References

Allen, H., Shraga-Heled, N., Blumenfeld, M., Dego-Ashto, T., Fuchs-Telem, D., Gilert, A., et al. (2018). Human placental-derived adherent stromal cells Co-induced with TNF-alpha and IFN-gamma inhibit triple-negative breast cancer in nude mouse xenograft models. *Sci. Rep.* 8 (1), 670. doi:10.1038/s41598-017-18428-1

Alshareeda, A. T., Rakha, E., Alghwainem, A., Alrfaei, B., Alsowayan, B., Albugami, A., et al. (2018). The effect of human placental chorionic villi derived mesenchymal stem cell on triple-negative breast cancer hallmarks. *PLoS One* 13 (11), e0207593. doi:10.1371/journal.pone.0207593

Ashraf, H., Font, K., Powell, C., and Schurr, M. (2019). Antimicrobial activity of an amnion-chorion membrane to oral microbes. *Int. J. Dent.* 2019, 1269534. doi:10.1155/2019/1269534

Ayuzawa, R., Doi, C., Rachakatla, R. S., Pyle, M. M., Maurya, D. K., Troyer, D., et al. (2009). Naive human umbilical cord matrix derived stem cells significantly attenuate growth of human breast cancer cells *in vitro* and *in vivo*. *Cancer Lett.* 280 (1), 31–37. doi:10.1016/j.canlet.2009.02.011

Bajetto, A., Pattarozzi, A., Corsaro, A., Barbieri, F., Daga, A., Bosio, A., et al. (2017). Different effects of human umbilical cord mesenchymal stem cells on glioblastoma stem cells by direct cell interaction or via released soluble factors. *Front. Cell. Neurosci.* 11, 312. doi:10.3389/fncel.2017.00312

Banerjee, A., Lindenmair, A., Hennerbichler, S., Steindorf, P., Steinborn, R., Kozlov, A. V., et al. (2018a). Cellular and site-specific mitochondrial characterization of vital human amniotic membrane. *Cell Transpl.* 27 (1), 3–11. doi:10.1177/0963689717735332

Banerjee, A., Lindenmair, A., Steinborn, R., Dumitrescu, S. D., Hennerbichler, S., Kozlov, A. V., et al. (2018b). Oxygen tension strongly influences metabolic parameters and the release of interleukin-6 of human amniotic mesenchymal stromal cells*in vitro*. *Stem Cells Int.* 2018, 11. doi:10.1155/2018/9502451

Banerjee, A., Weidinger, A., Hofer, M., Steinborn, R., Lindenmair, A., Hennerbichler-Lugscheider, S., et al. (2015). Different metabolic activity in placental and reflected regions of the human amniotic membrane. *Placenta* 36 (11), 1329–1332. doi:10.1016/j.placenta.2015.08.015

Bhatt, A. P., Redinbo, M. R., and Bultman, S. J. (2017). The role of the microbiome in cancer development and therapy. *CA A Cancer J. Clin.* 67 (4), 326–344. doi:10.3322/caac.21398

Björkholm, B., Bok, C. M., Lundin, A., Rafter, J., Hibberd, M. L., and Pettersson, S. (2009). Intestinal microbiota regulate xenobiotic metabolism in the liver. *PloS one* 4 (9), e6958. doi:10.1371/journal.pone.0006958

Bolle, E. C. L., Verderosa, A. D., Dhouib, R., Parker, T. J., Fraser, J. F., Dargaville, T. R., et al. (2020). An *in vitro* reconstructed human skin equivalent model to study the role of skin integration around percutaneous devices against bacterial infection. *Front. Microbiol.* 11, 670. doi:10.3389/fmicb.2020.00670

Bonomi, A., Silini, A., Vertua, E., Signoroni, P. B., Cocce, V., Cavicchini, L., et al. (2015). Human amniotic mesenchymal stromal cells (hAMSCs) as potential vehicles for drug delivery in cancer therapy: An *in vitro* study. *Stem Cell Res. Ther.* 6 (1), 155. doi:10.1186/s13287-015-0140-z

Borghesi, J., Caceres, S., Mario, L. C., Alonso-Diez, A., Silveira Rabelo, A. C., Illera, M. J., et al. (2020). Effects of doxorubicin associated with amniotic membrane stem cells in the treatment of canine inflammatory breast carcinoma (IPC-366) cells. *BMC Vet. Res.* 16 (1), 353. doi:10.1186/s12917-020-02576-0

Bu, S., Zhang, Q., Wang, Q., and Lai, D. (2017). Human amniotic epithelial cells inhibit growth of epithelial ovarian cancer cells via TGF-β1-mediated cell cycle arrest. *Int. J. Oncol.* 51 (5), 1405–1414. doi:10.3892/ijo.2017.4123

Cafforio, P., Viggiano, L., Mannavola, F., Pellè, E., Caporusso, C., Maiorano, E., et al. (2017). pIL6-TRAIL-engineered umbilical cord mesenchymal/stromal stem cells are highly cytotoxic for myeloma cells both *in vitro* and *in vivo*. *Stem Cell Res. Ther.* 8 (1), 206. doi:10.1186/s13287-017-0655-6

Carmody, R. N., and Turnbaugh, P. J. (2014). Host-microbial interactions in the metabolism of therapeutic and diet-derived xenobiotics. *J. Clin. Invest.* 124 (10), 4173–4181. doi:10.1172/jci72335

Chai, L., Bai, L., Li, L., Chen, F., and Zhang, J. (2018). Biological functions of lung cancer cells are suppressed in co-culture with mesenchymal stem cells isolated from umbilical cord. *Exp. Ther. Med.* 15 (1), 1076–1080. doi:10.3892/etm.2017.5456

Chao, K. C., Yang, H. T., and Chen, M. W. (2012). Human umbilical cord mesenchymal stem cells suppress breast cancer tumourigenesis through direct cell-cell contact and internalization. *J. Cell. Mol. Med.* 16 (8), 1803–1815. doi:10.1111/j.1582-4934.2011.01459.x

Chen, Q., Cheng, P., Song, N., Yin, T., He, H., Yang, L., et al. (2012). Antitumor activity of placenta-derived mesenchymal stem cells producing pigment epithelium-derived factor in a mouse melanoma model. *Oncol. Lett.* 4 (3), 413–418. doi:10.3892/ol.2012.772

Chen, X., Wang, K., Chen, S., and Chen, Y. (2019). Effects of mesenchymal stem cells harboring the Interferon-β gene on A549 lung cancer in nude mice. *Pathology - Res. Pract.* 215 (3), 586–593. doi:10.1016/j.prp.2019.01.013

Chetty, S. S., Praneetha, S., Vadivel Murugan, A., Govarthanan, K., and Verma, R. S. (2020). Human umbilical cord wharton's jelly-derived mesenchymal stem cells labeled with Mn(2+) and Gd(3+) Co-doped CuInS(2)-ZnS nanocrystals for multimodality imaging in a tumor mice model. *ACS Appl. Mat. Interfaces* 12 (3), 3415–3429. doi:10.1021/acsami.9b19054

Choi, J. H., Lim, S. M., Yoo, Y. I., Jung, J., Park, J. W., and Kim, G. J. (2016). Microenvironmental interaction between hypoxia and endothelial cells controls the migration ability of placenta-derived mesenchymal stem cells via α4 integrin and rho signaling. *J. Cell. Biochem.* 117 (5), 1145–1157. doi:10.1002/jcb.25398

Ciavarella, S., Caselli, A., Tamma, A. V., Savonarola, A., Loverro, G., Paganelli, R., et al. (2015). A peculiar molecular profile of umbilical cord-mesenchymal stromal cells drives their inhibitory effects on multiple myeloma cell growth and tumor progression. *Stem Cells Dev.* 24 (12), 1457–1470. doi:10.1089/scd.2014.0254

Dabrowski, F. A., Burdzinska, A., Kulesza, A., Sladowska, A., Zolocinska, A., Gala, K., et al. (2017). Comparison of the paracrine activity of mesenchymal stem cells derived from human umbilical cord, amniotic membrane and adipose tissue. *J. Obstet. Gynaecol. Res.* 43 (11), 1758–1768. doi:10.1111/jog.13432

Del Fattore, A., Luciano, R., Saracino, R., Battafarano, G., Rizzo, C., Pascucci, L., et al. (2015). Differential effects of extracellular vesicles secreted by mesenchymal stem cells from different sources on glioblastoma cells. *Expert Opin. Biol. Ther.* 15 (4), 495–504. doi:10.1517/14712598.2015.997706

Di Germanio, C., Bernier, M., Petr, M., Mattioli, M., Barboni, B., and de Cabo, R. (2016). Conditioned medium derived from rat amniotic epithelial cells confers protection against inflammation, cancer, and senescence. *Oncotarget* 7, 39051–39064. doi:10.18632/oncotarget.9694

Di, G. H., Liu, Y., Lu, Y., Liu, J., Wu, C., and Duan, H. F. (2014). IL-6 secreted from senescent mesenchymal stem cells promotes proliferation and migration of breast cancer cells. *PLoS One* 9 (11), e113572. doi:10.1371/journal.pone.0113572

Dong, L., Pu, Y., Zhang, L., Qi, Q., Xu, L., Li, W., et al. (2018). Human umbilical cord mesenchymal stem cell-derived extracellular vesicles promote lung adenocarcinoma growth by transferring miR-410. *Cell Death Dis.* 9 (2), 218. doi:10.1038/s41419-018-0323-5

Drago, L., Cappelletti, L., De Vecchi, E., Pignataro, L., Torretta, S., and Mattina, R. (2014). Antiadhesive and antibiofilm activity of hyaluronic acid against bacteria responsible for respiratory tract infections. *Apmis* 122 (10), 1013–1019. doi:10.1111/apm.12254

Du, T., Ju, G., Wu, S., Cheng, Z., Cheng, J., Zou, X., et al. (2014). Microvesicles derived from human Wharton's jelly mesenchymal stem cells promote human renal cancer cell growth and aggressiveness through induction of hepatocyte growth factor. *PLoS One* 9 (5), e96836. doi:10.1371/journal.pone.0096836

Dubus, M., Scomazzon, L., Chevrier, J., Ledouble, C., Baldit, A., Braux, J., et al. (2022). Antibacterial and immunomodulatory properties of acellular wharton's jelly matrix. *Biomedicines* 10 (2), 227. doi:10.3390/biomedicines10020227

Dubus, M., Varin-Simon, J., Prada, P., Scomazzon, L., Reffuveille, F., Alem, H., et al. (2020). Biopolymers-calcium phosphate antibacterial coating reduces the pathogenicity of internalized bacteria by mesenchymal stromal cells. *Biomater. Sci.* 8 (20), 5763–5773. doi:10.1039/d0bm00962h

Dzobo, K., Vogelsang, M., Thomford, N. E., Dandara, C., Kallmeyer, K., Pepper, M. S., et al. (2016). Wharton's jelly-derived mesenchymal stromal cells and fibroblast-derived extracellular matrix synergistically activate apoptosis in a p21-dependent mechanism in WHCO1 and MDA MB 231 cancer cells*in vitro*. *Stem Cells Int.* 2016, 1–17. doi:10.1155/2016/4842134

El-Mahdy, T. S., Mongaret, C., Varin-Simon, J., Lamret, F., Vernet-Garnier, V., Rammal, H., et al. (2021). Interaction of implant infection-related commensal bacteria with mesenchymal stem cells: A comparison between cutibacterium acnes and *Staphylococcus aureus*. *FEMS Microbiol. Lett.* 368 (4), fnab014. doi:10.1093/femsle/fnab014

Fan, S., Gao, H., Ji, W., Zhu, F., Sun, L., Liu, Y., et al. (2020). Umbilical cord-derived mesenchymal stromal/stem cells expressing IL-24 induce apoptosis in gliomas. *J. Cell. Physiol.* 235 (2), 1769–1779. doi:10.1002/jcp.29095

Faraj, L., Stewart, E., Albert, R., Allen, C., Petrovski, G., Dua, H., et al. (2015). *In-vitro* anti angiogenic effects of cryo-preserved amniotic membrane. *Acta Ophthalmol.* 93 (S255). doi:10.1111/j.1755-3768.2015.0635

Faridvand, Y., Nozari, S., Vahedian, V., Safaie, N., Pezeshkian, M., Haddadi, P., et al. (2019). Nrf2 activation and down-regulation of HMGB1 and MyD88 expression by amnion membrane extracts in response to the hypoxia-induced injury in cardiac H9c2 cells. *Biomed. Pharmacother.* 109, 360–368. doi:10.1016/j.biopha.2018.10.035

Fong, C. Y., Chak, L. L., Biswas, A., Tan, J. H., Gauthaman, K., Chan, W. K., et al. (2011). Human Wharton's jelly stem cells have unique transcriptome profiles compared to human embryonic stem cells and other mesenchymal stem cells. *Stem Cell Rev. Rep.* 7 (1), 1–16. doi:10.1007/s12015-010-9166-x

Ganjibakhsh, M., Mehraein, F., Koruji, M., Aflatoonian, R., and Farzaneh, P. (2019). Three-dimensional decellularized amnion membrane scaffold as a novel tool for cancer research; cell behavior, drug resistance and cancer stem cell content. *Mater. Sci. Eng. C* 100, 330–340. doi:10.1016/j.msec.2019.02.090

García-Díaz, M., Cendra, M. D. M., Alonso-Roman, R., Urdániz, M., Torrents, E., and Martínez, E. (2022). Mimicking the intestinal host-pathogen interactions in a 3D *in vitro* model: The role of the mucus layer. *Pharmaceutics* 14 (8), 1552. doi:10.3390/pharmaceutics14081552

Gauthaman, K., Yee, F. C., Cheyyatraivendran, S., Biswas, A., Choolani, M., and Bongso, A. (2012). Human umbilical cord Wharton's jelly stem cell (hWJSC) extracts inhibit cancer cell growth *in vitro*. *J. Cell. Biochem.* 113 (6), 2027–2039. doi:10.1002/jcb.24073

Gnaiger, E. (2008). Polarographic oxygen sensors, the oxygraph, and high-resolution respirometry to assess mitochondrial function. in *Drug-induced mitochondrial dysfunction*. New Jersey, USA: John Wiley & Sons (Wiley), 325–352.

Grzywocz, Z., Hoser, G., Sabalinska, S., Ladyzynski, P., Czubak, J., Dworczynska, M., et al. (2018). Response of human normal and leukemia cells to factors released by amnion fragments *in vitro*. *PLOS ONE* 13 (3), e0195035. doi:10.1371/journal.pone.0195035

Haiser, H. J., and Turnbaugh, P. J. (2012). Is it time for a metagenomic basis of therapeutics? *Science* 336 (6086), 1253–1255. doi:10.1126/science.1224396

Han, I., Yun, M., Kim, E. O., Kim, B., Jung, M. H., and Kim, S. H. (2014). Retracted article: Umbilical cord tissue-derived mesenchymal stem cells induce apoptosis in PC-3 prostate cancer cells through activation of JNK and downregulation of PI3K/AKT signaling. *Stem Cell Res. Ther.* 5 (2), 54. doi:10.1186/scrt443

Hanahan, D., and Weinberg, R. A. (2011). Hallmarks of cancer: The next generation. *Cell* 144 (5), 646–674. doi:10.1016/j.cell.2011.02.013

Haney, E. F., Trimble, M. J., Cheng, J. T., Vallé, Q., and Hancock, R. E. W. (2018). Critical assessment of methods to quantify biofilm growth and evaluate antibiofilm activity of host defence peptides. *Biomolecules* 8 (2), 29. doi:10.3390/biom8020029

Hasan, S., Sebo, P., and Osicka, R. (2018). A guide to polarized airway epithelial models for studies of host-pathogen interactions. *FEBS J.* 285 (23), 4343–4358. doi:10.1111/febs.14582

Hendijani, F., Javanmard, S. H., and Sadeghi-aliabadi, H. (2015). Human Wharton's jelly mesenchymal stem cell secretome display antiproliferative effect on leukemia cell line and produce additive cytotoxic effect in combination with doxorubicin. *Tissue Cell* 47 (3), 229–234. doi:10.1016/j.tice.2015.01.005

Hütter, E., Unterluggauer, H., Garedew, A., Jansen-Dürr, P., and Gnaiger, E. (2006). High-resolution respirometry--a modern tool in aging research. *Exp. Gerontol.* 41 (1), 103–109. doi:10.1016/j.exger.2005.09.011

Iravani, A., and Hicks, R. J. (2020). Imaging the cancer immune environment and its response to pharmacologic intervention, Part 2: The role of novel PET agents. *J. Nucl. Med.* 61 (11), 1553–1559. doi:10.2967/jnumed.120.248823

Jain, T., Sharma, P., Are, A. C., Vickers, S. M., and Dudeja, V. (2021). New insights into the cancer-microbiome-immune Axis: Decrypting a decade of discoveries. *Front. Immunol.* 12, 622064. doi:10.3389/fimmu.2021.622064

Janev, A., Ramuta, T. Ž., Tratnjek, L., Sardoč, Ž., Obradović, H., Mojsilović, S., et al. (2021). Detrimental effect of various preparations of the human amniotic membrane homogenate on the 2D and 3D bladder cancer *in vitro* models. *Front. Bioeng. Biotechnol.* 9, 690358. doi:10.3389/fbioe.2021.690358

Jiao, H., Guan, F., Yang, B., Li, J., Song, L., Hu, X., et al. (2012). Human amniotic membrane derived-mesenchymal stem cells induce C6 glioma apoptosis *in vivo* through the Bcl-2/caspase pathways. *Mol. Biol. Rep.* 39 (1), 467–473. doi:10.1007/s11033-011-0760-z

Jiao, Y., Zhao, H., Chen, G., Sang, X., Yang, L., Hou, Z., et al. (2018). Pyroptosis of MCF7 cells induced by the secreted factors of hUCMSCs. *Stem Cells Int.* 2018, 1–12. doi:10.1155/2018/5912194

Jorgensen, J. H., and Ferraro, M. J. (2009). Antimicrobial susceptibility testing: A review of general principles and contemporary practices. *Clin. Infect. Dis.* 49 (11), 1749–1755. doi:10.1086/647952

Josse, J., Velard, F., Mechiche Alami, S., Brun, V., Guillaume, C., Kerdjoudj, H., et al. (2014). Increased internalization of *Staphylococcus aureus* and cytokine expression in human Wharton's jelly mesenchymal stem cells. *Biomed. Mat. Eng.* 24 (1), 27–35. doi:10.3233/bme-140971

Kalamegam, G., Sait, K. H. W., Ahmed, F., Kadam, R., Pushparaj, P. N., Anfinan, N., et al. (2018). Human wharton's jelly stem cell (hWJSC) extracts inhibit ovarian cancer cell lines OVCAR3 and SKOV3 *in vitro* by inducing cell cycle arrest and apoptosis. *Front. Oncol.* 8, 592. doi:10.3389/fonc.2018.00592

Kalamegam, G., Sait, K. H. W., Anfinan, N., Kadam, R., Ahmed, F., Rasool, M., et al. (2019). Cytokines secreted by human Wharton's jelly stem cells inhibit the proliferation of ovarian cancer (OVCAR3) cells *in vitro*. *Oncol. Lett.* 17 (5), 4521–4531. doi:10.3892/ol.2019.10094

Kamalabadi-Farahani, M., Vasei, M., Ahmadbeigi, N., Ebrahimi-Barough, S., Soleimani, M., and Roozafzoon, R. (2018). Anti-tumour effects of TRAIL-expressing human placental derived mesenchymal stem cells with curcumin-loaded chitosan nanoparticles in a mice model of triple negative breast cancer.

Artif. Cells Nanomed. Biotechnol. 46 (3), S1011–s1021. doi:10.1080/21691401.2018.1527345

Kang, N. H., Yi, B. R., Lim, S. Y., Hwang, K. A., Baek, Y. S., Kang, K. S., et al. (2012). Human amniotic membrane-derived epithelial stem cells display anticancer activity in BALB/c female nude mice bearing disseminated breast cancer xenografts. *Int. J. Oncol.* 40 (6), 2022–2028. doi:10.3892/ijo.2012.1372

Khalil, C., Moussa, M., Azar, A., Tawk, J., Habbouche, J., Salameh, R., et al. (2019). Anti-proliferative effects of mesenchymal stem cells (MSCs) derived from multiple sources on ovarian cancer cell lines: An *in-vitro* experimental study. *J. Ovarian Res.* 12 (1), 70. doi:10.1186/s13048-019-0546-9

Kim, H. S., Cho, J. H., Park, H. W., Yoon, H., Kim, M. S., and Kim, S. C. (2002). Endotoxin-neutralizing antimicrobial proteins of the human placenta. *J. Immunol.* 168 (5), 2356–2364. doi:10.4049/jimmunol.168.5.2356

Kim, J.-Y., Park, S.-C., Lee, J.-K., Choi, S. J., Hahm, K.-S., and Park, Y. (2012). Novel antibacterial activity of β2-microglobulin in human amniotic fluid. *PLOS ONE* 7 (11), e47642. doi:10.1371/journal.pone.0047642

Kim, S.-H., Bang, S. H., Kang, S. Y., Park, K. D., Eom, J. H., Oh, I. U., et al. (2015). Human amniotic membrane-derived stromal cells (hAMSC) interact depending on breast cancer cell type through secreted molecules. *Tissue Cell* 47 (1), 10–16. doi:10.1016/j.tice.2014.10.003

King, A. E., Kelly, R. W., Sallenave, J. M., Bocking, A. D., and Challis, J. R. (2007a). Innate immune defences in the human uterus during pregnancy. *Placenta* 28 (11-12), 1099–1106. doi:10.1016/j.placenta.2007.06.002

King, A. E., Paltoo, A., Kelly, R. W., Sallenave, J. M., Bocking, A. D., and Challis, J. R. (2007b). Expression of natural antimicrobials by human placenta and fetal membranes. *Placenta* 28 (2-3), 161–169. doi:10.1016/j.placenta.2006.01.006

Kjaergaard, N., Hein, M., Hyttel, L., Helmig, R. B., Schønheyder, H. C., Uldbjerg, N., et al. (2001). Antibacterial properties of human amnion and chorion *in vitro*. *Eur. J. Obstet. Gynecol. Reprod. Biol. X.* 94 (2), 224–229. doi:10.1016/s0301-2115(00)00345-6

Klaffenbach, D., Friedrich, D., Strick, R., Strissel, P. L., Beckmann, M. W., Rascher, W., et al. (2011). Contribution of different placental cells to the expression and stimulation of antimicrobial proteins (AMPs). *Placenta* 32 (11), 830–837. doi:10.1016/j.placenta.2011.08.004

Komaki, M., Numata, Y., Morioka, C., Honda, I., Tooi, M., Yokoyama, N., et al. (2017). Exosomes of human placenta-derived mesenchymal stem cells stimulate angiogenesis. *Stem Cell Res. Ther.* 8 (1), 219. doi:10.1186/s13287-017-0660-9

Kramer, N., Walzl, A., Unger, C., Rosner, M., Krupitza, G., Hengstschläger, M., et al. (2013). *In vitro* cell migration and invasion assays. *Mutat. Research/Reviews Mutat. Res.* 752 (1), 10–24. doi:10.1016/j.mrrev.2012.08.001

Lang, D. S., Marwitz, S., Zeiser, T., Seehase, S., Watermann, I., Vollmer, E., et al. (2015). Placenta-derived conditioned medium with anti-tumor properties on human NSCLC. *Eur. Respir. J.* 46 (59), OA4983. doi:10.1183/13993003

Laroye, C., Boufenzer, A., Jolly, L., Cunat, L., Alauzet, C., Merlin, J.-L., et al. (2019). Bone marrow vs Wharton's jelly mesenchymal stem cells in experimental sepsis: A comparative study. *Stem Cell Res. Ther.* 10 (1), 192. doi:10.1186/s13287-019-1295-9

Lehouritis, P., Cummins, J., Stanton, M., Murphy, C. T., McCarthy, F. O., Reid, G., et al. (2015). Local bacteria affect the efficacy of chemotherapeutic drugs. *Sci. Rep.* 5, 14554. doi:10.1038/srep14554

Leng, L., Wang, Y., He, N., Wang, D., Zhao, Q., Feng, G., et al. (2014). Molecular imaging for assessment of mesenchymal stem cells mediated breast cancer therapy. *Biomaterials* 35 (19), 5162–5170. doi:10.1016/j.biomaterials.2014.03.014

Li, T., Zhang, C., Ding, Y., Zhai, W., Liu, K., Bu, F., et al. (2015). Umbilical cord-derived mesenchymal stem cells promote proliferation and migration in MCF-7 and MDA-MB-231 breast cancer cells through activation of the ERK pathway. *Oncol. Rep.* 34 (3), 1469–1477. doi:10.3892/or.2015.4109

Li, X., Ling, W., Pennisi, A., Wang, Y., Khan, S., Heidaran, M., et al. (2011). Human placenta-derived adherent cells prevent bone loss, stimulate bone formation, and suppress growth of multiple myeloma in bone. *Stem Cells* 29 (2), 263–273. doi:10.1002/stem.572

Li, X., Liu, L. l., Yao, J. l., Wang, K., and Ai, H. (2019). Human umbilical cord mesenchymal stem cell-derived extracellular vesicles inhibit endometrial cancer cell proliferation and migration through delivery of exogenous miR-302a. *Stem Cells Int.* 2019, 1–11. doi:10.1155/2019/8108576

Liepke, C., Baxmann, S., Heine, C., Breithaupt, N., Ständker, L., and Forssmann, W. G. (2003). Human hemoglobin-derived peptides exhibit antimicrobial activity: A class of host defense peptides. *J. Chromatogr. B* 791 (1-2), 345–356. doi:10.1016/s1570-0232(03)00245-9

Lin D, D. H., Biswas, A., Choolani, M., Fong, C. Y., and Bongso, A. (2017). Induction of immunogenic cell death in lymphoma cells by wharton's jelly mesenchymal stem cell conditioned medium. *Stem Cell Rev. Rep.* 13 (6), 801–816. doi:10.1007/s12015-017-9767-8

Lin H, H., Fang, Z., Su, Y., Li, P., Wang, J., Liao, H., et al. (2017). DHX32 promotes angiogenesis in colorectal cancer through augmenting β-catenin signaling to induce expression of VEGFA. *EBioMedicine* 18, 62–72. doi:10.1016/j.ebiom.2017.03.012

Lin, H. D., Fong, C. Y., Biswas, A., Choolani, M., and Bongso, A. (2016). Human umbilical cord wharton's jelly stem cell conditioned medium induces tumoricidal effects on lymphoma cells through hydrogen peroxide mediation. *J. Cell. Biochem.* 117 (9), 2045–2055. doi:10.1002/jcb.25501

Lin, H. D., Fong, C. Y., Biswas, A., Choolani, M., and Bongso, A. (2014). Human Wharton's jelly stem cells, its conditioned medium and cell-free lysate inhibit the growth of human lymphoma cells. *Stem Cell Rev. Rep.* 10 (4), 573–586. doi:10.1007/s12015-014-9514-3

Liu, J., Han, G., Liu, H., and Qin, C. (2013). Suppression of cholangiocarcinoma cell growth by human umbilical cord mesenchymal stem cells: A possible role of wnt and akt signaling. *PLoS ONE* 8 (4), e62844. doi:10.1371/journal.pone.0062844

Ma, F., Chen, D., Chen, F., Chi, Y., Han, Z., Feng, X., et al. (2015). Human umbilical cord mesenchymal stem cells promote breast cancer metastasis by interleukin-8- and interleukin-6-dependent induction of CD44(+)/CD24(-) cells. *Cell Transpl.* 24 (12), 2585–2599. doi:10.3727/096368915x687462

Magatti, M., De Munari, S., Vertua, E., and Parolini, O. (2012). Amniotic membrane-derived cells inhibit proliferation of cancer cell lines by inducing cell cycle arrest. *J. Cell. Mol. Med.* 16 (9), 2208–2218. doi:10.1111/j.1582-4934.2012.01531.x

Magatti, M., Vertua, E., De Munari, S., Caro, M., Caruso, M., Silini, A., et al. (2017). Human amnion favours tissue repair by inducing the M1-to-M2 switch and enhancing M2 macrophage features. *J. Tissue Eng. Regen. Med.* 11 (10), 2895–2911. doi:10.1002/term.2193

Mamede, A. C., Guerra, S., Laranjo, M., Carvalho, M. J., Oliveira, R. C., Goncalves, A. C., et al. (2015). Selective cytotoxicity and cell death induced by human amniotic membrane in hepatocellular carcinoma. *Med. Oncol.* 32 (12), 257. doi:10.1007/s12032-015-0702-z

Mandal, S., Arfuso, F., Sethi, G., Dharmarajan, A., and Warrier, S. (2019). Encapsulated human mesenchymal stem cells (eMSCs) as a novel anti-cancer agent targeting breast cancer stem cells: Development of 3D primed therapeutic MSCs. *Int. J. Biochem. Cell Biol.* 110, 59–69. doi:10.1016/j.biocel.2019.02.001

Mao, Y., Hoffman, T., Johnson, A., Duan-Arnold, Y., Danilkovitch, A., and Kohn, J. (2016). Human cryopreserved viable amniotic membrane inhibits the growth of bacteria associated with chronic wounds. *J. Diabet. Foot Complicat.* 8 (2), 8.

Mao, Y., Hoffman, T., Singh-Varma, A., Duan-Arnold, Y., Moorman, M., Danilkovitch, A., et al. (2017). Antimicrobial peptides secreted from human cryopreserved viable amniotic membrane contribute to its antibacterial activity. *Sci. Rep.* 7 (1), 13722. doi:10.1038/s41598-017-13310-6

Mao, Y., Singh-Varma, A., Hoffman, T., Dhall, S., Danilkovitch, A., and Kohn, J. (2018). The effect of cryopreserved human placental tissues on biofilm formation of wound-associated pathogens. *J. Funct. Biomater.* 9 (1), 3. doi:10.3390/jfb9010003

Marcuzzo, A. V., Tofanelli, M., Boscolo Nata, F., Gatto, A., and Tirelli, G. (2017). Hyaluronate effect on bacterial biofilm in ENT district infections: A review. *Apmis* 125 (9), 763–772. doi:10.1111/apm.12728

Marleau, A. M., McDonald, G., Koropatnick, J., Chen, C.-S., and Koos, D. (2012). Reduction of tumorigenicity by placental extracts. *Anticancer Res.* 32 (4), 1153–1161.

Marrazzo, P., Maccari, S., Taddei, A., Bevan, L., Telford, J., Soriani, M., et al. (2016). 3D reconstruction of the human airway mucosa *in vitro* as an experimental model to study NTHi infections. *PLoS One* 11 (4), e0153985. doi:10.1371/journal.pone.0153985

Marshall, J. (2011). Transwell(®) invasion assays. *Methods Mol. Biol.* 769, 97–110. doi:10.1007/978-1-61779-207-6_8

Martin, T. A., and Jiang, W. G. (2009). Loss of tight junction barrier function and its role in cancer metastasis. *Biochimica Biophysica Acta - Biomembr.* 1788 (4), 872–891. doi:10.1016/j.bbamem.2008.11.005

Martin, T. A., Ye, L., Sanders, A. J., Lane, J., and Jiang, W. G. (2013). *Cancer invasion and metastasis: Molecular and cellular perspective*. Austin (TX): Landes Bioscience.

Meng, M. Y., Li, L., Wang, W. J., Liu, F. F., Song, J., Yang, S. L., et al. (2019). Assessment of tumor promoting effects of amniotic and umbilical cord mesenchymal stem cells *in vitro* and *in vivo*. *J. Cancer Res. Clin. Oncol.* 145 (5), 1133–1146. doi:10.1007/s00432-019-02859-6

Menyhárt, O., Harami-Papp, H., Sukumar, S., Schäfer, R., Magnani, L., de Barrios, O., et al. (2016). Guidelines for the selection of functional assays to evaluate the hallmarks of cancer. *Biochimica Biophysica Acta (BBA) - Rev. Cancer* 1866 (2), 300–319. doi:10.1016/j.bbcan.2016.10.002

Modaresifar, K., Azizian, S., Zolghadr, M., Moravvej, H., Ahmadiani, A., and Niknejad, H. (2017). The effect of cryopreservation on anti-cancer activity of human amniotic membrane. *Cryobiology* 74, 61–67. doi:10.1016/j.cryobiol.2016.12.001

Nelson, D. L., and Cox, M. M. (2004). *Lehninger principles of biochemistry*. New York, NY: W. H. Freeman.

Niknejad, H., Khayat-Khoei, M., Peirovi, H., and Abolghasemi, H. (2014). Human amniotic epithelial cells induce apoptosis of cancer cells: A new anti-tumor therapeutic strategy. *Cytotherapy* 16 (1), 33–40. doi:10.1016/j.jcyt.2013.07.005

Palanker, N. D., Lee, C. T., Weltman, R. L., Tribble, G. D., van der Hoeven, R., Hong, J., et al. (2019). Antimicrobial efficacy assessment of human derived composite amnion-chorion membrane. *Sci. Rep.* 9 (1), 15600. doi:10.1038/s41598-019-52150-4

Paris, J. L., de la Torre, P., Manzano, M., Cabañas, M. V., Flores, A. I., and Vallet-Regi, M. (2016). Decidua-derived mesenchymal stem cells as carriers of mesoporous silica nanoparticles. *in vitro* and *in vivo* evaluation on mammary tumors. *Acta Biomater.* 33, 275–282. doi:10.1016/j.actbio.2016.01.017

Parolini, O., Souza-Moreira, L., O'Valle, F., Magatti, M., Hernandez-Cortes, P., Gonzalez-Rey, E., et al. (2014). Therapeutic effect of human amniotic membrane-derived cells on experimental arthritis and other inflammatory disorders. *Arthritis Rheumatol.* 66 (2), 327–339. doi:10.1002/art.38206

Pearce, S. C., Coia, H. G., Karl, J. P., Pantoja-Feliciano, I. G., Zachos, N. C., and Racicot, K. (2018). Intestinal *in vitro* and *ex vivo* models to study host-microbiome interactions and acute stressors. *Front. Physiol.* 9, 1584. doi:10.3389/fphys.2018.01584

Poženel, L., Lindenmair, A., Schmidt, K., Kozlov, A. V., Grillari, J., Wolbank, S., et al. (2019). Critical impact of human amniotic membrane tension on mitochondrial function and cell viability *in vitro*. *Cells* 8 (12), 1641. doi:10.3390/cells8121641

Predojević, L., Keše, D., Žgur Bertok, D., Železnik Ramuta, T., Veranič, P., Erdani Kreft, M., et al. (2022). A biomimetic porcine urothelial model for assessing *Escherichia coli* pathogenicity. *Microorganisms* 10 (4), 783. doi:10.3390/microorganisms10040783

Puaux, A. L., Ong, L. C., Jin, Y., Teh, I., Hong, M., Chow, P. K., et al. (2011). A comparison of imaging techniques to monitor tumor growth and cancer progression in living animals. *Int. J. Mol. Imaging* 2011, 321538. doi:10.1155/2011/321538

Ramuta, T., Jerman, U. D., Tratnjek, L., Janev, A., Magatti, M., Vertua, E., et al. (2020a). The cells and extracellular matrix of human amniotic membrane hinder the growth and invasive potential of bladder urothelial cancer cells. *Front. Bioeng. Biotechnol.* 8, 554530. doi:10.3389/fbioe.2020.554530

Ramuta, T., Šket, T., Starčič Erjavec, M., and Kreft, M. E. (2021a). Antimicrobial activity of human fetal membranes: From biological function to clinical use. *Front. Bioeng. Biotechnol.* 9, 691522. doi:10.3389/fbioe.2021.691522

Ramuta, T., Starčič Erjavec, M., and Kreft, M. E. (2020b). Amniotic membrane preparation crucially affects its broad-spectrum activity against uropathogenic bacteria. *Front. Microbiol.* 11, 469. doi:10.3389/fmicb.2020.00469

Ramuta, T., Tratnjek, L., Janev, A., Seme, K., Starčič Erjavec, M., and Kreft, M. E. (2021b). The antibacterial activity of human amniotic membrane against multidrug-resistant bacteria associated with urinary tract infections: New insights from normal and cancerous urothelial models. *Biomedicines* 9 (2), 218. doi:10.3390/biomedicines9020218

Ramuta, T. Z., Starčič Erjavec, M., and Kreft, M. E. (2020c). Amniotic membrane preparation crucially affects its broad-spectrum activity against uropathogenic bacteria. *Front. Microbiol.* 11, 469. doi:10.3389/fmicb.2020.00469

Ramuta, T. Ž., Tratnjek, L., Janev, A., Seme, K., Starčič Erjavec, M., and Kreft, M. E. (2021c). The antibacterial activity of human amniotic membrane against multidrug-resistant bacteria associated with urinary tract infections: New insights from normal and cancerous urothelial models. *Biomedicines* 9 (2), 218. doi:10.3390/biomedicines9020218

Raza, M. H., Gul, K., Arshad, A., Riaz, N., Waheed, U., Rauf, A., et al. (2019). Microbiota in cancer development and treatment. *J. Cancer Res. Clin. Oncol.* 145 (1), 49–63. doi:10.1007/s00432-018-2816-0

Rezaei-Tazangi, F., Alidadi, H., Samimi, A., Karimi, S., and Kahorsandi, L. (2020). Effects of Wharton's jelly mesenchymal stem cells-derived secretome on colon carcinoma HT-29 cells. *Tissue Cell* 67, 101413. doi:10.1016/j.tice.2020.101413

Riedel, R., Pérez-Pérez, A., Carmona-Fernández, A., Jaime, M., Casale, R., Dueñas, J. L., et al. (2019). Human amniotic membrane conditioned medium inhibits proliferation and modulates related microRNAs expression in hepatocarcinoma cells. *Sci. Rep.* 9 (1), 14193. doi:10.1038/s41598-019-50648-5

Robson, M. C., and Krizek, T. J. (1973). The effect of human amniotic membranes on the bacterial population of infected rat burns. *Ann. Surg.* 177 (2), 144–149. doi:10.1097/00000658-197302000-00003

Rolfo, A., Giuffrida, D., Giuffrida, M. C., Todros, T., and Calogero, A. E. (2014). New perspectives for prostate cancer treatment: *In vitro* inhibition of LNCaP and PC3 cell proliferation by amnion-derived mesenchymal stromal cells conditioned media. *Aging Male* 17 (2), 94–101. doi:10.3109/13685538.2014.896894

Roy, S., and Trinchieri, G. (2017). Microbiota: A key orchestrator of cancer therapy. *Nat. Rev. Cancer* 17 (5), 271–285. doi:10.1038/nrc.2017.13

Segev-Zarko, L. A., and Shai, Y. (2017). Methods for investigating biofilm inhibition and degradation by antimicrobial peptides. *Methods Mol. Biol.* 1548, 309–322. doi:10.1007/978-1-4939-6737-7_22

Selwyn, F. P., Cheng, S. L., Bammler, T. K., Prasad, B., Vrana, M., Klaassen, C., et al. (2015). Developmental regulation of drug-processing genes in livers of germ-free mice. *Toxicol. Sci.* 147 (1), 84–103. doi:10.1093/toxsci/kfv110

Selwyn, F. P., Cheng, S. L., Klaassen, C. D., and Cui, J. Y. (2016). Regulation of hepatic drug-metabolizing enzymes in germ-free mice by conventionalization and probiotics. *Drug Metab. Dispos.* 44 (2), 262–274. doi:10.1124/dmd.115.067504

Shen, C. J., Chan, T. F., Chen, C. C., Hsu, Y. C., Long, C. Y., and Lai, C. S. (2016). Human umbilical cord matrix-derived stem cells expressing interferon-β gene inhibit breast cancer cells via apoptosis. *Oncotarget* 7 (23), 34172–34179. doi:10.18632/oncotarget.8997

Silini, A. R., Magatti, M., Cargnoni, A., and Parolini, O. (2017). Is immune modulation the mechanism underlying the beneficial effects of amniotic cells and their derivatives in regenerative medicine? *Cell Transpl.* 26 (4), 531–539. doi:10.3727/096368916x693699

Silini, A. R., Masserdotti, A., Papait, A., and Parolini, O. (2019). Shaping the future of perinatal cells: Lessons from the past and interpretations of the present. *Front. Bioeng. Biotechnol.* 7, 75. doi:10.3389/fbioe.2019.00075

Silva, M., Monteiro, G. A., Fialho, A. M., Bernardes, N., and da Silva, C. L. (2020). Conditioned medium from azurin-expressing human mesenchymal stromal cells demonstrates antitumor activity against breast and lung cancer cell lines. *Front. Cell Dev. Biol.* 8, 471. doi:10.3389/fcell.2020.00471

Sivandzade, F., Bhalerao, A., and Cucullo, L. (2019). Analysis of the mitochondrial membrane potential using the cationic JC-1 dye as a sensitive fluorescent probe. *Bio. Protoc.* 9 (1), e3128. doi:10.21769/bioprotoc.3128

Šket, T., Ramuta, T., Starčič Erjavec, M., and Kreft, M. E. (2019). Different effects of amniotic membrane homogenate on the growth of uropathogenic *Escherichia coli*, *Staphylococcus aureus* and *Serratia marcescens*. *Infect. Drug Resist.* 12, 3365–3375. doi:10.2147/IDR.S215006

So, K. A., Min, K. J., Hong, J. H., and Lee, J. K. (2015). Interleukin-6 expression by interactions between gynecologic cancer cells and human mesenchymal stem cells promotes epithelial-mesenchymal transition. *Int. J. Oncol.* 47 (4), 1451–1459. doi:10.3892/ijo.2015.3122

Subramanian, A., Shu-Uin, G., Kae-Siang, N., Gauthaman, K., Biswas, A., Choolani, M., et al. (2012). Human umbilical cord Wharton's jelly mesenchymal stem cells do not transform to tumor-associated fibroblasts in the presence of breast and ovarian cancer cells unlike bone marrow mesenchymal stem cells. *J. Cell. Biochem.* 113 (6), 1886–1895. doi:10.1002/jcb.24057

Sung, D. K., Chang, Y. S., Sung, S. I., Yoo, H. S., Ahn, S. Y., and Park, W. S. (2016). Antibacterial effect of mesenchymal stem cells against *Escherichia coli* is mediated by secretion of beta- defensin- 2 via toll- like receptor 4 signalling. *Cell. Microbiol.* 18 (3), 424–436. doi:10.1111/cmi.12522

Svitina, H., Skrypkina, I., Areshkov, P., Kyryk, V., Bukreieva, T., Klymenko, P., et al. (2018). Transplantation of placenta-derived multipotent cells in rats with dimethylhydrazine-induced colon cancer decreases survival rate. *Oncol. Lett.* 15 (4), 5034–5042. doi:10.3892/ol.2018.7996

Talmi, Y. P., Sigler, L., Inge, E., Finkelstein, Y., and Zohar, Y. (1991). Antibacterial properties of human amniotic membranes. *Placenta* 12 (3), 285–288. doi:10.1016/0143-4004(91)90010-d

Tehrani, F. A., Ahmadiani, A., and Niknejad, H. (2013). The effects of preservation procedures on antibacterial property of amniotic membrane. *Cryobiology* 67 (3), 293–298. doi:10.1016/j.cryobiol.2013.08.010

Tehrani, F. A., Modaresifar, K., Azizian, S., and Niknejad, H. (2017). Induction of antimicrobial peptides secretion by IL-1β enhances human amniotic membrane for regenerative medicine. *Sci. Rep.* 7 (1), 17022. doi:10.1038/s41598-017-17210-7

Thadepalli, H., Appleman, M. D., Maidman, J. E., Arce, J. J., and Davidson, E. C., Jr (1977). Antimicrobial effect of amniotic fluid against anaerobic bacteria. *Am. J. Obstet. Gynecol.* 127 (3), 250–254. doi:10.1016/0002-9378(77)90463-x

Tian, K., Yang, S., Ren, Q., Han, Z., Lu, S., Ma, F., et al. (2010). p38 MAPK contributes to the growth inhibition of leukemic tumor cells mediated by human umbilical cord mesenchymal stem cells. *Cell. Physiol. biochem.* 26 (6), 799–808. doi:10.1159/000323973

Touboul, C., Lis, R., Al Farsi, H., Raynaud, C. M., Warfa, M., Althawadi, H., et al. (2013). Mesenchymal stem cells enhance ovarian cancer cell infiltration through IL6 secretion in an amniochorionic membrane based 3D model. *J. Transl. Med.* 11 (1), 28. doi:10.1186/1479-5876-11-28

Vaught, D. B., Stanford, J. C., and Cook, R. S. (2015). Efferocytosis creates a tumor microenvironment supportive of tumor survival and metastasis. *Cancer Cell Microenviron.* 2 (1), e666. doi:10.14800/ccm.666

Wang M, M., Cai, J., Huang, F., Zhu, M., Zhang, Q., Yang, T., et al. (2015). Pre-treatment of human umbilical cord-derived mesenchymal stem cells with interleukin-6 abolishes their growth-promoting effect on gastric cancer cells. *Int. J. Mol. Med.* 35 (2), 367–375. doi:10.3892/ijmm.2014.2019

Wang W, W., Zhong, W., Yuan, J., Yan, C., Hu, S., Tong, Y., et al. (2015). Involvement of Wnt/β-catenin signaling in the mesenchymal stem cells promote metastatic growth and chemoresistance of cholangiocarcinoma. *Oncotarget* 6 (39), 42276–42289. doi:10.18632/oncotarget.5514

Wang, X., Xie, J., Tan, L., Huo, J., and Xie, H. (2012). A new vision of definition, commentary, and understanding in clinical and translational medicine. *Clin. Transl. Med.* 6 (21), 5. doi:10.1186/2001-1326-1-5

Wiegand, I., Hilpert, K., and Hancock, R. E. (2008). Agar and broth dilution methods to determine the minimal inhibitory concentration (MIC) of antimicrobial substances. *Nat. Protoc.* 3 (2), 163–175. doi:10.1038/nprot.2007.521

Wilson, I. D., and Nicholson, J. K. (2017). Gut microbiome interactions with drug metabolism, efficacy, and toxicity. *Transl. Res.* 179, 204–222. doi:10.1016/j.trsl.2016.08.002

Wolbank, S., Hildner, F., Redl, H., van Griensven, M., Gabriel, C., and Hennerbichler, S. (2009). Impact of human amniotic membrane preparation on release of angiogenic factors. *J. Tissue Eng. Regen. Med.* 3 (8), 651–654. doi:10.1002/term.207

Wu, M., Yu, Z., Matar, D. Y., Karvar, M., Chen, Z., Ng, B., et al. (2022). Human amniotic membrane promotes angiogenesis in an oxidative stress chronic diabetic murine wound model. *Adv. Wound Care (New Rochelle)* [Epub ahead of print]. doi:10.1089/wound.2022.0005

Wu, S., Ju, G. Q., Du, T., Zhu, Y. J., and Liu, G. H. (2013). Microvesicles derived from human umbilical cord Wharton's jelly mesenchymal stem cells attenuate bladder tumor cell growth *in vitro* and *in vivo*. *PLoS One* 8 (4), e61366. doi:10.1371/journal.pone.0061366

Yadav, M. K., Go, Y. Y., Kim, S. H., Chae, S.-W., and Song, J.-J. (2017). Antimicrobial and antibiofilm effects of human amniotic/chorionic membrane extract on Streptococcus pneumoniae. *Front. Microbiol.* 8, 1948. doi:10.3389/fmicb.2017.01948

Yan, C., Li, S., Li, Z., Peng, H., Yuan, X., Jiang, L., et al. (2013). Human umbilical cord mesenchymal stem cells as vehicles of CD20-specific TRAIL fusion protein delivery: A double-target therapy against non-hodgkin's lymphoma. *Mol. Pharm.* 10 (1), 142–151. doi:10.1021/mp300261e

Yang, C., Lei, D., Ouyang, W., Ren, J., Li, H., Hu, J., et al. (2014a). Conditioned media from human adipose tissue-derived mesenchymal stem cells and umbilical cord-derived mesenchymal stem cells efficiently induced the apoptosis and differentiation in human glioma cell lines *in vitro*. *Biomed. Res. Int.* 2014, 109389. doi:10.1155/2014/109389

Yang, X., Li, Z., Ma, Y., Gao, J., Liu, S., Gao, Y., et al. (2014b). Human umbilical cord mesenchymal stem cells promote carcinoma growth and lymph node metastasis when co-injected with esophageal carcinoma cells in nude mice. *Cancer Cell Int.* 14 (1), 93. doi:10.1186/s12935-014-0093-9

Yuan L, L., Liu, Y., Qu, Y., Liu, L., and Li, H. (2019). Exosomes derived from MicroRNA-148b-3p-overexpressing human umbilical cord mesenchymal stem cells restrain breast cancer progression. *Front. Oncol.* 9, 1076. doi:10.3389/fonc.2019.01076

Yuan, Y., Lu, X., Tao, C. L., Chen, X., Shao, H. W., and Huang, S. L. (2013). Forced expression of indoleamine-2, 3-dioxygenase in human umbilical cord-derived mesenchymal stem cells abolishes their anti-apoptotic effect on leukemia cell lines *in vitro*. *Vitro Cell. Dev. Biol. -Animal.* 49 (10), 752–758. doi:10.1007/s11626-013-9667-4

Yuan, Y., Zhou, C., Chen, X., Tao, C., Cheng, H., and Lu, X. (2018). Suppression of tumor cell proliferation and migration by human umbilical cord mesenchymal stem cells: A possible role for apoptosis and wnt signaling. *Oncol. Lett.* 15 (6), 8536–8544. doi:10.3892/ol.2018.8368

Yuan Z, Z., Bian, Y., Ma, X., Tang, Z., Chen, N., and Shen, M. (2019). LncRNA H19 knockdown in human amniotic mesenchymal stem cells suppresses angiogenesis by associating with EZH2 and activating vasohibin-1. *Stem Cells Dev.* 28 (12), 781–790. doi:10.1089/scd.2019.0014

Zhang, J., Huang, J., Lin, X., Fei, K., Xie, Y., Peng, Q., et al. (2022). Phosphoglycerate mutase 5 promotes necroptosis in trophoblast cells through activation of dynamin-related protein 1 in early-onset preeclampsia. *Am. J. Reprod. Immunol.* 87 (6), e13539. doi:10.1111/aji.13539

Zhang, W., Yang, H., Zhang, Y., Lu, Y., Zhou, T., Li, M., et al. (2015). A biotherapy based on PSCs-in-3D spheroid-ameliorated biologics depletes *in vivo* cancer-sustaining stem cells. *Oncotarget* 6, 40762–40774. doi:10.18632/oncotarget.5691

Zhang, X., Yang, Y., Zhang, L., Lu, Y., Zhang, Q., Fan, D., et al. (2017). Mesenchymal stromal cells as vehicles of tetravalent bispecific Tandab (CD3/CD19) for the treatment of B cell lymphoma combined with Ido pathway inhibitor D-1-methyl-tryptophan. *J. Hematol. Oncol.* 10 (1), 56. doi:10.1186/s13045-017-0397-z

frontiers | Frontiers in Bioengineering and Biotechnology

TYPE Original Research
PUBLISHED 24 October 2022
DOI 10.3389/fbioe.2022.968346

OPEN ACCESS

EDITED BY
Heinz Redl,
Institute for Experimental and Clinical Traumatology (LBG), Austria

REVIEWED BY
Jingang An,
Peking University Hospital of Stomatology, China
Jochen Salber,
Ruhr-University Bochum, Germany

*CORRESPONDENCE
Florelle Gindraux,
fgindraux@chu-besancon.fr

SPECIALTY SECTION
This article was submitted to Tissue Engineering and Regenerative Medicine, a section of the journal Frontiers in Bioengineering and Biotechnology

RECEIVED 13 June 2022
ACCEPTED 23 September 2022
PUBLISHED 24 October 2022

CITATION
Odet S, Solecki L, Meyer C, Weber E, Chatelain B, Euvrard E, Barrabé A, Gualdi T, Parmentier A-L, Tatu L, Pouthier F, Louvrier A and Gindraux F (2022), Human amniotic membrane application in oral surgery—An ex vivo pilot study.
Front. Bioeng. Biotechnol. 10:968346.
doi: 10.3389/fbioe.2022.968346

Human amniotic membrane application in oral surgery—An *ex vivo* pilot study

Stéphane Odet[1], Lauriana Solecki[2], Christophe Meyer[1,3], Elise Weber[1], Brice Chatelain[1], Edouard Euvrard[1,2], Aude Barrabé[1], Thomas Gualdi[4], Anne-Laure Parmentier[4], Laurent Tatu[5,6], Fabienne Pouthier[7,8], Aurélien Louvrier[1,8] and Florelle Gindraux[1,3]*

[1]Service de chirurgie maxillo-faciale, stomatologie et odontologie hospitaliéère, CHU Besançon, Besançon, France, [2]Service d'ophtalmologie, CHU Besançon, Besançon, France, [3]Laboratoire de Nanomédecine, Imagerie, Thérapeutique EA 4662, Université Bourgogne Franche-Comté, Besançon, France, [4]INSERM Centre d'Investigation Clinique 1431, CHU Besançon, Besançon, France, [5]Service de neurologie, CHU Besançon, Besançon, France, [6]Laboratoire d'anatomie, Université Bourgogne Franche-Comté, Besançon, France, [7]AICT, Établissement français du sang Bourgogne Franche-Comté, Besançon, France, [8]Université Bourgogne Franche-Comté, INSERM, EFS BFC, UMR1098, RIGHT Interactions Greffon-Hôte-Tumeur/Ingénierie Cellulaire et Génique, Besançon, France

Objectives: The purpose of this pilot porcine study was to explore and illustrate the surgical application of human amniotic membrane (hAM) in an *ex vivo* model of medication-related osteonecrosis of the jaw (MRONJ).

Material and methods: Five oral and maxillofacial surgeons participated to this study. MRONJ was simulated on porcine mandible specimens. hAM was applied using four different techniques: implantation with complete coverage, implantation with partial coverage, apposition and covering graft material. At the same time, the surgeons evaluated how well the hAM handled and its physical properties during the surgery.

Results: Surgeons found that hAM had suitable mechanical properties, as it was easy to detach from the support, handle, bind to the defect and bury. hAM was also found to be strong and stable. The "implantation with complete coverage" and "implantation with partial coverage" techniques were the preferred choices for the MRONJ indication.

Conclusion: This study shows that hAM is a graft material with suitable properties for oral surgery. It is preferable to use it buried under the gingiva with sutures above it, which increases its stability. This technical note aims to educate surgeons and provide them with details about the handling of hAM in oral surgery.

Clinical relevance: Two surgical techniques for hAM application in MRONJ were identified and illustrated. hAM handling and physical properties during surgery were reported.

10.3389/fbioe.2022.968346

KEYWORDS

amniotic membrane, porcine jaw, oral mucosa, xenograft, *ex vivo*, osteonecrosis of the jaw and illustrations

Introduction

Human amniotic membrane (hAM) is the innermost layer of fetal membranes. It is composed of a single layer of epithelial cells, a basement membrane, and an avascular stroma containing amniotic mesenchymal stem cells, underlayered by the chorion. Its thickness (70–180 μm) varies among individuals (Chen et al., 2012; Gremare et al., 2019). The beneficial effects of hAM use have been widely described in the literature. To date, ophthalmology is one of the most popular applications of hAM (John, 2003).

Since the mid-1990s, there has been a growing interest in using hAM for oral surgery to accelerate tissue regeneration. One systematic review of literature explored the different indications for hAM use in oral surgery (Fenelon et al., 2018). In this line, two hAM configurations were identified (Odet et al., 2021): "implanted graft material" and "covering graft material". The first one was applied to gingival recession, bone defects in the furcation, bone defects in interproximal areas and surgical wounds after implant surgery. The second one was applied to mandibular vestibuloplasty and mucosal defects. Whereas hAM use in ophthalmology has been accompanied by informative surgical illustrations (Dua and Azuara-Blanco, 1999; Letko et al., 2001; John, 2003), its use in oral surgery is not described to the same extent, specifically its handling and surgical application. As a

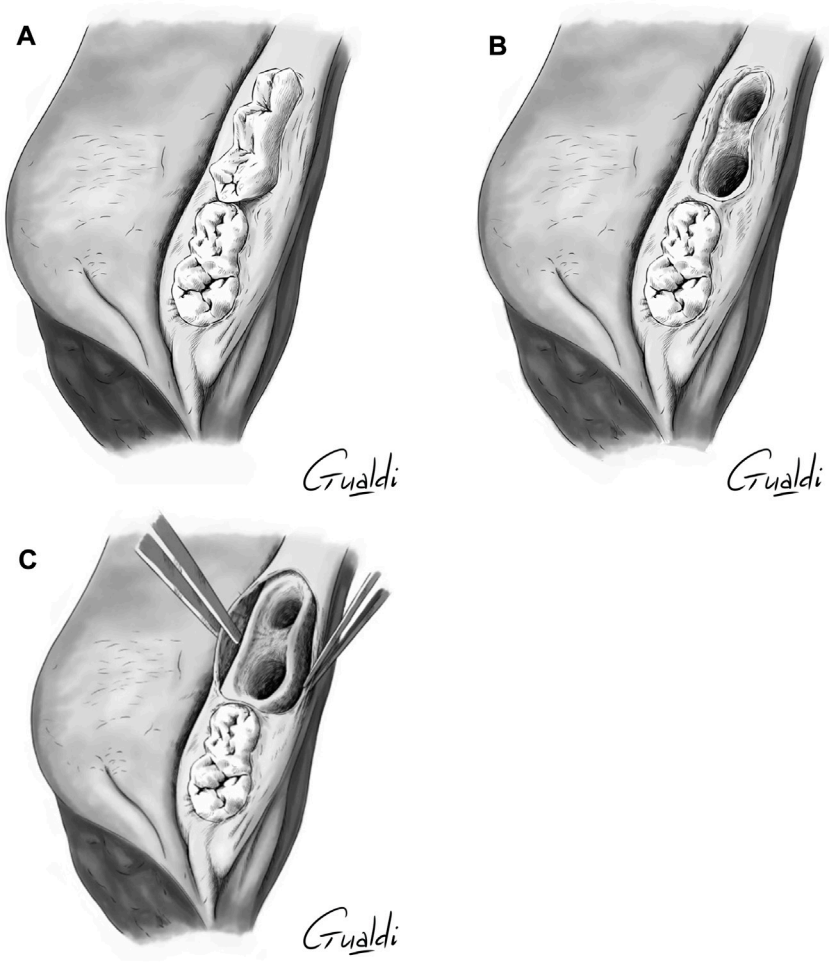

FIGURE 1
Simulation of MRONJ on porcine mandible specimen (upper view illustration): **(A)** Before premolar extraction; **(B)** After premolar extraction; **(C)** After gingival detachment from the alveolar bone.

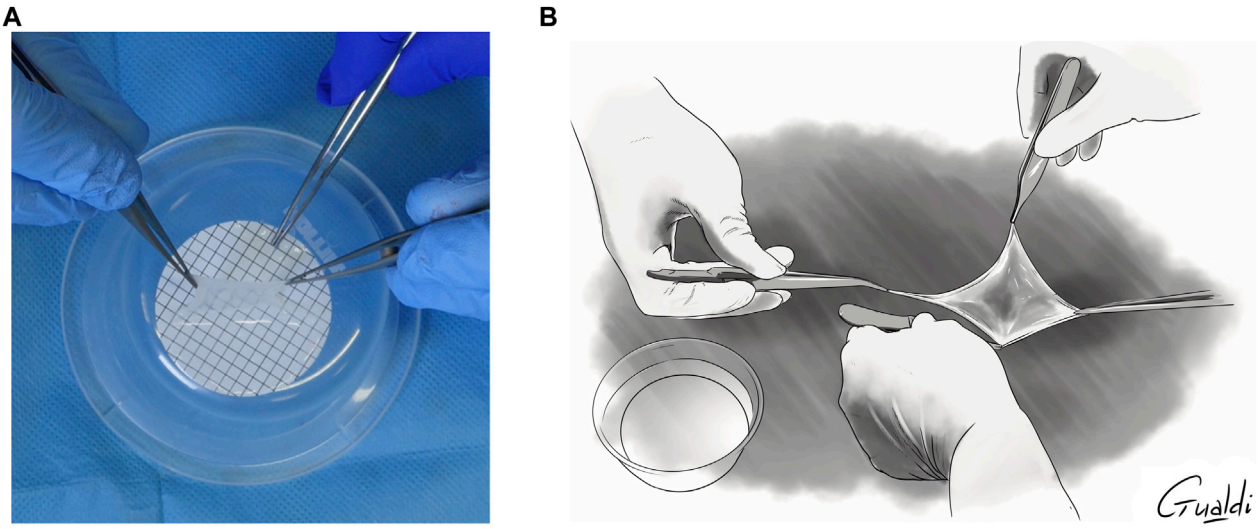

FIGURE 2
(A) hAM detachment from the nitrocellulose support. **(B)** "Four hands" application of hAM.

consequence, a specific nomenclature beyond the previously mentioned terms—"implanted graft material" and "covering graft material"—was necessary (Odet et al., 2021). Along these lines, four theorical types of hAM surgeries are proposed:

1) *"implantation"*, where the hAM is buried and completely covered by the gingiva
2) *"apposition"*, where the hAM is applied against the site to be treated, not sutured, left exposed in the mouth and stabilized by any means (cross stitches, pressure dressing, palatal plates, etc.)
3) *"whole covering graft material"*, where the hAM is applied against the site to be treated, sutured to adjacent mucosa or underlying mucosa, fully left exposed in the mouth and protected by any means (cross stitches, pressure dressing, palatal plates, etc.)
4) *"partial covering graft material"*, where the hAM is applied against the bone, buried under the wound edges, sutured to adjacent mucosa or underlying mucosa, left partially exposed in the mouth and protected by any means (cross stitches, pressure dressing, palatal plates, etc.).

However, no study has provided details about how to handle cryopreserved hAM which is more challenging to cut, orient (mesenchymal versus epithelial side), manipulate and apply than the lyophilized or dehydrated amnion or amnion-chorion often used in oral surgery (Fenelon et al., 2018; Gulameabasse et al., 2020; Odet et al., 2021).

As previously investigated by Ragazzo et al. (Ragazzo et al., 2018; Ragazzo et al., 2021), our team wanted to use hAM to manage medication-related osteonecrosis of the jaw (MRONJ) in a compassionate clinical trial (Odet et al., 2022). Despite our extensive experience with hAM banking, its *in vitro*/*in vivo* osteogenic potential, and its use in oral, bone and nerve surgeries (Gindraux and Obert, 2010; Obert et al., 2012; Gindraux et al., 2013; Laurent et al., 2014a; Laurent et al., 2014b; Laurent et al., 2014c; Gindraux et al., 2017; Laurent et al., 2017; Fénelon et al., 2018; Bourgeois et al., 2019; Fenelon et al., 2019; Gualdi et al., 2019; Fenelon et al., 2020; Etchebarne et al., 2021; Fénelon et al., 2021; Fenelon et al., 2021; Odet et al., 2021), we failed to identify how to handle and apply hAM during surgery in the oral cavity. Thus, an *ex vivo* pilot study was required to fill these voids and train the surgeons.

Porcine jaw specimens are common *in vivo* models for oral and maxillofacial surgery, as the bone, teeth and mucosa have similar appearance, size and structure as the human jaw (Deppe et al., 2018; Kniha et al., 2021). So, MRONJ was simulated in fresh porcine mandible specimens to investigate 1) the handling of cryopreserved hAM and its related physical properties for oral surgery, and 2) the four previously listed theorical types of hAM surgeries. No specific MRONJ grade was targeted in this study. A questionnaire was developed to collect surgeon feedback. Thus, this technical note only defines hAM handling, its

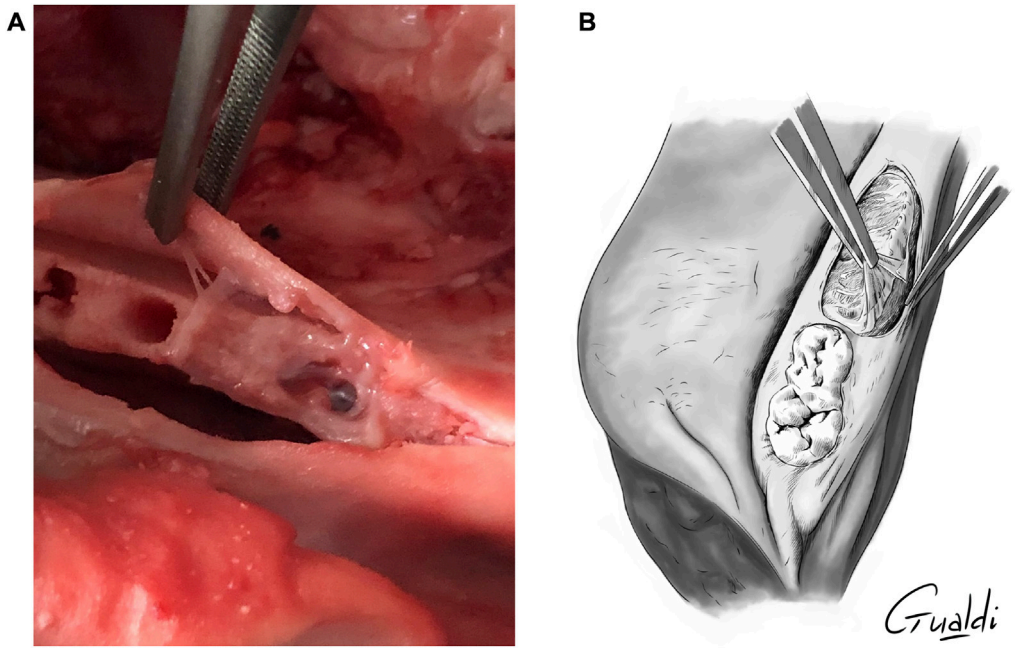

FIGURE 3
(A) hAM application on MRONJ simulation site. **(B)** hAM burying between bone and gingiva (upper view illustration).

physical properties and surgical application in an *ex vivo* MRONJ model. It provides surgeons with tips and tricks for hAM application in oral surgery or more broadly, in soft tissue regeneration.

Material and methods

The work for this technical note was performed at the anatomy laboratory of the University of Franche-Comté (Besançon, France). Five maxillofacial and oral surgeons (CM, EE, EW, AB, SO), one ophthalmologist and one methodologist participated in the training. The fresh porcine mandible specimens were provided by Chevillotte Breeders (Valdahon, France). All the hAM application techniques were filmed by the group "Tête de Com", and all the illustrations were made by Mr. Thomas Gualdi, a scientific illustrator.

hAM suitable for scientific purposes were provided by the AICT bank from the French Blood Institute (Etablissement Français du Sang). A 4.7-cm diameter cryopreserved hAM stored in glycerol on a nitrocellulose support (epithelial layer facing the support) was thawed for 2 h at room temperature. After three 5 min rinses in saline or hypotonic injection solution, the hAM was cut either on the nitrocellulose support or after being detached from it.

MRONJ simulation

A sulcular incision on two adjacent teeth was made in the premolar area of the porcine mandible (Figures 1A–C). Two teeth were extracted, and a 3-mm wide defect was created by resecting the mucosa on the vestibular edge of the incision, simulating MRONJ. The alveolar bone was resected over approximately 3 mm using a rongeur. Here, no specific MRONJ grade was targeted.

For the "hAM implantation with complete coverage" technique (see below), a horizontal periosteum incision was made on the two full thickness vestibular and lingual flaps to allow tensionless closure on the mucosal edges.

hAM applications

Two surgeons were needed to separate the hAM from its support: one detached the hAM with two forceps (without teeth) while the other held the support with another set of forceps (Figure 2A). The hAM tended to fold upon itself once detached from the support. Two options were used to unfold and apply it. The first one needed two surgeons: one held the membrane while the second unfolded it using two forceps without teeth. Later, both surgeons applied it on the surgical site ("with four hands") in the desired orientation (Figure 2B). In the second option, only one

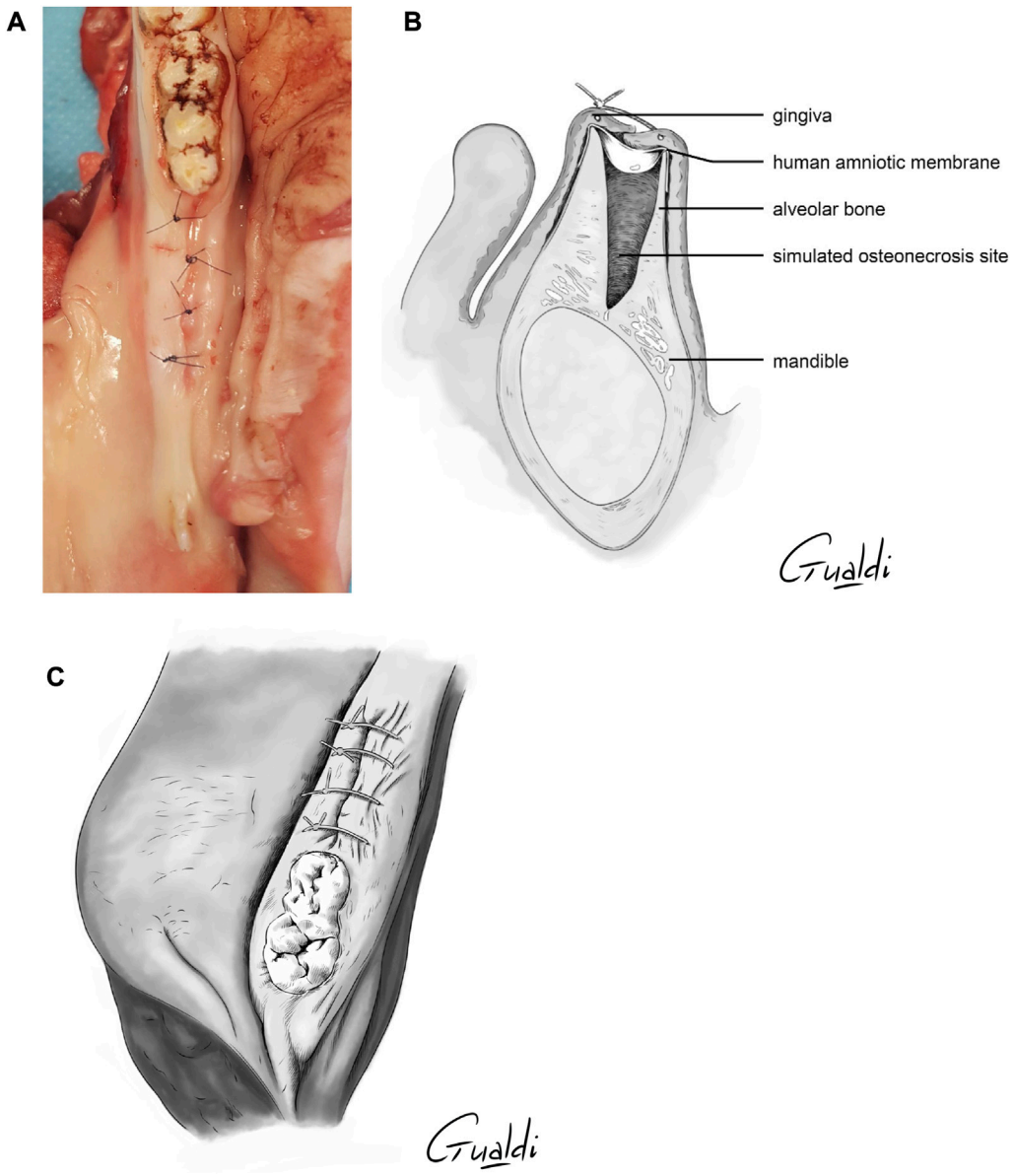

FIGURE 4
hAM implantation with complete coverage. The sutures were realized above the implanted hAM which was thus not visible. **(A)** Photography; **(B)** Sagittal section illustration; **(C)** Upper view illustration.

surgeon was required: once the hAM was detached from the support, it was directly applied on the surgical site, and then unfolded using two forceps. The hAM's orientation was quite difficult to maintain in this case.

The four theoretical techniques identified by Odet et al. (Odet et al., 2021) were attempted and adapted to this experimental study. After hAM application at the MRONJ site (Figure 3A), hAM was buried between bone and gingiva when necessary (Figure 3B). In all cases, hAM could be cut into the desired shape and size and then applied with the mesenchymal side facing the bone and the epithelial side facing the gingiva. One to two hAM units were manipulated by the surgeon.

Evaluation by surgeons

hAM handling and physical properties during the surgery were evaluated with a questionnaire. The studied parameters were:

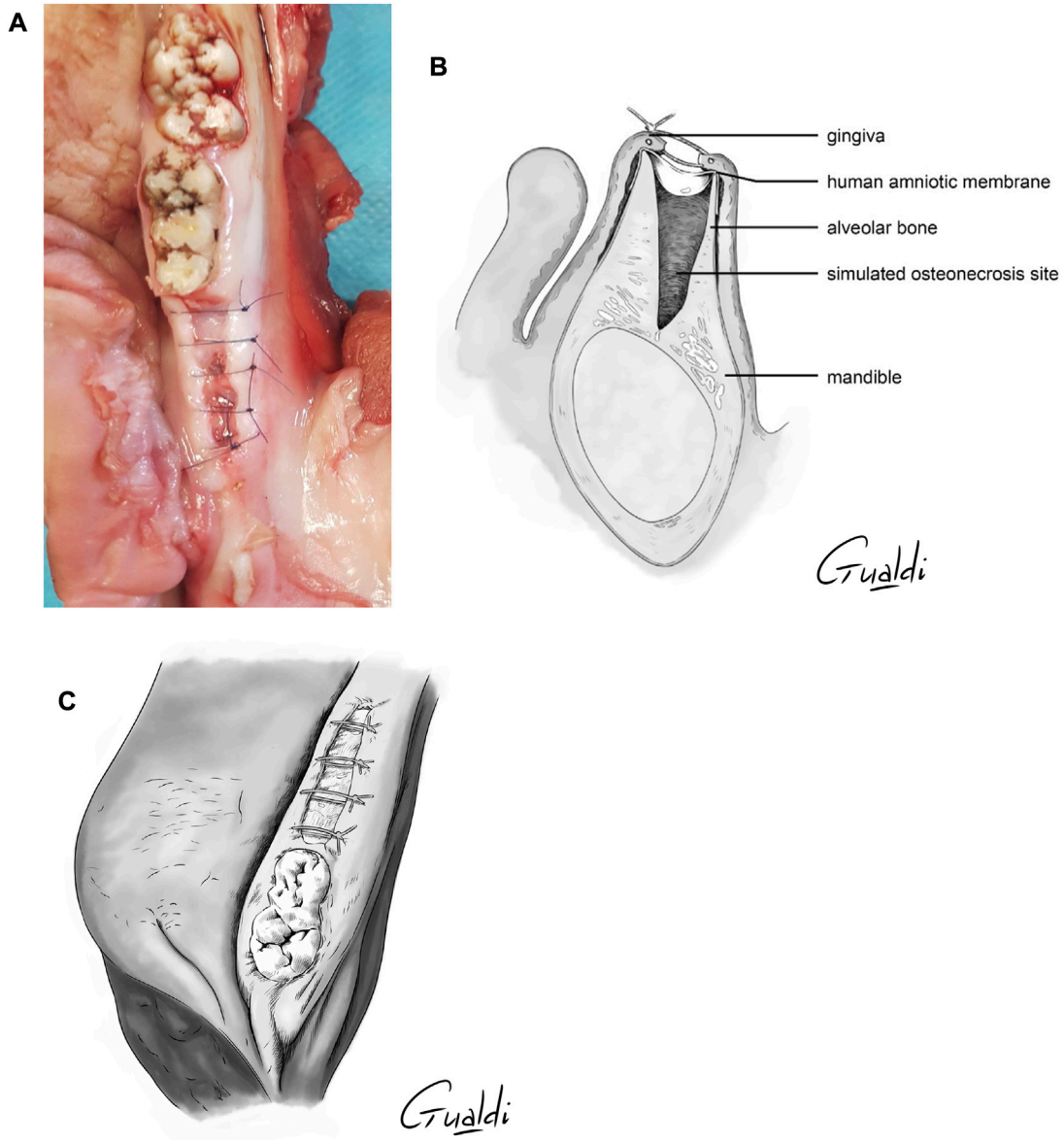

FIGURE 5
hAM implantation with partial coverage. The gingiva was sutured above the hAM, but leaving the hAM exposed in the oral cavity. **(A)** Photography; **(B)** Sagittal section illustration; **(C)** Upper view illustration.

1) ease of detaching the hAM from the nitrocellulose support
2) hAM handling
3) hAM adhesion once applied on the defect (bone)
4) hAM strength
5) ease of suturing the hAM
6) ease of burying the hAM between the bone and mucosa.

These parameters were evaluated on a scale of 0–10 (0 = impossible to handle the hAM/failure of the procedure; 10 = perfect handling/success of the procedure). Grading was left up to each surgeon.

Additional parameters included

1) easiest way to cut the hAM: when still bound to the support or after being detached
2) easiest way to apply the hAM on the surgical site: flat or folded on itself
3) stability of hAM during suturing once applied on the surgical site.

TABLE 1 Evaluation by the surgeons. ND: not done.

Operators	Easiest localization to cut the hAM	Facility to detach hAM from nitrocellulose support	hAM handling	hAM adhesion once applied on the defect	hAM resistance	Facility to suture the hAM	Facility to bury hAM between the bone and the mucosa	Easiest way to apply hAM on the surgical site	Stability of hAM during sutures
CM	Support	7	4	6	3	0	5	Folded on itself	YES
EE	Support	6	7	9	8	ND	7	Folded on itself	YES
EW	Support	8	8	7	10	5	9	Flat	NO
AB	Support	8	8	7	10	5	9	Flat	NO
SO	Support	8	8	8	9	4	8	Flat	NO
MEAN	-	7.4	7	7.4	8	3.5	7.6	-	-

Results

hAM applications

The four theoretical techniques previously mentioned were attempted and adapted to this practical study as follows:

1) *Implantation with complete coverage* (Figures 4A–C): the hAM was applied and buried between the bone and mucosa (Figure 3B). The mucoperiosteal flap was reapplied over the hAM and sutured hermetically above it, using simple or cross stitches.
2) *Implantation with partial coverage* (Figures 5A–C): the hAM was applied and buried between the bone and mucosa (Figure 3B). The mucoperiosteal flap was then sutured above it, non-hermetically. In this case, the hAM was left exposed in the oral cavity.
3) *Apposition*: the hAM was simply applied "in apposition" against the defect, without burying it between the bone and mucosa. The mucosa was then closed above it as hermetically as possible, using simple or cross stitches. Compared to the initial nomenclature, the hAM was not sutured.
4) *Covering graft material*: The hAM was cut into the desired shape, applied on the defect and sutured directly to the adjacent mucosa, using single stitches.

Video of the procedure:

https://https://youtu.be/GKy3I-n3NRQ

Surgeon evaluation

The surgeons noted that hAM was easy to work with overall (Table 1).

1) To detach from the nitrocellulose support: mean of 7.4 (6–8)
2) To handle: mean of 7.0 (4–8)
3) To bind to the defect: mean of 7.4 (6–9)
4) To bury between the bone and mucosa once applied on the defect: mean of 7.6 (5–9).

With a mean of 8 (3–10), surgeons found the hAM was very strong during manipulation, particularly when detached from the nitrocellulose support. However, all surgeons had difficulties when suturing it due to its fragility (because the stitch caused a crack during tightening) and its tendency to fold upon itself, making it hard to suture. After thawing and rinsing, wet hAM tended to fold on itself, making it difficult to manipulate and cut it from its nitrocellulose support. All surgeons agreed that it was easier to cut hAM when it was still bound to its support.

Two surgeons mentioned that hAM was easier to apply on the surgical site when it was folded upon itself. They noticed that the folding increased its thickness but that it was impossible to maintain its orientation. The other surgeons found that it was easier to use it flat and mentioned two advantages: hAM orientation and burying between the bone and mucosa.

hAM was found to be unstable at the surgical site during suturing by three surgeons. In these cases, hAM tended to rise up between the stitches when the mucosal edges were approximated. However, it was stable enough that it was not expelled from the surgical site. In contrast, two surgeons found that hAM was quite stable during suturing, without any movement or oral exposition from the hAM.

Discussion

The aim of this pilot porcine study was to reproduce MRONJ in fresh porcine mandible specimens and to describe hAM

handling and physical properties during surgery. First it allowed us to refine the theorical nomenclature previously proposed for MRONJ (Odet et al., 2021). Second it assisted us in the practical aspects of our clinical study (Odet et al., 2022).

Of the four techniques evaluated, only two proved to be useful in MRONJ surgery: implantation with complete coverage and implantation with partial coverage. In both techniques, the hAM was very stable as it adhered to the bone and did not move when placing sutures above it. The common aspect of these the two techniques was that wet hAM was buried between the bone and mucosa, which increased its stability.

In contrast, there was no burying of hAM in the apposition technique. Compared to the initial nomenclature, the hAM was not sutured due to its fragility. Thus, wet hAM applied without burying on mucosa/bone nor suturing was unstable and the instability increased with suturing of the gingiva above it. Similarly, the absence of burying in the covering graft technique made hAM unstable on mucosa/bone. In this last technique, suturing of hAM to the gingiva was the hardest part. Suturing of hAM to the mucosa shifted the allograft from the surgical site and made it fold upon itself. This makes hAM unsuitable for the suturing performed during oral surgery. Indeed, the dimensions of the suture material usually range from 3/0 (largest) to 6/0 (thinnest). These types of sutures lacerated the hAM because it is relatively thin. This is in contrast with hAM use in ophthalmology where the allograft is always sutured with smaller suture material—10/0 nylon or 8/10 to 10/0 VICRYL or PROLENE sutures (Sippel et al., 2001)—which produce less cracking of the hAM.

Odet's review of literature distinguished two types of hAM application in the oral cavity (Odet et al., 2021). First, hAM could be used as an "implanted graft material" in periodontology and implantology. In these cases, the procedure was similar to our "implantation with complete coverage" technique, as the hAM was completely covered by the mucosa. Second, hAM was used as a "covering graft material" in mucosal defects of the oral cavity or in mandibular vestibuloplasties. In these cases, hAM was either directly sutured to the adjacent mucosa or simply applied on the defect to be filled and secured by any means (splints, sutured gauze, etc.) (Samandari et al., 2004; Arai et al., 2012; Amemiya et al., 2015). Here, this second type of surgery involves suturing of hAM which makes it unsuitable to MRONJ.

This technical note supplements the existing literature (Dua and Azuara-Blanco, 1999; Letko et al., 2001; John, 2003) and provides information on how to handle cryopreserved hAM in MRONJ. Detailed and novel illustrations are provided to assist maxillofacial and oral surgeons who want to use hAM in this application.

Conclusion

This technical note showed that hAM implantation with complete or partial coverage techniques is the preferred choice in an *ex vivo* MRONJ model. Directly suturing to the adjacent mucosa is hardly feasible because of the suture size and the relative thinness of hAM. In oral surgery, cryopreserved hAM has adequate adherence to both bone and mucosa and good stability once applied. This technical note also describes tips and tricks on hAM handling and provides practical illustrations to assist maxillofacial and oral surgeons in hAM application.

Data availability statement

The original contributions presented in the study are included in the article/supplementary materials, further inquiries can be directed to the corresponding author.

Ethics statement

Ethical review and approval was not required for the animal study because porcine jaw specimens.

Author contributions

FG, CM, LT, and SO elaborated the design of the study and organized the educational school at the University. FG supervised the training. SO and LS taught the technique to the surgeons. CM, EW, BC, EE, AB, and AL did the experimentations. TG elaborated the illustrations. AP studied the methodology to transfer it to clinical situation. FP provided the hAM. SO and FG wrote the manuscript. All authors contributed to manuscript revision, read, and approved the submitted version.

Funding

This study was supported by a grant from the French Ministry of Health (PHRCI-2020). This publication is based upon work from COST Action 17116 "SPRINT", supported by COST (European Cooperation in Science and Technology)—www.cost.eu.

Acknowledgments

The authors are grateful to Éleveurs de la Chevillotte (Valdahon, Besançon) and Société Bisontine d'Abattage-SBA (Besançon, France) for porcine mandible specimens; Hughes Grandin (Laboratoire d'Anatomie, Université de Franche-Comté, Besançon) for his high availability; TG (thomas-gualdi.fr) for the high quality of his illustrations and Franck Daval (Bibliothèque Universitaire Santé, Université Bourgogne Franche-Comté, Besançon, France) for the very helpful bibliographic support. The

authors acknowledge the language support provided by Joanne Archambault.

Conflict of interest

The authors declare that the research was conducted in the absence of any commercial or financial relationships that could be construed as a potential conflict of interest.

Publisher's note

All claims expressed in this article are solely those of the authors and do not necessarily represent those of their affiliated organizations, or those of the publisher, the editors and the reviewers. Any product that may be evaluated in this article, or claim that may be made by its manufacturer, is not guaranteed or endorsed by the publisher.

References

Amemiya, T., Nakamura, T., Yamamoto, T., Kinoshita, S., and Kanamura, N. (2015). Autologous transplantation of oral mucosal epithelial cell sheets cultured on an amniotic membrane substrate for intraoral mucosal defects. *PLoS One* 10, e0125391. doi:10.1371/journal.pone.0125391

Arai, N., Tsuno, H., Okabe, M., Yoshida, T., Koike, C., Noguchi, M., et al. (2012). Clinical application of a hyperdry amniotic membrane on surgical defects of the oral mucosa. *J. Oral Maxillofac. Surg.* 70, 2221–2228. doi:10.1016/j.joms.2011.09.033

Bourgeois, M., Loisel, F., Obert, L., Pluvy, I., and Gindraux, F. (2019). Can the amniotic membrane be used to treat peripheral nerve defects? A review of literature. *Hand Surg. Rehabilitation* 38, 223–232. doi:10.1016/j.hansur.2019.05.006

Chen, B., Jones, R. R., Mi, S., Foster, J., Alcock, S. G., Hamley, I. W., et al. (2012). The mechanical properties of amniotic membrane influence its effect as a biomaterial for ocular surface repair. *Soft Matter* 8, 8379–8387. doi:10.1039/c2sm26175h

Deppe, H., Wolff, C., Bauer, F., Ruthenberg, R., Sculean, A., and Mücke, T. (2018). Dental implant surfaces after insertion in bone: An *in vitro* study in four commercial implant systems. *Clin. Oral Investig.* 22, 1593–1600. doi:10.1007/s00784-017-2262-4

Dua, H. S., and Azuara-Blanco, A. (1999). Amniotic membrane transplantation. *Br. J. Ophthalmol.* 83, 748–752. doi:10.1136/bjo.83.6.748

Etchebarne, M., Fricain, J.-C., Kerdjoudj, H., Di Pietro, R., Wolbank, S., Gindraux, F., et al. (2021). Use of amniotic membrane and its derived products for bone regeneration: A systematic review. *Front. Bioeng. Biotechnol.* 9, 661332. doi:10.3389/fbioe.2021.661332

Fenelon, M., B Maurel, D., Siadous, R., Gremare, A., Delmond, S., Durand, M., et al. (2019). Comparison of the impact of preservation methods on amniotic membrane properties for tissue engineering applications. *Mater. Sci. Eng. C* 104, 109903. doi:10.1016/j.msec.2019.109903

Fenelon, M., Catros, S., and Fricain, J. C. (2018). What is the benefit of using amniotic membrane in oral surgery? A comprehensive review of clinical studies. *Clin. Oral Investig.* 22, 1881–1891. doi:10.1007/s00784-018-2457-3

Fénelon, M., Catros, S., Meyer, C., Fricain, J.-C., Obert, L., Auber, F., et al. (2021). Applications of human amniotic membrane for tissue engineering. *Membranes* 11, 387. doi:10.3390/membranes11060387

Fénelon, M., Chassande, O., Kalisky, J., Gindraux, F., Brun, S., Bareille, R., et al. (2018). Human amniotic membrane for guided bone regeneration of calvarial defects in mice. *J. Mat. Sci. Mat. Med.* 29, 78. doi:10.1007/s10856-018-6086-9

Fenelon, M., Etchebarne, M., Siadous, R., Grémare, A., Durand, M., Sentilhes, L., et al. (2021). Comparison of amniotic membrane versus the induced membrane for bone regeneration in long bone segmental defects using calcium phosphate cement loaded with BMP-2. *Mater. Sci. Eng. C* 124, 112032. doi:10.1016/j.msec.2021.112032

Fenelon, M., Etchebarne, M., Siadous, R., Grémare, A., Durand, M., Sentilhes, L., et al. (2020). Assessment of fresh and preserved amniotic membrane for guided bone regeneration in mice. *J. Biomed. Mat. Res. A* 108, 2044–2056. doi:10.1002/jbm.a.36964

Gindraux, F., Laurent, R., Nicod, L., De Billy, B., Meyer, C., Zwetyenga, N., et al. (2013). Human amniotic membrane: Clinical uses, patents and marketed products. *Recent Pat. Regen. Med.* 3, 193–214. doi:10.2174/22102965113039990021

Gindraux, F., and Obert, L. (2010). "Human amniotic membranes: Benefits for bone repair/regeneration," in *Bioreconstruction : De l'os à la peau tome 2*. Editor S. M. France, 85–91.

Gindraux, F., Rondot, T., De Billy, B., Zwetyenga, N., Fricain, J.-C., Pagnon, A., et al. (2017). Similarities between induced membrane and amniotic membrane: Novelty for bone repair. *Placenta* 59, 116–123. doi:10.1016/j.placenta.2017.06.340

Gremare, A., Jean-Gilles, S., Musqui, P., Magnan, L., Torres, Y., Fenelon, M., et al. (2019). Cartography of the mechanical properties of the human amniotic membrane. *J. Mech. Behav. Biomed. Mat.* 99, 18–26. doi:10.1016/j.jmbbm.2019.07.007

Gualdi, T., Laurent, R., Moutarlier, V., Fenelon, M., Nallet, A., Pouthier, F., et al. (2019). *In vitro* osteodifferentiation of intact human amniotic membrane is not beneficial in the context of bone repair. *Cell Tissue Bank.* 20, 435–446. doi:10.1007/s10561-019-09778-3

Gulameabasse, S., Gindraux, F., Catros, S., Fricain, J. C., and Fenelon, M. (2020). Chorion and amnion/chorion membranes in oral and periodontal surgery: A systematic review. *J. Biomed. Mat. Res.* 109, 1216–1229. doi:10.1002/jbm.b.34783

John, T. (2003). Human amniotic membrane transplantation: Past, present, and future. *Ophthalmol. Clin. North Am.* 16, 43–65. vi. doi:10.1016/s0896-1549(02)00110-4

Kniha, K., Buhl, E. M., Hermanns-Sachweh, B., Al-Sibai, F., Bock, A., Peters, F., et al. (2021). Implant removal using thermal necrosis—An *in vitro* pilot study. *Clin. Oral Investig.* 25, 265–273. doi:10.1007/s00784-020-03361-x

Laurent, R., . Brennan, M., . Renaud, A., . D'arros, C., . Obert, L., . Layrolle, P., et al. (2014b). Osteodifferenciation of intact human amniotic membrane through a jet sprayed polycaprolactone nanofibre scaffold. *Orthop. Proc.* 96, 113.

Laurent, R., Nallet, A., De Billy, B., Obert, L., Nicod, L., Meyer, C., et al. (2017). Fresh and *in vitro* osteodifferentiated human amniotic membrane, alone or associated with an additional scaffold, does not induce ectopic bone formation in Balb/c mice. *Cell Tissue Bank.* 18, 17–25. doi:10.1007/s10561-016-9605-2

Laurent, R., Nallet, A., Obert, L., Nicod, L., and Gindraux, F. (2014c). Storage and qualification of viable intact human amniotic graft and technology transfer to a tissue bank. *Cell Tissue Bank.* 15, 267–275. doi:10.1007/s10561-014-9437-x

Laurent, R., . Nicod, L., . Layrolle, P., . de Billy, B., . Obert, L., and . Gindraux, F. (2014a). Osteogenic potential and immunogenicity of human amniotic membrane: *In vitro* and *in vivo* studies. *Orthop. Proc.* 96-B, 112.

Letko, E., Stechschulte, S. U., Kenyon, K. R., Sadeq, N., Romero, T. R., Samson, C. M., et al. (2001). Amniotic membrane inlay and overlay grafting for corneal epithelial defects and stromal ulcers. *Arch. Ophthalmol.* 119, 659–663. doi:10.1001/archopht.119.5.659

Obert, L., Genestier, L., Froidevaux, L., Averlant, E., Laurent, R., Wajszczak, L., et al. (2012). "Amniotic membrane for bone repair? Reflection around of the masquelet technique to one stage/membrane amniotique pour la réparation osseuse ? Réflexion autour de la simplification de la technique de Masquelet à une chirurgie," in *Technique de Masquelet. Sauramps médical.*

Odet, S., Louvrier, A., Meyer, C., Nicolas, F. J., Hofman, N., Chatelain, B., et al. (2021). Surgical application of human amniotic membrane and amnion-chorion membrane in the oral cavity and efficacy evaluation: Corollary with ophthalmological and wound healing experiences. *Front. Bioeng. Biotechnol.* 9, 685128. doi:10.3389/fbioe.2021.685128

Odet, S., Meyer, C., Gaudet, C., Weber, E., Quenot, J., Derruau, S., et al. (2022). Tips and tricks and clinical outcome of cryopreserved human amniotic membrane application for the management of medication-related osteonecrosis of the jaw (MRONJ): A pilot study. *Front. Bioeng. Biotechnol.* 10, 936074. doi:10.3389/fbioe.2022.936074

Ragazzo, M., Trojan, D., Spagnol, L., Paolin, A., and Guarda Nardini, L. (2018). Use of amniotic membrane in the treatment of patients with BRONJ: Two case reports. *J. Surg. Case Rep.* 2018, rjy073. doi:10.1093/jscr/rjy073

Ragazzo, M., Val, M., Montagner, G., Trojan, D., Fusetti, S., and Guarda Nardini, L. (2021). Human amniotic membrane: An improvement in the treatment of medication-related osteonecrosis of the jaw (MRONJ)? A case–control study. *Cell Tissue Bank.* 23 (1), 129–141. doi:10.1007/s10561-021-09922-y

Samandari, M. H., Yaghmaei, M., Ejlali, M., Moshref, M., and Saffar, A. S. (2004). Use of amnion as a graft material in vestibuloplasty: A preliminary report. *Oral Surg. Oral Med. Oral Pathology, Oral Radiology, Endodontology* 97, 574–578. doi:10.1016/j.tripleo.2003.10.031

Sippel, K. C., Ma, J. J. K., and Foster, C. S. (2001). Amniotic membrane surgery. *Curr. Opin. Ophthalmol.* 12, 269–281. doi:10.1097/00055735-200108000-00006

frontiers | Frontiers in Bioengineering and Biotechnology

TYPE Review
PUBLISHED 08 November 2022
DOI 10.3389/fbioe.2022.969927

OPEN ACCESS

EDITED BY
Guei-Sheung Liu,
Centre for Eye Research Australia, Australia

REVIEWED BY
Guido Moll,
Charité Universitätsmedizin Berlin, Germany
La-ongsri Atchaneeyasakul,
Mahidol University, Thailand

*CORRESPONDENCE
Esmeralda Costa,
esmeraldaguedes@gmail.com
Marta Agudo-Barriuso,
martabar@um.es

SPECIALTY SECTION
This article was submitted to Tissue Engineering and Regenerative Medicine, a section of the journal Frontiers in Bioengineering and Biotechnology

RECEIVED 15 June 2022
ACCEPTED 17 October 2022
PUBLISHED 08 November 2022

CITATION
Norte-Muñoz M, Botelho MF, Schoeberlein A, Chaves J, Neto Murta J, Ponsaerts P, Agudo-Barriuso M and Costa E (2022), Insights and future directions for the application of perinatal derivatives in eye diseases: A critical review of preclinical and clinical studies.
Front. Bioeng. Biotechnol. 10:969927.
doi: 10.3389/fbioe.2022.969927

Insights and future directions for the application of perinatal derivatives in eye diseases: A critical review of preclinical and clinical studies

María Norte-Muñoz[1], Maria Filomena Botelho[2,3,4], Andreina Schoeberlein[5,6], João Chaves[7], Joaquim Neto Murta[3,4,7,8], Peter Ponsaerts[9], Marta Agudo-Barriuso[1]* and Esmeralda Costa[3,4,7,8]*

[1]Experimental Ophthalmology Group, IMIB-Arrixaca, University of Murcia, Murcia, Spain, [2]Institute of Biophysics and Institute for Clinical and Biomedical Research (iCBR), Area of Environment Genetics and Oncobiology (CIMAGO), Faculty of Medicine, University of Coimbra, Coimbra, Portugal, [3]Center for Innovative Biomedicine and Biotechnology (CIBB), University of Coimbra, Coimbra, Portugal, [4]Clinical and Academic Centre of Coimbra (CACC), Coimbra, Portugal, [5]Department of Obstetrics and Feto-maternal Medicine, Inselspital, Bern University Hospital, University of Bern, Bern, Switzerland, [6]Department for BioMedical Research (DBMR), University of Bern, Bern, Switzerland, [7]Ophthalmology Department, Centro Hospitalar e Universitário de Coimbra, Coimbra, Portugal, [8]Ophtalmology Universitary Clinic and Institute for Clinical and Biomedical Research (iCBR), Faculty of Medicine, University of Coimbra, Coimbra, Portugal, [9]Laboratory of Experimental Hematology, Vaccine and Infectious Disease Institute (Vaxinfectio), University of Antwerp, Antwerp, Belgium

Perinatal derivatives (PnD) are gaining interest as a source for cell-based therapies. Since the eye is easily accessible to local administration, eye diseases may be excellent candidates to evaluate novel therapeutic approaches. With this work, we performed a systematic review of published preclinical and clinical studies addressing PnD in the treatment of ocular diseases. We have set two specific objectives: (i) to investigate the current level of standardization in applied technical procedures in preclinical studies and (ii) to assess clinical efficacy in clinical trials. Hereto, we selected studies that applied amniotic membrane (hAM) and mesenchymal stromal cells derived from amniotic membrane (hAMSC), placenta (hPMSC), umbilical cord (hUC-MSC) and Wharton's Jelly (hUC-WJ-MSC), excluding those where cells were not transplanted individually, following a systematic PubMed search for preclinical studies and consultation of clinical studies on https://clinicaltrials.gov and https://www.clinicaltrialsregister.eu/. Our bibliographic search retrieved 26 pre-clinical studies and 27 clinical trials. There was a considerable overlap regarding targeted ocular structures. Another common feature is the marked tendency towards (i) locally administered treatments and (ii) the PnD type. In the cornea/ocular surface, hAM was preferred and usually applied directly covering the ocular surface. For neuroretinal disorders, intra-ocular injection of umbilical or placental-derived cells was preferred. In general, basic research reported favourable outcomes. However, due to lack of standardization between different studies, until now there is no clear consensus regarding the fate of administered PnD or their mode of action.

This might be accountable for the low index of clinical translation. Regarding clinical trials, only a minority provided results and a considerable proportion is in "unknown status". Nevertheless, from the limited clinical evidence available, hAM proved beneficial in the symptomatic relief of bullous keratopathy, treating dry eye disease and preventing glaucoma drainage device tube exposure. Regarding neuroretinal diseases, application of Wharton's Jelly MSC seems to become a promising future approach. In conclusion, PnD-based therapies seem to be beneficial in the treatment of several ocular diseases. However, much is yet to be done both in the pre-clinical and in the clinical setting before they can be included in the daily ophthalmic practice.

KEYWORDS

perinatal derivates, ophthalmology, preclinical models, clinical trials and database search, mesenchymal stromal cells

1 Introduction

Cell therapy encompasses a wide range of treatment strategies that use cells as therapeutic agents. Although cellular therapies have multiple beneficial properties, the rationale supporting the application of cellular medicines varies depending on the source of cells, the target organ or disease. Focusing on research using stem cells, based on their developmental status they can be classified into (i) embryonic stem cells (ESC) and (ii) adult stem cells (ASC). ESCs are extracted from the inner cell mass of blastocysts. They actively divide and applied as such are tumorigenic *in vivo*, which, together with their implicit ethical problems, means that they are of little benefit to patients in an undifferentiated stage. ASC encompass a wide variety of (stem) cell types that can be obtained postnatal from neonate to adulthood, but also from extra-embryonic perinatal tissues. Several examples of well-known ASC are those derived from bone marrow, dental pulp or adipose tissue (AT). They are widely investigated in novel regenerative medicine strategies because they can be isolated from the patient with little discomfort, and there are no ethical concerns. However, the efficacy of ASC therapy, apart from bone marrow transplantation for hematological malignancies, varies depending on their source, the age of the donors and, importantly, their health (Torre and Flores, 2020). On the other hand, perinatal derivatives (PnD) are prepared from fetal discarded annexes (i.e., amniotic membrane, placenta, umbilical cord). These tissues not only have been less exposed to infections and diseases, come from "young tissue" and are not burdened with ethical concerns, but also could be used as biological structure or scaffold (Abbaspanah et al., 2018).

Three decades ago, the first therapeutic mesenchymal stromal/stem cells (MSC) were isolated from bone-marrow (BM) (Moll et al., 2019). However, throughout the years, MSC originating in other locations have gained increasing interest, with PnD representing 27% and AT up to 22% of the chosen MSCs in registered clinical trials between 2008 and 2018 (Moll et al., 2019). But in contrast to BM, whose safety has been well established, AT and PnD have been associated with severe adverse effects when administered intra-vascularly, some of them fatal. These adverse reactions involve pro-thrombotic and pro-inflammatory mechanisms that were demonstrated to be linked with the presence of high levels of procoagulant Tissue Factor (TF) in those cells (Caplan et al., 2019; Moll et al., 2019; Moll et al., 2022). In addition, intra-vascular injection activates the host immune system, which on the one hand seems to convey the MSC immunomodulatory function, but on the other hand, promotes the sequestration and inactivation of MSC, thereby decreasing their potential therapeutic effect (Moll et al., 2019).

There is an increasing body of evidence from pre-clinical and clinical studies showing that those deleterious effects can be minimized with several strategies, such as modifying MSC manufacture, improving MSC characterization, establishing optimal concentrations and administering simultaneous anticoagulant therapy (Moll et al., 2019; Caplan et al., 2019; Moll et al., 2022). In this context, local administration *via* direct injection in the target organ/tissue, when possible, presents some advantages. In theory, it can eliminate the need for hemocompatibility and minimize the risk of life-threatening complications [thrombosis and severe systemic inflammatory reaction—Instant Blood-Mediated Inflammatory Reaction (IBMIR)]. Over the years, there has been a tendency among clinical trials to move from intra-vascular delivery to locally administered treatments, with the latter being the choice in about half of the clinical trials currently performed (Moll et al., 2019).

The eye is, *per se*, considered a sanctuary, protected from the bloodstream by hemato-ocular barriers, rendering him a target difficult to reach endovenously, similarly to central nervous system (Caplan et al., 2019). On the other hand, it is easily accessible, either topically or by intra-ocular administration (intra-vitreal, intra-cameral, subconjunctival, subtenon injection). These surgical procedures are widely and routinely performed worldwide, in an outpatient basis and are well tolerated, with little discomfort. Local administration to the eye easily bypasses the ocular barriers, probably increasing cell delivery efficiency and lowering the incidence of complications

TABLE 1 Papers selected for pre-clinical studies and PnD analysis. (PMID: PubMed ID; PnD: Perinatal Derivates; RCS: Royal College Surgeons; hUC-MSC: human Umbilical Cord Mesenchymal Stromal Cells; hAM: human Amniotic Membrane; hAMSC: human Amniotic Membrane Mesenchymal Stromal Cells; hPMSC: human Placenta Mesenchymal Stromal Cells; hUC-WJ-MSC: human Umbilical Cord Wharton's Jelly Mesenchymal Stromal Cells).

PMID	Animal	Injury	Tissue	PnD	Administration	Immunosuppression	Size of experimental groups	Outcome
31523119 Call et al. (2019)	$Col5a1^{\Delta st/\Delta st}$ and $Col5a1^{f/f}$ mice	Keratectomy	Cornea	hUC-MSC	Single subconjunctival injection	No	Not mentioned	Reduction of corneal opacity at 7 days in treated $Col5a1^{f/f}$ with no improvement at 14 days. Significant reduction in $Col5a1^{\Delta st/\Delta st}$ mice at 7 and 14 days
31727008 Zhou et al. (2019)	C57BL/6J mice	Fungal keratitis	Cornea	hUC-MSC	Repeted subconjunctival injection	No	$n = 6$ for each group	Collagen destruction was restored by uMSCs treatment with an AOD 69,97 ± 7.09 at 14 days post-injury, vehicle group (28.98 ± 3.32)
16249483 Heiligenhaus et al. (2005)	BALB/c mice	Viral keratitis	Cornea	hAM	Sutured to cornea	No	$n = 12$ for each group	Severity of corneal keratitis is significant reduced after 2 days. (1.2± 0.8 vs. no transplanted 3.1 ± 1.1)
17637463 Bauer et al. (2007)	BALB/c mice	Viral keratitis	Cornea	hAM	Sutured to cornea	No	$n = 12$ for each group	Severity of corneal keratitis is significantly reduced after 2 days of AMT (1.2 ± 0.8 vs. no transplanted 3.1 ± 1.1)
19255156 Bauer et al. (2009)	BALB/c mice	Viral keratitis	Cornea	hAM	Sutured to cornea	No	Not specifically mentioned in transplants but from *in vitro* assays n = 8	AM reduces infiltering cells but not well detailed
18172088 Barequet et al. (2008)	Wistar rats	Bacterial keratitis	Cornea	hAM	Sutured to cornea	No	$n = 16$ saline group $n = 15$ antibiotics group $n = 16$ antibiotics-AM	One week after transplantation, significant reduction of opacity, and neovascularization in AM group than antibiotics (p value = 0.007) and saline group ($p = 0.014$)
24695478 Zeng et al. (2014)	New Zealand white rabbits	Alkali burns	Cornea	hAMSC	Single subconjunctival injection	No	vehicle $n = 10$, for all transplanted groups $n = 12$	At 7 days, control (PBS) exhibited significant higher opacity score (3.9) than transplanted ones (hAMSC 3.15, AM graft 3.20 and combination 2.45)
28704317 Subasi et al. (2017)	New Zealand white rabbits	Alkali burns	Cornea	hAM	Sutured to cornea	No	$n = 8$ for each group	Less neovascularization was observed in the collagen group than in the AM group. No differences in opacity
21431286 Reza et al. (2011)	New Zealand white rabbits	Keratectomy	Cornea	hAM	Sutured to cornea	No	$n = 4$ for each group	AM exhibited more transparent up to 10 weeks after injury with no neovascularzation or irregularities

(Continued on following page)

10.3389/fbioe.2022.969927

TABLE 1 (*Continued*) Papers selected for pre-clinical studies and PnD analysis. (PMID: PubMed ID; PnD: Perinatal Derivates; RCS: Royal College Surgeons; hUC-MSC: human Umbilical Cord Mesenchymal Stromal Cells; hAM: human Amniotic Membrane; hAMSC: human Amniotic Membrane Mesenchymal Stromal Cells; hPMSC: human Placenta Mesenchymal Stromal Cells; hUC-WJ-MSC: human Umbilical Cord Wharton's Jelly Mesenchymal Stromal Cells).

PMID	Animal	Injury	Tissue	PnD	Administration	Immunosuppression	Size of experimental groups	Outcome
29929442 Yamashita et al. (2018)	Japan white rabbits	Keratectomy	Cornea	hUC-MSC	Sutured to cornea over a collagen sheet	No	n = 6 for each group	At 8 days after transplantation, red cells can be detected in transplant group and there is no edema
21310014 Guo et al. (2011)	New Zealand white rabbits	Keratectomy	Cornea	hAM	Sutured to cornea	No	n = 11 for each group	At 7 days the diameter of lesion decreased significantly in AM group
30260581 Navas et al. (2018)	New Zealand white rabbits	Alkali burns	Cornea	hAMSC	Single injection in anterior chamber	No	n = 6 for each group	At 12 days after injury, hAMSC group presents a signifcant inhibition (0.5 ± 0.05 vs. NaOH 4.11 ± 0.26) of neovascularitation and the lowest corneal opacity (1.24 ± 0.06 vs. NaOH 3.21 ± 0.34)
31399042 Park et al. (2019)	BALB/c mice	Graves' Ophthalmopathy induced by immunization with hTSHR	Optic nerve surrounding tissues	hPMSC	Single intraorbital injection	No	n = 12 in saline + n = 14 steroids + n = 14 hPMSC	At 4 weeks hPMSC decrease % of orbital volume like steroid treatment but also attenuate pro inflammatory cytokine production
34051850 Park et al. (2021)	BALB/c mice	Graves' Ophthalmopathy induced by immunization with hTSHR	Optic nerve surrounding tissues	hPMSC	Single intraorbital injection	No	n = 6 for each group	1 week after transplantation, $hPMSCs^{PRL1}$ and hPMSCs found to reduce the thickness of the optic nerve but steroid did not have the same effect. Also, WAT (white adipose tissue) area immunodeteted by perilipin was significantly reduced in hPMSC group
25734497 Xie et al. (2015)	Sprague Dawley rats	Optic nerve transection	Optic nerve	hAMSC	Single intranerve injection	No	n = 18 for sham and n = 21 for the rest of groups	28 days after transplantation, GAP-43 integral optical density value in control group was lower than transplantation group (p < 0.0001)
28857477 Park et al. (2018)	Sprague Dawley rats	Optic nerve crush	Optic nerve	hPMSC	Single intranerve injection	No	n = 5 for each group	2 weeks after injection axon survival ratio was higher in the hPMSC group
32524519 Kwon et al. (2020)	Sprague Dawley rats	Optic nerve crush	Optic nerve	hPMSC	Single subtenon injection	No	n = 4 for sham and n = 6 for transplanted groups	4 weeks after transplantation, expression of GAP43 was significantly increased in all treated groups
30389962 Millán-Rivero et al. (2018)	Sprague Dawley rats	Optic nerve crush	Retina and optic nerve	hUC-WJ-MSC	Single intravitreal injection	No	n = 4 for each group	At 7 days, hUC-WJ-MSCs protected retinal ganglion cells from death after axotomy

(Continued on following page)

10.3389/fbioe.2022.969927

TABLE 1 (*Continued*) Papers selected for pre-clinical studies and PnD analysis. (PMID: PubMed ID; PnD: Perinatal Derivates; RCS: Royal College Surgeons; hUC-MSC: human Umbilical Cord Mesenchymal Stromal Cells; hAM: human Amniotic Membrane; hAMSC: human Amniotic Membrane Mesenchymal Stromal Cells; hPMSC: human Placenta Mesenchymal Stromal Cells; hUC-WJ-MSC: human Umbilical Cord Wharton's Jelly Mesenchymal Stromal Cells).

PMID	Animal	Injury	Tissue	PnD	Administration	Immunosuppression	Size of experimental groups	Outcome
29210653 Wang et al. (2017)	RCS rats	Photoreceptor degeneration	Retina	hUC-MSC	Single subretinal injection	No	$n = 6$ for each group	8 weeks after transplantation there are GFP positive cells in both groups. Between 1 and 8 weeks after transplantation, hUC-MSCs demonstrated significant protective effect in b waves of ERG.
26107378 Leow et al. (2015)	RCS rats	Photoreceptor degeneration	Retina	hUC-WJ-MSC	Single subretinal injection	Yes Dexamethasone + Cyclosporine A	$n = 8$ for each group	At 2 weeks, cells remained in subretinal localization. No significant differences between groups in waves amplitude of ERG at 15 and 30 days. However, outer nuclear layer (ONL) thickness at 70 days was higher in transplanted group ($p < 0.001$)
17053209 Lund et al. (2007)	RCS rats	Photoreceptor degeneration	Retina	hUC-MSC and hPMSC	Single intrascleral injection	Yes Dexamethasone + Cyclosporine A	$n = 23$ for hUC-MSC group $n = 8$ for hPMSC group	At 1 month, hUC-MSCs rescued amplitude of ERG waves and not hPMSCs
21629576 Scalinci et al. (2011)	Lewis rats	Diabetic ophthalmopathy induced by streptozotocin	Retina	hPMSC	Single intravitreal injection	No	$n = 3$ for sham and $n = 12$ for transplanted groups	At 21 days, hPMSC group presented less hypofluorescence areas with means less isquemic zones than sham group. Only qualitative
32210708 Yu et al. (2020)	Sprague Dawley rats	Diabetic ophthalmopathy induced by streptozotocin	Retina	hUC-MSC	Single tail-vein injection	No	$n = 15$ for each group	After 1 month, hUC-MSCs reduced retinal microvascular permeability ($p < 0.05$)
31737079 Ji et al. (2019)	Sprague Dawley rats	Ocular hypertension (OHT)	Retina	hUC-MSC	Single intravitreal injection	No	$n = 12$ for each group	After 14 days, in OHT animals retinal thickness decreased significantly (89.09 ± 3.04 μm) while hUC-MSCs significantly increased that value (105.4 ± 3.37)
26065854 Kim et al. (2016)	C57BL/6J mice	Oxygen-induced retinopathy (OIR) by hyperoxic room	Retina	hAMSC	Single intraperitoneal injection	No	$n = 18$ for each group	After 5 days, hAMSCs were found surrounded vasculature in retina but not differentiated into endothelium or pericytes
22550516 Kiilgaard et al. (2012)	Domestic pigs	Choroidal neovascularitation induction (CNV) by removing RPE	Retina	hAM	Single subretinal injection	No	$n = 9$ control and $n = 15$ transplanted group	At 42 days, AM was covered by RPE cell in a monolayer

10.3389/fbioe.2022.969927

(Caplan et al., 2019), which makes the eye a suitable candidate for PnD-based therapies.

With this work, we aimed to perform a systematic review of published preclinical and clinical studies involving therapeutic approaches of PnD in the field of ocular diseases. We have set forward two specific objectives: (i) to investigate the current level of standardization in applied technical procedures, regarding cell therapeutic interventions in preclinical studies, and (ii) to assess how clinical efficacy of PnD was evaluated in view of current and future clinical relevance

This work was performed in the framework of The International Network for Translating Research on Perinatal Derivatives into Therapeutic Approaches (SPRINT, CA17116), funded by COST (European Cooperation in Science and Technology).

2 Materials and methods

We performed a review of published preclinical and clinical studies selecting those that used perinatal derivatives (PnD). We included amniotic membrane and mesenchymal stromal cells derived from amniotic membrane (hAMSC), placenta (hPMSC), umbilical cord (hUC-MSC) and Wharton's jelly (hUC-WJ-MSC), excluding those where cells were not transplanted individually or were not used in combination with other derivatives such as conditioned medium.

For preclinical studies, the SPRINT consortium performed a systematic search of the PubMed database (Linares-Espinós et al., 2018) using a Boolean search string including perinatal derivatives such as tissues, membranes, cells, and secretome derived from them, but excluding cord blood and hematopoietic products, as well as non-original publications. The search string was supplemented with terms covering preclinical animal or *in vivo* models, and publications from 2004 to the present were collected in a searchable database as described in detail elsewhere (https://doi.org/10.5281/zenodo.6334077). The filter "*ophthalmology OR eye OR vision OR retina OR cornea*" was then used to select preclinical studies in the ophthalmology field, that were manually curated to exclude adult MSC.

The search for Clinical Trials (CTs) using PnD in the treatment of ocular conditions was carried out in the https://clinicaltrials.gov and https://www.clinicaltrialsregister.eu/ databases, using the following terms: "*Ophthalmopathy OR ocular OR vision OR eye OR ophthalmic OR Eye Disease OR Eye OR Ocular OR optic OR retina AND mesenchymal*". Next, the retrieved CTs (n = 41) were manually curated to exclude those testing adult MSCs (n = 14) (Supplementary Figure S1). In addition, CTs that used hAM as a carrier for other cell types, such as in limbal cell transplant, were excluded from this search, since their primary goal was not the use of AM. We also excluded CTs that had been withdrawn. Data were analyzed and plotted using GraphPad Prism 9 (GraphPad, San Diego, CA, United States).

3 Results

Our bibliographic search, as outlined in Materials and Methods section, retrieved 26 pre-clinical studies and 27 randomized clinical trials (CTs), that are listed in Tables 1, 2.

Both pre-clinical studies and CTs addressed diseases of the cornea/ocular surface and the retina/optic nerve (Figure 1). No other ocular structure was object of study.

3.1 Preclinical studies: Animal models

Most of the reports studied the effects of PnD in rats (n = 11), mice (n = 8) and rabbits (n = 6). Only one of them used higher mammals, namely domestic pigs, to assess the effect of amniotic membrane in retinal neovascularization (Kiilgaard et al., 2012). The used species and applied disease models are summarized in Table 1 and Figure 2.

Rabbits are exclusively used as keratectomy model (Figure 2), where corneal ablation is performed by placing a NaOH soaked disk over the cornea (Guo et al., 2011; Reza et al., 2011; Zeng et al., 2014; Subasi et al., 2017; Navas et al., 2018; Yamashita et al., 2018).

Rodents are the most common model to study either keratitis using bacterial (Barequet et al., 2008), fungal (Zhou et al., 2019) or viral infection (Heiligenhaus et al., 2005; Bauer et al., 2007; Barequet et al., 2008) and retinal injuries or diseases such as photoreceptor degeneration (Lund et al., 2007; Leow et al., 2015; Wang et al., 2017), optic nerve trauma (Xie et al., 2015; Millán-Rivero et al., 2018; Park et al., 2018; Kwon et al., 2020), hypoxia (Kim et al., 2016), ocular hypertension (Ji et al., 2019), Grave's ophthalmopathy (Park et al., 2019, 2021) and diabetic retinopathy (Scalinci et al., 2011; Yu et al., 2020).

All selected papers analyzed a large enough sampling size (12 papers had a "number of animals" higher than 10) to perform consistent statistical analyses. Furthermore, according to the ethical committees' recommendations, most of the studies explicitly mentioned the age or weight of animals, although neither explored how transplantation effects differ among interindividual variables.

3.2 Preclinical studies: Type of cells and route of administration

As we expected for their translational potential to the clinic, all the selected studies used human PnDs (Figure 3); thus, in these works, PnDs were xenotransplanted. Surprisingly, among

TABLE 2 Clinical trials selected for the present review. (hAM: human Amniotic Membrane; hAMSC: human Amniotic Membrane Mesenchymal Stromal Cells; hUC-MSC: human Umbilical Cord Mesenchymal Stromal Cells; hUC-WJ-MSC: human Umbilical Cord Wharton's Jelly Mesenchymal Stromal Cells).

Type of tissues	Type of cell used	Route of administration	Ocular therapeutic target	Disease treated	RCT References	Status	Published results
hAM	hAM as a tissue	over tissue	Cornea	Bullous keratopathy	https://ClinicalTrials.gov/show/NCT01926535	Completed	yes
hAM	AM Extract Eye Drop	topical	Cornea	Epithelial defects	https://ClinicalTrials.gov/show/NCT02746848	Completed	No
hAM	hAM as a tissue	over tissue	Cornea	Corneal perforation	https://ClinicalTrials.gov/show/NCT03500796	Completed	No
hAM	hAM as a tissue	over tissue	Cornea/Dry Eye	Dry Eye	https://ClinicalTrials.gov/show/NCT04553432	Recruiting	No
hAM	AM Extract Eye Drop	topical	Cornea	Limbal insufficiency	https://ClinicalTrials.gov/show/NCT02649621	Completed	No
hAM	hAM as a tissue	over tissue	Cornea	Limbal insufficiency	https://ClinicalTrials.gov/show/NCT02102776	Unknown	No
hAM	hAM as a tissue	over tissue	Cornea	Limbal insufficiency	https://ClinicalTrials.gov/show/NCT02015000	Unknown	Submitted
hAM	hAM as a tissue	over tissue	Cornea	Limbal insufficiency	https://ClinicalTrials.gov/show/NCT01319721	Completed	Yes
hAM	hAM as a tissue	over tissue	Cornea	Corneal ulcer	https://ClinicalTrials.gov/show/NCT01765244	Completed	no
hAM	hAM as a tissue	over tissue	Scleral	Scleral thinning	https://clinicaltrials.gov/ct2/show/study/NCT00801073	Unknown	Yes
hAM	hAM as a tissue	over tissue	Cornea	Bullous keratopathy	https://clinicaltrials.gov/ct2/show/study/NCT00659308	Completed	yes
hAM	hAM as a tissue	over tissue	Cornea	Limbal insufficiency	https://clinicaltrials.gov/ct2/show/study/NCT00457223	Completed	No
hAM	hAM as a tissue	over tissue	Cornea	Limbal insufficiency	https://clinicaltrials.gov/ct2/show/study/NCT00802620	Unknown	No
hAM	hAM as a tissue	over tissue	Cornea	Corneal ulcer	https://clinicaltrials.gov/ct2/show/study/NCT00915759	Unknown	Yes
hAM	hAM as a tissue	over tissue	Cornea	Corneal ulcer/melting	https://clinicaltrials.gov/ct2/show/study/NCT02168790	Completed	Yes
hAM	hAM as a tissue	over tissue	Cornea	Corneal ulcer	https://clinicaltrials.gov/ct2/show/study/NCT00238862	Completed	No
hAM	hAM as a tissue	over tissue	Sclera/conjunctiva	Shunt tube exposure	https://clinicaltrials.gov/ct2/show/study/NCT01551550	Completed	Yes
hAM	hAM Extract Eye Drop	topical	Cornea/Dry Eye	Dry Eye	https://www.clinicaltrialsregister.eu/ctr-search/trial/2011-006287-50/ES	Prematurely ended	Yes
hAM	hAM conditioned media	topical	Cornea/Dry Eye	Dry Eye	https://clinicaltrials.gov/ct2/show/study/NCT02369861	Completed	No
hUC	UC MSC	not stated (systemic administration?)	Optic nerve	Neuromyelitis Optica/Multiple sclerosis	https://ClinicalTrials.gov/show/NCT01364246	Unkonown	No
hUC	UC MSC	subconjunctival injection	Cornea	Ocular Corneal Burn	https://ClinicalTrials.gov/show/NCT03237442	Unknown	No
hUC	UC MSC and UC MSC-Exo	intravitreal injection	Retina	Macular Hole	https://ClinicalTrials.gov/show/NCT03437759	Active, not recruiting	No
hUC	UC MSC-Exo	topical	Cornea/Dry Eye	Dry eye/GVHD	https://ClinicalTrials.gov/show/NCT04213248	Recruiting	No
hUC	WJ MSC	subtenon injection	Retina	Retinitis pigmentosa	https://ClinicalTrials.gov/show/NCT04224207	Completed	yes
hUC	UC MSC and UC MSC conditioned media	peribulbar injection	Retina	Retinitis pigmentosa	https://ClinicalTrials.gov/show/NCT04315025	Completed	No

(Continued on following page)

TABLE 2 (*Continued*) Clinical trials selected for the present review. (hAM: human Amniotic Membrane; hAMSC: human Amniotic Membrane Mesenchymal Stromal Cells; hUC-MSC: human Umbilical Cord Mesenchymal Stromal Cells; hUC-WJ-MSC: human Umbilical Cord Wharton's Jelly Mesenchymal Stromal Cells).

Type of tissues	Type of cell used	Route of administration	Ocular therapeutic target	Disease treated	RCT References	Status	Published results
hUC	UC MSC	subtenon injection and suprachoroidal injection	Retina	Retinitis pigmentosa	https://ClinicalTrials.gov/show/NCT04763369	Recruiting	No
hUC	WJ MSC	subtenon space	Optic nerve	Toxic optic neuropathy	https://ClinicalTrials.gov/show/NCT04877067	Completed	Yes

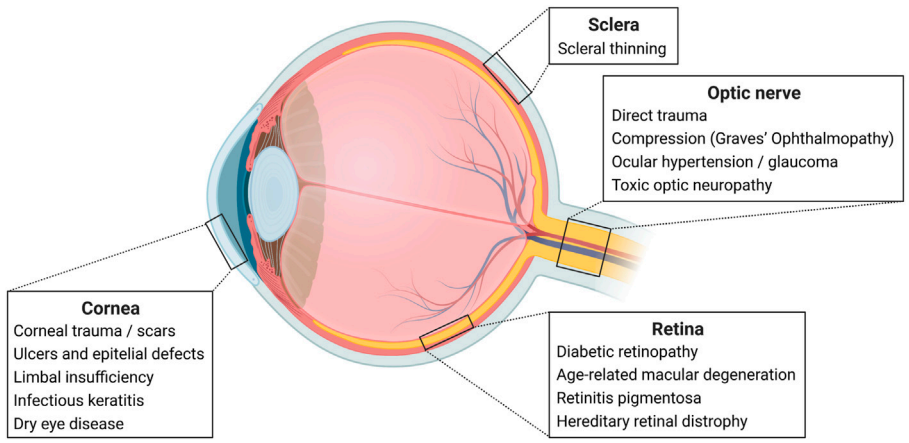

FIGURE 1
Ocular Anatomy and Diseases. Examples of eye diseases per ocular structure. Created with BioRender.com.

all 26 studies, only two applied an immunosuppressive regimen (Lund et al., 2007; Leow et al., 2015).

Regarding corneal diseases, we identified 12 studies using PnD: five aiming to treat corneal infections, four evaluating corneal epithelialization in keratectomy models and three evaluating its effect in alkali burns. The majority (n = 8) was treated with hAM as an over tissue, three with subconjunctival injections of hUC-MSC or hAMSC and one with an intracameral injection of hAMSC (Heiligenhaus et al., 2005; Bauer et al., 2007, 2009; Barequet et al., 2008; Guo et al., 2011; Reza et al., 2011; Kiilgaard et al., 2012; Subasi et al., 2017).

There were 14 studies focusing on retinal and optic nerve disorders. In contrast to corneal pathologies, umbilical cord derived cells were preferred (n = 6), followed by hPMSC (n = 5) and hAMSC (n = 2).

In retinal diseases (n = 8), subretinal injections (n = 3) and intra-vitreal injections (n = 2) were the most frequently performed procedures. Of notice, there were two studies where cells were systemically administered, either *via* the tail or injected in intraperitoneal space. In none of those two studies systemic immunosuppression was administered. (Lund et al., 2007; Wang et al., 2017; Yamashita et al., 2018; Call et al., 2019; Ji et al., 2019; Zhou et al., 2019; Yu et al., 2020) (Lund et al., 2007; Scalinci et al., 2011; Park et al., 2018, 2019, 2021; Kwon et al., 2020).

In optic nerve disorders (n = 6), cells were injected directly in the nerve (n = 2), in the orbit (n = 2), in the subtenon space (n = 1) and in the vitreous (n = 1).

3.3 Pre-clinical studies: Cell fate and outcome reports

A major strength of preclinical animal models is that they allow to determine the cell fate of transplanted cells. However, only ten studies identified the graft *post-mortem*, using diverse techniques that include immunofluorescence (Millán-Rivero et al., 2018), membrane staining with lipophilic fluorophores (Scalinci et al., 2011; Yamashita et al., 2018; Kwon et al., 2020) or nuclei stains (Xie et al., 2015; Navas et al., 2018). Of notice, Kim et al., 2016 proved that intraperitoneally injected hAMSCs can migrate into the retina, resulting in supressed neovascularization in the retina. The rest of studies that identified cells agreed on transplanted cells remaining in the local of injection (Millán-Rivero et al.,

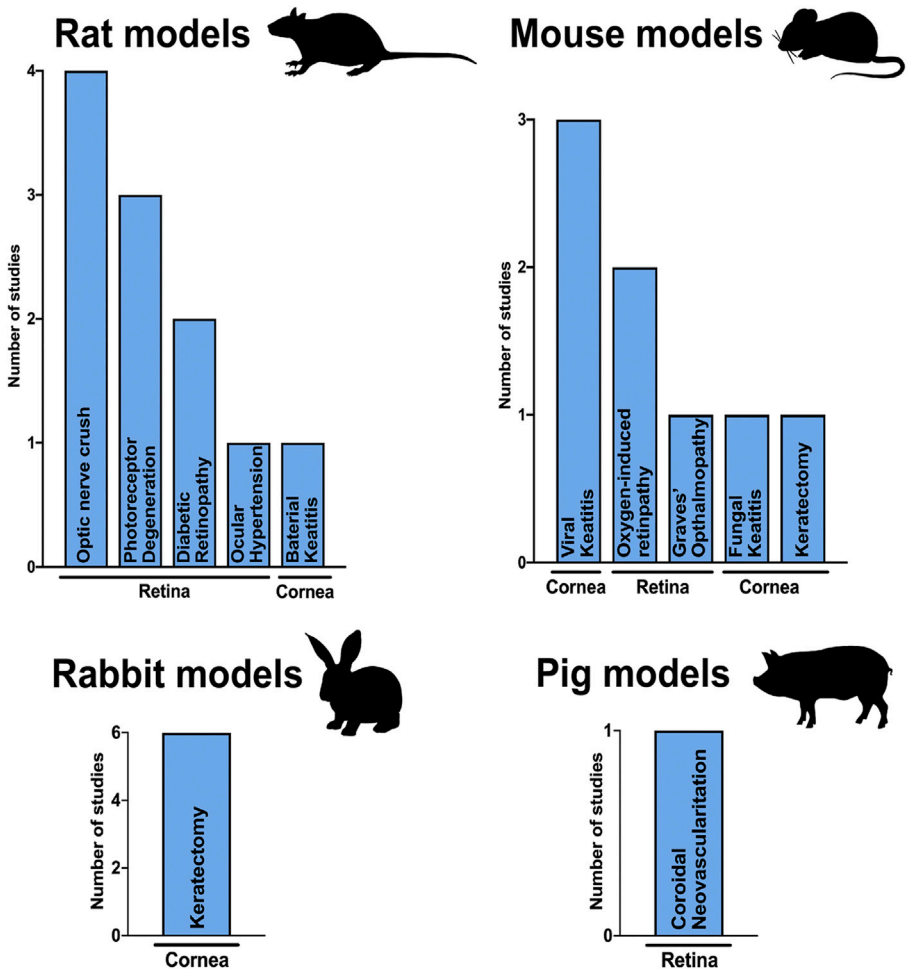

FIGURE 2
Animal models. Column graphs showing the species used to test PnDs in ophthalmology and the number of articles published for every injury model in the cornea and retina.

2018; Kwon et al., 2020), and their effects are locally potentiated but detectable all over retina.

Regarding the route of administration, most of the studies report beneficial effects of PnD when applied locally. The two studies that investigated systemic administration also report beneficial effects, with no severe adverse reactions (Kim et al., 2016; Yu et al., 2020). More concerning is the absence of consensus regarding the optimal time points for analyses, so that positive effects can be reported as early as 2 days post-administration (Heiligenhaus et al., 2005; Bauer et al., 2007) or 2 months (Reza et al., 2011; Wang et al., 2017) after transplantation. Furthermore, the approach for measuring the beneficial effect of PnD transplants also lacks consensus. As shown in Figure 4, we selected those studies that assessed functional or anatomical outcomes in the same animal model and matched time points: for cornea, the clinical score for improvement was the corneal opacity after transplant (Heiligenhaus et al., 2005; Zeng et al., 2014; Navas et al., 2018; Yamashita et al., 2018) and for the retina, recordings of the b-wave in electroretinograms that measure post photoreceptors synapsis (Lund et al., 2007; Leow et al., 2015; Wang et al., 2017). In the studies graphed in Figure 4, PnD displayed a beneficial impact in decreasing corneal opacity, increasing the b-wave amplitude and ONL thickness, but results differed depending on PnD tissue origin. However, no clear statement can be made due to the low number of studies.

3.4 PnD in clinical trials

Our curated search for Clinical Trials (CT) retrieved 27 registries, that are summarized in Table 2. The vast majority addresses the use of human amniotic membrane,

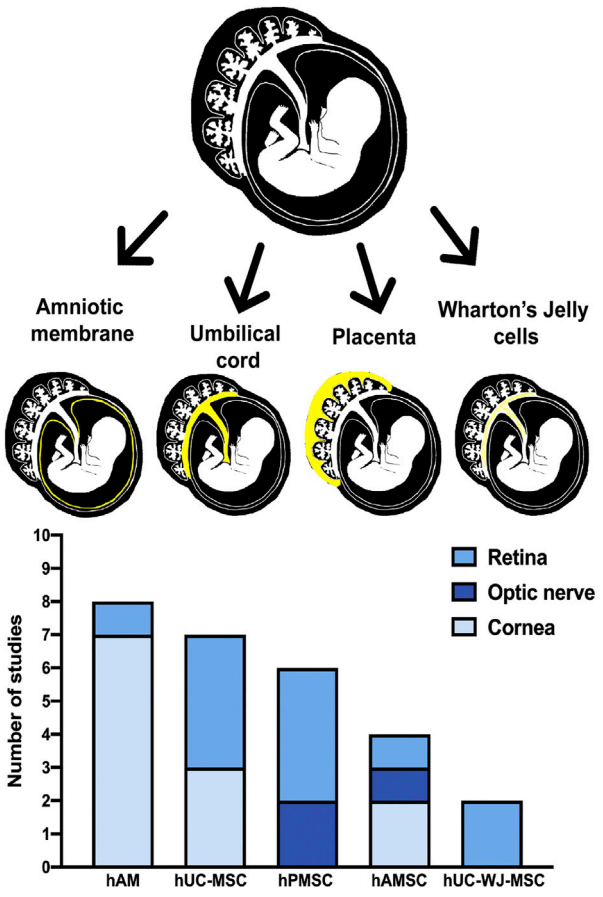

FIGURE 3
Types of PnD. Top, a schematic picture of different origins of fetal tissue for each PnD selected in this review. Below, grouped column graph showing the number of publications using each PnD type in retina, optic nerve, and cornea. (hAM: human Amniotic Membrane; hUC-MSC: human Umbilical Cord Mesenchymal Stromal Cells; hPMSC: human Placenta Mesenchymal Stroma Cells; hAMSC: human Amniotic Membrane Mesenchymal Stromal Cells; hUC-WJ-MSC: human Umbilical Cord Wharton's Jelly Mesenchymal Stromal Cells).

either as a tissue (n = 16) or as an extract/conditioned medium eye drop (n = 3). The remaining trials evaluate the use of umbilical cord mesenchymal stromal cells (hUC-MSC) (n = 3), Wharton's Jelly MSC (hUC-WJ-MSC) (n = 2), hUC-MSC-derived extracellular vesicles (n = 1), hUC-MSC plus hUC-MSC-derived extracellular vesicles (n = 1) and hUC-MSC plus hUC-MSC-conditioned media (n = 1) (Figure 5).

The majority of CTs have used the cornea as a therapeutic target (n = 19) and are designed to treat limbal insufficiency (n = 7), epithelial defects and ulcers (n = 5), bullous keratopathy (n = 2), dry eye disease (n = 3), and corneal perforations (n = 1). The usefulness of hAM in treating scleral/conjunctival thinning is the object of two CTs (Figure 6).

The remaining six CT are designed to treat retinal diseases (n = 4) and optic neuropathies (n = 2): retinitis pigmentosa (n = 3), macular hole (n = 1), neuromyelitis optica/multiple sclerosis (n = 1) and toxic optic neuropathy (n = 1) (Figure 6). Of notice, all these six RCT are designed to evaluate the therapeutic value of umbilical cord and Wharton's Jelly-derived products, rather than hAM, which is not a choice in treating these diseases (Figure 7).

In fact, it becomes apparent from Figure 7 that hAM is the PnD of choice to treat ocular surface conditions (the columns to the left of the dashed line), while retinal and optic nerve diseases are predominantly treated with hUC and hUC-WJ derivatives. The route of administration is inherent to that choice: while ocular surface conditions are treated with hAM applied to the surface or with PnD eyedrops, the retina and the optic nerve are not that easily accessible and therefore require PnD to be delivered through subconjunctival, subtenon, periocular or intravitreal injection (Table 2).

Fifteen of those 27 RCT are currently completed, three are still recruiting, one is active but not recruiting, and seven have an unknown recruiting status (Figure 8). Surprisingly, only ten RCT have published results.

Available results are compiled in Table 3 and detailed below, by pathology.

3.4.1 Bullous keratopathy

Two RCT evaluate the use of transplanted hAM in the management of BK (NCT01926535; NCT00659308). Both seem to favour hAM: hAM outperforms therapeutic contact lenses in pain relief up to 6 months and is more effective in achieving a regular epithelium at 6 months, compared to anterior stromal puncture.

3.4.2 Pterygium

One randomized, interventional, and comparative study on recurrent pterygium surgery compared conjunctival-limbal autograft (CLAU) with hAM and concluded the superiority of CLAU in all parameters evaluated (healing of epithelial defect, post-operative conjunctival inflammation, and recurrence rate at 1 year) (NCT01319721).

3.4.3 Scleral thinning

A randomized, interventional, comparative study compared hAM with pericardial graft covering to prevent glaucoma drainage device tube exposure and found that hAM was more effective at the 2-year time point (NCT01551550).

Another RCT compared the use of multilayer amniotic membrane transplantation (AMT) with lamellar corneal transplantation (LCT) and lamellar scleral transplantation (LST) for the treatment of scleral thinning after pterygium surgery (NCT00801073). It found that AMT performed significantly worse than LCT or LST. A high rate of reabsorption was noted with AMT, which was the least

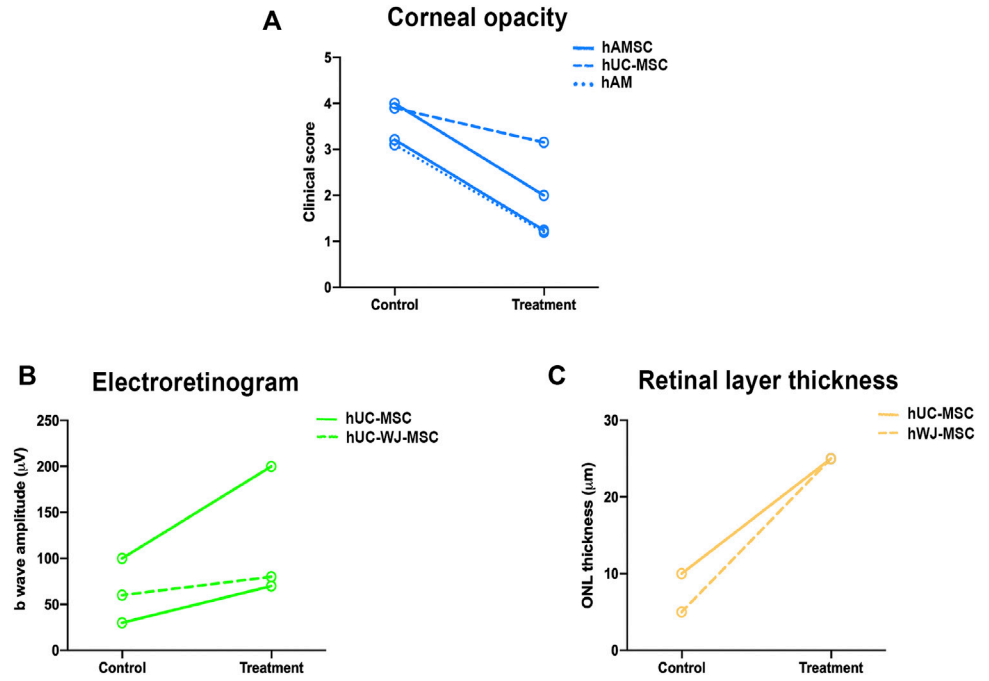

FIGURE 4
Preclinical scores to measure PnD therapeutic success. Graphs representing the functional or anatomical changes after PnD treatment between control and treated groups. Clinical score measuring corneal opacity in keratitis corneal model 15 days after the transplant **(A)**, b wave amplitude (μV) recorded from rats with retinal dystrophy measured 30 days after injection **(B)** and measurement of the thickness of outer nuclear layer (ONL) (μm) in the same model but measured at 60 days after injection **(C)**. (hAM: human Amniotic Membrane; hUC-MSC: human Umbilical Cord Mesenchymal Stromal Cells; hAMSC: human Amniotic Membrane Mesenchymal Stromal Cells; hUC-WJ-MSC: human Umbilical Cord Wharton's Jelly Mesenchymal Stromal Cells).

effective of the three therapeutic options and should not be used for this condition.

3.4.4 Corneal ulcer

Two RCTs evaluated the role of sutureless hAM in the treatment of corneal ulcers. One was designed to prove its safety and wearability as a prerequisite to obtaining regulatory approval. Eight eyes of seven patients were enrolled and showed good tolerance with no complications (NCT02168790).

The largest RCT compared hAM and bandage contact lens (BCL) in aiding corneal re-epithelialization after photorefractive keratectomy in 40 patients. One eye of each patient was treated with hAM, and the other eye with BCL. Published results show shorter healing times for BCL, but no statistical analysis was performed, so clear conclusions cannot be drawn (NCT00915759).

3.4.5 Dry eye disease

One phase III comparative clinical trial evaluated the efficacy of amniotic membrane extract for treating severe dry eye disease compared with autologous serum eyedrops (2011-006287-50). Among the group of 12 patients enrolled, no statistical differences were noted between the two treatments. Since autologous serum eyedrops are a world-wide accepted treatment option for dry eye disease, this RCT proved the non-inferiority of hAM extract.

3.4.6 Neuroretinal diseases

There are two RCTs with the focus on neuroretinal disease that have published results, both using hUC-WJ-MSC.

One prospective, sequential, open-label phase III clinical study enrolled 34 eyes of 32 patients with retinitis pigmentosa (RP) (NCT04224207). In this RCT, subtenon transplantation of WJ-MSCs was effective and safe in the treatment of RP during the first year.

Similarly, the beneficial effect of hUC-WJ-MSC combined with electromagnetic stimulation in toxic optic neuropathy was evidenced in another RCT involving 36 eyes of 18 patients (NCT04877067).

4 Discussion

Our thorough review of pre-clinical studies and clinical trials has shown a considerable overlap with regard to the ocular structures being targeted. The cornea, the retina and the optic nerve are the main targets of PnD therapeutic interventions.

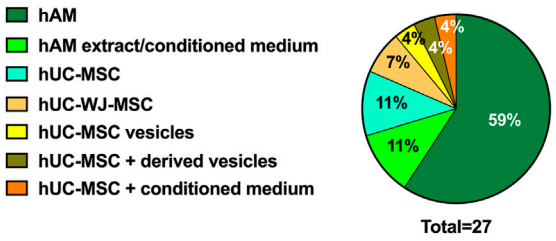

FIGURE 5
Randomized Clinical Trials (RCT) and PnD used. Pie graph representing the type of PnD used in RCTs.

Another common feature is the marked tendency towards locally administered treatments, as opposed to systemic delivery. This is in agreement with the current world-wide trends in mesenchymal stromal/stem cell clinical applications (Moll et al., 2019).

Another similarity between pre-clinical and clinical studies is the preferred cell type used: in the cornea and ocular surface, hAM is the PnD of choice, while retinal and optic nerve diseases are predominantly treated with umbilical cord derived and placenta mesenchymal stromal cells. This also implicitly conditions the route of administration, ocular surface conditions being treated with hAM applied as a tissue or with PnD eyedrops, while the retina and the optic nerve are treated with injected cells.

The existence of clinical trials register platforms is a scientific, ethical and moral responsibility (https://www.who.int/clinical-trials-registry-platform/network/trial-registration). Databases for clinical trials registration are a valuable source of information. However, we noticed that the follow-up is frequently missing and results are not published; it is very common to find clinical trials in "unknown status". Having a follow-up from clinical failure studies could also help to re-drive pre-clinical and clinical works to better targets.

The cornea is a specialized, transparent tissue placed in the anterior part of the eye, that allows the passage of light to the retina, the light sensory tissue (Figure 1). Thus, corneal integrity

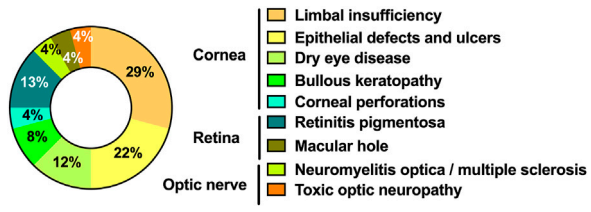

FIGURE 6
Ophtalmic diseases object of RCT grouped by ocular target. Circular graph representing the distribution of ocular diseases that were object of RCT.

and transparency are essential for a clear vision. Once damaged, the cornea's ability to heal relies on stem cells located around its periphery, the so-called limbal stem cells. Not unfrequently, this healing process leads to scar formation and transparency loss, especially in extensive lesions and long-standing disease. PnD-based therapies have immunoregulatory properties that may be useful in modulating wound healing (Bukowiecki et al., 2017). Both pre-clinical studies and CTs have addressed this subject, and demonstrated that PnDs are useful in corneal re-epithelialization in keratectomy animal models. In the clinical setting, hAM was proven useful in the symptomatic relief of bullous keratopathy and was well tolerated and safe in treating corneal ulcers and epithelial defects; however, it did not seem to outperform bandage contact lenses—only one CT with published results was performed, and it seemed to favour contact lens wear compared to hAM, but did not present statistical analysis.

Limbal insufficiency is an ocular surface disease involving the cornea that has attracted the attention of basic and clinical researchers. It is a devastating condition often leading to blindness, that is mostly caused by chemical injuries and typically affects young males, that are more prone to that kind of accidents (Deng et al., 2019). In limbal insufficiency, the cornea becomes opaque and neovascularized, which erodes ocular immune privilege (Bukowiecki et al., 2017) and therefore turns corneal grafts into very high-risk procedures due to the increased risk of rejection. The potential beneficial effect of PnD was evaluated in animal alkali burn models, with favourable results. Regarding clinical trials, there were seven registered studies. Of those, only one had their results published, and it evaluated pterygium, a localized form of limbal insufficiency that does not entail the severity of chemical burns. In pterygia surgery, hAM presented poor results, but the comparative treatment was conjunctival-limbal autograft, whose superiority is well known since it contains limbal stem cells.

There are other diseases of the ocular surface where the treatment with biological products has proven benefits. That is the case of dry eye disease, where the treatment with blood derived products is beneficial, due to the presence of growth factors, among other molecules, and is part of the current treatment guidelines (Jones et al., 2017). The discovery of other biological options that might be even more effective and wider available could be advantageous. In fact, hAM extract can be an option in treating dry eye disease, since a CT proved its non-inferiority compared to autologous serum eyedrops, a gold-standard treatment for this condition. hAM also proved helpful in preventing glaucoma drainage device tube exposure. On the contrary, a CT has shown that in the case of scleral thinning, the use of hAM should be discouraged since there are better alternatives (corneal or scleral grafts).

The optic nerve and retina are projections of the brain and therefore part of the central nervous system. They are highly specialized tissues where neuronal death can occur as a result of

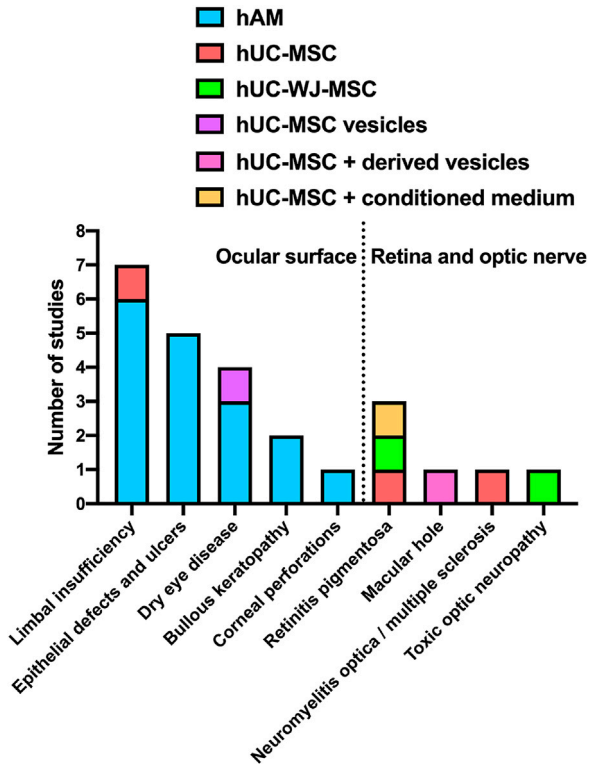

FIGURE 7
Type of PnD used in every disease. Column graph representing the type of PnD used in each pathology; the dashed line separates pathologies associated with the ocular surface on the left and the retina or optic nerve on the right.

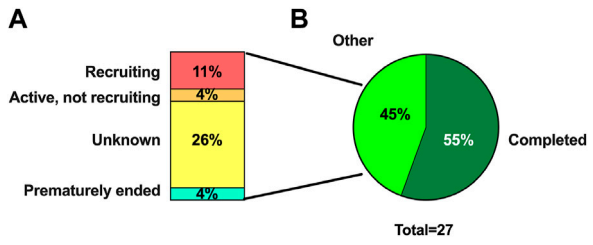

FIGURE 8
Recruiting status of RCT. Column graph **(A)** representing percentage of RCT not completed and circular graph **(B)** with percentage of RCT completed and not completed of twenty-seven RCT included.

varied diseases: age-related macular degeneration (AMD), retinitis pigmentosa (RP), diabetic retinopathy (DR), trauma, ocular hypertension/glaucoma, etc. Regardless of their primary cause (mutations, aging, systemic disorder), these diseases share common underlying mechanisms, such as oxidative stress, excitotoxicity, inflammation, or cytokine imbalance (Holan et al., 2021). The current treatment for these diseases is varied, depending on the disease itself, but of limited success in visual recovery: it encompasses antiangiogenic intravitreal injections (for AMD and DR), laser applied to the retina and metabolic control (in DR), lowering intra-ocular pressure (in glaucoma), etc. There is currently no treatment available for end-stage retinal/optic nerve diseases, where the discovery of nerve cell regeneration therapies remains the holy grail. Of notice, two CT addressing neuroretinal diseases showed very promising results on the use of Wharton's Jelly MSC, bringing hope to otherwise irreversible diseases. However, one must say that the current belief is that these cells do not differentiate into neurons, rather they facilitate neurorestorative mechanisms (Caplan et al., 2019).

When clinical trials and pre-clinical studies are compared, it becomes evident that research does not easily translate to the clinic, despite reported beneficial effects. That is especially noticeable in neuroretinal diseases, where the amount of CTs is considerably lower. Likely, this is related to the lack of standardization in terms of models, techniques, doses, optimal time points for evaluation and outcome measures of efficacy definition. The lack of similarity of the preclinical and the clinical settings, immunosuppressive treatments, or animal models that do not fully reflect human disease could also contribute to that discrepancy. Also noteworthy is that ophthalmic diseases are multifactorial and progress over time, so more longitudinal or chronic preclinical studies are needed, exploring diverse analyses such as visual tests, functional assessment, and cellular fate in the tissue, to support their use in patients. Other of the greatest advantages of preclinical studies is to be able to document the consequences of an intervention, both *in vivo* and *ex vivo*. In these types of therapies, it is very important to determine cell fate and histological changes that may occur, and that is only possible in the preclinical setting.

Furthermore, based on the data extracted from the included studies, it is difficult to extract a unique working mechanism to explain PnD advantages in the ophthalmology field. For some authors, the primary molecular mechanism involved is immunomodulation by the production of cytokines such as TGF-β or IL-10 (Barequet et al., 2008; Guo et al., 2011), the upregulation of essential survival pathways such as NF-κB (Park et al., 2018), and modifying cellular adhesion and motility (Lee et al., 2004). However, each PnD has different properties and that needs to be addressed.

In order to gather all available data on PnD, the SPRINT consortium established a publication database on the Mendeley Reference Manager platform (https://www.mendeley.com/) and collected outcome data from selected publications in an Access database (Microsoft, Redmont WA, United States of America), linking PnD types, dosage, route and time point of applications to functional effects. However,

TABLE 3 Clinical trials with published results.

References	Title/Purpose/Description	Condition	n° of eyes	Parameters evaluated
NCT01926535	Amniotic Membrane Graft in Symptomathic Bullous Keratopathy Amniotic Membrane Transplantation (AMT) vs. contact lens (CL)	Bullous keratopathy	AMT 10 CL 10	Eye pain, visual acuity; bullae, corneal epithelial defects, corneal neovascularization and complications (6 months)
NCT00659308	Amniotic Membrane and Anterior Stromal Puncture to the Treatment of Symptomatic Bullous Keratopathy Compare AMT and anterior stromal puncture (ASP) in the management of pain in patients with symptomatic bullous keratopathy	Bullous keratopathy	AMT 20 ASP 20	Regular epithelium (6 months)
NCT01319721	Recurrent Pterygium Surgery Using Mitomycin C With Limbal Conjunctival or Amniotic Membrane Randomized, interventional, comparative: limbal-conjunctival autograft (CLAU) vs. AMT in recurrent pterygia	Pterygium	47 (CLAU) + 42 (AMT)	Recurrence at 1Year Healing Time of Corneal Defect Postoperative Conjunctival Inflammation
NCT01551550	Shunt Tube Exposure Prevention Study (STEPS) Randomized, interventional, comparative: AMT vs. pericardial graft covering glaucoma drainage device tube	Prevention of tube exposure	AMT 41 Peric 40	Tube exposure (2 Years)
NCT00801073	Comparison Amongst Scleral, Corneal and Amniotic Membrane Grafts to Restore Scleral Thinning Compare the use of multilayer amniotic membrane transplantation (AMT) with lamellar corneal transplantation (LCT) and lamellar scleral transplantation (LST) for the treatment of scleral thinning after pterygium surgery	Scleral thinning	Total 26	Increase in scleral thickness at 6 months
NCT00915759	Sutureless Cryopreserved Amniotic Membrane Graft (ProKera) and Wound Healing After Photorefractive Keratectomy (PRK) Compare sutureless AMT and bandage contact lens in aiding corneal re-epithelialization after PRK (both eyes of 40 patiens enrolled) Non randomized	Corneal ulcer	40 patients AMT 40 CL 40	Corneal Re-epithelialization measured as number of days to complete re-epithelialization
NCT02168790	Safety Study of a Sutureless Amniotic Membran Transplantation to Treat Ocular Surface Disorders (Expanded Access) (AmnioClip) Seven day-wearing period of AmnioClip to prove safety, wearability and fit of AmnioClip as a prerequisite to obtain a regulatory approval	Corneal ulcer/ erosion; Corneal scarring	8 eyes (7 patients)	Tolerance and complications
2011-006287-50	Phase III comparative clinical trial to evaluate the efficacy of amniotic membrane extract for the treatment of severe dry eye disease, in comparison with autologous serum eyedrops Amniotic membrane (AM) extract vs. autologous serum (AS)	Dry Eye	12 patients (6 AM. extract + 6 AS)	Schirmer Test, Fluorescein Clearance test, TBUT, Impression cytology: HLA-DR, MUC1; subjective improvement
NCT04224207	Management of Retinitis Pigmentosa by Mesenchymal Stem Cells by Wharton's Jelly Derived Mesenchymal Stem Cells (WJ-MSC) prospective, sequential, open-label phase-3 clinical study	Retinitis pigmentosa	34 eyes (32 patients)	outer retinal thickness, mean horizontal ellipsoid zone, BCVA, fundus perimetry deviation index, full-field flicker ERG parameters
NCT04877067	Therapy of Toxic Optic Neuropathy *via* Combination of Stem Cells With Electromagnetic Stimulation (Magnovision)	Toxic Optic Neuropathy	36 eyes (18 patients)	best corrected visual acuity, fundus perimetry deviation index, ganglion cell complex thickness, visual evoked potential

both databases remain to be further implemented in the scientific community (e.g. by the International Placenta Stem Cell Society, IPLASS).

Recently, also new non-cellular therapies have emerged to replace certain limitations of the use of live cells, such as maintaining viability upon allogeneic administration. In particular, extracellular vesicles derived from mesenchymal stromal cells are showing promising results (Thomi et al., 2019). However, it is difficult to draw conclusions about a common beneficial dose to treat a disease. For that, advancing our knowledge of cell-based regenerative mechanisms is still critical to reaching success in eye diseases.

5 Conclusion

The eye is a good candidate for PnD-based therapies and ocular diseases have gained attention from both pre-clinical and clinical researchers. However, the number of studies is considerably low, a sign that much work is still to be done.

Selected pre-clinical studies and clinical trials converge in a number of features. They targeted the same ocular structures (cornea/ocular surface and retina/optic nerve). They tended to choose the same type of PnD according to the target tissue and also their route of administration. In the cornea/ocular surface, hAM was preferred and usually applied directly covering the ocular surface. In neuroretinal disorders, cells of umbilical or placental origin were injected in the eye.

In general, basic research reported favourable outcomes in all animal models of disease treated with PnD. From the clinical perspective, hAM proved useful in the symptomatic relief of bullous keratopathy, treating dry eye disease and in preventing glaucoma drainage device tube exposure. hAM was well tolerated and safe in treating corneal ulcers and epithelial defects; however, it did not seem to outperform bandage contact lenses. In pterygia surgery and in scleral thinning, the use of isolated hAM should be discouraged. Regarding neuroretinal diseases, the use of Wharton's Jelly MSC seems very promising, giving hope to otherwise irreversible diseases.

Pre-clinical studies are very important because they ought to provide necessary evidence supporting translation to the clinic. This includes efficacy and safety data, as well as insights into mechanisms of action. What stands out from our selection of pre-clinical studies is a lack of standardization among them. Also, until now, they have failed to provide an explanation on how exactly do these PnD work and their fate.

Clinical trials register in dedicated platforms is a valuable source of information. Surprisingly, the effort to register clinical trials is not accompanied by the effort to keep theirs records updated. Only a minority of CT provided results, despite displaying "complete status" and there are some whose status is "unknown". Also, in the case of "withdrawn" CT, providing an explanation for this fact should be encouraged. Negative results are as important as positive results and becoming aware of them contributes to evolving knowledge.

In conclusion, PnD-based therapies seem to be beneficial in the treatment of several ocular diseases. However, much needs to be done both in the pre-clinical and in the clinical setting before they can be included in the daily ophthalmic practice.

Author contributions

MN-M, EC, MA-B, and AS analyzed the data and drafted the manuscript. PP, MB, and JN contributed to revising and editing the article and all authors approved the submitted version.

Funding

This review is based on work from the COST Action CA17116 "International Network for Translating Research on Perinatal Derivatives into Therapeutic Approaches (SPRINT)", supported by COST (European Cooperation in Science and Technology). This study was supported by the Spanish Ministry of Economy and Competitiveness, Instituto de Salud Carlos III, Fondo Europeo de Desarrollo Regional "Una manera de hacer Europa" project: PI19/00071 (MA-B).

Conflict of interest

The authors declare that the research was conducted in the absence of any commercial or financial relationships that could be construed as a potential conflict of interest.

Publisher's note

Supplementary material

The Supplementary Material for this article can be found online at: https://www.frontiersin.org/articles/10.3389/fbioe.2022.969927/full#supplementary-material

References

Abbaspanah, B., Momeni, M., Ebrahimi, M., and y Mousavi, S. H. (2018). Advances in perinatal stem cells research: A precious cell source for clinical applications. *Regen. Med.* 13, 595–610. doi:10.2217/rme-2018-0019

Barequet, I. S., Habot-Wilner, Z., Keller, N., Smollan, G., Ziv, H., Belkin, M., et al. (2008). Effect of amniotic membrane transplantation on the healing of bacterial keratitis. *Invest. Ophthalmol. Vis. Sci.* 49, 163–167. doi:10.1167/iovs.07-1005

Bauer, D., Wasmuth, S., Hennig, M., Baehler, H., Steuhl, K.-P., and y Heiligenhaus, A. (2009). Amniotic membrane transplantation induces apoptosis in T lymphocytes in murine corneas with experimental herpetic stromal keratitis. *Invest. Ophthalmol. Vis. Sci.* 50, 3188–3198. doi:10.1167/iovs.08-3041

Bauer, D., Wasmuth, S., Hermans, P., Hennig, M., Meller, K., Meller, D., et al. (2007). On the influence of neutrophils in corneas with necrotizing HSV-1 keratitis following amniotic membrane transplantation. *Exp. Eye Res.* 85, 335–345. doi:10.1016/j.exer.2007.05.009

Bukowiecki, A., Hos, D., Cursiefen, C., and y Eming, S. A. (2017). Wound-healing studies in cornea and skin: Parallels, differences and opportunities. *Int. J. Mol. Sci.* 18, 1257. doi:10.3390/ijms18061257

Call, M., Elzarka, M., Kunesh, M., Hura, N., Birk, D. E., and y Kao, W. W. (2019). Therapeutic efficacy of mesenchymal stem cells for the treatment of congenital and acquired corneal opacity. *Mol. Vis.* 25, 415–426.

Caplan, H., Olson, S. D., Kumar, A., George, M., Prabhakara, K. S., Wenzel, P., et al. (2019). Mesenchymal stromal cell therapeutic delivery: Translational challenges to clinical application. *Front. Immunol.* 10, 1645. doi:10.3389/fimmu.2019.01645

Deng, S. X., Borderie, V., Chan, C. C., Dana, R., Figueiredo, F. C., Gomes, J. A. P., et al. (2019). Global consensus on definition, classification, diagnosis, and staging of limbal stem cell deficiency. *Cornea* 38, 364–375. doi:10.1097/ICO.0000000000001820

Guo, Q., Hao, J., Yang, Q., Guan, L., Ouyang, S., and Wang, y. J. (2011). A comparison of the effectiveness between amniotic membrane homogenate and transplanted amniotic membrane in healing corneal damage in a rabbit model. *Acta Ophthalmol.* 89, e315–e319. doi:10.1111/j.1755-3768.2010.02097.x

Heiligenhaus, A., Li, H. F., Yang, Y., Wasmuth, S., Steuhl, K. P., and y Bauer, D. (2005). Transplantation of amniotic membrane in murine herpes stromal keratitis modulates matrix metalloproteinases in the cornea. *Invest. Ophthalmol. Vis. Sci.* 46, 4079–4085. doi:10.1167/iovs.05-0192

Holan, V., Palacka, K., and y Hermankova, B. (2021). Mesenchymal stem cell-based therapy for retinal degenerative diseases: Experimental models and clinical trials. *Cells* 10 (3), 588. doi:10.3390/cells10030588

Ji, S., Xiao, J., Liu, J., and y Tang, S. (2019). Human umbilical cord mesenchymal stem cells attenuate ocular hypertension-induced retinal neuroinflammation via toll-like receptor 4 pathway. *Stem Cells Int.* 2019, 1–17. doi:10.1155/2019/9274585

Jones, L., Downie, L. E., Korb, D., Benitez-Del-Castillo, J. M., Dana, R., Deng, S. X., et al. (2017). TFOS DEWS II management and therapy report. *Ocul. Surf.* 15, 575–628. doi:10.1016/j.jtos.2017.05.006

Kiilgaard, J. F., Scherfig, E., Prause, J. U., and y la Cour, M. (2012). Transplantation of amniotic membrane to the subretinal space in pigs. *Stem Cells Int.* 2012, 1–5. doi:10.1155/2012/716968

Kim, K.-S., Park, J.-M., Kong, T., Kim, C., Bae, S.-H., Kim, H. W., et al. (2016). Retinal angiogenesis effects of TGF-β1 and paracrine factors secreted from human placental stem cells in response to a pathological environment. *Cell Transpl.* 25, 1145–1157. doi:10.3727/096368915X688263

Kwon, H., Park, M., Nepali, S., and y Lew, H. (2020). Hypoxia-preconditioned placenta-derived mesenchymal stem cells rescue optic nerve axons via differential roles of vascular endothelial growth factor in an optic nerve compression animal model. *Mol. Neurobiol.* 57, 3362–3375. doi:10.1007/s12035-020-01965-8

Lee, J. H., Lee, H. K., Kim, J. K., Chang, J. H., Kim, S. E., Kim, E. K., et al. (2004). Expression of laminin-5 with amniotic membrane transplantation in excimer laser ablated rat corneas. *J. Cataract. Refract. Surg.* 30, 2192–2199. doi:10.1016/j.jcrs.2004.02.021

Leow, S. N., Luu, C. D., Hairul Nizam, M. H., Mok, P. L., Ruhaslizan, R., Wong, H. S., et al. (2015). Safety and efficacy of human Wharton's jelly-derived mesenchymal stem cells therapy for retinal degeneration. *PLoS One* 10, e0128973. doi:10.1371/journal.pone.0128973

Linares-Espinós, E., Hernández, V., Domínguez-Escrig, J. L., Fernández-Pello, S., Hevia, V., Mayor, J., et al. (2018). Methodology of a systematic review. *Actas Urol. Espanolas* 42, 499–506. doi:10.1016/j.acuroe.2018.07.002

Lund, R. D., Wang, S., Lu, B., Girman, S., Holmes, T., Sauvé, Y., et al. (2007). Cells isolated from umbilical cord tissue rescue photoreceptors and visual functions in a rodent model of retinal disease. *Stem Cells* 25, 602–611. doi:10.1634/stemcells.2006-0308

Millán-Rivero, J. E., Nadal-Nicolás, F. M., García-Bernal, D., Sobrado-Calvo, P., Blanquer, M., Moraleda, J. M., et al. (2018). Human Wharton's jelly mesenchymal stem cells protect axotomized rat retinal ganglion cells via secretion of anti-inflammatory and neurotrophic factors. *Sci. Rep.* 8, 16299. doi:10.1038/s41598-018-34527-z

Moll, G., Ankrum, J. A., Kamhieh-Milz, J., Bieback, K., Ringdén, O., Volk, H.-D., et al. (2019). Intravascular mesenchymal stromal/stem cell therapy product diversification: Time for new clinical guidelines. *Trends Mol. Med.* 25, 149–163. doi:10.1016/j.molmed.2018.12.006

Moll, G., Ankrum, J. A., Olson, S. D., and y Nolta, J. A. (2022). Improved MSC minimal criteria to maximize patient safety: A Call to embrace tissue factor and hemocompatibility assessment of MSC products. *Stem Cells Transl. Med.* 11, 2–13. doi:10.1093/stcltm/szab005

Navas, A., Magaña-Guerrero, F. S., Domínguez-López, A., Chávez-García, C., Partido, G., Graue-Hernández, E. O., et al. (2018). Anti-inflammatory and anti-fibrotic effects of human amniotic membrane mesenchymal stem cells and their potential in corneal repair. *Stem Cells Transl. Med.* 7, 906–917. doi:10.1002/sctm.18-0042

Park, M., Banga, J. P., Kim, G. J., Kim, M., and y Lew, H. (2019). Human placenta-derived mesenchymal stem cells ameliorate orbital adipogenesis in female mice models of Graves' ophthalmopathy. *Stem Cell Res. Ther.* 10, 246. doi:10.1186/s13287-019-1348-0

Park, M., Kim, H. C., Kim, O., and y Lew, H. (2018). Human placenta mesenchymal stem cells promote axon survival following optic nerve compression through activation of NF-κB pathway. *J. Tissue Eng. Regen. Med.* 12, e1441–e1449. doi:10.1002/term.2561

Park, M., Kim, J. Y., Kang, J. M., Lee, H. J., Banga, J. P., Kim, G. J., et al. (2021). PRL-1 overexpressed placenta-derived mesenchymal stem cells suppress adipogenesis in Graves' ophthalmopathy through SREBP2/HMGCR pathway. *Stem Cell Res. Ther.* 12, 304. doi:10.1186/s13287-021-02337-2

Reza, H. M., Ng, B.-Y., Gimeno, F. L., Phan, T. T., and y Ang, L. P.-K. (2011). Umbilical cord lining stem cells as a novel and promising source for ocular surface regeneration. *Stem Cell Rev. Rep.* 7, 935–947. doi:10.1007/s12015-011-9245-7

Scalinci, S. Z., Scorolli, L., Corradetti, G., Domanico, D., Vingolo, E. M., Meduri, A., et al. (2011). Potential role of intravitreal human placental stem cell implants in inhibiting progression of diabetic retinopathy in type 2 diabetes: Neuroprotective growth factors in the vitreous. *Clin. Ophthalmol.* 5, 691–696. doi:10.2147/OPTH.S21161

Subasi, S., Altintas, O., Yardimoglu, M., Yazir, Y., Karaman, S., Rencber, S. F., et al. (2017). Comparison of collagen cross-linking and amniotic membrane transplantation in an experimental alkali burn rabbit model. *Cornea* 36, 1106–1115. doi:10.1097/ICO.0000000000001276

Thomi, G., Surbek, D., Haesler, V., Joerger-Messerli, M., and y Schoeberlein, A. (2019). Exosomes derived from umbilical cord mesenchymal stem cells reduce microglia-mediated neuroinflammation in perinatal brain injury. *Stem Cell Res. Ther.* 10, 105. doi:10.1186/s13287-019-1207-z

Torre, P. D. I., and Flores, A. I. (2020). Current status and future prospects of perinatal stem cells. *Genes (Basel)* 12, 6. doi:10.3390/genes12010006

Wang, L., Li, P., Tian, Y., Li, Z., Lian, C., Ou, Q., et al. (2017). Human umbilical cord mesenchymal stem cells: Subpopulations and their difference in cell biology and effects on retinal degeneration in RCS rats. *Curr. Mol. Med.* 17, 421–435. doi:10.2174/1566524018666171205140806

Xie, J.-X., Feng, Y., Yuan, J.-M., You, Z.-D., Lin, H.-Y., Lu, C.-L., et al. (2015). Positive effects of bFGF modified rat amniotic epithelial cells transplantation on transected rat optic nerve. *PLoS One* 10, e0119119. doi:10.1371/journal.pone.0119119

Yamashita, K., Inagaki, E., Hatou, S., Higa, K., Ogawa, A., Miyashita, H., et al. (2018). Corneal endothelial regeneration using mesenchymal stem cells derived from human umbilical cord. *Stem Cells Dev.* 27, 1097–1108. doi:10.1089/scd.2017.0297

Yu, C., Yang, K., Meng, X., Cao, B., and Wang, y. F. (2020). Downregulation of long noncoding RNA MIAT in the retina of diabetic rats with tail-vein injection of human umbilical-cord mesenchymal stem cells. *Int. J. Med. Sci.* 17, 591–598. doi:10.7150/ijms.38078

Zeng, W., Li, Y., Zeng, G., Yang, B., and y Zhu, Y. (2014). Transplantation with cultured stem cells derived from the human amniotic membrane for corneal alkali burns: An experimental study. *Ann. Clin. Lab. Sci.* 44, 73–81.

Zhou, Y., Chen, Y., Wang, S., Qin, F., and Wang, y. L. (2019). MSCs helped reduce scarring in the cornea after fungal infection when combined with anti-fungal treatment. *BMC Ophthalmol.* 19, 226. doi:10.1186/s12886-019-1235-6

Frontiers in
Bioengineering and Biotechnology

Accelerates the development of therapies, devices, and technologies to improve our lives

A multidisciplinary journal that accelerates the development of biological therapies, devices, processes and technologies to improve our lives by bridging the gap between discoveries and their application.

Discover the latest Research Topics

See more →

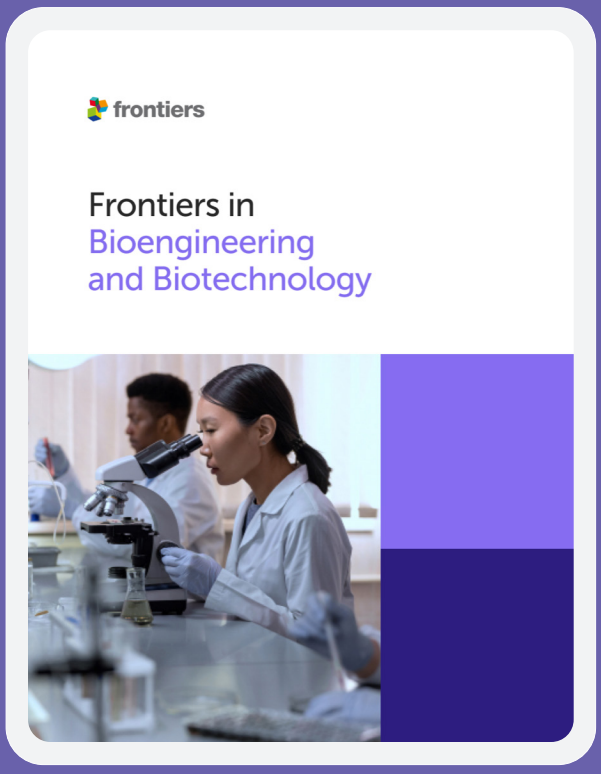

Frontiers

Avenue du Tribunal-Fédéral 34
1005 Lausanne, Switzerland
frontiersin.org

Contact us

+41 (0)21 510 17 00
frontiersin.org/about/contact